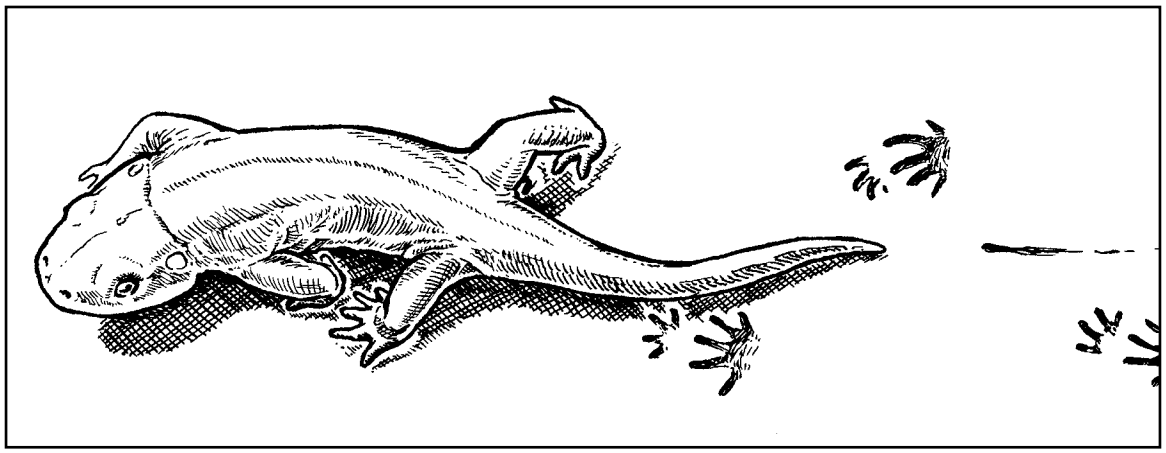
Bulletin 65

New Mexico Museum of Natural History & Science

A Division of the
DEPARTMENT OF CULTURAL AFFAIRS

Carboniferous-Permian Transition in the Robledo Mountains, Southern New Mexico



Edited by

Spencer G. Lucas and William A. DiMichele

Albuquerque, 2015

Bulletin 65

New Mexico Museum of Natural History & Science

A Division of the
DEPARTMENT OF CULTURAL AFFAIRS

Carboniferous-Permian Transition in the Robledo Mountains, Southern New Mexico

Edited by

Spencer G. Lucas and William A. DiMichele

New Mexico Museum of Natural History & Science
Albuquerque, 2015

Published with the support of the Vortman Fund

STATE OF NEW MEXICO
Department of Cultural Affairs
Veronica Gonzales, *Secretary*

NEW MEXICO MUSEUM OF NATURAL HISTORY AND SCIENCE
Gary Romero, *Interim Executive Director*

BOARD OF TRUSTEES
Susanna Martinez, Governor, State of New Mexico, *ex officio*
Gary Romero, *Interim Executive Director*, *ex officio*
Gary Friedman, *President*
Deborah Dixon
Maya Elrick, Ph.D.
Peter F. Gerity, Ph.D.
Laurence Lattman, Ph.D.
Morton Lieberman, Ph. D.
Imogene Lindsay, *Emerita*
Viola Martinez
Marvin Moss
John Montgomery, Ph.D.
Jennifer Riordan
Laura Smigielski-Garcia
David Smoak
Steve West

Cover illustration: The *Batrachichnus* trackmaker; artwork by Matt Celeskey. All filler page artwork also by Matt Celeskey.

Original Printing

ISSN: 1524-4156

Available from the New Mexico Museum of Natural History and Science,
1801 Mountain Road NW, Albuquerque, NM 87104; Telephone (505) 841-2800;
Fax (505) 841-2866; www.nmnaturalhistory.org

NMMNH Bulletins online at: http://nmnaturalhistory.org/bulletins

BULLETIN OF THE NEW MEXICO MUSEUM OF NATURAL HISTORY AND SCIENCE

EDITORS

Spencer G. Lucas	New Mexico Museum of Natural History and Science, Albuquerque, NM, USA (NMMNHS)
Robert Sullivan	NMMNHS
Lawrence H. Tanner	Le Moyne College, Syracuse, NY, USA

PRODUCTION EDITOR

Asher J. Lichtig	NMMNHS

ASSOCIATE EDITORS

Guillermo Alvarado	Asociación Costarricense de Geotecnica, San José, Costa Rica
Marco Avanzini	Museo Tridentino di Scienze Naturali, Trento, Italy
David Berman	Carnegie Museum of Natural History, Pittsburgh, PA, USA
Brent Breithaupt	Laramie, WY, USA
William DiMichele	National Museum of Natural History, Washington, D.C., USA
John R. Foster	Museum of Moab, Utah, USA
Gerard Gierlinski	Polish Geological Institute, Warsaw, Poland
Jean Guex	University of Lausanne, Lausanne, Switzerland
Jerald D. Harris	Dixie State College, St. George, UT, USA
Andrew B. Heckert	Appalachian State University, Boone, NC, USA
Adrian P. Hunt	Flying Heritage Collection, Everett, WA, USA
Hendrik Klein	Neumarkt, Germany
Karl Krainer	University of Innsbruck, Innsbruck, Austria
Martin G. Lockley	University of Colorado at Denver, Denver, CO, USA
Claudia Marsicano	Universidad de Buenos Aires, Buenos Aires, Argentina
Gary S. Morgan	NMMNHS
Donald R. Prothero	Natural History Museum, Los Angeles, CA, USA
Silvio Renesto	Università degli Studi dell'Insubria, Varese, Italy
Joerg W. Schneider	Technical University BergAkademie of Freiberg, Freiberg, Germany
Jingeng Sha	Nanjing Institute of Geology and Palaeontology, Nanjing, China
Sebastian Voigt	Urweltmuseum GEOSKOP/Burg Lichtenburg, Thallichtenberg, Germany
Ralf Werneburg	Naturhistorisches Museum Schloss Bertholdsburg, Schleusingen, Germany
Richard S. White, Jr.	International Wildlife Museum, Tucson, AZ, USA

NEW MEXICO MUSEUM OF NATURAL HISTORY AND SCIENCE BULLETINS

27. Late Triassic microvertebrates from the lower Chinle Group (Otischalkian-Adamanian: Carnian), 2004. by Andrew B. Heckert, 170 pp.
28. New Mexico's Ice Ages, 2005. edited by Spencer G. Lucas, Gary S. Morgan, and Kate E. Zeigler, 300+ pp.
29. Vertebrate Paleontology in Arizona, 2005. edited by Andrew B. Heckert & Spencer G. Lucas, 210 pp.
30. The Nonmarine Permian, 2005. edited by Spencer G. Lucas & Kate E. Zeigler, 362 pp.
31. Permian of Central New Mexico, 2005. edited by Spencer G. Lucas, Kate E. Zeigler & Justin A Spielmann, 176 pp.
32. Genética y Mamíferos Mexicanos: Presente y Futuro, 2006. edited by Ella Vázquez-Domínguez and David J. Hafner, 73 pp.
33. Skeletal Impact of Disease, 2006. by Bruce M. Rothschild and Larry D. Martin, 226 pp.
34. America's Antiquities: 100 Years of Managing Fossils on Federal Lands, 2006. edited by Spencer G. Lucas, Justin A. Spielmann, Patricia M. Hester, Jason P. Kenworthy and Vincent L. Santucci, 185 pp.
35. Late Cretaceous Vertebrates from the Western Interior, 2006. edited by Spencer G. Lucas and Robert M. Sullivan, 410 pp.
36. Paleontology and Geology of the Upper Jurassic Morrison Formation, 2006. edited by John R. Foster and Spencer G. Lucas, 249 pp.
37. The Triassic-Jurassic Terrestrial Transition, 2006. edited by Jerry D. Harris, Spencer G. Lucas, Justin A. Spielmann, Martin G. Lockley, Andrew R.C. Milner and James I. Kirkland, 607 pp.
38. Pennsylvanian-Permian Fusulinaceans of the Big Hatchet Mountains, New Mexico, 2006. by Garner L. Wilde, 331 pp.
39. Upper Aptian-Albian Bivalves of Texas and Sonora: Biostratigraphic, Paleoecologic and Biogeographic Implications, 2007. edited by Robert W. Scott, 39 pp.
40. Triassic of the American West, 2007. edited by Spencer G. Lucas and Justin A. Spielmann, 247 pp.
41. The Global Triassic, 2007. edited by Spencer G. Lucas and Justin A. Spielmann, 415 pp.
42. Cenozoic Vertebrate Tracks and Traces, 2007. edited by Spencer G. Lucas, Justin A. Spielmann and Martin G. Lockley, 330 pp.
43. The Late Triassic archosauromorph *Trilophosaurus*, 2008. by Justin A. Spielmann, Spencer G. Lucas, Larry F. Rinehart and Andrew B. Heckert, 177 pp.
44. Neogene Mammals, 2008. edited by Spencer G. Lucas, Gary S. Morgan, Justin A. Spielmann and Donald R. Prothero, 442 pp.
45. The Paleobiology of Coelophysis bauri (Cope) from the Upper Triassic (Apachean) Whitaker quarry, New Mexico, with detailed analysis of a single quarry block, 2009. by Larry F. Rinehart, Spencer G. Lucas, Andrew B. Heckert, Justin A. Spielmann and Matthew D. Celeskey, 260 pp.
46. The taxonomy and paleobiology of the Late Triassic (Carnian-Norian: Adamanian-Apachean) drepanosaurs (Diapsida: Archosauromorpha: Drepanosauromorpha, 2010. by Silvio Renesto, Justin A. Spielmann, Spencer G. Lucas and Giorgio Tarditi Spagnoli, 81 pp.
47. Ichnology of the Upper Triassic (Apachean) Redonda Formation, east-central New Mexico, 2010. by Spencer G. Lucas, Justin A. Spielmann, Hendrik Klein and Allan J Lerner, 75 pp.
48. New Smithian (Early Triassic) ammonoids from Crittenden Springs, Elko County, Nevada: Implications for taxonomy, biostratigraphy and biogeography, 2010. by James F. Jenks, Arnaud Brayard, Thomas Brühwiler and Hugo Bucher, 41 pp.
49. Carboniferous-Permian transition in Cañon del Cobre, northern New Mexico, 2010. edited by Spencer G. Lucas, Jörg W. Schneider and Justin A. Spielmann, 229 pp.
50. Review of the tetrapod ichnofauna of the Moenkopi Formation/Group (Early-Middle Triassic) of the American Southwest, 2010. by Hendrik Klein and Spencer G. Lucas, 67 pp.
51. Crocodyle tracks and traces, 2010. edited by Jesper Milàn, Spencer G. Lucas, Martin G. Lockley and Justin A. Spielmann, 244 pp.
52. Selachians from the Upper Cretaceous (Santonian) Hosta Tongue of the Point Lookout Sandstone, central New Mexico, 2011. by Jim Bourdon, Keith Wright, Spencer G. Lucas, Justin A. Spielmann and Randy Pence, 54 pp.
53. Fossil Record 3, 2011. edited by Robert M. Sullivan, Spencer G. Lucas and Justin A. Spielmann, 736 pp.
54. Ichnology of the Mississippian Mauch Chunk Formation, eastern Pennsylvania, 2012. by David L. Fillmore, Spencer G. Lucas and Edward L. Simpson, 136 pp.
55. Tetrapod fauna of the Upper Triassic Redonda Formation, east-central New Mexico: The characteristic assemblage of the Apachean land-vertebrate faunachron, 2012. by Justin A. Spielmann and Spencer G. Lucas, 119 pp.
56. Revision of the Lower Triassic tetrapod ichnofauna from Wióry, Holy Cross Mountains, Poland, 2012. by Hendrik Klein and Grzegorz Niedzwiedzki, 62 pp.
57. Vertebrate Coprolites, 2012. edited by Adrian P. Hunt, Jesper Milàn, Spencer G. Lucas and Justin A. Spielmann, 387 pp.
58. A new archaic basking shark (Lamniformes: Cetorhinidae) from the late Eocene of western Oregon, U.S.A., and description of the dentition, gill rakers and vertebrae of the recent basking shark Cetorhinus maximus (Gunnerus), 2013. by Bruce J. Welton, 48 pp.
59. The Carboniferous-Permian transition in central New Mexico, 2013. edited by Spencer G. Lucas, W. John Nelson, William A. DiMichele, Justin A. Spielmann, Karl Krainer, James E. Barrick, Scott Elrick and Sebastian Voigt, 389 pp.
60. The Carboniferous-Permian transition, 2013. edited by Spencer G. Lucas, William A. DiMichele, James E. Barrick, Joerg W. Schneider and Justin A. Spielmann, 465 pp.
61. The Triassic System: New Developments in Stratigraphy and Paleontology, 2013. edited by Lawrence H. Tanner, Justin A. Spielmann and Spencer G. Lucas, 612 pp.
62. Fossil Footprints of Western North America, 2014. edited by Martin G. Lockey and Spencer G. Lucas, 508 pp.
63. Variation in the Dentition of *Coelophysis bauri*, 2014. by Lisa G. Buckley and Philip J. Currie, 73 pp.
64. Conodonts from the Carnian-Norian Boundary (Upper Triassic) of Black Bear Ridge, Northeastern British Columbia, Canada, 2014, by Michael J. Orchard, 139 pp.

Lucas, S. G. and DiMichele, W. A., eds., 2015, Carboniferous-Permian Transition in the Robledo Mountains, Southern New Mexico. New Mexico Museum of Natural History and Science Bulletin 65.

Carboniferous-Permian Transition in the Robledo Mountains, Southern New Mexico

Contents

Foreword…….....Philip A. Gensler vi

Preface…….....Spencer G. Lucas and William A. DiMichele vii

Carboniferous-Permian transition in the Robledo Mountains, southern New Mexico: An overview…….. Spencer G. Lucas and William A. DiMichele 1

The Pennsylvanian-Permian section at Robledo Mountain, Doña Ana County, New Mexico, USA…..
.....Karl Krainer, Spencer G. Lucas, Daniel Vachard and James E. Barrick 9

The Lower Permian Hueco Group, Robledo Mountains, New Mexico.....Spencer G. Lucas, Karl Krainer and Daniel Vachard 43

Geology of Prehistoric Trackways National Monument, Doña Ana County, New Mexico….....Spencer G. Lucas, Karl Krainer, John Nelson and Scott Elrick 97

Walchian charcoalified wood from the Early Permian Community Pit Formation in Prehistoric Trackways National Monument, New Mexico, U.S.A., and its paleoecological implications.....
.....Howard Falcon-Lang, Francine Kurzawe and Spencer G. Lucas 115

A compositionally unique voltzian conifer-callipterid flora from a carbonate-filled channel, Lower Permian, Robledo Mountains, New Mexico, and its broader significance….William A. DiMichele, Dan S. Chaney, Howard Falcon-Lang, Hans Kerp, Cindy V. Looy, Spencer G. Lucas, Karl Krainer and Sebastian Voigt 123

Early Permian fossil floras from the red beds of Prehistoric Trackways National Monument, southern New Mexico…….....William A. DiMichele, Spencer G. Lucas, Cindy V. Looy, Dan S. Chaney and Sebastian Voigt 129

A *Selenichnites* ichnoassociation from Early Permian tidal flats of the Prehistoric Trackways National Monument of south-central New Mexico…….....Allan J Lerner and Spencer G. Lucas 141

Permian tetrapod ichnodiversity of the Prehistoric Trackways National Monument (south-central New Mexico, U.S.A.).....Sebastian Voigt and Spencer G. Lucas 153

Foreword



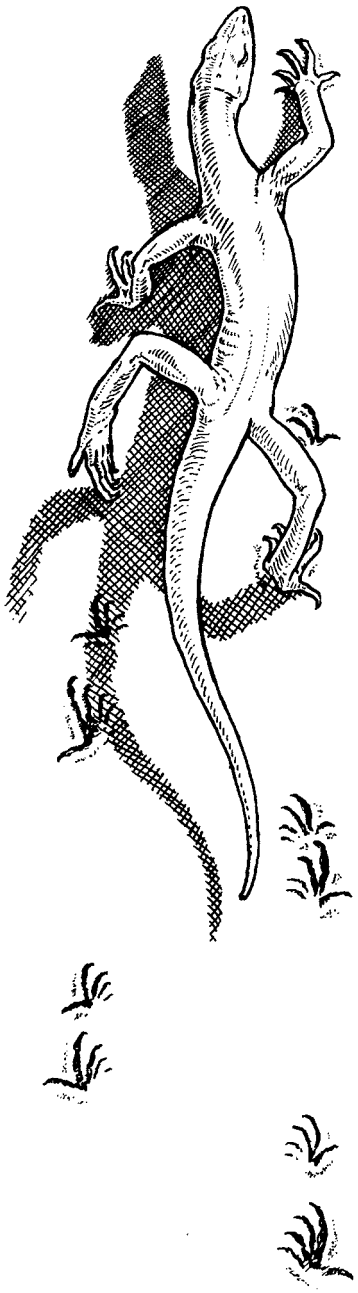
Today, the Robledo Mountains of southern New Mexico are characterized by a dry desert landscape with outcrops of sedimentary rock and sparse vegetation. In contrast to the current desert climate, the sedimentary outcrops found in the Robledos provide evidence that millions of years ago, the southern New Mexico landscape was very different. The sedimentary units consist predominantly of red sandstone and gray limestone that represent the transgression and regression of an ancient seacoast that existed here during the Permian Period, about 280 million years ago. This ancient seacoast is named the Hueco Seacoast. Owned and managed by the U. S. Bureau of Land Management (BLM), the Robledos provide opportunities for the public to recreate and experience the outdoors. The Robledos also provide an excellent opportunity for scientific research. During the 1980's, paleontologist Jerry MacDonald recognized the significance of the numerous trace fossils he was discovering in the area. Working with the BLM, Jerry started collecting what would turn out to be a large fossil collection that would capture the interest of scientists internationally. These rare trace fossils, which consist of trackways and impressions of numerous life forms, include those of reptiles, amphibians, fish, arthropods, including insects, soft-bodied marine animals, and plants that tell an in-depth story of life along the ancient Hueco Seacoast that is not found elsewhere.

In the 1990s, the major portion of MacDonald's fossil collection was transferred to the New Mexico Museum of Natural History & Science (NMMNHS), allowing for its long term care and a more in-depth study of the fossils. Since that time, Dr. Spencer Lucas has assembled an interdisciplinary team of scientists from around the world to describe and interpret the various trace fossils and geology found in the Robledo Mountains. Initial studies and publications of the Robledo Mountain trace fossils illustrated the rarity and scientific importance of the fossils MacDonald had discovered. Due to this scientific significance, the U. S. Congress, in 2009, set aside 5,280 acres of the Robledo Mountains by establishing the Prehistoric Trackways National Monument (PTNM). The BLM manages this monument to allow for public enjoyment and to provide for the protection, study, and educational opportunities that the fossils offer.

This volume presents the most current research that has been conducted on the various fossil groups and presents new evidence that refines the depositional timing of the Hueco Group. The research presented here certainly allows for a greater understanding of an ancient ecosystem during the Permian Period and will provide a basis with which the BLM will interpret the paleontological and geologic resources within the Monument.

—Philip A. Gensler
BLM Regional Paleontologist
Santa Fe, NM

Preface



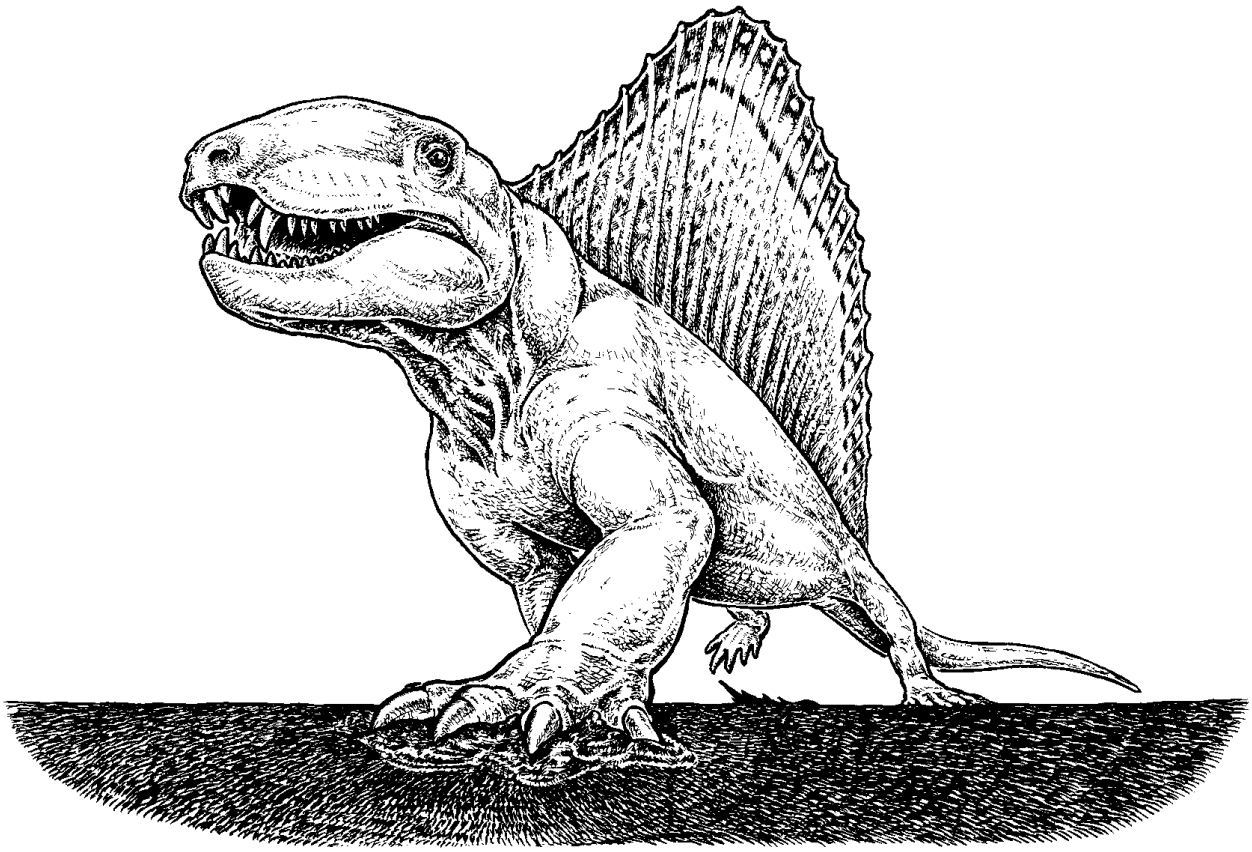
In 1987, paleontologist Jerry MacDonald discovered an extensive assemblage of fossil footprints in Lower Permian red beds exposed in the Robledo Mountains just northwest of Las Cruces, New Mexico. MacDonald collected at this site and other fossil localities he found nearby. In the early 1990s, McDonald's collection became part of the fossil collection of the New Mexico Museum of Natural History and Science (NMMNHS). Interest in the scientific significance of this collection drove a Federally-funded study of the collection and the tracksites by NMMNHS in collaboration with the Smithsonian Institution. The goal of that study was to provide a scientific assessment of the Lower Permian trace fossil assemblages and to recommend options for their preservation, future scientific research and public education.

The study, completed in 1994, identified the area with extensive trace fossil assemblages in the southern Robledo Mountains as an extremely significant record of traces, the most scientifically important such record known from red beds of Permian age. Subsequent research and scientific publications on the Robledo traces rewrote Permian nonmarine ichnology. Not only was Permian vertebrate ichnotaxonomy revised wholesale, but new ichnotaxa were discovered, aspects of invertebrate ichnology were clarified and new analyses of ichnofacies followed.

Ultimately, in 2009, the U. S. Government designated the approximately 5000-acre area in the southern Robledo Mountains that yields Lower Permian trace fossils as the Prehistoric Trackways National Monument (PTNM). In that year began a new, Federally-funded study of the trace fossils in and around the PTNM, undertaken by NMMNHS to re-evaluate all of the fossil sites and make specific recommendations to manage the paleontological resources. This required new research, and the NMMNHS worked with a team of collaborators in sedimentology, field geology, paleobotany, micropaleontology and ichnology. This project provided the evaluations and the recommendations asked for by BLM. It also produced a new round of research on the trace fossil assemblages, the associated plant, invertebrate macro- and microfossils and the geological context of the fossils. Some of the results of that research are published here. Other aspects of this research have already been published or will appear in print elsewhere.

The science presented in this volume owes a heavy debt to Jerry MacDonald, who worked extensively with the researchers in the field from 2009 through 2011, sharing his discoveries and deep knowledge of the paleontology of the southern Robledo Mountains. The financial and logistical support provided by the BLM was critical to all phases of the research presented here. Among the many BLM personnel who helped us, we are particularly grateful to Lori Allen, McKinney Briske, Phil Gensler and Pat Hester. Finally, we thank those who generously devoted time and effort to reviewing the articles in this volume: Bruce Allen, B. Mitchell Blake, Jr., Blaine Cecil, Pedro Cózar, David Haig, Martin Gibling, Peter Holterhoff, Adrian Hunt, Hendrik Klein, John Nelson, Mike Romano, Ed Simpson, Matt Stimson and several who wish to remain anonymous.

—Spencer G. Lucas and William A. DiMichele



Lucas, S. G. and DiMichele, W. A., eds., 2015, Carboniferous-Permian Transition in the Robledo Mountains, Southern New Mexico. New Mexico Museum of Natural History and Science Bulletin 65.

CARBONIFEROUS-PERMIAN TRANSITION IN THE ROBLEDO MOUNTAINS, SOUTHERN NEW MEXICO: AN OVERVIEW

SPENCER G. LUCAS[1] AND WILLIAM A. DIMICHELE[2]

[1]New Mexico Museum of Natural History and Science, 1801 Mountain Rd. NW, Albuquerque, NM 87104, spencer.lucas@state.nm.us; [2]Department of Paleobiology, NMNH Smithsonian Institution, Washington, DC 20560 dimichel@si.edu

Abstract—This volume presents eight articles on the Pennsylvanian-Permian geology and paleontology of the Robledo Mountains in Doña Ana County, southern New Mexico. The reported research resulted from a federally-funded study of the trace fossils in and around the Prehistoric Trackways National Monument (PTNM). We divide the overview by the main topics addressed—stratigraphy, sedimentology, paleobotany, micropaleontology, biostratigraphy and ichnology—and draw attention to the most significant research results. These indicate that the identification of glacio-eustatically driven sedimentary cyclicity in the Robledos Lower Permian strata, paralleling that seen in mid-continent and Appalachian basin cyclothems of Pennsylvanian age, is problematic. There may be some kind of allocyclic signature in the Robledo sections, but autocyclic drivers clearly were important forces in the local Early Permian sedimentary history. The red-bed fossil assemblages in the PTNM were early fit into a rather simple model of intertidal flat depositional environments, but studies here indicate much greater depositional complexity, and identify what are likely a mosaic of local paleonenvironments and taphonomic settings in which the trace fossils and red-bed plant assemblages accumulated. The Early Permian geological record indicates episodically increasing seasonality and climatic dryness around the equatorial regions of central and western Pangea, a trend that began in the late Middle Pennsylvanian. During this period of warming, terrestrial floras became increasingly heterogeneous spatially, and the Robledo paleofloras fit that pattern. Precise and extensive age data for the Hueco Group section based on non-fusulinid and fusulinid foraminiferans indicate that the base of the Leonardian (Artinskian) is very close to the base of the Robledo Mountains Formation. This means the upper part of the local Hueco section is Leonardian, not Wolfcampian as long supposed.

INTRODUCTION

The Robledo Mountains are an isolated fault block mountain range northwest of Las Cruces in southern New Mexico. Paleozoic strata are the primary bedrock exposed in the range (Fig. 1). The youngest Paleozoic rocks, Lower Permian strata of the Hueco Group, are as much as 565 m thick and crop out across most of the central and southern parts of the Robledo Mountains (Seager et al., 2008). In 2009, the U. S. Congress created a new national monument in the Robledo Mountains, primarily because of the world-class Early Permian trace-fossil assemblages preserved in the Hueco Group strata exposed in the southern Robledo Mountains (Lucas and Heckert, 1995; Lucas et al., 1998a, 2011; Minter and Braddy, 2009 and references cited therein).

The Prehistoric Trackways National Monument (PTNM) is approximately 2137 hectares (5280 acres) of land administered by the U. S. Bureau of Land Management (Fig. 1). In 2009, a Federally funded study began of the trace fossils in and around the PTNM, undertaken by the New Mexico Museum of Natural History and Science (NMMNHS) to re-evaluate all of the fossil sites and make specific recommendations to manage the paleontological resources. This required new research, and the NMMNHS worked with a team of collaborators in sedimentology, field geology, paleobotany, micropaleontology and ichnology.

This project provided the evaluations and the recommendations asked for by BLM. It also produced a new round of research on the trace fossil assemblages, the associated plant fossils, invertebrate microfossils and the geological context in which these fossils are found. Some of the results of that research are published here. Other aspects of this research have already been published (Lucas et al., 2011, 2013; Voigt et al., 2013a, b; Falcon-Lang et al., 2014) or will appear in print elsewhere.

Here, we present a brief overview of the articles in this volume. We divide the overview by the main topics addressed—stratigraphy, sedimentology, paleobotany, micropaleontology, biostratigraphy and ichnology. We conclude by drawing attention to the most significant research results to emerge from the studies of the PTNM published here.

LITHOSTRATIGRAPHY

Most of the bedrock exposed in the Robledo Mountains is of Early Permian age (Fig. 1), and most of the articles in this volume are about those Lower Permian strata and their fossils. However, Pennsylvanian strata do crop out along the northern and western periphery of the Robledo Mountains (Fig. 1). Kottlowski (1960) first described these strata in some detail, assigning them Atokan ("Derryan"), Desmoinesian, Missourian and Virgilian ages. He also identified a stratigraphic interval just below the Hueco strata as equivalent to the lower Wolfcampian Bursum Formation to the north.

Seager et al. (2008) mapped these chronostratigraphic subdivisions, and Wahlman and King (2002) described some fusulinids from the Bursum-equivalent and lower Hueco strata (Thompson, 1954 had first described fusulinids from the same interval). Lucas et al. (1995, 1998b) created formal lithostratigraphic nomenclature for the Hueco Group strata in the Robledo Mountains (Fig. 2)

In this volume, **Krainer, Lucas, Vachard and Barrick** present a detailed study of the Pennsylvanian-Permian section on the northern end of the Robledo Mountains. This ~ 418 m thick section is carbonate dominated with diverse fusulinid assemblages. **Krainer et al.** assign this section to the Horquilla Formation (lower 300 m) overlain by the Shalem Colony Formation of the Hueco Group (upper 118 m). They divide the Horquilla Formation into five informal members, in ascending order: member A (~ 82 m thick), characterized by cherty limestone; member B (~ 24 m thick), a slope-forming, shale-dominated interval; member C (~ 52 m thick), consisting of alternating beds of limestone and shale; member D (~ 75 m thick), bedded to massive, non-cherty limestone; and member E (~ 62 m thick), composed of bedded limestone with intercalated shale (Fig. 2).

A detailed study of the entire Lower Permian Hueco Group section in the Robledo Mountains is presented by **Lucas, Krainer and Vachard.** They assign the Hueco Group strata to (in ascending order) the Shalem Colony, Community Pit, Robledo Mountains and Apache Dam formations (Fig. 2). The Shalem Colony Formation is about 127-156 m thick and is a relatively thick-bedded and coarse-grained succession of wackestones, grainstones, rudstones and some oolitic limestones intercalated with mostly covered intervals that represent shale and/or nodular limestone. It rests with apparent conformity on the Pennsylvanian-Permian Horquilla Formation. The Community Pit Formation, 93-177 m thick, is mostly a slope-forming interval of shale and siltstone intercalated with relatively thin intervals of limestone, many of which are mudstones and dolomitic mudstones. The formation has a characteristic brownish gray to grayish orange color. The Robledo Mountains Formation is about 90-125 m thick and is mostly drab-colored marine shale and limestone, but is readily identified by its characteristic siliciclastic red beds (mudstone, siltstone and sandstone), which are intercalated with the marine rocks. At least 107 m thick, the Apache Dam Formation is composed mainly of algal limestone and shale/covered intervals.

The general geology of the PTNM is described in this volume by **Lucas, Krainer, Nelson and Elrick.** Most of the bedrock exposed in

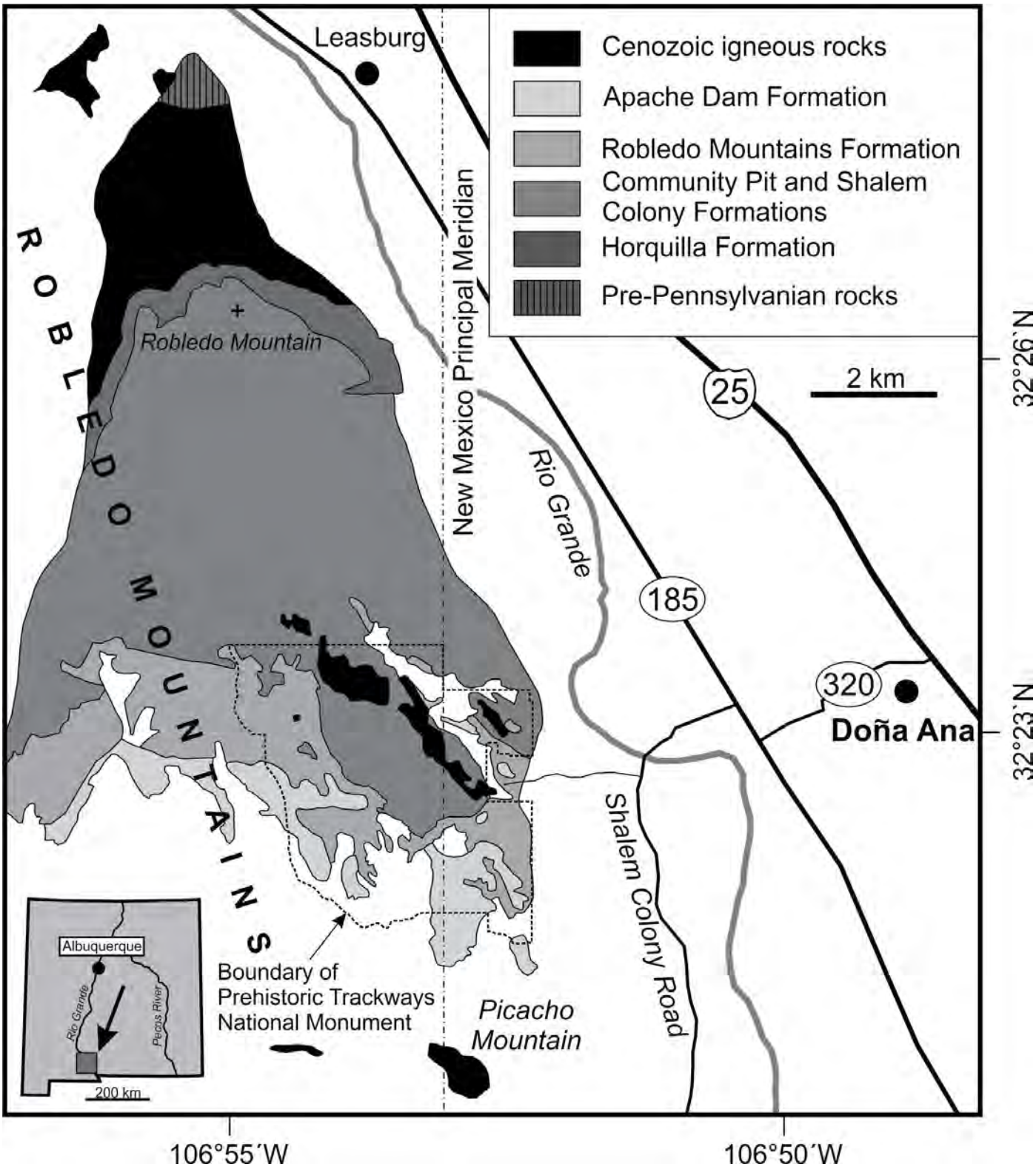


FIGURE 1. Generalized geologic map of the Robledo Mountains in south-central New Mexico (drawn by Karl Krainer). Boundary of Prehistoric Trackways National Monument (PTNM) is shown in the southern part of the range.

group/ fmn	formation/ member	maximum thickness	principal lithologies
Hueco Group	Apache Dam Formation	107+ m	algal limestone and shale
	Robledo Mountains Formation	90-125 m	grainy limestone, shale and red-bed siliciclastics (sandstone, siltstone, mudstone)
	Community Pit Formation	93-177 m	shale, muddy limestone, dolomitic limestone
	Shalem Colony Formation	127-156 m	thick-bedded, coarse-grained limestone (wackestone, grainstone, etc.)
Horquilla Formation	member E	62 m	bedded limestone with intercalated shale
	member D	75 m	bedded to massive, non-cherty limestone
	member C	52 m	alternating beds of limestone and shale
	member B	24 m	mostly shale
	member A	82 m	cherty limestone

FIGURE 2. Brief summary of Horquilla Formation and Hueco Group stratigraphy in the Robledo Mountains, after **Krainer et al.** and **Lucas et al.**, this volume.

the PTNM can be assigned to the four formations of the Lower Permian Hueco Group. These strata are mainly limestone and mudstone of shallow marine origin, but the Robledo Mountains Formation also includes red-bed siliciclastic coastal plain deposits that yield the trace fossil assemblages that justified creation of the PTNM.

Rocks of Cenozoic age crop out much less extensively in the PTNM than do Hueco Group strata. Cenozoic strata include Eocene fluvial, playa and volcaniclastic deposits of the Laramide orogeny (Love Ranch and Palm Park formations) and Miocene to Pliocene alluvial sediments (Rincon Valley and Camp Rice formations) or igneous rocks (Bell Top Formation, Robledo rhyolite, basalt) associated with late Cenozoic development of the Rio Grande rift. Quaternary rocks are mostly superficial alluvial and terrace deposits. The Rio Grande rifting event, which commenced in the Miocene, determined the current geological structure of the Robledo Mountains and the PTNM. The geological history of the PTNM can thus be divided into two principal phases—Early Permian shoreline and shallow marine environments of the Hueco seaway and late Cenozoic continental rifting and basin-margin sedimentation. The more than 250 million years that divide these two phases left little geological evidence in the PTNM.

SEDIMENTOLOGY

During Pennyslvanian-Permian time, the area of the Robledo Mountains lay along the western edge of the late Paleozoic Orogrande basin (Fig. 3). To the southwest, what has been called the Florida islands or Florida uplift separated the Orogrande basin from the late Paleozoic Pedregosa basin, which covered much of southwestern New Mexico, southeastern Arizona and adjacent portions of the Mexican states of Chihuahua and Sonora. Based on currently posited paleogeography, Pennsylvanian-Permian deposition in the Robledo Mountains area took place on the Robledo shelf, and was part of deposition in the Orogrande basin.

However, as Lucas and Krainer (2011) first pointed out, the Pennsylvanian section at Robledo Mountain differs substantially from the closest Pennsylvanian sections in the Orogrande basin, which are in the Doña Ana Mountains 10 km to the northeast and in the Caballo Mountains-Derry Hills, 40 km to the northwest. Indeed, **Krainer, Lucas, Vachard and Barrick** assign the section at Robledo Mountain to the Horquilla Formation, which is the Pennsylvanian-lowermost Permian lithostratigraphic unit in the Pedregosa basin.

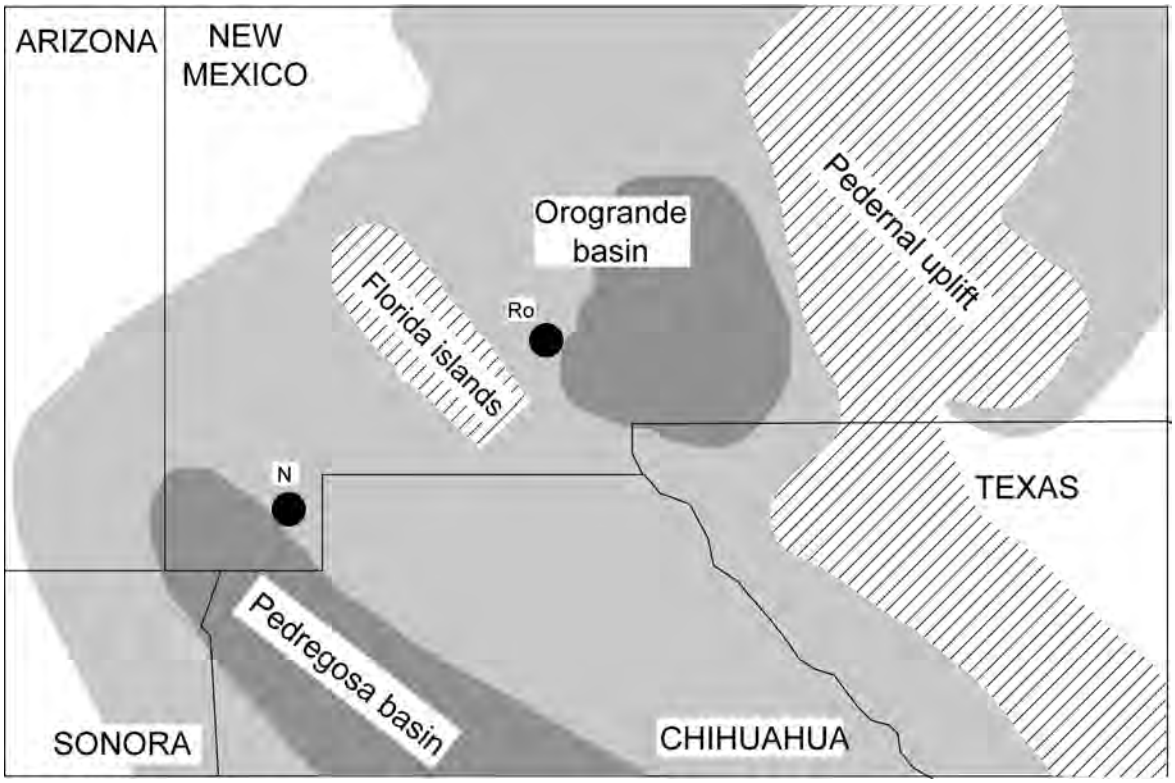


FIGURE 3. Pennsylvanian paleogeography of the divide between the Orogrande and Pedregosa basins during the Pennsylvanian, showing relatively small area of islands and straits dividing the Pedregosa and Orogrande basins, from **Krainer et al.**, this volume. N = Newwell Peak, Big Hatchet Mountains; Ro = Robledo Mountain.

Because of the lithologic similitude of strata to the southwest, **Krainer et al.** argue that the Pennsylvanian strata at Robledo Mountain are more closely related genetically to deposition in the Pedregosa basin than to deposition in the Orogrande basin. Thus, subsidence in the Pedregosa basin and along the Florida shelf (including the Robledo shelf) was relatively even during the Virgilian-Wolfcampian, so that glacio-eustatic cycles are better recorded in these sections than in the more tectonically-influenced sections to the east, within the Orogrande basin. Assignment of most of the Robledo Mountain section to the Horquilla Formation casts doubt on the idea that the Robledo shelf was significantly separated from Horquilla deposition in the Pedregosa basin to the southwest by an intervening Florida uplift (highland). Instead, the original idea of a Florida island, and a strait to the southeast of it, separating the late Paleozoic Orogrande and Pedregosa basins, is more compatible with the stratigraphic and sedimentologic data (Fig. 3).

Based in large part on microfacies and paleontology, **Krainer et al**. interpret the depositional environments of the five informal members of the Horquilla Formation at Robledo Mountain. The microfacies and biota of member A are characteristic of open marine, well-oxygenated and well-circulated conditions with normal marine salinity, deposited below the fair weather wave base in a relatively deep, open marine shelf environment with water depths of at least some tens of meters. These limestones are part of well-developed cycles, and the microfacies and biota indicate a relatively shallow depositional environment. The bulk of member B (shale, wavy and nodular limestone) was deposited in an open marine shelf environment in deeper water and in a more outer shelf position than member A.

Microfacies and biota (particularly algae and fusulinids) indicate that the limestone units of members C, D, and E formed in a shallower depositional environment than the wavy-bedded to nodular limestone units of members A and B. Indistinctly bedded to massive limestone formed in an open, shallow marine, well-oxygenated environment with normal salinity. Water depth did not exceed a few tens of meters. High-energy microfacies (grainstone, packstone, rudstone) and bindstone are also indicative of a shallow marine setting. Thin intercalated conglomerate beds containing marine fossils also point to a high-energy shallow marine environment.

In the Horquilla Formation at Robledo Mountain, the well-developed cyclic pattern with subaerial exposure surfaces on top of many limestone units indicates rapid sea-level fluctuations during deposition of members C, D, and E. Water depth varied between deeper shelf (deposition of offshore mudstone and wavy bedded to nodular limestone) and subaerial exposure, indicating sea-level fluctuations on the order of some tens of meters. Glacio-eustasy seems a likely driver of such cycles.

In their study of the Hueco Group, **Lucas, Krainer and Vachard** analyze microfacies, paleontology and stratigraphic architecture to conclude that: (1) the Shalem Colony Formation accumulated on a platform interior environment of open, normal marine to less common, restricted marine settings; (2) the Community Pit Formation was deposited in shelf settings ranging from shallow, low-energy (rarely high-energy) open marine to restricted marine environments; (3) the Robledo Mountains Formation represents deposition in a restricted to open marine shallow shelf setting where intercalated red beds were deposited on a distal, extensive flood plain (exhibiting crevasse splay deposits, rare channels, and distal sheet flood deposits) during periods of strong siliciclastic influx from uplifts located to the north and northeast; and (4) the Apache Dam Formation was deposited in an open shelf to shelf lagoon environment with normal salinity and open circulation.

The Community Pit and Robledo Mountains formation strata were deposited during a portion of the Early Permian characterized by intense southern hemisphere glaciation (Fielding et al., 2008). However, **Lucas et al.** find the imprint of allocyclicity to be difficult to identify, primarily because of the generally disorganized (chaotic) facies stacking patterns in the Community Pit and Robledo Mountains formations. Instead, the stratigraphic patterns indicate that autocyclic processes strongly influenced deposition. These findings conflict with some earlier interpretations of the stratigraphic framework in the PTNM and surrounding area (Mack, 2007; Mack et al., 2010, 2013).

PALEOBOTANY

Paleobotanical material from the PTNM is known from the Community Pit and Robledo Mountains formations. This consists of numerous fossil logs in shallow marine strata of the Community Pit Formation and one locality where compression foliage of conifers and callipterids is preserved in a small channel-fill deposit (Fig. 4). In the Robledo Mountains Formation, impressions of foliage are present in the siliciclastic red beds. Thus, at least three Lower Permian taphofloras are present.

Among the Early Permian deposits in the PTNM is a localized, limestone-filled paleochannel in the Community Pit Formation discussed in this volume by **DiMichele, Chaney, Falcon-Lang, Kerp, Looy, Lucas, Krainer and Voigt** and by **Falcon-Lang, Kurzawe and Lucas.** The paleochannel, which is ~ 140 m wide and 5-6 m maximum depth, contains a complex fill sequence that yields two distinct fossil plant assemblages (Fig. 4). The base of the channel is a limestone conglomerate that contains permineralized logs and charcoal attributable to indeterminate walchian conifers. The middle channel fill consists of multiple lenses of lime mudstone with a sparse brackish-to-marine water invertebrate fauna and a macroflora consisting largely of an undescribed voltzian conifer, the earliest known occurrence of this plant group, and the callipterid *Lodevia oxydata*, previously known from two areas, one in Central Europe and the other in the Central Appalachian basin. The deposit also contains in situ fossil roots, indicating at least sporadic plant colonization of the micritic muds.

Falcon-Lang et al. describe the stratigraphically lower plant assemblage, which includes large chunks of charcoalified wood, attributed to walchian conifers, associated with a limestone conglomerate in the base of the channel. This charcoalified wood shows dominantly uniseriate, contiguous tracheidal pitting, cupressoid cross-field pits that are solitary or, if paired, show an opposite arrangement, and short uniseriate rays, 1–18 cells high. These anatomical characters match closely the wood of *Macdonaldodendron*, recently described from other sites in PTNM (Falcon-Lang et al., 2014), which is demonstrably a walchian conifer based on aspects of its pith with sclerotic nests, endarch cauline bundles, triangular leaves, and whorled branch pattern. Therefore – while accepting that precise identification of isolated pieces of wood is fraught with difficulties – the overwhelming likelihood is that the charcoalified material from the channel deposit is walchian.

The occurrence of burned fragments of walchian wood in an incised fluvio-estuarine channel suggests that fire-prone walchian trees grew at a time when sea-level was temporarily lowered and the shoreline of the Hueco Seaway had regressed southward. Diverse data indicate that this coastline was subject to strongly seasonal rainfall, but a remarkable feature of the charcoalified woods is that they completely lack growth rings. These facts can be reconciled if the walchian conifers were somehow buffered against seasonal drought. The most likely explanation, consistent with taphonomic considerations, is that they were growing along wet riparian corridors, where elevated water tables provided a reliable year-round water supply. High fuel loads might be expected to have accumulated in these "wet spots" on an otherwise dry landscape, which would have been vulnerable to conflagration in the event of extreme droughts; this fire dynamic may explain the predominant preservation of fossil wood as charcoal.

DiMichele et al. review the stratigraphically higher plant assemblage in the channel fill to note that the voltzian conifer from the channel fill is the earliest member of this evolutionary lineage, extending the known range by approximately 25 million years. Similarly, the geographic range of *Lodevia oxydata* is extended nearly 2500 km, from its previously most westerly known occurrence in West Virginia. Together with the only other report from the Rotliegendes of Poland, this species now has a total known range of approximately 9000 km on today's earth, based on three widely separated and localized occurrences.

Clearly, prior to the latest Permian, when such conifers were abundant, the voltzians were significant tropical landscape elements somewhere, but have been incorporated into the fossil record rarely, so their early history remains largely unknown. For the callipterid, temporal continuity throughout its known range cannot be established, so it cannot be determined if the plant occupied the full range at any given time, or only portions thereof. Nonetheless, the geographic sparseness of its appearances, in light of the high density of plant remains from the sites where it does occur, indicates that its fossil record also is very incomplete.

DiMichele, Lucas, Looy, Chaney and Voigt review the floras of the Robledo Mountains Formation red beds to conclude that they are compositionally similar to those found in the Abo Formation to the north (Hunt, 1983; DiMichele et al., 2007, 2013). These floras are dominated by walchian conifers most similar to the form taxon *Walchia piniformis*. Isolated occurrences of other taxa include the peltasperm *Supaia thinnfeldioides*, the possible peltasperm *Gigantopteridium* sp., the cycadophyte *Taeniopteris* and callipterid peltasperms. The monotony

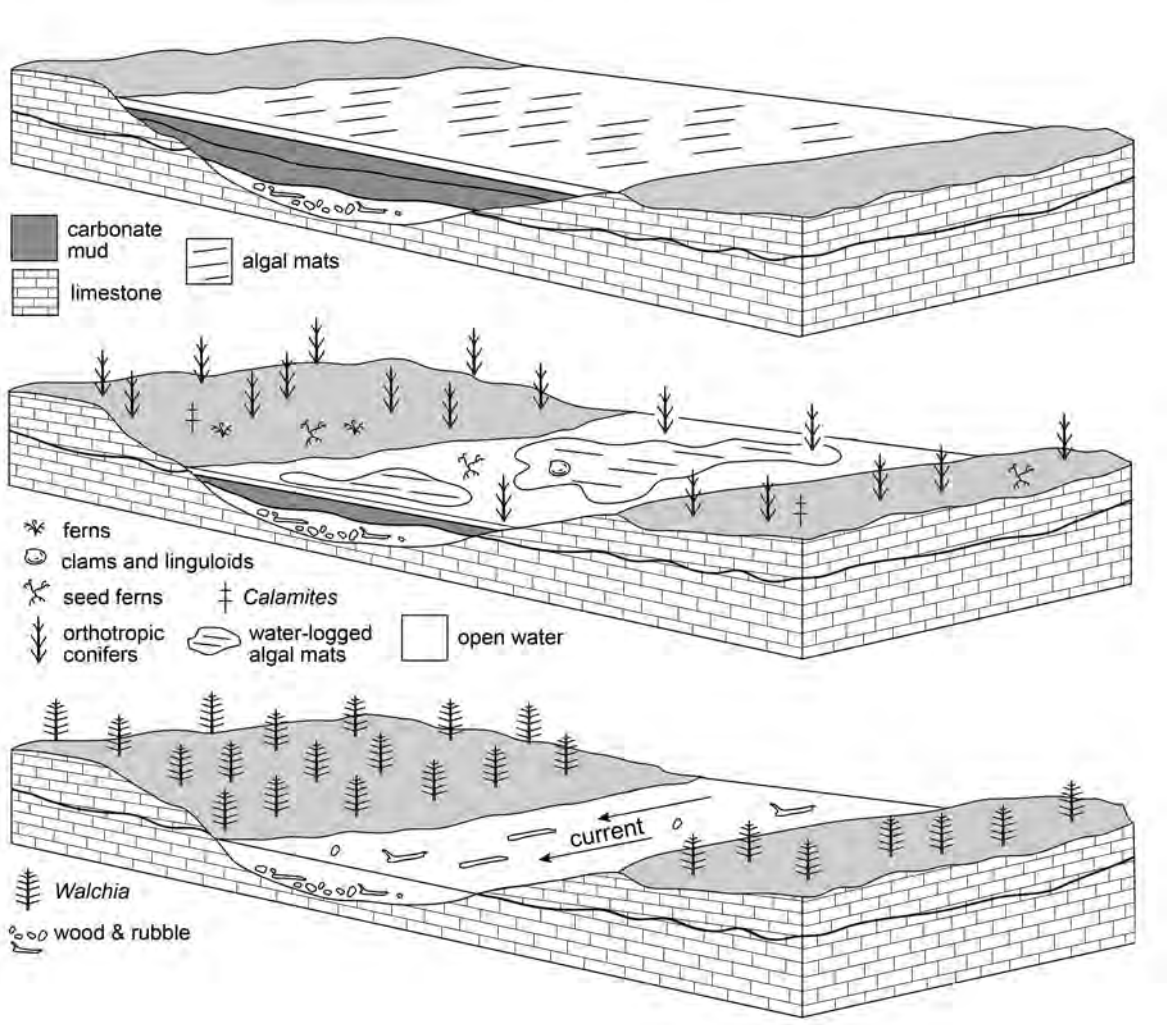


FIGURE 4. Channel-fill progression model of localized deposit in the Community Pit Formation, from **DiMichele et al.** this volume. Bottom— active flow during incision phase and early back filling. Middle— as channel flow volume decreases and carbonate precipitation ensues; surrounding flora changes and plants are incorporated into the micritic muds. Top— evaporitic conditions intensify in final channel fill phases and gypsum is deposited in association with micritic muds. Drawing by Mary Parrish, NMNH.

of these Early Permian red-bed floras over a very large area of New Mexico is noteworthy and perplexing. Notably, other facies from strata within this same time interval, elsewhere in the region, preserve either strikingly different floras or floras of considerably higher diversity. The red-bed floras do not appear to reflect a persistent preservational bias, but suggest that large areas were covered by low diversity forests of conifers. At the outcrops in the Robledo Mountains, the proximity of the red-bed facies to marine conditions bordering the Hueco seaway does not seem to have had any discernible effect on floral composition.

MICROPALEONTOLOGY AND BIOSTRATIGRAPHY

In the Robledo Mountains, marine limestones of the Horquilla Formation and Hueco Group contain diverse assemblages of calcareous microfossils, mostly algae and foraminiferans (including fusulinds). Some of the non-fusulinid foraminiferans and the fusulinids provide the most precise age control of the Pennsylvanian-Permian section in the Robledos. Some conodont biostratigraphy is also available, but it is only based on preliminary sampling (Kozur and LeMone, 1995; Lucas et al., 1995). Ostracods have also been documented in a preliminary way from part of the Robledo Mountains Formation (Kietzke and Lucas, 1995).

Krainer, Lucas, Vachard and Barrick describe microfossils (mostly foraminiferans, including fusulinids, and conodonts) of Morrowan-Wolfcampian age from the section at Robledo Mountain to assign reasonably precise ages, though more data are needed to refine placement of some of the stage boundaries. Thus, the oldest strata of the Horquilla Formation at Robledo Mountain are late Morrowan, and the overlying remainder of member A is of Atokan-Desmoinesian age. Member B is Desmoinesian. The base of the Missourian is not precisely constrained, but conodonts tentatively place the base of the Missourian near the base of member C. The base of the Virgilian is better constrained as high in member C, and the Wolfcampian base is very close to the top of member E, which is just below the base of the Shalem Colony Formation of the Hueco Group. Most of the Shalem Colony Formation section at Robledo Mountain is early Wolfcampian (Newwellian or "Bursumian"), but the uppermost ~50 m of the section are of middle Wolfcampian age.

Lucas, Krainer and Vachard similarly document numerous microfossils from the Hueco Group strata, primarily from in and immediately around the PTNM. They build on work by Vachard et al. (2015) to establish different lineages of foraminiferans, miliolates and nodosariates in the regional Lower Permian, especially the group *Calcivertella*, *Hedraites*, *Hedraites*? and *Pseudovermiporella*, and the group *Nodosinelloides*, *Protonodosaria*, true *Nodosaria*, *Geinitzina*, *Pseudolangella*?, *Rectoglandulina*, and *Pachyphloia*? Thus, a complete Early Permian biozonation by smaller foraminiferans is constructed (Fig. 5).

Lucas et al. thus present new age data, primarily from fusulinids and non-fusulinid foraminiferans, to conclude that the Shalem Colony Formation is early-middle Wolfcampian (Asselian), the Community Pit Formation is middle Wolfcampian-early Leonardian (Asselian-early Artinskian), the Robledo Mountains Formation is early Leonardian (middle-late/latest Artinskian) and the Apache Dam Formation is late Leonardian (latest Artinskian/earliest Kungurian). This indicates

ZONATION	FORMATIONS		Thickness (m)	BIOMARKERS (and representative samples)		REGIONAL STAGES	INTERNATIONAL STAGES
Zone 15	SAN ANDRES FORMATION			*Olgaorlovella davydovi* *Tubiphytes epimonellaeformis* *Geinitzina indepressa*	LEONARDIAN	CATHEDRALIAN	LATE KUNGURIAN
Zone 14				*Hemigordiellina* spp.			MIDDLE KUNGURIAN
Zone 13	GLORIETA SANDSTONE			barren of foraminifers			
Zone 12	YESO GROUP			*Frondicularia* aff. *turae*			EARLY KUNGURIAN
Zone 11				*Ellesmerella rara* *Nestellorella* ? sp.			
Zone 10				*Globivalvulina novamexicana* *Orthovertellopsis protaeformis* *Globomidiella infrapermica*			
Zone 9	HUECO GROUP	Apache Dam Formation					LATE ARTINSKIAN
Zone 8		Robledo Mountains Formation	53	*Pseudoreichelina* sp. *Geinitzina* sp. 2 (?*multicamerata*)		HESSIAN	MIDDLE ARTINSKIAN
Zone 7		Community Pit Formation	10	*Praeneodiscus* sp. *Globivalvulina novamexicana* *Globivalvulina praegraeca* DAB 13 + DAB 14/DAC 1-DAC 5			EARLY ARTINSKIAN
Zone 6			20	*Pseudovermiporella* sp. DAB 10 - DAB 12	WOLFCAMPIAN	LENOXIAN	LATEST SAKMARIAN
Zone 5			50	*Pachyphloia*? sp. *Geinitzina postcarbonica* *Nodosinelloides longissima* DAB 7 - DAB 9			LATE SAKMARIAN
Zone 4			7	*Nodosinelloides pinardae* *Globivalvulina parapiciformis* *Geinitzina postcarbonica* DAA 59 - DAA 69/DAB 2 - DAB 6			EARLY SAKMARIAN
Zone 3			50	*Hedraites* sp. DAA 53 - DAA 58		NEALIAN	LATE ASSELIAN
Zone 2			20	*Geinitzina postcarbonica* *Nodosinelloides netschajewi* DAA 45 - DAA 52			MIDDLE ASSELIAN
Zone 1		Shalem Colony Formation	65	*Leptotriticites* sp. (DAA 43) *Nodosinelloides longissima* *Tubiphytes* sp., *Geinitzina* sp. (DAA 38) *Pseudovidalina* sp., *Pseudoschwagerina* sp. DAA 42	BURSUMIAN		EARLY ASSELIAN - LATEST GZHELIAN

FIGURE 5. Biozonation by foraminiferans and correlation of the Lower Permian strata of the Robledo Mountains, New Mexico, after Lucas et al., this volume.

that the Wolfcampian and Leonardian regional stages/superstages are remarkably complete in New Mexico, where the base of the Wolfcampian is at (or very close to) the base of the Shalem Colony Formation, and the base of the Leonardian is within the Hueco-Abo lithosome.

Note that earlier, Kozur and LeMone (1995) and Lucas et al. (1995) assigned an Artinskian age to the Robledo Mountains Formation based on limited samples of conodonts. Much more conodont sampling and biostratigraphy needs to be undertaken in the Carboniferous-Permian transition section in the Robledo Mountains.

ICHNOLOGY

The trace fossil assemblages from the Robledo Mountains Formation of the Hueco Group are, of course, the basis of the PTNM. Indeed, the PTNM contains one of the most abundant and most extensively discussed assemblages of Paleozoic tetrapod footprints in the world. The red-bed ichnofossil assemblages from the Robledo Mountains Formation (e. g., Minter and Braddy, 2009; Lucas et al., 2011 and references therein) represent an arthropod-dominated invertebrate fauna of terrestrial herbivores and predators such as apterygote insects, myriapods and scorpionids that can be assigned to the *Scoyenia* ichnoguild of the *Scoyenia* ichnofacies. The invertebrate trace fossils are dominated by arthropod trackways, resting traces, jumping traces and grazing traces. Other invertebrate feeding traces, grazing traces, graphoglyptids and helical-shaped burrows are less common. Vertebrate footprints are mostly of small temnospondyls, araeoscelids and pelycosaurs. Tracks of larger amphibians and of primitive amniotes are much less common, and fish swimming traces and tetrapod "swim tracks" are present.

An important issue concerns the amount of tidal influence in the trace-fossil-bearing red beds. The abundance of small amphibian and arthropod traces suggests that the trace fossil assemblages were made in a freshwater setting. However, in apparent contradiction, most sedimentological studies have argued for deposition of the trace-fossil-bearing red beds in the intertidal zone of tidal flats (e.g., Mack and James, 1986; Lucas et al., 1995; Minter and Braddy, 2009). The answer to this lies in Voigt et al. (2013b), who concluded that the red beds of the Robledo Mountains Formation were deposited in the distal parts of an extensive coastal flood plain during alternating dry and wet climatic conditions. Flaser- to wavy-bedded siltstone and fine-grained sandstone represent distal crevasse splay deposits. Most of the trace fossils in the Robledo Mountains Formation occur on mud-draped bedding planes of this lithofacies. The red-bed intervals thus do not show any evidence of marine or tidal influence

An exception to the interpretation of Voigt et al. (2013b) is identified in this volume by **Lerner and Lucas**. They describe a local ichnoassociation of vertebrate and invertebrate ichnotaxa from stratigraphically high in the Robledo Mountains Formation near the eastern border of the PTNM. The vertebrate ichnotaxa of this ichnoassociation include tetrapod "swim tracks" and fish swimming traces. The invertebrate ichnotaxa are dominated by limulid (horseshoe crab) traces, notably the head shield (feeding) trace *Selenichnites*. **Lerner and Lucas** argue that this "*Selenichnites* ichnoassociation" formed subaqueously in two differing nearshore settings: (1) a lower energy setting that contains relatively abundant *Selenichnites;* and (2) a higher energy setting, in which *Selenichnites* is scarce. The higher energy setting includes marine bivalves and possible storm indicators (pot casts), which are not found at the lower energy locality. The ichnogeneric composition and marine-influenced depositional setting of this local *Selenichnites* ichnoassociation distinguish it from those well-known nonmarine Robledo Mountains Formation red bed ichnoassemblages that formed in freshwater settings.

Most prominent among the trace fossils of the Robledo Mountains Formation are those made by vertebrates. In this volume, **Voigt and Lucas** subject more than 700 specimens with tetrapod footprints from the PTNM to an anatomical-feature-based ichnotaxonomic analysis. Based on the results of this study, the tracks belong to eight tetrapod ichnotaxa—*Matthewichnus caudifer*, *Batrachichnus salamandroides*, *Amphisauropus kablikae*, *Dimetropus leisnerianus*, *Notalacerta missouriensis*, *Robledopus macdonaldi*, *Hyloidichnus bifurcatus*, and *Dromopus lacertoides*. These can be referred to lepospondyl, temnospondyl, seymouriamorph, pelycosaurian-grade synapsid, protorothyridid, captorhinid, and araeoscelid trackmakers, respectively. Notable features are the rare occurrence of two more typically Pennsylvanian ichnotaxa (*Matthewichnus*, *Notalacerta*) as well as the only occurrence of the proposed basal non-diapsid eureptilian track *Robledopus*.

About 90% of the material comprises tracks of *Batrachichnus*, *Dimetropus*, and *Dromopus*, suggesting that temnospondyl amphibians, pelycosaurs, and early diapsids represented the most common individuals of the ancient terrestrial tetrapod fauna of the study area. The ichnoassemblage is of typical Early Permian aspect and, in view of the low number and diversity of advanced captorhinomorph footprints, supports assignment to the Artinskian stage.

SIGNIFICANT RESULTS

We can identify four significant results of the research reported here:

1. There is strong evidence for glaciation in the Southern Hemisphere during part of Early Permian time, an interval that is well represented in the PTNM, but the identification of clear cyclicity, paralleling that seen in mid-continent and Appalachian basin cyclothems of Pennsylvanian age, is problematic in the Robledo sections. This does not mean that there are not allocyclic signatures in these rocks. Rather, it indicates how difficult these can be to identify in an area with strong contemporaneous tectonism, complex paleogeography, and a background climate not conducive to the formation and preservation of terrestrial wetland facies, such as coal. Furthermore, this difficulty is not unique to the western regions of Pangea. There have been difficulties identifying clear signatures of glacial-interglacial cycles on 100,000 and 400,000 year time scales throughout the world, though there have been attempts at identification in such areas as carbonate platforms, where one would expect to see incision (see Koch and Frank, 2011). In other cases, however, there is a clear terrestrial vegetational change associated with lithological changes, but seemingly reflecting broad changes in equatorial climate (e.g., Tabor et al., 2013). So, there may be some kind of allocyclic signature in the Robledo sections, but autocyclic drivers clearly were important forces in the local Early Permian sedimentary history.
2. The red-bed fossil assemblages in the PTNM were initially fit into a rather simple model of intertidal flat depositional environments. Studies here indicate much greater depositional complexity, and identify what are likely a mosaic of local paleonenvironments and taphonomic settings in which the trace fossils and red-bed plant assemblages accumulated.
3. The Early Permian was marked by a series of glaciations separated by periods of global warmth. In addition, the geological record indicates episodically increasing seasonality and climatic dryness around the equatorial regions of central and western Pangea, a trend that began in the late Middle Pennsylvanian. During this period of warming, terrestrial floras became increasingly heterogeneous spatially, which might be expected in a world where generally increasing aridity magnifies habitat variability at all scales from the local landscape to broad regions. The Robledo paleofloras fit that pattern.
4. Precise and extensive age data for the Hueco Group section based on non-fusulinid and fusulinid foraminiferans are provided for the first time. These data indicate that the base of the Leonardian (Artinskian) is very close to the base of the Robledo Mountains Formation. This means the upper part of the Hueco section is Leonardian, not Wolfcampian as long supposed.

ACKNOWLEDGMENTS

First, we thank the contributors to this volume as well as the reviewers. BLM provided financial and logistical support for much of the research reported here. Jerry MacDonald generously shared his discoveries and assisted in various ways.

REFERENCES

DiMichele, W. A., Chaney, D. S., Lucas, S. G., Kerp, H. and Voigt, S., 2013, Flora of the Lower Permian Abo Formation red beds, western equatorial Pangea, New Mexico: New Mexico Museum of Natural History and Science, Bulletin 59, p.265-288.

DiMichele, W. A., Chaney, D. S., Nelson, W. J., Lucas, S. G., Looy, C. V., Quick, K. and Jun, W., 2007, A low diversity, seasonal tropical landscape dominated by conifers and peltasperms: Early Permian Abo Formation, New Mexico: Review of Palaeobotany and Palynology, v. 145, p. 249-273.

Falcon-Lang, H. J., Kurzawe, F., and Lucas, S. G., 2014, Coniferopsid tree-trunks preserved in sabkha facies in the Permian (Sakmarian) Community Pit Formation in south-central New Mexico, U.S.A.: Systematics and palaeoecology: Review of Palaeobotany and Palynology, v. 200, p. 138-160.

Fielding, C. R., Frank, T. D. and Isbell, J. L., 2008. The late Paleozoic ice age—a

review of current understanding and synthesis of global climate patterns: Geological Society of America Special Papers 441, p. 343-354.

Hunt, A., 1983, Plant fossils and lithostratigraphy of the Abo Formation (Lower Permian) in the Socorro area and plant biostratigraphy of Abo red beds in New Mexico: New Mexico Geological Society Annual Field Conference Guidebook 34, p. 157-163.

Kietzke, K. K. and Lucas, S. G., 1995, Some microfossils from the Robledo Mountains Member of the Hueco Formation, Doña Ana County, New Mexico: New Mexico Museum of Natural History and Science, Bulletin 6, p. 57-62.

Koch, J. T. and Frank, T. D., 2011, The Pennsylvanian–Permian transition in the low-latitude carbonate record and the onset of major Gondwanan glaciation: Palaeogeography, Palaeoclimatology, Palaeoecology 308, p. 362-372.

Kottlowski, F. E., 1960b, Summary of Pennsylvanian sections in southwestern New Mexico and southeastern Arizona: New Mexico Bureau of Mines and Mineral Resources, Bulletin 66, 187 p.

Kozur, H. and LeMone, D.V., 1995, The Shalem Colony section of the Abo and upper Hueco members of the Hueco Formation of the Robledo Mountains, Doña Ana County, New Mexico: Stratigraphy and new conodont-based age determinations: New Mexico Museum of Natural History and Science, Bulletin 6, p. 39-55.

Lucas, S.G. and Heckert, A.B., eds., 1995, Early Permian footprints and facies: New Mexico Museum of Natural History and Science, Bulletin 6, 301 p.

Lucas, S. G. and Krainer, K., 2011, Pennsylvanian section in the Robledo Mountains, Doña Ana County, New Mexico and its paleogeographic significance: New Mexico Geology, v. 33, p. 48.

Lucas, S. G., Estep, J. W. and Hoffer, J. M., eds., 1998a, Permian stratigraphy and paleontology of the Robledo Mountains, New Mexico: New Mexico Museum of Natural History and Science, Bulletin 12, 98 p.

Lucas, S. G., Lerner, A. J. and Voigt, S., 2013, Scorpionid resting trace from the Lower Permian of southern New Mexico, USA: Ichnos, v. 20, p. 195-201.

Lucas, S. G., Heckert, A. B., Estep, J. W. and Cook, C. W., 1998b, Stratigraphy of the Lower Permian Hueco Group in the Robledo Mountians, Doña Ana County, New Mexico: New Mexico Museum of Natural History and Science, Bulletin 12, p. 43-54.

Lucas, S. G., Anderson, O. J., Heckert, A. B. and Hunt, A. P., 1995, Geology of Early Permian tracksites, Robledo Mountains, south-central New Mexico: New Mexico Museum of Natural History and Science, Bulletin 6, p. 13-32.

Lucas, S. G., Voigt, S., Lerner, A. J., MacDonald, J. P., Spielmann, J. A. and Celeskey, M. D., 2011, The Prehistoric Trackways National Monument, Permian of southern New Mexico, U. S. A.: Ichnology Newsletter, no. 28, p. 10-14.

Mack, G. H., 2007, Sequence stratigraphy of the Lower Permian Abo member in the Robledo and Doña Ana Mountains near Las Cruces, New Mexico: New Mexico Geology, v. 29, p. 3-12.

Mack, G. H. and James, W. C., 1986, Cyclic sedimentation in the mixed siliclastic-carbonate Abo-Hueco transitional zone (Lower Permian), southwestern New Mexico: Journal of Sedimentary Petrology, v. 50, p. 635-647.

Mack, G. H., Tabor, N. J. and Zollinger, H. J., 2010, Palaeosols and sequence stratigraphy of the Lower Permian Abo Member, south-central New Mexico, USA: Sedimentology 57, p. 1566-1583.

Mack, G. H., Giles, K. A. and Durr, C. W., 2013, Sequence stratigraphy of the lower-middle Hueco transition interval (Lower Permian, Wolfcampian), Robledo Mountains, New Mexico: New Mexico Geology, v. 35, p. 27-37.

Minter, N. J. and Braddy, S. J., 2009, Ichnology of an Early Permian intertidal flat: The Robledo Mountains Formation of southern New Mexico, USA: Special Papers in Palaeontology, v. 82, p. 1-107.

Seager, W. R., Kottlowski, F. E. and Hawley, J. W., 2008, Geologic map of the Robledo Mountains and vicinity, Doña Ana County, New Mexico: New Mexico Bureau of Geology and Mineral Resources, Open-file Report 509, scale 1:24,000.

Tabor, N. J., DiMichele, W. A., Montañez, I. P. and Chaney, D. S, 2013, Late Paleozoic continental warming of a cold tropical basin and floristic change in western Pangea: International Journal of Coal Geology 119, p. 177-186.

Thompson, M. L., 1954, American Wolfcampian fusulinids: University of Kansas, Paleontological Contributions, Protozoa, Article 5, 226 pp.

Vachard, D., Krainer, K., and Lucas, S. G. 2015, Kungurian algae and microproblematica from the Yeso Group and San Andres Formation (New Mexico; U.S.A.): Palaeontologia Electronica, in press.

Voigt, S., Lucas, S. G., Buchwitz, M. and Celeskey, M. D., 2013a, *Robledopus macdonaldi*, a new kind of basal eureptile footprint from the Early Permian of New Mexico: New Mexico Museum of Natural History and Science, Bulletin 60, p. 445-459.

Voigt, S., Lucas, S. G. and Krainer, K., 2013b, Coastal-plain origin of trace-fossil bearing red beds in the Early Permian of southern New Mexico, U. S. A.: Palaeogeography, Palaeoclimatology, Palaeoecology, v. 369, p. 323-334.

Wahlman, G. P. and King, W. E., 2002, Latest Pennsylvanian and earliest Permian fusulinid biostratigraphy, Robledo Mountains and adjacent ranges, south-central New Mexico: New Mexico Bureau of Geology and Mineral Resources, Circular 208, p. 1-26.

Lucas, S. G. and DiMichele, W. A., eds , 2015, Carboniferous-Permian transition in the Robledo Mountains, southern New Mexico. New Mexico Museum of Natural History and Science, Bulletin 65.

THE PENNSYLVANIAN-PERMIAN SECTION AT ROBLEDO MOUNTAIN, DOÑA ANA COUNTY, NEW MEXICO, USA

KARL KRAINER[1], SPENCER G. LUCAS[2], DANIEL VACHARD[3] AND JAMES E. BARRICK[4]

[1]Institute of Geology, University of Innsbruck, Innsbruck, A-6020, Austria, Karl.Krainer@uibk.ac.at;
[2]New Mexico Museum of Natural History, 1801 Mountain Road N.W., Albuquerque, New Mexico, 87104, USA, Spencer.lucas@state.nm.us;
[3]Université Lille 1, UMR 8217 Géosystèmes, SN 5, F-59655 Villeneuve d'Ascq Cédex, France, daniel.vachard@univ-lille1.fr;
[4]Department of Geosciences, Texas Tech University, Box 41053, Lubbock, Texas, 79409, Jim.Barrick@ttu.edu

Abstract—The Pennsylvanian-Permian stratigraphic section exposed at Robledo Mountain, in the northern Robledo Mountains of Doña Ana County, New Mexico, is ~ 418 m thick and is a carbonate-dominated section with diverse fusulinid assemblages. We assign this section to the Horquilla Formation (lower 300 m) overlain by the Shalem Colony Formation of the Hueco Group (upper 118 m). We divide the Horquilla Formation into five informal members, in ascending order: member A (~ 82 m thick), characterized by cherty limestone; member B (~ 24 m thick), slope-forming, shale-dominated interval; member C (~ 52 m thick), alternating beds of limestone and shale; member D (~ 75 m thick), bedded to massive, non-cherty limestone; and member E (~ 62 m thick), bedded limestone with intercalated shale. This section yields fusulinids and conodonts that indicate the Horquilla Formation is Morrowan-early Wolfcampian, and the lower part of the Shalem Colony Formation is of middle Wolfcampian age. Subsidence in the Pedregosa basin and along the Florida shelf (including the Robledo shelf) was relatively even during the Virgilian-Wolfcampian, so that glacio-eustatic cycles are better recorded in these sections than in the more tectonically-influenced sections to the east, within the Orogrande basin. Assignment of most of the Robledo Mountain section, which was deposited on the western edge of the Orogrande basin, to the Horquilla Formation casts doubt on the idea that the Robledo shelf was significantly separated from Horquilla deposition in the Pedregosa basin to the southwest by an intervening Florida uplift (highland). Instead, the original idea of a Florida island, and a strait to the southeast of it, separating the late Paleozoic Orogrande and Pedregosa basins, is more compatible with the stratigraphic and sedimentologic data.

INTRODUCTION

The Robledo Mountains are a wedge-shaped horst of Paleozoic and Cenozoic rocks tilted 10-14° to the southwest, located along the western margin of the southern Rio Grande rift just northwest of Las Cruces, New Mexico (Fig. 1). The horst exposes a thick, carbonate-dominated section of Paleozoic strata overlain locally by upper Cenozoic siliciclastic rocks and cut locally by Cenozoic intrusives (Hawley et al., 1975; Seager et al., 1987, 2008). Near the northern end of the Robledo Mountains, on the north face of Robledo Mountain *sensu stricto* (the summit of the range), an ~ 418 m thick section of Pennsylvanian-Permian strata is exposed. Relatively little studied, this section is unusual in its lithostratigraphic differences from nearby Pennsylvanian sections, notably the Pennsylvanian section in the southern Caballo Mountains and Derry Hills (Lucas and Krainer, 2011). Here, we provide the first detailed description of the Pennsylvanian section at Robledo Mountain, focusing on its lithostratigraphy, microfacies, sedimentology and cycle stratigraphy as well as the biostratigraphy of its fusulinids and conodonts. We refer this section to the Horquilla Formation, and discuss its implications for the Pennsylvanian paleogeography of southern New Mexico.

PREVIOUS STUDIES

Geologists have known about Pennsylvanian rocks of the Robledo Mountains for nearly 90 years. Although the age of these rocks has been firmly established via microfossils, little has been published about their lithologic features or relationships to coeval rocks in neighboring areas. In fact, most authors did not bother to assign formation names.

The earliest geologists who described the geology of the Robledo Mountains (e.g., Darton, 1928; Dunham, 1935) were aware that Pennsylvanian strata are exposed in the range, though most of the strata they deemed Pennsylvanian are now referred to the Lower Permian Hueco Group. They referred to these strata as Magdalena "Formation," "Group" or "Series," but provided no data on them. Thompson (1954, fig. 8) presented a stratigraphic section and fusulinid data for a section across the Pennsylvanian-Permian boundary at Robledo Mountain (Fig. 2). He assigned these strata to the Virgilian Fresnal Group (undivided) and the Wolfcampian Bursum formation(?), Bursum formation and Hueco limestone. Thompson's (1954, p. 18) text makes it clear that these lithostratigraphic assignments were based on fusulinid biostratigraphy, not on lithologic correlation.

Kottlowski (1960b, p. 71-72, fig. 16) published a measured section of the Pennsylvanian-Permian succession at Robledo Mountain (Fig. 3). He described this section as relatively thin (~ 670 ft [204 m] thick) and indicated it rests on and is in part intruded by a Tertiary sill of non-flow-banded, slightly porphyritic rhyolite. Using fusulinid biostratigraphy, Kottlowski (1960b) assigned the Pennsylvanian-Permian strata at Robledo Mountain to the Derryan, Desmoinesian, Missourian, Virgilian and Wolfcampian series, but he made no lithostratigraphic assignments. He drew attention to some characteristic lithologies of the different series, notably the cherty limestones of the Desmoinesian, the slope-forming shale and limestone of the Missourian and the massive, non-cherty limestone cliffs of the Virgilian. Kottlowski (1960b, p. 72), referring to the work of Thompson (1954), stated that "early Wolfcampian beds attributed to the Bursum formation by Thompson (1948 [sic], p. 23) are similar to upper Virgilian beds but include some lenses of reddish-brown shale." Subsequent regional geologic mapping (e.g., Kottlowski, 1960a; Seager et al., 1987) simply referred the Pennsylvanian strata at Robledo Mountain to the Magdalena Formation.

Wahlman and King (2002) analyzed the fusulinid biostratigraphy across the Pennsylvanian-Permian boundary at Robledo Mountain to reach essentially the same results as had Thompson (1954). The fusulinids they studied came from three stratigraphic sections, one at Robledo Mountain, and two other sections to the southeast. They assigned the strata that yield the Pennsylvanian-Permian fusulinids to the Fresnal Group, "Bursum equivalent" and lower Hueco member (Fig. 4). Wahlman and King (2002) concluded that the section at and around Robledo Mountain is "an important regional reference section" across the Pennsylvanian-Permian boundary. However, as Wilde (2002) noted, the absence of *Triticites* in this section suggests that a significant part of early Wolfcampian ("Bursumian") time is not represented by strata at Robledo Mountain.

Krainer et al. (2003) described the microfacies and microfossils across the Pennsylvanian-Permian boundary at a section west of Robledo Mountain, with a primary focus on the Shalem Colony Formation of the Hueco Group. They referred to the strata immediately beneath the Hueco Group as the Atrasado Formation of the Madera Group (Fig. 4).

Seager et al. (2008) published a geologic map of the Robledo Mountains that included stratigraphic sections, one of which is a complete Pennsylvanian section measured at Robledo Mountain (Fig. 5). They assigned the Pennsylvanian strata to series, much as Kottlowski (1960b) had: Derryan + Desmoinesian (76 m), Missourian (66 m), Virgilian (64 m) and "Bursum equivalent" (109 m). Seager et al. (2008) mapped these chronostratigraphic intervals around the northern end of the Robledo Mountains, but we infer the mapping was not based

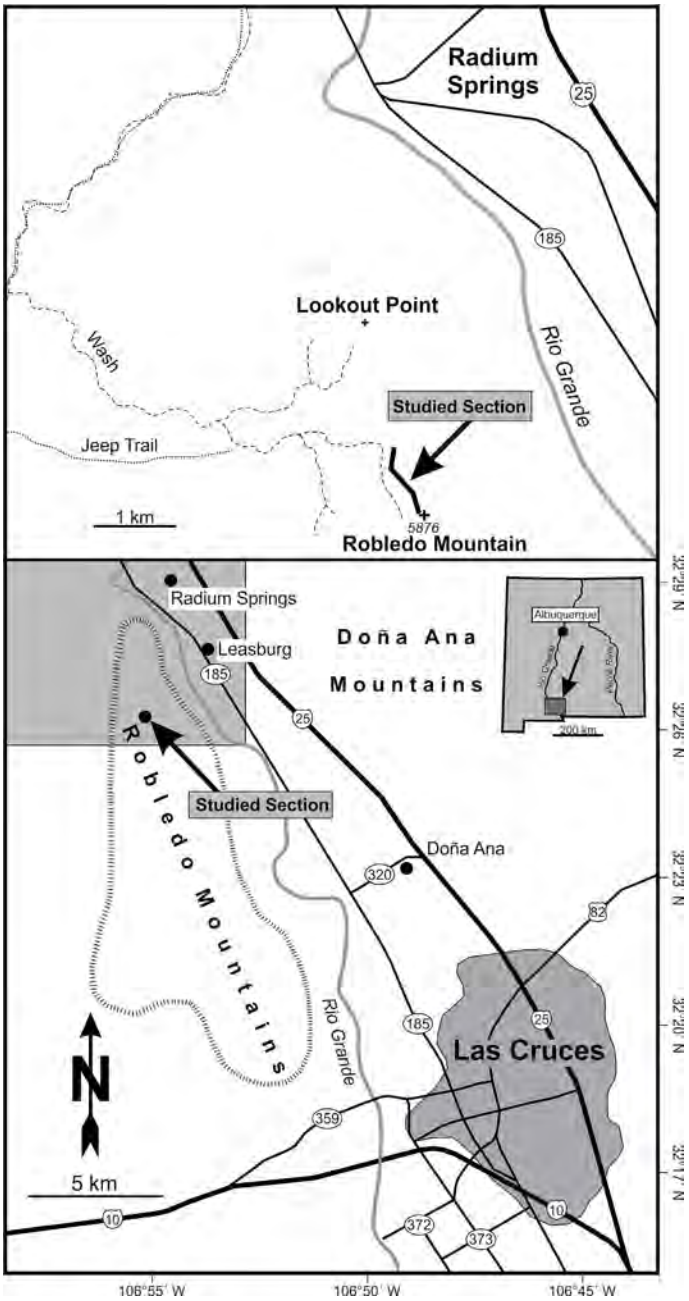


FIGURE 1. Index map showing location of the studied section at Robledo Mountain, Doña Ana County, New Mexico.

on biostratigraphy but instead on the different lithologic/topographic expression of the intervals first drawn attention to by Kottlowski, and further discussed by us below. Thus, to Seager et al. (2008) the Derryan + Desmoinesian is dominated by cherty limestones; the Missourian is a shaley, slope-forming interval; the Virgilian is represented by cliffs of massive, chert-free limestone; and the "Bursum equivalent" is mostly composed of thin bedded limestones and shales.

Lucas and Krainer (2011), in an abstract, briefly reviewed the Pennsylvanian stratigraphic section at Robledo Mountain that we describe here in detail. They stressed how different the section is lithologically from nearby and correlative Pennsylvanian strata in the southern Caballo Mountains and Derry Hills, only 40-60 km to the northwest (see Kelley and Silver, 1952; Lucas et al., 2012a, b). They assigned the Pennsylvanian strata at Robledo Mountain to the Horquilla Formation and thus questioned how much separation existed between the western Orogrande basin, where the Robledo Mountain section was deposited, and the Pedregosa basin to the southwest, where the Horquilla Formation was deposited.

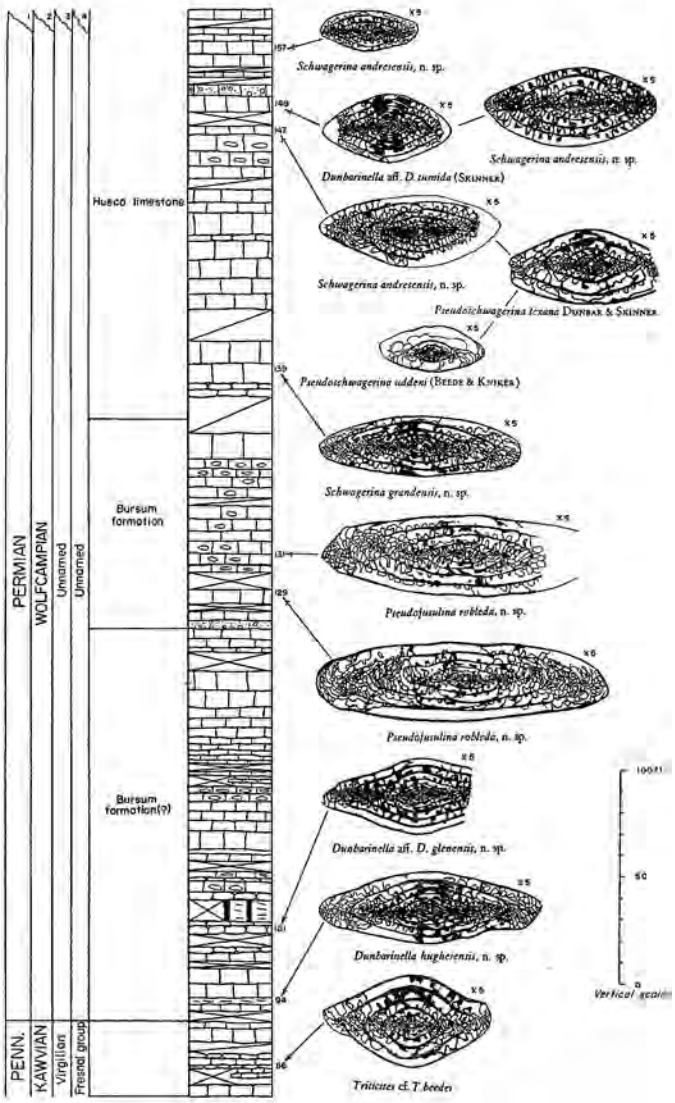


FIGURE 2. Section across the Pennsylvanian-Permian boundary at Robledo Mountain, from Thompson (1954).

METHODS

In 2010, we first measured and sampled the Pennsylvanian section at Robledo Mountain (Figs. 6-8). We returned in 2011 to restudy the section, checking our previous observations and taking additional samples. We selected a traverse up steep spurs on the north face of Robledo Mountain (Fig. 1), which offered the most complete exposures of bedrock available. From the samples we have prepared petrographic as well as microfossil data based on the study of 102 thin sections, presented here.

Robledo Mountain offers one of the most complete Pennsylvanian and Lower Permian sections in southern New Mexico. These rocks dip gently; faults are few and small. However, exposures extend only about 6 km along strike (Seager et al., 2008). The next nearest Pennsylvanian outcrops are located 30 to 35 km away, in the Caballo Mountains to the north and the southern San Andres and Organ Mountains to the east and southeast. Pennsylvanian rocks of the Franklin Mountains, north of El Paso, Texas, are more than 50 km south of Robledo Mountain. Outcrops in ranges west and southwest of the Robledo Mountains are 75 or more km distant. Thus, Robledo Mountain provides a key control point in regional understanding of Pennsylvanian sedimentation.

LITHOSTRATIGRAPHY

The section we measured at Robledo Mountain is ~ 418 m thick (Fig. 6). We assign this section to the Horquilla Formation (lower 300 m) overlain by the Shalem Colony Formation of the Hueco Group (upper 118 m). We divide the Horquilla Formation into five informal members

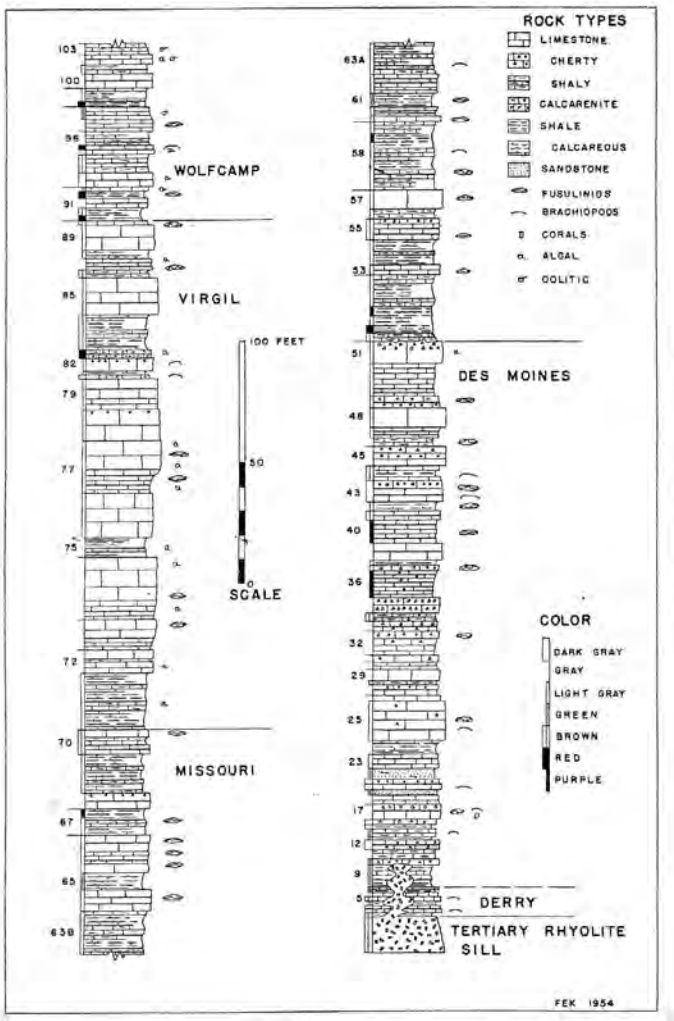


FIGURE 3. Pennsylvanian section at Robledo Mountain, from Kottlowski (1960b).

(Fig. 6), in ascending order: member A (units 1-68), characterized by cherty limestone; member B (units 69-87), slope-forming, shale-dominated interval; member C (units 88-113), alternating beds of limestone and shale; member D (units 114-146), bedded to massive, non-cherty limestone; and member E (units 146-201), bedded limestone with intercalated shale.

Younger Permian rocks of the Hueco Group crop out in the central and southern part of the Robledo Range, where they have been studied extensively (e.g. Krainer and Lucas, 1995, Lucas et al., 1995, 1998, Mack, 2007, Mack et al., 1988, 2013; Voigt et al., 2013)

Horquilla Formation

As will be explained more thoroughly in a later section of this article, we are assigning the Pennsylvanian and lowermost Permian rocks of Robledo Mountain to the Horquilla Formation. In the section we measured, five subdivisions of the Horquilla Formation are apparent. Because no members have been assigned to the Horquilla Formation elsewhere in New Mexico, and because Horquilla outcrops near Robledo Mountain extend laterally only about 6 km, coining formal member names was deemed inadvisable. Accordingly, we designated these five units informally as Members A through E.

Member A

This member (units 1-68) rests on Tertiary igneous rocks and is 82.2 m thick (Fig. 6). The underlying igneous rocks are part of the Lookout Peak sill, composed of non-flow-banded rhyolite of the ~ 35 Ma (latest Eocene) Robledo rhyolite (Seager et al., 2008). Although the contact with the sill was not cleanly exposed, this contact is apparently simple and concordant. Overlying sedimentary rocks have not been significantly deformed or metamorphosed beyond a few meters from the boundary of the sill. However, an unknown thickness of basal Pennsylvanian strata may have been removed or assimilated by the intrusion.

Member A is composed of limestone intervals (0.3-10.1 m) separated by covered intervals (0.3-4 m), which probably represent shale intervals (Fig. 7). Covered intervals constitute 36.6% of the total thickness of the member. This member erodes to a moderately steep slope, punctuated by limestone ledges that range from less than 1 to more than 5 m high.

Limestone intervals are composed of: (a) thick-bedded to massive limestone, mostly cherty, (b) thin- to medium- and even-bedded, cherty and non-cherty limestone, and (c) wavy bedded to nodular, mostly cherty limestone (Fig. 8A). Limestone is mostly muddy (mudstone to wackestone) and gray to dark gray. Chert occurs as dark gray to black chert nodules with diameters up to 30 cm and, subordinately, in the lower part, as chert layers that are 10-20 cm thick.

Fossils are common in some of the limestone (crinoidal wackestone to packstone) beds with echinoderm fragments and brachiopods are most abundant; less common are bryozoans, calcareous algae (upper part), gastropods, and, in one bed, syringoporid corals. In individual beds, the fossils are silicified. Two limestone beds display strong bioturbation. In the upper part of member A, rhizoliths are developed at the top of three limestone beds, indicating subaerial exposure surfaces.

Cycles are not well developed in the lower and middle parts of member A. But, shallowing upward cycles composed of wavy-bedded, cherty limestone, grading into thick-bedded to massive limestone with rhizoliths near the top, are present (Fig. 6).

Wackestone is by far the most common microfacies type, locally grading into packstone and floatstone. Wackestone contains a diverse fossil assemblage (bioclastic wackestone: Fig. 9.2). As shown by thin section study, the most abundant fossils are fragments of echinoderms (mainly crinoids), brachiopods (shells and spines) and bryozoans. Less common are smaller foraminifers, fusulinids (Fig. 9.5), ostracods and bivalves. Echinoderm spines, gastropods and trilobite fragments are rare. Locally, sponge spicules are abundant (Fig. 9.1). Individual beds contain abundant phylloid algae (phylloid algal wackestone to floatstone: Fig. 9.7) and smaller foraminifers (foraminiferal wackestone). Peloidal wackestone is rare and contains large recrystallized skeletons (?bivalves, phylloid algae; Fig. 9.6), a few echinoderm fragments, rare ostracods, bryozoans and smaller foraminifers. Bioclastic packstone (Fig. 9.4) is composed of strongly fragmented skeletons, mainly derived from echinoderms (Fig. 9.3), brachiopods and bryozoans. Non-skeletal grains include peloids (rarely forming peloidal wackestone and grainstone), fecal pellets, detrital quartz grains and rare micritic intraclasts. Smaller foraminifers include taxa of the following genera: *Bradyina, Climacammina, Globivalvulina, Tetrataxis, Tuberitina* and tubular forms.

Unit 58 in the upper part of member A is a gray micritic limestone bed with rhizoliths. In thin section, a clotted fabric typical of paleocalcrete is observed with abundant calcrete peloids and pisoids (Fig. 9.8). A few micritic grains display dark micritic rims. Irregular voids are filled with calcite cement. Ostracods are very rare.

Member B

Member B stands apart from the remainder of the Horquilla Formation by the abundance of shale. This member includes units 69-87, measures 23.9 m thick and is composed of shale and intercalated limestone units and two conglomerate beds (Fig. 6). Marly shale contains abundant limestone nodules. One shale unit with limestone nodules in the upper part contains fossil fragments. Shale and shale with limestone nodules constitute 71% of the member, limestone 22.7%, conglomerate 3.3% and covered intervals 3%. In most places, Member B erodes to a gentle, vegetated slope where bedrock outcrops are few (Fig. 7). However, our measured section encompassed a deeply gullied area where the member is almost completely exposed.

Shale units are 0.5-5.6 m thick and partly poorly exposed. The color ranges from gray to purple-gray, pink and pale green. Most shale intervals are composed of marly shale and contain limestone nodules or thin layers of nodular limestone. One shale interval contains abundant limestone nodules and isolated brachiopods.

Intercalated limestone units are either individual, thin limestone beds (0.1-0.2 m thick) or, more commonly, wavy bedded to nodular limestone intervals (0.7-1.6 m thick). Some of the limestone beds contain chert nodules. Fossils observed on outcrop are brachiopods and crinoid debris. Rhizoliths are developed on top of one limestone unit (Fig. 8B).

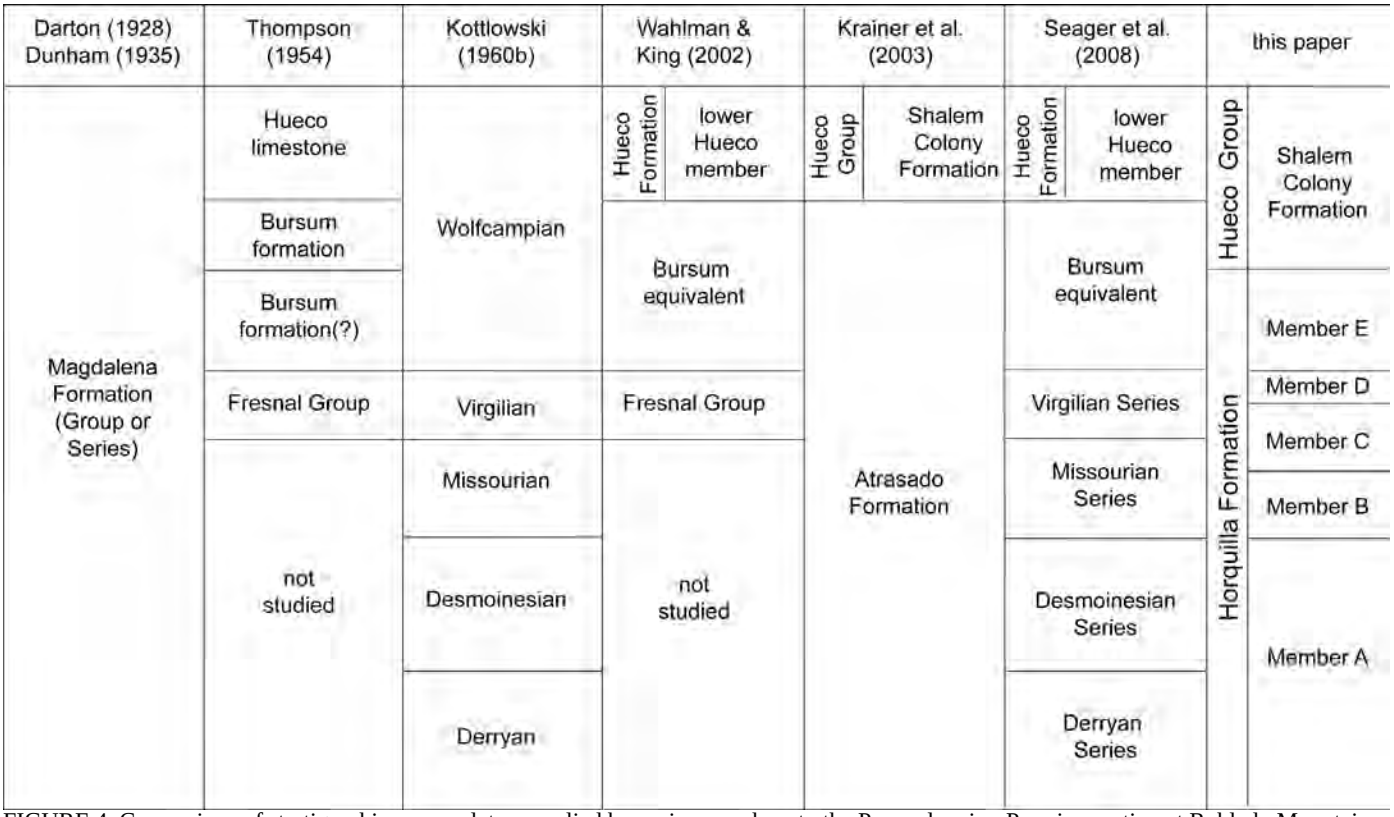


FIGURE 4. Comparison of stratigraphic nomenclature applied by various workers to the Pennsylvanian-Permian section at Robledo Mountain.

Limestone is composed of wackestone that may grade into floatstone (Fig. 10.1), and subordinately of packstone to rudstone. All microfacies types contain a diverse fossil assemblage, which is similar to that of member A. Most common are fragments of echinoderms (crinoids), brachiopods and bryozoans and recrystallized skeletons; subordinate are ostracods, smaller foraminifers (*Bradyina, Climacammina, Endothyra, Globivalvulina, Spireitlina* and *Syzrania*), fusulinids, brachiopod spines and gastropods. Locally abundant recrystallized skeletons of probable algae are present. In a few beds, *Bacinella* and cyanobacteria are present, encrusting skeletons and locally forming bindstone. Packstone contains abundant subrounded to rounded micritic intraclasts and detrital quartz grains up to 2 mm in diameter.

The lower conglomerate bed (Fig. 6, unit 82) is 0.7 m thick, cross bedded and polymict, containing various types of limestone clasts and abundant chert clasts (Fig. 10.2). The conglomerate is clast-supported and poorly sorted; the clasts are subangular to rounded; and the maximum clast size is 5 cm. The conglomerate contains fossil fragments. Limestone clasts are reworked from mudstone to wackestone microfacies. The clasts are embedded in a fine-grained packstone matrix composed of abundant echinoderm fragments and intraclasts, subordinate shell fragments of brachiopods, ostracods and common bone fragments. Detrital quartz grains are rare.

The upper conglomerate bed (Fig. 6, unit 86) is thin (0.1 m) and similar in composition. It contains shark teeth and other ichthyoliths (Ivanov and Lucas, 2014).

Member C

Like member A, member C consists of alternating limestone and shale or mudstone (largely covered) in roughly equal proportions, and eroding to a step-and-ledge topography. Nodular to wavy-bedded limestone is prominent at the top of the member. Unlike member A, limestone beds of member C contain little or no chert.

Member C is 51.7 m thick (Fig. 6, units 88-113) and is composed of alternating limestone (43.7%), shale (11.8%) and covered intervals (44.5%) (Fig. 6). Limestone units are mostly indistinctly bedded to massive, 0.5-6.1 m thick. Wavy bedded to nodular limestone units, 0.6-1.8 m thick, are subordinate. Chert nodules are rare. Limestone units alternate with covered intervals that are 1.2-7.2 m thick. In the upper part, red shale with limestone nodules is intercalated (1.1 and 3.9 m thick). Fossils observed in the field are calcareous algae in the indistinctly bedded to massive limestone units, fusulinids, rare brachiopods and syringoporid corals, which are present in the lowermost limestone bed (Fig. 6, unit 88).

Limestone is commonly wackestone (Fig. 10.4), which may grade into packstone and floatstone. Grainstone is rare. All limestone types are characterized by a diverse fossil assemblage, including abundant recrystallized indeterminable skeletons, echinoderm fragments, bryozoans, brachiopods, subordinate ostracods, smaller foraminifers (*Bradyina, Climacammina, Globivalvulina, Spireitlina, Syzrania, Tetrataxis, Tuberitina*; locally *Bradyina* and *Globivalvulina* are common), echinoid spines, rare gastropods, recrystallized phylloid algae and *Epimastopora*. Fusulinids are abundant in this member, forming many beds of fusulinid wackestone (Fig. 10.5), packstone and rudstone (Fig. 10.7). Many fusulinid tests are abraded and fragmented. Skeletons in wackestone to floatstone are embedded either in micrite or peloidal micrite. Locally, irregular voids filled with coarse blocky calcite cement occur.

Grainstone (Fig. 10.6) is rare, fine-grained (0.1-0.3 mm), moderately sorted, and, besides a diverse fossil assemblage, contains abundant peloids, a few aggregate grains and very few detrital quartz grains and intraclasts. In the lowermost limestone unit (Fig. 6, unit 88), small colonies of syringoporid corals are present (Fig. 10.3). Micritic matrix between the syringoporid coral branches contains a few fossils such as fusulinids, smaller foraminifers (*Bradyina, Tetrataxis*), brachiopods, ostracods and echinoderms. Pore space between the syringoporid coral branches is filled with coarse calcite cement.

On top of many limestone beds, rhizoliths are present, indicating subaerial exposure surfaces. The uppermost part of one limestone bed is strongly bioturbated. On top of unit 102, rhizoliths are present, and the limestone is composed of laminated microbialite that grades into paleocalcrete (Fig. 10.8). Laminated microbialite contains fenestral fabrics and grades into agglutinated microbialite composed of amalgamated peloids, overlain again by laminated microbialite. Microbialite is overlain by paleocalcrete with nodular texture and composed of calcrete peloids and abundant micritic nodules, some displaying circumgranular fractures.

The succession shows a cyclic pattern of either shale-limestone cycles or shale overlain by wavy to nodular bedded limestone and indistinctly bedded to massive limestone with subaerial exposure

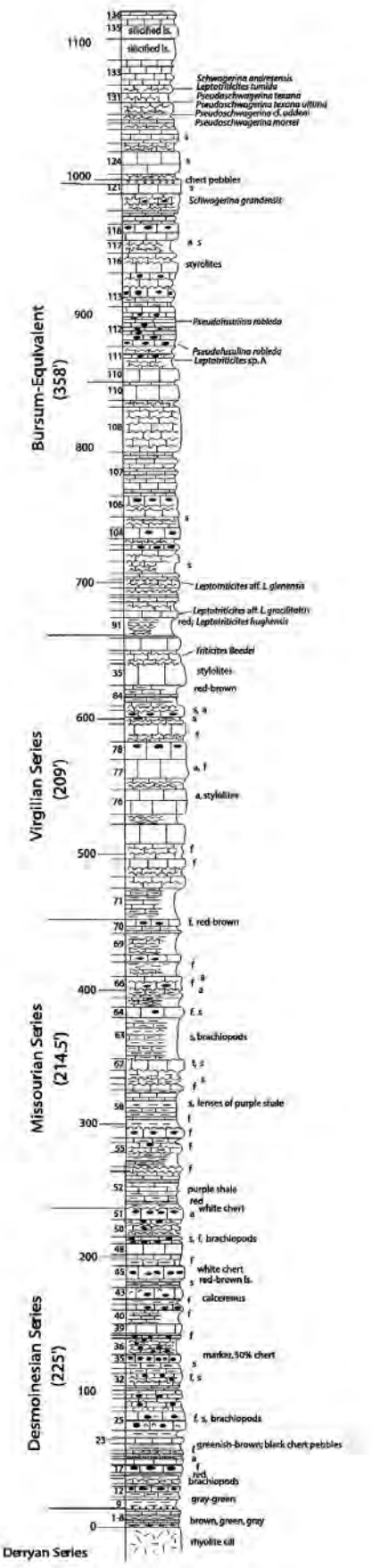


FIGURE 5. Pennsylvanian-Permian section at Robledo Mountain, from Seager et al. (2008).

surfaces on top, indicating shallowing upward cycles (Fig. 6).

Member D

Member D is characterized by light-colored, algal limestones that essentially lack chert and that form thick ledges or cliffs, separated by relatively thin covered (shale?) intervals (Fig. 7).

Member D is 74.8 m thick (units 114-146: Fig. 6). Limestone units alternate with shale and covered intervals. Limestone constitutes 67.4% of the section, shale 12.6% and covered intervals 19%. Limestone is dominated by indistinctly bedded to massive intervals (1.3-9.8 m thick); rare thin-bedded to nodular limestone units and individual limestone beds (0.2-0.8 m thick) are present. The two shale intervals are 4.3 and 4.6 m thick; shale is reddish and contains limestone nodules in unit 130. Covered intervals are 0.2-2.6 m thick. Member D is characterized by limestones that essentially lack chert and that form thick ledges separated by relatively thin covered (shale?) intervals. Fossils observed on outcrop are calcareous algae in the indistinctly bedded to massive limestone units, crinoidal debris, fusulinids and, locally, large gastropods.

Wackestone (Figs. 11.1-11.2), grainstone to rudstone and phylloid algal wackestone to floatstone are common microfacies. Packstone and peloidal mudstone are rare. All microfacies types contain diverse fossil assemblages, which, compared to the members below, are characterized by the abundance of completely recrystallized phylloid algae (Fig. 11.3) and *Eugonophyllum*, whereas bryozoans remain rare to absent. *Epimastopora* is present, too. Locally, fusulinids are abundant. Smaller foraminifers include *Bradyina, Climacammina, Globivalvulina, Pseudovidalina, Tetrataxis, Tuberitina* and calcivertellid tubular forms.

In grainstone to rudstone (Figs. 11.4, 11.5, 11.7), many skeletons display micritic envelopes (forming cortoids) or are encrusted by cyanobacteria (forming oncoids). Rarely, oncoidal grainstone (Figs. 11.6, 11.8) composed of small oncoids (0.5-2 mm) is present, in which the oncoids are abraded.

The tops of limestone units display bioturbation, rhizoliths, microkarst (unit 142), and a black mottled color (in unit 144). A thin, in-situ breccia is developed on top of unit 146. Cycles are common, typically starting with a covered interval/shale, overlain by thin-bedded or nodular limestone and finally by indistinctly bedded to massive limestone with subaerial exposure surfaces on top (shallowing upward cycles) (Fig. 6).

Member E

This member is 67.7 m thick (units 147-201: Fig. 6) and is characterized by alternating shale/covered intervals, limestone intervals and one conglomerate bed. Shale constitutes 8.7%, conglomerate 0.7%, limestone 64.9% and covered intervals 25.7% of the member. Unlike member D, limestone beds of member E are generally thinner and thinner bedded, so they do not form thick cliffs/ledges. Thin- to medium bedded limestone is more abundant and massive limestone is present but less abundant than in member D. This unit also shows more diverse types of limestone than member D, and shale or mudstone is largely confined to the basal 15 m of the member. Thus, member E is more of a slope-forming interval than the cliff-forming member D (Fig. 7).

The following limestone types are observed: (a) individual limestone beds, 0.1-0.9 m thick, (b) thin- to medium-bedded limestone intervals with even bedding, 0.4-2.5 m thick, (c) wavy bedded to nodular limestone, 0.6-1.3 m thick, (d) indistinctly bedded to massive limestone, 1.4-4.4 m thick and (e) one fine-grained limestone conglomerate, 0.5 m thick. A distinct stromatolite bed (0.5 m thick) is present at the base of a massive algal limestone (Fig. 6, unit 187: Fig. 8C). Rhizoliths are present on top of a few limestone intervals.

The most common microfacies types are grainstone-packstone-rudstone, wackestone-floatstone (Figs. 12.1-12.4) and rare bindstone. Grainstone-packstone-rudstone is moderately sorted and contains a diverse fossil assemblage (including abundant recrystallized skeletons, echinoderms, ostracods, brachiopods, bryozoans, phylloid algae, smaller foraminifers such as *Bradyina, Earlandia, Endothyra, Nodosinelloides, Pseudovidalina, Spireitlina, Syzrania, Tetrataxis* and *Tuberitina*, echinoid spines, brachiopod spines, rare *Epimastopora, Efluegelia*, and very rare trilobite fragments). Fossils are commonly strongly fragmented (Figs. 12.7-12.8). Many skeletons occur as coated grains (cortoids). Non-skeletal grains are present in varying amounts and include ooids, oncoids, peloids and micritic intraclasts. Locally, ooids are abundant, forming oolitic grainstone. Rarely, thin layers of peloidal mudstone alternate with grainstone. Another microfacies type

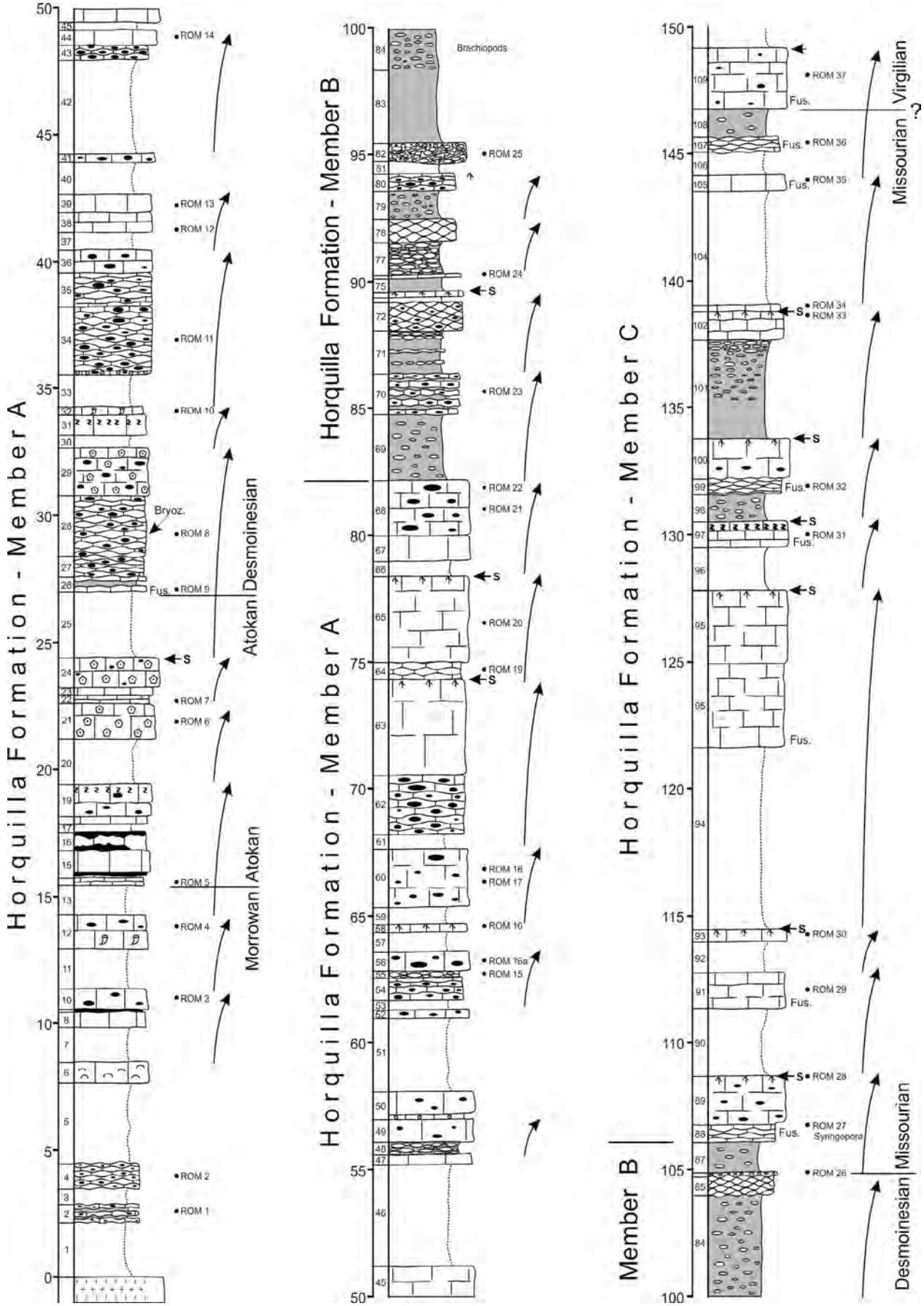


FIGURE 6. Measured section of the Pennsylvanian strata exposed at Robledo Mountain.

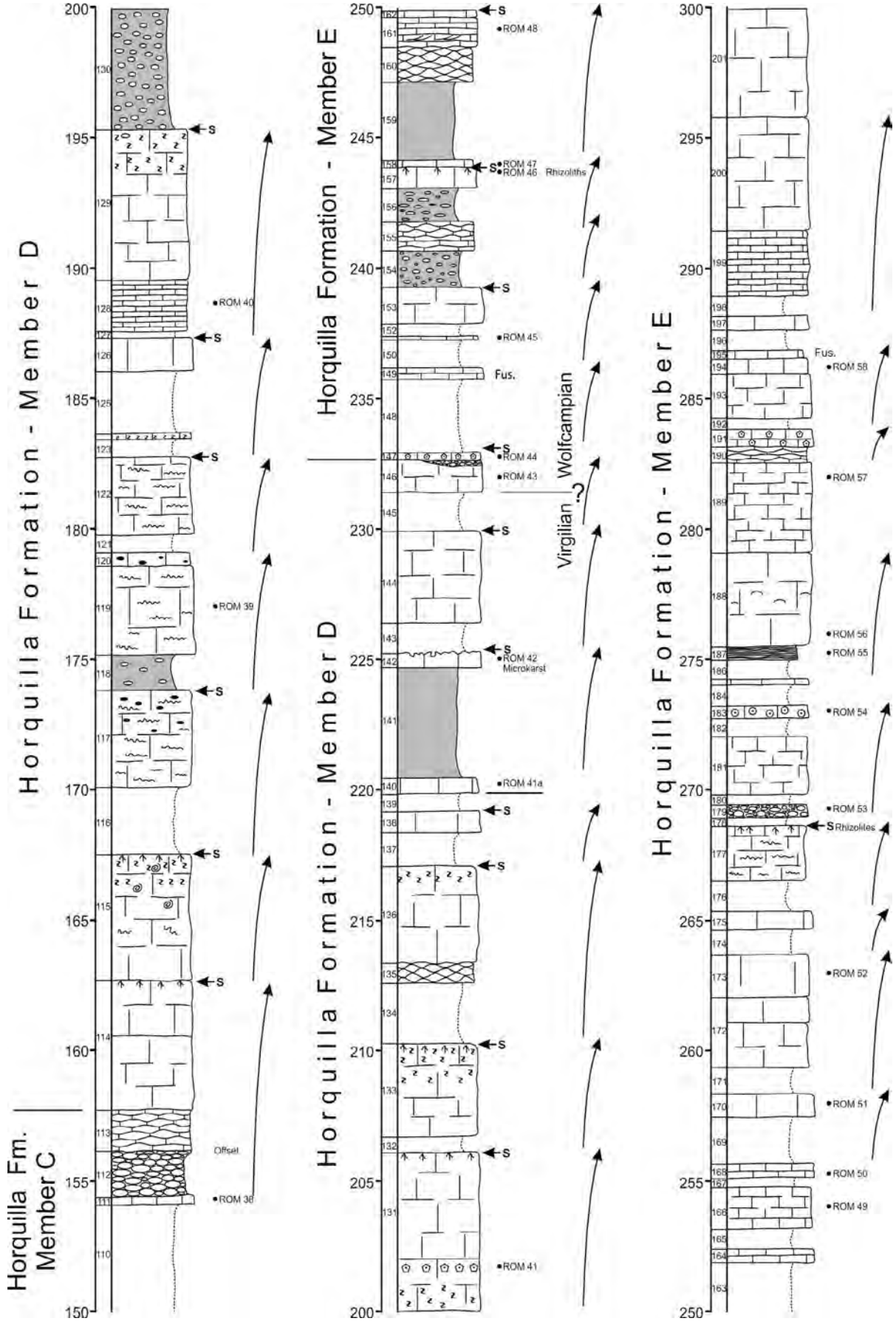


FIGURE 6 (continued).

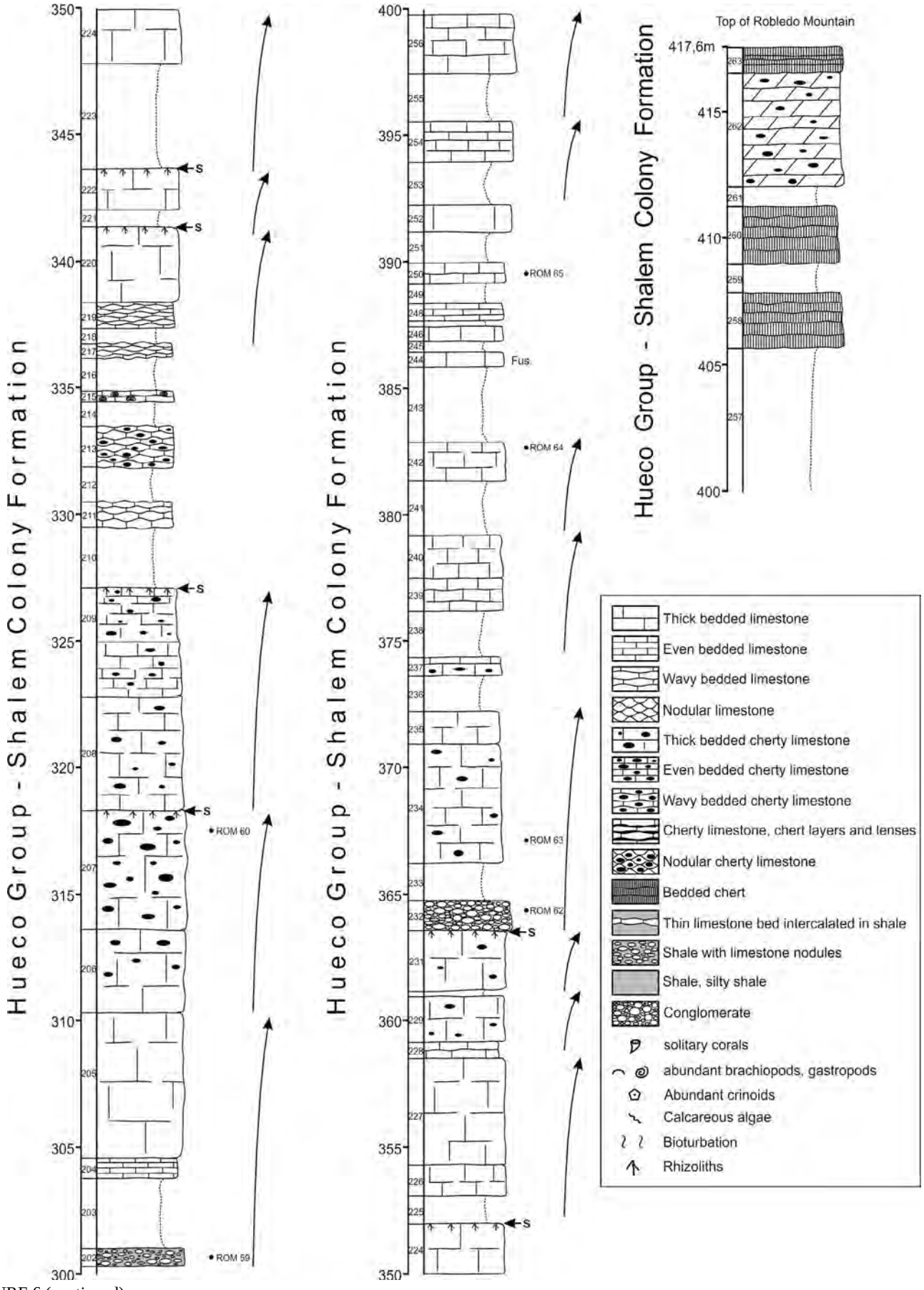


FIGURE 6 (continued).

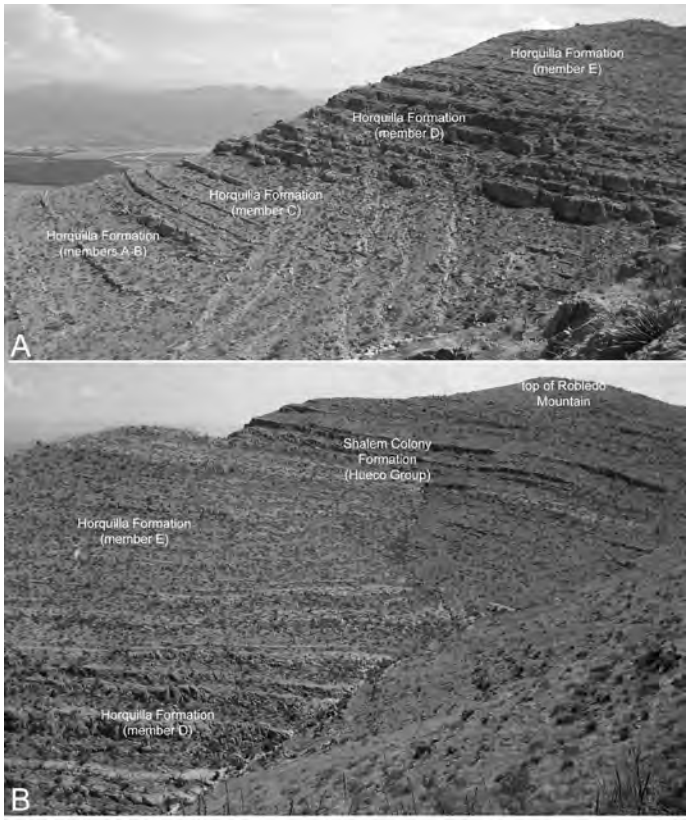


FIGURE 7. Overview of the Pennsylvanian-Permian section at Robledo Mountain; lower part of section (A) and upper part of section (B).

is oncoidal grainstone to rudstone (Fig. 12.6) containing well-rounded oncoid grains up to approximately 6 mm in diameter. Oncoids are commonly composed of a nucleus represented by a skeletal grain, which is encrusted by thicker layers of cyanobacteria. Ooids and coated grains as well as some skeletal grains are also present in oncoidal grainstones.

Bindstones are composed of *Archaeolithophyllum lamellosum*, which forms irregularly laminated crusts (Fig. 12.5). Subordinately, cyanobacteria, *Girvanella*, encrusting bryozoans and a few encrusting foraminifers (*Tuberitina*, calcivertellids) are present, too. Some micrite is intercalated as thin irregular laminae that contain a few ostracods and other small skeletons. Locally, calcite cement is present in the pore space between the algal laminae.

The conglomerate is poorly sorted and contains various limestone intraclasts (reworked mudstone-wackestone and rare grainstone), some fossil fragments such as recrystallized skeletons and echinoderms, and very rare, small detrital quartz grains. The sand fraction contains a few coated grains. The conglomerate is cemented by calcite; locally, some micritic matrix is present.

Shale units are 1.3-3 m thick, reddish, and contain limestone nodules. Covered intervals are 0.4-2.9 m thick and likely represent shale units. Fossils observed in the field are calcareous algae, crinoidal debris, fusulinids and rare gastropods and bivalves.

Depositional Environments

The microfacies of the Horquilla Formation can be assigned to the following standard microfacies types (SMF) of Flügel (2004): SMF 5--allochthonous bioclastic grainstone, rudstone, packstone and floatstone; SMF 10--bioclastic wackestone and packstone with abraded and worn skeletal grains; SMF 11--coated bioclastic grainstone; SMF 12--limestone with shell concentrations; SMF 13--oncoid rudstone and grainstone; and SMF 20--stromatolitic bindstone.

In members A and B, wavy bedded to nodular limestone with muddy texture and dark gray color is common. Chert is a common constituent of many limestone units. Indistinctly bedded to massive limestone occurs in the upper part of member A.

The microfacies types that predominate in members A and B are

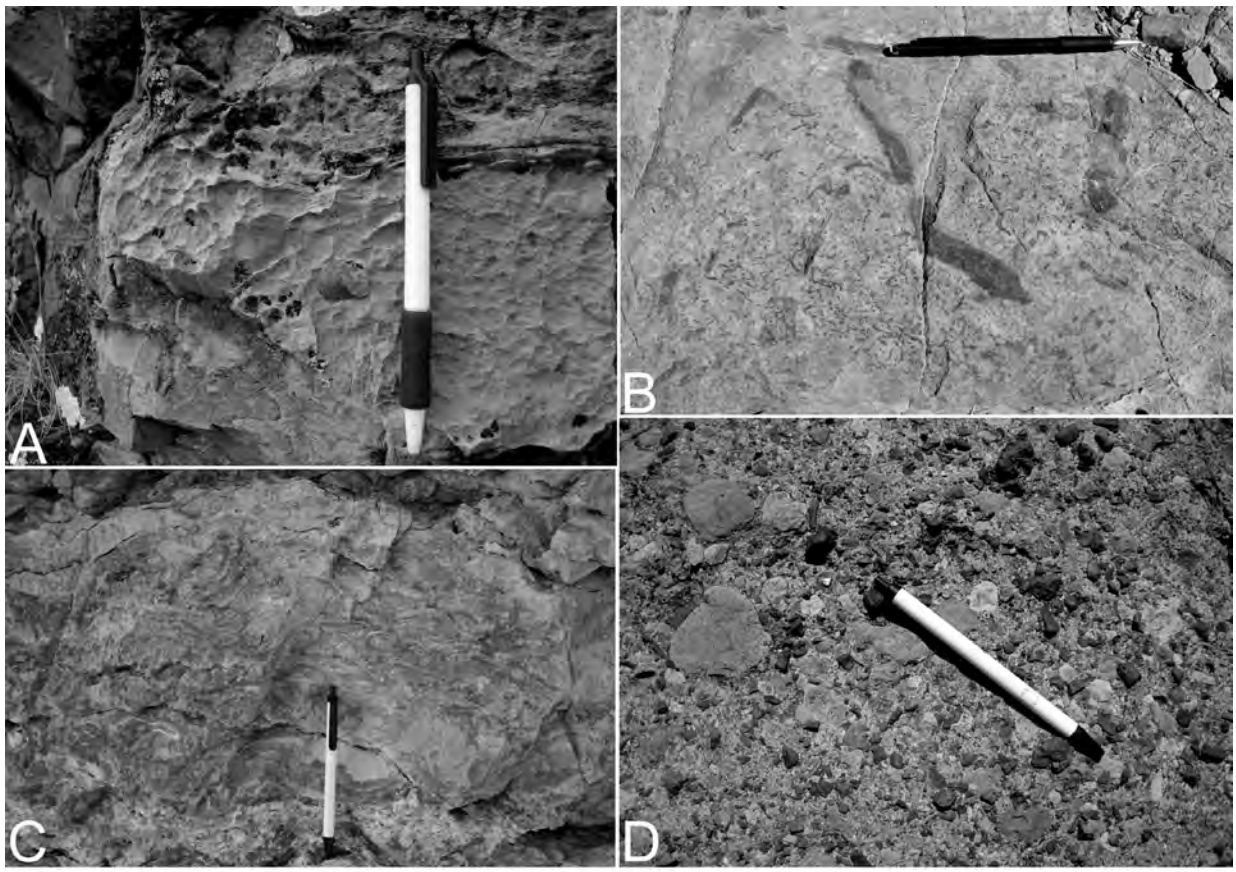
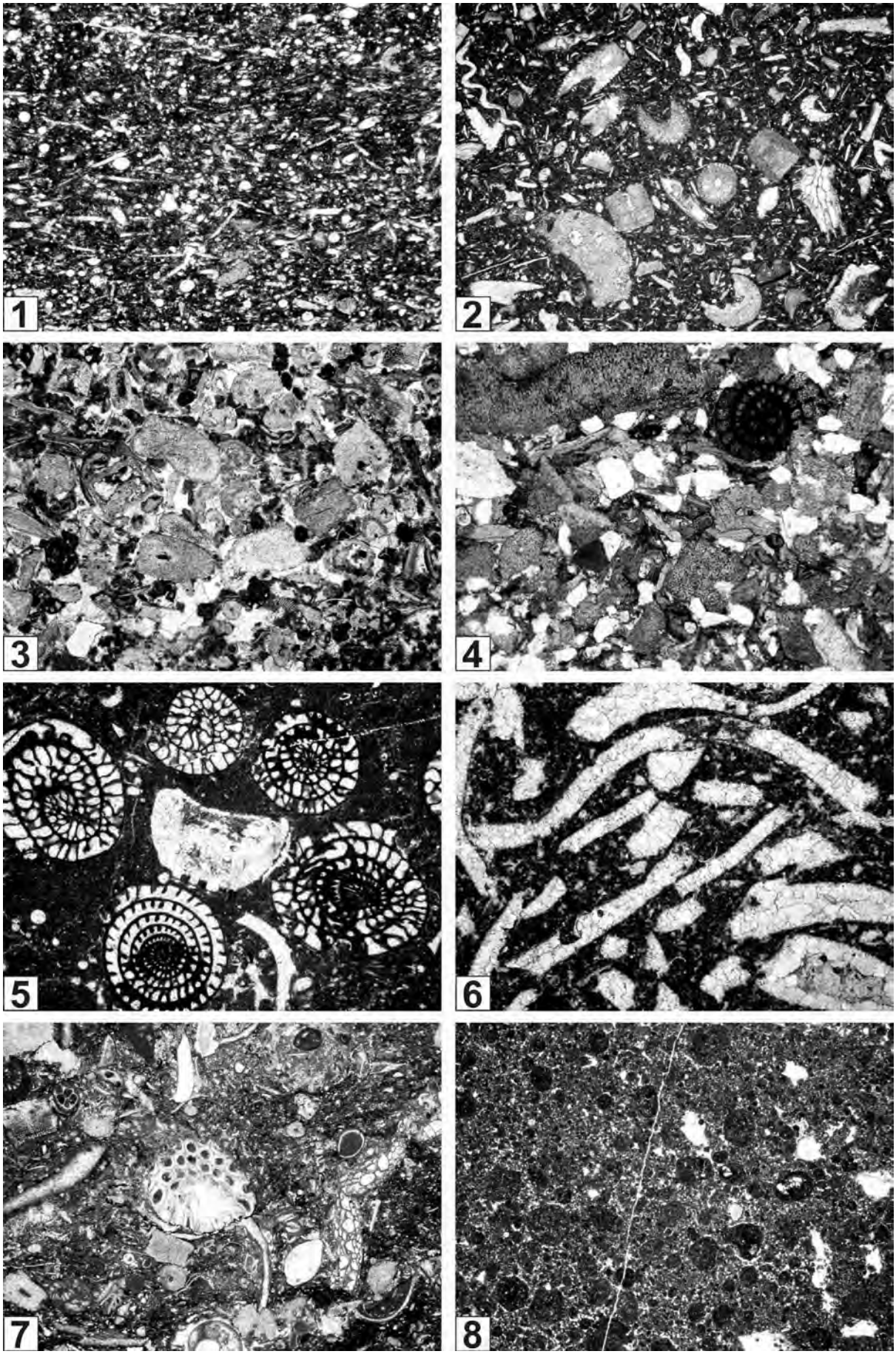


FIGURE 8. Selected lithotypes in the Robledo Mountain section. A, Cherty limestone with silicified brachiopods (unit 27). B, Rhizoliths and dark crust on top of limestone bed, indicative of subaerial exposure (unit 95). C, Stromatolites (unit 187). D, Conglomerate (unit 203).


1
2
3
4
5
6
7
8

wackestone to floatstone, subordinate packstone, rare rudstone and grainstone (mainly SMF 5 and 10, rarely SMF 11). All types contain a very diverse fauna including stenohaline forms such as brachiopods, echinoderms, trilobites and rare corals. The microfacies and biota are characteristic of open marine, well-oxygenated and well-circulated conditions with normal marine salinity, deposited below the fair weather wave base in a deeper, open marine shelf environment with water depths of at least some tens of meters. High-energy deposits (grainstone) are rare. At least part of the silica of the chert nodules and chert bands is probably derived from siliceous sponges, which is indicated by the presence of locally abundant sponge spicules.

These limestones are part of well-developed cycles, and the microfacies and biota indicate a more shallow depositional environment. Covered intervals in member A are difficult to interpret, but most probably represent shale intervals composed of shale and marly shale deposited in a deeper (outer) shelf environment.

Member B is dominantly shale and intercalated wavy-bedded to nodular limestone intervals composed of wackestone, packstone and floatstone (SMF 5 and 10). Indistinctly bedded to massive limestone is absent. One limestone bed (Fig. 6, unit 58) contains rhizoliths, indicating a subaerial exposure surface. We infer that the bulk of member B (shale, wavy and nodular limestone) was deposited on a deeper (outer), open marine shelf environment than member A.

Intercalated conglomerates contain marine fossils indicating a high-energy, shallow marine depositional environment. Shale is not exposed in member A, but is probably represented by covered intervals. Shale of member B most probably is all of marine origin, although the depositional environment is difficult to interpret. The marine character is documented for only one shale interval by the occurrence of brachiopods. Limestone nodules in the shale intervals also indicate a marine origin; calcrete nodules are absent.

In members C, D and E, wavy bedded to nodular, dark gray limestone and cherty limestone are rare. Indistinctly bedded to massive limestone (partly phylloid algal limestone) is most common. In limestone units of members C, D and E, the most common microfacies is bioclastic wackestone to floatstone (SMF 11), and subordinately (but more abundant than in members A and B) bioclastic grainstone, packstone and rudstone (SMF 5). Other microfacies such as cortoid grainstone (SMF 11), coquina (SMF 12), oncoidal grainstone-rudstone (SMF 13) and stromatolitic bindstone (SMF 20) are rare.

The fossil assemblage shows some differences when compared to members A and B: bryozoans are less abundant, calcareous algae (phylloid algae) are much more abundant (commonly forming phylloid algal wackestone to floatstone) and fusulinids are also more common. Phylloid algae are an abundant constituent in late Paleozoic shelf carbonates, forming reef mounds and banks, and they grew in shallow shelf settings controlled by short-term sea-level fluctuations (Flügel, 2004). Dasycladacean algae (*Epimastopora*) commonly grew in shallow water between approximately 5 and 30 m deep.

Microfacies and biota (particularly algae and fusulinids) indicate that the limestone units of members C, D, and E formed in a shallower depositional environment than the wavybedded to nodular limestone units of members A and B. Indistinctly bedded to massive limestone formed in an open, shallow marine, well-oxygenated environment with normal salinity. Water depth did not exceed a few tens of meters. High-energy microfacies (grainstone, packstone, rudstone) and bindstone are also indicative of a shallow marine setting. Thin intercalated conglomerate beds containing marine fossils also point to a high-energy shallow marine environment.

In members C, D and E, shale is rarely exposed, but the limestone units in most cases are separated by covered intervals that probably represent shale. Shale is commonly reddish and contains abundant limestone nodules; fossils are absent. The depositional environment – marine or nonmarine – is unclear. A few of the reddish shale intervals may be of nonmarine origin due to the presence of calcrete nodules.

The well-developed cyclic pattern with subaerial exposure surfaces on top of many limestone units indicates rapid sea-level fluctuations during deposition of members C, D, and E. Water depth varied between deeper shelf (deposition of offshore mudstone and nodular limestone) and subaerial exposure, indicating sea-level fluctuations on the order of some tens of meters.

Hueco Group-Shalem Colony Formation

Lucas et al. (1998) provided a new formal nomenclature of the Hueco strata in the Robledo Mountains. They elevated the Hueco Formation to group status and divided the Hueco Group into four formations, which in ascending order were named Shalem Colony, Community Pit, Robledo Mountains and Apache Dam formations.

The Shalem Colony Formation at its type section (incomplete) is composed of slope forming shale or siltstone (approximately 50%) and intercalated ledge-forming limestone (mainly calcarenite, calcirudite and grainstone, less abundant packstone, mudstone, algal bindstone and wackestone) (Lucas et al., 1998).

Petrography and Microfacies

At Robledo Mountain, above strata we assign to the Horquilla Formation, the exposed thickness of the overlying lower part of the Hueco Group is 117.3 m (units 202-263), and the entire succession is assigned to the Shalem Colony Formation (Fig. 6). The succession is composed mainly of limestone (60.3%), with intercalated conglomerate (1.6%), bedded chert (4.7%) and covered intervals (33.4%). We place the base of the Hueco Group at a conglomerate unit (Fig. 6, unit 202: Fig. 8D) at which the limestone facies change and cherty limestone beds again are present, features we judge characteristic of the lower Hueco Group. However, Seager et al. (2008; also see Wahlman and King, 2002, who used the llithostratigraphy of Seager et al. 2008) placed the base of the Hueco Group stratigraphically higher, at the conglomerate that is unit 232 of our measured section.

Limestone units are 0.4-23.3 m thick. The following lithotypes are distinguished: (a) thin- to medium-bedded limestone with even to slightly wavy bedding planes, up to 1.6 m thick; (b) wavy-bedded to nodular limestone, partly cherty, 0.4-1 m thick; and (c) indistinctly bedded to massive limestone, up to 5.8 m thick, partly cherty. Lithotypes (a) and (b) are rare; indistinctly bedded to massive limestone is most abundant (c). Fossils are rarely observed on outcrop and include gastropods, brachiopods, calcareous algae, crinoid debris and very rare fusulinids. Small oncoids (2-3 mm in size) are present in unit 215. The most common microfacies types are various types of grainstone-packstone (Fig. 13.1) and wackestone-floatstone; peloidal mudstone, wackestone and grainstone (Fig. 13.2) and oncoidal floatstone-rudstone are rare.

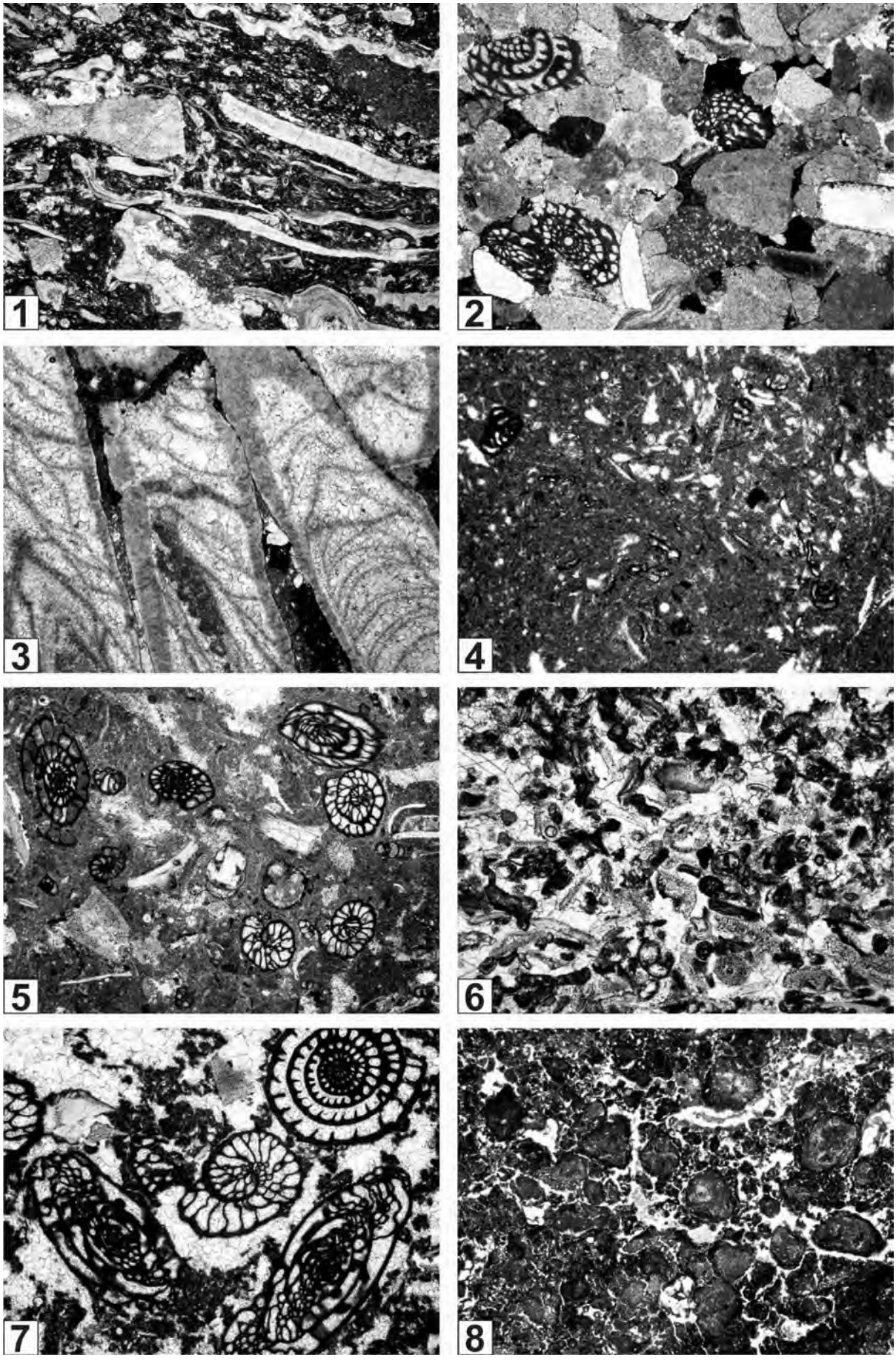
Grainstone contains a diverse assemblage of strongly fragmented fossils similar to that of member E of the underlying Horquilla Formation. Grainstone also contains many coated grains (Fig. 13.4). Typical foraminifers are *Climacammina, Globivalvulina, Spireitlina, Syzrania, Tetrataxis, Tuberitina*, nodosinelloid and tubular forms. Rarely, oolitic grainstone is present (Fig. 13.6)

Wackestone to floatstone is also characterized by a diverse fossil assemblage including many recrystallized skeletons, phylloid algae, echinoderms, bryozoans, fusulinids, smaller foraminifers (*Climacammina, Tetrataxis, Tuberitina*), ostracods, locally abundant *Tubiphytes* (Fig. 13.5) and *Koivaella*.

Oncoidal floatstone-rudstone (Fig. 13.3) contains oncoids with diameters up to 5 mm. Some oncoids display a nucleus formed by skeletal grains that are encrusted by *Girvanella* and rarely by tubular foraminifers. Most oncoids lack such a nucleus. Oncoids float in peloidal micrite that contains abundant tubular foraminifers, *Bradyina, Spireitlina, Tuberitina*, ostracods, *Girvanella*, gastropods, echinoderms, rare bryozoans and locally abundant sponge spicules.

Peloidal mudstone-wackestone-packstone is less diverse and

FIGURE 9 (facing page). Thin section photographs of limestone from the lower part of the Horquilla Formation (member A) at the Robledo Mountain section. All photos under plane light. **1,** Wackestone/packstone containing abundant sponge spicules and a few other skeletons (spiculite). Sample ROM 8, width is 3.2 mm. **2,** Bioclastic wackestone containing a diverse fossil assemblage dominated by fragments of echinoderms, bryozoans, foraminifers and ostracods. Sample ROM 7, width is 6.3 mm. **3,** Crinoidal packstone. Sample ROM 13, width is 6.3 mm. **4,** Packstone mainly composed of echinoderm fragments, subordinately fusulinids, bryozoans, recrystallized skeletons and detrital quartz grains. Sample ROM 6, width is 3.2 mm. **5,** Fusulinid floatstone containing a few fragments of bryozoans, foraminifers, recrystallized skeletons and many peloids. Sample ROM 11, width is 6.3 mm. **6,** Phylloid algal floatstone with broken fragments of completely recrystallized phylloid algae. Sample ROM 18, width is 6.3 mm. **7,** Wackestone/rudstone containing large fragments of echinoderms, bryozoans and brachiopods floating in fine bioclastic matrix. Sample ROM 9, width is 6.3 mm. **8,** Paleocalcrete displaying clotted fabric and containing abundant micritic grains, some showing micritic rims. Sample ROM 16, width is 6.3 mm.


1
2
3
4
5
6
7
8

contains a few recrystallized skeletons, echinoderms, foraminifers and ostracods. Locally, a few detrital quartz grains are present in peloidal grainstone (Figs. 13.7-13.8). Peloidal mudstone-wackestone is locally bioturbated.

Two conglomerate beds are present in the Shalem Colony Formation section, one at the base and one in the middle of the succession. The conglomerate bed at the base is 0.7 m thick, mud supported and composed of dark gray limestone clasts with diameters up to 3 cm floating in mudstone. The conglomerate bed in the middle is 1.2 m thick, fine grained, clast supported and composed of limestone and chert clasts with a maximum grain size of 3 cm. The conglomerate is poorly sorted, and most clasts are subangular to subrounded.

Near the top of the exposed succession, three bedded chert horizons are intercalated, ranging in thickness from 1 to 2.3 m. Covered intervals most likely represent shale and are 0.2-4.2 m thick.

Cycles are relatively poorly developed in the Shalem Colony Formation strata at Robledo Mountain (Fig. 6). Some shallowing upward cycles are present, starting with covered (shale) intervals, overlain by thin-bedded, wavy to nodular limestone and finally by indistinctly-bedded to massive limestone. Rhizoliths are developed at some cycle tops, indicating subaerial exposure surfaces.

Depositional Environments

Shale is not exposed in the Shalem Colony Formation of the Robledo Mountain section; however, we suggest that the covered intervals represent shale units. In the section studied by Krainer et al. (2003), approximately 1.5 km west of Robledo Mountain, shale is rarely exposed and, in the lower part of the Shalem Colony Formation, there is reddish marly shale with limestone nodules. In the Doña Ana Mountains, approximately 8 km ENE of Robledo Mountain (Fig. 1), shale is locally exposed between the limestone intervals. Several gray shale intervals that locally contain brachiopods and rare limestone nodules are interpreted as shallow marine deposits. One shale horizon containing limestone nodules is probably of pedogenic origin (Krainer et al., 2009).

Limestone of the Shalem Colony Formation is dominantly indistinctly bedded to massive; wavy bedded to nodular limestone is rare. Limestone consists of a variety of microfacies types that can be assigned to the following Standard Microfacies (SMF) types (Flügel, 2004): SMF 5 – allochthonous bioclastic grainstone, rudstone, packstone, floatstone; SMF 10 – bioclastic packstone and wackestone with worn and abraded skeletal grains; SMF 13 – oncoid rudstone and grainstone; SMF 15 – oolite, commonly oolitic grainstone, but also wackestone; and SMF 16 – peloidal grainstone and packstone.

SMF 5, 10 and 13 contain a diverse fossil assemblage including stenohaline forms, phylloid algae and rarely *Epimastopora*, indicating deposition in an open, shallow marine depositional environment with normal marine salinity. SMF 15 (oolitic grainstone) and SMF 16 contain a less diverse fossil assemblage. Oolitic grainstone indicates a very shallow, high-energy setting. Peloidal grainstone and packstone (SMF 16) with a less diverse fossil assemblage point to deposition in a shallow, restricted platform environment.

According to Jordan and Wilson (1971) and Wilson and Jordan (1983), the Hueco Group represents a gently inclined ramp profile across the late Paleozoic Orogrande basin, and the Hueco shelf facies is best described as a facies mosaic involving various mixtures and combinations of skeletal and pelletal particle types in dominantly muddy limestones. Shoal environments are represented by bioclastic grainstone and packstone. High-energy water conditions are also indicated by the presence of rounded grains. At Robledo Mountain, the Shalem Colony Formation of the Hueco Group was deposited on the western shelf of the Orogrande basin.

In the Shalem Colony Formation sections west of the Robledo Mountain section, and in the Doña Ana Mountains in the east studied by Krainer et al. (2003, 2009), indistinctly bedded to massive limestone is more common. Chert is also more common. At all three locations (Robledo Mountain, west of Robledo Mountain, Doña Ana Mountains), limestones of the Shalem Colony Formation formed in a shallow, open marine shelf environment with normal marine salinity. Limestone of a restricted shallow marine depositional environment is rare (Krainer et al., 2003, 2009). As pointed out by Wilson and Jordan (1983), the shelf was characterized by a facies mosaic of low-energy and high-energy settings and locally by phylloid algal biostromes. Carbonate conglomerate is rarely intercalated, and is probably of nonmarine origin. Siliciclastic sediment (crossbedded pebbly sandstone) occurs as a thin intercalation west of Robledo Mountain. Subaerial exposure surfaces on the tops of limestone intervals are present at Robledo Mountain where some poorly developed cycles are preserved, indicating high-frequency sea-level fluctuations.

BIOSTRATIGRAPHY

Introduction

Other than shark's teeth from unit 86 of the Horquilla Formation (Ivanov and Lucas, 2014), we made no effort to collect macrofossils from the section at Robledo Mountain. Instead, we collected samples for microfossils, primarily fusulinids and conodonts, to assign biostratigraphic ages to the section.

Algae and Foraminifers

Late Morrowan

The late Morrowan foraminifers (samples ROM 2, 3, 4; Fig. 6) are composed of endothyrids *Endothyra*, *Planoendothyra* (Fig. 14.2), palaeotextulariids, common millerellids, especially *Pseudonovella* cf. *P. irregularis* Kireeva, 1949 emend. Vachard et al., 2013 (Fig. 14.1), *Millerella marblensis* Thompson, 1942 (Fig. 14. 6?-7), *M.* cf. *M. pressa* Thompson, 1944 (Fig. 14.3-5), *M.* sp. 3 (Fig. 14.8?-9); rare eostaffellids *Eostaffella* cf. *E. pinguis* (Thompson, 1944) (Fig. 14.10), *E.* spp.; and rare Miliolata cornuspirids (*Hemigordiellina*, *Calcitornella*, *Trepeilopsis*), and a probable new genus (Fig. 14.11-13) corresponding to a parent of *Turrispiroides* having developed a porcelaneous filling in the umbilicus; this form was erroneously interpreted as *Monotaxinoides* by Mamet (1976, pl. 88, figs. 1-4) and Groves (1983, p. 21-22, pl. 13, figs. 15-19; 1984, pl. 5, figs. 10-17; 1992, pl. 3, figs. 27-33).

Late early Atokan

The late early Atokan strata (ROM 6, 7 and 7A) contain large, evolved *Profusulinella* cf. *P. spicata* Thompson, 1948 (Fig. 14.14-15), endothyrids, bradyinids, eostaffellids and millerellids. This interval is relatively thin, and it may only represent the first biozone of this substage, with its assemblage composed of *Spireitlina, Palaeonubecularia*, *Millerella*, palaeotextulariids and various fusulinellids: *Fusulinella* ex gr. *F. fugax* Thompson, 1948, *F.* ex gr. *F. juncea* Thompson, 1948, *F.* aff. *F. devexa* Thompson, 1948 (Fig. 14. 17), and *F.* cf. *F. fugafilia* Wilde, 2006 (Fig. 14.16).

Early Desmoinesian

Unit 26 contains numerous typical *Beedeina*? *insolita* (Thompson, 1948) (Fig. 15.1-10), typical of the earliest Desmoinesian. The early Desmoinesian again appears at ROM 11 (Fig. 6) with a questionable *Wedekindellina* (Fig. 14.18), and especially in ROM 11A with a diversified assemblage of *Wedekindellina euthysepta* (Henbest, 1928) (Fig. 14.19), *Beedeina pattoni* (Needham, 1937) (Fig. 14.23), *B.* aff. *B.apachensis* Ross and Sabins, 1965, *B.* aff. *B.leei* (Skinner, 1931) and *B.*aff. *B.pristina* (Thompson, 1945). A new taxon, *Cornuspira*? n. sp. (Fig. 14.20-22), is a large taxon of Miliolata homeomorph of the late Tournaisian *Eoforschia*. It may also include some Russian species like *Ammodiscus turbulentus* Reitlinger, 1950 and *A. gigas* Reitlinger, 1950.

FIGURE 10 (facing page). Thin section photographs of limestone from the lower part of the Horquilla Formation (members B, C) at the Robledo Mountain section. All photos under plane light. **1,** Floatstone containing a diverse fossil assemblage and larger skeletons (brachiopods, echinoderms and bryozoans) floating in fine bioclastic wackestone matrix. Sample ROM 23, width is 6.3 mm. **2,** Fine-grained packstone matrix in the conglomerate, many skeletons (fusulinids, echinodoerms, brachiopods), a few chert grains and rare detrital quartz grains. Sample ROM 25A, width is 6.3 mm. **3,** Syringoporid corals forming a small colony. Pore space between the branches is filled with micrite. Sample ROM 27, width is 6.3 mm. **4,** Bioclastic mudstone/wackestone containing tubular foraminiferans, subordinately bryozoans, ostracods and spicules. Sample ROM 29, width is 3.2 mm. **5,** Fusulinid wackestone containing a diverse fossil assemblage. Sample ROM 35, width is 6.3 mm. **6,** Grainstone containing a diverse fossil assemblage, some aggregate grains, many peloids and rare detrital quartz grains. Sample ROM 34, width is 3.2 mm. **7,** Fusulinid grainstone/rudstone. Sample RM unit 109, width is 6.3 mm. **8,** Paleocalcrete showing a nodular texture and containing abundant micritic nodules with circumgranular fractures. Irregular voids are filled with calcite. Sample ROM 33, width is 6.3 mm.

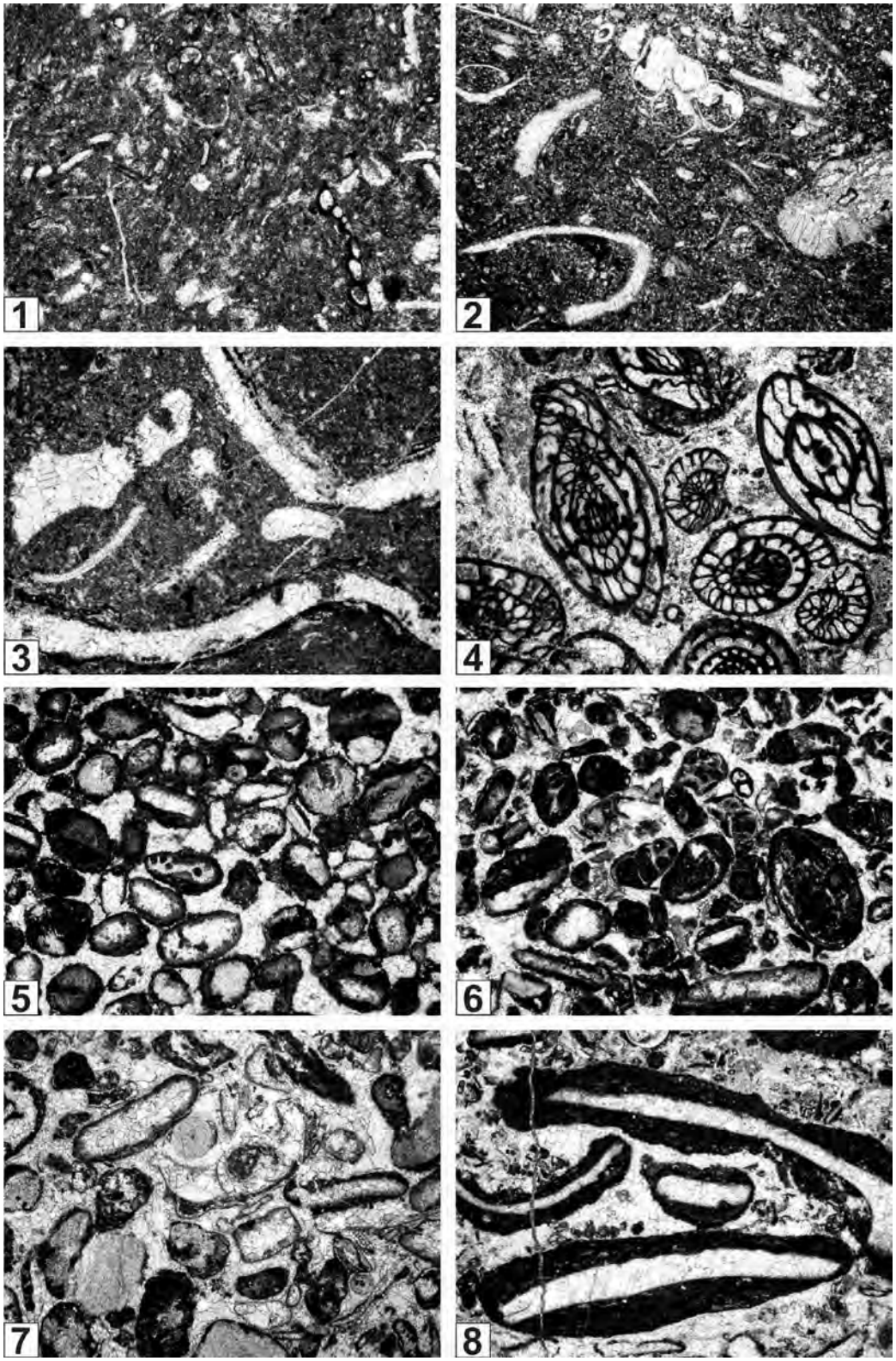


FIGURE 11. Thin section photographs of limestone from the middle part of the Horquilla Formation (member D) at the Robledo Mountain section. All photos under plane light. **1,** Bioclastic wackestone containing a diverse fossil assemblage including many tubular foraminifers and recrystallized skeletons. Sample ROM 40, width is 3.2 mm. **2,** Wackestone/floatstone containing a diverse fossil assemblage including bryozoans, echinoderms, foraminifers, ostracods and phylloid algae. Sample ROM 43, width is 6.3 mm. **3,** Phylloid algal floatstone with fragments of recrystallized phylloid algae, probably *Eugonophyllum*. Sample RM unit 122, width is 6.3 mm. **4,** Slightly washed fusulinid rudstone containing a few other bioclasts. Sample RM unit 119, width is 6.3 mm. **5,** Grainstone composed of abundant coated grains, a few intraclasts and rare detrital quartz grains. Sample RM unit 136, width is 6.3 mm. **6,** Oncoidal grainstone composed of abundant small oncoids, a few micritic intraclasts, diverse skeletons and peloids. Sample ROM 42, width is 6.3 mm. **7,** Grainstone/rudstone containing recrystallized skeletons (?phylloid algae), echinoderms and micritic intraclasts. Sample ROM 41, width is 6.3 mm. **8,** Oncoidal rudstone, moderately washed, containing elongate oncoids composed of recrystalized skeletons encrusted by cyanobacteria. Sample ROM 40a, width is 6.3 mm.

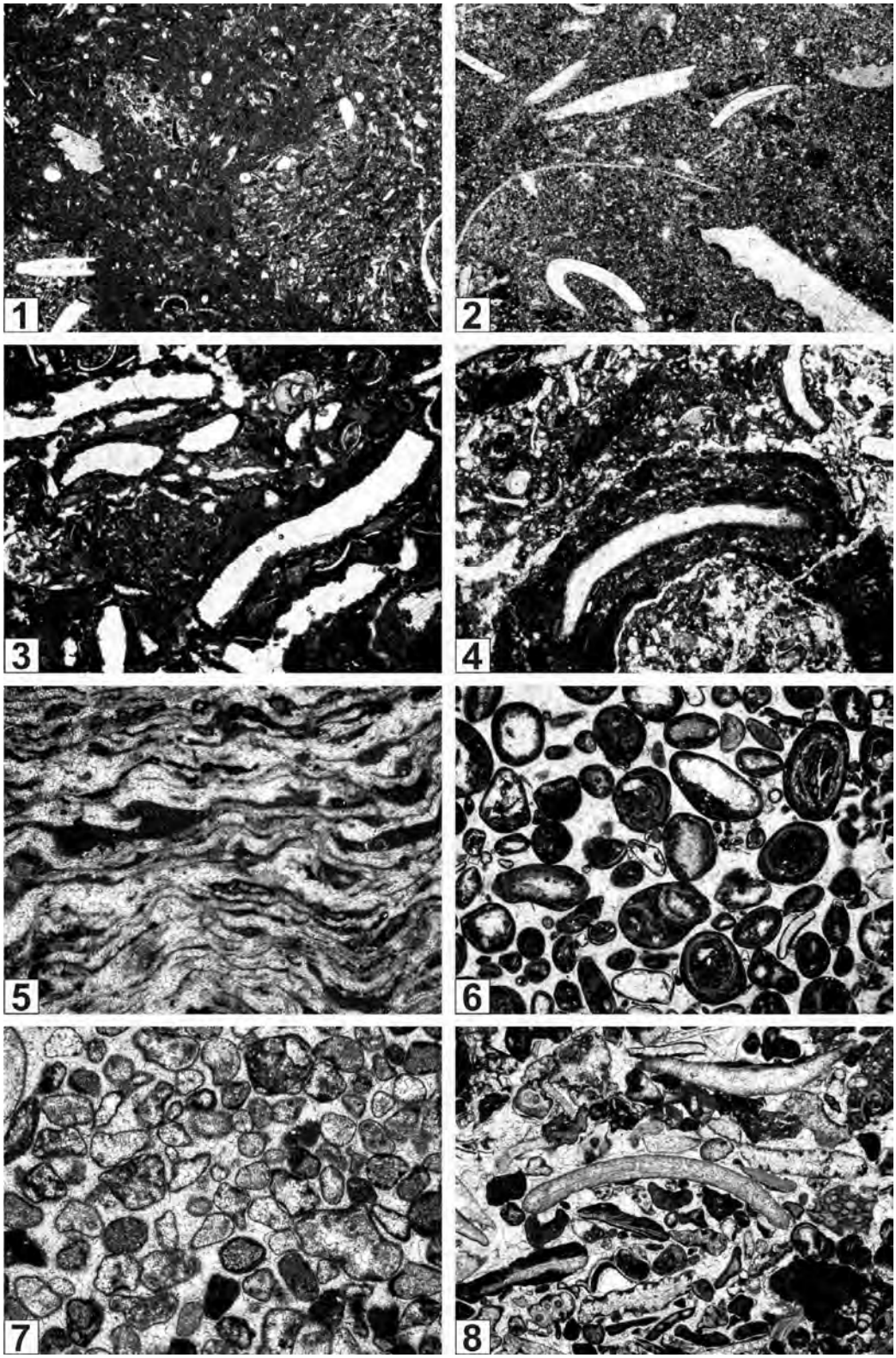


FIGURE 12. Thin section photographs of limestone from the upper part of the Horquilla Formation (member E) at the Robledo Mountain section. All photos under plane light. **1,** Wackestone, fine-grained and bioturbated, containing a diverse fossil assemblage, including echinoderms, brachiopods, foraminifers, ostracods and recrystallized skeletons. Sample ROM 54, width is 6.3 mm. **2,** Wackestone/floatstone containing a few large skeletons floating in fine bioclastic peloidal micrite. Sample ROM 47, width is 6.3 mm. **3,** Phylloid algal floatstone with completely recrystallized skeletons of phylloid algae. Sample RM unit 175, width is 6.3 mm. **4,** Oncoidal floatstone composed of oncoids up to 6 mm in diameter floating in grainstone to packstone containing a diverse fossil assemblage. Sample ROM 45, width is 6.3 mm. **5,** Bindstone composed of irregular crusts formed by *Archaeolithophyllum lamellosum*. Sample RM unit 187, width is 6.3 mm. **6,** Grainstone containing small oncoids, coated grains, ooids and recrystallized skeletons. Sample ROM 52, width is 6.3 mm. **7,** Grainstone composed of abundant recrystallized grains (?skeletons) with thin micritic envelopes and a few micritic intraclasts. Sample ROM 50, width is 3.2 mm. **8,** Rudstone, poorly sorted containing abundant intraclasts, coated grains, peloids and diverse skeletons. Sample ROM 58, width is 6.3 mm.

Middle? Desmoinesian

The middle? Desmoinesian (ROM 13-ROM 26) is probably characterized by the disappearance of *Wedekindellina*, and by some species of *Beedeina*: *B.* cf. *B. pararockymontana* Wilde, 2006 (ROM 13) (Fig. 14.24), *Plectofusulina* sp. (ROM 22) (Fig. 16.1), *Beedeina* cf. *B. leei* (Skinner, 1931) (Fig. 16.7) and *B.* cf. *B. pristina* Thompson, 1945 (Fig. 16.8) (both in ROM 26). In this interval, the smaller foraminifers are diversified: endothyrids (Fig. 16.4), bradyinids (Fig. 16.3), eostaffellids and palaeotextulariids (Fig. 16.6), cornuspirids and calcivertellids (Fig. 16.5), and syzraniids (FO [first occurrence] in ROM 15). *Bacinella* sp. are noticeable in ROM 24 (Fig. 16.15), *Archaeolithophyllum*? sp. in ROM 25, and *Efluegelia johnsoni* (Flügel, 1966) in ROM 22 (Fig. 16.2).

Late Desmoinesian?-early Missourian?

The late Desmoinesian? does not yield large fusulinids, but might be characterized by the transitional forms between palaeonubeculariids and tubiphytids (visible, for example, in ROM 28; Fig. 16.9) and associated with a smaller fusulinid *Fusiella*? sp. (Fig. 16.10). The earliest Missourian *Eowaeringella* zone is similarly not locally characterized. It might correspond to ROM 29 with *Eoschubertella*/*Schubertellina* sp., *Oketaella* cf. O. *campensis* Thompson, 1954 (Fig. 16.11), *Globivalvulina* ex gr. *G. mosquensis* Reitlinger, 1950, *Hemigordius* sp., *Calcitornella* sp., *Hemigordiellina* sp., *Palaeonubecularia* sp. and *Syzrania* sp. and/or to ROM 31 with *Eugonophyllum*.

Early/middle Missourian

The early/middle Missourian is present in unit 95 with *Triticites* cf. *T. ferayi* Bilelo, 1969 (Fig. 16.12), in unit 98 with *Bradyina lucida* Morozova, 1949, in ROM 32 with *Triticites acutuloides* Ross, 1965 (Fig. 17.5-6) and *Paraepimastopora kanumai* (Endo, 1954) n. comb. (Fig. 17.3-4), in ROM 32 with *T. acutuloides* (Fig. 17.1-2), and in ROM 32A with *Paraepimastopora* cf. *P. kanumai*, *T. acutuloides*, *T.* cf. *T. marathonensis* Ross, 1965 (Fig. 17. 7) and *Syzrania* sp.

Late Missourian

At Robledo Mountain, the late Missourian is well-characterized with *Triticites* cf. *T. marathonensis* (Fig. 17. 10), *T.* cf. *T. moorensis* Ross, 1965 (Fig. 17. 8, 11), *T.* cf. *T. yvani* Wilde, 2006 (Fig. 17.9?, 12), and *T. acutuloides* in ROM 35, 35A and 35B, associated with *Eotuberitina* sp., *Spireitlina*, a bradyinid, a palaeotextulariid, *Globivalvulina* ex gr. *G. bulloides* (Brady, 1876) (Fig. 18.3-4), *Syzranella arctica* Mamet and Pinard, 1992 (Fig. 18.1) and *Triticites* cf. *T. acutuloides* (Fig. 18. 5), *T.* sp. 6 (Fig. 18. 2) and *T.* cf. *T. coronadoensis* Ross and Tyrrell, 1965 (Fig. 18.8) in ROM 36 (unit 107).

Early Virgilian

The early Virgilian appears in ROM 37 with *Triticites* cf. *T. acutuloides* (Fig. 18.6), *Triticites secalicus* (Say, 1823) (Fig. 18.9-10) and in ROM 37 with *T.* cf. *T. coronadoensis* Ross and Tyrrell, 1965 (Fig. 18.7), in ROM 37A with *Triticites* ex gr. *T. plummeri* Dunbar and Condra, 1927 (Fig. 19.1), in ROM 38 with *Triticites* cf. *T. beedei* Dunbar and Condra, 1927 (Fig. 18.11), and in unit 114 with the alga *Epimastopora*? sp. (Fig. 19.9).

Late Virgilian

The late Virgilian starts in ROM 39 and unit 119 with *Triticites* cf. *T. bungerensis* Kauffman and Roth, 1966 (Fig. 18.12); *T.* aff. *T. jackboroensis* Kauffman and Roth, 1966 (Fig. 19.3-4); *T.* sp. 12 (Fig. 19.5-6); *T.* sp. 13 (Fig. 19.7-8); a primitive form of the group *T. ventricosus* (Meek and Hayden, 1865) assigned here to *T.* aff. *T. southensis* Ross and Tyrrell, 1965 (Fig. 20.1), a form transitional to the pseudoschwagerinids (specimen RM unit 119-17) (Fig. 20.2), and the smaller foraminifers *Bradyina* sp. (Fig. 20, fig. 9), *Tetrataxis* sp. (Fig. 18.15-16), *Timanella* sp. (Fig. 18.14) a genus from the Urals mentioned here, to our knowledge, for the first time in the USA, and calcivertellids indet. (Fig. 18.13). In unit 122, *Eugonophyllum* sp. with *Claracrusta* sp. and *Palaeonubecularia* sp are present (Figs. 19.2, 20.6-7) with *Latitubiphytes* sp. (Fig. 20.8). The late Virgilian is still present in ROM 41 with *T.* cf. *T. plummeri maximus* Kauffman and Roth, 1966 (Fig. 20.3) and *Epimastopora* ex gr. *E. alpina* (Pia, 1937) Kochansky-Devidé and Herak, 1960 (Fig. 19.10).

Early Wolfcampian

The Carboniferous-Permian interval encompasses the stratigraphic interval from units 136 to 142. It is characterized by the appearance of the Permian microfacies, i.e., grainstone with *Calcivertella* spp., *Ellesmerella-Girvanella* oncoids (Fig. 20.4), *Epimastopora* ex gr. *E. alpina* (Pia, 1937) Kochansky-Devidé and Herak, 1960 (Fig. 20.10), *Parapimastopora* ex gr. *P. kansasensis* (Johnson, 1946) (Fig. 20.11), and some surviving large *Triticites*. The last large fusulinids are *Triticites meeki* (Möller, 1879) emend. Thompson, 1954 in unit 149 (Fig. 21.1) associated with *Spireitlina* cf. *S. conspecta* (Reitlinger, 1950) (Fig. 21.2, 4) and *Bradyina* cf. *B. lucida* Morozova, 1949 (Fig. 21.3).

The typical Permian (i.e., Asselian) algal and foraminiferal assemblages are probably present as low as ROM 43 with algae *Epimastopora* ex gr. *E. japonica* Endo, 1951 (Fig. 20. 5) and *Epimastopora* sp. (Fig. 20.14) in ROM 44, and pseudovidalinids in ROM 43 due to the specific diversity of *Pseudovidalina* (= *Raphconilia* of the authors) with *P. modificata* (Potievskaya, 1962) (Fig. 20.12), and *P.* cf. *P. iranica* Alipour and Vachard in Alipour et al., 2013 (Figs. 20.13, 21.21). In ROM 44 the Permian algae *Epimastopora japonica* Endo, 1951 is present. In ROM 45, *Nodosinelloides longissima* (Suleimanov, 1945) (Fig. 21.5), *N. pinardae* Groves and Wahlman, 1997 (Fig. 21.6), and *N. netschajewi* (Cherdyntsev, 1914) sensu Groves and Wahlman, 1997 (Fig. 21.8) indicate possibly that the beds are already middle or late Asselian in age. In ROM 45, interesting specimens of *Tuberitina bulbacea* Galloway and Harlton, 1928 are present (Fig. 21.7). In unit 149, *Latitubiphytes* sp. 1 was found (Fig. 21.11). One large keriothecal fusulinid is present in ROM 45 but it is difficult to interpret, even generically, because it is cut in transverse section, and partly affected by cyanobacterial action. Nevertheless, it is either a reworked *Triticites* cf. *pinguis* Dunbar and Skinner, 1937 or a *Leptotriticites* or a *Thompsonites* (Fig. 21.12).

From strata we judge to encompass our units 149-162, Wahlman and King (2002) reported small species of *Leptotriticites* that overlap the *Leptotriticites* (as "*Dunbarinella*") records reported by Thompson (1954) (compare Figs. 2 and 5). This indicates an early Wolfcampian ("Bursumian") age.

Middle Wolfcampian

The upper part of the section from unit 157 to the top of the Horquilla Formation corresponds to the middle Wolfcampian; i.e., early Sakmarian. Our sample ROM 46 contains only *Latitubiphytes* sp. 2 (Fig. 21.13). The taxon *Hemigordius* cf. *H. schlumbergeri* (Howchin, 1895) in ROM 47 (Fig. 21.14? 15, 17?) might indicate the presence of (early?) Sakmarian beds, as well as *Nodosinelloides longa* (Lipina, 1949) in ROM 48 (Fig. 21.16), and *Pseudovidalina* cf. *P. helicis* Pinard and Mamet, 1998 in ROM 49-1 (Fig. 21.18). Up to ROM 59, no indications of a younger age (late Sakmarian-Artinskian) were encountered, because the taxa observed in this interval (*Pseudovidalina modificata* (Fig. 21.19?, 21) and *Archaeolithophyllum lamellosum* Wray, 1964 (Fig. 21.23-24) have a relatively long stratigraphic range. Only the latest staffellid of ROM 58 (Fig. 21.20), which eventually gave rise to the Leonardian genus *Pseudoreichelina* Leven, 1970 (see Krainer et al., 2009), might indicate the presence of late Wolfcampian beds in the top of the field section.

In the lower part of the Shalem colony Formation (unist 207-250), the foraminiferal genera have long biostratigraphic ranges, so we still judge the age to be middle Wolcampian. There are *Spireitlina conspecta* (Fig. 22.4-5), *Globivalvulina* sp. (Fig. 22.7), *Calcitornella* spp. (Fig. 22.1, 3), *Hedraites plummerae* Henbest, 1963 (Fig. 22.6), *Syzrania* sp. (Fig. 22.9 part), *Nodosinelloides potievskayae* Mamet and Pinard, 1996 (Fig. 22.2), *Protonodosaria* sp. 1 (Fig. 22.12-13), *P.* sp. 2 (Fig. 22.14). The oncoids remain frequent, but the *Ellesmerella* oncoids (Fig. 22.8, 11) are partly replaced by oncoids with *Girvanella* (Fig. 22. 9, 11, Fig. 23. 1) especially in unit 217. Some *Efluegelia* are present (Fig. 22.20, Fig. 23.12).

Thompson (1954) and Wahlman and King (2002) described fusulinids from our units 240-244 that include *Pseudoschwagerina*, indicative of the middle Wolfcampian. Nevertheless, our unit 244 contains typical *Tubiphytes obscurus* Maslov, 1956 (Figs. 22.21, 23.2-3, 5, 10) and *Pseudofusulina*? sp. (Fig. 23.8), which could be secondary markers of the middle/late Wolfcampian, because contrary to the situation in Russia, the first true *Tubiphytes* of the group *obscurus* Maslov, 1956 (i.e., the *Nigriporella* of Rigby, 1958) regionally appears only in the late Wolfcampian-Leonardian (= latest Sakmarian-Artinskian; Vachard et al., 2014, and work in progress).

Subordinate taxa are cyanobacteria *Koivaella permica* Chuvashov, 1974 (Fig. 22.15, Fig. 23.4), dasycladaleans *Epimastopora* sp. (Fig.

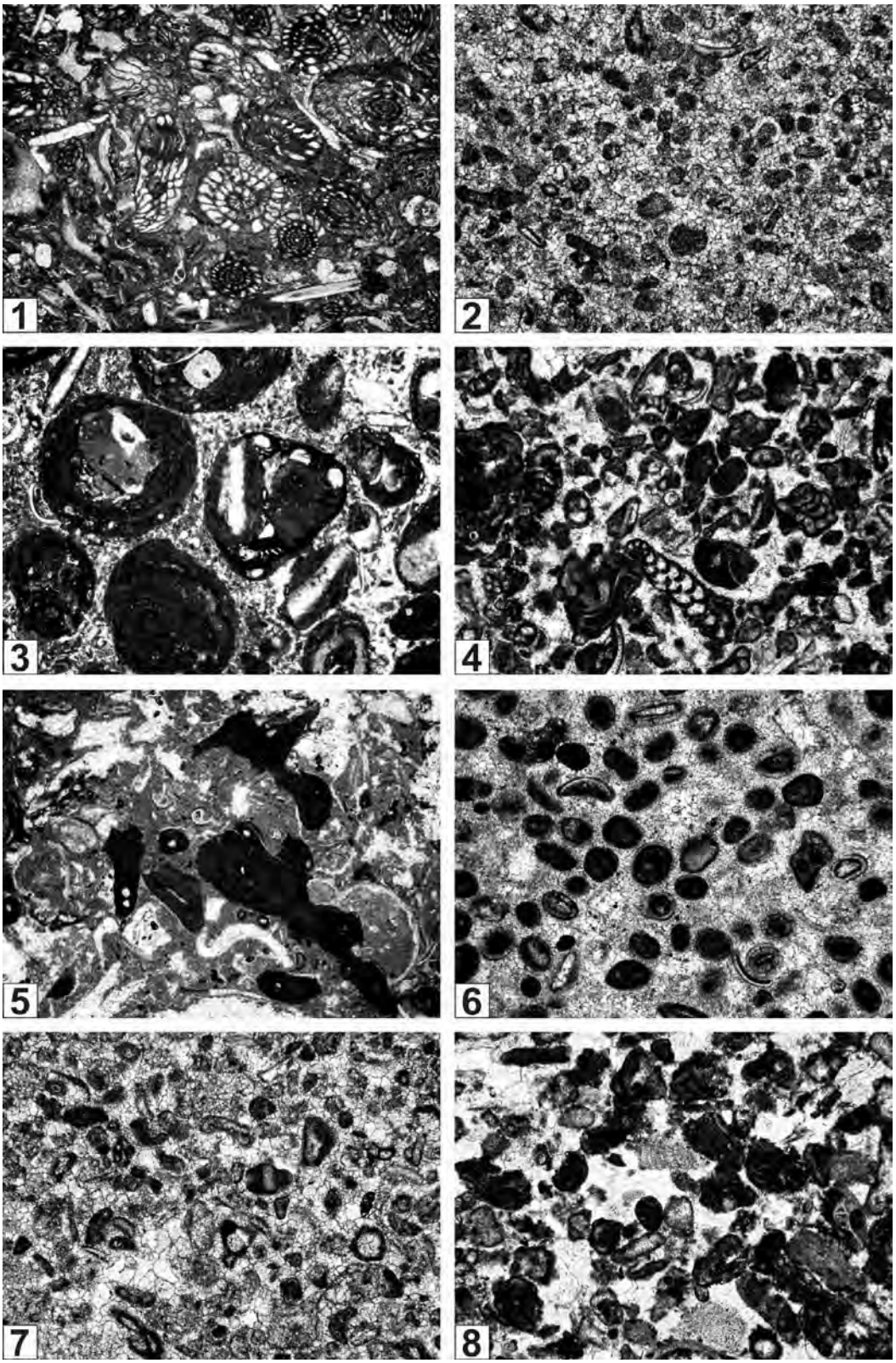


FIGURE 13. Thin section photographs of limestone from Hueco Group (Shalem Colony Formation) at the Robledo Mountain section. All photos under plane light. **1,** Fusulinid packstone with a few other skeletons such as echinoderms, brachiopods and bryozoans. Sample RM unit 226, width is 6.3 mm. **2,** Peloidal grainstone containing a few recrystallized skeletons. Sample RM unit 227, width is 3.2 mm. **3,** Oncoidal floatstone/rudstone. Oncoids float in fine bioclastic matrix containing a diverse fossil assemblage. Sample RM unit 217, width is 6.3 mm. **4,** Grainstone composed of small oncoids, coated grains, and partly recrystallized skeletons. Sample RM unit 234, width is 3.2 mm. **5,** Floatstone containing many large *Tubiphytes* and various skeletons. Sample RM unit 244, width is 6.3 mm. **6,** Oolitic grainstone containing a few skeletons (shell debris, echinoderms, ostracods). Sample RM unit 205, width is 3.2 mm. **7,** Grainstone composed of abundant peloids, tubular foraminiferans, ostracods, echinoderms and other skeletons. Sample RM unit 207, width is 3.2 mm. **8,** Grainstone/packstone composed of peloids, intraclasts and a diverse fossil assemblage. Sample RM unit 256, width is 3.2 mm.

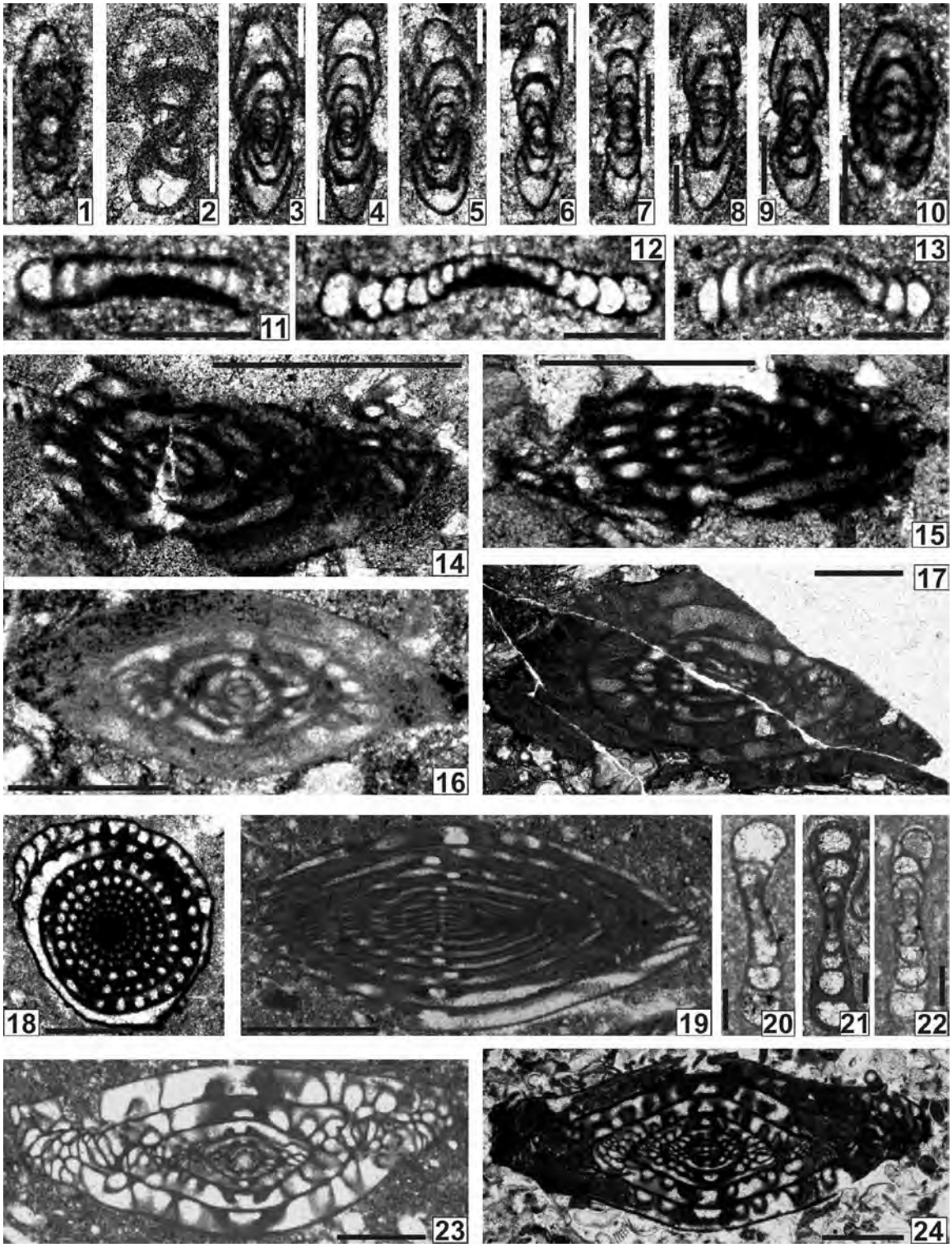


FIGURE 14. Foraminiferans from the Horquilla Formation at Robledo Mountain. **1,** *Pseudonovella* cf. *P. irregularis* Kireeva, 1949. Axial section. Early or late Morrowan. Sample ROM 2-1. **2,** *Planoendothyra* sp. Axial section. Early or late Morrowan. Sample ROM 2-10. **3-5,** *Millerella* cf. *pressa* Thompson, 1944. Three axial sections. Late Morrowan. Samples ROM 3-1, ROM 3-8, and ROM 3-13. **6?-7,** *Millerella marblensis* Thompson, 1942. Axial sections. Late Morrowan. Samples ROM 3-36 and 4-13. **8?-9,** *Millerella* sp. 3. Subaxial and axial sections. Late Morrowan. Samples ROM 4-18 and 4-16. **10,** *Eostaffella* cf. *E. pinguis* (Thompson, 1944). Axial section. Early or Late Morrowan. Sample ROM 3-29. **11-13,** N. gen. n. sp. = *Monotaxinoides transitorius* sensu Groves 1983, 1984, 1992 non Brazhnikova and Yartseva, 1956. Three axial sections showing the porcelaneous umbilical filling more or less developed. Late Morrowan. Samples ROM 3-5, 3-6 and 3-17.**14-15,** *Profusulinella* cf. *P. spicata* Thompson, 1948. Two subaxial sections. Early Atokan. Samples ROM 6-4 and 6-8.16, *Fusulinella* cf. *F. fugafilia* Wilde, 2006. Subaxial section. Late Atokan. Samples ROM 9-16.**16-17,** *Fusulinella* aff. *F. devexa* Thompson, 1948. Oblique axial section. Late Atokan. Samples ROM 9A-1.**18,** *Wedekindellina*? sp. Transverse section. Early Desmoinesian?. Sample ROM 11-5.**19,** *Wedekindellina euthysepta* (Henbest, 1928). Subaxial section. Early Desmoinesian. Sample ROM 11A-4. **20-22,** *Cornuspira*? n. sp. Three axial sections. Early Desmoinesian. Samples ROM 11A-1, 11A-2, 11A-7. **23,** *Beedeina pattoni* (Needham, 1937). Axial section. Early Desmoinesian. Sample ROM 11a-6. **24,** *Beedeina* cf. *B. pararockymontana* Wilde, 2006. Subaxial section. Early Desmoinesian. Sample ROM 13-1. Scale bars: 1-13, 20-22 = 0.10 mm; 14-19, 23 = 0.50 mm; 24 = 1.00 mm.

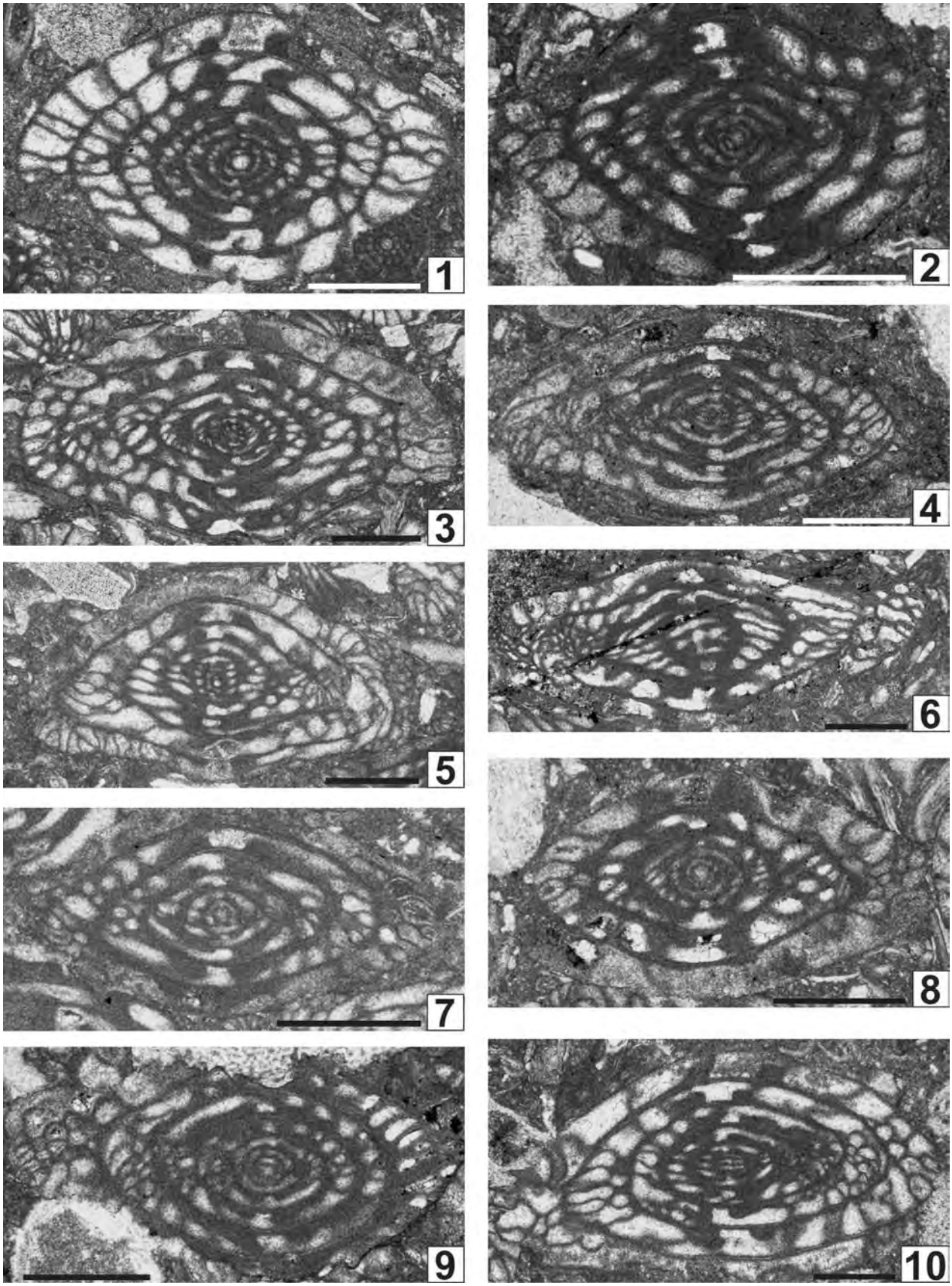


FIGURE 15. Middle Pennsylvanian (earliest Desmoinesian) fusulinids from unit 26. Various axial and subaxial sections. **1-10**, *Beedeina*? *insolita* (Thompson, 1948). **1**, Sample RM Unit 26-6. **2**, Sample RM Unit 226-1. **3**, Sample RM Unit 26-2. **4**, Sample RM Unit 26-19. **5**, Sample RM Unit 26-5. **6**, Sample RM Unit 26-11. **7**, Sample RM Unit 26-5a. **8**, Sample RM Unit 26-10. **9**, Sample RM Unit 26-17. **10**, Sample RM Unit 26-14. All figures are 0.5 mm wide.

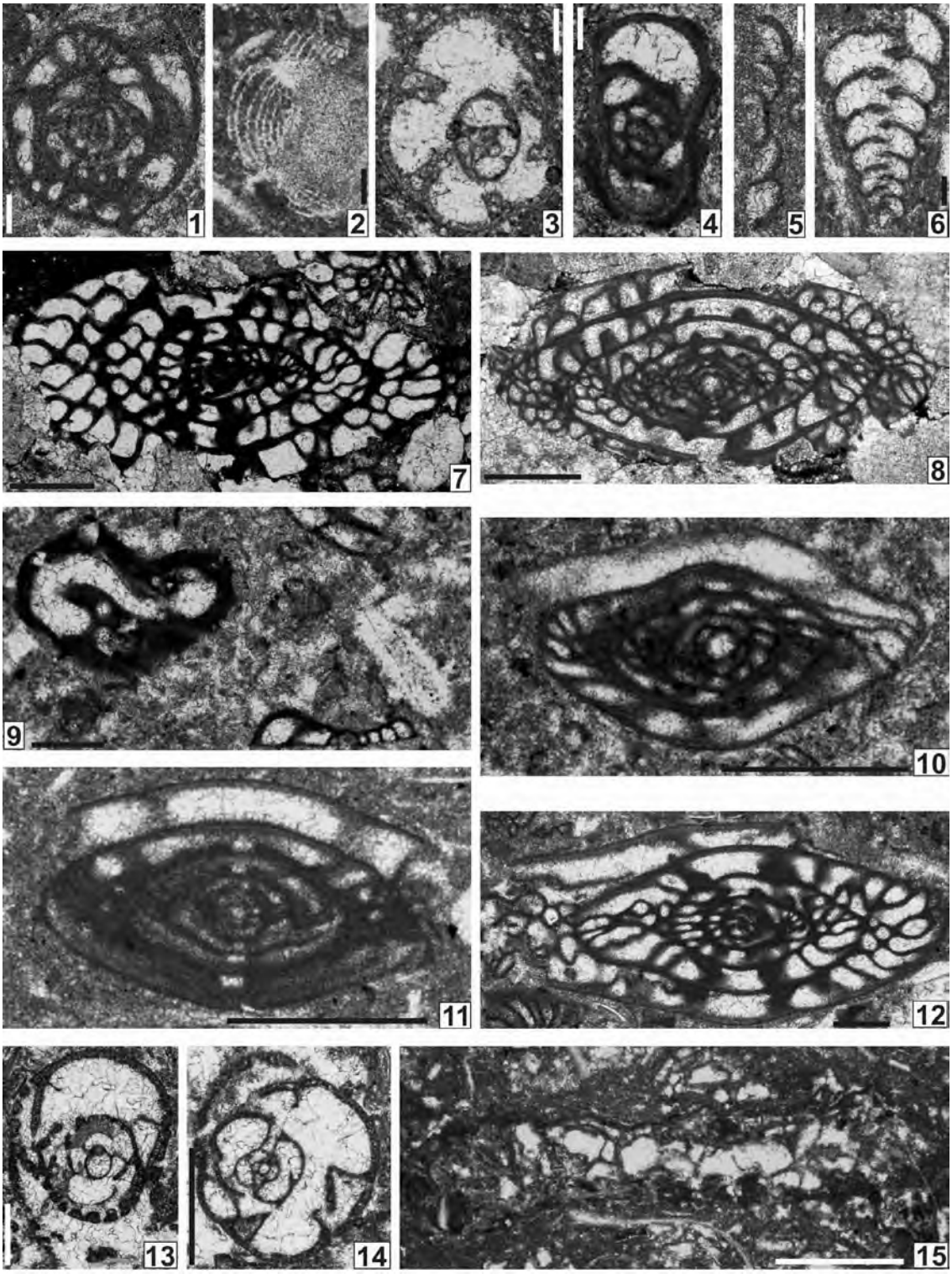


FIGURE 16. Foraminiferans from the Horquilla Formation at Robledo Mountain. **1,** *Plectofusulina* sp. Oblique section. Middle Desmoinesian. Sample ROM 22-2. **2,** *Efluegelia johnsoni* (Flügel, 1966).Axial section. Middle Desmoinesian. Sample ROM 22-5. **3,** *Bradyina samarica* Reitlinger, 1950. Transverse section. Middle Desmoinesian. Sample ROM 23-3. **4,** *Endothyra whitesidei* Galloway and Ryniker, 1930. Axial sections. Middle Desmoinesian. Sample ROM 23-7. **5,** *Calcivertella* sp. Subaxial section. Middle Desmoinesian. Sample RM unit 65-1. **6,** *Palaeotextulariaangusta* Reitlinger, 1950. Axial section. Early Missourian. Sample RM unit 91-2. **7,** *Beedeina* cf. *B.leei* (Skinner, 1931). Oblique subtransverse section. Robledo Mountains. Middle? Desmoinesian. Sample ROM 26-1. **8,** *Beedeina* cf. *B. pristina* (Thompson, 1945). Axial section. Middle? Desmoinesian. Sample ROM 26-3. **9,** Transition *Palaeonubecularia*/*Latitubiphytes* (oblique section; left) and *Calcivertella* sp. (axial section; right, bottom). Late Desmoinesian or early Missourian. Sample ROM 28-3. **10,***Fusiella*? sp. (sensu Wilde, 2006) or juvenile of *Eowaeringella* sp. Late Desmoinesian or earliest Missourian. Sample ROM 28-4. **11,** *Oketaella* cf. *O. campensis* Thompson, 1954. Axial section. Early Missourian. Sample RM unit 91-1. **12,** *Triticites* cf. *T. ferayi* Bilelo, 1969. Subaxial and oblique axial sections. Early/Middle Missourian. Sample RM unit 95A-1.**13-14,** *Bradyina lucida* Morozova, 1949. Axial and transverse sections. Early/middle Missourian. Samples RM unit 98-2 and unit 98-3. **15,** *Bacinella* sp. Random section. Middle/late Desmoinesian?. Sample ROM 24-2. Scale bars = 1-6 = 0.10 mm; 7-15 = 0.50 mm.

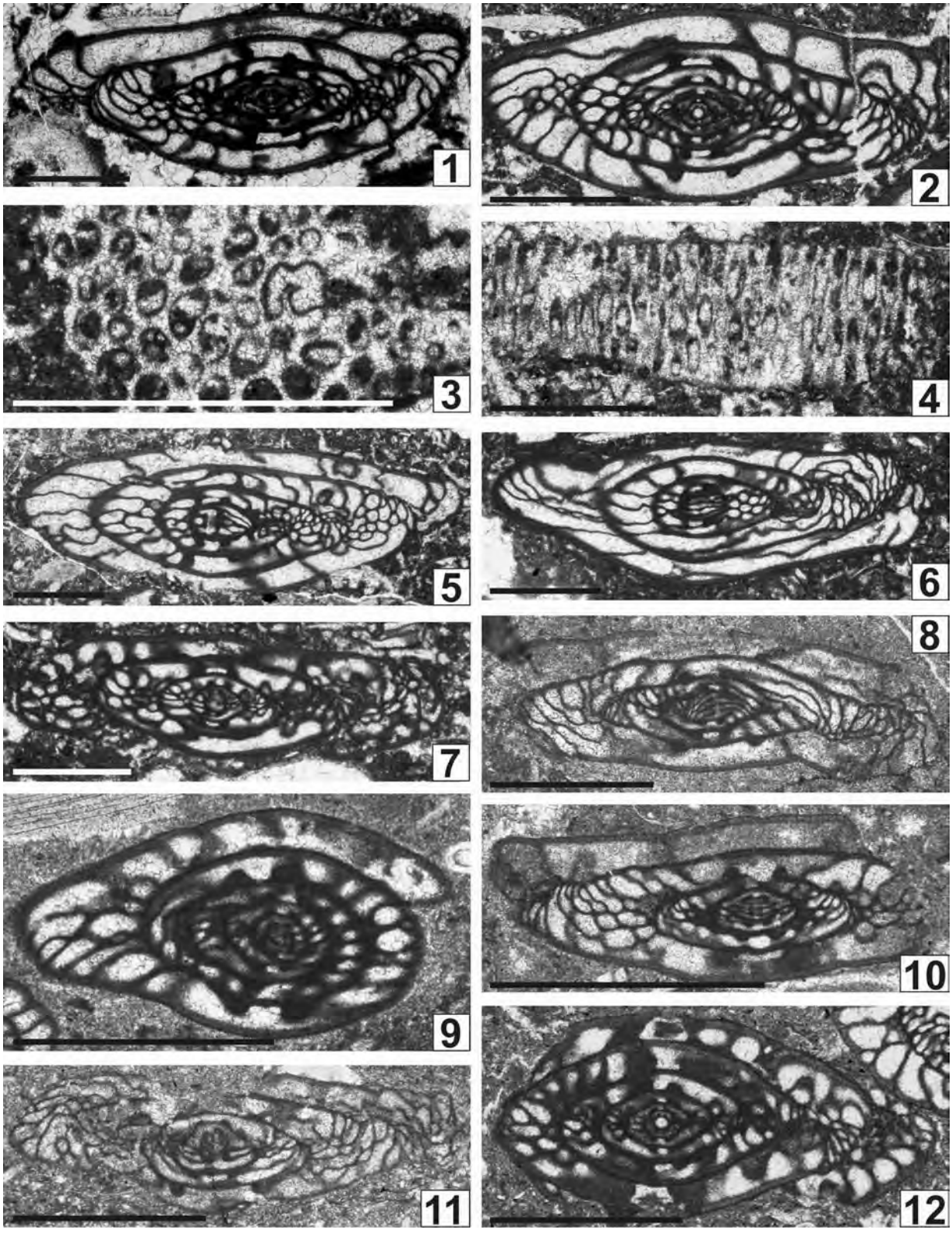


FIGURE 17. Foraminiferans from the Horquilla Formation at Robledo Mountain. **1-2,** *Triticites acutuloides* Ross, 1965. Two axial sections. Middle Missourian. Samples RM unit 99-5 and unit 99A-1. **3-4,** *Paraepimastopora kanumai* (Endo, 1954).Tangential and subaxial sections. Middle Missourian. Samples ROM 32-3 and 32-4. **5-6,** *Triticites acutuloides* Ross, 1965. Two subaxial sections. Middle Missourian. Samples ROM 32-5 and 32-7. **7, 10,** *Triticites* cf. *T. marathonensis* Ross, 1965. Two subaxial sections. Middle and late Missourian. Samples ROM 32A-6 and 35B-2. **8, 11,** *Triticites* cf. *T. moorensis* Ross, 1965. Two subaxial sections. Late Missourian. Samples ROM 35-1 and 35A-4. **9?, 12,** *Triticites* cf. *T. yvani* Wilde, 2006. Subaxial and axial sections. Late Missourian. Samples ROM 35-2 and RM unit 105A-1. Scale bars: 3 = 0.50 mm; 1, 2, 4-12 = 1.00 mm.

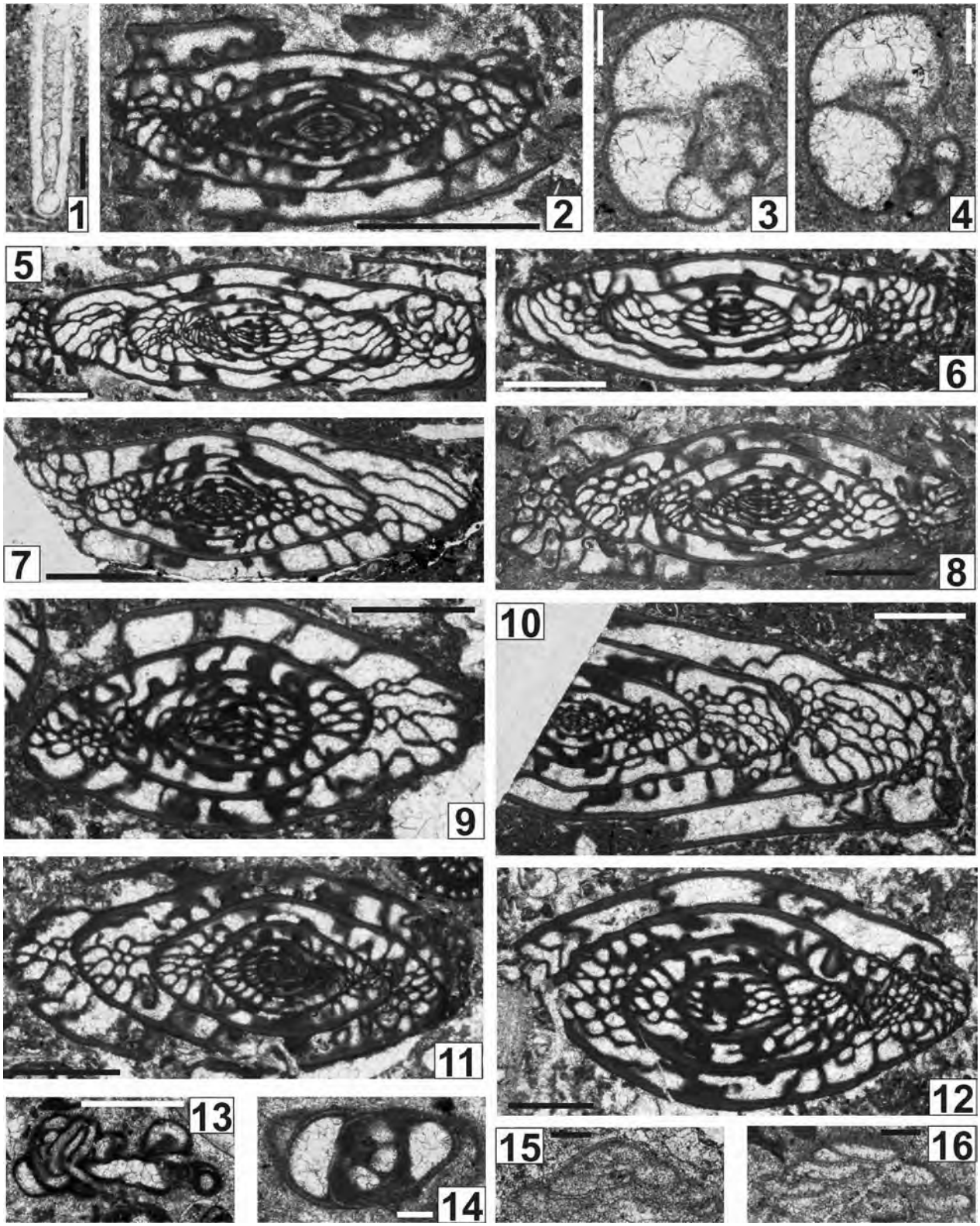


FIGURE 18. Foraminiferans from the Horquilla Formation at Robledo Mountain. **1,** *Syzranella arctica* Mamet and Pinard, 1992. Axial section. Latest Missourian. Sample RM unit 105A-3. **2,** *Triticites* sp. 6. Subxial section. Late Missourian. Sample RM 36-2a. **3-4,** *Globivalvulina* ex gr. *G.bulloides* (Brady, 1876). Axial and transverse sections. Latest Missourian. Samples RM units 105-3 and 105A-7. **5-6,** *Triticites* cf. *T. acutuloides* Ross, 1965. Two subaxial sections. Latest Missourian. Samples ROM 36-2 and 37-2. **7-8,** *Triticites* cf. *T. coronadoensis* Ross and Tyrrell, 1965. Two subaxial sections. Earliest Virgilian. Samples ROM 37-6 and RM unit 107-2. **9-10,** *Triticites secalicus* (Say, 1823). Two subaxial sections. Earliest Virgilian. Samples ROM 37-4a and 37A-3. **11,** *Triticites* cf. *T. beedei* Dunbar and Condra, 1927. Subaxial section. Early Virgilian. Sample ROM 38-3. **12,** *Triticites* cf. *T. bungerensis* Kauffman and Roth, 1966. Subaxial section. Early Virgilian. Sample ROM 39-1. **13,** Calcivertellid (n. gen.?). Subaxial section. Late Virgilian. Sample RM unit 119-10. **14,** *Timanella* sp. Subaxial section. Late Virgilian. Samples RM unit 119-11. **15-16,** *Tetrataxis* sp. Two subaxial sections. Late Virgilian. Samples RM unit 119-1 and unit 119-8. Scale bars: 1, 3, 4, 14, 15, 16 = 0.10 mm; 13 = 0.50 mm; 2, 5-12 =1.00 mm.

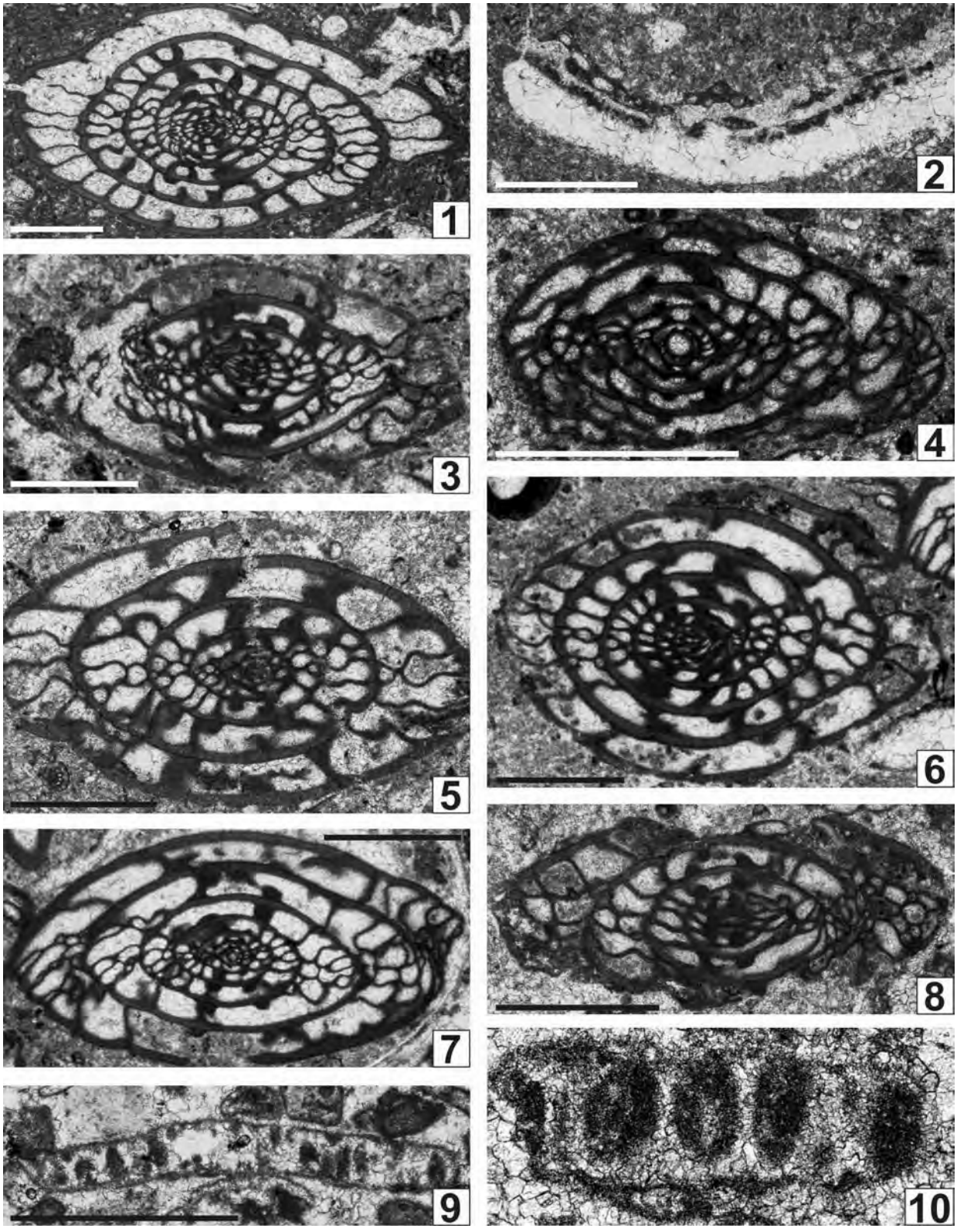


FIGURE 19. Foraminiferans from the Horquilla Formation at Robledo Mountain. **1,** *Triticites* ex gr. *T. plummeri* Dunbar and Condra, 1927. Subaxial section. Robledo Mountains. Earliest Virgilian. Sample ROM 37A-4. **2,** *Eugonophyllum* sp. with *Claracrusta* sp. and *Palaeonubecularia* sp. Subaxial section. Middle Virgilian. Sample RM unit 122-3a. **3-4,** *Triticites* aff. *T. jackboroensis* Kauffman and Roth, 1966. Subaxial and axial sections. Middle Virgilian. Samples RM unit 119-4 and unit 119-9. **5-6,** *Triticites* sp. 12. Two subaxial sections. Middle Virgilian. Samples RM unit 119-5 and unit 119-12a. **7-8,** *Triticites* sp. 13. Axial and subaxial sections. Middle Virgilian. Samples RM unit 119-12 and unit 119-13. **9,** *Epimastopora*? sp. Subaxial section. Early Virgilian. Sample RM unit 114-4. **10,** *Epimastopora* ex gr. *E.alpina* (Pia, 1937) Kochansky-Devidé and Herak, 1960. Subaxial section. Late Virgilian. Sample ROM 41-2. Scale bars: 1-9 = 1.00 mm; 10 = 0.10 mm.

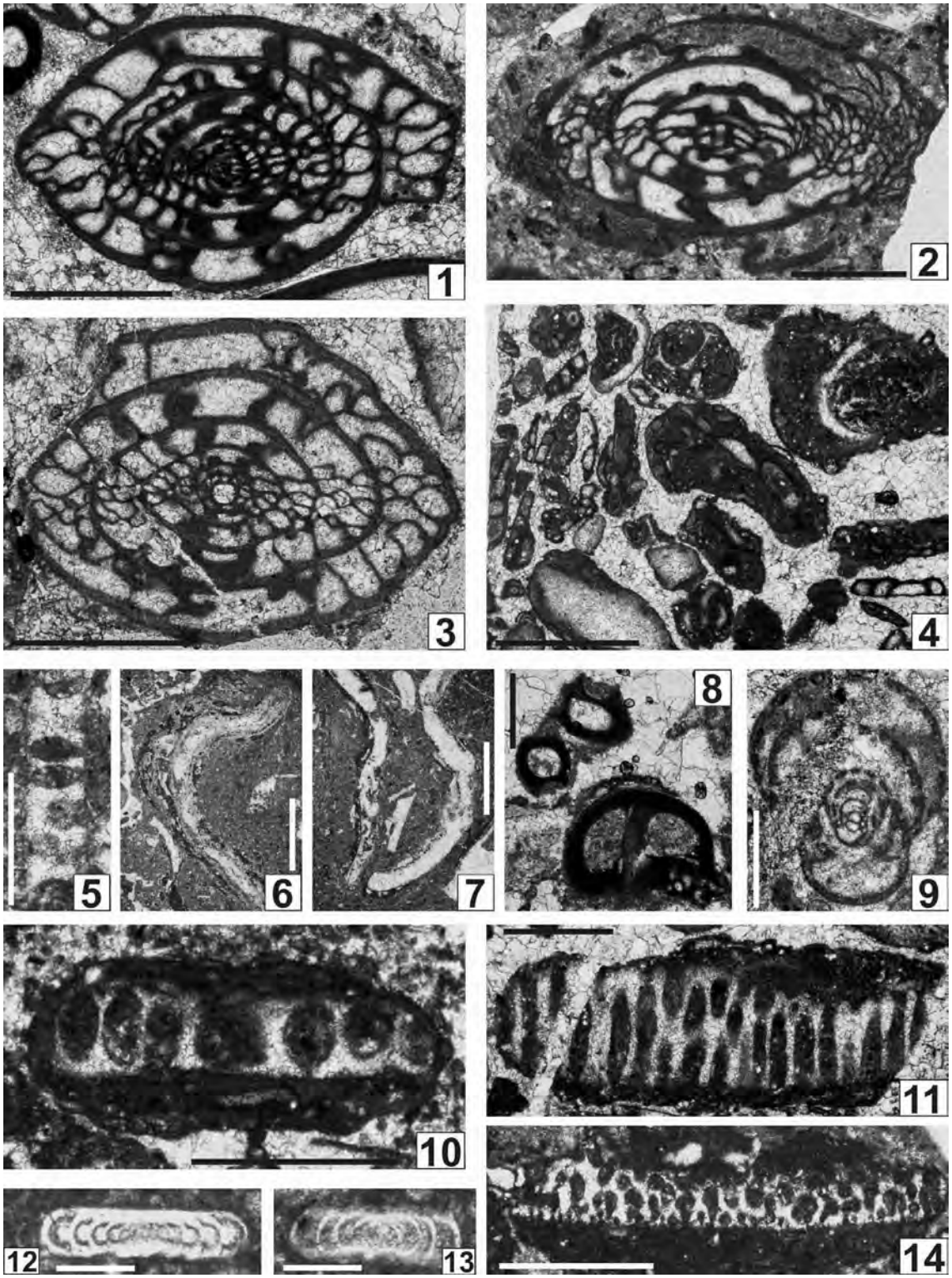


FIGURE 20. Foraminiferans from the Horquilla Formation at Robledo Mountain. **1,** *Triticites* aff. *T. southensis* Ross and Tyrrell, 1965. Subaxial section. Middle Virgilian. Sample RM unit 119-15. **2,** *Triticites* sp. indet transitional to pseudoschwagerininins. Oblique subaxial section. Middle Virgilian. Sample RM unit 119-17. **3,** *Triticites* cf. *T. plummeri maximus* Kauffmann and Roth, 1966. Axial section. Late Virgilian. Samples ROM 41-1. **4,** Bioclastic grainstone with *Calcivertella* sp. (left; bottom right) and biopisoids with *Ellesmerella* sp. (right). Earliest Wolfcampian (= early Asselian). Sample ROM 42-3. **5,** *Epimastopora* ex gr. *E. japonica* Endo, 1951. Subaxial section. Early Wolfcampian (= early/middle Asselian). Sample ROM 43-4. 6-**7,** *Eugonophyllum* sp. with *Claracrusta* sp. and *Palaeonubecularia* sp. Subaxial section. Middle Virgilian. Samples RM unit 122.2 and unit 122-3. **8,** *Latitubiphytes* sp. Various oblique sections. Middle Virgilian. Sample RM unit 122-1. **9,** *Bradyina* sp. Axial section. Middle Virgilian. Sample RM unit 119-14. **10,** *Epimastopora* ex gr. *E. alpina* (Pia, 1937) Kochansky-Devidé and Herak, 1960. Subaxial section. Late Virgilian. Sample RM unit 136-2. **11,** *Parapimastopora* ex gr. *P. kansasensis* (Johnson, 1946). Subaxial section. Earliest Wolfcampian. Sample ROM 42-1. **12,** *Pseudovidalina modificata* (Potievskaya, 1962). Axial section. Early Wolfcampian. Sample ROM 43-3. **13,** *Pseudovidalina* cf. *P. iranica* Alipour and Vachard in Alipour et al., 2013. Axial section. Early Wolfcampian. Sample ROM 43-6. **14,** *Epimastopora* sp. Subaxial section. Early Wolfcampian. Sample ROM 44-1. Scale bars: 12, 13 = 0.10 mm; 5, 9-11 = 0.50 mm; 1-4, 8, 14 = 1.00 mm; 6, 7 = 2.00 mm

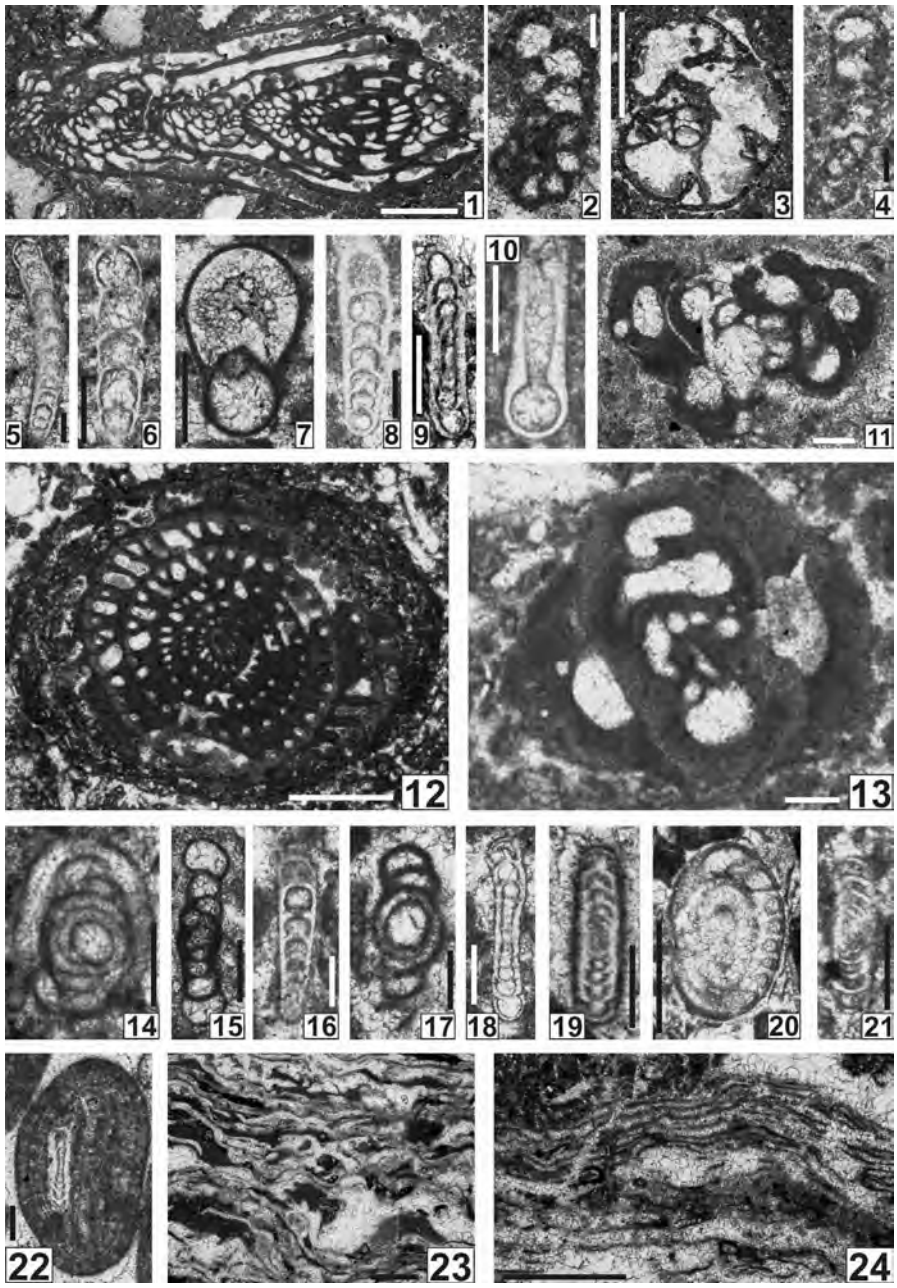


FIGURE 21. Foraminiferans from the Horquilla Formation at Robledo Mountain. **1,** *Triticites meeki* (Möller, 1879) emend. Thompson, 1954. Subaxial section. Early Wolfcampian. Sample RM unit 149-1. **2, 4,** *Spireitlina* cf. *S. conspecta* (Reilinger, 1950). Transverse and subaxial sections. Early Wolfcampian. Samples RM unit 149A-1 and unit 149A-2. **3,** *Bradyina* cf. *B.lucida* Morozova, 1949. Subtransverse section. Early Wolfcampian. Sample RM unit 149A-6. **5,** *Nodosinelloides longissima* (Suleimanov, 1945). Subaxial section. Robledo Mountain. Early Wolfcampian. Sample ROM 45-4. **6,** *Nodosinelloides pinardae* Groves and Wahlman, 1997. Subaxial section. Robledo Mountains. Early Wolfcampian. Sample ROM 45-6. **7,** *Tuberitina bulbacea* Galloway and Harlton, 1928. Axial section. Robledo Mountains. Early Wolfcampian Sample ROM 45-7. **8,** *Nodosinelloides netschajewi* (Chernysheva, 1941). Subaxial section. Robledo Mountains. Early Wolfcampian. Sample ROM 45-11. **9,** *Pseudovidalina modificata* (Potievskaya, 1962). Subaxial section. Robledo Mountains. Early Wolfcampian. Sample ROM 45-13. **10,** *Syzraniabella* Reitlinger, 1950. Axial section. Robledo Mountains. Early Wolfcampian. Sample ROM 46-5. **11,** *Latitubiphytes* sp. 1. Transverse sections. Robledo Mountains. Early Wolfcampian. Sample RM unit 149-8. **12,** *Triticites* cf. *T. pinguis* Dunbar and Skinner, 1937. Subtransverse section. Robledo Mountains. Early Wolcampian. Late Virgilian. Samples ROM 45-15. **13,** *Latitubiphytes* sp. 2. Transverse sections. Robledo Mountains. Early Wolfcampian. Sample ROM 46-7. **14?,** *Hemigordius* cf. *H. schlumbergeri* (Howchin, 1895). See also *Hemigordiellinapseudopusilla* (Baryshnikov in Zolotova and Baryshnikov, 1980). Subtransverse section. Early/middle? Wolfcampian. Sample ROM 47-1b. **15,** *Hemigordius* cf. *H. schlumbergeri* (Howchin, 1895). Subtransverse section. Early/middle? Wolfcampian. Sample ROM 47-4. **16,** *Nodosinelloides longa* (Lipina, 1949). Subaxial section. Robledo Mountains. Early/middle? Wolfcampian. Sample ROM 48-3. **17,** *Hemigordius*? sp. Subtransverse section. Robledo Mountains. Early/middle? Wolfcampian. Sample ROM 48-10. **18,** *Pseudovidalina* cf. *P. helicis* Pinard and Mamet, 1998. Subtransverse section. Robledo Mountains. Middle/late Wolfcampian. Sample ROM 49-1. **19,** *Pseudovidalina* cf. *P. modificata* (Potievskaya, 1962). Axial section. Middle/late Wolfcampian. Sample ROM 52-1. **20,** Staffellid indet. Subtransverse section. Middle/late Wolfcampian. Sample ROM 58-2. **21,** *Pseudovidalina* cf. *P. iranica* Alipour and Vachard in Alipour et al., 2013. Axial section. Early Wolfcampian. Sample ROM 43-5. **22,** *Pseudovidalina modificata* (Potievskaya, 1962). Axial section included in an ooid. Robledo Mountains. Middle/late Wolfcampian. Sample ROM 52-5. **23-24,** *Archaeolithophyllum lamellosum* Wray, 1964. Axial sections. Middle/late Wolfcampian. Samples RM unit 187-1 and ROM 55-1. Scale bars: 2, 4-11, 13, 14-19, 21, 22 = 0.10 mm; 20 = 0.50 mm; 1, 3, 12, 23, 24 = 1.00 mm.

23.13), tuberitinids (Fig. 23.2, 5, 11), *Tetrataxis* sp. (Fig. 23.9), *Hemigordiellina* sp. (Fig. 23.7), *Palaeonubecularia* sp. (Fig. 22.19), *Syzrania* sp. (Fig. 22.18), *Geinitzina* sp. 1 (Fig. 22.16-17), and *G*. sp. 2 (Fig. 23.6).

Conodonts

A series of 12 small (about 1.5 to 2 kg) samples from the Robledo Mountain section produced limited biostratigraphic information. The conodont faunas (Figs. 24-25) tend to be heavily fragmented, with fresh-appearing fracture surfaces. Perhaps, they were fractured by tectonic activity and subsequent processing separated most elements into fragments. The conodonts are mostly dark gray in color, approximately CAI 6 (gray).

Conodont faunas from the lower 10 m of the section (units 2 and 8) are small, consisting of only a few elements of *Hindeodus*, *Adetognathus*, and *Idiognathodus* P_1 elements similar to *I. klapperi* Lane and Straka (Fig. 24.20) and *I. sinuosus* Ellison and Graves. Three large fragments of Late Devonian (*Palmatolepis* sp.) and Early Mississippian (*Siphonodella*) conodonts were recovered from unit 8, reworked from older strata. A larger, more diverse fauna occurs in unit 14, at 15 m. This fauna is strongly dominated by *I. klapperi* (Fig. 24.14, 18, 19, 21) and advanced *I. sinuosus* morphotypes (Fig. 24.15, 22). A small number of *Declinognathodus marginodosus* Grayson (Fig. 24.11, 13, 16) and *Idiognathoides sinuatus* (Harris and Hollingsworth) (Fig. 24.12) elements were recovered. The presence of *I. klapperi* morphotypes in association with *D. marginodosus* indicates a latest Morrowan to early Atokan (late Bashkirian) age (Barrick et al., 2013).

In unit 21, at 22 m, larger, more complex forms of *Idiognathodus* appear that possess large caudal and rostral lobes and a distinct curvature. These are questionably referred to *I. incurvus* Dunn (Fig. 24.9, 10, 17). A few representatives of the *Neognathodus atokaensis* Grayson group are present; they show a range of development of the rostral dorsal platform margin (Fig. 24.1-3). A few *Hindeodus* and a single *Diplognathodus*, *D. orphanus?*, are also present. The *N. atokaensis* morphotypes and *I. incurvus?* suggest a middle Atokan (early Moscovian) age (Barrick et al., 2013).

Small, early Desmoinesian (Moscovian) conodont faunas occur from approximately 30 to 45 m in the section (units 29, 34, and 39). Early Desmoinesian conodonts are not well known, and species assignments are difficult to make for the small number of mostly broken specimens. Elements of *Adetognathus* are most common. The most distinctive elements are those of the few *Neognathodus* specimens. Examples of the *N. asymmetricus* Stibane group (e.g., *N. medadultimus* Merrill and *N. medexultimus* Merrill) occur (Fig. 24.8), and in unit 34, possibly *N. intrala* Stamm and Wardlaw (Fig. 24.7), which was described from the Verdigris cyclothem, near the top of the lower Desmoinesian section (Stamm and Wardlaw, 2003). The *Idiognathodus* specimens are early Desmoinesian forms for which species assignments are problematic (Fig. 24.4-6).

A sample taken from unit 78 was barren. The large sample taken from unit 86 to obtain shark's teeth also yielded a number of conodont elements, most of which are fragments of large *Idiognathodus* platforms. The most complete specimens include examples of *I. harkeyi* Gunnell (Fig. 25.7, 13, 14), *I. heckeli* Rosscoe and Barrick (Fig. 25.12), *I. swadei* Rosscoe and Barrick (Fig. 25.15-17), and *I. sulciferus* Gunnell (Fig. 25.8), characteristic early Missourian (early Kasimovian) species. The presence of *I. pseudocarinatus* Rosscoe and Barrick (Fig. 25.10, 11) and *I. cancellosus* (Gunnell) (Fig. 25.9) permits confident assignment of this bed to the *I. cancellosus* Zone, which characterizes the Swope cyclothem (*I. cancellosus* Zone) in the North America Midcontinent region (Rosscoe and Barrick, 2013; Barrick et al., 2013). Samples from unit 133 and unit 144 yielded just a few undiagnostic elements.

At 284 m, unit 191 produced a small, but diagnostic latest Pennsylvanian conodont fauna. The association of *Streptognathodus conjunctus* Barskov, Isakova, and Shchastlivceva (Fig. 25.1, 2) with *S. binodosus* Wardlaw, Boardman, and Nestell (Fig. 25.4-6), is diagnostic of the *S. binodosus* Zone, which is restricted to the Upper Hughes Creek Fifth-Order Sequence (upper Foraker Limestone), the highest early Wolfcampian cyclothem in the Midcontinent region (Boardman et al., 2009). *Streptognathodus elongatus* Gunnell (Fig. 25.3) and possibly *S. wabaunsensis* Gunnell are also present. A sample from unit 229 was barren.

Summary

To summarize the biostratigraphic data presented here and in earlier publications, we can assign reasonably precise ages to much of the section at Robledo Mountain, though more data are needed to refine placement of many of the stage boundaries (Fig. 26). Thus, the oldest strata of the Horquilla Formation at Robledo Mountain are late Morrowan (definite ages are only possible for units 4-12: Fig. 6). The base of the Atokan is close to unit 14, and units 21-22 are definitely Atokan. The base of the Desmoinesian is ~ unit 26.

The base of the Missourian is less precisely constrained because of a lack of age-significant data from ~ units 40-78. Conodonts from unit 86 are definitely early Missourian, so we place the base of the Missourian tentatively near the base of member C. The base of the Virgilian is better constrained as close to unit 109, and the Wolfcampian base is very close to unit 147. Only the uppermost ~50 m of the section, beginning at ~ unit 232 are of middle Wolfcampian age.

DISCUSSION

Assignment to Horquilla Formation

At Robledo Mountain, most previous workers either made no lithostratigraphic assignment for the Pennsylvanian section or they made a very general assignment, such as to the Magdalena Formation, an obsolete term that basically is synonymous with the Pennsylvanian (Fig. 4). In part, this is likely because these rocks do not closely resemble Pennsylvanian sections nearby, particularly the closest sections in the southern Caballo Mountains and Derry Hills, 40-60 km to the northwest.

The Pennsylvanian section in the Derry Hills and the Caballo and Fra Cristobal Mountains consists, in ascending order, of (1) the Red House Formation, 29-93 m of slope-forming shale, limestone and minor conglomerate and sandstone; (2) the Gray Mesa Formation, 118-210 m of mostly ledge- and cliff-forming cherty limestone; (3) the Bar B Formation, 72-107 m of slope-forming shale and relatively thin limestone; and (4) the Bursum Formation, as much as 107 m of interbedded siliciclastic red beds, limestone and shale (Kelley and Silver, 1952; Seager and Mack, 2003; Lucas et al., 2012a, b). The lower part of the Pennsylvanian section at Robledo Mountain does not resemble the Red House Formation and includes Morrowan strata evidently older than all of the Red House Formation, with the exception of local outcrop in the Derry Hills, where a very thin (< 5 m thick) part of the basal Red House Formation is Morrowan. The upper part of member A of the Robledo Mountain section does contain much cherty limestone, similar to the Gray Mesa Formation to the northwest, but the cherty-limestone interval is much thinner. Cliff-forming cherty limestone, the main characteristic feature of the Gray Mesa Formation, is absent. Members B, C and D at Robledo Mountain bear no close lithologic resemblance to the Bar B Formation. Particularly thick, massive algal limestones present in Member D are absent in the Bar B Formation.

Member E encompasses most of the strata that have been termed Bursum Formation or Bursum-equivalent by some previous workers (see Fig. 4). Based on fusulinid evidence, member E temporally overlaps the Bursum Formation to the north, but it is not lithostratigraphically assignable to the Bursum Formation because it lacks the siliciclastic red beds (mudstones, sandstones) and conglomerates that are characteristic of the Bursum Formation (cf. Lucas and Krainer, 2004; Krainer and Lucas, 2009). The "Bursum age" (early Wolfcampian) interval of the section at Robledo Mountain contains no siliciclastic red beds, as does the Bursum Formation to the north. Therefore, assignment of the Pennsylvanian-Permian section at Robledo Mountain to any formations recognized to the northwest in the Derry Hills and Caballo Mountains cannot be made based on lithologic similarities.

In the San Andres Mountains, ~40-60 km northeast of the Robledo Mountain section, the coeval strata are assigned to the Red House, Gray Mesa, Panther Seep and Hueco formations (e.g., Kottlowski et al., 1956; Lucas et al., 2002; Lucas and Krainer, 2009). The Panther Seep Formation here is up to 450 m of cyclically bedded limestone, sandstone, shale and gypsum, very different from the temporally overlapping members B, C and D at Robledo Mountain. Therefore, use of the lithostratigraphic name Panther Seep Formation at Robledo Mountain cannot be justified. The section at Robledo Mountain differs from that in the southern San Andres Mountains (Bachman and Myers, 1969) or in the northern Organ Mountains (Seager, 1981). In both places, the Pennsylvanian was divided into two formations: Lead Camp Limestone below and Panther Seep Formation above. The Lead Camp itself is divisible into a thinner shaly and sandy lower unit similar to the Red House, and a thicker, upper unit of thick-bedded cherty limestone, similar to the Gray Mesa (Nelson et al., 2013). Again, the Panther Seep is dramatically different from the upper Horquilla.

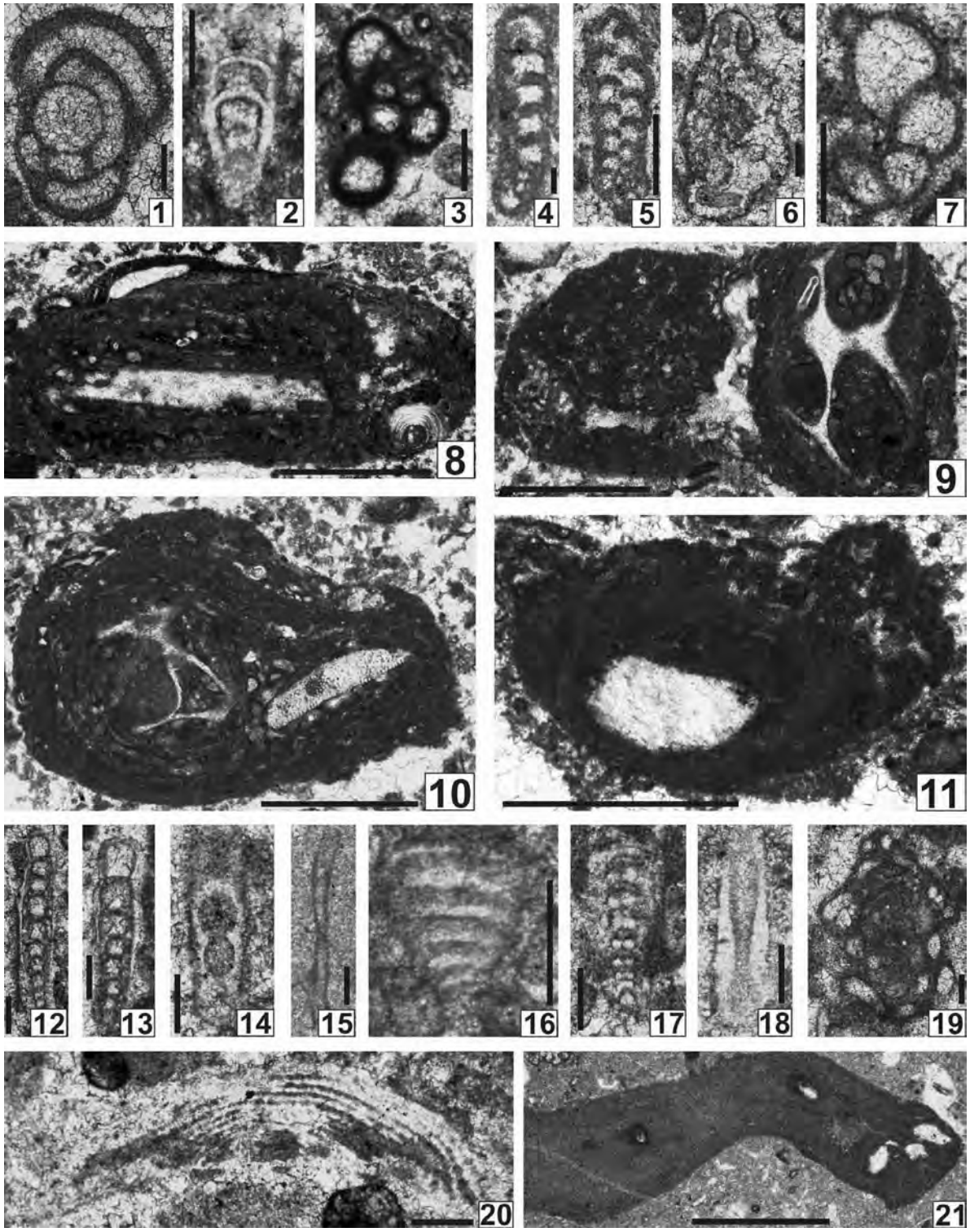


FIGURE 22. Foraminiferans from the Horquilla Formation at Robledo Mountain. **1,** *Calcitornella* sp. Oblique section. Middle Wolfcampian. Sample RM Unit 207-1. **2,** *Nodosinelloides potievskayae* Mamet and Pinard, 1996. Axial section. Middle Wolfcampian. Sample RM Unit 217-4. **3,** *Calcitornella*? sp. Axial section. Middle Wolfcampian. Sample RM Unit 217-6. **4-5,** *Spireitlina conspecta* Reitlinger, 1950. Oblique and transverse sections. Middle Wolfcampian. Sample RM Unit 217-6a and 234-6. **6,** *Hedraites plummerae* Henbest, 1963. Axial section. Middle Wolfcampian. Sample RM Unit 234-8. **7,** *Globivalvulina* sp. Subtransverse section. Middle Wolfcampian. Sample RM Unit 234-15. **8, 10,** Oncoids with *Ellesmerella* and cyanobacteria. Two longitudinal sections. Middle Wolfcampian. Sample RM Unit 217-3 and 217-5. **9, 11,** Oncoids with *Girvanella* and cyanobacteria. Two longitudinal sections. Middle Wolfcampian. Sample RM Unit 217-5 and 217-7. **12, 13,** *Protonodosaria* sp. 1. Two axial sections. Middle Wolfcampian. Sample RM Unit 234-2 and 234-1. **14,** *Protonodosaria* sp. 2. Subaxial section. Middle Wolfcampian. Sample RM Unit 234-5. **15,** *Koivaella permica* Chuvashov, 1974. Axial section. Middle/late Wolfcampian. Sample RM Unit 244-10. **16, 17?,** *Geinitzina* sp. 1. Subaxial and oblique sections. Middle/late Wolfcampian. Sample RM Unit 256-2 and 256-3. **18,** *Syzrania* sp. Axial section. Middle/late Wolfcampian. Sample RM Unit 256A-1. **19,** *Palaeonubecularia* sp. Subaxial section. Middle/late Wolfcampian. Sample RM Unit 256A-2. **20,** *Efluegelia johnsonii* (Flügel, 1966).Axial section. Middle Wolfcampian. Sample RM Unit 234-4. **21,** *Tubiphytes obscurus* Maslov, 1956. Subaxial section. Middle/late Wolfcampian. Sample RM Unit 244-3. Scales: figs. 1-7, 12-20: 0.1 mm; figs. 8-11, 21: 1 mm.

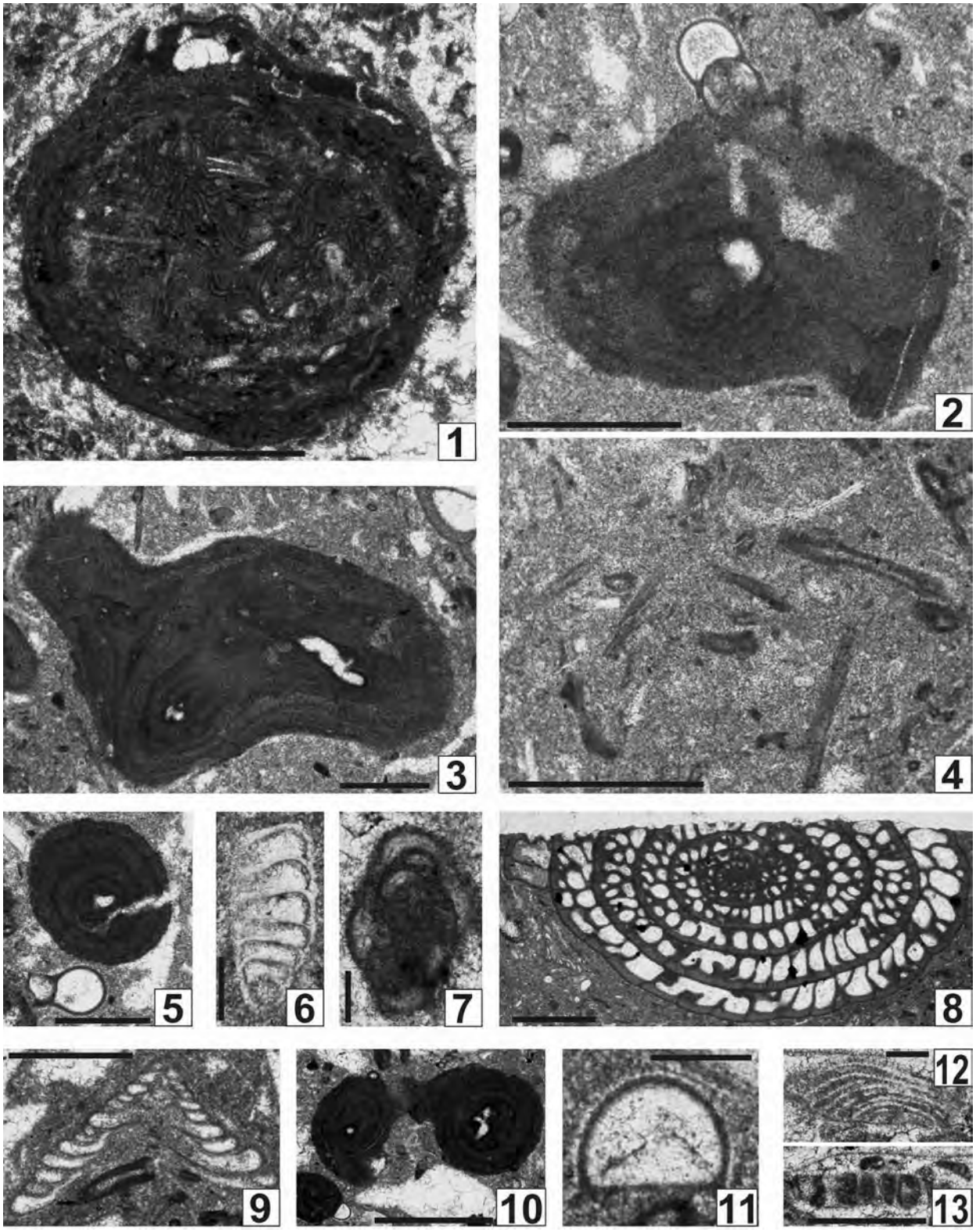


FIGURE 23. Foraminiferans from the Shalem Colony Formation at Robledo Mountain.**1,** Oncoid with *Girvanella* and cyanobacteria. Longitudinal section. Middle Wolfcampian. Sample RM Unit 217-9. **2, 3, 5, 10,** *Tubiphytes obscurus* Maslov, 1956. Various sections. Middle/late Wolfcampian. Samples RM Unit 244-3, 244-11, 244-12, 244-19, respectively. **2, 5, 11,** *Tuberitina* spp. Axial sections. Middle/late Wolfcampian. Samples RM Unit 244-3, 244-11, 244-1, respectively. **4,** *Koivaella permica* Chuvashov, 1974. Axial and obliquesections. Middle/late Wolfcampian. Sample RM Unit 244-6. **6,** *Geinitzina* sp. 2. Oblique axial sections. Middle/late Wolfcampian. Sample RM Unit 244-17. **7,** *Hemigordiellina* sp. section. Middle/late Wolfcampian. Sample RM Unit 256A-5. **8,** *Pseudofusulina*?sp. Oblique section. Middle/late Wolfcampian. Sample RM Unit 244-9. **9,** *Tetrataxis* sp. Axial section. Middle/late Wolfcampian. Sample RM Unit 244-13. **12,** *Efluegelia johnsonii* (Flügel, 1966).Axial section. Middle Wolfcampian. Sample RM Unit 236A-3. **13,** *Epimastopora* sp. Axial section. Middle/late Wolfcampian. Sample RM Unit 244-3. Fig. 6, 7, 11, 12: 0.1 mm. Scales: figs. 1-5, 9, 13: 0.5 mm; figs. 8, 10: 1 mm.

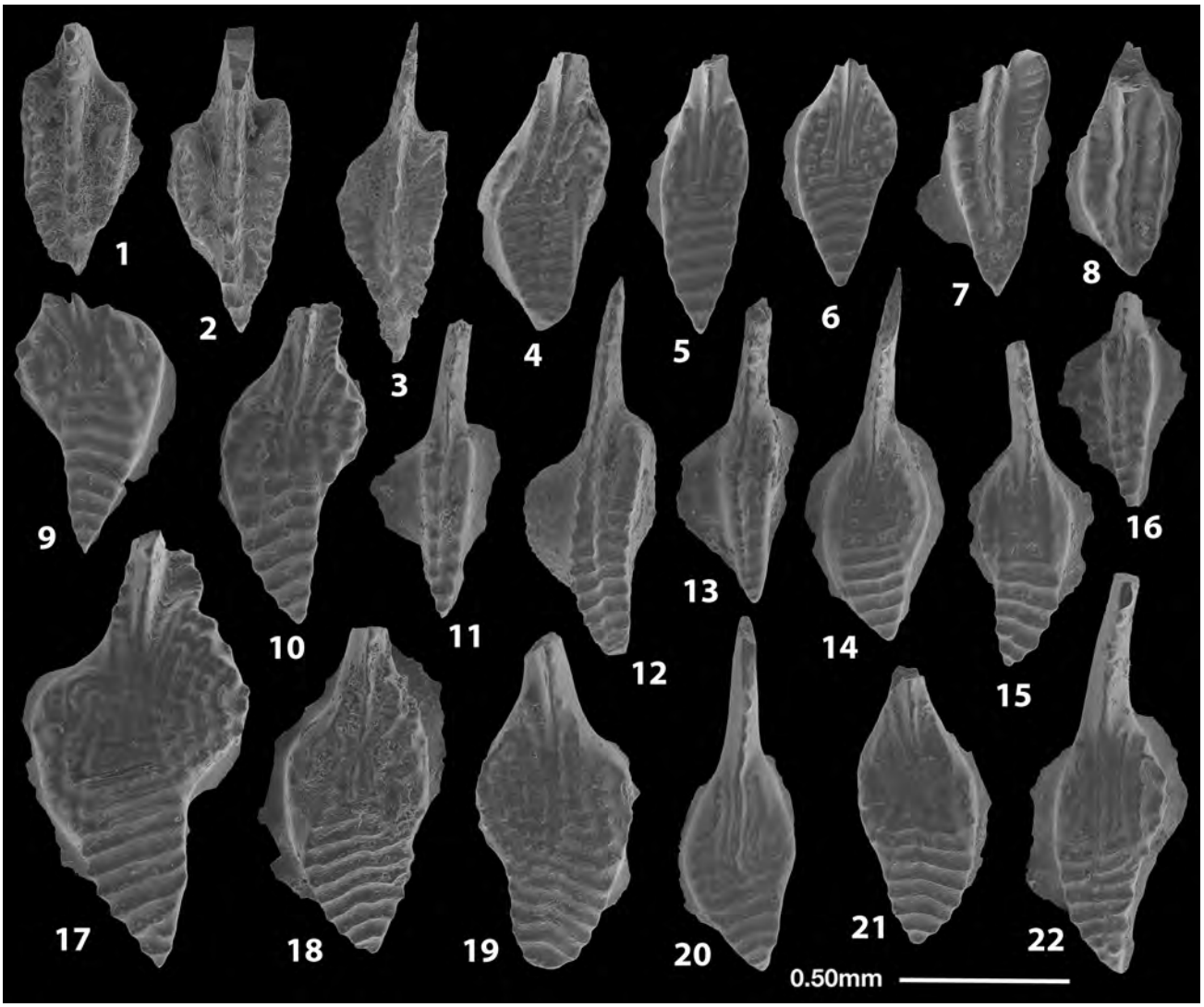


FIGURE 24. Conodonts from the Horquilla Formation at Robledo Mountain. All approximately 50X. **1-3,** *Neognathodus atokaensis* Grayson group, unit 21. **4-6,** *Idiognathodus* spp., **4,** unit 29. **5, 6,** unit 39. **7,** *Neognathodus intrala* Stamm and Wardlaw?, unit 34. **8,** *Neognathodus asymmetricus* Stibane group, unit 39. **9, 10, 17.** *Idiognathodus incurvus* Dunn?, unit 21. **11, 13, 16,** *Declinognathodus marginodosus* Grayson, unit 14. **12,** *Idiognathoides sinuatus* (Harris and Hollingsworth), unit 14. **14, 18-21,** *Idiognathodus klapperi* Lane and Straka. **14, 18, 19 21,** unit 14; **20,** unit 8. **15, 22,** *Idiognathodus sinuosus* Ellison and Graves, advanced morphotype, unit 14.

In contrast, in the Big Hatchet Mountains, ~ 160 km to the southwest of Robledo Mountain, the Pennsylvanian-Permian Horquilla Formation bears a striking resemblance to the Pennsylvanian-Permian section at Robledo Mountain. The Horquilla Formation is approximately 1050 m thick (including the Wolfcampian part, which measures about 200 m: Zeller, 1965; Wilde, 2006; Krainer and Lucas, 2007; Lucas et al., 2007) and is thus much thicker than the Horquilla Formation at Robledo Mountain (300 m). Nevertheless, the limestone facies (microfacies, biota) are similar (see Zeller 1965; Thompson and Jacka 1981; unpubl. data). Also, in the Big Hatchet Mountains, chert is common in the lower part of the Horquilla Formation, whereas indistinctly bedded to massive algal limestone is common in the upper part. High-frequency cycles are also well developed, particularly in the upper part. Therefore, lithologic similarity, similarity of stratigraphic architecture and overlapping ages justify assigning most of the Robledo Mountain section to the Horquilla Formation (Fig. 6).

It is also important to note that Pennsylvanian sections to the south-southeast of the Robledo Mountain section, at Bishop's Cap in southern Doña Ana County and at Vinton Canyon in the Franklin Mountains near El Paso, Texas, are much more similar to the section at Robledo Mountain than to sections to the north, in the Derry Hills, Caballo Mountains or San Andres Mountains (cf. Kottlowski, 1960a, b). This suggests continuity of deposition not only from the Robledo Mountains to the south-southeast, but also across southernmost New Mexico-northernmost Chihuahua, Mexico, from the Pedregosa basin to the southern Orogrande basin (see below).

Depositional Sequences and Cycle Stratigraphy

Pennsylvanian sediments in southern New Mexico (Orogrande and Pedregosa basins) were deposited during a time of major tectonic activity (Ancestral Rocky Mountains orogeny: ARM) and extensive glaciation in the southern hemisphere that caused substantial glacio-eustatic sea-level changes. High-frequency cycles related to glacio-eustatic sea-level fluctuations have been reported from the Pennsylvanian of central (Scott and Elrick, 2004; Elrick and Scott 2010) and southern New Mexico (e.g., Algeo et al., 1991; Raatz et al., 1994; Soreghan, 1994a, b) and southeastern Arizona (Conolly and Stanton, 1992) as well as by a multitude of authors in the U.S. Midcontinent and Illinois basins.

Working primarily in southern New Mexico, Soreghan (1994a) reported 9 cycles from the Missourian (Kasimovian) and 15 cycles from the Virgilian (Gzhelian). Cycles are also well developed within the Horquilla Formation of Robledo Mountain, particularly in the upper part of member A, in members C, D and E, and less well developed in the lower part of member A and in member B (Fig. 26). Cycle thickness is mostly in the range of 2–7 m, and, rarely, thicker cycles are developed. Cycle boundaries are drawn at exposure surfaces on cycle tops, represented by rhizoliths, rarely by thin calcrete crusts, laminated microbialite crusts, microkarst features and thin brecciated layers.

A critical point is the interpretation of covered intervals and shale intervals, which we interpret as offshore shales. Some of the limestone

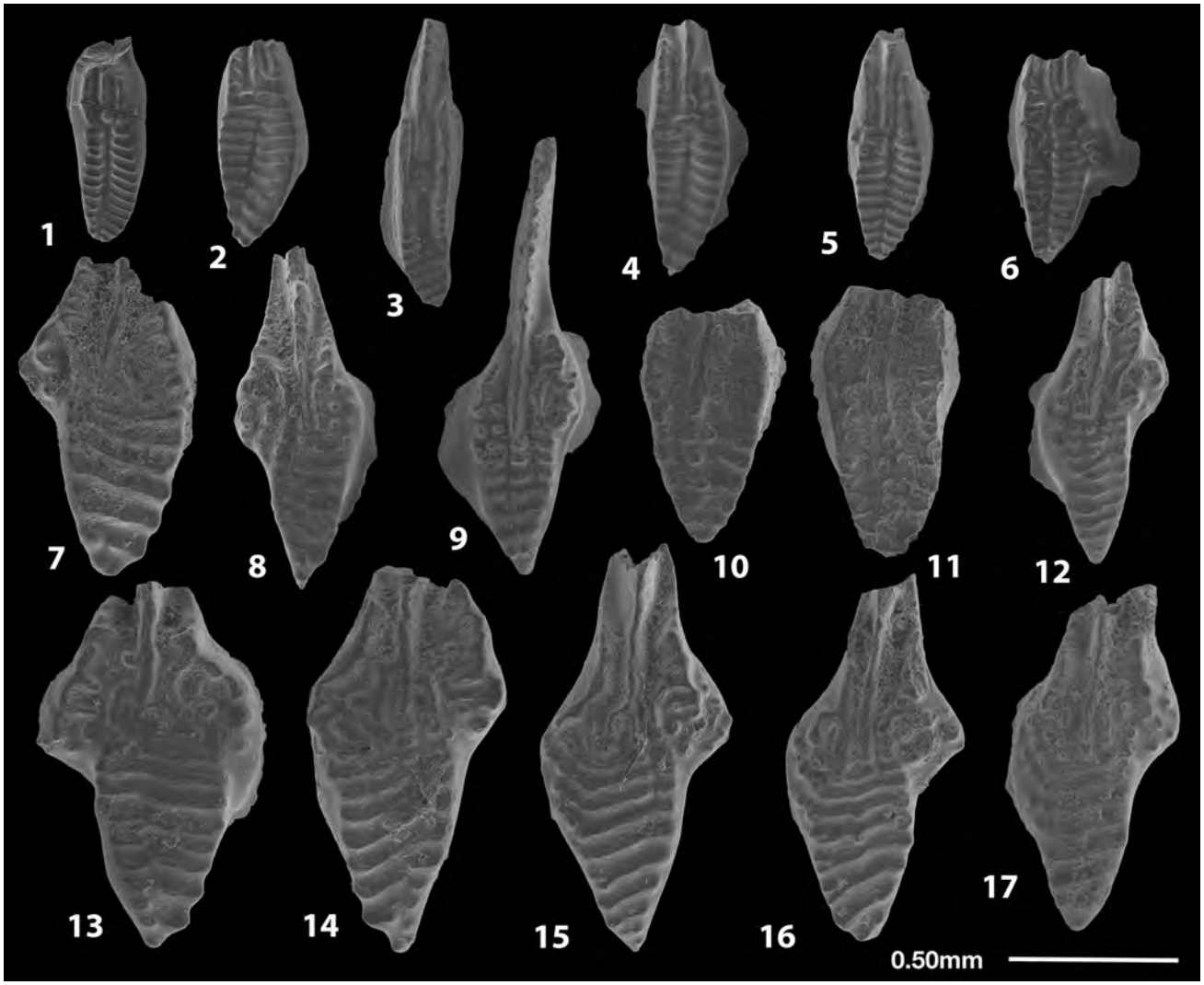


FIGURE 25. Conodonts from the Horquilla Formation at Robledo Mountain. All approximately 50X. **1, 2,** *Streptognathodus conjunctus* Barskov, Isakova, and Shchastlivceva, unit 191. **3,** *Streptognathodus elongatus* Gunnell, unit 191. **4-6,** *Streptognathodus binodosus* Wardlaw, Boardman, and Nestell, unit 191. **7, 13, 14,** *Idiognathodus harkeyi* Gunnell, unit 86. **8,** *Idiognathodus sulciferus* Gunnell, unit 86. **9,** *Idiognathodus cancellosus* (Gunnell), unit 86. **10, 11,** *Idiognathodus pseudocarinatus* Rosscoe and Barrick, unit 86. **12,** *Idiognathodus heckeli* Rosscoe and Barrick, unit 86. **15-17,** *Idiognathodus swadei* Rosscoe and Barrick, unit 86.

units display a clear shallowing upward trend that is expressed by bedding and microfacies: thin, wavy to nodular bedded limestone grades into indistinctly thick bedded and massive limestone. The microfacies changes from mudstone/wackestone into wackestone/floatstone and packstone/rudstone/grainstone near the top. Locally, laminated microbialite (stromatolite) is developed on top of the cycles. However, some of the cycles do not reflect a clear shallowing upward trend.

Similar shallowing upward cycles (parasequences) were reported by Soreghan (1994a). The number of cycles recognized by us at Robledo Mountain is also similar to that reported by Soreghan (1994a). Thus, in the Robledo Mountain section we recognize 8 cycles in the Missourian and 15 cycles in the Virgilian.

According to Schmitz and Davydov (2012), the duration of the Missourian is approximately 2.55 Ma (305.75-303.2 Ma) and of the Virgilian 7.6 Ma (303.2-295.6 Ma), which results in a cycle duration of 318 ky for the Missourian and 506 ky for the Virgilian. Soreghan (1994a) estimated a periodicity of 478 ky or 347 ky depending on the duration of the Missourian and Virgilian. In the Desmoinesian part of the section, we recognized 16 cycles, which, based on the duration of the Desmoinesian of approximately 6.85 Ma (Schmitz and Davydov 2012) results in a cycle duration of 428 ky. This 400 ky periodicity, which is also recognized in sections of the North American Midcontinent (e.g., Heckel 2003, 2004, 2006), is considered to be typical of orbital eccentricity.

Paleogeography

Recognition of two separate late Paleozoic depositional basins in southern New Mexico—Pedregosa and Orogrande—stems from the work of Lloyd Pray and Frank Kottlowski in the 1950s. The currently understood late Paleozoic paleogeography (e.g., Kues and Giles, 2004) identifies the site of deposition of the Pennsylvanian-Permian Robledo Mountain section as the western edge of the Orogrande basin, usually referred to as the Robledo shelf or platform. The boundary (or divide) between the Orogrande basin and the Pedregosa basin to the southwest is just west of the Robledo shelf and is generally called the Florida uplift (Fig. 27).

Identification of the Horquilla Formation at Robledo Mountain calls into question just how separate Pennsylvanian-Permian deposition was between the Pedregosa basin and the Robledo shelf. Indeed, early work by Kottlowski (1960b, 1963) identified an area lacking Pennsylvanian strata in the Florida Mountains, that he referred to as the "Florida islands." Other nearby areas lacking Pennsylvanian strata extend from Deming through Silver City in New Mexico, and northwest of Ciudad Juarez in Chihuahua, Mexico (Greenwood et al., 1977). These zero isopach areas of the Pennsylvanian define a southeast-northwest trending divided between the Pedregosa and Orogrande basins. However, they do not define a continuous highland separating the two basins, as has been published by some later workers (e.g., Wilson and Jordan, 1978; Kues and Giles, 2004).

Instead, we believe a marine strait between the Florida and

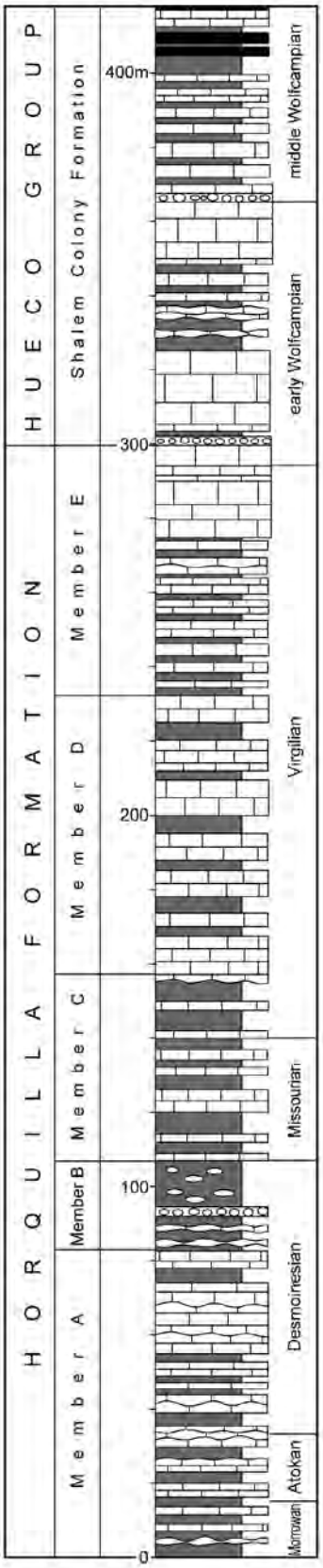


FIGURE 26. Generalized lithostratigraphy and age assignments for Pennsylvanian-Permian section at Robledo Mountain.

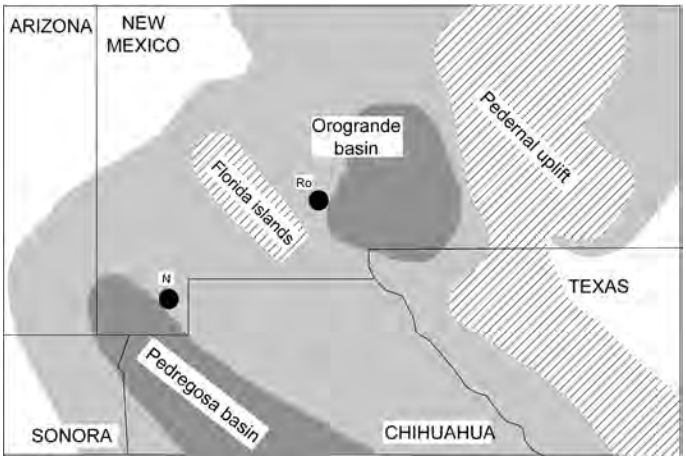


FIGURE 27. Pennsylvanian paleogeography of the divide between the Orogrande and Pedregosa basins during the Pennsylvanian, showing relatively small area of islands and straits dividing the Pedregosa and Orogrande basins. N = Newwell Peak, Big Hatchet Mountains; Ro = Robledo Mountain.

Deming uplifts connected the Pedregosa and Orogrande basins. This strait existed throughout most or all of the Pennsylvanian and into the early Wolfcampian. By middle Wolfcampian time, the Hueco seaway had spread to inundate the Florida uplift, so that there was no separation of deposition in the Pedregosa and Orogrande basins.

ACKNOWLEDGMENTS

We are grateful to John Nelson, Justin Spielmann and Sebastian Voigt for assistance in the field. We thank Julia Wallraf (Innsbruck) for the preparation of numerous thin sections. We thank Pedro Cózar and John Nelson, who reviewed the manuscript and provided helpful comments and suggestions that improved the manuscript.

REFERENCES

Algeo, T.J., Wilson, J. L. and Lohmann, K.C., 1991, Eustatic and tectonic controls on cyclic sediment accumulation patterns in Lower-Middle Pennsylvanian strata of the Orogrande basin, New Mexico: New Mexico Geological Society, Guidebook 42, p. 203-212.

Alipour, Z., Hosseini-Nezhad S. M., Vachard D. and Rashidi, K., 2013, Biostratigraphy and description of smaller foraminifers of Dorud Group (uppermost Gzhelian-lower Sakmarian) in Tang-e Shamshirbor section Eastern Alborz, Iran: Geological Journal, v. 48, p. 385-402.

Bachman, G. O. and Myers, D. A., 1969, Geology of the Bear Peak area, Doña Ana County, New Mexico: U. S. Geological Survey, Bulletin 1271-C, 46 p.

Barrick, J.E., Lambert, L.L., Heckel, P.H., Rosscoe, S.J. and Boardman, D.R., 2013, Midcontinent Pennsylvanian conodont zonation: Stratigraphy,v. 10, p. 55-72.

Bilelo, M. M., 1969, Fusulinidae of the Winchell Formation (Pennsylvanian), north-central Idaho: Journal of Paleontology, v. 43, p. 688-704.

Boardman, D.R., Wardlaw, B.R. and Nestell, M.K., 2009, Stratigraphy and conodont biostratigraphy of the uppermost Carboniferous and Lower Permian from the North American Midcontinent: Kansas Geological Survey, Bulletin 255, p. 1-42 and cd-rom.

Brady, H. B., 1876, A monograph of Carboniferous and Permian Foraminifera (the genus *Fusulina* excepted): Palaeontographical Society of London, no. 30, p. 1-166.

Brazhnikova, N.E. and Yartseva, M.V., 1956, K voprosu ob evolyutsii roda *Monotaxis* [On the question of the evolution of the genus *Monotaxis*]: Voprosy Mikropaleontologii, v. 1, p. 62-71 [in Russian; French translation, BRGM, n°1752, p. 1-13].

Cherdyntsev, W., 1914, K faune foraminifer Permskikh otlozhenii vostochnoi polosy Evropeiskoi Rossii [The fauna of foraminifera of Permian deposits of the eastern belt of European Russia]: Trudy Obsbchestva Estestvoispytateley pri Imperatorskomy Kazanskomy Universitet, v. 46, p. 3-88 [in Russian].

Chernysheva, N.E., 1941, A new genus of foraminifera from the Tournesian deposits of the Urals : Acad. Sci. U.R.R.S., Comptes Rendus (Doklady), Moscov, n.s., vol. 32, no. 1, p. 69.

Chuvashov, B. I.,1974, Permskie izvestkovye vodorosli Urala (Permian calcareous algae from Urals); *in* Papulov, G.N., Chuvashov, B. I., eds., Vodorosli, brakhiopodi i miospory iz permskikh otlozhenii zapadnogo Urala (Algae, brachiopods and miospores from the Permian deposits of western Urals): Akademiya Nauk SSSR, Uralskii Nautchnyi Tsentr, Trudy Instituta Géologii i Geokhimii,v. 109, p. 1-76. [in Russian]

Conolly, W.M. and Stanton, R.J., 1992, Interbasinal cyclostratigraphic correlation of Milankovitch band transgressive-regressive cycles: Correlation of

Desmoinesian-Missourian strata between southeastern Arizona and the midcontinent of North America: Geology, v. 20, p. 999-1002.
Darton, N.H., 1928, "Red beds" and associated formations in New Mexico with an outline of the geology of the state: U.S. Geological Survey, Bulletin 794, 356 p.
Dunbar, C.O. and Condra, G.E., 1927, The Fusulinidae of the Pennsylvanian System in Nebraska: Nebraska Geological Survey,2nd series, Bulletin 2, p. 1-135.
Dunbar, C.O. and Skinner, J.W., 1937, The geology of Texas. Vol. III. Pt. 2. Permian Fusulinidae of Texas: The University of Texas, Bulletin3701, p. 517-825.
Dunham, K. C., 1935, The geology of the Organ Mountains with an account of Doña Ana County, New Mexico: New Mexico Bureau of Mines and Mineral Resources, Bulletin 11, 272 p.
Elrick, M. and Scott, L.A., 2010, Carbon and oxygen isotope evidence for high-frequency (104-105 yr) and my-scale glacio-eustasy in Middle Pennsylvanian cyclic carbonates (Gray Mesa Formation), central New Mexico: Palaeogeography, Palaeoclimatology, Palaeoecology, v. 285, p. 307-320.
Endo, R., 1951, Stratigraphical and paleontological studies of the Later Paleozoic calcareous algae in Japan, I. Several new species from the Sakamotozawa section, Hikoroichi-mura, Kesen-gun, in the Kitakami Mountainous Land: Transactions and Proceedings of the Paleontological Society of Japan,new series, v. 4, p. 121-129.
Endo, R., 1954, Stratigraphical and paleontological studies of the later Paleozoic calcareous algae in Japan; IX. Interesting species from the Yayamadake Limestone Subgroup, Kyushu and new species from Sakato-mura, Taga-gun, Ibaraki-ken: The Science Reports of the Saitama University,series B, v. 1, p. 217-221.
Flügel, E., 1966, Algen aus dem Perm der Karnischen Alpen: Carinthia II,Sonderheft 25, p. 3-76.
Flügel, E., 2004, Microfacies of Carbonate Rocks. Analysis, Interpretation and Application. Springer, Berlin, 976 p.
Galloway, J. J. and Harlton, B. H., 1928, Some Pennsylvanian Foraminifera of Oklahoma with special reference to the genus *Orobias*: Journal of Paleontology, v. 2, p. 338-357.
Galloway, J. J. and Ryniker, C., 1930, Foraminifera from the Atoka Formation of Oklahoma: Oklahoma Geological Survey, Circular21, p. 1-36.
Greenwood, E., Kottlowski, F. E. and Thompson, S. III, 1977, Petroleum potential and stratigraphy of Pedregosa basin: Comparison with Permian and Orogrande basins: American Association of Petroleum Geologists Bulletin, v. 61, p. 1448-1469.
Groves, J. R., 1983, Calcareous foraminifers and algae from the type Morrowan (Lower Pennsylvanian) region of northeastern Oklahoma and northwestern Arkansas: Oklahoma Geological Survey, Bulletin 133, p. 1-39.
Groves, J.R., 1984, Foraminifers and biostratigraphy of the Arco Hills, Bluebird Mountain, and lower Snaky Canyon formations (mid-Carboniferous) of east-central Idaho: Journal of Foraminiferal Research, v. 14, p. 282-302.
Groves, J. R., 1992, Stratigraphic distribution of non-fusulinacean foraminifers in the Marble Falls Limestone (Lower-Middle Pennsylvanian), western Llano region, central Texas: Oklahoma Geological Survey, Circular 94, p. 145-161.
Groves, J.R. and Wahlman, G.P., 1997, Biostratigraphy and evolution of late Carboniferous and early Permian smaller foraminifers from the Barents Sea (offshore Arctic Norway): Journal of Paleontology, v. 71, p. 758-779.
Hawley, J. W., Seager, W. R. and Clemons, R. E., 1975, Third day road log from Las Cruces to north Mesilla Valley, Cedar Hills, San Diego Mountain, and Rincon area: New Mexico Geological Society, Guidebook 26, p. 35-53.
Heckel, P.H., 2003, Updated cyclothem constraints on radiometric dating of the Pennsylvanian succession in North America and its correlation with dates from Europe: Newsletter on Carboniferous Stratigraphy, vol. 21, p. 12-20.
Heckel, P.H., 2004, Updated cyclothem grouping chart and observations on the grouping of Pennsylvanian cyclothems in Midcontinent North America: Newsletter on Carboniferous Stratigraphy, vol. 22, p. 18-22.
Heckel, P.H., 2006, Latest calibration of Middle to Late Pennsylvanian time scale using succession of Midcontinent cyclothems: Newsletter on Carboniferous Stratigraphy, vol. 24, p. 35-39.
Henbest, L.G., 1928, Fusulinellas from the Stonefort limestone member of the Tidewater formation: Journal of Paleontology, v. 2, p. 70-85.
Henbest, L. G., 1963, Biology, mineralogy, and diagenesis of some typical late Paleozoic sedimentary foraminifera and algal-foraminiferal colonies:Cushman Foundation for Foraminiferal Research, Special Publication 6, p. 1-44.
Howchin, W., 1895, Carboniferous Foraminifera of Western Australia, with descriptions of new species: Transactions and Proceedings of the Royal Societies of South Australia, v. 19, p. 198-200.
Ivanov, A.O. and Lucas, S.G., 2014, Fish assemblage from the Late Pennsylvanian of the Robledo Mountains, New Mexico: Geological Society of America, Abstracts with Programs, v. 46, no. 1, p. 2.
Johnson, H. L., 1946, Lime-secreting algae from the Pennsylvanian and Permian of Kansas: Geological Society of America Bulletin, v. 57, p. 1080-1120.
Jordan, C.F., Jr., and Wilson, J.L., 1971, The Late Paleozoic section of the Franklin Mountains : Field Conference Guidebook, Permian Basin Section, SEPM, p. 77-86.
Kauffman, A.E. and Roth, R.L., 1966, Upper Pennsylvanian and Lower Permian fusulinids from north-central Texas: Cushman Foundation Foraminiferal Research,Special Publication, v. 8, p. 1-49.
Kelley, V.C. and Silver, C., 1952, Geology of the Caballo Mountains: University of New Mexico, Publications in Geology 4, 286 p.
Kireeva, G.D., 1949, Psevdofuzuliny tastubskogo i sterlitamakskogo gorizontov pogrebennykh massivov Bashkirii (Pseudofusulinid from Tastub and Sterlitamak horizons of buried massifs of Bashkiria) :Akademiya Nauk SSSR, Trudy Instituta Geologicheskh Nauk, v. 35, p. 171-191. [in Russian]
Kochansky-Devidé, V. and Herak, M., 1960, On the Carboniferous and Permian Dasycladaceae of Yugoslavia: Geoloski Vjesnik, v. 13 (1959), p. 65-94.
Kottlowski, F. E., 1960a, Reconnaissance geologic map of Las Cruces thirty-minute quadrangle: New Mexico Bureau of Mines and Mineral Resources, Geologic Map 14.
Kottlowski, F.E., 1960b, Summary of Pennsylvanian sections in southwestern New Mexico and southeastern Arizona: New Mexico Bureau of Mines and Mineral Resources, Bulletin 66, 187 p.
Kottlowski, F.E., 1963, Paleozoic and Mesozoic strata of southwestern and central New Mexico: New Mexico Bureau of Mines and Mineral Resources, Bulletin 79: 100 pp.
Kottlowski, F. E., Flower, R. H., Thompson, M. L., and Foster, R. W., 1956, Stratigraphic studies of the San Andres Mountains, New Mexico: New Mexico Bureau of Mines and Mineral Resources, Memoir 1, 132 p.
Krainer, K. and Lucas, S.G., 1995, The limestone facies of the Abo-Hueco transitional zone in the Robledo Mountains, southern New Mexico: New Mexico Museum of Natural History and Science, Bulletin 6, p. 33-38.
Krainer, K. and Lucas, S.G., 2007, Facies of the Horquilla Formation across the Pennsylvanian-Permian boundary at New Well Peak (Big Hatchet Mountains, SW New Mexico, USA). Geo.Alp, v. 4, p. 22.
Krainer, K. and Lucas, S.G., 2009, Cyclic sedimentation of the Upper Pennsylvanian (lower Wolfcampian) Bursum Formation, central New Mexico: Tectonics versus glacioeustasy: New Mexico Geological Society, Guidebook 60, p. 167-182.
Krainer, K., Vachard, D. and Lucas, S. G., 2003, Microfacies and microfossil assemblages (smaller foraminifers, algae, pseudoalgae) of the Hueco Group and Laborcita Formation (Upper Pennsylvanian-Lower Permian), south-central New Mexico, USA: Rivista Italiana di Paleontologia e Stratigrafia, v. 109, p. 3-36.
Krainer, K., Vachard, D. and Lucas, S. G., 2009, Facies, microfossils (smaller foraminifers, calcareous algae) and biostratigraphy of the Hueco Group, Doña Ana Mountains, southern New Mexico, USA: Rivista Italiana di Paleontologia e Stratigrafia, v. 115, p. 3-26.
Kues, B. S. and Giles, K. A., 2004, The late Paleozoic ancestral Rocky Mountains system in New Mexico; *in* Mack, G. H. and Giles, K. A., eds., The geology of New Mexico: A geologic history: New Mexico Geological Society, Special Publication 11 p. 95-136.
Leven, E.Ya., 1970, O proiskhozhdenii vysshikh fuzulinid [On the origin of the advanced fusulinids]: Paleontologicheskiy Zhurnal, v. 1970 (3), p. 18-25 [in Russian; English translation: Paleontological Journal, 1970, 3, p. 303-309].
Lipina, O.A., 1949, Melkie foraminifery pogrebennykh massivov Bashkirii [Smaller foraminifers from the buried massifs of Bashkiria]: Akademiya Nauk SSSR, Trudy Instituta Geologicheskikh Nauk, v. 105, geologicheskaya seriya, v. 35, p. 198-235 [in Russian; French translation BRGM, n° 791].
Lucas, S. G. and Krainer, K., 2004, The Red Tanks Member of the Bursum Formation in the Lucero uplift and regional stratigraphy of the Bursum Formation in New Mexico: New Mexico Museum of Natural History and Science, Bulletin 25, p. 43-52.
Lucas, S. G. and Krainer, K., 2009, Pennsylvanian stratigraphy in the northern Oscura Mountains, Socorro County, New Mexico: New Mexico Geological Society, Guidebook 60, p. 153-166.
Lucas, S. G. and Krainer, K., 2011, Pennsylvanian section in the Robledo Mountains, Doña Ana County, New Mexico and its paleogeographic significance: New Mexico Geology, v. 33, p. 48.
Lucas, S. G., Krainer, K. and Kues, B. S., 2002, Stratigraphy and correlation of the Lower Permian Hueco Group in the southern San Andres Mountains, Doña Ana County, New Mexico: New Mexico Geological Society, Guidebook 53, p. 223-240.
Lucas, S. G., Krainer, K. and Spielmann, J. A., 2012a, Pennsylvanian stratigraphy in the Fra Cristobal and Caballo Mountains, Sierra County, New Mexico: New Mexico Geological Society, Guidebook 63, p. 327-344.
Lucas, S.G., Heckert, A.B., Estep, J.W. and Cook, C.W., 1998, Stratigraphy of the Lower Permian Hueco Group in the Robledo Mountians, Doña Ana County, New Mexico: New Mexico Museum of Natural History and Science, Bulletin 12, p. 43-54.
Lucas, S. G., Anderson, O. J., Heckert, A. B. and Hunt, A. P., 1995, Geology of Early Permian tracksites, Robledo Mountains, south-central New Mexico: New Mexico Museum of Natural History and Science, Bulletin 6, p. 13-32
Lucas, S. G., Krainer, K., Barrick, J. E. and Spielmann, J. A., 2012b, The Pennsylvanian Red House Formation, central Sierra County, New Mexico: New Mexico Geological Society, Guidebook 63, p. 305-326.
Lucas, S. G., Krainer, K., Barrick, J., Ritter, S. and Spielmann, J. A., 2007, The New Well Peak section of the Pennsylvanian-Permian Horquilla Formation, Big Hatchet Mountains, southwestern New Mexico: New Mexico Geology, v. 29, p. 56.

Mack, G. H., 2007, Sequence stratigraphy of the Lower Permian Abo member in the Robledo and Doña Ana Mountains near Las Cruces, New Mexico: New Mexico Geology, v. 29, p. 3-12.

Mack, G. H., Giles, K. A. and Durr, C. W., 2013, Sequence stratigraphy of the lower-middle Hueco transition interval (Lower Permian, Wolfcampian), Robledo Mountains, New Mexico: New Mexico Geology, v. 35, p. 27-37.

Mack, G. H., James, W. C., and Seager, W. C., 1988, Wolfcampian (Early Permian) stratigraphy and depositional environments in the Doña Ana and Robledo Mountains, south-central New Mexico; *in* Robichaud, S. R. and Gallick, C. M., eds., Basin to shelf facies transition of the Wolfcampian stratigraphy of the Orogrande basin: Las Cruces, Permian Basin Section of SEPM Publication 88-28, p. 97-106.

Mamet, B., 1976, An atlas of microfacies in Carboniferous carbonates of the Canadian Cordillera. Geological Survey Canada, v. 255, p.1-131.

Mamet, B. and Pinard, S., 1992, Note sur la taxonomie des petits foraminifères du Paléozoïque supérieur: Bulletin de la Société belge de Géologie, v. 99 (1990), p. 373-398.

Mamet, B. and Pinard, S., 1996, *Nodosinelloidespotievskayae*,nomen novum (foraminifère):Revue de Micropaléontologie,v. 39, p. 223.

Maslov, V. P., 1956, Iskopaemye izvestkovye vodorosli SSSR (Fossil calcareous algae from USSR]: Trudy Instituta Geologichesnikh Nauk SSSR, v. 160, p. 1-301 [in Russian; French translation BRGM. n° 3517].

Meek, F.B. and Hayden, F.V., 1865, Paleontology of the upper Missouri: Smithsonian Contributions to Knowledge, v. 14, p. 1-135.

Möller, V. von, 1879, Die Foraminiferen der russischen Kohlenkalk: Mémoires de l'Académie Impériale des Sciences de St. Petersbourg,7th series, v. 27 (5), p. 1-131.

Morozova, V.G., 1949, Predstaviteli semeytsv Lituolidae i Textulariidae iz verkhnekamennougolnykh i artinski otlozhenii bashkirskogo Priuralya [Members of families Lituolidae and Textulariidae from late Carboniferous and Artinskian from the Bashkir Pre-Urals]: Akademyia Nauk SSSR, Trudy Instituta Geologicheskikh Nauk, v. 105, geologicheskaya seriya, v. 35, p. 244-275 [in Russian; French translation: BRGM, n° 783].

Needham, C. E., 1937, Some New Mexico Fusulinidae: New Mexico School of Mines, Bulletin 14, p. 1-88.

Nelson, W. J., Lucas, S.G., Krainer, K. and Elrick, S., 2013, The Gray Mesa Formation (Middle Pennsylvanian) in New Mexico : New Mexico Museum of Natural History and Science Bulletin, vol. 59, p. 101–122.

Pia, J. von, 1937, Die wichtigsten Kalkalgen des Jungpaläozoikums und ihre geologische Bedeutung: Compte Rendu du 2e Congrès Avancement Etudes de Stratigraphie du Carbonifère, Heerlen, 1935, v. 2, p. 765-856.

Pinard, S. and Mamet, B., 1998, Taxonomie des petits foraminifères du Carbonifère supérieur-Permien inférieur du bassin de Sverdrup, Arctique canadien: Paleontographica Canadiana, v. 15 (1), p. 1-253.

Potievskaya, P.D., 1962, Predstaviteli nekotorykh semeystv melkikh foraminifer iz nizhney permi severozapadnoy okrainy Donbassa [Representatives of certain families of small foraminifers from the Early Permian of the northwestern border of the Donets Basin]: Akademiya Nauk Ukrainskoi SSR, Instituta Geologicheskikh Nauk, Trudy, seriya stratigrafii i paleontologii, v. 44, p. 49-94 (in Russian).

Raatz, W.D., Schutter, S.R. and Wilson, J.L., 1994, Missourian strata of the northern Sacramento Mountains and Orogrande Basin, New Mexico. Permian basin Section-SEPM, 1994 Annual Field Trip Guidebook, Publication 94-35, p. 61-69.

Reitlinger, E. A., 1950, Foraminifery srednekamennougolnykh otlozhenii tsentralnoi chasti Russkoi platformy (isklyuchaya semeistvo Fusulinidae) [Foraminifera from middle Carboniferous deposits of the central part of the Russian Platform (except the family Fusulinidae)]:Trudy Instituta Geologicheskikh Nauk, v.126, geologichevskaya seriya, v. 47, p. 1-126 [in Russian, French translation BRGM n° 1456].

Rigby, J. K., 1958, Two new Upper Paleozoic hydrozoans: Journal of Paleontology, v. 32, p. 583-586.

Ross, C.A., 1965, Late Pennsylvanian Fusulinidae from the Gaptank Formation, West Texas: Journal of Paleontology, v. 39, p. 1175-1176.

Ross, C.A. and Sabins, F.F., 1965, Early and Middle Pennsylvanian fusulinids from southeast Arizona: Journal of Paleontology, v.39, p. 173-209.

Ross, C.A. and Tyrrell, W.W., 1965, Pennsylvanian and Permian fusulinids from the Whetstone Mountains, southeast Arizona: Journal of Paleontology, v. 39, p. 615-635.

Rosscoe, S.J. and Barrick, J.E., 2013, North American species of the conodont genus *Idiognathodus* from the Moscovian-Kasimovian boundary composite sequences and correlartion of the Moscovian-Kasimovian boundary: New Mexico Museum of Natural History and Science, Bulletin 60, p. 354-371.

Say, T., 1823, In: James, E., Account of an Expedition from Pittsburgh to the Rocky Mountains, Carey and Lea, Philadelphia, v. 1, p. 146-152.

Schmitz, M.D. and Davydov, V.I., 2012, Quantitative radiometric and biostratigraphic calibration of the Pennslyvanian-Early Permian (Cisuralian) time scale and pan-Euramerican chronostratigraphic correlation. GSA Bulletin, vol. 124, p. 549-577.

Scott, L.A. and Elrick, M.B., 2004, Cycle and sequence stratigraphy of Middle Pennslyvanian (Desmoinesian) strata of the Lucero Basin, central New Mexico. In : Lucas, S.G and Zeigler, K.E. (eds), Carboniferous-Permian Transition at Carrizo Arroyo, Central New Mexico. New Mexico Museum of Natural History & Science, Bulletin 25, p. 31 – 42.

Seager, W.R., 1981, Geology of Organ Mountains and southern San Andres Mountains, New Mexico: New Mexico Bureau of Mines and Mineral Resources Memoir 36, 97 p.

Seager, W.R., Kottlowski, F.E. and Hawley, J.W., 2008, Geologic map of the Robledo Mountaisn and vicinity, Doña Ana County, New Mexico: New Mexico Bureau of Geology and Mineral Resources, Open-file Report 509, scale 1:24,000.

Seager, W.R., Hawley, J.W., Kottlowski, F.E. and Kelly, S.A., 1987, Geology of east half of Las Cruces and northeast El Paso 1° by 2° sheets: New Mexico Bureau of Mines and Mineral Resources, Geologic Map 57.

Skinner, J.W., 1931, Primitive fusulinids of the Mid-Continent region: Journal of Paleontology, v. 5, p. 253-259.

Soreghan, G.S., 1994a, Stratigraphic response to geologic processes: Late Pennsylvanian eustasy and tectonics in the Pedregosa and Orogrande basins, Ancestral Rocky Mountains: Geological Society of America Bulletin, v. 106, p. 1195-1211.

Soreghan, G.S., 1994b, Upper Pennsylvanian facies and cyclostratigraphy in Rhodes and Hembrillo canyons, San Andres Mountains: Permian basin Section-SEPM, 1994 Annual Field Trip Guidebook, Publication 94-35, p. 71-85

Stamm, R.G. and Wardlaw, B.R., 2003, Conodont faunas of the late Middle Pennsylvanian (Desmoinesian) Lower Kittanning cyclothem, U.S.A. 2003; *in* Cecil, C. B. and Edgar, N. T., eds., Climate Controls on Stratigraphy: SEPM (Society for Sedimentary Geology), Special Publication 77, p. 95-121.

Suleimanov, I. S., 1945, Novye vidy melkikh foraminifer iz Turneyskogo yarusa Ishimbaevskogo Neftenosnogo rayona [New species of smaller foraminifers from the Tournaisian of the petroliferous region of Ishimbayev]: Doklady Akademii Nauk SSSR, v. 48, p. 124-127 [in Russian].

Thompson, M.L.,1936, Pennsylvanian fusulinids from Ohio: Journal of Paleontology, v. 10, p. 673-683.

Thompson, M.L., 1942, New genera of Pennsylvanian fusulinids: American Journal of Science, 5th series, v. 240, p. 403-420.

Thompson, M.L., 1944, Pennsylvanian Morrowan rocks and fusulinids of Kansas: University of Kansas Publications, State Geological Survey, Bulletin 52, Part 7, p. 409-431.

Thompson, M.L., 1945, Pennsylvanian rocks and fusulinids of east Utah and northwest Colorado correlated with Kansas section: Kansas Geological Survey, Bulletin 60, p. 17-84.

Thompson, M.L., 1948, Studies of American fusulinids: University of Kansas, Paleontological Contributions, Protozoa, Article 1, 184 p.

Thompson, M.L., 1954, American Wolfcampian fusulinids: University of Kansas, Paleontological Contributions, Protozoa, Article 5, 226 p.

Thompson, S. III and Jacka, A.D., 1981, Pennsylvanian stratigraphy, petrography, and petroleum geology of Big Hatchet Peak section, Hidalgo County, New Mexico : New Mexico Bureau of Mines & Mineral Resources, Circular 176 : 125p.

Vachard D., Krainer K. and Lucas S. 2013, Pennsylvanian (Late Carboniferous) calcareous microfossils from Cedro Peak (New Mexico, USA); Part 2: Smaller foraminifers and fusulinids. Annales de Paléontologie, v. 99 (1), p. 1-42.

Vachard D., Krainer, K. and Lucas, S.G., 2014, Kungurian (late Early Permian) algae, microproblematica, and smaller foraminifers from the Yeso Group and San Andres Formation (New Mexico; USA): Palaeontologia Electronica (in press).

Voigt, S., Lucas, S. G. and Krainer, K., 2013, Coastal-plain origin of trace-fossil bearing red beds in the Early Permian of southern New Mexico, U. S. A.: Palaeogeography, Palaeoclimatology, Palaeoecology, v. 369, p. 323-334.

Wahlman, G.P. and King, W.E., 2002, Latest Pennsylvanian and earliest Permian fusulinid biostratigraphy, Robledo Mountains and adjacent ranges, south-central New Mexico: New Mexico Bureau of Geology and Mineral Resources, Circular 208, p. 1-26.

Wilde, G. L., 2002, The Newwellian Substage: Rejection of the Bursumian Stage: Permophiles, no. 41, p. 53-62.

Wilde, G.L., 2006, Pennsylvanian-Permian fusulinaceans of the Big Hatchet Mountains, NewMexico: New Mexico Museum Natural History and Science, Bulletin 38, 311 p.

Wilson, J.L. and Jordan, C.F., 1983, Middle Shelf Environments. In : Scholle, P.A., Bebout, D.G. and Moore, C.H. (eds), Carbonate Depositional Environments. American Association of Petroleum Geologists, Memoir 33, p. 298-343, Tulsa.

Wray, J. L., 1964, *Archaeolithophyllum*, an abundant calcareous alga in limestones of the Lansing Group (Pennsylvanian), southeastern Kansas: State Geological Survey of Kansas, v. 170 (1), p. 3-13.

Zeller, R.A., Jr., 1965, Stratigraphy of the Big Hatchet Mountains area, New Mexico: New Mexico Bureau of Mines and Mineral Resources, Memoir 16, 128 p.

Zolotova, V.P. and Baryshnikov, V.V., 1980, Foraminifer kungurskogo yarusa stratotipicheskoi mestnosti [Foraminifer from Kungurian stage stratotype locality]; *in* Rauzer-Chernousova, D.M. and Chuvashov, B.I., eds., Biostratigrafiya Artinskogo i Kungurskogo yarusov Urala [Biostratigraphy of Artinskian and Kungurian stages of Urals]: Akademiya Nauk SSSR, Uralskii Nauchnyi Tsentr, p. 72-109 [in Russian].



Lucas, S. G. and DiMichele, W. A., eds., 2015, Carboniferous-Permian Transition in the Robledo Mountains, Southern New Mexico. New Mexico Museum of Natural History and Science Bulletin 65.

THE LOWER PERMIAN HUECO GROUP, ROBLEDO MOUNTAINS, NEW MEXICO (U.S.A.)

SPENCER G. LUCAS[1], KARL KRAINER[2] AND DANIEL VACHARD[3]

[1]New Mexico Museum of Natural History, 1801 Mountain Road N.W., Albuquerque, New Mexico, 87104, USA; [2]Institute of Geology and Paleontology, University of Innsbruck, Innsbruck, A-6020, Austria; [3]CIRCAS, 1. rue de Tilleul, F-59152, Gruson, France

Abstract—Strata of the Lower Permian Hueco Group exposed in the Robledo Mountains of Doña Ana County, New Mexico, are assigned to the (ascending order) Shalem Colony, Community Pit, Robledo Mountains and Apache Dam formations. The Shalem Colony Formation is about 127-156 m thick and is a relatively thick-bedded and coarse-grained succession of wackestones, grainstones, rudstones and some oolitic limestones intercalated with mostly covered intervals that are shale and/or nodular limestone. It rests with apparent conformity on the Pennsylvanian-Permian Horquilla Formation. The Community Pit Formation, 93-177 m thick, is mostly an interval of shale and siltstone intercalated with relatively thin interbeds of limestone, many of which are lime mudstones and dolomitic mudstones. The formation has a characteristic brownish gray to grayish orange color. The Robledo Mountains Formation is about 90-125 m thick and is mostly drab-colored marine shale and limestone, but is readily identified by its characteristic siliciclastic red beds (mudstone, siltstone and sandstone), which are intercalated with the marine rocks. At least 107 m thick, the Apache Dam Formation is composed mainly of algal limestone and shale/covered intervals. Analyses of microfacies, paleontology and stratigraphic architecture indicate that the Shalem Colony Formation accumulated on a platform interior environment characterized by open, normal marine to less common, restricted marine conditions; the Community Pit Formation formed in a shelf setting exhibiting shallow, low-energy (rarely high-energy) open marine to restricted marine conditions; the Robledo Mountains Formation represents deposition in a restricted to open marine shallow shelf setting where intercalated red beds were deposited on a distal, extensive flood plain (exhibiting crevasse splay deposits, rare channels, and distal sheet flood deposits) during periods of strong siliciclastic influx from uplifts located to the north and northeast; and the Apache Dam Formation was deposited in an open shelf to shelf lagoon environment with normal salinity and open marine circulation. Previously published analyses that posit cycles of deposition in the Community Pit and Robledo Mountains formations driven by glacio-eustasy or another allocyclic process are rejected primarily because they failed to demonstrate any lateral extent to the inferred cycles and are based on insufficiently detailed analyses of microfacies. Different lineages of foraminifers, especially miliolates and nodosariates, are more accurately documented in the regional Lower Permian, especially the group *Calcivertella*, *Hedraites*, *Hedraites*? and *Pseudovermiporella*, and the group *Nodosinelloides*, *Protonodosaria*, true *Nodosaria*, *Geinitzina*, *Pseudolangella*?, *Rectoglandulina*, and *Pachyphloia*?. A first complete biozonation by smaller foraminifers is presented. These new age constraints, primarily from fusulinids and non-fusulinid foraminifers, indicate the Shalem Colony Formation is early-middle Wolfcampian (Asselian), the Community Pit Formation is middle Wolfcampian-early Leonardian (Asselian-early Artinskian), the Robledo Mountains Formation is early Leonardian (middle-late/latest Artinskian) and the Apache Dam Formation is late Leonardian (latest Artinskian/earliest Kungurian). Neither physical nor biostratigraphic evidence was found for any significant gaps in the succession. This means that the Wolfcampian and Leonardian regional stages/superstages are remarkably complete in New Mexico, where the base of the Wolfcampian is at the base of the Shalem Colony Formation, and the base of the Leonardian is within the Hueco-Abo lithosome.

INTRODUCTION

The Hueco Group encompasses Lower Permian marine strata, predominantly limestone, that crop out across parts of West Texas and southern New Mexico. These strata represent marine deposition on extensive carbonate platforms and relatively shallow sea bottoms along part of the Pangean near-equatorial and tropical shoreline during the Wolfcampian-early Leonardian (e.g., Kottlowski, 1963; Jordan, 1975). The Robledo Mountains near Las Cruces in southern New Mexico expose substantial outcrops of the Hueco Group (Fig. 1). As much as 565 m thick, Hueco Group strata in the Robledo Mountains are assigned to four formations. Here, we present new data and a comprehensive review of the lithostratigraphy, microfacies and paleontology of Hueco Group strata in the Robledo Mountains to analyze their depositional systems and correlation.

PREVIOUS STUDIES

Because of their lack of mineral deposits, the Robledo Mountains attracted little notice from pioneer geologists. The earliest definite reference is Darton (1928, p. 326), who mentioned the Robledo Mountains (as "Roblero Mountain"), and believed that most of the limestones in the range belonged to the "Magdalena Group" and therefore are pre-Hueco and of Pennsylvanian age (Fig. 2). Indeed, in far western Texas and in southern New Mexico, Darton (1928, p. 20) only identified Hueco strata in the northern Franklin Mountains (see Lucas et al., 2011a) and in the Sacramento Mountains (see Pray, 1961). Dunham (1935, p. 166-167, 247) also identified most of the Paleozoic limestones exposed in the Robledo Mountains as Magdalena "Series" (Pennsylvanian) and noted that these strata are intertongued with red beds of the Abo "Sandstone."

Richardson (1904) introduced the name "Hueco formation" for largely massive, gray, fossiliferous limestone in the Hueco Mountains east of El Paso in what is now Hudspeth County, Texas. Thompson (1942, pl. 20) first identified the Hueco Limestone in the Robledo Mountains (also see Thompson, 1954, figs. 5, 8). Thompson (1954) documented Lower Permian fusulinids from the lowermost Hueco strata in the Robledo Mountains, including species of *Schwagerina*, *Pseudoschwagerina* and *Dunbarinella* (i.e., currently, *Thompsonites*, *Pseudoschwagerina*, "*Pseudoschwagerina*," and *Leptotriticites*). Regionally, the Hueco Limestone, Formation, or Group is a succession of shallow marine limestone with local interbeds of shale and sandstone. The Hueco was deposited on a broad shelf north and west of the Delaware Basin, largely during Wolfcampian time. As Thompson (1942, pl. 2) illustrated, limestone of the Hueco intertongues northward on a large scale with red, nonmarine mudstone and sandstone of the Abo Formation.

Kottlowski (1960a), in his geologic map of the Las Cruces quadrangle, mapped all of the Paleozoic strata in the Robledo Mountains, south of Robledo Mountain, as Hueco Formation. He indicated a total Hueco thickness in the Robledo Mountains of 523 m, including in the upper half of the Hueco an "Abo tongue" or "Abo clastic tongue" (Fig. 2). Kottlowski (1960b, fig. 31; 1963; Kottlowski et al., 1975) also used this stratigraphy.

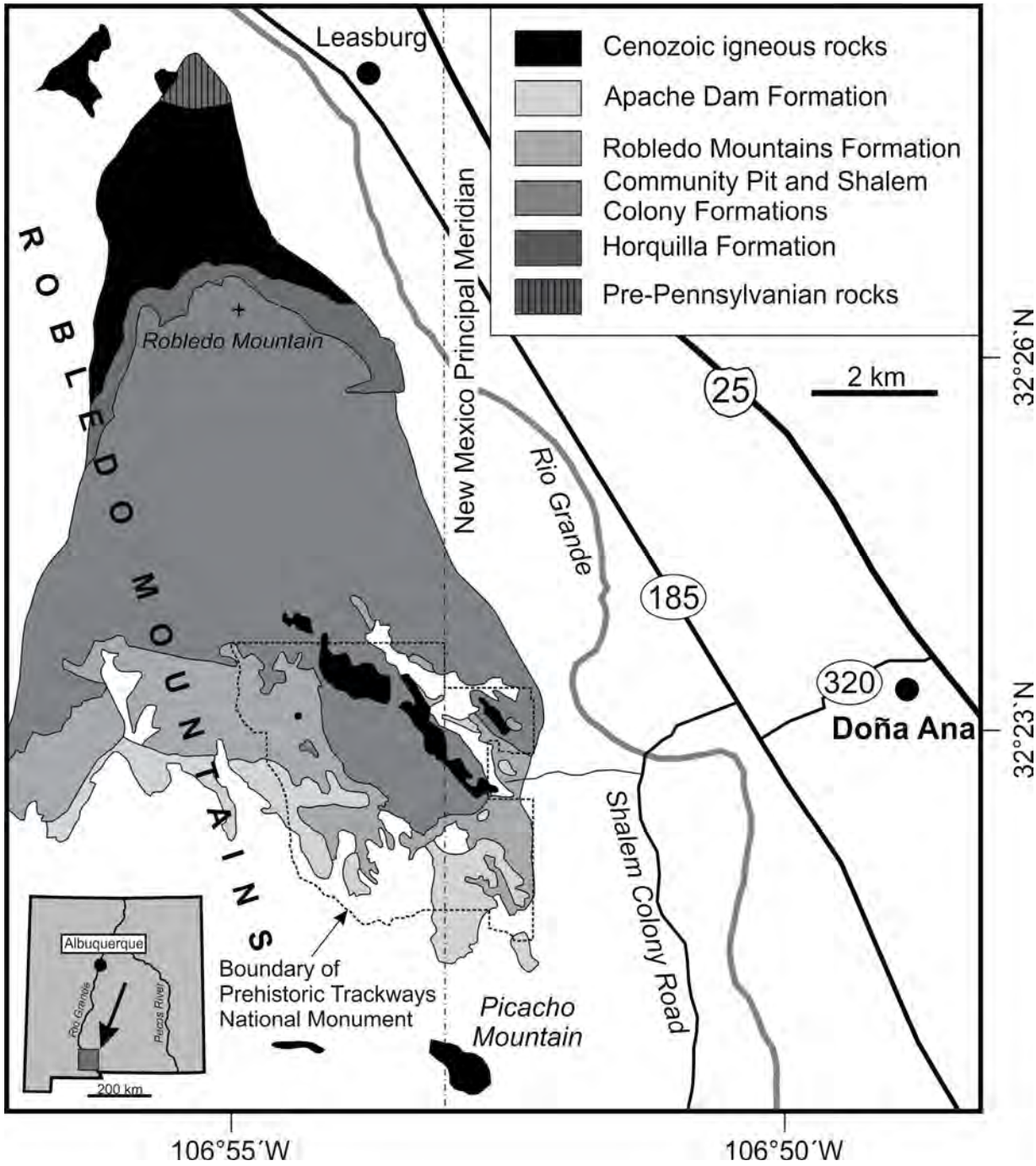


FIGURE 1. Generalized geologic map of the Robledo Mountains in south-central New Mexico. Boundary of Prehistoric Trackways National Monument (PTNM) is shown in the southern part of the range.

Jordan (1971, 1975) published much more detailed data on the Hueco stratigraphy in the Robledo Mountains (Fig. 3). He informally divided the Hueco strata into four units: (1) lower member, about 210 m of oolitic grainstone, rudstone and minor crossbedded sandstone and siltstone interpreted as shoal water deposits; (2) middle member, about 61 m of carbonate mudstone, shale and minor packstone and grainstone interpreted as shallow-water shelf deposits; (3) Abo Formation (tongue), 125 m of red-bed clastics, marine limestone and shale interpreted as nearshore to terrestrial deposits; and (4) upper member, 122 m of algal plate limestone, thin biostromes and interbedded siltstones interpreted as very shallow-water shelf deposits (Fig. 3). Jordan (1971, 1975) regarded the entire Hueco lithosome as early Wolfcampian, based on fusulinids from its two lower members and regional correlations.

Simpson (1976, 1984; also, see LeMone et al., 1971, 1975) presented detailed stratigraphic and paleontologic data on the "Abo Tongue" and the "upper member" of the Hueco in the Robledo Mountains. Simpson's studies were particularly focused on the shelly benthos of these units, especially the brachiopods. He reconstructed their marine communities along the lines of Stevens (1966), and assigned them a late Wolfcampian age. Simpson (1976, 1984) used Jordan's (1971, 1975) stratigraphic framework, as did Seager et al. (1987) in a geologic map that included the Robledo Mountains.

A volume edited by Lucas and Heckert (1995) included diverse articles on the Hueco Group in the southern Robledo Mountains, and focused primarily on the paleontology (especially ichnology) of the unit Kottlowski and Jordan referred to as the "Abo Tongue" or "Abo Formation." Indeed, Lucas et al. (1995) replaced the name "Abo Tongue" with Robledo Mountains Member, making it a formal lithostratigraphic unit in the Hueco Formation. That article provided a stratigraphic and sedimentologic context to all of the Robledo Mountains Member. Other articles in the volume edited by Lucas and Heckert (1995) described the history of footprint discoveries (MacDonald, 1995), the microfacies

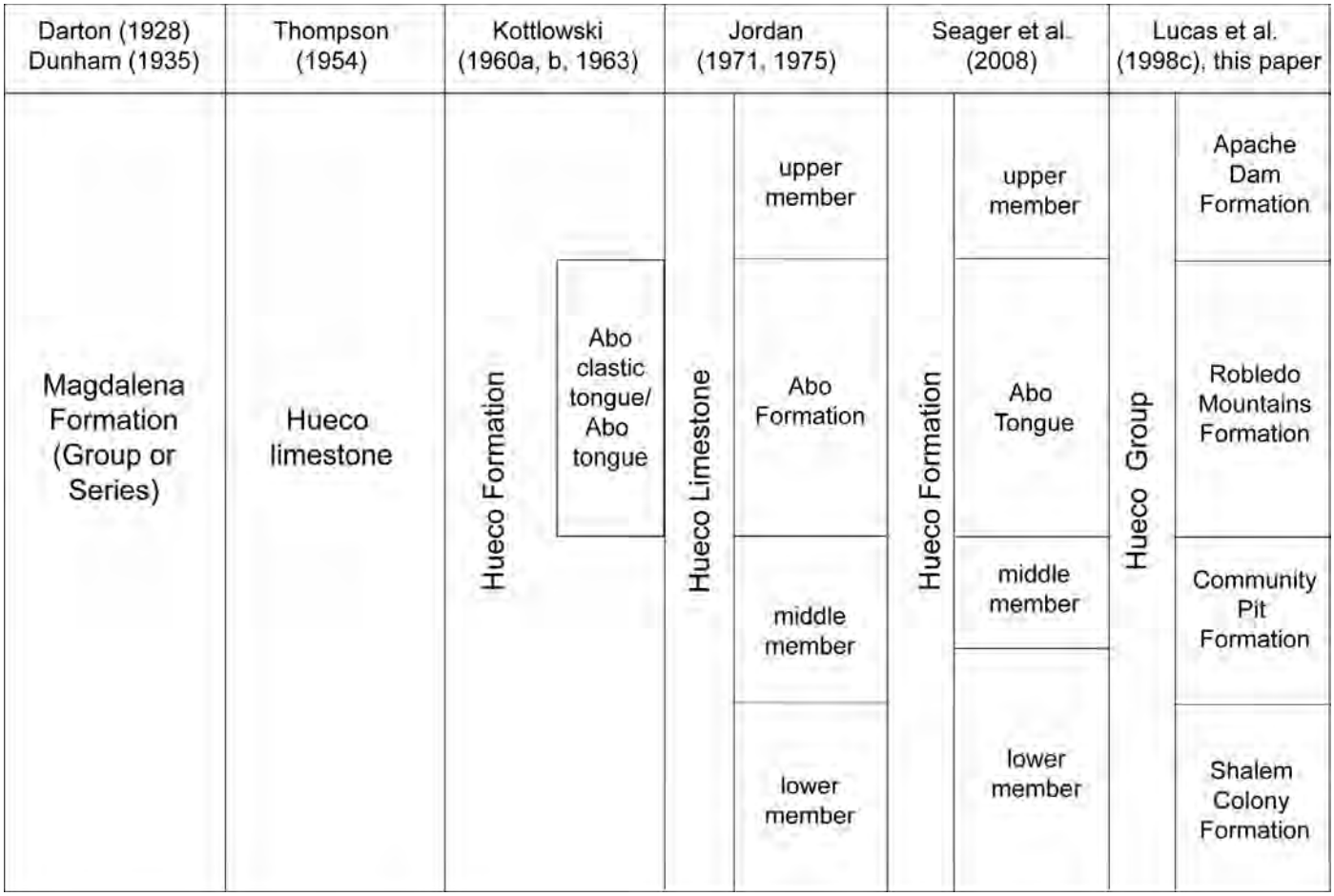


FIGURE 2. Development of lithostratigraphic nomenclature of the Hueco Group in the Robledo Mountains.

(Krainer and Lucas, 1995), the microfossils (Kietzke and Lucas, 1995; Kozur and LeMone, 1995a), the invertebrate macrofauna (Kues, 1995), invertebrate ichnofossils (Braddy, 1995; Kozur and LeMone, 1995b) and vertebrate ichnofossils (Schult, 1995a, b; Haubold et al., 1995; Hunt et al., 1995) of the Robledo Mountains Member. Tidwell and Munzing (1995) documented some fossil wood from the Community Pit Formation. Important conclusions reached by these workers included: (1) recognition that the so-called "Abo Tongue" is dominantly limestone and shale of marine origin, so it belongs in the Hueco lithosome; (2) assignment of a late Wolfcampian age to the Robledo Mountains Member based on ostracod, ammonoid and conodont biostratigraphy; and (3) recognition of the ichnoassemblages of the Robledo Mountains Member as the most extensive and well-preserved terrestrial red-bed ichnoassemblages of Permian age in the world.

Lucas et al. (1998a) later edited another volume on the Robledo Mountains Hueco Group that included a field guide to part of the area later designated as the Prehistoric Trackways National Monument (PTNM). The field guide (Lucas et al., 1998b) was followed by an article that reviewed the stratigraphy, paleontology and depositional environments of the Robledo Mountains Member (Lucas et al., 1998d), and an article that presented formal nomenclature for all of the Hueco Group subdivisions in the Robledo Mountains (Lucas et al., 1998c). Three other articles in that volume further analyzed the invertebrate and vertebrate ichnology of the Hueco Group in the southern Robledo Mountains (Braddy, 1998; Hunt and Lucas, 1998a, b).

Lucas et al. (1998c) elevated the Hueco Formation to Hueco Group, comprising four formations: Shalem Colony (oldest), Community Pit, Robledo Mountains, and Apache Dam (Fig. 2). Seager et al. (2008) mapped the geology of the Robledo Mountains and surrounding area at a scale of 1:24,000. On this map, they continued to apply an informal subdivision of the Hueco Limestone.

Three kinds of research results have been published on the Hueco Group strata during the last decade. Most have been on the ichnology of the Robledo Mountains Formation (see review by Minter and Braddy, 2009 and the bibliography of Lucas et al., 2011b). Almost all others have been on sedimentary cyclicity of the Community Pit and Robledo Mountains formations (Mack, 2007; Mack et al., 2010, 2013). In addition, Wahlman and King (2002) published some fusulinids from the Shalem Colony Formation at the northern end of the Robledo Mountains, Krainer et al. (2003) published data on the microfacies and micropaleontology of part of the Shalem Colony Formation at the northern end of the Robledo Mountains, Lucas et al. (2013a) described a scorpion resting impression from the Robledo Mountains Formation and Falcon-Lang et al. (2014) reported on fossil wood from the Community Pit Formation in the Prehistoric Trackways National Monument.

MATERIALS AND METHODS

Our studies of the Hueco Group in the Robledo Mountains began more than 20 years ago. However, most of the data reported on here were collected by us in 2009-2012, as part of a Federally-funded study of the newly created Prehistoric Trackways National Monument. As part of this study, we measured and sampled 27 stratigraphic sections of parts of the Hueco Group in the southern Robledo Mountains (Fig. 4; Table 1). These sections are identified both by numbers (1-27) and names given to them during fieldwork (Table 1). We add these unpublished sections to those of Jordan (1971, 1975), LeMone et al. (1971, 1975), Lucas et al. (1995, 1998c), Krainer and Lucas (1995), Wahlman and King (2002, which are from Seager et al., 2008), Seager et al. (2008) and Krainer et al. (this volume).

From the measured stratigraphic sections, we collected samples to prepare more than 300 thin sections for petrographic and microfossil analysis, trace fossils, plant macrofossils and selected invertebrate macrofossils. All of these fossils are part of the collections of the New Mexico Museum of Natural History and Science (NMMNH). Conodont samples were collected by us and processed by James Barrick (Texas Tech University) but did not yield age-diagnostic material.

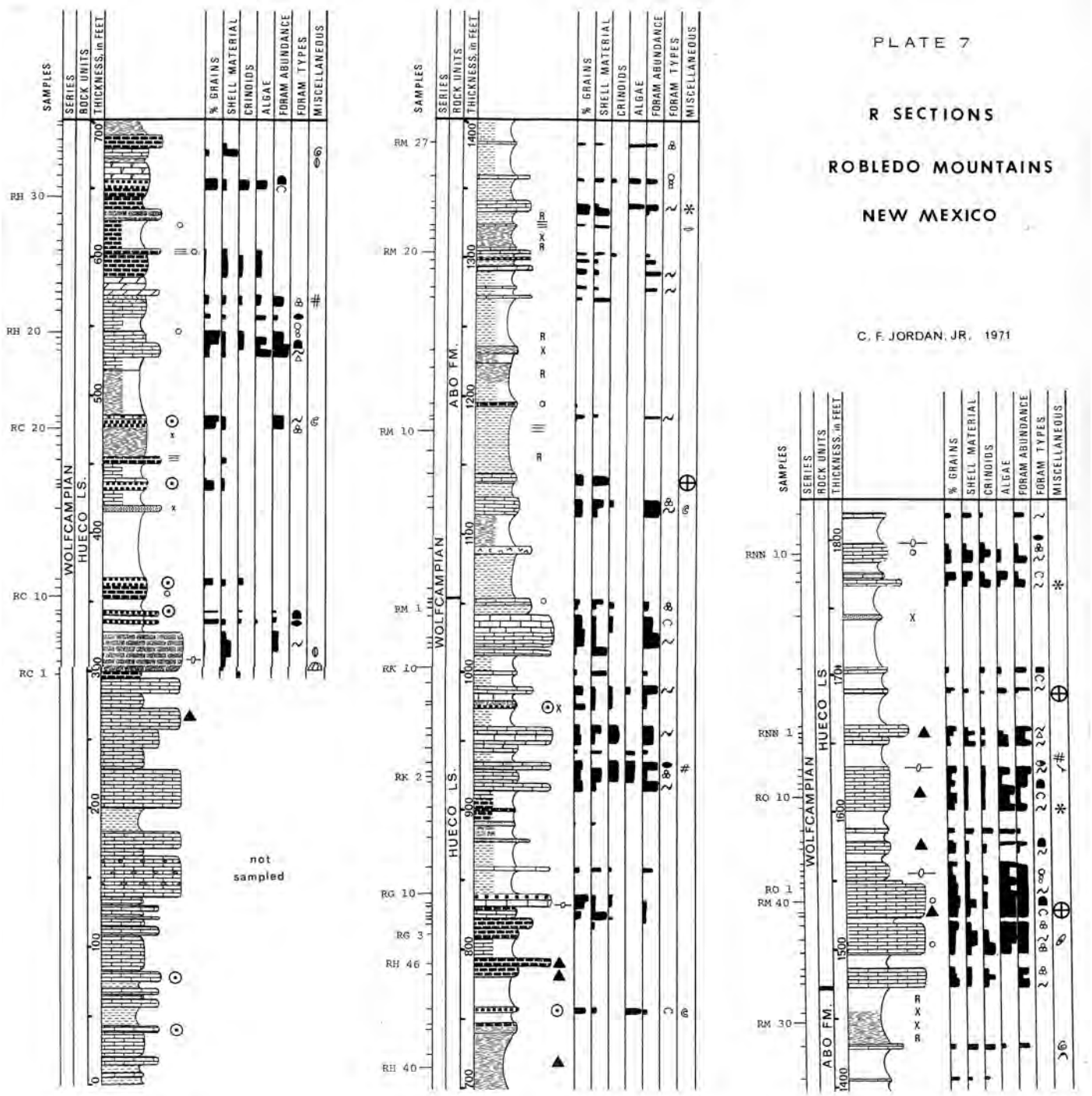


FIGURE 3. Jordan's (1971, pl. 7) composite section of Hueco Group strata in the Robledo Mountains.

LITHOSTRATIGRAPHY

Stratigraphic Nomenclature

Lucas et al. (1995, 1998c) proposed formal lithostratigraphic nomenclature for the Hueco Group strata in the Robledo Mountains, dividing the Hueco Group into the (ascending order) Shalem Colony, Community Pit, Robledo Mountains and Apache Dam formations (Fig. 2). In so doing, they divided the lower member of the Hueco Formation of Jordan (1971, 1975) into the Bursum Formation and overlying Shalem Colony Formation. They equated the overlying formal units to Jordan's informal units: Community Pit Formation = middle member, Robledo Mountains Formation = Abo Tongue and Apache Dam Formation = upper member. However, Bursum Formation as a lithostratigraphic unit is not recognized in the Robledo Mountains, though strata of "Bursum" age (early Wolfcampian) are present (Krainer et al., this volume).

Like Jordan (1971, 1975), working in the structurally complex eastern side of the Robledo Mountains, Lucas et al. (1998c) could not locate complete stratigraphic sections of the Shalem Colony, Community Pit and Apache Dam formations (actually, the Apache Dam Formation has no complete section anywhere in the range). Therefore, they described type sections that were not complete stratigraphic sections of the formations, but that well represent characteristic lithologies.

The term Hueco is generally used as a group-rank unit, simply because its subdivisions are relatively thick and distinctive lithosomes readily mapped at a scale of 1:24,000 (e.g., King et al., 1945; Williams, 1963; Harbour, 1972, Seager et al., 2008, who mapped Hueco subdivisions in the Robledos, but did not recognize it as a group). This is the case in the Robledo Mountains, where we recognize a Hueco Group divided into four mappable formations (Fig. 5).

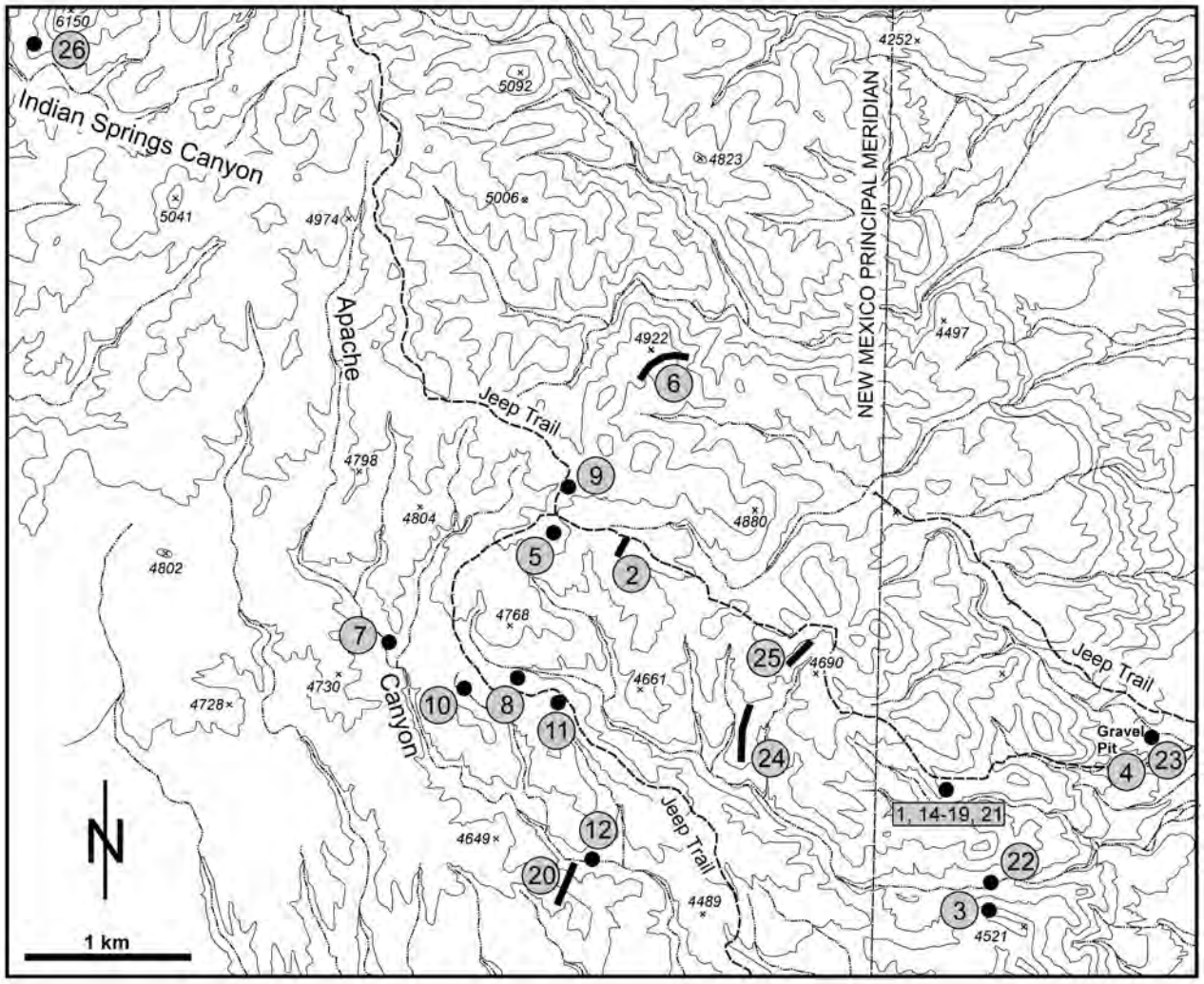


FIGURE 4. Map of the Prehistoric Trackways National Monument in the southern Robledo Mountains (see Fig. 1) and vicinity showing location of Hueco Group sections discussed here (see Table 1 for map coordinates of sections). Sections not shown on this map are at Robledo Mountain (see Krainer et al, this volume), and Apache Dam (Table 1, section 13), which is south of the map area.

The terms Abo Formation, Abo Tongue or Abo Member were previously applied to part of the Hueco Group section in the Robledo Mountains, because this part of the section includes red-bed siliciclastic strata. These red beds have long (and we believe correctly) been equated to part of the Abo Formation, red beds of fluvial origin as much as 309 m thick in central New Mexico, well north of the Robledo Mountains (Lucas et al., 2013b). Nevertheless, more than 50% of the stratigraphic interval previously termed "Abo" in the Robledo Mountains is drab-colored (gray, yellow and tan) marine limestone and shale, characteristic Hueco Group lithologies. Therefore, Lucas et al. (1995, 1998c) assigned this stratigraphic interval to the Hueco Group as a distinct Robledo Mountains Formation. There is thus no justification for using the term Abo to refer to any Permian strata in the Robledo Mountains. The southernmost outcrops of the Abo Formation in the Rio Grande Valley are in the southern Caballo Mountains of Sierra County, about 60 km northwest of the Robledo Mountains (Lucas et al., 2012, 2013b).

Lucas et al. (1998c) indicated that the formations of the Hueco Group they named correspond precisely to the informal subdivisions of the Hueco used by Jordan (1971, 1975). However, this is not the case in the usage of Seager et al. (2008), in which the contact of their lower and middle Hueco members is well above the contact of the Shalem Colony and Community Pit formations. Thus, Jordan's (1971) lower member of the Hueco in the Robledo Mountains has its contact with the middle member at the change from ledge- and cliff-forming, thick intervals of limestone to slope-forming shale intercalated with thin, muddy limestone intervals (Fig. 3). This is the contact between the Shalem Colony and Community Pit formations of Lucas et al. (1998c) used here.

However, Seager et al. (2008) included the lower ~ 30-50 m of our Community Pit Formation in their lower Hueco member, describing these strata in their map legend as "slope or ledge-forming, thin to medium-bedded carbonate mudstone and dolomitic mudstone that weathers to shades of cream, yellow, light gray, buff and orange." These are characteristic lithologies and colors of overlying strata of the Community Pit Formation, so we place the base of the Community Pit well below the top of this stratigraphic interval. This is most easily seen at our Indian Springs and Monument North sections (Figs. 6-8). In particular, at Monument North, Seager et al. (2008) map the base of their middle Hueco member at about our bed 68, which is about 40 m above the base of the Community Pit Formation of our stratigraphy. Thus, we advocate the most mappable contact between the Shalem Colony and Community Pit formations at a stratigraphic level lower than the mapped boundary between the lower and middle Hueco members of Seager et al. (2008). This means that the upper part of section J of Wahlman and King (2002, fig. 4), beginning with their unit 4, is assigned by us to the Community Pit Formation.

Indeed, the geologic map of PTNM that appears elsewhere in this volume was adapted from the map of Seager et al. (2008), with minor changes. The most important change is that the boundary between the Shalem Colony and Community Pit formations was adjusted downward from the contact between the lower and middle members of the Hueco limestone, as mapped by Seager et al. (2008).

The lithostratigraphic nomenclature introduced by Lucas et al. (1998c) was applied to Hueco Group strata in southern New Mexico in the Doña Ana Mountains (Krainer et al., 2005, 2009; Spielmann et

group	formation	maximum thickness	principal lithologies
Hueco Group	Apache Dam Formation	107+ m	algal limestone and shale
	Robledo Mountains Formation	90-125 m	grainy limestone, shale and red-bed siliciclastics (sandstone, siltstone, mudstone)
	Community Pit Formation	93-177 m	shale, muddy limestone, dolomitic limestone
	Shalem Colony Formation	127-156 m	thick-bedded, coarse-grained limestone (wackestone, grainstone, etc.)

FIGURE 5. Brief summary of Hueco Group stratigraphy in the Robledo Mountains.

al., 2005), the southern San Andres Mountains (Lucas et al., 2002) and the Jarilla Mountains (Lucas and Krainer, 2002). Published work on the Hueco strata in the Robledo Mountains since Lucas et al. (1998c) either uses the formal lithostratigraphic nomenclature (e. g., Minter and Braddy, 2009; Lucas et al., 2013a; Voigt et al., 2013) or continues to use the informal nomenclature of Jordan (Mack, 2007; Seager et al., 2008; Mack et al., 2013). The strata immediately beneath the Hueco Group in the Robledo Mountains are assigned to the Horquilla Formation by Krainer et al. (this volume), who explain and justify that lithostratigraphic assignment.

Shalem Colony Formation

The basal unit of the Hueco Group in the Robledo Mountains is the Shalem Colony Formation, a relatively thick-bedded and coarse-grained succession of wackestones, grainstones and rudstones intercalated with mostly covered intervals of shale and/or nodular limestone (Figs. 6-10). We place the base of the Shalem Colony Formation in the Robledo Mountains at the change from thinner-bedded, slope-forming limestone and shale of the uppermost Horquilla Formation to thicker-bedded, cliff- and bench-forming limestones of the Shalem Colony Formation (Figs. 6A, 7). Locally, a conglomerate bed is at the base of the Shalem Colony Formation above Horquilla Formation wackestone (see Krainer et al., this volume).

At the type section, the Shalem Colony Formation is 106 m thick,

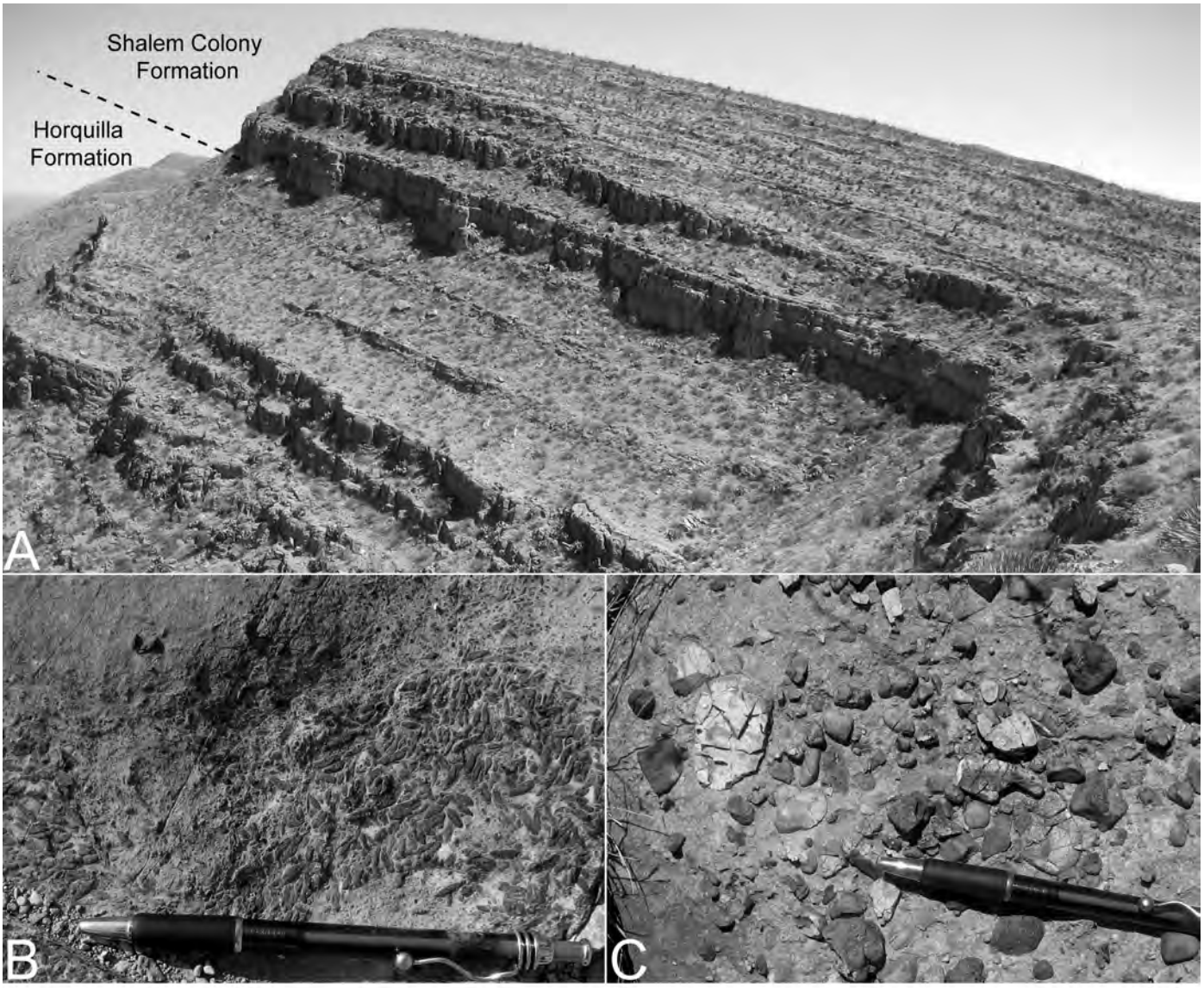


FIGURE 6. Photographs of selected outcrops of the Shalem Colony Formation at the Indian Springs Canyon section in the Robledo Mountains. **A,** Overview of lower part of section, showing contact of Horquilla and Shalem Colony formations. **B,** Fusulinid packstone in Shalem Colony Formation (Fig. 7, unit 28). **C,** Conglomerate bed in Shalem Colony Formation (Fig. 7, unit 41).

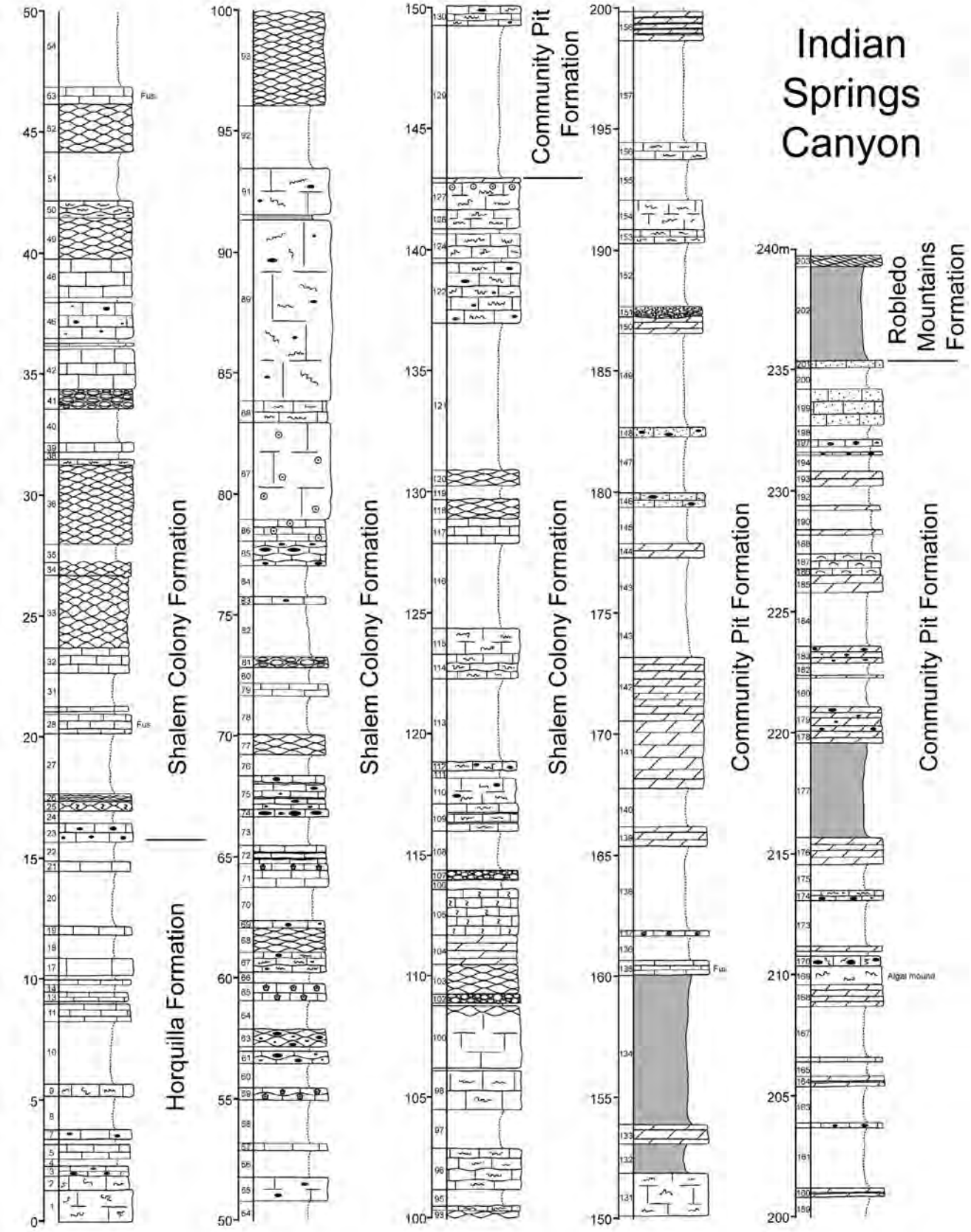


FIGURE 7. Measured stratigraphic section of the Shalem Colony and Community Pit formations at Indian Springs Canyon (see Figure 4 and Table 1 for location of section). See Figure 8 for legend to lithologic symbols.

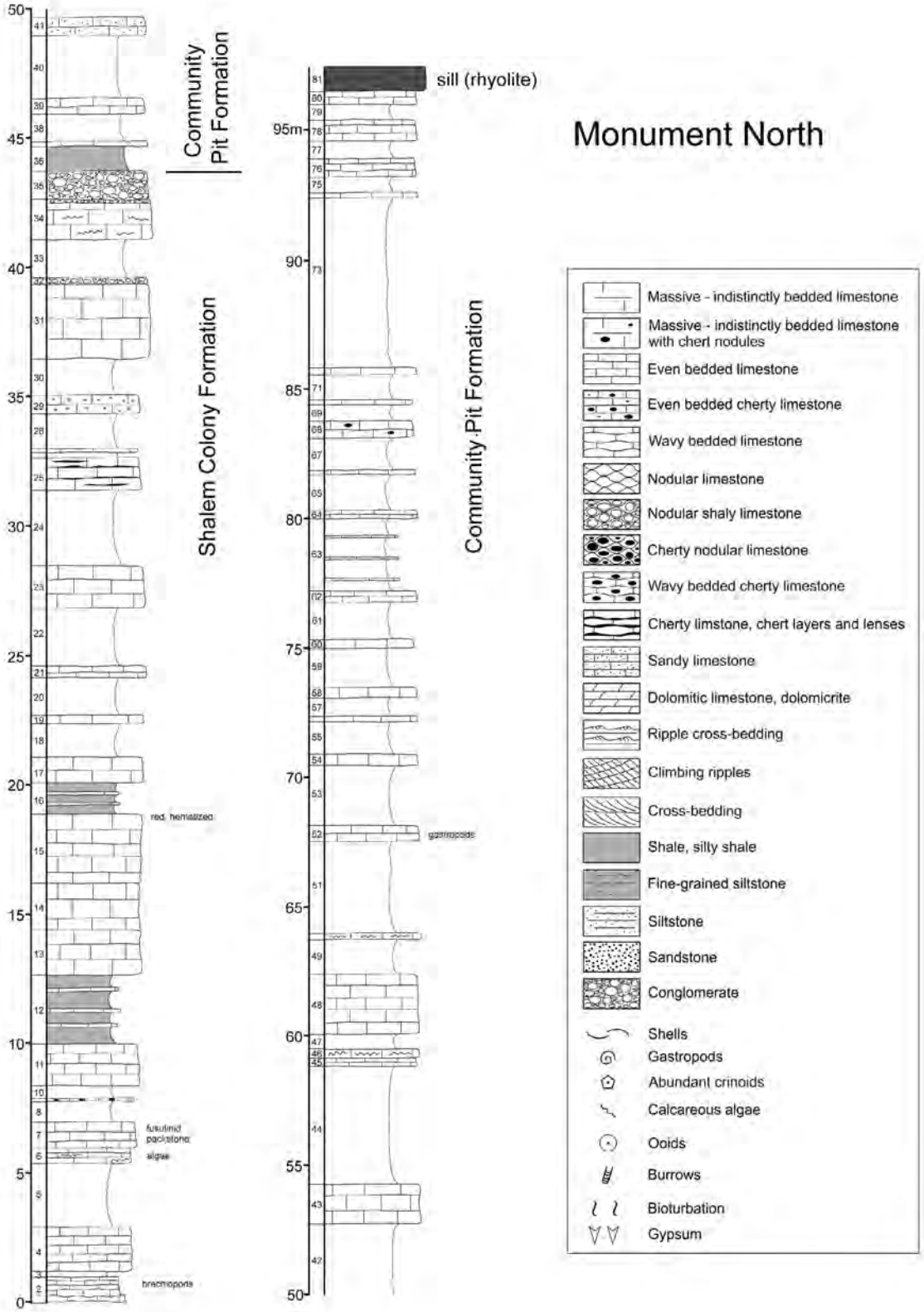


FIGURE 8. Measured stratigraphic section of parts of the Shalem Colony and Community Pit formations at Monument North (see Figure 4 and Table 1 for location of section).

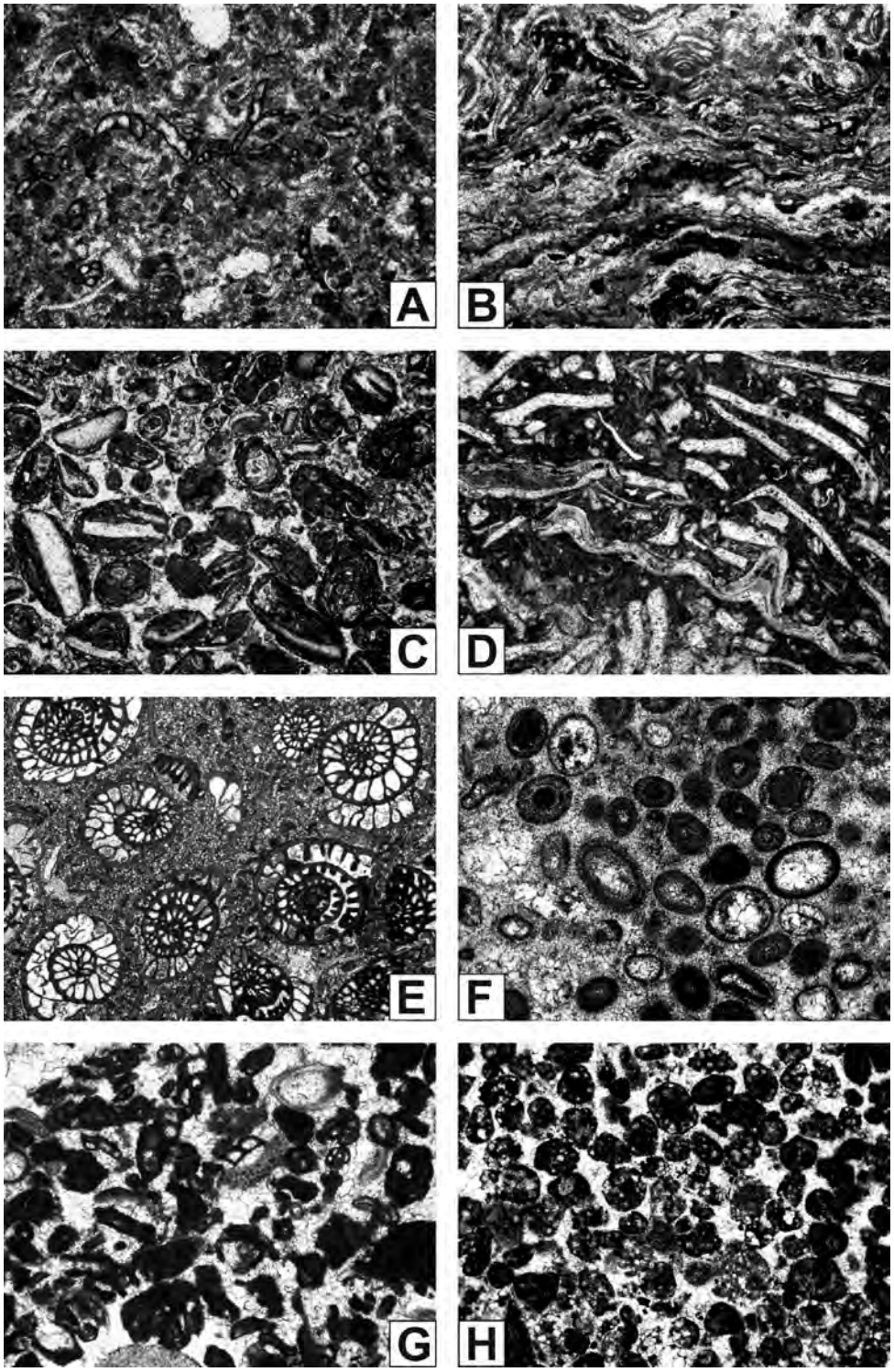


FIGURE 9. Thin section photographs of common microfacies types of uppermost Horquilla and Shalem Colony formations, Robledo Mountains. All photographs under plane light. **A,** Bioclastic wackestone to packstone containing a moderately diverse fossil assemblage (mainly calcivertellid foraminifers, ostracodes, bivalves, gastropods) and abundant peloids. Indian Springs Canyon, unit 17, width of photograph is 6.3 mm. **B,** Large oncoid composed of *Archaeolithophyllum lamellosum* Wray and calcivertellid foraminifers, embedded in a bioclastic wackestone. Indian Springs Canyon, unit 21, width of photograph is 6.3 mm. **C,** Oncoidal wackestone to grainstone. Oncoids (mostly 1-2 mm) are encrusted by *Ellesmerella* ex gr. *permica* (Pia) and calcivertellids. Locally peloids and peloidal micrite are present. Indian Springs Canyon, unit 87, width of photograph is 6.3 mm. **D,** Phylloid algal floatstone. Abundant recrystallized fragments of phylloid algae and debris of shells are embedded in micrite. Indian Springs Canyon, unit 9, width of photograph is 6.3 mm. **E,** Fusulinid wackestone containing partly abraded and fragmented tests of fusulinids *Leptotriticites* and *Paraschwagerina*, and subordinately other fossil fragments. Monument North, unit 1, width of photograph is 6.3 mm. **F,** Grainstone, well sorted, composed of ooids, peloids, cortoids (recrystallized skeletons with micritic envelopes), fossil fragments and rare detrital quartz grains. Indian Springs Canyon, unit 127, width of photograph is 3.2 mm. **G,** Grainstone containing abundant calcivertellid foraminifers, peloids and micritic intraclasts and a few other fossil fragments. Indian Springs Canyon, unit 81, width of photograph is 3.2 mm. **H,** Grainstone composed of abundant crustacean coprolites, a few intraclasts and rare bioclastic fragments. Indian Springs Canyon, unit 26, width of photograph is 3.2 mm.

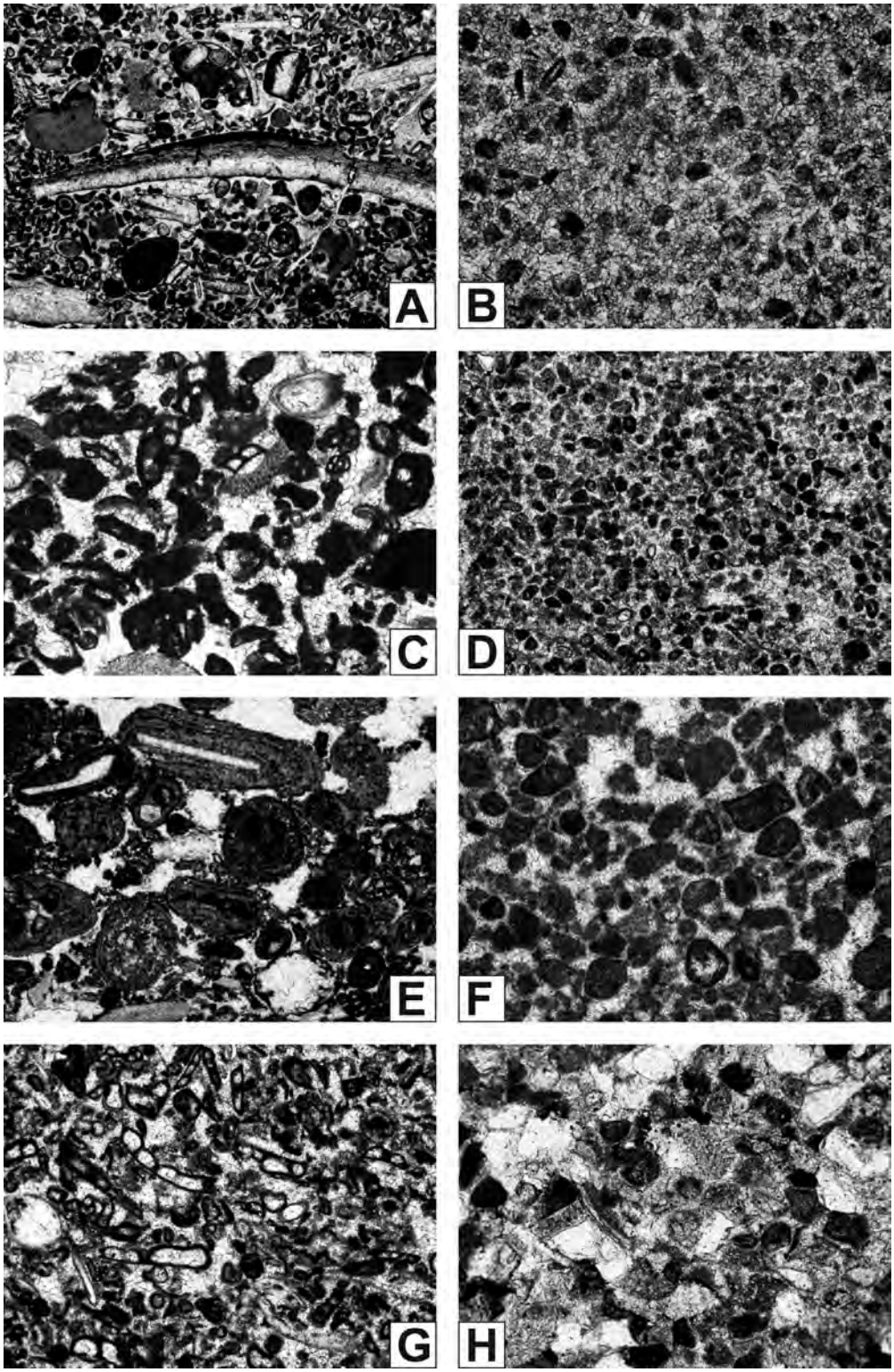


FIGURE 10. Thin section photographs of common microfacies types of the Shalem Colony Formation, Robledo Mountains. All photographs under plane light. **A,** Grainstone-rudstone containing ooids, peloids, intraclasts and skeletons. Well washed but poorly sorted with a few large skeletons. Some skeletons display thin micritic envelopes (cortoids). Indian Springs Canyon, unit 118, width of photograph is 6.3 mm. **B,** Peloidal grainstone, recrystallized. Indian Springs Canyon, unit 37, width of photograph is 1.2 mm. **C,** Oncoidal grainstone composed of abundant oncoids formed of cyanobacteria and few cortoids. Locally some peloidal micrite is present. Indian Springs Canyon, unit 110, width of photograph is 6.3 mm. **D,** Peloidal grainstone with rare intraclasts, ooids, fossil fragments and detrital quartz grains. Indian Springs Canyon, unit 100, width of photograph is 3.2 mm. **E,** Oncoidal grainstone-rudstone containing oncoids that are partly fragmented and abraded, peloids and some fossil fragments. Sample ISC 71 (Indian Springs Canyon), width of photograph 6.3 mm. **F,** Grainstone composed of intraclasts and peloids and rare ostracodes. Indian Springs Canyon, unit 89, width of photograph is 3.2 mm. **G,** Foraminiferal grainstone-packstone containing abundant calcivertellid foraminifers, some ooids, intraclasts and other fossil fragments. Indian Springs Canyon, unit 88, width of photograph is 3.2 mm. **H,** Fine-grained, mixed siliciclastic-carbonate sandstone composed of detrital quartz grains, rare detrital feldspars, many micritic intraclasts and subordinate fossil fragments. Monument North, unit 29, width of photograph is 1.2 mm.

but, the base of the formation is not exposed (Lucas et al., 1998c). At the type section, slope-forming shale and siltstone comprise approximately 50% of the section; intercalated limestones consist of rudstone (13%), calcarenite (11%), and grainstone (9%) and a lesser amount of packstone (9%), mudstone (4%), algal boundstone (4%), and wackestone (< 1%) (Lucas et al., 1998c). Shale intervals in the Shalem Colony Formation are mostly covered but where exposed are drab colored (gray, tan) and calcareous.

According to Jordan (1971), the total thickness of the Shalem Colony Formation of our usage (his "lower member") is about 210 m, but our data suggest this is an overestimate by at least one-third of actual thickness. Seager et al. (2008) estimate the thickness of their lower Hueco as ~156 m, but if we substract the ~50 m that we would assign to the Community Pit Formation, then the Shalem Colony Formation thickness by this estimate is close to 106 m. A complete section of the Shalem Colony Formation is exposed in Indian Springs Canyon, and we consider this section an important reference section of the unit (Figs. 6-7). At Indian Springs Canyon, the Shalem Colony Formation is 127 m thick, underlain by the Horquilla Formation and overlain by the Community Pit Formation.

Here, the Shalem Colony Formation is composed of limestone, two thin conglomerate beds (each 0.4 m thick: Fig. 6C) and covered intervals that most likely represent shale units. Covered intervals are 0.1-6.1 m thick and constitute 39% of the total thickness of the formation. Limestone intervals are up to 14.3 m thick. Within the limestone facies several lithotypes are distinguished: (1) thin, even-bedded limestone; (2) medium, even-bedded limestone; (3) indistinctly bedded to massive limestone (1.9-7.5 m thick); (4) wavy bedded limestone, bed thickness mostly 10-30 cm (0.5-1 m thick); (5) nodular limestone (0.4-4.2 m thick); and (6) rare individual limestone beds (0.3 m thick). Chert is rare and occurs as nodules, rarely as thin bands and predominantly in wavy-bedded limestone.

At the Monument North section (Fig. 8), the upper 44 m of the Shalem Colony Formation are exposed. These strata are composed of limestone lithofacies (thin- to medium-bedded limestone, wavy bedded, rare nodular limestone) similar to those at Indian Springs Canyon. Limestone intervals are 0.1-6.2 m thick, and covered intervals are 0.2-2.9 m thick. Calcareous algae occur in limestone near the top and near the base of the exposed section. Fusulinids are present in two limestone beds in the lower part of the section (Fig. 8, units 1 and 7). Chert is rare in the limestone facies. A carbonate conglomerate bed is present at the top of the Shalem Colony Formation.

At Robledo Mountain, above strata we assign to the Horquilla Formation, the exposed thickness of the overlying lower part of the Hueco Group is 117.3 m, and the entire succession is assigned to the Shalem Colony Formation (Krainer et al., this volume). The succession is composed mainly of limestone (60.3%), with intercalated conglomerate (1.6%), bedded chert (4.7%) and covered intervals (33.4%). We place the base of the Hueco Group at a conglomerate unit at which the limestone facies change and and relatively thick limestone beds are present, features we judge characteristic of the Shalem Colony Formation of the Hueco Group (see Krainer et al., this volume).

Compared to the Shalem Colony Formation in the Doña Ana Mountains (Krainer et al., 2005, 2009), the formation is: (1) thicker in the Robledo Mountains (maximum of 127 m vs. 63 m); and (2) nodular and indistinctly bedded/massive limestone beds are more abundant in the Robledo Mountains.

Microfacies

Limestone of the Shalem Colony Formation is composed of a large variety of microfacies types, most of them containing a diverse fossil assemblage (Figs. 9-15). Most common are various types of wackestone and grainstone-rudstone, and less common are floatstone, mudstone and bindstone.

Bioclastic wackestone (Fig. 9A) is characterized by a diverse fossil assemblage, locally contains abundant peloids and may grade into floatstone or peloidal mudstone. Oncoidal wackestone to floatstone (Fig. 9C) contains oncoids up to 3 mm in diameter that float in the bioclastic wackestone matrix with a diverse fossil assemblage, and are composed of a nucleus (commonly recrystallized skeletons) encrusted by *Ellesmerella* and calcivertellid tubular foraminifers (Fig. 9C). Phylloid algal wackestone to floatstone (Fig. 9D) contains large fragments of recrystallized phylloid algal blades that are commonly encrusted by cyanobacteria, rarely by calcivertellid tubular foraminifers and by *Efluegelia*. Other fossils are rare.

Fusulinid wackestone (Fig. 9E) is present at the base of the Monument North section and contains abundant, complete and abraded fusulinid tests. Grainstone-rudstone (Figs. 9F, H) is poorly sorted, and contains peloids, intraclasts, locally abundant ooids, rare detrital quartz grains and a diverse fossil assemblage. Fossils are commonly strongly fragmented and include recrystallized skeletons, which display micritic envelopes (cortoids). Locally, thin layers of peloidal grainstone alternate with coarser-grained layers of peloidal-bioclastic grainstone.

Oncoidal grainstone-rudstone (Fig. 10C) contains oncoids, mostly up to 3 mm, rarely up to 10 mm in diameter, peloids, rare ooids and a diverse biota. Skeletons are encrusted by *Girvanella* and tubular foraminifers forming oncoids that are partly abraded and fragmented. Foraminiferal grainstone (Fig. 9G and Fig. 10G) is composed of abundant calcivertellids and subordinate other bioclasts, peloids, intraclasts and locally ooids. Oolitic grainstone (Figs. 9F and 10A, E-F) is well sorted. Ooids are 0.2-0.5 mm in diameter and display tangential structure. Many ooids are micritized or recrystallized. Very rare oncoids are present, too. Fossil fragments are rare. Peloidal grainstone (Figs. 10B, D) contains a few ooids, quartz grains and fossils, including calcivertellid foraminifers and ostracodes. Intraclast-peloidal grainstone is also characterized by a sparse fossil assemblage.

Floatstone contains large recrystallized skeletons of bivalves, gastropods and brachiopods that float in peloidal wackestone with a moderately diverse fossil assemblage. Many skeletons are encrusted by *Girvanella* and calcivertellids.

Mudstone is locally peloidal, bioturbated and contains a low diversity assemblage of mainly calcivertellids and ostracodes, as well as rare echinoderms. Silty mudstone contains small angular quartz grains, peloids, rare ostracodes and foraminifers, and is locally bioturbated.

Bindstone is composed of microbial crusts (stromatolite) with fenestral fabrics, alternating with fine-grained bioclastic wackestone containing a few fossil fragments.

Sandstone Petrography

A single bed of carbonate sandstone (grainstone) of the Shalem Colony Formation in the Indian Springs Canyon section (Fig. 7, unit 107) is composed of different types of reworked carbonate grains, mostly rounded with grain diameters of 0.2-1 mm. A few chert grains and detrital quartz grains, rare ooids and oolitic limestone fragments are present, too. Recrystallized skeletons are rare. The sandstone contains both micritic matrix and calcite cement.

One bed of fine-grained sandstone of the Shalem Colony Formation at the Monument North section (Fig. 8, unit 29) is mixed siliciclastic-carbonate in composition and contains angular to subangular detrital monocrystalline quartz grains, rare polycrystalline quartz grains and muscovite, and very rare schistose metamorphic rock fragments composed of quartz and mica. Detrital feldspar grains are rare and mostly replaced by calcite. The sandstone contains abundant gray micritic carbonate grains and subordinate fossil fragments, including echinoderms, ostracodes, smaller foraminifers and recrystallized skeletons. The grains are cemented by calcite (Fig. 10H).

Fossils

Fusulinids occur in two limestone beds in the lower part of the Indian Springs Canyon section (Figs. 6B, 7 units 28 and 53). Calcareous algae are common in bedded and massive limestone in the middle and upper parts of this section. Other fossils observed on outcrop are brachiopods and crinoidal debris. Peloidal grainstone contains a few calcivertellids and ostracodes. Also, lime mudstone is characterized by a low-diversity assemblage of ostracodes, calcivertellids, and rare echinoderm fragments. Foraminifers and algae (Figs. 11-15) are as follows:

Fusulinids: "*Nankinella*?" sp. (Figs. 12. 24-25), reworked late Moscovian *Beedeina*? cf. *primitiva* (Thompson) (Fig. 12.13), *Triticites* ex gr. *meeki* (Moeller) (Fig. 11.1), *T.* spp., *Thompsonites* cf. *longissimoidea* (Beede) (Fig. 11.5-6) *T.* aff. *longissimoidea* (Fig. 11.2-4) *T.* ex gr. *longissimoidea*, *T.* sp. (Fig. 11.7), *Leptotriticites* spp. (Figs. 13.1-6, 14.1-2, 5, 15.1), and *Paraschwagerina* cf. *acuminata* Dunbar and Skinner (Figs. 13.8, 15.5-6).

Smaller foraminifers: *Tuberitina bulbacea* Galloway and Harlton (Fig. 12.12), *Endothyra* spp., *Endothyranella* sp., *Planoendothyra* sp., *Neoendothyra*? sp. (Fig. 21.14), *Pseudobradyina pauciseptata* (Reitlinger) (Fig. 12.20), *Bradyina lucida* Morozova (Fig. 12.23), *Globivalvulina* sp., *Climacammina* sp., *Deckerella* sp., other palaeotextulariids, *Spireitlina baschkirica* (Rauzer-Chernousova) (Fig. 21.13), *S. tokmovensis* Reitlinger, *Tetrataxis* sp., *Hemigordiellina* sp., *Palaeonubecularia* sp. (Fig. 12.2), *Calcivertella* sp., *Orthovertella*

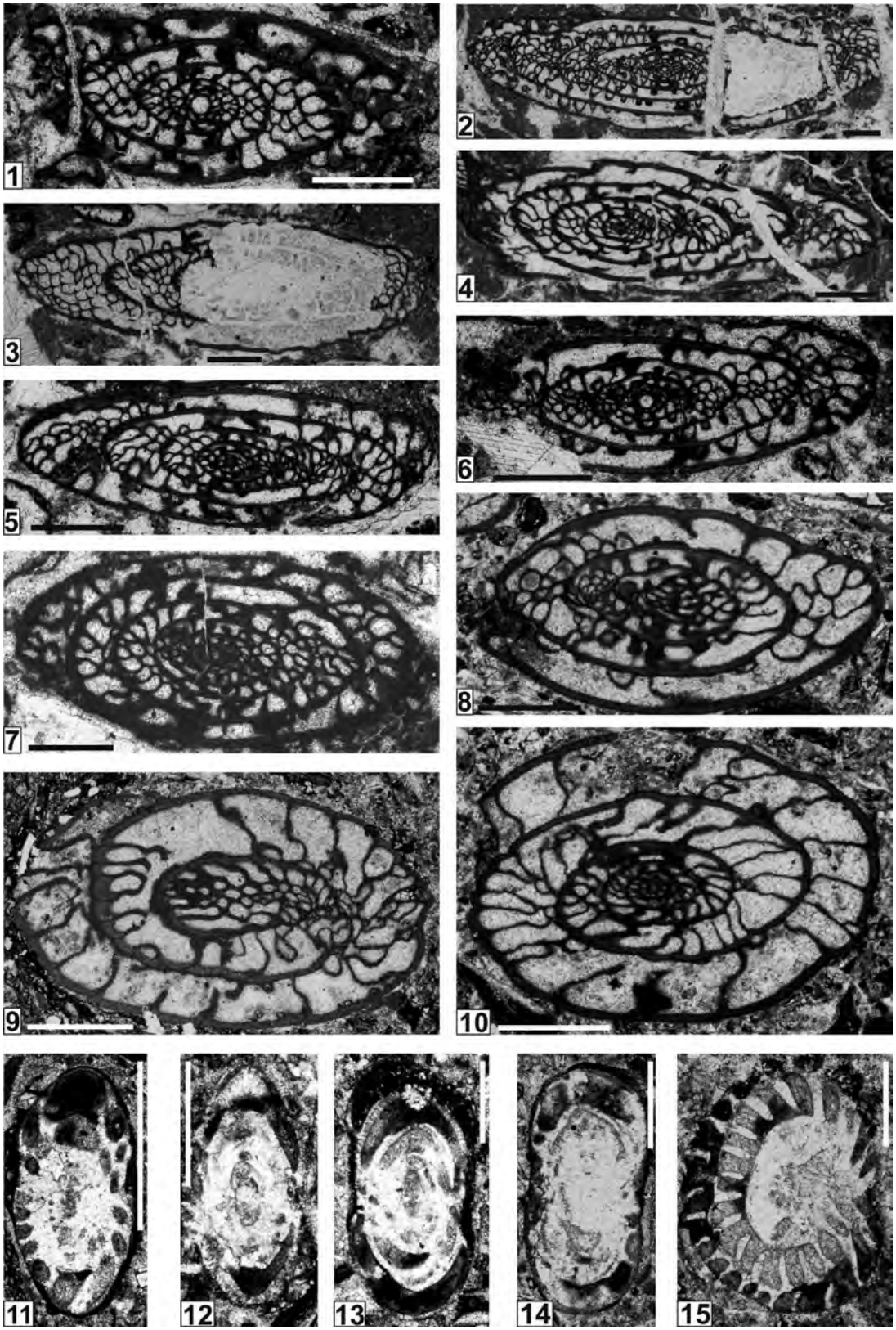


FIGURE 11. Indian Springs Canyon section, fusulinids of Shalem Colony and lowermost Community Pit formations. Scale bars: 1-10 = 1.0 mm; 11-15 = 0.5 mm. **1,** *Triticites* ex gr. *meeki* (Möller). Oblique axial section. Sample ISC 53-1-2. **2-4,** *Thompsonites* aff. *longissimoidea* (Beede). 2. Axial section (weakly silicified). Sample ISC 53-3-2. 3. Subaxial section (partly silicified). Sample ISC 53-2-1. 4. Subxial section. Sample ISC 53-2-2. **5-6,** *Thompsonites* cf. *longissimoidea* (Beede). 5. Subaxial section. Sample ISC 53-1-3. 6. Oblique axial section. Sample ISC 53-3-1. **7,** *Thompsonites* sp. Oblique section. Sample ISC 53-4-4. **8-10,** *Pseudoschwagerina* cf. *needhami* Thompson. 8. Oblique subaxial section. Sample ISC 135-2-6. 9. Oblique section. Sample ISC 135-6. 10. Oblique subtransverse section. Sample ISC 135-4-3. **11-15,** "*Nankinella*?" cf. *loeiensis* Igo, Ueno and Sashida. 11. Subaxial section. Sample ISC 135-1-1. 12. Axial section. Sample ISC135-1-2. 13. Axial section. Sample ISC 135-4-1. 14. Subaxial section. Sample 135-7-9. 15. Subtransverse section. Sample ISC 135-6-1.

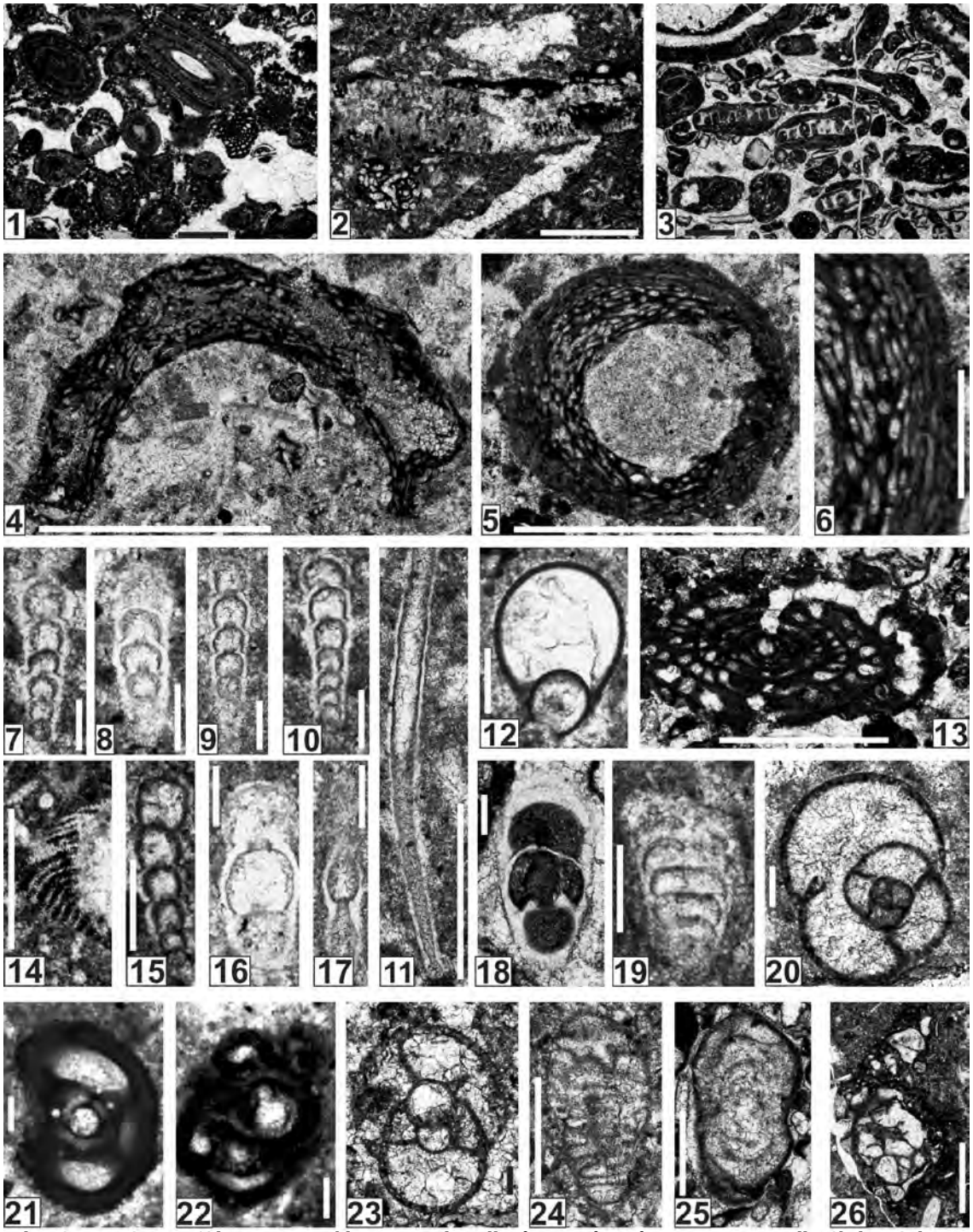


FIGURE 12. Indian Springs Canyon (Algae, microproblematica and smaller foraminifers of uppermost Horquilla, Shalem Colony and lowermost Community Pit formations). Scale bars: 1-5, 13 = 1.0 mm; 6, 11, 14, 24-26 = 0.5 mm; 7-10, 12, 15-23 = 0.1 mm. **1,** Oncoidal grainstone (perhaps built by rivulariacean algae) and some abraded but minreralogically well preserved staffellid fusulinids (S). Sample ISC 71-3. **2,** Phylloid alga *Anchicodium funile* Johnson encrusted by tubular foraminifers *Palaeonubecularia* sp. Sample ISC 109.1. **3,** Oncoidal grainstone with cortices of *Ellesmerella* ex gr. *permica* and nuclei of *Epimastopora* ex gr. *alpina* Pia. Sample ISC 110-7. **4-6,** *Ellesmerella* cf. *subparallella* (Flügel and Flügel). 4. Longitudinal section. Sample ISC 135-7-8. 5. Transverse section. Sample ISC 135-4-6. 6. Detail of 5 showing the tubes. Sample ISC 135-4-6. **7, 9-10,** *Nodosinelloides sikhanica* (Lipina). Axial and subaxial sections. 7. Sample ISC 1-2. 9. Sample ISC 17-1. 10. Sample ISC 17-6. **8,** *Nodosinelloides* cf. *potievskayae* Mamet and Pinard. Sample ISC 7-5. **11,** *Syzrania gigas* Stepanova. Axial section. Sample ISC 109-8. **12,** *Tuberitina bulbacea* Galloway and Harlton. Axial section. Sample ISC 67-5. **13,** Reworked *Beedeina*? *primitiva* (Thompson). Oblique axial section. Sample ISC 28-1. **14,** *Efluegelia johnsoni* (Flügel). Oblique section. Sample ISC 109-7a. **15,** *Nodosinelloides* cf. *sikhanica* (Lipina). Axial section. Sample ISC 17-3. **16,** *Protonodosaria* aff. *globifrondina* Sellier de Civrieux and Dessauvagie. Subaxial section. Sample ISC 7-6. **17,** *Vervilleina bradyi* (Spandel). Oblique section. Sample ISC 50-5. **18,** *Nestellorella*? sp. Oblique section. Sample ISC 28-8. **19,** *Geinitzina linguliformis* Lipina. Subaxial section. Sample ISC 109-5. **20,** *Pseudobradyina pauciseptata* (Reitlinger). Transverse section. Sample ISC 9-1. **21-22,** *Hedraites* n. sp. (probably similar to *Lituotuba* (?) sp. 1 and 2 of Bogush and Yuferev, 1966). 21. Axial section. Sample ISC 67-2a. 22. Subaxial section with a flexostyle canal. Sample ISC 67-2b. **23,** *Bradyina lucida* Morozova. Subaxial section. Sample ISC 28-12. **24?-25,** *Nankinella*? sp. 24. Oblique section. Sample ISC 23-2. 25. Subaxial section. Sample ISC 23-5. **26,** *Bacinella* sp. Random section. Sample ISC 50-2.

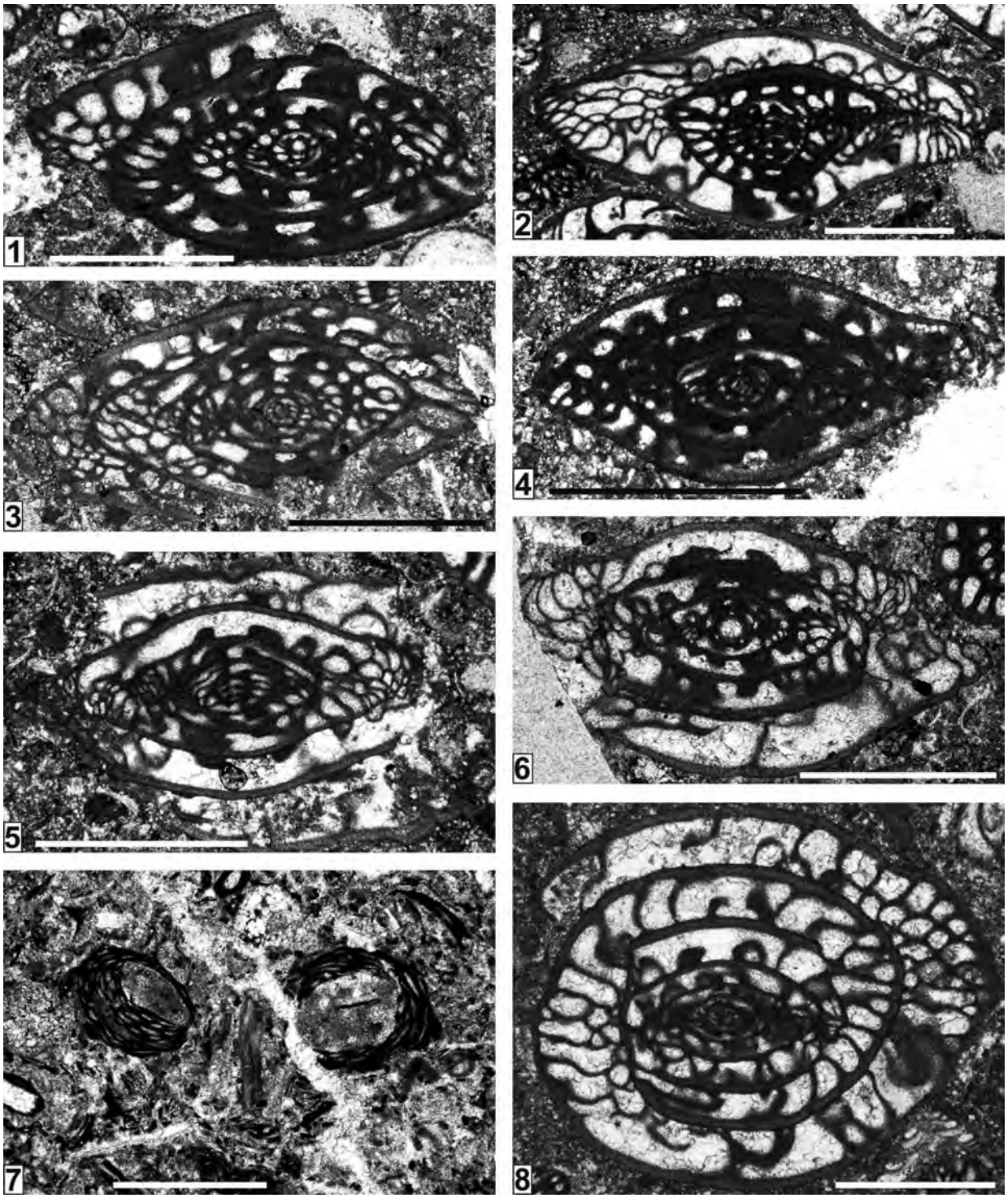


FIGURE 13. Fusulinids of the Shalem Colony Formation at the Monument North section. Scale bars = 1.0 mm. **1-4,** *Leptotriticites* sp. 1. Four subaxial sections. 1. Sample MON 1c-4. 2. Sample MON 1b-1. 3. Sample MON 1a-7. 4. Sample MON 1a-1. **5-6,** *Leptotriticites* sp. 2. Subaxial and axial sections. 5. Sample MON 1a-3. 6. Sample MON 1c-1. **7,** *Ellesmerella* cf. *subparallella* (Flügel and Flügel). Two sections in a bioclastic grainstone. Sample MON 1-6. **8,** *Paraschwagerina* cf. *acuminata* Dunbar and Skinner. Subaxial section. MON 1b-6.

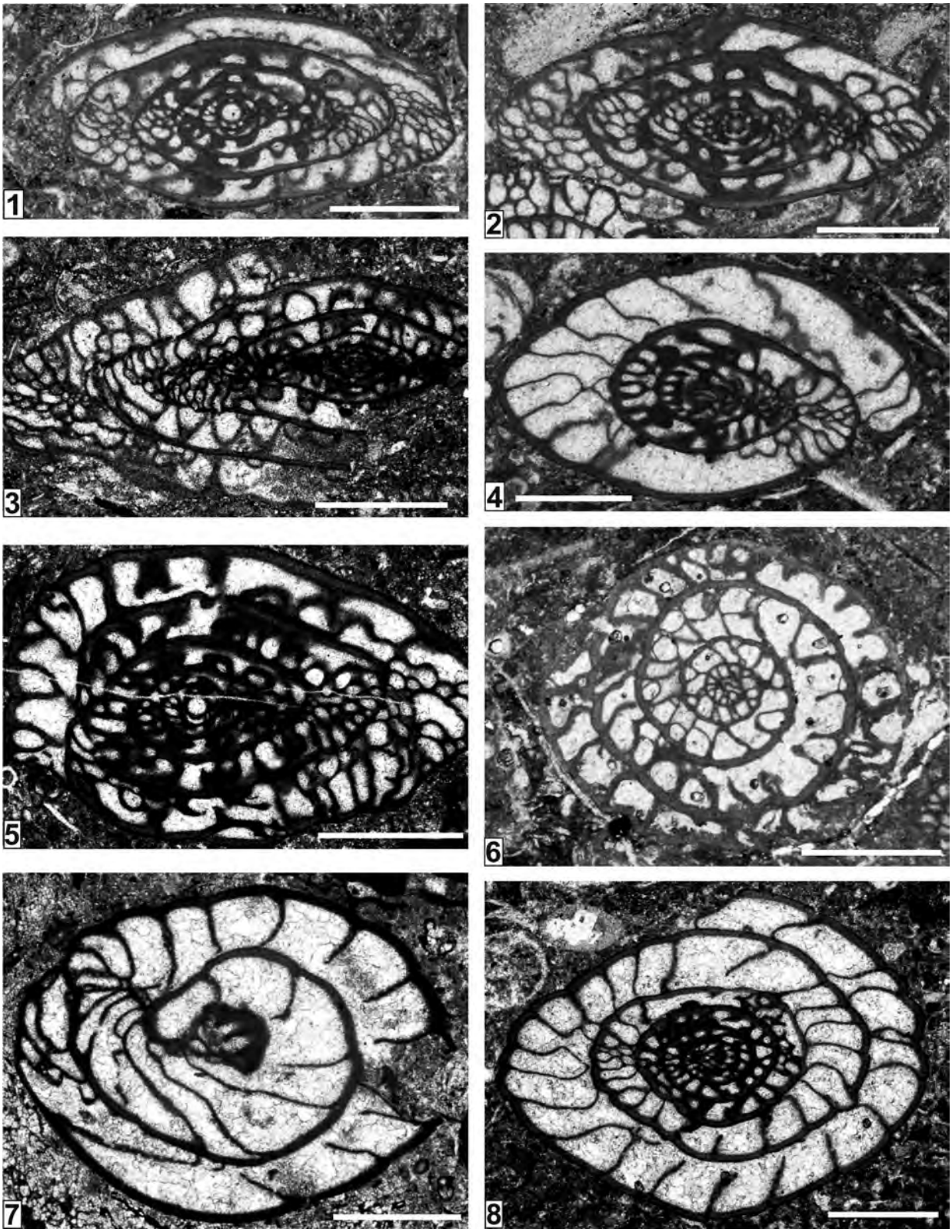


FIGURE 14. Fusulinids of the Community Pit Formation at the Flood section. Scale bars = 1.0 mm. **1-2,** *Leptotriticites* cf. *hughesensis* (Thompson). 1. Axial section. Sample 010-040e. 2. Subaxial section. Sample 010-040f. **3,** "*Pseudoschwagerina*" *texana* Dunbar and Skinner. Subaxial section. Sample 40-5-1. **4,** *Pseudoschwagerina* aff. *needhami* Thompson. Oblique section. Sample 40-6-4. **5,** *Leptotriticites* sp. 3. Deformed axial section. Sample 010-040c. **6,** *Paraschwagerina*? aff. *phrenessa* Wilde. Subtransverse section showing the phrenothecae. Sample 010-049a. **7,** *Pseudoschwagerina* ex gr. *uddeni* (Beede and Knicker). Oblique tangential section. Sample 72-1-3-2. **8,** *Pseudoschwagerina* cf. *morsei* Needham. Oblique subtransverse section. Sample 010-040.

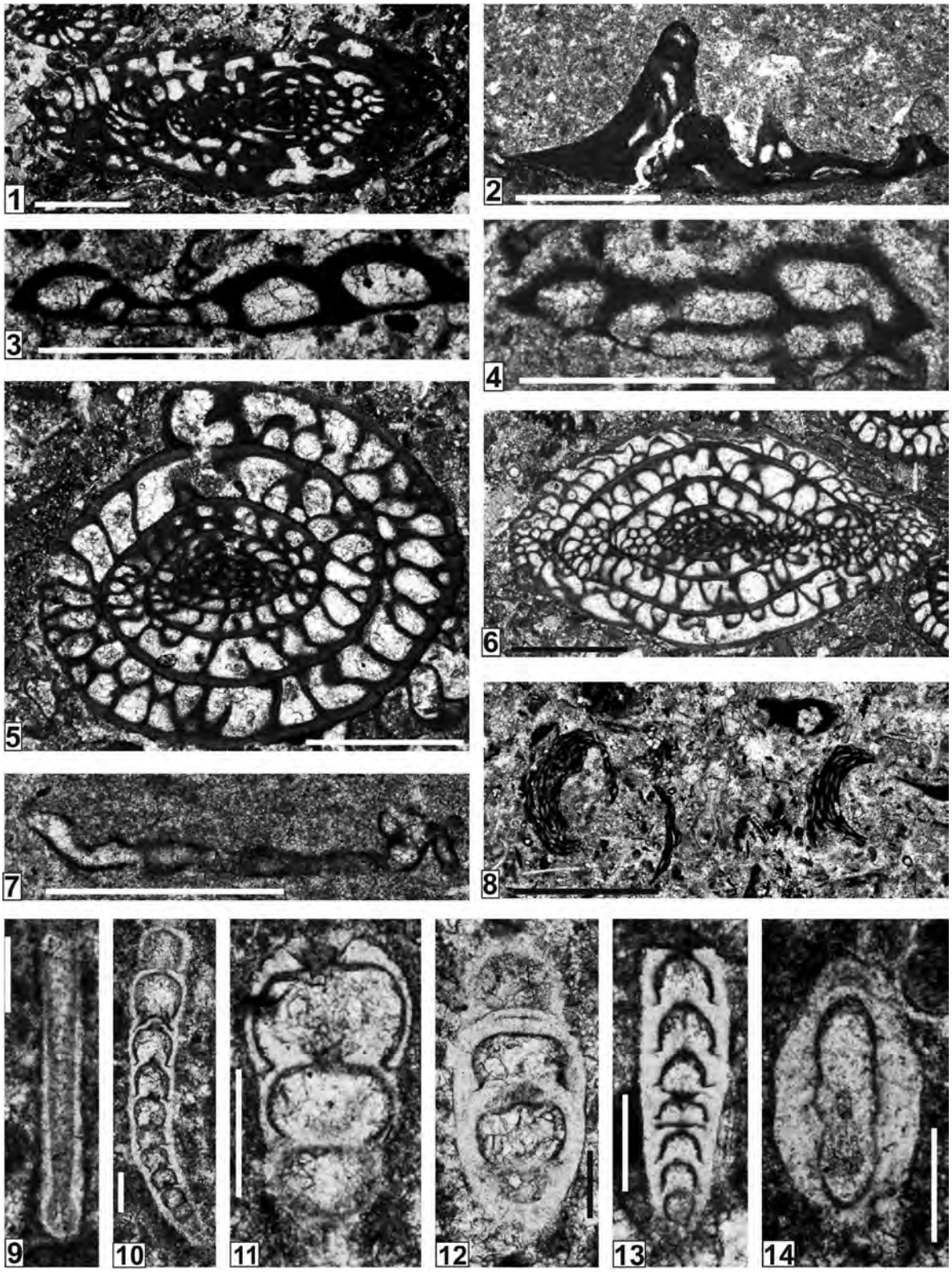


FIGURE 15. Algae, microproblematica, fusulinids and smaller foraminifers of uppermost Horquilla and Shalem Colony formations (Indian Springs Canyon, and Monument North sections). Scale bars: Figs. 1, 2, 5, 6, 14 = 1.0 mm, Figs. 3, 4, 13 = 0.5 mm, Figs. 7–12 = 0.1 mm; FLD = Flood, ISC = Indian Springs Canyon, MON = Monument North. **1,** *Leptotriticites* sp. 4. Subaxial section. Sample ISC 28-10. **2,** *Tubiphytes* ex gr. *obscurus* Maslov. Longitudinal section. Sample MON 1-6a. **3-4,** *Hedraites plummerae* Henbest. Axial section. Sample ISC 28-9. 4. Subaxial section. Sample ISC 21-14. **5-6,** *Paraschwagerina* cf. *acuminata* Dunbar and Skinner. 5. Oblique section. Sample MON 1c-9. 6. Subaxial section. Sample MON 1a-11. **7,** *Orthovertella* sp. Subaxial section. Sample ISC 13-4. **8,** *Ellesmerella* cf. *subparallella* (Flügel and Flügel). Various sections in the microfacies. Sample MON 2-1. **9,** *Syzrania confusa* Reitlinger. Axial section. Sample ISC 1-4. **10,** *Nodosinelloides longa* (Lipina). Axial section. Sample ISC 17-7. **11,** *Protonodosaria* cf. *irwinensis* (Howchin sensu Palmieri). Subaxial section. Sample ISC 109-10. **12,** *Nodosinelloides pinardae* Groves and Wahlman. Subaxial section. Sample ISC 28-3. **13,** *Nodosinelloides*? *pseudoovoidea* (Lipina). Axial section. Sample ISC 127-2. **14,** *Geinitzina*? sp. Transverse section. Sample ISC 109-11.

sp. (Fig. 15.7), *Hedraites plummerae* Henbest (Fig. 15.3-4), *H.* "cf. *graiferi*" (Baryshnikov) sensu Vachard and Krainer, 2001b (Fig. 21.1); *H.* n. sp. cf. "*Lituotuba* (?)" sensu Bogush and Yuferev, (1966, pl. 2, figs. 8-13) (Fig. 12.21-22), *Hemigordius*? sp., *Syzrania gigas* Stepanova (Fig. 12.11), *S. confusa* Reitlinger (Fig. 15.9), *Syzranella* cf. *higginsi* Pinard and Mamet, *Tezaquina clivuli* Vachard (Fig. 21.11), *Vervilleina bradyi* (Spandel) (Fig. 12.17), *Protonodosaria* aff. *globifrondina* Sellier de Civrieux and Dessauvagie (Fig. 12.16), *P.* cf. *irwinensis* (Howchin sensu Palmieri) (Figs. 12.18, 15.11), *Nodosinelloides* cf. *potievskayae* Mamet and Pinard (Fig. 12.8), *N. shikhanica* (Lipina) (Fig. 12.7, 9-10, 15?), *N. longa* (Lipina) (Figs. 15.10, 22.18), *N.* cf. *aequiampla* (Lipina), *N.* cf. *pinardae* Groves and Wahlman (Fig. 15.12), *N.*? *pseudoovoidea* (Lipina) (Fig. 15.13), *Geinitzina linguliformis* (Lipina) (Fig. 12.19), *G.* sp. (Fig. 21.12), and *G.*? sp. (Figs. 15.14, 21.2-5).

Calcareous algae: They are locally present, mainly phylloid algae that are completely recrystallized and therefore undeterminable; nevertheless, some *Anchicodium funile* Johnson (Fig. 12.2) and *Calcipatera* sp. (Fig. 21.18) were identified. Rarely, *Bacinella* sp. (Fig. 12.26), *Epimastopora* ex gr. *alpina* Pia (Figs. 12.3, 21.16), *Archaeolithophyllum lamellosum* Wray (Fig. 9B) and *Efluegelia johnsoni* (Flügel) ex Vachard (Fig. 12.14) are present.

Microproblematic foraminifers and/or algae: The girvanelliform, encrusting miliolate, nubeculariid-like foraminifers appear with *Ellesmerella* cf. *permica* in Indian Springs Canyon units 85 and 87 (Fig. 9C), and are rapidly replaced by *Ellesmerella* cf. *subparallela* (Flügel and Flügel) observed in the upper part of the Indian Springs Canyon section (unit 135; Fig. 12.4-6) and near the base of the Monument North section (units 1 and 2) (Figs. 13.7, 15.8). *Tubiphytes* is present with the first specimens of the group *T. obscurus* Maslov in a few wackestone and grainstone samples (Fig. 15.2). Oncoids are frequent in the form of skeletons encrusted by *Girvanella* (Fig. 21. 1, 17), rivulariaceans (Fig. 12.1), *Ellesmerella* and other calcivertellids (Fig. 9B), and rare *Efluegelia*.

Depositional Environments

The carbonate microfacies types of the Shalem Colony Formation belong to the following Standard Microfacies Types (SMF) of Wilson (1975) and Flügel (2010): SMF 5 (allochthonous bioclastic grainstone, rudstone, packstone, floatstone), indicating deposition adjacent to reef mounds (FZ 6) or inner ramp settings; SMF 10 (bioclastic packstone and wackestone with abraded and worn skeletal grains), indicating an open marine shelf setting (FZ 7) or inner to mid-ramp setting; SMF 11 (coated bioclastic grainstone), indicating deposition in areas of normal marine salinity and constant wave action at or above the fair weather wave base (winnowed platform edge sands; FZ 6)--coatings by microborers that typically form in very shallow environments; SMF 13 (oncoid rudstone and grainstone) is common in open-marine, winnowed edge-sand areas (FZ 6) and open shelf lagoons (FZ 7) or shallow inner ramp settings; SMF 15 (oolitic grainstone with tangential structures) indicates high-energy settings (FZ 6) such as oolitic shoals or shallow inner ramps; SMF 16 (non-laminated peloidal grainstone) commonly forms in shallow platform interiors with protected shallow marine environments of moderate water circulation (FZ 8) or inner ramp settings; SMF 18 (bioclastic grainstone and packstone with abundant benthic foraminifers) is typical of restricted platform environments (FZ 8), shelf lagoons with open circulation (FZ 7) or inner ramp settings; SMF 21 (fenestral bindstone) indicates deposition in inter- to supratidal environments or restricted lagoons (FZ 8); and SMF 22 (oncoid floatstone and wackestone) is formed in low-energy environments of shallow lagoons and tidal zones (FZ 8).

The SMF types recognized within the Shalem Colony Formation indicate that the limestones formed adjacent to platform margin algal-reef-mound environments (FZ 5) and platform margin sand shoals (FZ 6), mostly in platform interior environments of open, normal marine to (less common) restricted marine settings (FZ 7 and 8). Sandstones are interpreted to have formed in high-energy sand shoal environments.

The mostly covered intervals of the Shalem Colony Formation are more difficult to interpret depositionally. Many of them likely represent shale, which may have been deposited in an offshore environment. At the Robledo Mountain section (see Krainer et al., this volume), there are several limestone surfaces in the Shalem Colony Formation that contain rhizoliths and calichification indicative of subaerial exposure. These surfaces can be interpreted as the tops of shallowing-upward cycles driven by glacio-eustasy (Krainer et al., this volume). However, in the Shalem Colony Formation in general, the alternation of limestone and covered/shale intervals could also be the product of non-glacial eustatic sea-level changes caused by tectonic subsidence or uplift in the hinterland and increased siliciclastic input.

Community Pit Formation

Above the Shalem Colony Formation, the Community Pit Formation is mostly a slope-forming interval of shale beds intercalated with relatively thin intervals of limestone, many of which are micritic and dolomicritic mudstones (Figs. 16-20). The bedrock of the formation has a characteristic brownish gray to grayish orange color and forms thick slopes between the cliff- and ledge-forming outcrops of the Shalem Colony and Robledo Mountains formations (Fig. 16A). Typically, its base is a shale slope above the stratigraphically highest, relatively thick (3-5 m) limestone interval of the Shalem Colony Formation (Figs. 7-8).

Jordan (1971, 1975) estimated the thickness of the Community Pit Formation (i.e., his middle member of the Hueco Formation) as 61 m in the Robledo Mountains. Seager et al. (2008) estimated a thickness of 177 m (= 122 m of their middle member, plus 50 m of the upper part of their lower member, see earlier discussion). At the type section in the Robledo Mountains, an incomplete section of the Community Pit Formation is 59 m thick (Lucas et al., 1998c). However, Jordan's estimate and the type section are in the northeastern part of the range. A complete section of the Community Pit Formation to the southwest, at Indian Springs Canyon, is 93 m thick (Fig. 7). At the Monument North section (Fig. 8), the lower part of the Community Pit Formation is ~ 53 m thick. The rhyolitic sill at the top of that section is under the base of the Flood section, where the Community Pit Formation (no base is exposed) is ~ 91 m thick (Fig. 17). If the sill is simply injected along a bedding plane in the Community Pit Formation, then the formation is ~ 146 m thick in the northern part of the PTNM. In the Doña Ana Mountains, Krainer et al. (2005, 2009) reported a thickness of 108-156 m. Thus, it seems that a range in thickness of the Community Pit Formation from 93 to 177 m is supported by available data. Jordan's thickness estimate is too low.

At the type section, 42% of the Community Pit Formation is formed by slope-forming shale (Lucas et al., 1998c). Ledge-forming limestone is mostly composed of packstone (26%) and mudstone (19%). Grainstone (11%) and calcarenite (2%) are common near the top (Lucas et al., 1998c). At other localities in the Robledo Mountains (Figs. 16-18), measured thickness ranges from 53 m to 92.6 m: (1) Indian Springs Canyon, 92.6 m, a complete section with the contacts to underlying and overlying formations exposed (Fig. 7); (2) Flood, 90 m, a minimum, underlain by a rhyolitic sill, overlain by the Robledo Mountains Formation (Fig. 17); (3) Orin, 81 m, base and top not exposed, though the section evidently ends very close to the base of the overlying Robledo Mountains Formation (Fig. 18); (4) Upper Branson Canyon (an informal name), 60 m, base not exposed (Fig. 18); (5) Dead Man´s Curve, 60 m, base not exposed (Fig. 18); and (6) Monument North, 53 m, underlain by Shalem Colony Formation, overlain by a rhyolitic sill (Fig. 8).

At Indian Springs Canyon, which we regard as a reference section of the Community Pit Formation (Fig. 7), shale constitutes 11.3% of the total thickness, covered intervals (presumably shale) 56.4%, sandstone/conglomerate 0.4% and limestone 31%. The amount of covered intervals (shale) in the studied sections ranges from 44% at Upper Branson Canyon to 77% at Monument North, and the amount of limestone ranges from 23% at Monument North to 52% at Upper Branson Canyon. Covered intervals are up to 6.6 m thick (Monument North), and shale intervals are up to 6.2 m thick (Indian Springs Canyon).

Limestone units range in thickness from 0.2 to 5.4 m at Indian Springs Canyon. At Upper Branson Canyon, the section with the greatest amount of limestone, limestone units are up to 8.3 m thick. In all the sections, most of the limestone units are less than 2 m thick. Locally (Orin, Indian Springs Canyon, and Dead Man´s Curve), a few carbonate sandstone and conglomerate beds (0.1-0.7 m thick) are intercalated. At Upper Branson Canyon, a 2.5-m-thick carbonate breccia is intercalated in the upper part of the formation.

Limestone occurs as thin individual beds or thin- to medium-bedded limestone units, partly containing chert nodules. Bedding is commonly even. Wavy bedded to nodular limestone is very rare and forms less than 1-m-thick intervals at Upper Branson Canyon and Dead Man´s Curve. Massive algal limestone up to 1.9 m thick (Indian Springs Canyon) is very rare. Most limestone intervals display a muddy texture; sandy limestone and laminated limestone are subordinate. At Indian Springs Canyon, many dolomitic limestone (dolomicrite) intervals are present. Limestone units containing chert nodules are rare (Orin,

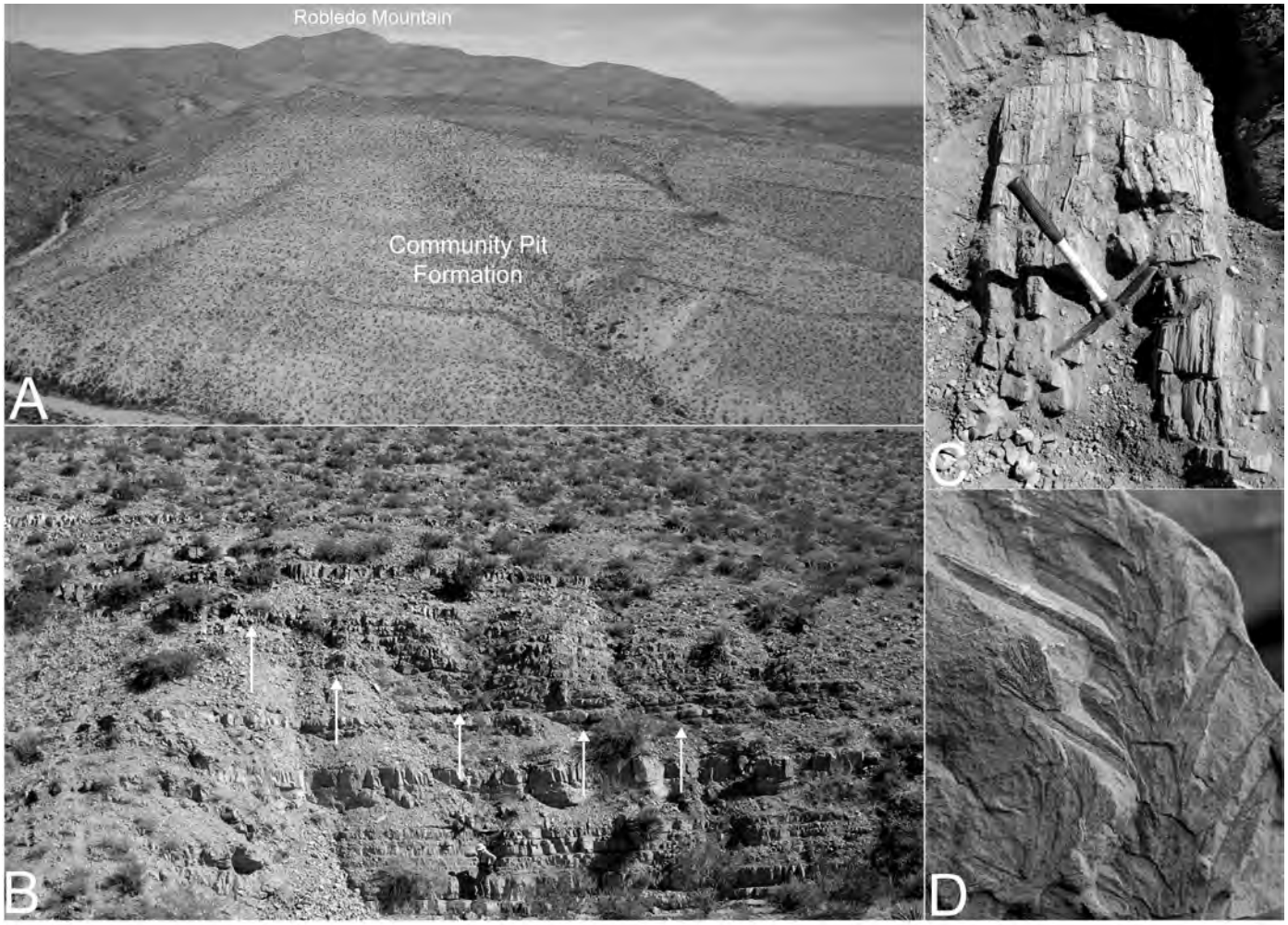


FIGURE 16. Photographs of selected outcrops of the Community Pit Formation in the Robledo Mountains. **A,** Overview of Community Pit Formation outcrops just north of the Prehistoric Trackways National Monument, with Robledo Mountain on the skyline. **B,** Incised channel in Community Pit Formation at Flood section. Arrows mark incised surface (see Fig. 19). **C,** Fossil log in Community Pit Formation (photograph courtesy of Jerry MacDonald). D, Fossil foliage at Flood section (photograph courtesy of Jerry MacDonald).

Flood, Indian Springs Canyon, Dead Man´s Curve) to almost absent (Upper Branson Canyon, Monument North) at most of the sections we measured. Chert nodules in limestone are most abundant at Dead Man´s Curve.

Shale in the Community Pit Formation is medium gray, olive gray and brownish gray, weakly to strongly fissile, and calcareous. Thin interbeds, lenses and/or nodules of limestone are commonly present. Some shale layers in the Community Pit Formation are gypsiferous, and there may be some bedded gypsum in these strata.

Flood

At the Flood locality, an incomplete section of the Community Pit Formation has a thickness of 90 m (Fig. 17). The succession rests on a Tertiary rhyolitic sill and is overlain by ripple-laminated, fine-grained red sandstone at the base of the Robledo Mountains Formation.

The Community Pit Formation at Flood consists of bedded limestone intervals and thicker limestone beds alternating with shale intervals and covered intervals. Bedded limestone intervals are 0.2 to 5.9 m thick. Limestone is dominantly thin bedded (5-30 cm), and, rarely, thicker bedded limestone and massive limestone beds up to 1.2 m thick are present. Limestone is dominantly gray to dark gray lime mudstone, and subordinate grainy limestone (wackestone to packstone). Bedded cherty limestone intervals are rare in the middle part of the section.

In the lower part of the section, two sandy carbonate conglomerate beds, 1.2 m (Fig. 17, unit 22) and 0.7 m thick (Fig. 17, unit 24) are intercalated. Shale intervals in the lower part of the section are up to 2.2 m thick; covered intervals (most are probably shale) are up to 5.8 m thick. Fossils observed on outcrop are brachiopods, gastropods (upper part), calcareous algae (upper part), rare bryozoans, plant foliage, mostly conifers (lower part, unit 19; Fig. 16D), and fossil wood (upper part, units 74 and 77).

In the Flood section, fossil wood and foliage (Figs. 16B, 19) is preserved in a 5-6 m deep channel, cut into a succession of shale, limestone and dolomite. The channel cuts down from a horizon about 15.5 m above the base of the section (Fig. 19). Measured on an east-west outcrop, sub-perpendicular to the channel axis, the apparent channel width is approximately 140 m (Fig. 19). The eastern channel margin appears steeper than the western margin, but this may be an artifact of outcrop orientation. In addition, the western margin is truncated by a fault.

Seven sections (Fig. 19A-G) were measured across the channel. Two distinct units filling the channel, each containing a different fossil plant assemblage, were recognized. The basal unit, which is only in the central part of the channel (Fig. 19, sections B-E), is a lens of limestone pebble-to-cobble conglomerate, 0.05-1.1 m thick, and is a rudstone composed mostly of sub-angular to sub-rounded, elongate clasts of gray-orange lime mudstone, 20-150 mm long, and accumulations of detrital crinoids and bryozoans (locally comprising multiple, cemented, randomly arranged fossil fragments, clearly reworked from underlying beds), within a poorly sorted matrix of medium- to coarse-grained mixed carbonate-siliciclastic sandstone and mudstone. Specimens of coalified tree-trunks, up to 0.17 m in diameter, co-occur with cubic, sub-rounded, 20-50 mm diameter blocks of charcoalified wood in the basal rudstone (see DiMichele et al., this volume; Falcon-Lang et al., this volume).

The middle unit, up to 4 m thick, is more laterally extensive, and oversteps the margins of the underlying rudstone. Lime mudstone beds, up to 1.4 m thick, displaying undulatory or wavy lamination are

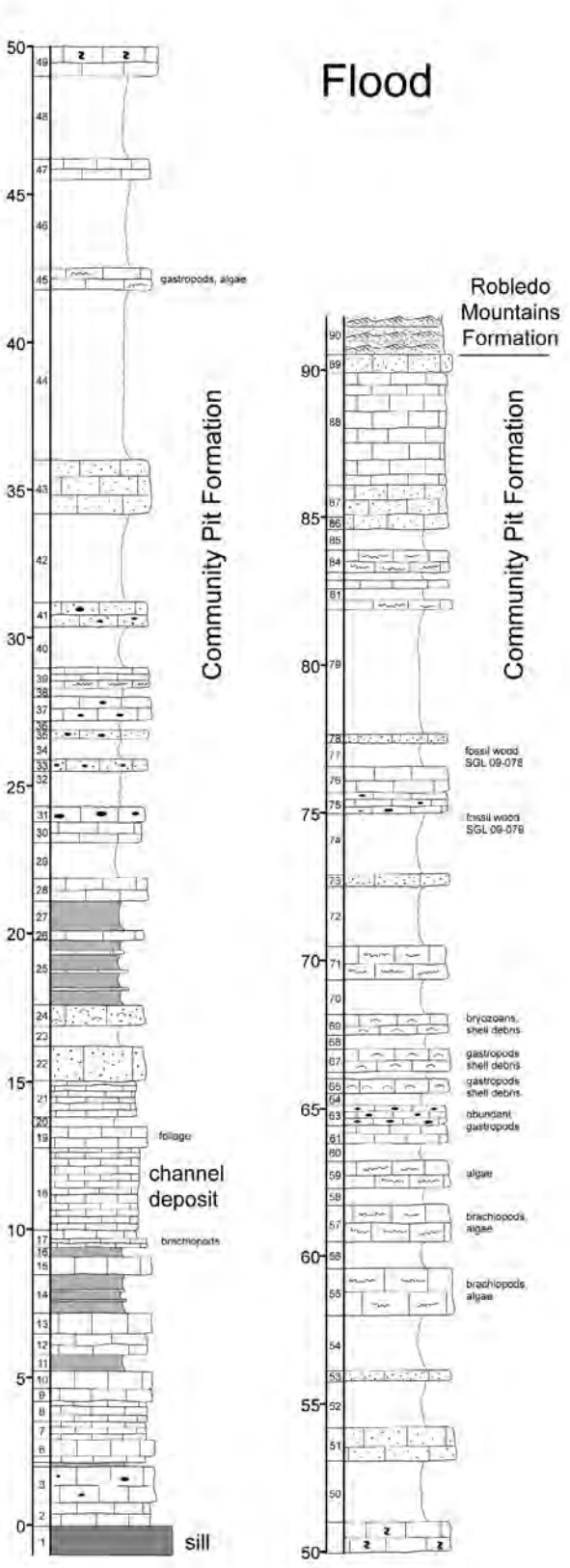


FIGURE 17. Measured stratigraphic section of part of the Community Pit Formation at Flood (see Figure 4 and Table 1 for location of section). See Figure 8 for legend to lithologic symbols.

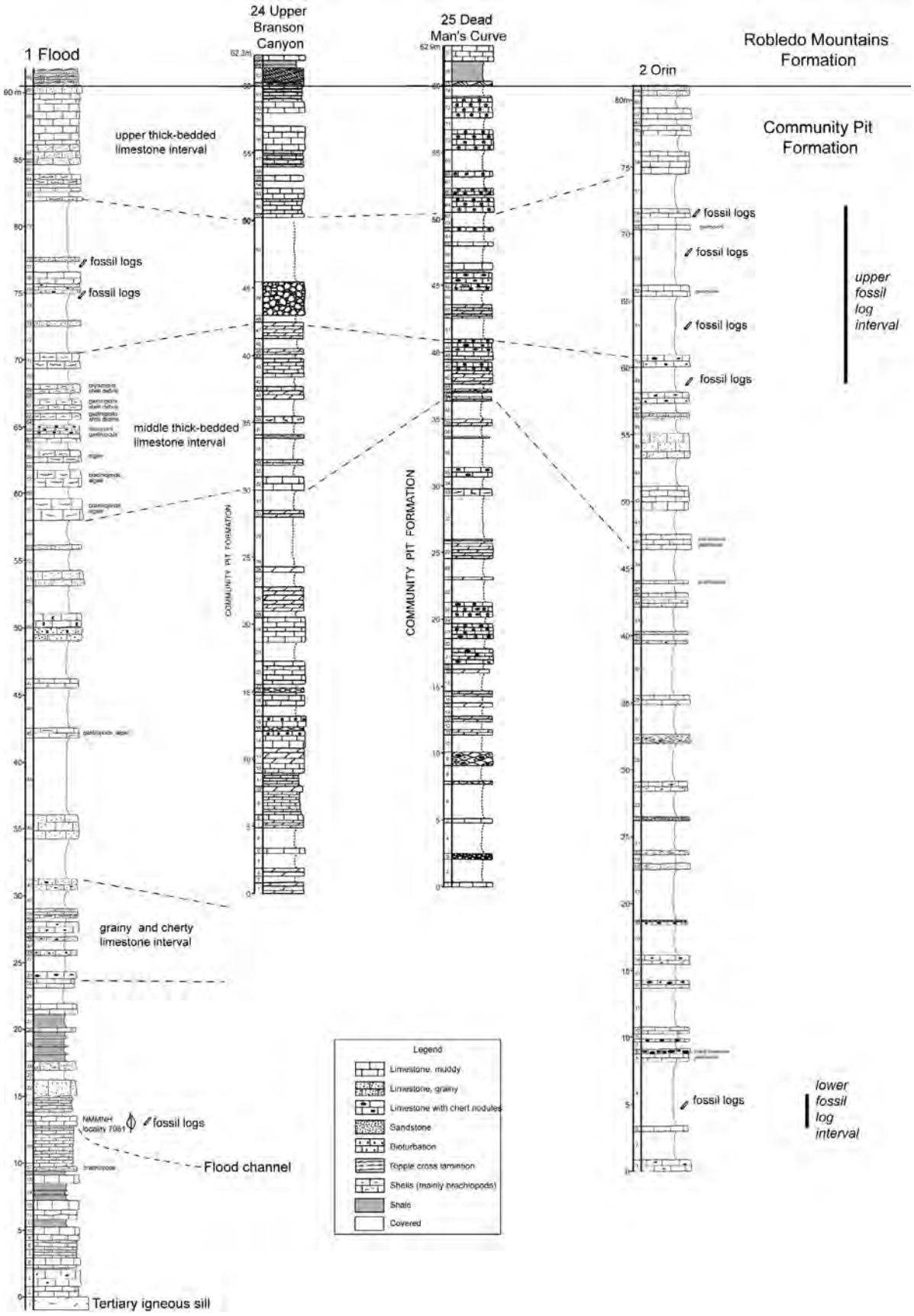


FIGURE 18. Correlation of measured stratigraphic sections of part of the Community Pit Formation from Flood through Orin (see Figure 4 and Table 1 for locations of sections).

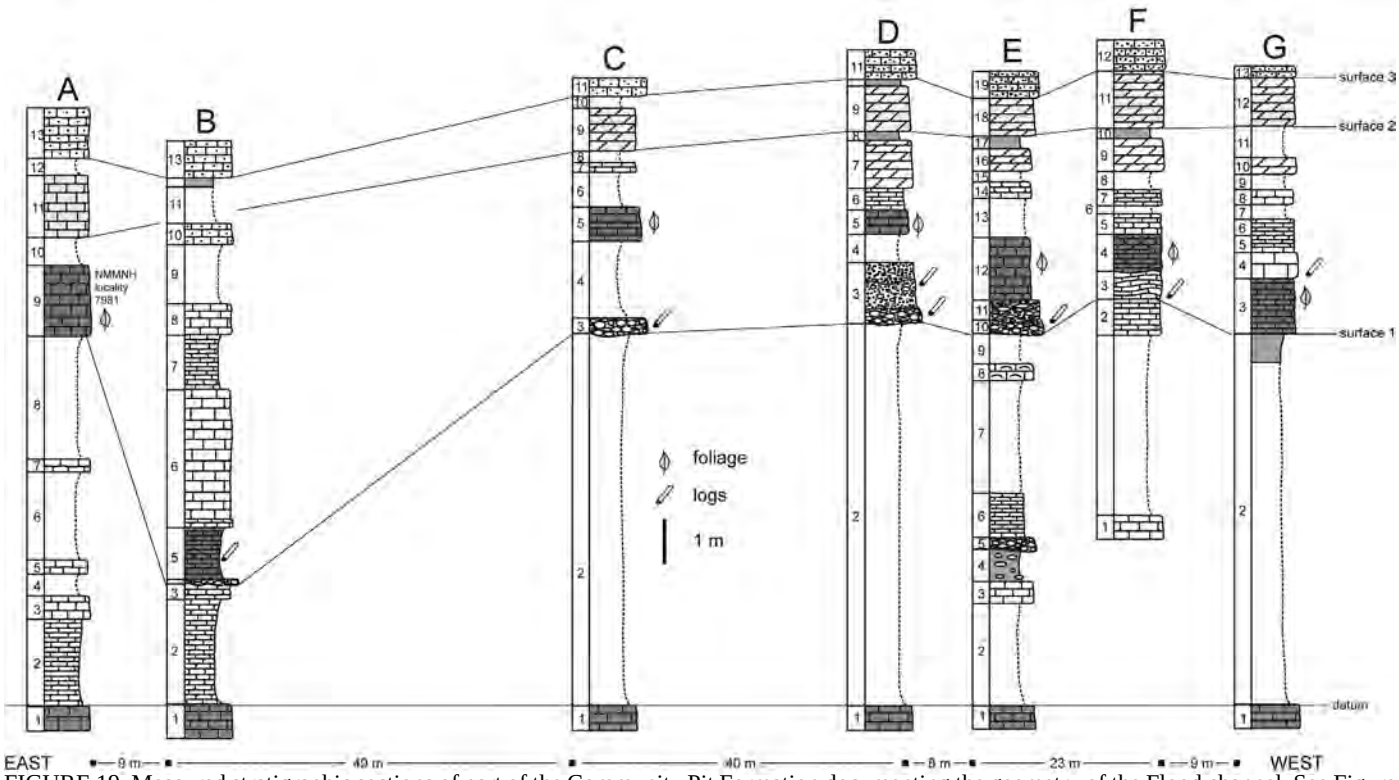


FIGURE 19. Measured stratigraphic sections of part of the Community Pit Formation documenting the geometry of the Flood channel. See Figure 8 for legend to lithologic symbols.

the most prominent feature of this unit. These beds contain scattered pectinid bivalves and rare lingulid brachiopods, and show horizons with vertical burrows. Also present at multiple horizons are rooted zones associated with adpressed megaflora. A few weakly calcified tree-trunks, up to 0.18 m in diameter and > 1.4 m long, occur in the undulatory beds. These logs have an orientation sub-perpendicular to the channel margins. In addition, there are poorly exposed siliciclastic shale beds and a single, thin calcarenite lens, 0.14 m thick and several meters wide. The calcarenite, which contains some medium- to coarse-grained siliciclastic sand and shows climbing ripple cross-laminations, is confined to the central part of the channel (Fig. 19, section B). The uppermost channel-fill unit is a distinctive yellow dolomite, up to 1.2 m thick, showing prominent calcite-filled vugs and nodular gypsum.

A very important aspect of this channel is its local nature. To the west of the outcrops measured (Fig. 19), there is no evidence of it. Thus, at the Orin section, about 3 km to the northwest, no evidence of a surface (unconformity?) corresponding to the base of the channel can be seen on outcrop (Fig. 18).

Orin

At the Orin section of the Community Pit Formation (Fig. 18), covered (shale) intervals comprise 72.3%, limestone 26%, sandstone 0.9% and conglomerate 0.8% of the section. Covered intervals are 0.4-4.4 m thick. In mostly covered shale intervals near the base and in the upper part of the section, fossil logs are present (Fig. 16C). Limestone intervals are 0.2-1.8 m thick. Thicker limestone intervals are thick bedded. A few limestone intervals contain chert nodules. Brachiopods and gastropods are observed in limestone mainly in the upper part of the section. Two thin carbonate conglomerates (each 0.3 m thick) are intercalated in the lower part of the section. A crossbedded carbonate sandstone bed (0.7 m thick) is intercalated 32 m above the base. The top of the Orin section is, within resolution, very close to the top of the Community Pit Formation.

Upper Branson Canyon

At Upper Branson Canyon (Fig. 18), the Community Pit Formation is at least 60 m thick; the contact with the underlying Shalem Colony Formation is not exposed. This section is dominated by limestone and dolomitic limestone (51.9% of the exposed section); covered intervals comprise 44%; and a limestone breccia (Fig. 18, unit 49) is 4.1% of the section. Limestone intervals are commonly 0.2-2 m thick, and, in the lower part, an 8.8-m-thick limestone succession is present. Limestone occurs as individual limestone beds, thin-bedded and thick-bedded limestone intervals and rarely as thin, nodular limestone. Chert is absent. A few limestone beds contain crinoidal debris and a few brachiopods. One bed (unit 32) contains abundant echinoid spines and one bed (unit 38) has calcareous algae. Many limestone beds are dolomitic (dolomicrite). Covered intervals (shale) are 0.2-4.7 m thick. The boundary with the overlying Robledo Mountains Formation is drawn at the base of the first red sandstone bed.

Dead Man´s Curve

At Dead Man´s Curve (Fig. 18), the exposed thickness of the Community Pit Formation is 60 m. The contact with the underlying Shalem Colony Formation is not exposed; the boundary with the overlying Robledo Mountains Formation is at the base of the first red, ripple-laminated sandstone bed.

Covered intervals (shale) comprise 60.8%, limestone is 38.5% and conglomerate is 0.7% of the exposed section. Limestone intervals are 0.1-1.5 m thick and are represented by individual limestone beds (0.1-0.5 m), thin- to medium-bedded limestone and nodular limestone. Many limestone beds contain chert nodules. Crinoidal limestone is abundant in the upper part of the section. Gastropods and rare brachiopods are present in some beds in the upper part. One algal limestone bed occurs in the middle of the section. Many limestone beds in the lower and middle part are dolomitized (dolomicritic).

Monument North

At the Monument North section (Fig. 8), the exposed thickness of the Community Pit Formation measures 52.8 m. The contact with the underlying Shalem Colony Formation is exposed, but the contact with the overlying Robledo Mountains Formation is not exposed. The section is overlain by a Tertiary rhyolitic sill.

Most of the section (77%) is covered (shale); consequently, limestone forms 23% of the rock volume. Shale is rarely exposed, with thicknesses ranging from 1 to 2.7 m. Covered intervals are 0.2-6.6 m thick. Limestone occurs as single beds (0.1-0.4 m thick), and thin- to medium-bedded limestone intervals are up to 2.3 m thick (mostly < 1 m). Limestone is commonly mudstone; a few beds contain calcareous algae and rare gastropods. Chert nodules are very rare.

Microfacies

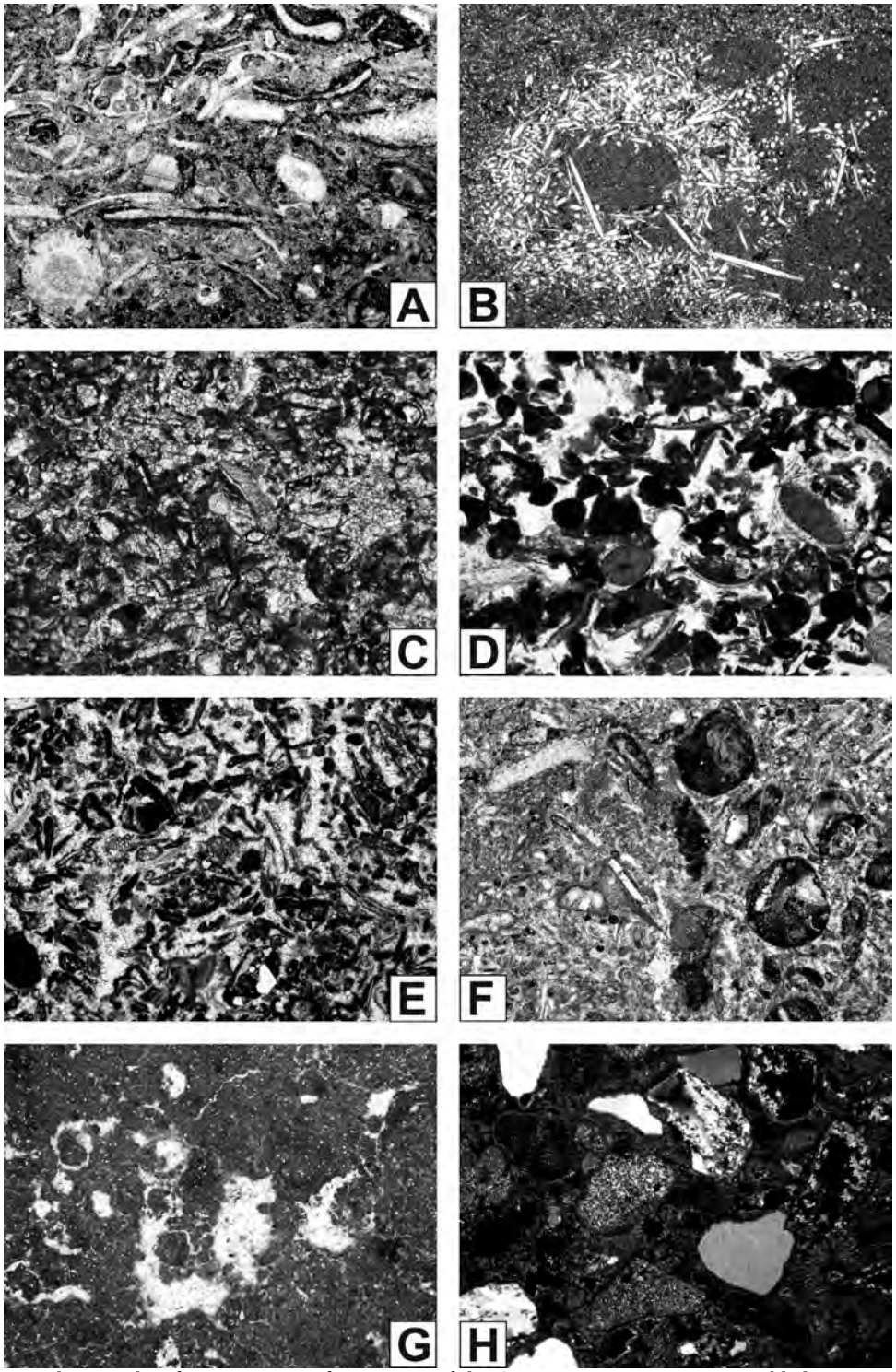


FIGURE 20. Thin section photographs of common microfacies types of the Community Pit Formation, Robledo Mountains. Photographs A-G under plane light, H under polarized light. **A,** Floatstone-rudstone composed of up to several mm diameter bioclasts; some of them display micritic envelopes or are encrusted by cyanobacteria to form oncoids. Monument North, unit 52, width of photograph is 6.3 mm. **B,** Sponge network composed of abundant small monaxone and rare triaxone spicules well preserved in micritic matrix. Monument North, unit 76, width of photograph is 3.2 mm. **C,** Foraminiferal wackestone composed of abundant calcivertellid foraminifers, many ostracodes and a few other fossil fragments. Indian Springs Canyon, unit 199, width of photograph is 3.2 mm. **D,** Grainstone, moderately sorted and poorly washed, containing abundant micritic intraclasts and skeletons of a diverse biota, a few quartz grains and locally some micrite. Indian Springs Canyon, unit 166, width pf photograph is 3.2 mm. **E,** Grainstone composed of peloids, intraclasts, and diverse skeletons, some encrusted by cyanobacteria and tubular foraminifers. Indian Springs Canyon, unit 133, width of photograph is 6.3 mm. **F,** Rudstone containing large intraclasts, large recrystallized shell fragments, many foraminifers and some other fossil fragments. Monument North, unit 41, width of photograph is 6.3 mm. **G,** Paleocaliche: mudstone displaying a nodular texture and containing micritic nodules of various sizes which locally show well-developed circumgranular fissures. Irregular voids are cemented by calcite spar. Indian Springs Canyon, unit 156, width of photograph is 6.3 mm. **H,** Coarse-grained sandstone composed of detrital quartz grains (mostly polycrystalline), some chert grains and few carbonate grains embedded in fine-grained carbonate matrix displaying irregular lamination. Indian Springs Canyon, unit 151, width of photograph is 3.2 mm.

Limestones of the Community Pit Formation are composed of various microfacies types (Fig. 20). The dominant microfacies is wackestone, which occurs as various types and locally grades into packstone and floatstone. Other microfacies such as mudstone, packstone, grainstone, floatstone and rudstone are subordinate.

Bioclastic wackestone is poorly sorted and contains a diverse fossil assemblage, mostly fragmented skeletons floating in micrite and peloidal micrite. Wackestone (spiculite) is subordinate and has abundant small, mostly monaxone sponge spicules and a few other skeletons embedded in peloidal micrite (Fig. 20B). Most of the spicules are calcified, but a few spicules are still siliceous. Wackestone with a low diversity fossil assemblage contains small echinoderm fragments and ostracodes.

Foraminiferal wackestone (Fig. 20C) contains abundant calcivertellids or a more diversified assemblage in peloidal micritic matrix. Wackestone to packstone is moderately sorted and contains a diverse fossil assemblage, many micritic intraclasts and approximately 5% siliciclastic grains, mostly monocrystalline quartz, subordinately chert and rare polycrystalline quartz in micritic matrix. This type locally grades into grainstone.

Poorly sorted crinoidal wackestone to packstone contains micritic intraclasts, and a few peloids in the micritic matrix. Floatstone contains large bivalve shell fragments, gastropods and brachiopods floating in peloidal micrite containing small bioclasts, intraclasts and peloids. Wackestone to floatstone (Fig. 20A) contains abundant, thin shell fragments (bivalves), other skeletons and intraclasts. A few skeletons are encrusted by cyanobacteria. Packstone to grainstone (Figs. 20D-E) is fine grained and moderately sorted, and contains a diverse fossil assemblage, abundant peloids, micritic intraclasts, and locally detrital quartz grains. Locally, the cement is silicified. Foraminiferal grainstone contains abundant tubular foraminifers, other skeletons, micritic intraclasts and peloids. The rock is fine grained, well washed and calcite cemented.

Rudstone (coquina bed: Fig. 20F) at the Flood section contains abundant recrystallized fragments of bivalves and gastropods, other skeletons, and small micritic intraclasts. At the Monument North section, rudstone is poorly washed and composed of dark micritic intraclasts containing fossil fragments, and a diverse, fragmented fossil assemblage.

Peloidal mudstone containing many spicules and some ostracodes is overlain by rudstone (coquina). Peloidal carbonate siltstone contains a few small quartz grains, ostracod shells and small gypsum (?) crystals. The siltstone is bioturbated. Indistinctly laminated, bioturbated silty mudstone containing a few ostracodes is observed in unit 9 of the Flood section (Fig. 17). Mudstone containing a few fossil fragments, particularly ostracodes and sponge spicules, is common in the Monument North section.

Lime mudstone, indistinctly laminated and recrystallized, forms the base of the Flood section (Fig. 17, unit 2). Inhomogeneous mudstone displaying a clotted to nodular texture and irregular voids filled with calcite cement and thin microbial crusts is present in the middle of the Indian Springs Canyon section. Mudstone, partly peloidal, with abundant shrinkage fissures filled with calcite cement occurs in unit 3 of the Flood section (Fig. 17). Nodular mudstone (paleocaliche; Fig. 20G) composed of abundant micritic nodules up to 1 cm in size is present in the Indian Springs Canyon section (Fig. 7, units 146, 156, 170). The mudstone lacks fossils, and contains irregular voids and fissures filled with calcite cement. Locally, circumgranular fractures, also filled with calcite cement, are developed.

Sandstone Petrography

A single bed of sandstone in the Indian Springs Canyon section (Fig. 7, unit 151) is coarse grained and composed of abundant polycrystalline quartz grains and many schistose metamorphic quartz grains, a few chert grains and monocrystalline quartz grains, rare altered and replaced detrital feldspars, rare muscovite and a few micritic rock fragments (Fig. 20H). Grains are embedded in fine-grained, locally laminated carbonate matrix. Siltstone is composed of carbonate and quartz grains and rare muscovite, and is locally bioturbated.

Fossil Assemblage

On outcrop, fossils observed in the Community Pit Formation are mostly brachiopods, gastropods and crinoid debris. Microfacies (wackestone, packstone, grainstone, floatstone, rudstone) with a high biological diversity contain echinoderms (mostly crinoid ossicles), gastropods, brachiopods, rare bryozoans, calcareous algae (*Epimastopora*), palechinid radioles, bivalve shells, ostracodes, smaller foraminifers and rare fusulinids (listed below and illustrated in Figs. 21-23). Sporadically, microconchiids (previously misinterpreted as *Spirorbis* annelids) are common, and there are skeletons encrusted by *Girvanella*.

Spiculite wackestone contains a low diversity assemblage of sponge spicules (mostly monaxone), a few foraminifers (*Globivalvulina*) and ostracodes. In foraminiferal wackestone, calcivertellid foraminifers are the most common bioclasts, whereas *Globivalvulina*, recrystallized shell fragments, echinoderms, ostracodes and brachiopods are subordinate.

Low diversity grainstone contains recrystallized shell (?bivalve) fragments and gastropods. Low diversity wackestone mostly contains small echinoderm fragments and ostracodes. Mudstone yields only rare ostracodes, echinoderms and bivalve shells. At Monument North, mudstone beds contain monaxone spicules (and some connected networks; Fig. 20B), rare echinoderm fragments, gastropods and calcivertellids.

Fusulinids: Unit 135, near the base of the Community Pit Formation of the Indian Springs Canyon section (Fig. 7), contains the stratigraphically highest, regionally diversified assemblage of fusulinids, with "*Nankinella*?" cf. *loiensis* Igo, Ueno and Sashida (Fig. 11.11-15), *Thompsonites*, transitional forms towards *Pseudoschwagerina*, and true *Pseudoschwagerina* represented by *Pseudoschwagerina* cf. *needhami* Thompson (Fig. 11.8-10). Stratigraphically higher, the fusulinid assemblages are poorer and less diversified: (1) two levels of the Flood section (Fig. 17, units 40 and 49) contain *Paraschwagerina*? aff. *phrenesa* Wilde (Fig. 14.6), *Pseudoschwagerina* spp. (Figs. 11.8-10, 14.4, 7-8, 21.7, 15), and "*P.*"? *texana* Dunbar and Skinner (Fig. 14.3); and (2) the upper beds of the Community Pit Formation yielded only *Oketaella* n. sp. aff. *waldrupensis* Thompson (Fig. 22.6-8), which possibly appears early, in Indian Springs Canyon unit 133 (Fig. 21.8), a schubertellid *Grovesella*? sp. (Fig. 21.9-10), and an indeterminate staffellid (Fig. 22.21).

Smaller foraminifers: *Earlandia* ex gr. *elegans* (Rauzer-Chernousova and Reitlinger) (Fig. 22.15), *Globivalvulina novamexicana* Vachard, Krainer and Lucas (Fig. 23.3), *G. parapiciformis* Vachard, Krainer and Lucas, *G. praegraeca* Vachard, Krainer and Lucas (Fig. 22.1-5, 23.4), *G. retroseptata* Vachard, Krainer and Lucas, *Spireitlina* sp., calcivertellids, *Orthovertellopsis calcitornellaeformis* Vachard, Krainer and Lucas (Fig. 23.11), *Cornuspira* sp., *Hemigordiellina*? sp. (Fig. 23.14), *Glomomidiella*? sp. (Fig. 23.1-2), *Syzrania confusa* Reitlinger (Fig. 23.7), *Protonodosaria* cf. *pirula* (Miklukho-Maklay) (Fig. 23.17), *P.* cf. *globifrondina* Sellier de Civrieux and Dessauvagie (Fig. 23.19), *P.*? sp. (Fig. 22.11), *Nodosinelloides longa* (Lipina) (Fig. 23.18); *N.* cf. *netschajewi* (Chernyntsev) (Figs. 21.5, 22.19), *N. subquadrata* (Lipina) (Fig. 22.10), *N.* cf. *ronda* (Fig. 23.9, 13), *N.* cf. *longissima* (Suleimanov) (Fig. 22.17), *N.* cf. *aequiampla* (Lipina), *N.* cf. *pinardae* (Fig. 23.5), "*Tauridia*" aff. *nudiseptata* Gaillot and Vachard (Fig. 22.18), *Geinitzina* cf. *indepressa* Cherdyntsev (Fig. 22.20), *G.* cf. *postcarbonica* Spandel (Fig. 23.10), *G.* cf. *spandeli* Cherdyntsev (Fig. 21.6), *G.* sp. 1 (Fig. 21.2-4), *G.* sp. 2 (Fig. 21.12), *G.*? sp. (Figs. 22.9, 23.6), *Pseudolangella*? sp. (Fig. 23.15), *Pachyphloia*? cf. *densa* (Lipina) (Fig. 22.12-13), *P.*? aff. *cubanica* (Miklukho-Maklay) (Fig. 22.16), *Nodosaria* cf. *camerata* (Miklukho-Maklay) (Fig. 23.8), and *N.*? sp. (Figs. 22.14, 23.16).

Depositional Environments

In the Community Pit Formation, limestone with a low-diversity fossil assemblage and muddy texture indicates deposition in a shallow-marine, low-energy restricted environment, whereas limestone containing a high-diversity normal marine fossil assemblage and dominantly muddy texture points to deposition in a shallow, low-energy, open marine environment with normal salinity. Microfacies indicating high-energy conditions such as grainstone are very rare.

In general, limestones in the lower part of the Community Pit Formation indicate dominantly restricted marine conditions, and in the upper part more open marine conditions. Crossbedded, coarse-grained sandstone and limestone conglomerate are interpreted as tidal channel deposits. Compared to the Community Pit Formation in the Doña Ana Mountains (Krainer et al., 2009), limestones with a low-diversity fossil assemblage such as mudstone, peloidal mudstone and wackestone, and ostracodal mudstone to wackestone, are less abundant at the Flood section, whereas limestones containing a diverse fossil assemblage are more abundant. This indicates that during deposition of the Community Pit Formation at Flood, shallow, open-marine conditions were more prevalent, particularly in the upper part of the section, than in the Doña

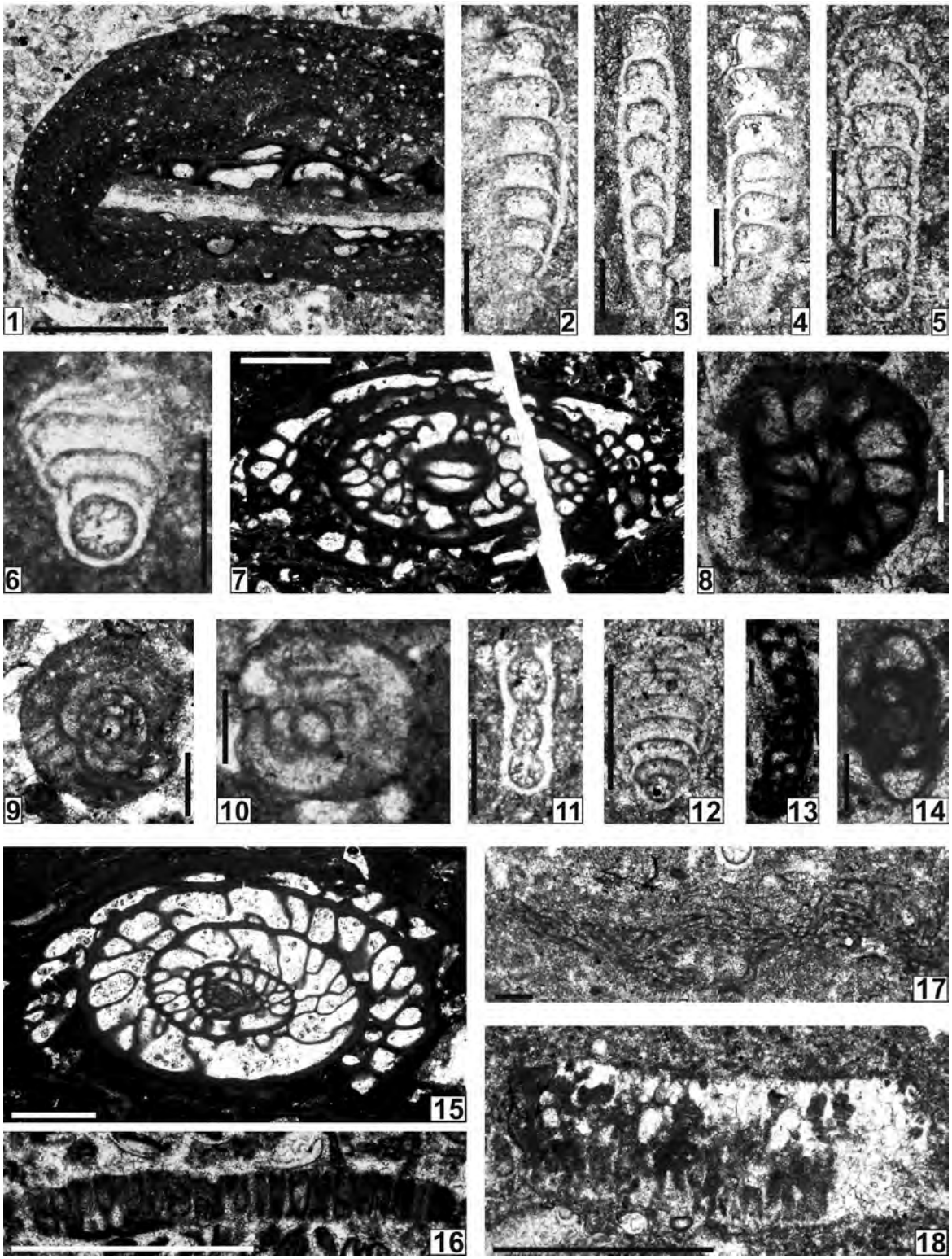


FIGURE 21. Microfossils from the lower Community Pit Formation, Shalem Colony Formation and uppermost Horquilla Formation. Scale bars for Figs. 1, 7, 15, 16 18 = 1 mm, for all other figures = 0.1 mm. ISC = Indian Springs Canyon, MON = Monument North.**1,** *Hedraites*? *graiferi* (Baryshnikov) sensu Vachard and Krainer, 2001b. A test encrusting a shell fragment, and included in an oncoid of *Girvanella* sp. Sample ISC 112-2. **2-5,** *Geinitzina*? sp. Four different types of subaxial and axial sections. 2. Sample MON 11-1.1. 3. Sample MON 11-9. 4. Sample MON 11-12. 5. Sample MON 12-3. **6,** *Geinitzina* cf. *spandeli* Cherdyntsev. Axial section. Sample ISC 127.6. **7, 15,** *Pseudoschwagerina* spp. 7. Subaxial section. Sample 49.1.1. 15. Oblique section. Sample 49.2.1. **8,** *Oketaella* sp. Subtransverse section. Sample ISC 133-2. 9-10. *Grovesella*? spp. Two oblique axial sections. 9. Sample ISC 166-2. 10. Sample ISC 186-5. **11,** *Tezaquina clivuli* Vachard. Axial section. Sample MON 11-11. **12,** *Geinitzina* sp. Axial section. Sample MON 12-6. **13,** *Spireitlina baschkirica* (Rauzer-Chernousova). Oblique section. Sample ISC 21-7. **14,** *Endothyra* transitional to *Neoendothyra* sp. Oblique axial section. Sample ISC 21-15. **16,** *Epimastopora* ex gr. *alpina* Pia. Longitudinal section. Sample ISC 89-1. **17,** *Girvanella* sp. Axial section of a set of trichomes. Sample MON 11-4. **18,** *Calcipatera* sp. (phylloid alga). Longitudinal section. Sample MON 11-5.

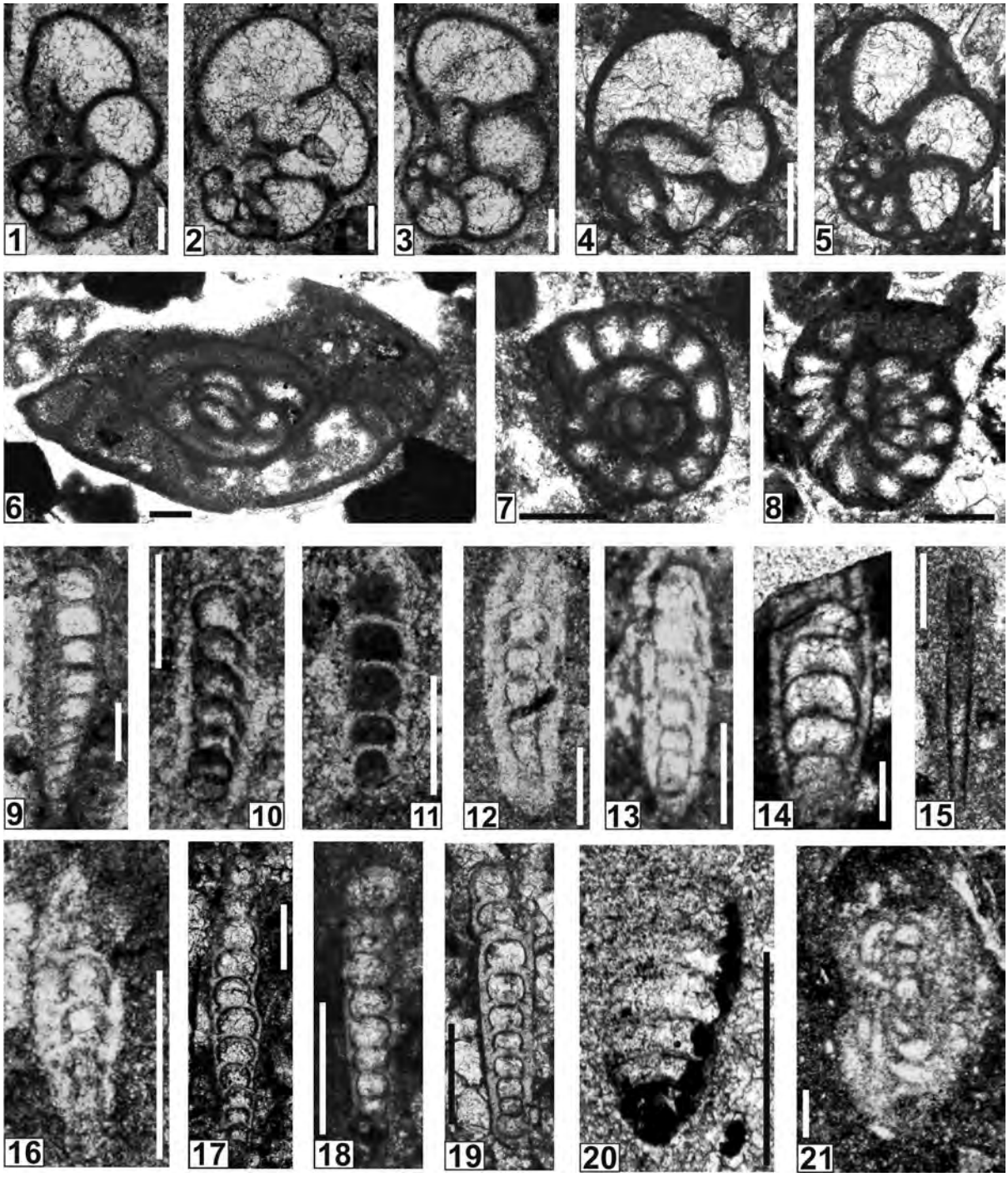


FIGURE 22. Community Pit Formation foraminifers. Scale bars = 0.1 mm**.** FLD = Flood, ISC = Indian Springs Canyon, MON = Monument North. **1-5,** *Globivalvulina praegraeca* Vachard, Krainer and Lucas. 1. Transverse section. Sample FLD 45A.2. 2. Transverse section. Sample FLD 47.1. 3. Transverse section (the proloculus has a pseudofibrous wall). Sample FLD 47.10a. 4. Axial section. Sample ISC 199.7. 5. Axial section (pseudofibrous proloculus). Sample ISC 199.8a. **6-8,** *Oketaella* n. sp. aff. *waldrupensis* Thompson. 6. Subaxial section. Sample ISC 166.7. 7. Transverse section. Sample ISC 166.4. 8. Subtransverse section. Sample ISC 166.6. **9,** *Geinitzina*? sp. Oblique subaxial section. Sample FLD 45.4. **10,** *Nodosinelloides subquadrata* (Lipina). Oblique axial section. Sample FLD 47.2. **11,** *Protonodosaria*? sp. Subaxial section. Sample FLD 86.2. **12-13,** *Pachyphloia*? cf. *densa* (Lipina). 12. Sample FLD 89.1. 13. Sample FLD 89.4. **14,** *Nodosaria*? sp. Sample FLD 186.1. **15,** *Earlandia* ex gr. *elegans* (Rauzer-Chernousova and Reitlinger). Sample MON 52.1. **16,** *Pachyphloia*? aff. *cubanica* (Miklukho-Maklay). Axial section. Sample ISC 186.9. **17,** *Nodosinelloides* cf. *longissima* (Suleimanov). Subaxial section. Sample ISC 189.6. **18,** "*Tauridia*" aff. *nudiseptata* Gaillot and Vachard. Axial section. Sample ISC 199.9. **19,** *Nodosinelloides* cf. *netschajewi* (Cherdyntsev). Sample ISC 199.10. **20,** *Geinitzina* cf. *indepressa* Cherdyntsev. Sample MON 41.1. **21,** Staffellid indet. Sample ISC 186.12.

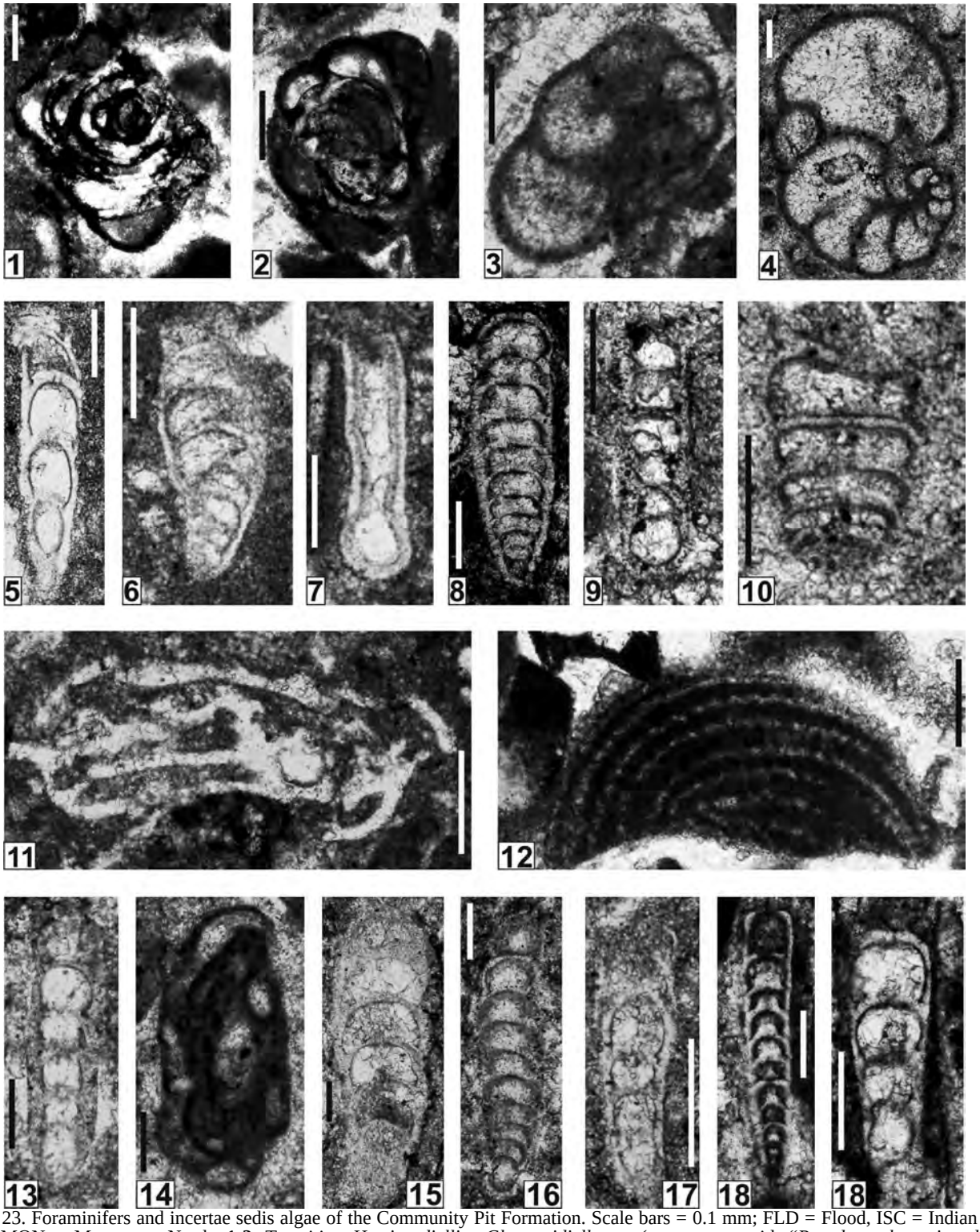


FIGURE 23. Foraminifers and incertae sedis algae of the Community Pit Formation. Scale bars = 0.1 mm; FLD = Flood, ISC = Indian Springs Canyon, MON = Monument North. **1-2,** Transition *Hemigordiellina-Glomomidiella* sp. (to compare with "*Pseudoagathammina dublicata* (Lipina)" sensu Filimonova, 2010 non Lipina, 1949). 1. Subtransverse section. Sample ISC 166-8. 2. Subaxial section. Sample ISC166-10. **3,** *Globivalvulina novamexicana* Vachard, Krainer and Lucas. Subtransverse section. Sample FLD 37-3. **4,** *Globivalvulina praegraeca* Vachard, Krainer and Lucas. Subtransverse section. Sample FLD 47-5. **5,** *Nodosinelloides* cf. *pinardae* Groves and Wahlman. Subaxial section. Sample ISC 186-10. **6,** *Geinitzina*? sp. Subaxial section (with axis slightly deviated). Sample ISC 186-11. **7,** *Syzrania confusa* Reitlinger. Subaxial section. Sample ISC 186-14. **8,** *Nodosaria* cf. *camerata* Miklukho-Maklay. Axial section. Sample ISC 199-1. **9, 13,** *Nodosinelloides* cf. *ronda* (Lipina). 9. Axial section. Sample MON 41-3. 13. Axial section. Sample FLD 45a-1. **10,** *Geinitzina* cf. *postcarbonica* Spandel. Axial section. Sample MON 41-2. **11,** *Orthovertellopsis calcitornellaeformis* Vachard, Krainer and Lucas. Subtransverse section. Sample FLD 78-4a. **12,** *Efluegelia johnsoni* (Flügel). Axial section. Sample ISC 166-5. **14,** *Hemigordiellina*? sp. (or calcivertellid indet.). Subaxial section. Sample FLD 47-10. **15,** *Pseudolangella*? sp. Subaxial section. Sample FLD 55-4. **16,** "*Tauridia*" aff. *nudiseptata* Gaillot and Vachard. Axial section. Sample FLD 86-3. **17,** *Protonodosaria* cf. *pirula* (Miklukho-Maklay). Subaxial section. Sample FLD 89-6. **18,** *Nodosinelloides longa* (Lipina). Axial section. Sample ISC 133-1. **19,** *Protonodosaria* cf. *globifrondina* (Sellier de Civrieux and Dessauvagie). Subaxial section. Sample ISC199-4.

Ana Mountains where restricted shallow marine conditions dominated.

Most of the shale in the Community Pit probably was deposited in shallow subtidal seawater having near-normal oxygen and salinity. This conclusion is based on drab colors, weak to string fissility, carbonate content and particularly the numerous interbeds of fossiliferous limestone. No paleosol features were observed and no indications of red or variegated (oxidized) layers are present. The common occurrence of fossilized logs at several distinct levels in the formation implies proximity to the shoreline. Evidently they accumulated as driftwood that became waterlogged and sank. No stumps in growth position were seen. The local occurrence of gypsum crystal casts and molds, together with beds of microgranular dolomite indicate that at times the waters became hypersaline.

Evidence of Cyclicity

The Community Pit Formation corresponds to the lower-middle Hueco transitional interval of Mack et al. (2013). From this interval, Mack et al. (2013, fig. 5) assembled a composite section based on 12 measured sections in the area where we measured our sections Flood through Orin (Figs. 4, 18). The base of the Mack et al. composite section apparently corresponds to the conglomerate at our Monument North section (Fig. 8). However, the overlying ~ 96 m of Mack et al.'s (2013, fig. 5) composite section bears little resemblance to our measured stratigraphic sections of the same outcrops. In particular, the fact that Mack et al. identified three well-separated petrified wood horizons in their composite section is at variance with our data, which indicate two intervals of petrified wood occurrence separated by about 60 m of section. Our sections also identify more and thicker covered intervals (shale?) and more cherty beds than does the composite section of Mack et al. Indeed, the facies stacking patterns depicted by Mack et al. are not evident in most of our sections, largely because we identified many more facies than did Mack et al.

Mack et al. (2013, fig. 5) posit that their composite section shows two levels of cyclicity: decimeter- to meter-thick, shallowing upward parasequences and meter- to decameter-thick megasequences, seven total, that are broadly shallowing upward. However, a critical review of their composite section calls into question these interpretations. Thus, some successions of cover (shale?) to dolomite can reasonably be interpreted as shallowing upward parasequences. However, the claim that the bases of overlying covered intervals represent the maximum flooding surfaces is conjectural at best. Moreover, Mack et al. (2013, fig. 5) also identify maximum flooding surfaces in other lithologies, including fenestral dolomudstone, peloidal dolomudstone and even at the bases of some beds of foraminiferal packstone and grainstone. Indeed, there is no consistent criterion by which Mack et al. identified maximum flooding surfaces in their composite section—these surfaces occur in a variety of lithologies and at diverse lithological boundaries, so the criteria by which they are identified is not clear.

Similarly, the so-called megasequences of Mack et al. (2013) have no consistent criteria by which to identify them or their bases (which should be unconformable sequence boundaries). The internal stratigraphic architecture of these "megasequences" is extremely variable, so that we cannot replicate identification of the seven megasequences based on any lithostratigraphic criteria presented by Mack et al. (2013). Our outcrop work discloses a lack of internal disconformities and of intertidal and supratidal facies in this formation.

According to Mack et al. (2013), using the Permian timescale of Henderson et al. (2012), the 49 parasequences they identified represent about 4.1 million years, so each parasequence has a duration of about 87 kyr. They considered that this "is in the range of the fourth-order cycles of…(100,000 years) which are assumed to result from eustatic sea-level changes associated with the waxing and waning of continental glaciers…" (Mack et al., 2013, p. 35). Mack et al. (2013) assigned each of their seven composite megasequences a duration of about 600 kyr, and suggested that "the composite megasequences may be a response to subsidence and/or non-glacial eustasy" (p. 36). Instead, we suggest that the composite megasequences of Mack et al. (2013) do not exist and that the number of parasequences they estimate is too high, divided into a very inexact estimate of the temporal span of Community Pit Formation deposition. Indeed, we would describe the composite stratigraphic section of Mack et al. (2013, fig. 5) as an extremely disordered vertical succession, one that shows little convincing evidence of sedimentary cyclicity above the scale of some cover (shale?)-carbonate couplets.

Mack et al. (2013) reported the following carbonate lithofacies and depositional interpretations: (1) fenestral dolomudstone (supratidal to high intertidal); (2) peloidal dolomudstone (low intertidal to lagoon); (3) foraminiferal packstone and grainstone (restricted marine); (4) intraclast fossiliferous grainstone (tidal channel); and (5) fossiliferous packstone (open marine). Shale is interpreted as an offshore marine facies. According to Mack et al. (2013) alternating shale and carbonate sediments of the Community Pit Formation may reflect not only eustatic sea-level changes but may also have been influenced by paleoclimate: carbonate deposited during more arid and shale during more humid climatic periods.

We measured one complete and several almost complete sections through the Community Pit Formation and observed marked lateral facies changes between the individual sections (Fig. 18). Lateral facies changes do not allow a bed-to-bed correlation between the individual sections (Fig. 18). Thus, the limestone facies of the Community Pit Formation are much more complex than reported by Mack et al. (2013). Indeed, we recognized several microfacies types not reported by Mack et al. (2013): (1) bioclastic wackestone containing a diverse fossil assemblage, a common microfacies type; (2) wackestone with a low diversity biota, including spiculite; (3) low-diversity foraminiferal wackestone; (4) intraclast wackestone-packstone-grainstone with a diverse fossil assemblage; and (5) crinoidal wackestone to packstone. Furthermore, Mack et al. (2013) did not report rudstone-floatstone, paleocaliche, sandstone and conglomerate as lithotypes of the Community Pit Formation, though they are present. Shale is rarely exposed, mostly represented by covered intervals, but it is not clear if all shale/covered intervals represent offshore deposits. Some of the carbonate and shale/covered intervals of the Community Pit Formation are much thicker than reported by Mack et al. (2013). At the Monument North section (Fig. 8), limestone comprises only 23% of the section, whereas at Upper Branson Canyon (Fig. 18) limestone comprises 52% of the section. At Upper Branson Canyon limestone units are up to 8.3 m thick. At Monument North, covered intervals are up to 6.6 m thick.

Thus, the work of Mack et al. (2013) failed to recognize many of the limestone facies present in the Community Pit Formation; therefore, the facies stacking pattern of Mack et al. (2013) relied on to identify cycles of deposition is, at best, greatly oversimplified. The fact that individual beds within the Community Pit Formation can be traced laterally over only very short distances (hundreds of meters at most) indicates that the formation lacks a stratigraphic architecture consistent with an allocyclic driver of cyclicity, such as glacio-eustasy or climate. Instead, the vertical disorder in facies stacking within the Community Pit Formation points to a more complex set of factors driving sedimentation, including local carbonate productivity, clastic sediment supply, subsidence rates and even stochastic processes.

Robledo Mountains Formation

The Robledo Mountains Formation is exposed in the southern Robledo Mountains, in and around the PTNM (Figs. 1, 24-29). The unit is mostly marine shale and limestone, but is readily identified by its characteristic siliciclastic red beds (mudstone, siltstone and sandstone), which comprise about one third of the unit, and are intercalated with the marine rocks (Fig. 24). The base of the Robledo Mountains Formation is the stratigraphically lowest red clastic bed above Community Pit Formation limestone or gray shale, and the top of the Robledo Mountains Formation is the stratigraphically highest red bed below Apache Dam Formation limestone. Long referred to as "Abo Tongue" or "Member," the Robledo Mountains Formation is a lithosome dominantly of Hueco Group lithologies (marine limestone and shale) with minor but conspicuous red beds that are laterally equivalent to part of the red-bed Abo Formation lithosome to the north.

The Robledo Mountains Formation at the type section is 125.4 m thick and composed of marine shale and nodular limestone, nonmarine reddish and variegated sandstone, siltstone and mudstone and ledgy marine limestone and gray shale (Lucas et al., 1995, 1998c; Krainer and Lucas, 1995). We studied the Robledo Mountains Formation at the following localities: (1) Branson Canyon, a complete section, with lower and upper boundaries exposed, 90 m thick, adjacent to the formation type section (Figs. 24, 26); (2) Apache Canyon Sabkha, lower contact not exposed, upper contact exposed, 80 m thick (Fig. 28); (3) Community Pit, lower contact not exposed, upper contact exposed, 67 m thick (Fig. 27); (4) Mack 4, upper contact not exposed, 54.5 m thick (Fig. 28); (5) Scorpion Hill, upper contact not exposed, 40 m thick (Fig. 29); (6) Scorpion Hill B, incomplete, 39 m thick (Fig. 29) (Scorpion Hill A and B are superposed, so together they constitute about 79 m of the Robledo Mountains Formation); (7) Excavation, incomplete, 20 m thick (Fig. 27); and (8) North Apache Canyon, incomplete, 14 m thick (Fig. 28).

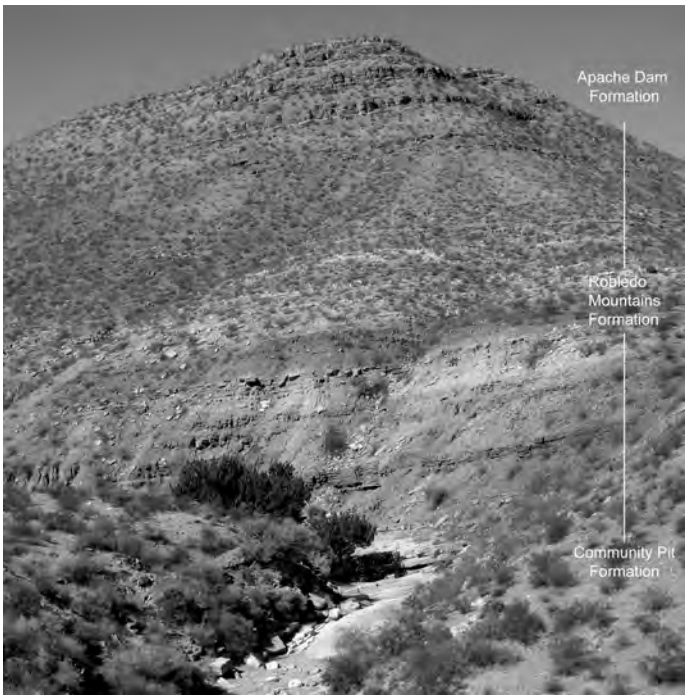


FIGURE 24. Exposure of the Robledo Mountains Formation in Branson Canyon.

Typical lithofacies of the Robledo Mountains Formation are: (1) non-fissile mudstone that is red, purple greenish-gray and rarely yellow; (2) red siltstone to fine-grained sandstone, commonly ripple laminated or horizontally laminated, rare trough crossbedded or massive (Fig. 25C-F); (3) limestone that occurs as single limestone beds (0.1-0.5 m) or thin, mostly even bedded, rarely wavy bedded limestone intervals mostly < 2 m, rarely up to 5.2 m thick (Fig. 25A-B); and (4) covered intervals, most probably representing shale or mudstone intervals. We measured numerous sections of the Robledo Mountains Formation, largely to establish the stratigraphic succession of its fossil plants, invertebrates and ichnofossils (Figs. 27-29). These sections indicate a relatively consistent internal stratigraphy of 4-6 red-bed intervals dominated by fine sandstone and siltstone that display climbing ripple stratification intercalated with thicker intervals of drab (yellow, gray) marine shale and limestone.

Branson Canyon

At Branson Canyon (Figs. 24, 26), the Robledo Mountains Formation is composed of the following lithofacies types:

1. Siltstone to calcareous fine-grained sandstone, partly micaceous, commonly displaying horizontal and ripple lamination (Fig. 25C-E). A few thin sandstone beds (0.1 m) appear massive. Rarely, mudcracks are present on the bedding surface. In one bed bi-directional ripples occur. Other sedimentary structures rarely observed are low-angle crossbedding and soft sediment deformation. This lithofacies is commonly red, and individual siltstone-sandstone beds are commonly 0.1-0.5 m thick, alternating with thinly laminated siltstone to mudstone, a few cm up to 1.6 m thick (mostly 0.1-0.5 m). The color is greenish gray in the lowermost part (lowermost 5 m) and red. Siltstone-sandstone and intercalated mudstone are common in the lowermost 5 m, between 11 and 32 m, and in the uppermost part (80-90 m). Between 32 and 80 m, siltstone to fine-grained sandstone is very rare (one interval, 0.7 m thick).

2. Limestone in the lower part of the section (5-11 m) occurs as limestone beds and bedded limestone units 0.2-1 m thick. Most beds are composed of lime mudstone; some beds are arenitic limestone containing crinoidal debris. A few lime mudstone beds contain calcite nodules (replaced gypsum) or are bioturbated. A few beds also contain myalinid bivalves on top. Limestone beds alternate with greenish and gray shale, which is partly laminated. Shale intervals are 0.1-0.7 m thick. Between 11 and 32 m, limestone is rare and occurs as thin limestone beds (0.2-0.3 m) that alternate with thin mudstone beds (0.1-0.3 m). Micritic and arenitic limestone beds are present.

The stratigraphic interval between 32 and 80 m is mainly composed of limestone and covered intervals. Limestone occurs as thin limestone beds and bedded limestone units up to 1.8 m thick. Bedding is mostly even; rarely, wavy bedding is observed. Bed thickness is 0.1-0.3 m. Between 32 and 43 m, many limestone beds are dolomitic, and some limestone beds contain crinoidal debris. Wavy bedded limestone (units 132, 136) contains abundant echinoid spines up to 5 cm long. Gastropods are present in limestone units 124 and 130. Limestone units 138 and 140 contain crinoidal debris, brachiopods and bryozoans. Algae occur in unit 142.

3. Limestone units are separated by covered intervals up to 5.2 m thick. Covered interval 131 seems to be underlain by nodular limestone and shale containing brachiopods. Covered interval 137 is underlain by a shaly slope containing abundant invertebrate macrofossils, mostly brachiopods, bryozoans and bivalves (Kues, 1995).

Community Pit

The Community Pit is a large (about 300 x 500 m) quarry that operated for several decades as a source of flagstone. It provides the best available exposures of the Robledo Mountains Formation, particularly its non-resistant lithologies. The Community Pit section (Fig. 27) can be lithologically divided into: (1) lower part (0-29 m) composed mainly of sandstone/siltstone and alternating mudstone, and rare thin limestone beds, (2) middle part (29-55 m) composed of alternating limestone and mudstone, and (3) upper part (55-66 m) composed of sandstone/siltstone with thin mudstone intercalations. The top of the section is represented by bedded limestone containing brachiopods and ostracodes. Layering throughout the quarry is more or less tabular. Lenticular and channel-form features were not observed.

1. Lower part: siltstone/sandstone units (0.2-1.7 m) alternate with mudstone (0.3-2.5 m; rarely, up to 8.9 m). Siltstone/sandstone is red, and intercalated mudstone is red and green. Near the base, a few thin limestone beds are intercalated. Siltstone/sandstone displays horizontal and ripple lamination and rare, small-scale trough crossbedding.

2. Middle part: limestone beds (0.1-1m) and bedded, rare nodular limestone units (up to 1.3 m thick) alternate with shale units (0.3-4.4 m) that are gray to dark gray and locally contain brachiopods (Fig. 25B). One thick limestone bed contains *Thalassinoides* up to 0.4 m long and 4 cm thick.

3. Upper part (55-66 m): red to purplish gray and variegated siltstone-sandstone units (up to 1.2 m thick), displaying horizontal lamination, ripples and rare mudcracks, alternate with thin (0.1-0.3 m) shale intervals.

Apache Canyon Sabkha

At the Apache Canyon Sabkha section (Fig. 28), siltstone/sandstone units displaying horizontal lamination, ripple cross lamination and rare small-scale trough crossbedding are 0.3-1.5 m thick and occur in the lower 9 m of the exposed section and between 25 and 39 m. Siltstone/sandstone units alternate with mudstone (0.1-4.5 m) and a few intercalated thin limestone beds (0.3-0.6 m), which are occasionally dolomicritic. From 5-40 m, the succession is composed of limestone units alternating with shale/covered intervals. Limestone units are up to 3.1 m thick and medium bedded (0.2-0.5 m). Bedding is even or rarely wavy. In the lower part of this succession, thin dolomicritc beds are present. In the middle, crinoidal limestone beds are present. Shale/covered intervals are up to 2.2 m thick.

The upper part of the section (39-81 m) is composed of limestone beds and limestone units up to 1.2 m thick, separated by covered intervals that are up to 8.3 m thick. Limestone intervals are even to wavy bedded and contain *Thalassinoides* in the lower part (unit 50: Fig. 25A). Limestone beds in the middle of this succession contain crinoidal debris, gastropods and brachiopods. Palechinid radioles occur in the limestone bed of unit 64. The thick covered interval in the uppermost part (unit 71) shows red sandstone in the slope. The Robledo Mountains Formation is overlain by black, wavy bedded cherty limestone containing gastropods and palechinid radioles at the base of the Apache Dam Formation.

Mack 4 Section

This section (Fig. 28) starts with a thin, red, fine-grained sandstone bed displaying ripple cross lamination, overlain by yellow shale. Red siltstone/sandstone is poorly exposed between 17 and 24 m in the section. Two thicker, fine-grained sandstone ledges (5.5 and 2.3 m thick) and several thin sandstone beds (0.1-0.7 m) occur in the upper part of the section and are separated by covered intervals. Sandstone/siltstone displays horizontal lamination and ripple cross lamination,

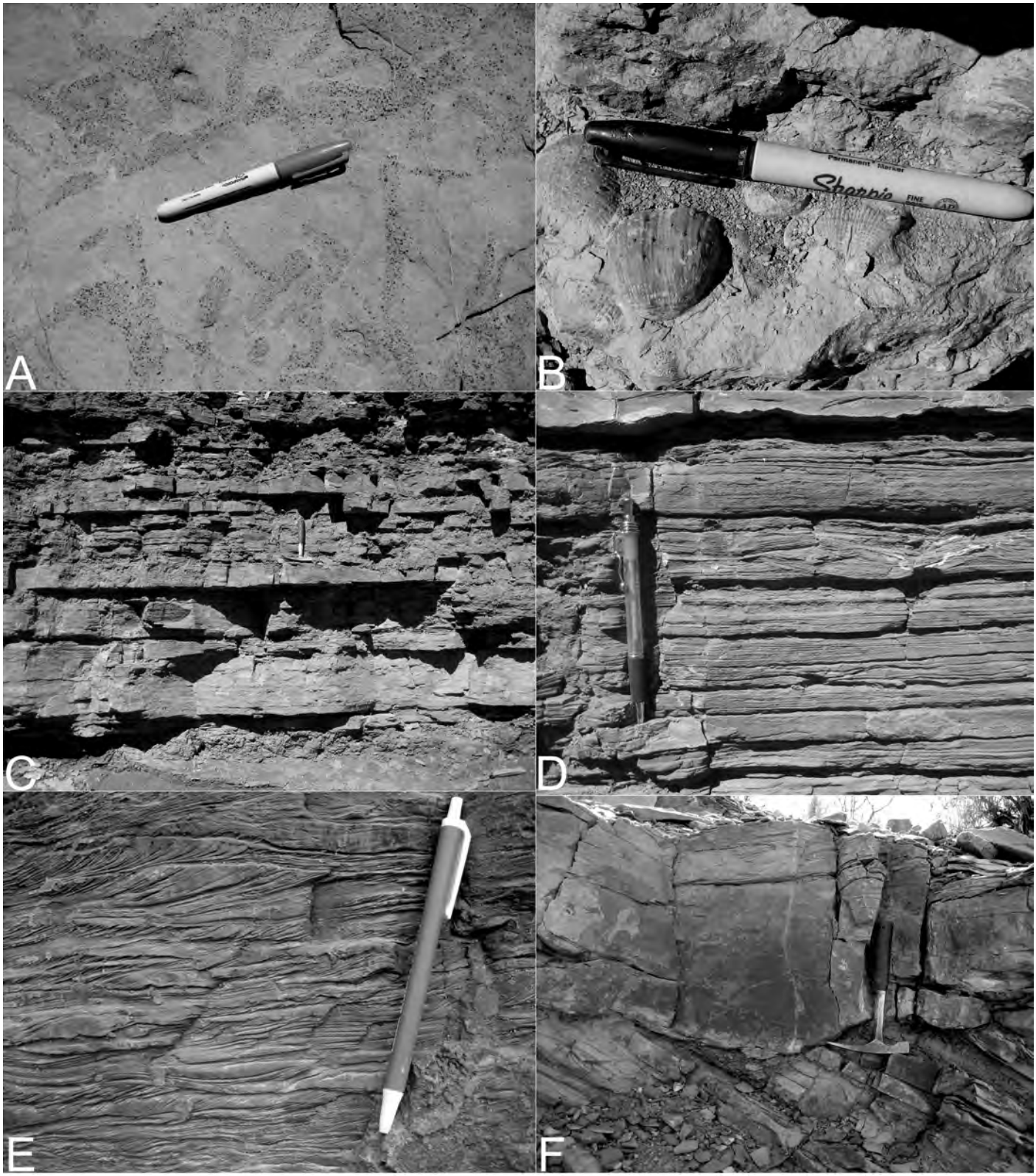


FIGURE 25. Photographs of selected outcrops of the Robledo Mountains Formation in the Robledo Mountains. A, *Thalassinoides* burrows in Apache Canyon Sabkha section. B, Brachiopods in Community Pit section. C-D, Thinly laminated and ripple laminated sandstones in Branson Canyon section. E, Climbing ripples in Community Pit section. F, Within formation angular unconformity, evidence of local Permian tectonism, Apache Canyon.

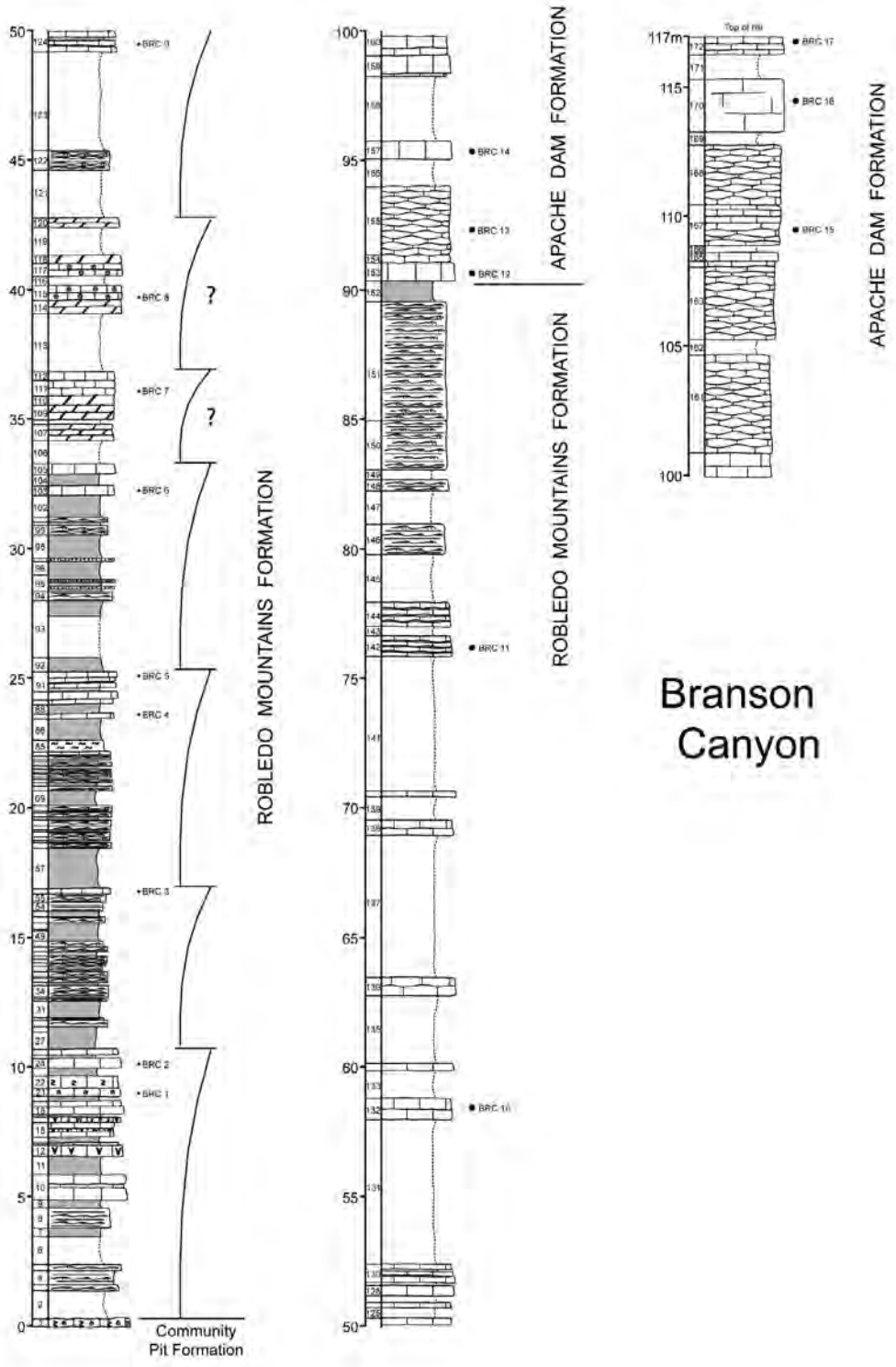


FIGURE 26. Measured stratigraphic section of the Robledo Mountains Formation at Branson Canyon (see Figure 4 and Table 1 for location of section). Inferred cycles in lower part of section are indicated. See Figure 8 for legend to lithologic symbols.

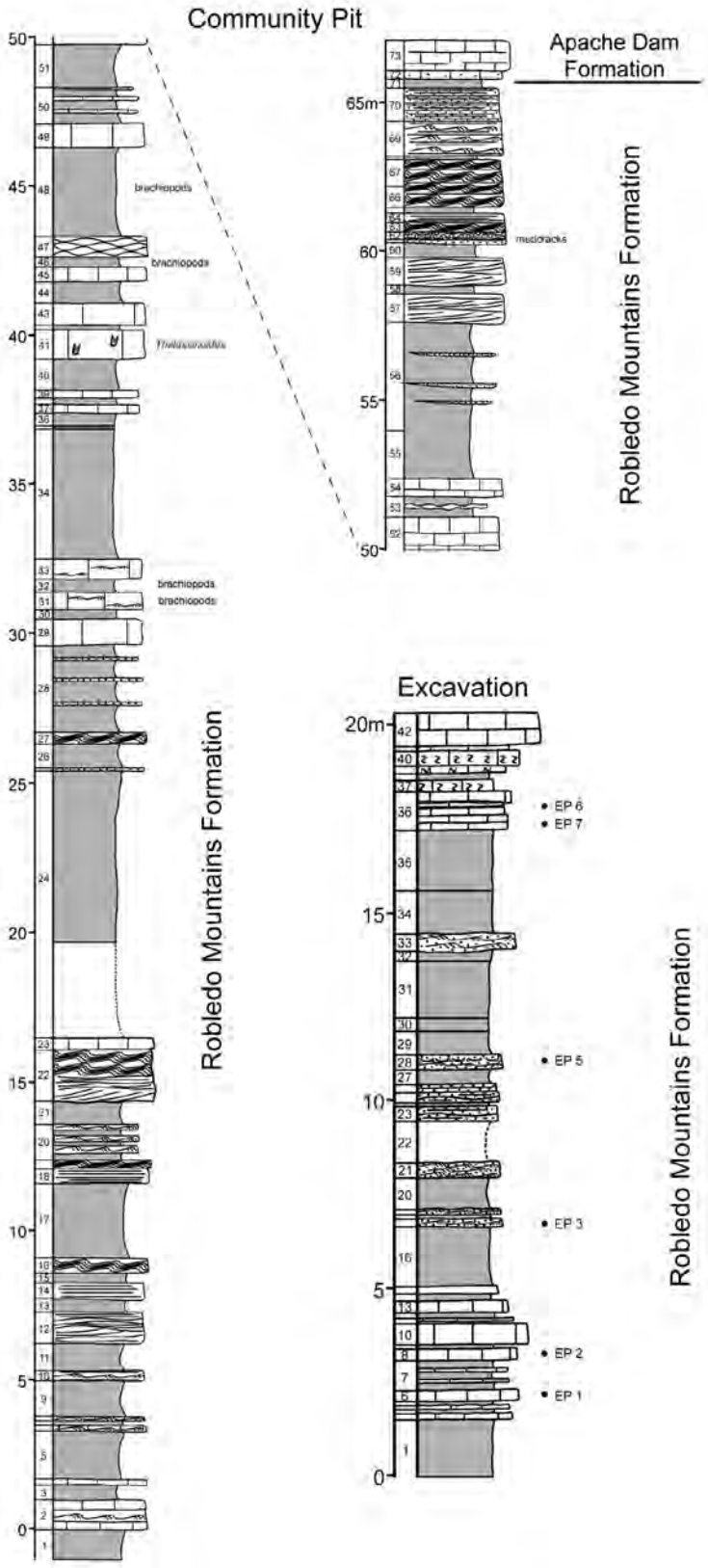


FIGURE 27. Measured stratigraphic sections of the Robledo Mountains Formation in the Community Pit (see Figure 4 and Table 1 for location of sections). See Figure 8 for legend to lithologic symbols.

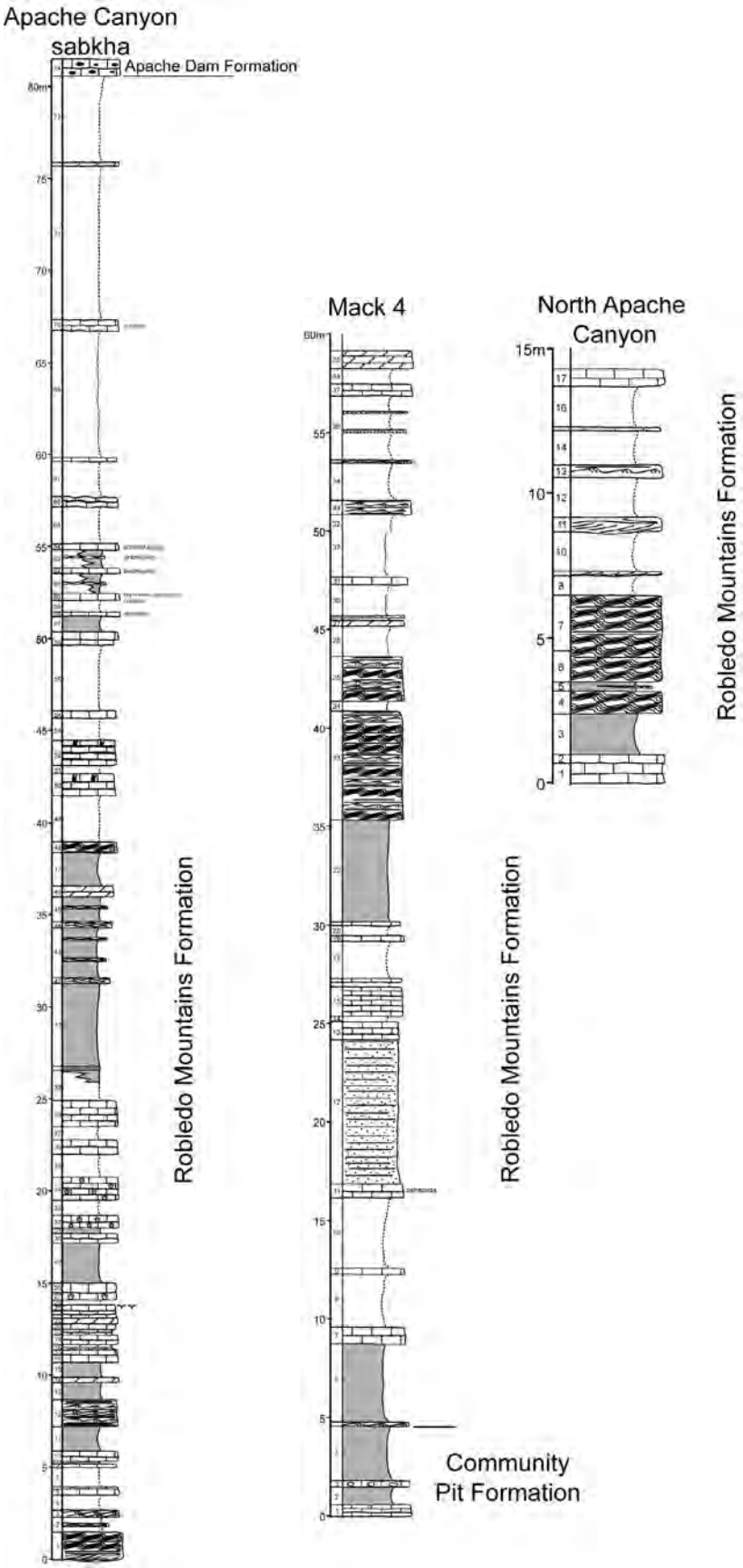


FIGURE 28. Measured stratigraphic section of parts of the Robledo Mountains Formation at Apache Canyon Sabkha, Mack 4 and North Apache Canyon (see Figure 4 and Table 1 for location of sections). See Figure 8 for legend to lithologic symbols.

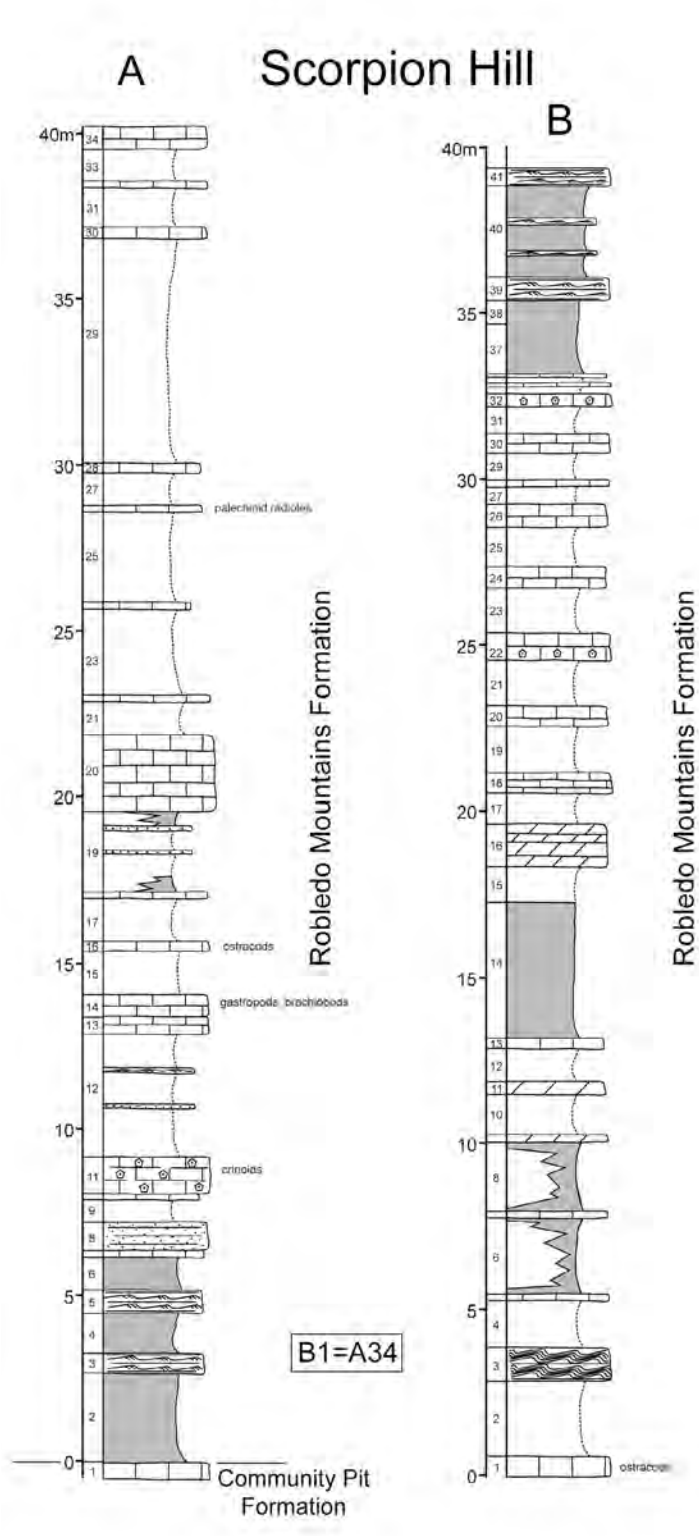


FIGURE 29. Measured stratigraphic sections of the Robledo Mountains Formation at Scorpion Hill (see Figure 4 and Table 1 for location of sections). See Figure 8 for legend to lithologic symbols.

and rare, thin, massive sandstone beds are present.

Limestone is rare in this section and occurs as 0.1-0.4 m thick limestone beds and 0.8-1.5 m thick, even bedded limestone intervals, separated by covered intervals that are 0.1-3.2 m thick. The topmost limestone interval is dolomitic. Note that this is section 4 of Mack (2007) and Mack et al. (2010), and is discussed below.

Scorpion Hill Section

Scorpion Hill section A (Fig. 29) represents the lower 40 m of the Robledo Mountains Formation. The topmost bed of section A (unit 34) is unit 1 of Scorpion Hill section B, and thus B is the continuation of section A. Total thickness of both sections combined is approximately 79 m, and this represents most of the thickness of the Robledo Mountains Formation at this location.

Section A starts with 7 m of red mudstone (1-2.7 m), alternating with red, fine-grained sandstone intervals (0.6-0.8 m thick) and one thin dolomitic limestone bed (0.2 m). Sandstone beds display ripple cross lamination and horizontal lamination. This succession is overlain by limestone beds (0.2-0.3 m thick) and a few thicker, even-bedded limestone intervals (0.5-2.3 m thick), alternating with covered intervals that are 1-6.8 m thick. One limestone interval in the lower part is composed of crinoidal wackestone. Fossils are rare and include gastropods, brachiopods and palechinid radioles in unit 26.

In section B (Fig. 29), fine-grained, red, ripple-laminated sandstone occurs in the lower part (1 m thick) and in the upper part (0.5-0.7 m thick), alternating with red mudstone. Most of the section is represented by limestone beds (0.1-0.4 m thick) and thin, even-bedded limestone intervals (0.6-1.3 m thick), separated by shale (up to 4.1 m) and covered intervals (0.1-1.4 m thick). In the lower part, a few limestone beds are dolomitic. Two limestone beds contain crinoidal debris, and other fossils are traces from the red beds, including the resting trace and trackways of a scorpion (Lucas et al., 2013a). Scorpion Hill B is section 3 of Mack (2007) and Mack et al. (2010), and is discussed below.

North Apache Canyon Section

At North Apache Canyon (Fig. 28), only a small portion of the Robledo Mountains Formation (14 m) is exposed, which is composed of: (1) limestone (0.1-1 m thick, medium bedded); (2) fine-grained, red sandstone, ripple-laminated (0.4-1.9 m thick); (3) fine-grained, red sandstone with trough crossbedding (0.1-0.5 m); (4) limestone and sandstone that are separated by shale intervals (0.3 and 1.4 m); and (5) covered intervals (0.7-1.4 m). Sandstone units 4-7 display well-developed climbing ripples, have a scour base and form a bench that thins laterally ~ 30 m on strike. This is the largest sandstone body we have seen in the Robledo Mountains Formation and is likely a tidal channel deposit (Voigt et al., 2013).

Excavation Section

The total thickness of the measured section at Excavation (Fig. 27) is 20.4 m. This is at the excavation documented in detail by Voigt et al. (2013). The lower 5 m are composed of alternating gray limestone beds 0.1-0.4 m thick and intercalated gray and yellowish-brown shale units 0.1-0.2 m thick (units 1-15). Burrows are observed in the limestone bed of unit 6. At the base, 1.5 m of red and green shale is exposed. The top of this succession (unit 15) is formed by yellowish-brown marl containing a few small brachiopods.

Above this alternating limestone and shale facies, 12 m of red, subordinately greenish-gray and purple mudstone with intercalated siltstone to fine-grained sandstone beds (units 16-35) are exposed. The shale at the base is 1.7 m thick, thinly laminated, greenish-gray and purple and contains plant debris. Shale units above are either laminated, mottled or massive.

Intercalated siltstone to fine-grained sandstone beds are 0.1-0.4 m thick, red, rarely greenish-gray (near the base), micaceous and partly calcareous. Sedimentary structures observed in the siltstone to fine-grained sandstone are ripple crossbedding, climbing ripples (rare), horizontal lamination, low-angle crossbedding (rare) and synsedimentary deformation structures. Siltstone is mixed siliciclastic-carbonate in composition, containing small quartz and carbonate grains and a few micas (muscovite). Lamination is caused by coarser- and finer-grained laminae. Coarser laminae are rich in quartz, and finer-grained laminae contain higher amounts of carbonate.

This redbed unit is overlain by gray, bedded marly limestone and marl (units 36-42). The marl of unit 37 contains burrows. These marly limestone and marl units are overlain by 0.2 m of greenish and gray shale.

Microfacies

In the lower part of the Robledo Mountains Formation (lower 50 m at Branson Canyon), the dominant microfacies types of the limestones are ostracodal wackestone (Fig. 30A-C) and foraminiferal wackestone to grainstone (Fig. 30D-F). Both contain a low diversity fossil assemblage. The skeletons are embedded in micrite and peloidal micrite. Mudstone containing a few ostracodes and bindstone (stromatolite), which occurs as thin LLH-type (laterally linked hemispheroids) microbial crusts, alternating with thin layers of peloidal micrite, are subordinate. The bindstone displays prominent fenestral fabrics filled with coarse calcite spar. In the upper part of this section, limestone is mainly composed of bioclastic wackestone to floatstone and phylloid algal wackestone to floatstone. Compared to the lower part, the diversity of the fossil assemblage is higher.

In wackestone to floatstone (Fig. 30G), echinoderms are a common constituent, and phylloid algal wackestone to floatstone contains abundant recrystallized fragments of phylloid algae. Some of the skeletons are encrusted by cyanobacteria, locally forming small oncoids. Both microfacies contain a diverse fossil assemblage.

In the Excavation section, limestone of the lower part is composed of bioclastic wackestone containing diverse fossil fragments embedded in the micritic matrix. The marly limestone in the upper part of the Excavation section consists of ostracodal wackestone to packstone containing many whole ostracod carapaces. The interior of the ostracod carapaces is commonly filled with cement, less commonly with internal micritic sediment. Other common fossils are foraminifers, microconchids and a few larger shell fragments, probably derived from bivalves. The fossils are embedded in micrite.

Sandstone Petrography

Siltstone and fine-grained sandstone of the Robledo Mountains Formation are mixed siliciclastic-carbonate in composition (Fig. 30H). The dominant grain types in fine-grained ripple-laminated sandstone and siltstone near the base are monocrystalline quartz and carbonate grains. Other grain types include polycrystalline quartz, rare feldspar grains, muscovite and opaque grains.

Fossils

The Robledo Mountains Formation yields marine macro- and microfossils from marine shale and limestone beds, and nonmarine plant and trace fossils from its siliciclastic red beds. Fossils observed in marine beds on outcrop include crinoidal debris, palechinid radioles, gastropods, brachiopods, bryozoans, bivalves, ammonoids and *Thalassinoides* (Simpson, 1976, 1984; Kues, 1995). Besides ostracodes (Kietzke and Lucas, 1995) and tubular foraminifers *Hedraites*? spp., ostracodal wackestone and foraminiferal wackestone to grainstone contain microconchids, rare thin bivalve shells, rare gastropods, and very rare bryozoans.

In wackestone to floatstone, echinoderm fragments (mostly derived from crinoids, with a few palechinid radioles) are a common constituent, and phylloid algal wackestone to floatstone contains abundant recrystallized fragments of phylloid algae (*Neoanchicodium*). Other fossils include brachiopod shells and spines, bivalve shells, bryozoans, small gastropods, ostracodes, rare microconchids, and foraminifers listed below. In the Apache Canyon Sabkha section, dasycladacean algae (*Epimastopora*), large tubular foraminifers (*Hedraites*? sp.) and rare trilobite fragments are present.

Bioclastic wackestone at the Excavation section contains abundant recrystallized fossil fragments probably derived from bivalves and calcareous algae (*Epimastopora*, phylloid algae *Eugonophyllum*, and *Claracrusta*). Less abundant are echinoderm fragments, gastropods, ostracodes, smaller foraminifers, and rare bryozoan fragments. The ostracodal wackestone to packstone contains, among abundant ostracodes, *Hedraites*? spp. and rare other foraminifers (nodosariates, globivalvulinids), microconchids and a few larger shell fragments, probably derived from bivalves.

Foraminifers (Figs. 31-34): *Eotuberitina* sp., *Tuberitina* sp., *Earlandia* sp., *Tetrataxis* sp., *Abadehella* n. sp. (Figs. 31.7, 33.12-13), *Globivalvulina* cf. *novamexicana*, *G. praegraeca* (Fig. 31.3-4), *G.* sp., *Pseudoreichelina* sp. (Figs. 32.8, 12, 34.5, 21), *Schubertella* sp., schubertelloid indet. (Fig. 32.18), *Calcivertella* sp., *Orthovertella* sp. (Fig. 34.20), *Hedraites*? n. sp. 1 (Fig. 31.1, 6, 8, 32.1-2, 33.1-7, 9), *H.*? n. sp. 2 (Fig. 34.15-16), *Pseudovermiporella* sp. (Fig. 31.2), *Hemigordius* sp. 1 (Fig. 31.5), *H.* sp. 2 (Fig. 32.13-14, 16), *H.* sp. 3 (Fig. 33.1-2), *H.* sp. 4 (Fig. 33.10.11), *H.* sp. 5 (Fig. 34.7-8), *Rectogordius* sp. (Fig. 34.7-8), *Glomomidiella* n. sp. 1 (Figs. 31.18-19, 32.3-7, 34.4, 9, 11-12), *G.* n. sp. 2 (Fig. 32.10, 15), *Syzrania pulchra* Kireeva (Figs. 32.11, 34.17), *Amphoratheca*? sp. (Fig. 31.10), *Protonodosaria*? sp. (Fig. 31.12), *Nodosinelloides aequiampla* (Lipina) (Fig. 34.3, 6, 13), *N. subquadrata* (Lipina) (Fig. 32.17), *N. longissima* (Suleimanov) (Fig. 34.25), "*Tauridia*" sp. (Fig. 31.13), *Nodosaria* cf. *opima* Lin (Fig. 34.18-19), *N.* sp. (Fig. 33.8), *Geinitzina* cf. *postcarbonica* Spandel (Fig. 31.14), *G. gigantea* Miklukho-Maklay (Fig. 34.23-24), *G.* sp., *G.*? *frondicularieaformis* Sosipatrova (Fig. 34.22), *Pseudolangella*? sp. (Fig. 31.11), *Rectoglandulina pigmaeformis supera* Gerke (Fig. 34.10, 14), *R.* sp. (Fig. 31.15-16) and *Pachyphloia*? sp. (Fig. 31.9, 17).

Fossil plants: Plant fossils from the reds beds of the Robledo Mountains Formation are a low diversity assemblage dominated by walchian conifers (Lucas et al., 1995; DiMichele et al., this volume). They indicate a coastal forest dominated by conifers, characteristic of the low diversity, drought-resistant paleoflora found in the Abo depositional system across much of New Mexico (DiMichele et al., 2007, this volume; Lucas et al., 2012, 2013b).

Ichnofossils: The red-bed ichnofossil assemblages from the Robledo Mountains Formation (e. g., Minter and Braddy, 2009; Lucas et al., 2011b and references therein) indicate an arthropod-dominated invertebrate fauna of terrestrial herbivores and predators such as apterygote insects, myriapods and scorpionids that well represent the *Scoyenia* ichnoguild of the *Scoyenia* ichnofacies. The invertebrate trace fossils are dominated by arthropod trackways (*Dendroidichnites, Diplichnites, Diplopodichnus, Kouphichnium, Lithographus, Octopodichnus, Palmichnium* and *Stiaria*), arthropod resting traces (*Lockeia, Rotterodichium, Selenichnites, Tonganoxichnus*), arthropod jumping traces (some *Tonganoxichnus*) and arthropod grazing traces (*Stiallia, Striatichnium*). Invertebrate feeding traces (*Treptichnus*), grazing traces (*Cochlichnus*), graphoglyptids and helical-shaped burrows (*Augerinoichnus*) are less common. Vertebrate footprints are mostly of small temnospondyls (*Batrachichnus*), areoscelids (*Dromopus*) and pelycosaurs (*Dimetropus*). Tracks of larger amphibians (*Limnopus*) and of primitive amniotes (*Hyloidichnus, Varanopus, Robledopus*) are much less common, and fish swimming traces (*Undichna*) and swim tracks (*Lunichnium, Characichnos*) are present (Voigt and Lucas, this volume).

Depositional Environments

Limestone microfacies types of the Robledo Mountains Formation containing a low-diversity fossil assemblage are interpreted as deposits of a restricted, very shallow, low-energy shelf environment. Limestone microfacies containing a diverse fossil assemblage accumulated in an open, normal marine shallow shelf environment, mostly under low-energy conditions (Krainer and Lucas, 1995; Krainer et al., 2009). The microfacies types include SMF (standard microfacies) 10, 18 and 20, indicating deposition in an open marine to restricted platform interior environment.

According to Lucas et al. (1995, 1998c) and Mack (2007), up to 11 red bed intervals occur within the Robledo Mountains Formation. The depositional environment of these red beds has variously been interpreted as deltaic to tidal flat (LeMone et al., 1975), intertidal flat (Mack and James, 1986), tidal flat (Lucas et al., 1995, 1998b), or as fluvial deposits composed of crevasse splay siltstone, overbank mudstone and fine-grained channel-fill sandstone and siltstone (Mack, 2007; Voigt et al., 2013). Minter and Braddy (2009) suggested they are intertidal deposits that formed a long distance inshore under essentially freshwater conditions.

Mack (2007) distinguished the following depositional environments within the Robledo Mountains Formation: fluvial (channel sandstone, crevasse splay siltstone, red overbank mudstone), estuarine (gray and green very fine sandstone and siltstone), lower shoreface (gray shale and siltstone), shallow marine lagoonal, restricted and normal marine limestone, peritidal dolomicrite and mature, polygenetic paleosols. Krainer et al. (2009) interpreted thick, crossbedded sandstone in the Robledo Mountains Formation of the Doña Ana Mountains as fluvial channel fill deposits, thin crossbedded and ripple laminated sandstone to siltstone as crevasse splay deposits, and red mudstone as overbank deposits (also see Voigt et al., 2013). Thicker, ripple laminated intervals probably represent a tidal flat or deltaic environment. Greenish and dark gray fissile shale was interpreted as marine deposits of the lower shoreface (Krainer et al., 2009).

According to Voigt et al. (2013), trace-fossil bearing red beds were deposited in the distal parts of an extensive coastal flood plain during alternating dry and wet climatic conditions. Flaser- to wavy-

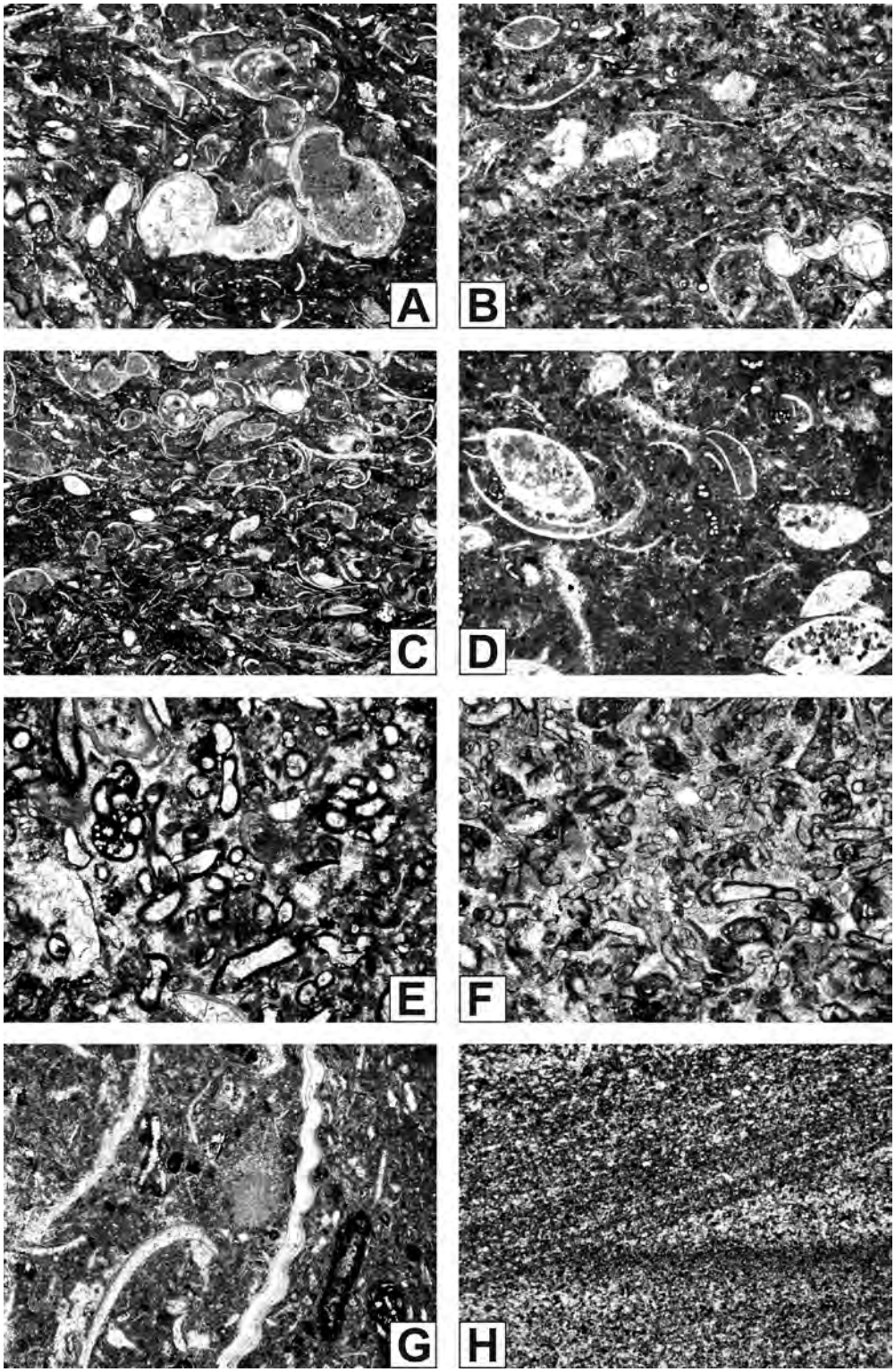


FIGURE 30. Thin section photographs of common microfacies types of the Robledo Mountains Formation, Robledo Mountains. All photographs under plane light. **A,** Ostracodal wackestone containing abundant ostracodes, subordinate tubular foraminifers (*Hedraites*? n. sp. 1) and microconchids. Branson Canyon, BRC 4, width of photograph is 6.3 mm. **B-C,** Ostracodal wackestone containing abundant ostracodes, subordinate tubular foraminifers (*Hedraites*? n. sp. 1), microconchids, many peloids and rare nodosariate foraminifers. Branson Canyon, BRC 9, width of photograph is 3.2 mm. **D,** Wackestone composed of abundant ostracodes and tubular foraminifers (*Hedraites*? n. sp. 1), few microconchids, rare bivalve shell fragments. The matrix contains abundant peloids. Branson Canyon, BRC 7, width of photograph is 3.2 mm. **E,** Foraminiferal wackestone to grainstone, composed of abundant tubular foraminifers (*Hedraites*? n. sp. 1), subordinate ostracodes and rare other skeletons. Locally micrite is present. Branson Canyon, BRC 2, width of photograph is 3.2 mm. **F,** Foraminiferal wackestone containing abundant tubular foraminifers (*Hedraites*? n. sp. 1), a few ostracodes, rare *Globivalvulina*, small gastropods, other skeletons and micritic intraclasts. Branson Canyon, BRC 5, width of photograph is 3.2 mm. **G,** Wackestone to floatstone containing few larger and many small bioclasts. Branson Canyon, BRC 10, width of photograph is 6.3 mm. **H,** Mixed siliciclastic-carbonate siltstone composed of detrital quartz grains and carbonate grains, displaying small-scale crossbedding. Indian Springs Canyon, unit 203, width of photograph is 3.2 mm.

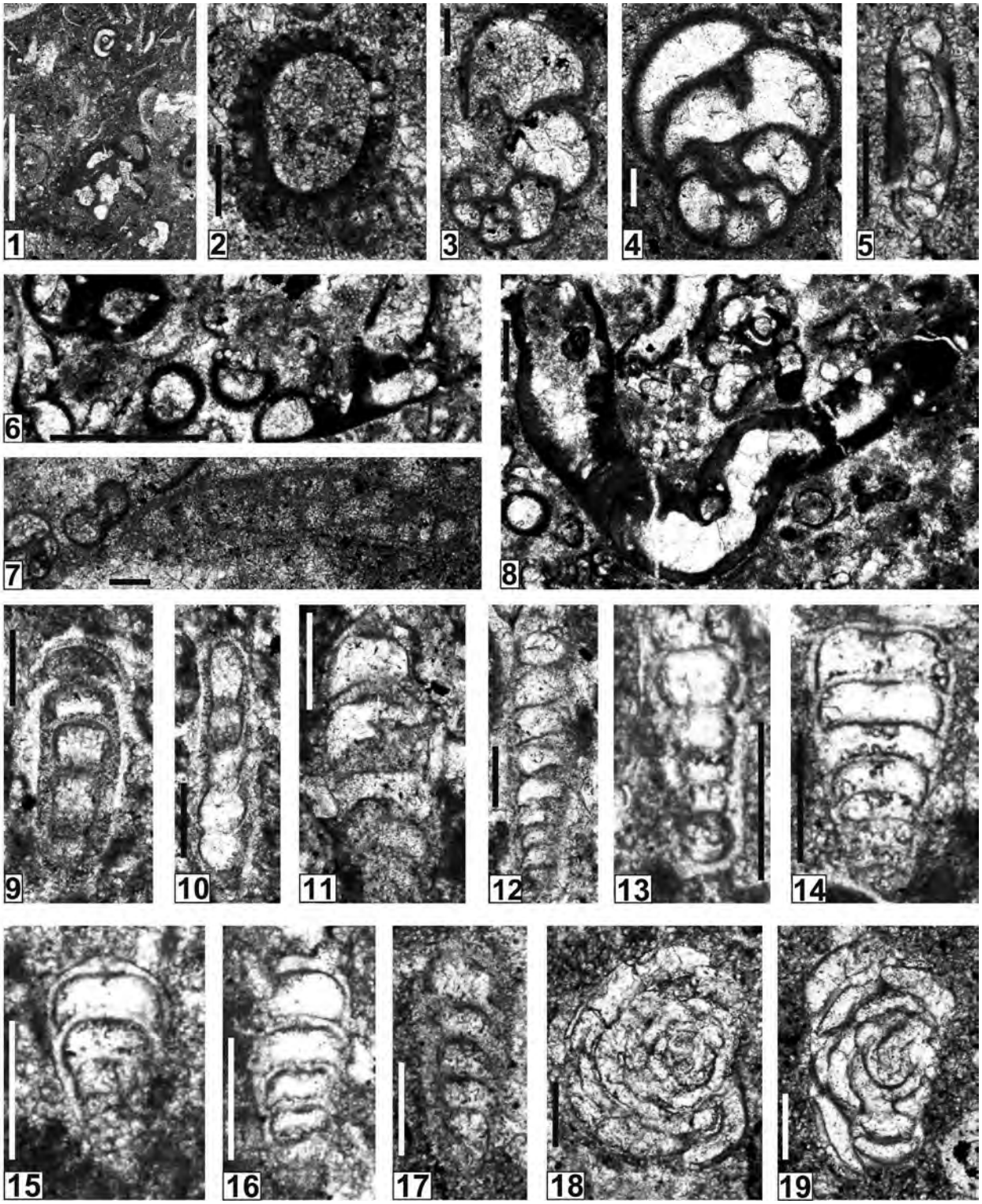


FIGURE 31. Microfossils from the Robledo Mountains Formation, Branson Canyon. Scale bars: Figs. 1, 6 = 0.5 mm, all other figures: 0.1 mm; BRC = Branson Canyon. **1, 6, 8,** *Hedraites*? n. sp. 1. 1. Various sections in a wackestone. Sample BRC 4-8. 6. Various sections in a bioclastic grainstone. Sample BRC 2-1. 8. Longitudinal section. Sample BRC 2-4. **2,** *Pseudovermiporella* sp. Transverse section. Sample BRC 1-4. **3-4,** *Globivalvulina praegraeca* Vachard, Krainer and Lucas. 3. Transverse section. Sample BRC 1-8. 4. Axial section. Sample BRC 8-1. **5,** *Hemigordius* sp. 1. Axial section. Sample BRC 11-9. **7,** *Abadehella* n. sp. Subaxial section. Sample BRC 11.17. **9, 17,** *Pachyphloia*? sp. 9. Subaxial section. Sample BRC 8-3. 17. Oblique subaxial section. Sample BRC 11-2. **10,** *Amphoratheca*? sp. Subaxial section. Sample BRC 8-13. **11,** *Pseudolangella*? sp. Subaxial section. Sample BRC 8-14. **12,** *Protonodosaria*? sp. Subaxial section. Sample BRC 8-17. **13,** "*Tauridia*" sp. Axial section. Sample BRC 8-18. **14,** *Geinitzina* cf. *postcarbonica.* Subaxial section. Sample BRC 9-4. **15-16,** *Rectoglandulina*? sp. 15. Subaxial section. Sample BRC 9-5. 16. Subaxial section. Sample BRC 11-1. **18-19,** *Glomomidiella* n. sp. 1. 18. Subtransverse section. Sample BRC 11-23. 19. Subaxial section. Sample BRC 11-30.

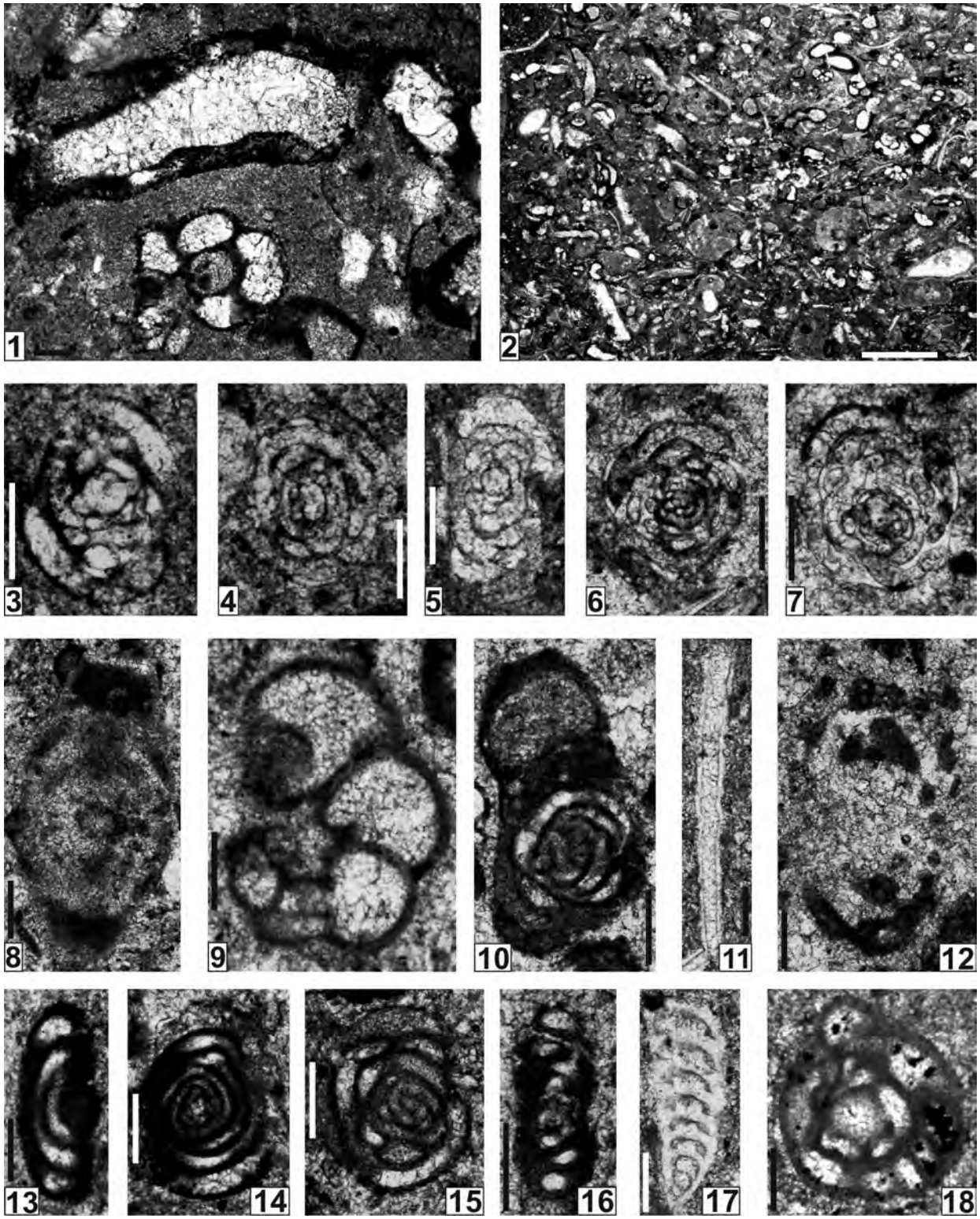


FIGURE 32. Foraminifers from the Robledo Mountains Formation, Apache Canyon Sabkha. Scale bars = 0.1 mm, for Fig. 2 = 1.0 mm. **1-2,** *Hedraites*? n. sp. 1. Two oblique sections (in an adult stage, top; and a juvenile stage bottom, center). Sample ACS 8.6. 2. Microfacies showing the numerous and relatively broad sections of this taxon. Sample ACS 8.8. **3-7,** *Glomomidiella* n. sp. 1. 5 random sections showing: 3. A flexostyle canal at the top of a spherical proloculus. Sample ACS 61.8. 4. A reniform proloculus. Sample ACS 61-6. 5. A more compressed test. Sample ACS 68-4. 6. More tighly coiled initial whorls. Sample ACS 68-5. 7. A typical test and coiling. Sample ACS 68-6. **8, 12,** *Pseudoreichelina* sp. 8. Broken axial section. Sample ACS 69-7. 12. Oblique section. Sample ACS 69-12. **9,** *Globivalvulina praegraeca* Vachard, Krainer and Lucas with a pseudofibrous-walled proloculus. Sample ACS 69-10. **10, 15,** *Glomomidiella* n. sp. 2. 10: A specimen in an aggregate grain or showing an additional ontogeny more or less uncoiled and semi-evolute. Sample ACS 69-11. 15. A typical specimen. Sample ACS 69-16. **11,** *Syzrania pulchra* sp. Longitudinal section. Last regional occurrence of this genus. Sample ACS 69a-11. **13-14, 16,** *Hemigordius* sp. 2. 13. Oblique axial section. Sample ACS 69-8. 14. Transverse section. Sample ACS 69.9. 16. ?Axial section, eventually belonging to another species. Sample ACS 69.18. **17,** *Nodosinelloides subquadrata* (Lipina). Oblique axial section. Sample 69a-7. **18,** Schubertelloid indet. Transverse section. Sample 69a-15.

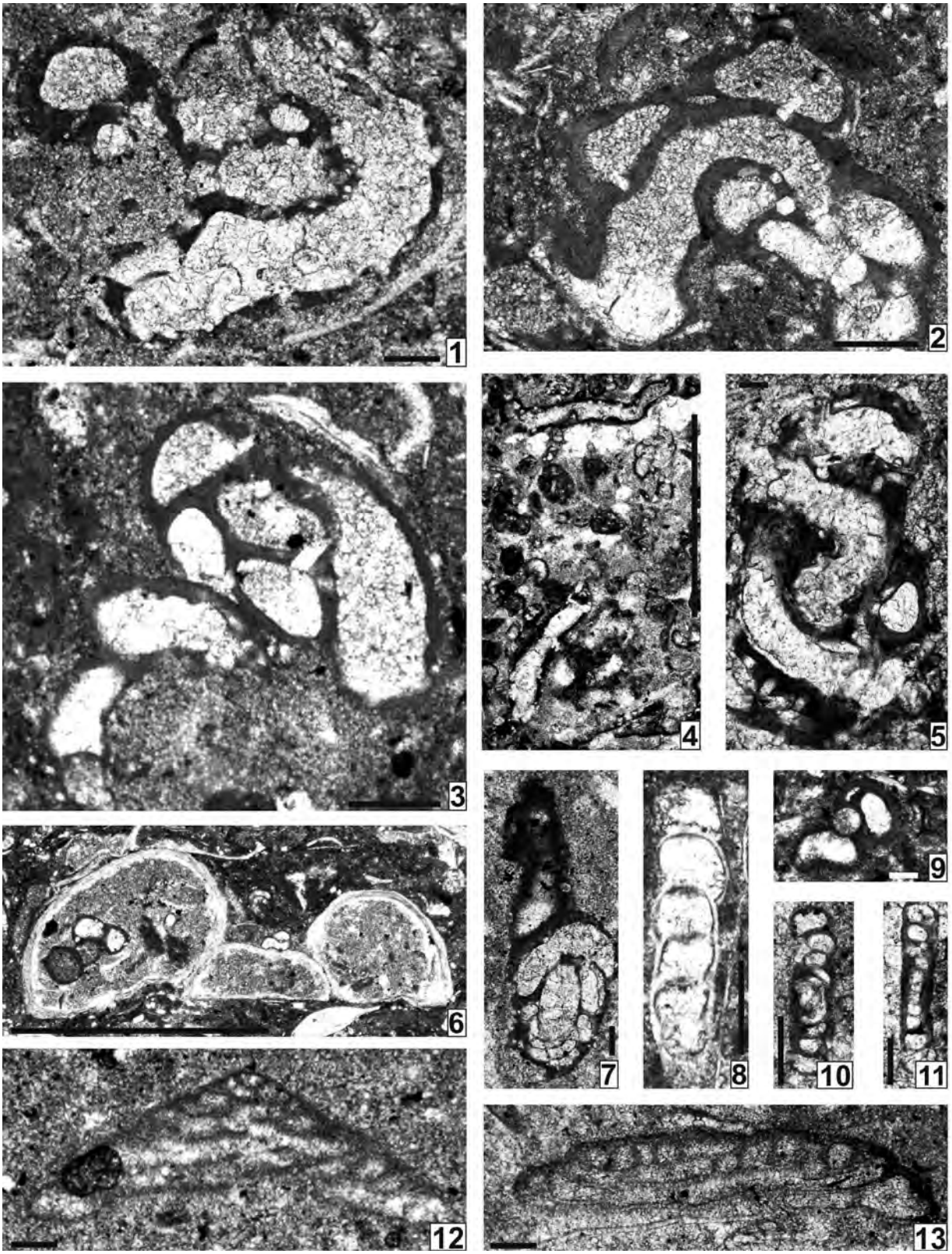


FIGURE 33. Foraminifers from the Robledo Mountains Formation, Branson Canyon. Scale bars = 0.1 mm, for Figs. 4 and 6 = 1.0 mm. **1-7, 9,** *Hedraites*? n. sp. 1, various longitudinal and transverse sections. 1. Oblique pits relatively well visible in the porcelaneous wall. Sample BRC 1-11. 2. Relatively compact wall. Sample BRC 4-1. 3. Oblique section showing the increasing of diameter of tubular chamber and of thickness of wall. Sample BRC 4-6. 4. Numerous tubular chambers cut in a microfacies. Sample BRC 5-5. 5. Very visible pits. Sample BRC 11-28. 6. Small porcelaneous tubular chamber within a microconchid shell. Sample BRC 4-4. 7. Tubular chamber *Orthovertella*-like Sample BRC 11-18. 9. A tubular chamber within a microfacies in order to indicate the great difference of size with the other grains. Sample BRC 9-18. **8,** *Nodosaria* sp. Subaxial section. Sample BRC 9-10. **10-11,** *Hemigordius* sp. 4. 10. Axial section. Sample BRC 11-20. 11. Subaxial section. Sample BRC 11-27. **12-13,** *Abadehella* n. sp. 12. Axial section with rare subdivisions in the chambers. Sample BRC 11-10. 13. Subaxial section showing the partitions. Sample BRC 11-36.

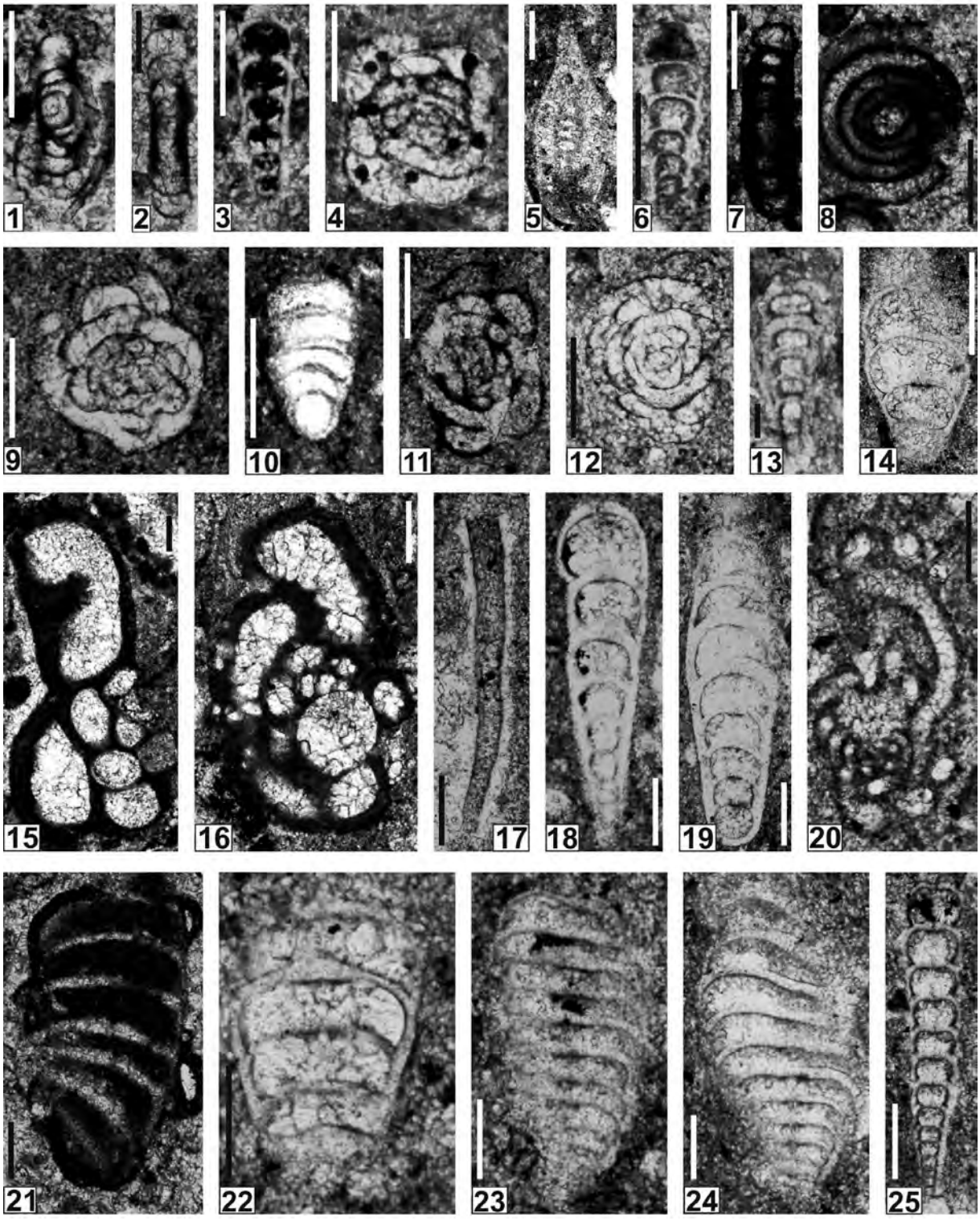


FIGURE 34. Foraminifers from the Robledo Mountains Formation, Apache Canyon Sabkha. Scale bars = 0.1 mm. **1-2,** *Hemigordius* sp. 4. (see also "*Neohemigordius*" *umbilicatus* (Kireeva) sensu Filimonova, 2008). Subaxial section. Sample ACS 66-8. 2. Axial section. Sample ACS 66-9. **3, 6, 13?,** *Nodosinelloides aequiampla* (Lipina). 3. Axial section. Sample ACS 66-15. 6. Axial section. Sample ACS 69-4. 13. Axial section. Sample ACS 69-20. **4, 9, 11-12,** *Glomomidiella* n. sp. 1. Axial section. Sample ACS 68-1. 9. Random section. Sample ACS 68-2. 11. Random section. Sample ACS 61-3. 12. Random section. Sample ACS 66-2. **5, 21,** *Pseudoreichelina* sp. 5. Oblique subaxial section. Sample ACS 69-2. 21. Axial section. Sample ACS 69-13. **7-8,** *Hemigordius* sp. 5. 7 Axial section. Sample ACS 69-5. 8. Transverse section. Sample ACS 69-66. **10, 14,** *Rectoglandulina pigmaeformis supera* Gerke. 10. Axial section. Sample ACS 17-1. 14. Subaxial section. Sample ACS 69a-3. **15-16,** *Hedraites*? n. sp. 2. Two longitudinal sections. 14. Sample ACS 8-4. 15. Sample ACS 8-7. **17,** *Syzrania pulchra* Kireeva. Longitudinal section. Sample ACS 61-1. **18-19,** *Nodosaria* cf. *opima* Lin. 18. Axial section. Sample ACS 61-4. 19. Axial section. Sample ACS 61-5. **20,** *Orthovertella* sp. Axial section. Sample ACS 66-7. **22,** *Geinitzina*? *frondiculariaeformis* Sosipatrova. Subtransverse section in the uncoiled part. Sample ACS 69-22b. **23-24,** *Geinitzina gigantea* Miklukho-Maklay. Two subaxial sections. 23. Sample ACS 69a-2. 24. Sample ACS 69a-8. **25,** *Nodosinelloides longissima* (Suleimanov). Axial section. Sample ACS 69a-9.

bedded siltstone and fine-grained sandstone were interpreted to represent distal crevasse splay deposits. Most of the trace fossils in the Robledo Mountains Formation occur on mud-draped bedding planes of this lithofacies (Fig. 25D-E). Laminated and homogeneous mudstone with well-preserved plant fossils and a lungfish aestivation burrow are interpreted as distal flood deposits. The red-bed intervals generally do not show any evidences of marine or tidal influence (for an exception, see Lerner and Lucas, this volume). The red beds thus represent a fluvially controlled freshwater ecosystem with loose plant cover and with arthropod and tetrapod inhabitants (Voigt et al., 2013).

In the Robledo Mountains Formation, Mack (2007) and Mack et al. (2010) identified 16-18 fourth-order sequences, each 3-15 m thick, and fifth-order cycles that they related to glacio-eustatic sea-level fluctuations. In contrast, Krainer et al. (2009) described six depositional sequences in the Robledo Mountains Formation in the Doña Ana Mountains. Red bed intervals alternate with marine shale and limestone. According to Krainer et al., red beds represent periods of increased siliciclastic influx onto the Hueco shelf, probably resulting from increased tectonic activity in the hinterland (uplift).

In the Branson Canyon section, six depositional cycles are developed in the lower 50 m (Fig. 26). Each cycle is 6-11 m thick, starts with siliciclastic sediments (mostly red mudstone and ripple laminated siltstone to fine-grained sandstone), and grades into marine shale and limestone. Compared to the Doña Ana Mountains, trough-crossbedded, fine-grained sandstone is less common in the Robledo Mountains, indicating a more distal position of deposition. Correlation of cycles or bed-to-bed correlation between individual sections in the Robledo Mountains is not possible, indicating that deposition was mainly controlled by factors other than glacio-eustatic sea-level changes.

Our data and analyses (Krainer et al., 2009; Voigt et al., 2013), stand in marked contrast to those of Mack (2007) and Mack et al. (2010), who presented a sequence stratigraphy of the Robledo Mountains Formation in the PTNM area that identified 16-18 "fourth-order" sequences supposedly bounded by unconformities that reflect the cutting of incised valleys. These incised valleys, according to Mack et al., were filled with lowstand fluvial red beds or by transgressive/highstand estuarine deposits. Mack et al. also identified cm- to m-scale cycles consisting of limestone-shale couplets ("fifth order" cycles), and concluded that both scales of cyclicity in the Robledo Mountains Formation were driven by glacio-eustasy. They further posited that the alternation of arid and humid climates influenced carbonate (arid) and siliciclastic (humid) deposition.

Nevertheless, this work suffers from many of the problems of the similar work by Mack et al. (2013) on the Community Pit Formation discussed above. Thus, the basic stratigraphic and facies data presented by Mack (2007) and Mack et al. (2010) diverge substantially from our field observations. Mack et al. only recognize five facies in the Robledo Mountains Formation: (1) fluvial, which refers to most of the siliciclastic red beds and is supposedly characterized by crossbedding and lateral accretion sets, although such strata are very rare or absent at the Robledo Mountains Formation outcrops in the PTNM area; (2) estuarine, applied to siliciclastics that are mostly ripple laminated and horizontally laminated, which we have interpreted as floodplain or sheetflood deposits (Voigt et al., 2013); (3) lower shoreface shale-siltstone, which encompasses most of the marine shale units and whose position relative to the shoreface is not certain; (4) shallow-marine limestone, which refers to limestones with a "micritic matrix" and thus ignores the varied other limestone microfacies of the Robedo Mountains Formation documented above; and (5) peritidal dolomicrite, a lithofacies also identified by us. Mack et al.'s facies identifications are thus a mixture of inaccurate reporting, incomplete analysis and questionable depositional interpretations.

These problems are best revealed by comparing three of the sections analyzed by Mack (2007) and Mack et al. (2010) to our remeasuring of exactly those sections:

1. Our section Mack 4 (Fig. 28) is the same as section 4 of Mack (2007) and Mack et al. (2010). Mack et al. show "ss-1" (sandstone 1) at the base of the section, but our section shows 4.2 m of red-bed mudstone with a very thin (0.2-m-thick) ripple laminated sandstone bed intercalated. Mack et al. show two higher, thin sandstone beds "ss-1a" and "ss2a," ~ 5 and 12 m above the base of the Robledo Mountains Formation. These are not in our section—they would be in covered intervals (Fig. 28, units 8 and 10). Mack et al.'s "ss3" is our unit 12 and their "ss-5" is our units 23-25. Our unit 12 is mostly laminar sandstone, whereas units 23-25 are a complex of mudstone intercalated with climbing-ripple sandstones, so to equate these as a single facies, as do Mack et al., is an oversimplification. Furthermore, the intervening facies are much more complex in the remainder of our section than are represented by Mack (2007) and Mack et al. (2010). Thus, two thin grainstones separated by a covered interval (our units 19-21) underlie their ss-5. Beneath that is more cover and limestone, including a thin dolostone bed, down to the level of their ss-3. In contrast, Mack et al. represent this interval as about 2 m of cover followed by a thick interval (about 5 m thick) of marine limestone with a thin peritidal dolomite (in our section, this is mostly covered and shale). Based on our observations, section 4 of Mack et al. bears only a superficial resemblance to the outcropping strata.

2. Section 3 of Mack (2007) and Mack et al. (2010) is the same as our section Scorpion Hill B (Fig. 29). Both sections are about 40 m thick and have relatively thick sandstone intervals near their bases and tops (ss-1 and ss-5 of Mack et al.). However, this section is not in the lower part of the Robledo Mountains Formation, as indicated by Mack (2007) and Mack et al. (2010). Instead, it is stratigraphically higher in the formation. Therefore, their correlations of it to other sections low in the Robledo Mountains Formation are not supportable.

3. Our Branson Canyon section (Fig. 26) is the same as sections 1 and 5 (together they are the entire Robledo Mountains Formation) of Mack (2007) and Mack et al. (2010). Again, our section shows much more facies complexity and this leads to a very different interpretation of cycles of deposition in this section (Fig. 26) than is inferred by Mack et al. Particularly problematic is the complex intercalation of red bed siliciclastics and carbonate beds evident in the lower 17 m of this section as we measured it (Fig. 26). Instead, Mack et al.'s section here simply shows a sandstone layer in the lower 3 m (ss-1) and then a thick, sandstone-dominated interval from about 13 m up (their ss's 2a, 2 b and 3).

According to Mack (2007) and Mack et al. (2010), the bases of each of the sandstone intervals in the Robledo Mountains Formation are sequence boundaries that are the supposed erosional bases of incised valleys overlying marine carbonate. However, none of these surfaces is demonstrably erosional and at many places red mudrock, not sandstone rests on carbonate. There is no geometry of incision observable on outcrop, as there is, for example, in the Community Pit Formation at the Flood section (Figs. 16B, 19). Where red beds rest on marine carbonate, the surfaces are flat and no basal conglomerate, rip-ups or other evidence of scour can be observed. The red-bed sandstones are not crossbedded, and the presence of incised valleys and their supposed interfluves is conjectural, not observable on outcrop.

Yet, Mack (2007, p. 5) states that "the base of each fluvial sandstone-siltstone interval defines a sequence boundary, because it is erosional and because it constitutes a non-Waltherian seaward shift in facies." But, as just stated, there is no evidence of erosion at these surfaces, and the "non-Waltherian seaward shift in facies" is at best conjectural, because the Waltherian equivalents of the red bed facies are outside of the outcrop area. Mack (2007, p. 5) went on to state that "the existence of incised valleys is inferred by the presence of estuarine facies overlying fluvial deposits, as well as the ability to correlate some sequence boundaries to adjacent interfluves." These supposed estuarine facies, however, refer mostly to floodplain mudrocks (Voigt et al., 2013), so, again, the evidence for incised valleys in the Robledo Mountains Formation is questionable. Claims by Mack et al. (2010) of numerous polygenetic paleosols in these strata also do not match our observations.The few paleosols we have seen are associated with floodplain mudrock (Lucas et al., 1995).

We thus conclude that the description of facies of the Robledo Mountains Formation by Mack (2007) and Mack et al. (2010) is an oversimplification. Their identification of sequence boundaries, and incised valley fill and interfluves in the Robledo Mountains Formation lacks supporting data, so at most is conjectural. Therefore, the "fourth order" cycles and sequences of Mack and Mack et al. are not supported. As noted above, Mack (2007) and Mack et al. (2010) also identified "fifth-order cycles" in the Robledo Mountains Formation represented by cm-to-m-thick "parasequences" of marine limestone overlain by peritidal dolomicrite or by marine limestone overlain by marine shale. Indeed, such similar alternating facies are present in parts of the Community Pit Formation (Mack et al., 2013). In both the Community Pit and Robledo Mountains formations, these cycles are part of vertically disorganized successions and cannot be correlated across the outcrop for long distances. Their origin thus does not necessarily reflect an allocyclic driver of deposition, such as glacio-eustasy or climate (see earlier discussion).

Apache Dam Formation

Lucas et al. (1998c) proposed the name Apache Dam Formation for the uppermost, limestone-dominated interval of the Hueco Group in the Robledo Mountains (Figs. 35-36). This unit is dominantly algal limestone (Fig. 35) and it is the stratigraphically highest Permian unit in the Robledo Mountains, overlain by Tertiary-Quaternary rocks.

According to Lucas et al. (1998c), the Apache Dam Formation is 61.7 m thick at the type section (Fig. 35A), but they note that this is an incomplete section. Jordan (1971) estimated a maximum thickness of 122 m, which is also incomplete, as younger Permian sediments are missing in the Robledo Mountains. However, our data do not support an Apache Dam Formation more than about 100 m thick, so we believe that Jordan overestimated its thickness. Seager et al. (2008) estimated a thickness of 107 m and this may be an acceptable preserved maximum.

The Apache Dam Formation is exposed in the southern Robledo Mountains, between the PTNM and Picacho Mountain, where it caps cuestas and benches above the slope-forming Robledo Mountains Formation (Figs. 1, 35A). The Apache Dam Formation is composed mainly of algal limestone and shale/covered intervals; algal biopackstone (48%) and slope forming shale-siltstone (48%) are the dominant lithologies (Lucas et al., 1998c). We studied the Apache Dam Formation at the following localities: (1) type Apache Dam, the lower 25 m, lower contact exposed; (2) Branson Canyon, 26.5 m, lower contact exposed; (3) lower Apache Canyon, 28 m, lower contact exposed; (4) middle Apache Canyon, 13 m, lower and upper contacts not exposed; and (5) upper Apache Canyon, 22 m, lower contact exposed (Fig. 36).

Lithology

The Apache Dam Formation is composed of limestone intervals alternating with covered (shale) intervals. On outcrop, the limestone is largely medium to dark gray and bluish gray and it exhibits wavy beds about 20 to 30 cm thick. The limestone is siliceous and contains scattered chert nodules, together with brown silica crusts on weathered surfaces. The limestone commonly forms cliffs.

The following limestone lithotypes are present: (1) wavy-bedded limestone, thin to medium bedded (5-40 cm); (2) nodular to wavy bedded limestone; (3) even bedded limestone, medium bedded; (4) thin-bedded limestone with thin shale intercalations (rare); (5) indistinctly bedded to massive limestone, up to 2 m thick; (6) thicker limestone beds containing crinoidal debris (up to 0.7 m thick); and (7) crossbedded arenitic limestone (very rare).

Limestone units are up to 5.6 m thick, and covered intervals up to 4 m. In some of the limestone units, chert occurs as nodules, and rarely as thin bands.

Microfacies

The most common microfacies types of the Apache Dam Formation are bioclastic wackestone to packstone (Figs. 37A-D) and algal wackestone to floatstone (Figs. 37E-H). Packstone to rudstone is rare. All microfacies contain a diverse fossil assemblage. Only at the base of the type Apache Dam section, wackestone with a low diversity assemblage dominated by tubular foraminifers and ostracodes; some microconchids and rare gastropods are present. Wackestone locally contains abundant peloids, and rare fecal pellets.

Fossils

Fossils commonly observed on outcrop are calcareous algae, crinoidal debris, large gastropods, brachiopods, and rare palechinid radioles. Simpson (1984) listed numerous taxa of invertebrate macrofossils from his "upper Hueco member," including ammonoid taxa, but we are skeptical of this list as we cannot verify that most of these taxa are present. Seager et al. (2008) stated cephalopods are "abundant" in the Apache Dam Formation, but we believe this is a mistaken reference to the large gastropods (especially bellerophontids) that are locally common on outcrop. In many limestone beds, fossils are silicified.

Algal limestone contains abundant phylloid algae (Fig. 37H), which are in most cases completely recrystallized. Rarely, phylloid algae are partly preserved and can be identified as *Neoanchicodium* cf. *catenoides* Endo (Fig. 40.1). Subordinate are dasycladacean algae (*Epimastopora alpina, E. japonica*; *E.* sp., Fig. 41.9, 24-25), as well as microproblematical *Tubiphytes* ex gr. *obscurus* (Figs. 38.2-7, 39.5); *Efluegelia* is very rare. Smaller foraminifers are common in all limestones and represented by *Eotuberitina reitlingerae, Tuberitina* sp., *Earlandia* sp., *Endothyra* sp., the first true *Neoendothyra* sp. (Fig. 39.15), palaeotextulariid, *Globivalvulina novamexicana, G. praegraeca, G. retroseptata, G.* ex gr. *kamensis, G.* n. sp., *Staffella* sp., *Nankinella* sp., *Pseudoreichelina* sp. (Fig. 38.3), *Eostaffella*? sp, *Schubertella* sp., *Calcivertella* sp., *Palaeonubecularia, Pseudospira* sp., *Hedraites* cf. *plummerae* Henbest (Fig. 40.7-8), *H.* n. sp. 2 (Fig. 38.9-10), *H.*? n. sp. 3 (Fig. 39.1), *Pseudovermiporella* ex gr. *sodalica* Elliott (Fig. 39.4), *P.* ex gr. *nipponica* Endo (Figs. 38.1, 7?-8, 40.6, 10), *Hemigordiellina, Hemigordius?,* hemigordiid *Glomomidiella* n. sp. 3 (Figs. 38.4, 39.3, 6), Miliolata indet. (Fig. 39.2), *Nodosinelloides aequiampla, N.* cf. *longissima* (Suleimanov) (Fig. 39.7-8), *N. subquadrata* (Fig. 39.9), *N. netschajewi, N. pinardae, Protonodosaria* sp. (Fig. 39.13), *P.*? sp. (Fig. 40.20), *"Tauridia"*? cf. *tenuiseptata* (Lipina) (Fig. 40.23). *"T."*? sp. (Fig. 40.19, 21?, 22?), *Nodosaria teretra* sensu Filimonova (Fig. 40.11, 12?, 16?), *N. opima* Lin (Fig. 40.14), *N.*? cf *caucasica* (Miklukho-Maklay) (Fig. 40.17), *N.*? sp. (Fig. 39.11), *Geinitzina* cf. *magna* Lipina (Fig. 39.10), *G. multicamerata* Lipina. (Fig. 39.14), *G.* sp. (Fig. 39.12?, 16), *Pachyphloia*? aff. *linae* (Miklukho-Maklay) (Fig. 40.15, 18?) and *P.* sp. (Fig. 40.13).

Ostracodes and echinoderm fragments (crinoids) are present in all samples. A few samples contain palechinid radioles. Other fossils include brachiopods, gastropods, bryozoans, rare small fusulinids and *Tubiphytes*. In many samples, larger skeleton fragments are encrusted by cyanobacteria, subordinately by tubular foraminifers and *Efluegelia*, locally forming oncoids (Fig. 37H).

Depositional Environments

Limestone microfacies of the Apache Dam Formation can be assigned to the following SMF types: SMF 5 (allochthonous bioclastic grainstone, rudstone, packstone and floatstone), indicating deposition adjacent to reef mounds (FZ 6) or inner ramp settings; SMF 10 (bioclastic packstone and wackestone with abraded and worn skeletal grains), indicating an open marine shelf setting (FZ 7) or inner to mid-ramp setting; and SMF 18 (bioclastic grainstone and packstone with abundant benthic foraminifers), which is typical of restricted platform environments (FZ 8), shelf lagoons with open circulation (FZ 7) or inner ramp settings.

These microfacies indicate deposition in an open shelf to shelf lagoon setting with open circulation. Calcareous algae are a common constituent in limestones of the Apache Dam Formation (Fig. 37E-H); they are much more common than in the other formations of the Hueco Group in the Robledo Mountains. Phylloid algae are common in shelf settings and shelf margin environments. Dasycladacean algae are commonly found in shallow shelf environments. A shallow marine, restricted environment is only indicated near the base of the formation.

BIOSTRATIGRAPHY AND CORRELATION

Chronostratigraphic Framework

Before discussing the biostratigraphy and correlation of the Hueco Group section in the Robledo Mountains, we briefly establish a chronostratigraphic framework for correlation (Figs. 41-42). We do so in large part because of the currently confused and confusing state of Early Permian chronostratigraphy. The reason for most of the confusion stems from destabilization during the last 20 years (1990s-present) of what was a well-accepted Early Permian chronostratigraphy for the previous 50-70 years (1920s-1990s). This well-accepted chronostratigraphy was largely rooted in fusulinid and ammonoid biostratigraphy, and the effort to redefine Early Permian chronostratigraphy by reliance on conodont biostratigraphy has caused diverse problems. This topic merits more discussion and justification than we can present here (key references we rely on include Wardlaw, 2005; Boardman et al., 2009; Ross and Ross, 2012; Davydov et al., 2013), so we just make a few key points:

1. Lucas (2013a, b) has well explained the problematic nature of the newly defined base of the Permian that relies on a conodont datum (FAD of *Streptognathodus isolatus* Chernykh, Ritter & Wardlaw) as its primary signal for correlation. Based on his arguments, we reject that conodont datum as useful for chronostratigraphic definition, and return to the fusulinid-based datum. Thus, the base of the Permian is the FAD of *Schwagerina sensu lato* (currently, *Thompsonites*), which means the base of the Permian is equivalent to the base of the North American Wolfcampian, which we regard as a stage. For book-keeping purposes, we thus return to equating the base of the Wolfcampian to the base of the Russian Asselian Stage (Figs. 41-42).

2. We divide the North American Wolfcampian into three fusulinid-based substages: Newwellian, Nealian and Lenoxian, which are lower, middle and upper Wolfcampian sensu Wilde (1990, 2006). For reasons

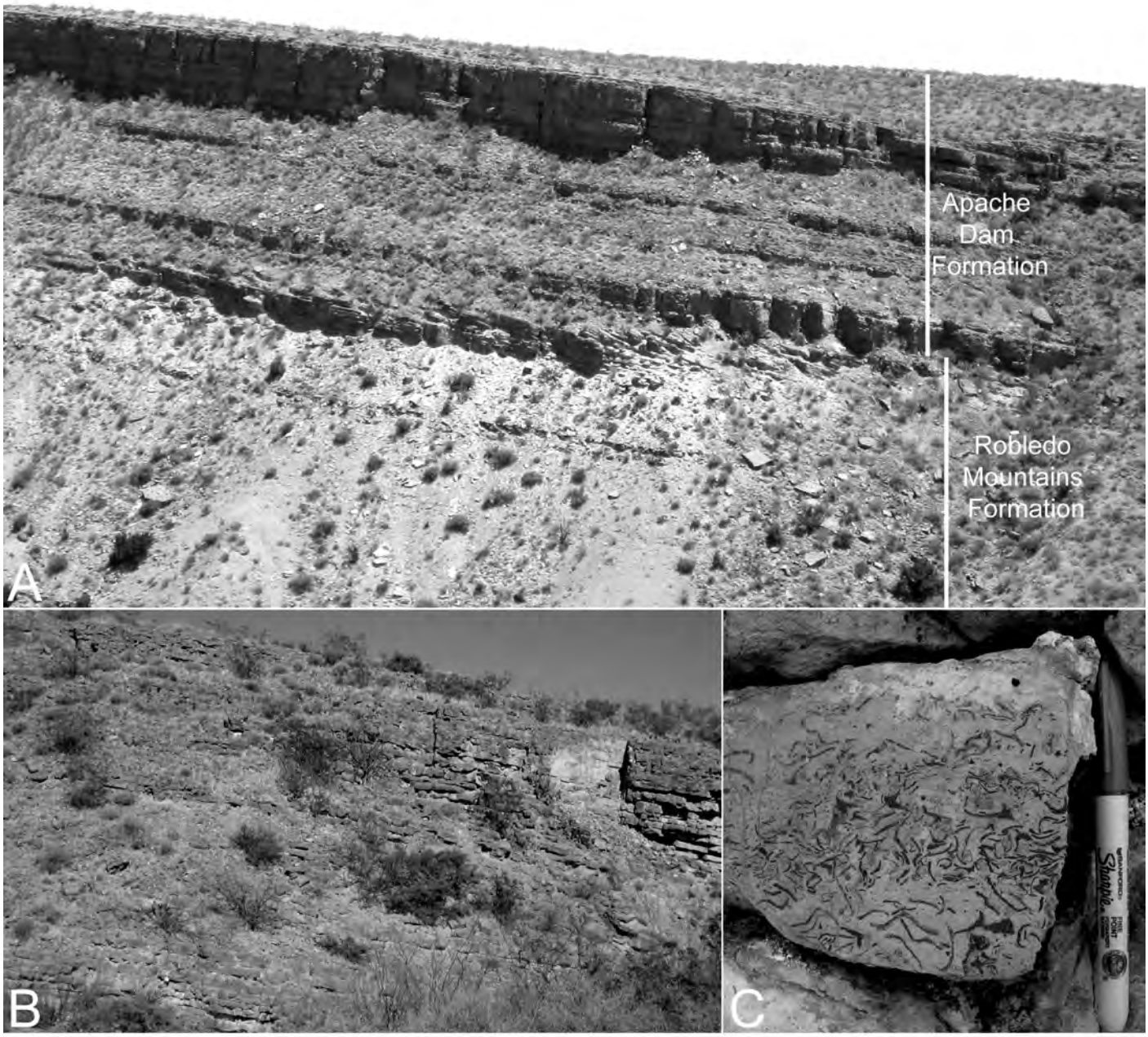


FIGURE 35. Photographs of selected outcrops of the Apache Dam Formation in the Robledo Mountains. **A,** Overview of Apache Dam type section. **B,** Overview of upper Apache Canyon section. **C,** Characteristic algal limestone at upper Apache Canyon section.

best articulated by Wilde (2002), we reject the term Bursumian and instead use Newwellian.

3. The FAD of the conodont *Sweetognathus merrilli* Kozur is the working definition of the Sakmarian base. This FAD in the Texas section is within Nealian strata (e.g., Wardlaw, 2005), so the Sakmarian correlates to the upper part of the Nealian and to the Lenoxian.

4. The base of the North American Leonardian is the FAD of the fusulinid *"Schwagerina"* (currently *Praeskinnerella*) *crassitectoria* Dunbar and Skinner. This stratigraphic level is higher than the FAD of the conodont *Sweetognathus "whitei"* (Rhodes), which is being used as the working definition of the base of the Artinskian. This means that most or all of Artinskian is Leonardian (note that in some earlier correlations, particularly in the 1990s, the Leonardian base was being correlated higher, to the Kungurian base).

5. Some chronological correlations (Fig. 41) were also modified because reference-sections in Austria and Russia have been re-interpreted (Davydov et al., 2013).

Perhaps the most important point to stress here is correlation of the Leonardian base to a point within the Artinskian. As discussed below, this correlation indicates that the upper part of the Hueco Group in the Robledo Mountains (Robledo Mountains and Apache Dam formations) is of early Leonardian age (Figs. 41-42). This is younger than the ages previously reported (Lucas et al., 1998a, c).

Shalem Colony Formation

Previous workers (Thompson, 1954; Wahlman and King, 2002) reported two biostratigraphically distinct fusulinid assemblages from the Shalem Colony Formation in the Robledo Mountains: (1) an older, lower Wolfcampian (Newwellian = "Bursumian") assemblage with small *Leptotriticites*, *Pseudofusulina* and primitive "*Schwagerina*" (i.e., *Thompsonites*); and (2) a younger, middle Wolfcampian (Nealian) assemblage with large *Leptotriticites*, diverse *Pseudoschwagerina* and *Sakmarella andresensis* (Thompson). Our data (also see Krainer et al., this volume) confirm that the Shalem Colony Formation contains

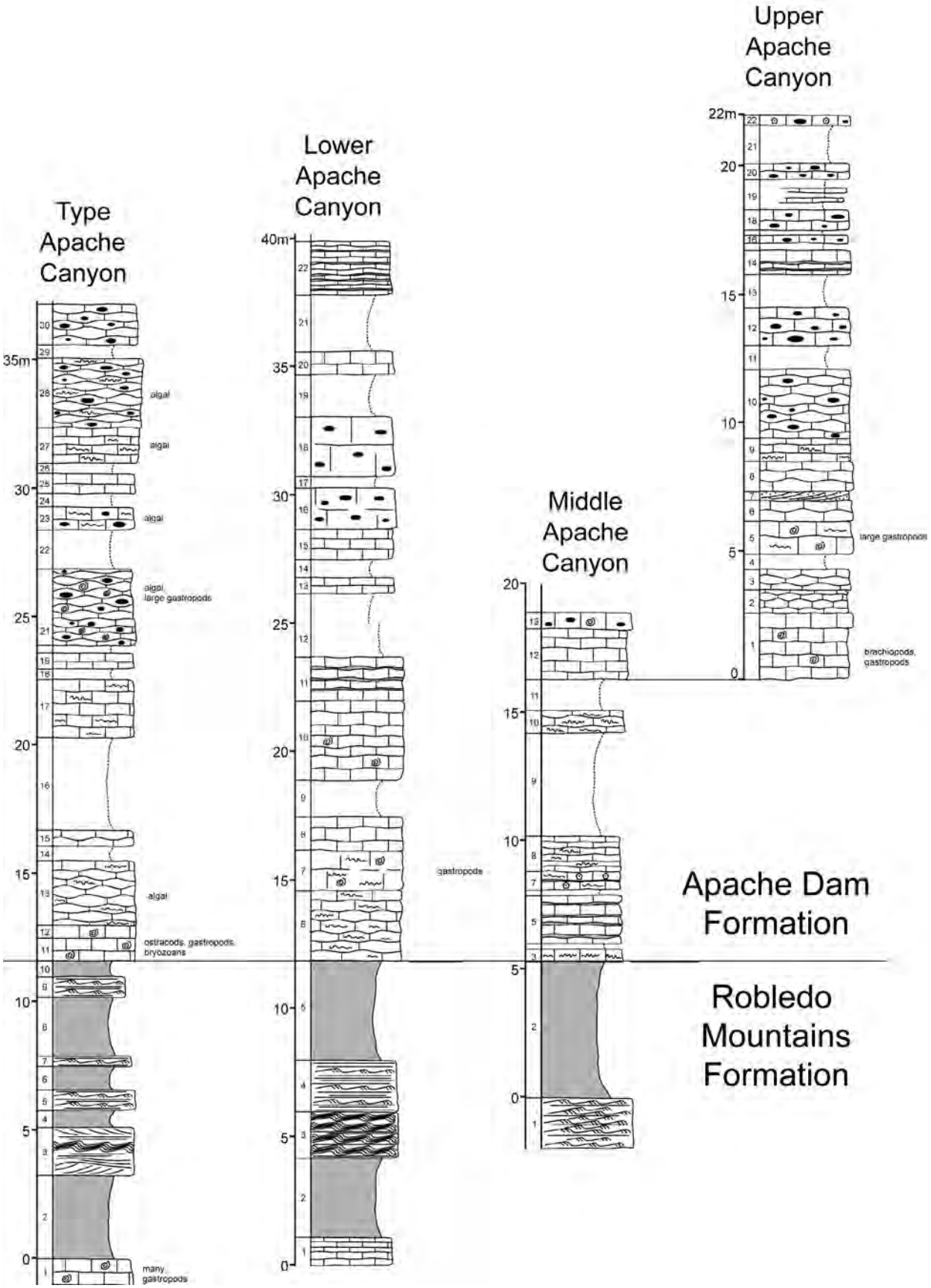


FIGURE 36. Measured stratigraphic section of parts of the Apache Dam Formation in the Robledo Mountains (see Figure 4 and Table 1 for location of sections). See Figure 8 for legend to lithologic symbols.

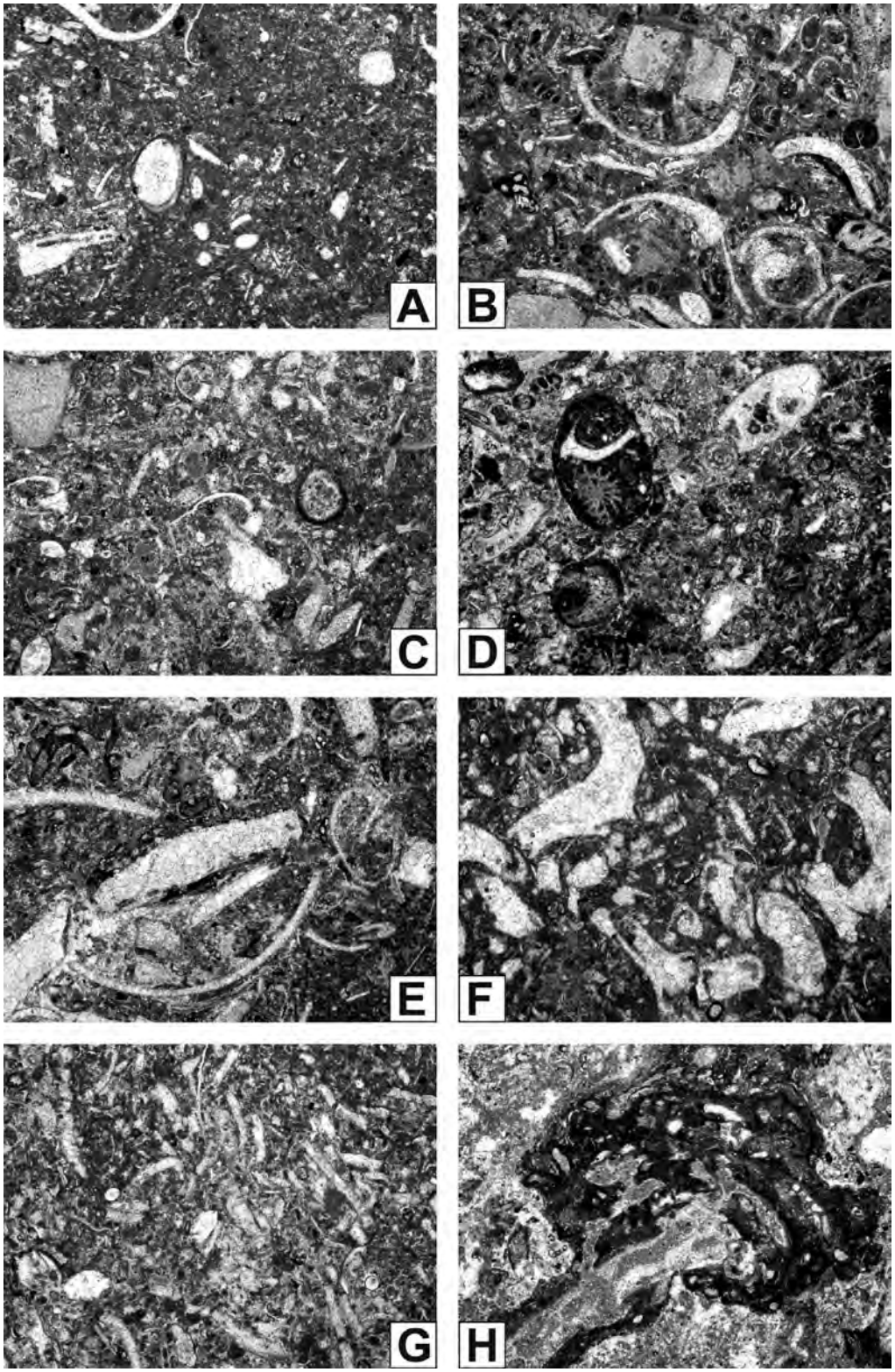


FIGURE 37. Thin section photographs of common microfacies types of the Apache Dam Formation, Robledo Mountains. All photographs under plane light. **A,** Bioclastic wackestone containing a moderately diverse fossil assemblage, mainly phylloid algae and foraminifers. Branson Canyon, BRC 13, width of photograph is 6.3 mm. **B-D,** Bioclastic wackestone to floatstone containing some larger and many small fossil fragments (echinoderms, phylloid algae, bivalves, brachiopods, foraminifers, bryozoans). A few skeletons are encrusted by cyanobacteria. Branson Canyon, B, C = BRC 15, D = BRC 16, width of photograph is 6.3 mm. **E,** Floatstone: large phylloid algal fragments and other skeletons float in wackestone containing abundant tubular foraminifers, ostracodes and subordinate other fossils. Some phylloid algae are encrusted by cyanobacteria. Type Apache Dam, unit 13, width of photograph is 6.3 mm. **F,** Algal wackestone to floatstone containing abundant recrystallized skeletons of phylloid algae (?*Neoanchicodium*), many foraminifers and some other fossils. Some skeletons are encrusted by tubular foraminifers. Type Apache Dam, unit 27, width of photograph is 6.3 mm. **G,** Algal wackestone containing abundant recrystallized skeletons of dasycladacean algae (*Epimastopora*), foraminifers and a few other fossils. Type Apache Dam, unit 21, width of photograph is 6.3 mm. **H,** Phylloid algal fragment encrusted by cyanobacteria and tubular foraminifers forming large oncoids. Type Apache Dam, unit 13, width of photograph is 6.3 mm.

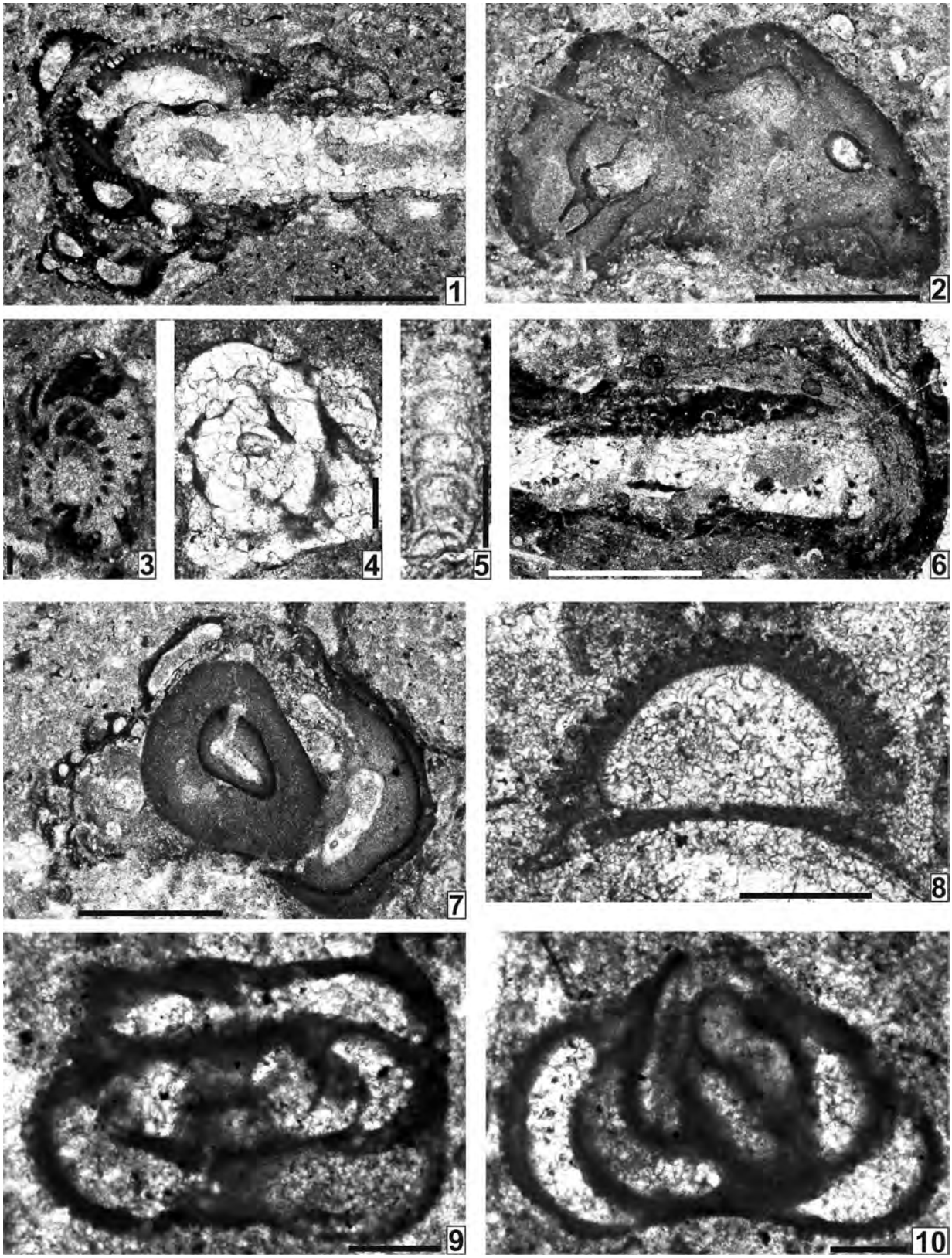


FIGURE 38. Algae and foraminifers from the Robledo Mountains and Apache Dam formations. Scale bars for Figs. 3, 4, 5, 8, 9, 10 = 0.1 mm, for Figs. 1, 2, 6 and 7 = 1 mm. BRC = Branson Canyon; LAC = Lower Apache Canyon; TAD = Type Apache Dam. **1, 7,** *Pseudovermiporella* sp. 1. Transverse section encrusting the extremity of a shell. Sample TAD 13-13. 7. Forming a crust on *Tubiphytes*. Sample TAD 13-13a. **2, 7,** *Tubiphytes obscurus* Maslov. 2. Typical colony. Sample TAD 13-10. 7. Large inner cavities with crust of *Pseudovermiporella* sp. Sample TAD 13-13a. **3,** *Pseudoreichelina* sp. Subtransverse section showing the terminal elevation of the whorl. Sample BRC 14-25. **4,** *Glomomidiella* n. sp. 3. Random section. Sample LAC 6-4. **5,** *Nodosaria* sp. Subaxial section. Sample LAC 1-12. **6,** *Eugonophyllum* and crust. Longitudinal section. Sample BRC 11-33. **8,** *Pseudovermiporella* ex gr. *nipponica* (Endo). Transverse section with typical pits. Sample UBL 14-5. **9-10,** *Hedraites* n. sp. 2. 9. Pits poorly visible. Sample LAC 13-5. 10. Pits more visible at the last whorl. Sample LAC 13-14.

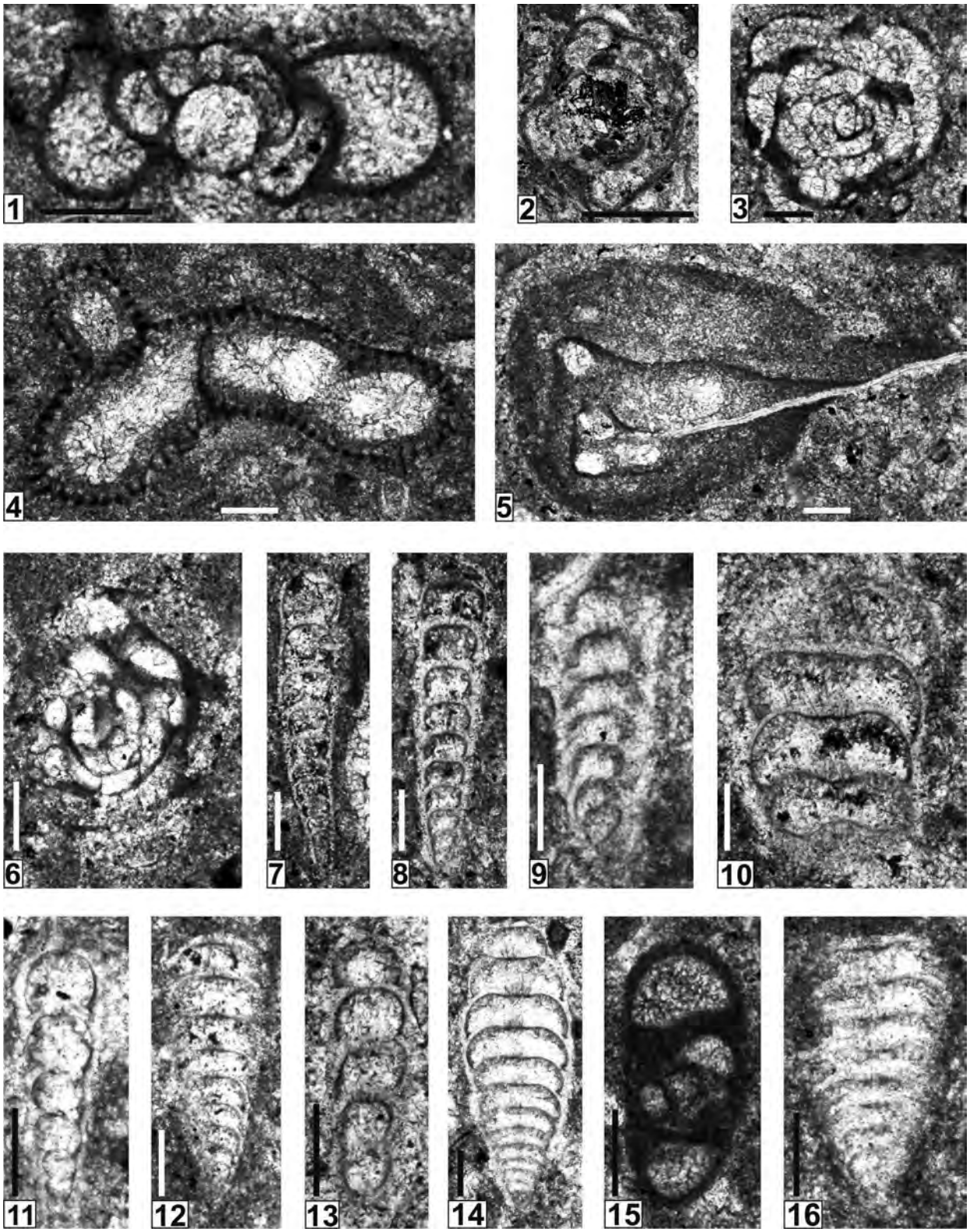


FIGURE 39. Microfossils from the Apache Dam Formation. Scale bars: Fig. 1 = 1. 0 mm, all other figures = 0.1 mm; BRC = Branson Canyon, TAD = Type Apache Dam. **1,** *Hedraites*? sp. 3. Axial section. Sample TAD 11-18. **2,** Miliolata gen. indet. Subaxial section. Sample BRC 16-1. **3, 6,** *Glomomidiella* n. sp. 3. Axial section. Sample TAD 13a-3. 6. Subaxial section. Sample BRC 13-16. **4,** *Pseudovermiporella* ex gr. *sodalica* Elliott. Oblique section. Sample TAD 27-6. **5,** *Tubiphytes* ex gr. *obscurus* Maslov. Axial section. Sample BRC 15-20. **7-8,** *Nodosinelloides* cf. *longissima* (Suleimanov). 7. Axial section. Sample BRC 13-4. 8. Subaxial section. Sample BRC 13-18. **9,** *Nodosinelloides subquadrata* (Lipina). Subaxial section. Sample TAD 21-2. **10,** *Geinitzina* cf. *magna* Lipina. Subaxial section. Sample TAD 13a-4. **11,** *Nestellorella*? sp. Subaxial section. Sample BRC 15-3. **12?,** *Geinitzina* sp. Axial section. Sample BRC 13-8. **13,** *Protonodosaria* sp. Subaxial section. Sample BRC 15-21. **14,** *Geinitzina multicamerata* Lipina. Axial section. Sample BRC 15a-18. **15,** *Neoendothyra* sp. Axial section. Sample TAD 21-6. **16,** *Geinitzina* sp. Axial section. Sample TAD 21-9.

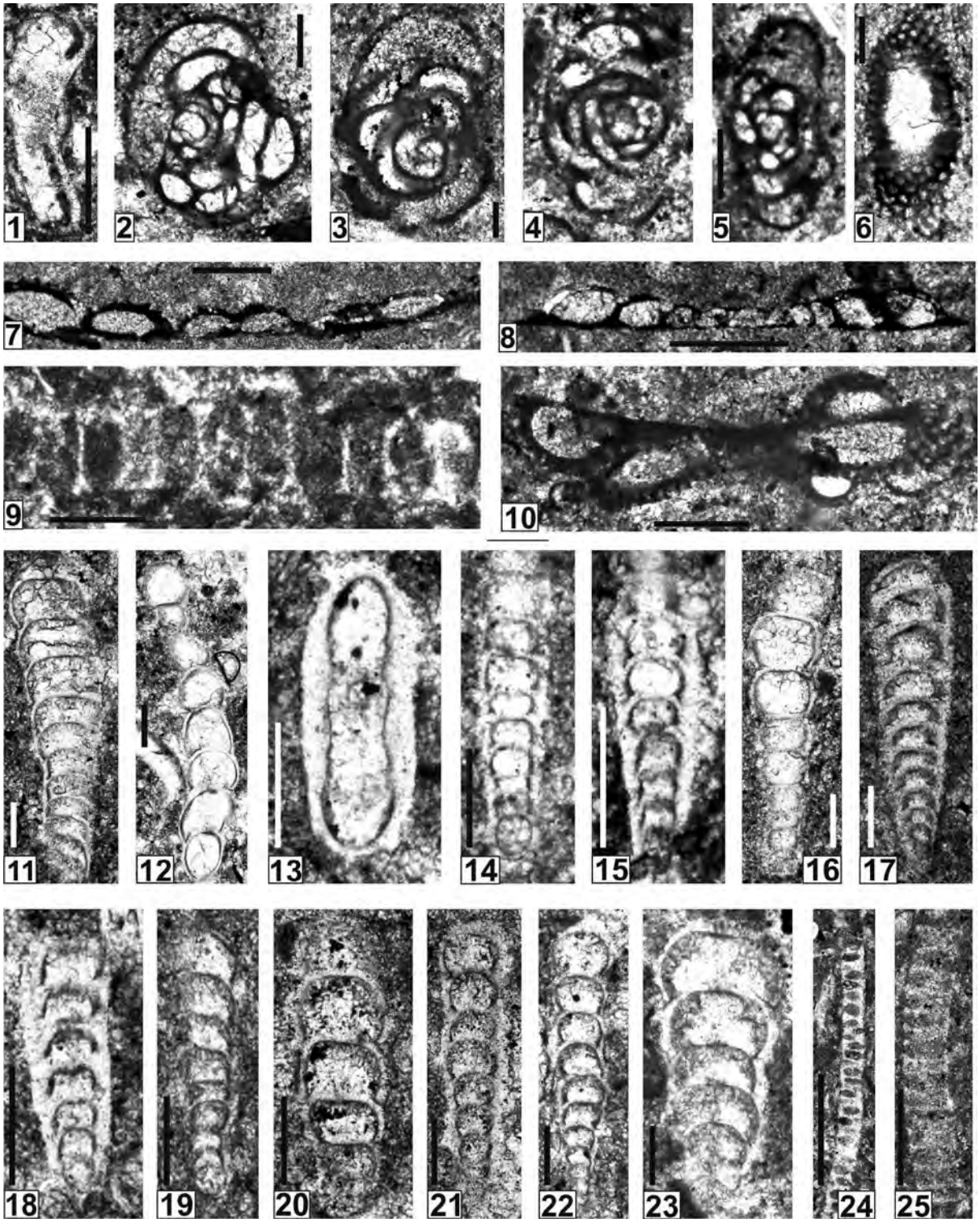


FIGURE 40. Microfossils from the Apache Dam Formation, Lower Apache Canyon. Scale bars: Figs. 1, 24 = 1. 0 mm, Fig. 25 = 0.5 mm, Figs. 7, 8, 9, 10, 12 = 0.2 mm, Figs. 2-6, 11, 13- 23 = 0.1 mm. **1,** *Neoanchicodium* cf. *catenoides* Endo. Longitudinal section. Sample LAC 18-5a. **2-5,** *Glomomidiella* n. sp. transition to *Praeneodiscus*. 2. Axial section. Sample LAC 13-17. 3. Subtransverse section with flexostyle canal. Sample LAC 13-9. 4. Subaxial section. Sample LAC 13-14. 5. Axial section. Sample LAC 13-15. **6, 10,** *Pseudovermiporella* ex gr. *nipponica* (Endo). 6. Oblique section. Sample LAC 13-17a. 10. Subaxial section. Sample LAC 13-11. **7-8,** *Hedraites* cf. *plummerae* Henbest. 7. Subaxial section. Sample LAC 6-9. 8. Subaxial section. Sample LAC 6-2. **9,** *Epimastopora alpina* Pia. Longitudinal section. Sample LAC 24-10. **11,** *Nodosaria teretra* sensu Filimonova. Subaxial section. Sample LAC 1-3. **12,** *Protonodosaria*? sp. Subaxial section. Sample LAC 1-4. **13,** *Pachyphloia* sp. Transverse section. Sample LAC 1-5. **14,** *Nodosaria opima* Lin. Axial section. Sample LAC 10-1. **15, 18?,** *Pachyphloia*? aff. *linae* (Miklukho-Maklay). 15. Subaxial section. Sample LAC 1-13. 18. Axial section. Sample LAC 1-19a. **17,** *Nodosaria*? cf. *caucasica* (Miklukho-Maklay). Axial section. Sample LAC 6-13. **19, 21?-22?,** "*Tauridia*"? sp. 19. Axial section. Sample LAC 6-15. 21. Subaxial section. Sample LAC 7-6. 22. Subaxial section. Sample LAC 10-7. **20,** *Protonodosaria*? sp. Subaxial section. Sample LAC 7-1. **23,** "*Tauridia*"? cf. *tenuiseptata* (Lipina). Subaxial section. Sample LAC 11-5. **24,** *Epimastopora japonica* Endo. Longitudinal section. Sample LAC 6-5. **25,** *Epimastopora alpina* Pia. Longitudinal section. Sample LAC 6-14.

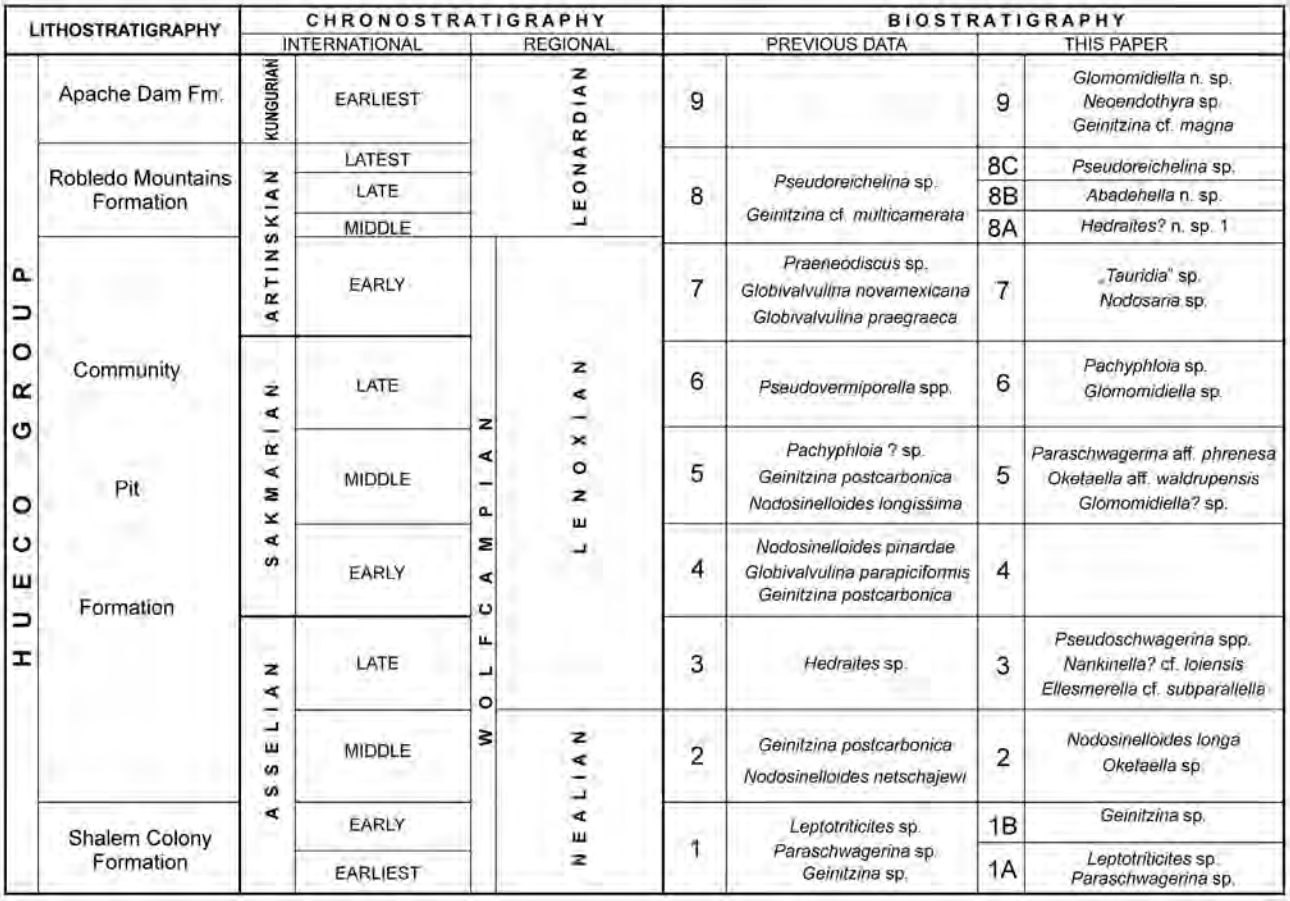


FIGURE 41. Biostratigraphy of the Lower Permian Hueco Group in the Robledo Mountains presented in this work and proposed chronostratigraphic correlations.

two biostratigraphically distinct microfossil assemblages, and both are assigned to the Wolfcampian because we consider that *Thompsonites* indicates the base of the regional Permian (see above, and Figs. 41-42).

The first assemblage is composed of *Triticites* spp., *Leptotriticites* spp., *Thompsonites* spp., *Paraschwagerina* spp., and *Hedraites plummerae*, and the second assemblage shows a diversification of the primitive nodosariates, with *Nodosinelloides longa*, *Geinitzina linguliformis* as well as *Protonodosaria* cf. *irwinensis*, *Nodosinelloides* cf. *pinardae*, *N.*? *pseudoovoidea*, and *Geinitzina*? sp. Consequently, within zone 1 of the scheme presented here (Fig. 41), we include two subzones: 1A with *Trititicites*, *Leptotriticites*, *Thompsonites*, and *Paraschwagerina*; 1B with the FO (FAD?) of *Geinitzina* in Indian Springs Canyon unit 109. Nevertheless, this lower limit might be extended downward to the FO of *Ellesmerella* cf. *permica* in Indian Springs Canyon units 85 and 87. The Permian age of our biozone 2 (at the base of the Community Pit Formation; see below) with *Pseudoschwagerina* and *Leptotriticites*, was previously established by Wahlman and King (2002). The same authors, between their assemblages with *Triticites* and those with *Pseudoschwagerina*, found a *Pseudofusulina robleda* assemblage, which is therefore probably coeval with our zone 1B.

Besides the fusulinid genera, biozone 1A may be also characterized by three taxa: *Hedraites plummerae*, indeterminate crustacean coprolites and *Ellesmerella*. *Hedraites plummerae* is defined by its calcivertellid test morphology, its dimensions and its few marked pits. The crustacean coprolites of biozone 1A (Fig. 9H), correspond to a potentially new genus different from the *Palaxius* and *Favreina* ordinarily described in the Late Palaeozoic and Triassic strata (Brönnimann and Zaninetti, 1972; Senowbari et al., 1992; Herbig, 1993; Masse and Vachard, 1996).

Subzone 1B displays abundant oncoids with *Ellesmerella* cf. *permica*, whereas *E.* cf. *subparallela* has its acme at the base of zone 2. It is noteworthy that *Osagia incrusta* Twenhofel as emended by Henbest (1963, p. 36-37, pl. 6, figs. 1-5) is probably synonymous with *Ellesmerella permica* and, therefore, *Ellesmerella* is possibly a junior synonym of *Osagia.*

Community Pit Formation

The Community Pit Formation was divided into 6 biozones (Zone 2 to Zone 7) in the Doña Ana Mountains (Krainer et al., 2009; Vachard et al., 2014; and Figs. 41-42). If the same number of subdivisions may be established in the Robledo Mountains, their biomarkers are distinct (Figs. 41-42). Zone 2, at the base of the formation, may be defined by *Nodosinelloides longa* (Fig. 23.18) and the FO of *Oketaella* sp. Zone 3 appears the richest with its assemblages with *Pseudoschwagerina* spp. (Fig.11.8-10, 14.3-4, 7), *Nankinella*? cf. *loiensis* (Fig. 11.11-15), and *Ellesmerella* cf. *subparallella* (Figs. 12.4, 6, 13.7, 15.8) of fusulinids. This latter genus is an atypical miliolate, and appears more precociously in New Mexico than in the Carnic Alps (Austria-Italy); it is indeed late Asselian in New Mexico, whereas the type material of the Carnic Alps (Flügel and Flügel-Kahler, 1980) belong to the latest Sakmarian-Kungurian uppermost Grenzland, Zweikofel, Trogkofel and Goggau formations (see e.g., Sanders and Krainer, 2005, as up-dated by Davydov et al., 2013).

Zone 4 is probably devoid of foraminifers and corresponds to calcareous paleosols and/or stratigraphical gaps due to a local phase of subaerial exposure. Zone 5 is characterized by *Paraschwagerina*? aff. *phrenesa*, *Oketaella* aff. *waldrupensis*, and the most primitive *Glomomidiella*. Zone 6 is characterized by the first true *Pachyphloia* and true *Glomomidiella*. However, the new markers do not permit more accurate correlations of the Community Pit Formation, which remains, in our proposed correlations, correlated with the Sakmarian and includes at its base a possible middle-late Asselian interval and at its top a possible early Artinskian interval.

Biozones 2, 3 and 5 of the Community Pit Formation are well characterized in the Robledo Mountains. On the other hand, biozones 6 and 7 were not identified in the Robledo Mountains. Two explanations are possible: they are absent because of stratigraphic gap(s) or, more likely, the correlative part of the Community Pit Formation in the Doña

ZONATION	FORMATIONS		Thickness (m)	BIOMARKERS (and representative samples)		REGIONAL STAGES	INTERNATIONAL STAGES
Zone 15	SAN ANDRES FORMATION			*Olgaorlovella davydovi* *Tubiphytes epimonellaeformis* *Geinitzina indepressa*	LEONARDIAN	CATHEDRALIAN	LATE KUNGURIAN
Zone 14				*Hemigordiellina* spp.			MIDDLE KUNGURIAN
Zone 13	GLORIETA SANDSTONE			barren of foraminifers			
Zone 12	YESO GROUP			*Frondicularia* aff. *turae*			EARLY KUNGURIAN
Zone 11				*Ellesmerella rara* *Nestellorella* ? sp.			
Zone 10				*Globivalvulina novamexicana* *Orthovertellopsis protaeformis* *Globomidiella infrapermica*			
Zone 9	HUECO GROUP	Apache Dam Formation					LATE ARTINSKIAN
Zone 8		Robledo Mountains Formation	53	*Pseudoreichelina* sp. *Geinitzina* sp. 2 (?*multicamerata*)		HESSIAN	MIDDLE ARTINSKIAN
Zone 7		Community Pit Formation	10	*Praeneodiscus* sp. *Globivalvulina novamexicana* *Globivalvulina praegraeca* DAB 13 + DAB 14/DAC 1-DAC 5			EARLY ARTINSKIAN
Zone 6			20	*Pseudovermiporella* sp. DAB 10 - DAB 12	WOLFCAMPIAN	LENOXIAN	LATEST SAKMARIAN
Zone 5			50	*Pachyphloia*? sp. *Geinitzina postcarbonica* *Nodosinelloides longissima* DAB 7 - DAB 9			LATE SAKMARIAN
Zone 4			7	*Nodosinelloides pinardae* *Globivalvulina parapiciformis* *Geinitzina postcarbonica* DAA 59 - DAA 69/DAB 2 - DAB 6			EARLY SAKMARIAN
Zone 3			50	*Hedraites* sp. DAA 53 - DAA 58		NEALIAN	LATE ASSELIAN
Zone 2			20	*Geinitzina postcarbonica* *Nodosinelloides netschajewi* DAA 45 - DAA 52			MIDDLE ASSELIAN
Zone 1		Shalem Colony Formation	65	*Leptotriticites* sp. (DAA 43) *Nodosinelloides longissima* *Tubiphytes* sp., *Geinitzina* sp. (DAA 38) *Pseudovidalina* sp., *Pseudoschwagerina* sp. DAA 42		Newwellian	EARLY ASSELIAN - LATEST GZHELIAN

FIGURE 42. Biozonations by foraminifers of the Lower Permian sucessions (Asselian, Sakmarian, Artinskian and Kungurian) of New Mexico (U.S.A.) (modified from Krainer et al., 2009; Vachard et al., 2015).

Ana Mountains corresponds to the lowermost part of the Robledo Mountains Formation in the Robledo Mountains.

Three assemblages of fusulinids with the last schwagerinoids and advanced schubertelloids of the series may be mentioned: (1) unit 135 of the Indian Springs Canyon section contains "*Nankinella*?" cf. *loiensis*, *Thompsonites*, transitional forms towards *Pseudoschwagerina*, true *Pseudoschwagerina* spp. and *Pseudoschwagerina*? *texana*; (2) *Paraschwagerina*? aff. *phrenesa* is present in Flood; and (3) *Oketaella* aff. *waldrupensis* is present at Indian Springs Canyon unit 166 (its FO is at Indian Springs Canyon unit 133, at the base of biozone 2)

Robledo Mountains Formation

The Robledo Mountains Formation is relatively poor in biostratigraphically useful microfossils, but confirms, in the Apache Canyon Sabkha section, that it belongs to the *Pseudoreichelina* Zone with the presence of this biomarker. Consequently, we can confirm its middle Artinskian age as proposed by Krainer et al. (2003) and Vachard et al. (2015) (Fig. 42).

Some other taxonomic groups further confirm this Artinskian age assignment. The few conodonts documented from the lower-middle Robledo Mountains Formation include *Sweetognathus expansus* (Perlmutter) and *S. merrilli* Kozur and were deemed to be of Artinskian age by Lucas et al. (1995) and Kozur and LeMone (1995b). Kietzke and Lucas (1995) described ostracodes from the upper part of the Robledo Mountains Formation and considered them (especially *Cavellina edmistonae* Harris & Lalicker) to be close in age to the Wolfcampian-Leonardian boundary (see Menyk and Maddocks, 1988). Kues (1995) stated that brachiopods from the upper part of the Robledo Mountains include taxa of both Wolfcampian and Leonardian age, notably the very abundant taxon *Squamaria moorei* Muir-Wood and Cooper, which was originally described from the Leonardian of Texas (Muir-Wood and Cooper, 1960). Two ammonoid taxa documented by Kues (1995) from the upper part of the Robledo Mountains Formation--*Properrinites boesei* (Plummer and Scott) and *Metalegoceras baylorense* (White)—are also taxa that cross the Wolfcampian-Leonardian boundary. Thus, biostratigraphic analyses prior to our work assigned the Robledo Mountains Formation an Artinskian age (conodonts) or an age very close to the Wolfcampian-Leonardian boundary (ostracodes, brachiopods, ammonoids). Our conclusion that the Robledo Mountains Formation is middle to latest Artinskian, and therefore early Leonardian (Figs. 41-42), thus is consistent with regional work, and the distribution of the genus *Pseudoreichelina* in Tethyan areas and Japan.

In fact, in our new collections *Pseudoreichelina:* (1) appears only in the upper part of the Robledo Mountains Formation; (2) locally survives in the base of the Apache Dam Formation (Fig. 38.3); and (3) is now considered as late Artinskian to early Kungurian in age in the Austrian Trogkofel Formation (Davydov et al., 2013). The lower part of the Robledo Mountains Formation contains in abundance a taxon kept here in open nomenclature: *Hedraites*? n. sp. 1. This taxon is not known in the Russian stratotype or Tethyan successions. Nevertheless, between the *Hedraites*? n. sp. 1 assemblages and the *Pseudoreichelina* assemblages, a FO of *Abadehella* n. sp. is noticeable. Similar primitive *Abadehella* appear in the Zottachkopf Formation in the Carnic Alps, which is probably middle to late Artinskian in age. Consequently, we introduce three subzones into biozone 8, the chronostratigraphy of which might be proposed as follows: 8A with *Hedraites*? n. sp. 1 is probably middle Artinskian in age; 8B with *Abadehella* n. sp., possibly late Artinskian; and 8C with *Pseudoreichelina* sp., possibly latest Artinskian.

Apache Dam Formation

Due to its microfossil assemblage, which is intermediate between that of the middle Artinskian Robledo Mountains Formation and that of the early Kungurian Yeso Group, the Apache Dam Formation is probably latest Artinskian and/or earliest Kungurian in age (Fig. 41). It yields, as possible secondary markers, the first true *Neoendothyra* sp. of the series (Fig. 39.15); numerous *Hedraites*? spp. (Fig. 39.1); rare true *Hedraites* spp. (Figs. 38.9-10, 40.7-8); several species of *Pseudovermiporella* (Figs. 38.1, 7-8, 39.4, 40.6, 10); *Tubiphytes* ex gr. *obscurus* Maslov (Figs. 38. 2, 7, 39.5); *Glomomidiella* spp. (Figs. 38.4, 39.3, 6, 40.2-5); *Nodosinelloides* cf. *mirabilis*; *N.* sp.; *Protonodosaria* sp.; *Geinitzina multicamerata*; *G.* cf. *magna*; *G.* sp.; and the first true *Pachyphloia* sp. (Fig. 40.13). The corresponding biozone 9, not yet characterized (Figs. 41-42), is defined here (Fig. 41) as a zone with true *Neoendothyra*, *Glomomidiella* n. sp. and *Geinitzina* cf. *magna*. Its age is supposed to be earliest Kungurian because it is between the latest Artinskian zone 8C and the early Kungurian zone 10 (Figs. 41-42).

Correlation

The new data permit a comparison with those already obtained in several localities of New Mexico, and the synthesis of all the data (Fig. 41). The previously published age of the Community Pit Formation and its biozonation are confirmed. Some further precision can be provided for the other formations. The Shalem Colony Formation corresponds to two distinct bio- and chronostratigraphical units within the Early Permian (Fig. 41). The Robledo Mountains Formation is confirmed as corresponding to the middle Artinskian; its top *Pseudoreichelina* Zone is even probably latest Artinskian. In this case, the overlying Apache Dam Formation corresponds probably to the earliest Kungurian, and to a unique regional zone 9 with *Neoendothyra* sp., *Glomomidiella* n. sp., and *Geinitzina* cf. *magna* as biomarkers.

Zone 1 contains classical schwagerinoid fusulinids, but this superfamily becomes very rare or absent in the subsequent zones. Only the staffelloid fusulinid *Pseudorechelina* is used as a marker of zone 8C. Endothyrida do not provide many markers, other than the FO of true *Neoendothyra* in zone 9. The LO of *Abadehella* permits characterization of zone 8B. Rare *Globivalvulina* are selected as zone markers, especially zones 4, 7 and 10 (Figs. 41-42).

The main markers are the Miliolata and the Nodosariata (these two classes are interpreted here as emended by Gaillot and Vachard, 2007). Among the typical Miliolata, the following genera were used for the biozonation (Figs. 41-42): *Praeneodiscus* (zone 10), *Olgaorlovella* (zones 9?, 15); *Orthovertellopsis* (zone 10); *Glomomidiella* (zones 9-10) and *Hemigordiellina* (zone 14). Atypical encrusting Miliolata (as interpreted by Vachard and Krainer, 2001a, b), neglected prior to our studies, are useful, especially *Hedraites* (zone 3), *Pseudovermiporella* (zone 6), and *Hedraites*? (zone 8A). A regional scale based on the different species of *Tubiphytes* and those of tubiphytids might be also refined (zones 1, 13), notably in order to characterize exactly the replacement of *Latitubiphytes* by true *Tubiphytes*, as well as the local evolution of the group *Tubiphytes obscurus*. *Ellesmerella* (often considered as a *Girvanella*, but, that belongs in reality to this group of atypical encrustiong Miliolata), permitted the characterization of two zones (9 and 11).

Nodosariata characterize zones 1B, 2, 4-9, 12 and 15; more accurate biozonation with *Nodosinelloides* and/or *Geinitzina* seems to be possible. Indeed, four different species of *Geinitzina* are designated as markers in our biozonation (zones 1B, 4-5, 8-9 and 15).

CONCLUSIONS

We offer the following conclusions based on this study:

1. As proposed by Lucas et al. (1998c), strata of the Lower Permian Hueco Group in the Robledo Mountains are assigned to the (ascending order) Shalem Colony, Community Pit, Robledo Mountains and Apache Dam formations.

2. The Shalem Colony Formation (127-156 m thick) is a relatively thick bedded and coarse-grained succession of wackestones, grainstones, rudstones and some oolites intercalated with mostly covered intervals that represent shale and/or nodular limestone. It rests with apparent conformity on the Pennsylvanian-Permian Horquilla Formation.

3. The Community Pit Formation (93-177 m thick) is mostly a slope-forming interval of shale and siltstone beds intercalated with relatively thin intervals of limestone, many of which are mudstones and dolomitic mudstones. The formation has a characteristic brownish gray to grayish orange color.

4. The Robledo Mountains Formation (90-125 m thick) is mostly drab-colored marine shale and limestone, but is readily identified by its characteristic siliciclastic red beds (mudstone, siltstone and sandstone), which are intercalated with the marine rocks.

5. At least 107 m thick, the Apache Dam Formation is composed mainly of algal limestone and shale/covered intervals.

6. Analyses of microfacies, paleontology and stratigraphic architecture indicate that the Shalem Colony Formation accumulated on a platform interior environment of open, normal marine to less common, restricted marine settings; the Community Pit Formation formed in shelf settings ranging from shallow, low-energy (rarely high-energy) open marine to restricted marine environments; the Robledo Mountains Formation represents deposition in a restricted to open marine shallow shelf setting where intercalated red beds were deposited on a distal, extensive flood plain (exhibiting crevasse splay deposits, rare channels, and distal sheet flood deposits) during periods of strong

siliciclastic influx from uplifts located to the north and northeast; and the Apache Dam Formation was deposited in an open shelf to shelf lagoon environment with normal salinity and open circulation.

7. Previously published analyses that posit cycles of deposition in the Community Pit and Robledo Mountains formations driven by glacio-eustasy or another allocyclic process are rejected because they failed to demonstrate any lateral extent to the inferred cycles and are based on insufficiently detailed analyses of microfacies, so that the facies stacking patterns interpreted to reflect cyclicity only approximate those evident on outcrop. Indeed, vertical successions of facies in the Community Pit and Robledo Mountains formations are generally so disorganized that an allocyclic driver of sedimentation appears unlikely.

8. New age data, primarily from fusulinids and non-fusulinid foraminifers, indicate the Shalem Colony Formation is early-middle Wolfcampian (Asselian), the Community Pit Formation is middle Wolfcampian-early Leonardian (Asselian-early Artinskian), the Robledo Mountains Formation is early Leonardian (middle-late Artinskian) and the Apache Dam Formation is Leonardian (Artinskian/Kungurian boundary interval). This indicates that the base of the Leonardian is within the Hueco-Abo lithosome.

ACKNOWLEDGMENTS

The U. S. Bureau of Land Management permitted our work, funded some of it and provided diverse logistical support. In particular, we are grateful to these BLM personnel for assistance: Lori Allen, McKinney Briske, Phil Gensler and Pat Hester. Jerry MacDonald, Larry Rinehart, Justin Spielmann and Sebastian Voigt assisted in diverse ways in the field. KK wishes to thank the Austrian Science Foundation (FWF), project P20178-N10, for financial support. Bruce Allen, David Haig, John Nelson and Ed Simpson provided helpful reviews of the manuscript that improved its content and clarity.

REFERENCES

Baryshnikov, V. V., Zolotova, V. P. and Koshaleva, V. F., 1982, Novye vidy foraminifer Artinskogo yarusa Permskogo Priuralya [New species of foraminifers from Artinskian stage of the Pre-Ural]: Akademiya Nauk SSSR, Uralskii Nauchnyi Tsentr, Institut Geologii i Geokhimii, Preprint, 54 p. [in Russian]

Boardman, D. R., II, Wardlaw, B. R. and Nestell, M. K., 2009, Stratigraphy and conodont biostratigraphy of the uppermost Carboniferous and Lower Permian from the North American midcontinent: Kansas Geological Suevey, Bulletin 255, p. 1-253.

Bogush, O. I. and Yuferev, O. V., 1966, Foraminifery karbona i permi Verkhoyanya [Carboniferous and Permian foraminifers from Verkhoiansk]: Akademiya Nauk SSSR, Sibirskoe Otdelenie, Institut Geologii i Geofiziki, 208 p. [in Russian].

Braddy, S. J., 1995, A new arthropod trackway and associated invertebrate ichnofauna from the Lower Permian Hueco Formation of the Robledo Mountains, southern New Mexico: New Mexico Museum of Natural History and Science, Bulletin 6, p. 101-105.

Braddy, S. J., 1998, An overview of the invertebrate ichnotaxa from the Robledo Mountains ichnofauna (Lower Permian), southern New Mexico: New Mexico Museum of Natural History and Science, Bulletin 12, p. 93-98.

Brönnimann, P. and Zaninetti, L. 1972, Revision of the micro-coprolite *Palaxius*? *triassicus* (Elliott), 1962, and description of a new Triassic thalassinid anomuran (Crustacea, Decapoda) coprolite from France, Austria and Libya: Mitteilungen Gesellschaft Geologie und Bergbaustuden, v. 21, p. 929-940.

Darton, N. H., 1928, "Red beds" and associated formations in New Mexico with an outline of the geology of the state: U.S. Geological Survey, Bulletin 794, 356 p.

Davydov, V. I., Krainer, K. and Chernykh, V., 2013. Fusulinid biostratigraphy of the Lower Permian Zweikofel Formation (Rattendorf Group; Carnic Alps, Austria) and Lower Permian Tethyan chronostratigraphy: Geological Journal, v. 48, p. 57-100.

DiMichele, W. A., Chaney, D. S., Nelson, W. J., Lucas, S. G., Looy, C. V., Quick, K. and Jun, W., 2007, A low diversity, seasonal tropical landscape dominated by conifers and peltasperms: Early Permian Abo Formation, New Mexico: Review of Palaeobotany and Palynology, v. 145, p. 249-273.

Dunham, K. C., 1935, The geology of the Organ Mountains with an account of Doña Ana County, New Mexico: New Mexico Bureau of Mines and Mineral Resources, Bulletin 11, 272 p.

Falcon-Lang, H. J., Kurzawe, F., and Lucas, S. G., 2014, Coniferopsid tree-trunks preserved in sabkha facies in the Permian (Sakmarian) Community Pit Formation in south-central New Mexico, U.S.A.: Systematics and palaeoecology: Review of Palaeobotany and Palynology, v. 200, p. 138-160.

Filimonova, T. V., 2008, Smaller foraminifers from type sections of the Bolorian stage, Lower Permian of Darvas: Stratigraphy and Geological Correlation, v. 16, p. 599-617.

Filimonova, T. V., 2010, Smaller foraminifers of the Lower Permian from western Tethys: Stratigraphy and Geological Correlation, v. 18, p. 687-811.

Flügel, E., 2010, Microfacies of carbonate rocks. Analysis, interpretation and application (2nd ed.). Springer, Berlin, 984 p.

Flügel, E. and Flügel-Kahler, E., 1980, Algen aus den Kalken der Trogkofel-Schichten der Karnischen Alpen: Carinthia II, Sonderheft, v. 36, p. 113-182.

Gaillot, J. and Vachard, D., 2007, The Khuff Formation (Middle East) and time equivalents in Turkey and South China: Biostratigraphy from Capitanian to Changhsingian times (Permian), new foraminiferal taxa, and palaeogeographical implications: Coloquios de Paleontología, v. 57, p. 37-223.

Harbour, R. L. 1972. Geology of the northern Franklin Mountains, Texas and New Mexico: U. S. Geological Survey, Bulletin 1298, 129 p.

Haubold, H., Hunt, A. P., Lucas, S. G. and Lockley, M. G., 1995, Wolfcampian (Early Permian) vertebrate tracks from Arizona and New Mexico: New Mexico Museum of Natural History and Science, Bulletin 6, p. 135-165.

Henbest, L. G., 1963, Biology, mineralogy, and diagenesis of some typical late Paleozoic sedimentary foraminifera and algal-foraminiferal colonies: Cushman Foundation for Foraminiferal Research, Special Publication 6, p. 1-44.

Henderson, C. M., Davydov, V. I., Wardlaw, B. R., Gradstein, F. M. and Hammer, O., 2012, The Permian Period; in Gradstein, F. M., Ogg, J. G., Schmitz, M. D. and Ogg, G. M., eds., The geologic time scale 2012, volume 2: Amsterdam, Elsevier, p. 653-679

Herbig, H. G., 1993, First upper Devonian crustacean coprolites: *Favreina prima* n. sp. from northern Morocco: Journal of Paleontology, v. 67, p. 98-103.

Hunt, A. P. and Lucas, S. G., 1998a, Vertebrate ichnofaunas of New Mexico and their bearing on Early Permian tetrapod ichnofacies: New Mexico Museum of Natural History and Science, Bulletin 12, p. 63-65.

Hunt, A. P. and Lucas, S. G., 1998b, Vertebrate tracks and the myth of the belly-dragging, tail-dragging tetrapods of the late Paleozoic: New Mexico Museum of Natural History and Science, Bulletin 12, p. 67-69.

Hunt, A. P., Lucas, S. G., Haubold, H. and Lockley, M. G., 1995, Early Permian (late Wolfcampian) tetrapod tracks from the Robledo Mountains, south-central New Mexico: New Mexico Museum of Natural History and Science, Bulletin 6, p. 167-180.

Igo, H., Ueno, K., and Sashida, K., 1993, Lower fusulinaceans from Bhan Phia, Changwat Loei, northeastern Thailand. Transactions and Proceedings Paleontological Society of Japan, new series, v. 169, p. 15-43.

Jordan, C. F., 1971, Lower Permian stratigraphy of southern New Mexico and West Texas [Ph.D. dissertation]: Houston, Rice University, 140 p.

Jordan, C. F., 1975, Lower Permian (Wolfcampian) sedimentation in the Orogrande basin, New Mexico: New Mexico Geological Society, Guidebook 26, p. 109-117.

Kietzke, K. K. and Lucas, S. G., 1995, Some microfossils from the Robledo Mountains Member of the Hueco Formation, Doña Ana County, New Mexico: New Mexico Museum of Natural History and Science, Bulletin 6, p. 57-62.

King, P. B., King, R. E. and Knight, J. B., 1945, Geology of Hueco Mountains, El Paso and Hudspeth Counties, Texas: U. S. Geological Survey, Oil and Gas Investigations Map 36.

Kottlowski, F. E., 1960a, Reconnaissance geologic map of Las Cruces thirty-minute quadrangle: New Mexico Bureau of Mines and Mineral Resources, Geologic Map 14.

Kottlowski, F. E., 1960b, Summary of Pennsylvanian sections in southwestern New Mexico and southeastern Arizona: New Mexico Bureau of Mines and Mineral Resources, Bulletin 66, 187 p.

Kottlowski, F., 1963, Paleozoic and Mesozoic strata of southwestern and south-central New Mexico: State Bureau of Mines and Mineral Resources, New Mexico Institute of Mining and Technology, Bulletin 79, 100 p.

Kottlowski, F. E., LeMone, D. V. and Seager, W. R., 1975, Marginal marine and continental facies of the Lower Permian in central New Mexico: Permian Basin Section SEPM, Publication 75-65, p. 119-124.

Kozur, H. and LeMone, D.V., 1995a, The Shalem Colony section of the Abo and upper Hueco members of the Hueco Formation of the Robledo Mountains, Doña Ana County, New Mexico: Stratigraphy and new conodont-based age determinations: New Mexico Museum of Natural History and Science, Bulletin 6, p. 39-55.

Kozur, H. and LeMone, D.V., 1995b, New terrestrial arthropod trackways from the Abo Member (Sterlitamakian, late Sakmarian, late Wolfcampian) of the Shalem Colony section, Robledo Mountains, New Mexico: New Mexico Museum of Natural History and Science, Bulletin 6, p. 107-113.

Krainer, K. and Lucas, S.G., 1995, The limestone facies of the Abo-Hueco transitional zone in the Robledo Mountains, southern New Mexico: New Mexico Museum of Natural History and Science, Bulletin 6, p. 33-38.

Krainer, K., Lucas, S. G. and Spielmann, J. A., 2005, Hueco Group (Lower Permian) stratigraphy in the Doña Ana Mountains, southern New Mexico: New Mexico Museum of Natural History and Science, Bulletin 31, p. 60-73.

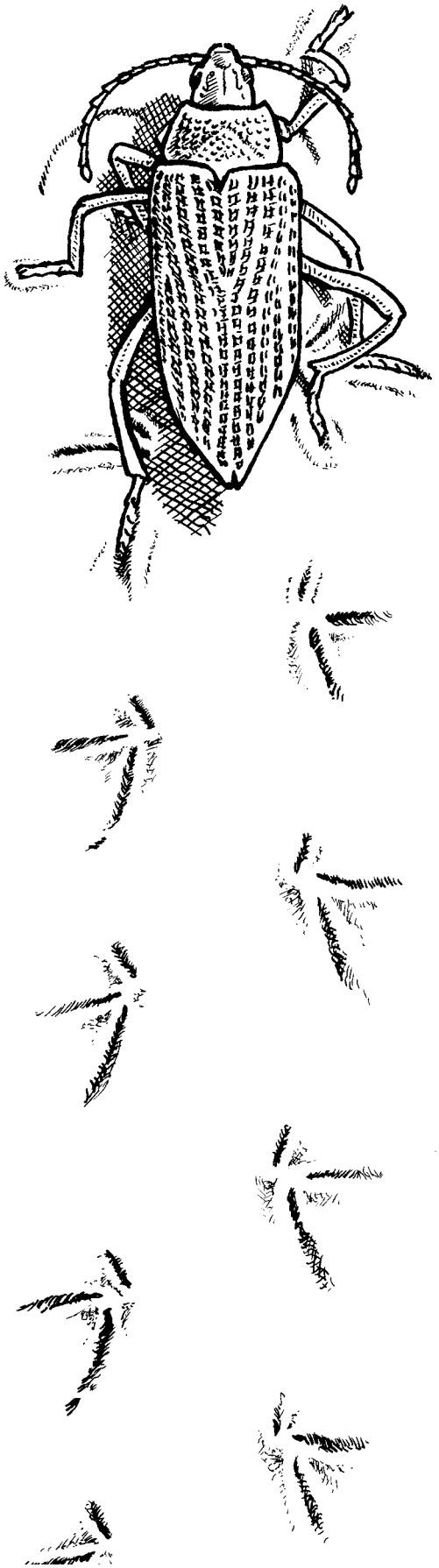
Krainer, K., Vachard, D. and Lucas, S. G., 2003, Microfacies and microfossil assemblages (smaller foraminifers, algae, pseudoalgae) of the Hueco Group and Laborcita Formation (Upper Pennsylvanian-Lower Permian), south-central New Mexico, USA: Rivista Italiana di Paleontologia e Stratigrafia, v. 109, p. 3-36.

Krainer, K., Vachard, D. and Lucas, S. G., 2009, Facies, microfossils (smaller foraminifers, calcareous algae) and biostratigraphy of the Hueco Group, Doña Ana Mountains, southern New Mexico, USA: Rivista Italiana di Paleontologia e Stratigrafia, v. 115, p. 3-26.
Kues, B. S., 1995, Marine fauna of the Early Permian (Wolfcampian) Robledo Mountains Member, Hueco Formation, southern Robledo Mountains, New Mexico: New Mexico Museum of Natural History and Science, Bulletin 6, p. 63-90.
LeMone, D. V., Klement, K. W. and King, W. E., 1971, Abo-Hueco facies of the upper Wolfcamp Hueco Formation of the southeastern Robledo Mountains, Doña Ana County, New Mexico; *in* Cys, J. M., ed., Robledo Mountains New Mexico Franklin Mountains Texas, 1971 Field Conference Guidebook, Permian Basin Section SEPM, p. 137-172.
LeMone, D.V., Simpson, R.D. and Klement, K.W., 1975, Wolfcampian upper Hueco Formation of the Robledo Mountains, Doña Ana County, New Mexico: New Mexico Geological Society, Guidebook 26, p. 119-121.
Lipina, O. A., 1949, Melkie foraminifery pogrebennykh massivov Bashkirii [Smaller foraminifers from the buried massifs of Bashkiria]. Akademiya Nauk SSSR, Trudy Instituta Geologicheskikh Nauk, v. 105, sér. géol. 35, p. 198-235. [in Russian; French translation BRGM, n° 791].
Lucas, S. G., 2013a, Reconsideration of the base of the Permian System: New Mexico Museum of Natural History and Science, Bulletin 60, p. 230-232.
Lucas, S. G., 2013b, We need a new GSSP for the base of the Permian: Permophiles, no. 58, p. 8-12.
Lucas, S.G. and Heckert, A.B., eds., 1995, Early Permian footprints and facies: New Mexico Museum of Natural History and Science, Bulletin 6, 301 p.
Lucas, S. G. and Krainer, K., 2002, Permian stratigraphy in the Jarilla Mountains, Otero County, New Mexico: New Mexico Geological Society, Guidebook 53, p. 211-222.
Lucas, S. G., Estep, J. W. and Hoffer, J. M., eds., 1998a, Permian stratigraphy and paleontology of the Robledo Mountains, New Mexico: New Mexico Museum of Natural History and Science, Bulletin 12, 98 p.
Lucas, S. G., Estep, J. W. and Hunt, A. P., 1998b, Road log to Early Permian tracksites in the Robledo Mountains, Doña Ana County, New Mexico: New Mexico Museum of Natural History and Science, Bulletin 12, p. 1-7.
Lucas, S. G., Krainer, K. and Kues, B. S., 2002, Stratigraphy and correlation of the Lower Permian Hueco Group in the southern San Andres Mountains, Doña Ana County, New Mexico: New Mexico Geological Society, Guidebook 53, p. 223-240.
Lucas, S. G., Lerner, A. J. and Voigt, S., 2013a, Scorpionid resting trace from the Lower Permian of southern New Mexico, USA: Ichnos, v. 20, p. 195-201.
Lucas, S. G., Anderson, O. J., Heckert, A. B. and Hunt, A. P., 1995, Geology of Early Permian tracksites, south-central New Mexico: New Mexico Museum of Natural History and Science, Bulletin 6, p. 13-32.
Lucas, S. G., Heckert, A. B., Estep, J. W. and Cook, C. W., 1998c, Stratigraphy of the Lower Permian Hueco Group in the Robledo Mountains, Doña Ana County, New Mexico: New Mexico Museum of Natural History and Science, Bulletin 12, p. 43-54.
Lucas, S.G., Heckert, A.B., Estep, J. W., Hunt, A.P. and Anderson, O. J., 1998d, Stratigraphy, pal;ontology and depositional environments of the Lower Permian Robledo Mountains Formation of the Hueco Group, Robledo Mountains, New Mexico: New Mexico Museum of Natural History and Science, Bulletin 12, p. 29-41.
Lucas, S. G., Krainer, K., Corbitt, L., DiBenedetto, J. and Vachard, D., 2011a, The Trans Mountain Road Member, a new stratigraphic unit of the Lower Permian Hueco Group, northern Franklin Mountains, Texas: New Mexico Museum of Natural History and Science, Bulletin 53, p. 93-109.
Lucas, S. G., Voigt, S., Lerner, A. J., MacDonald, J. P., Spielmann, J. A. and Celeskey, M. D., 2011b, The Prehistoric Trackways National Monument, Permian of southern New Mexico, U. S. A.: Ichnology Newsletter, no. 28, p. 10-14.
Lucas, S. G., Krainer, K., Chaney, D. S., DiMichele, W. A., Voigt, S., Berman, D. S and Henrici, A. C., 2012, The Lower Permian Abo Formation in the Fra Cristobal and Caballo Mountains, Sierra County, New Mexico: New Mexico Geological Society, Guidebook 63, p. 345-376.
Lucas, S. G., Krainer, K., Chaney, D. S., DiMichele, W. A., Voigt, S., Berman, D. S and Henrici, A. C., 2013b, The Lower Permian Abo Formation in central New Mexico: New Mexico Museum of Natural History and Science, Bulletin 59, p. 161-179.
MacDonald, J.P., 1995, History of the discovery of fossil footprints in southern New Mexico: New Mexico Museum of Natural History and Science, Bulletin 6, p. 1-12.
Mack, G. H., 2007, Sequence stratigraphy of the Lower Permian Abo member in the Robledo and Doña Ana Mountains near Las Cruces, New Mexico: New Mexico Geology, v. 29, p. 3-12.
Mack, G. H. and James, W. C., 1986, Cyclic sedimentation in the mixed siliclastic-carbonate Abo-Hueco transitional zone (Lower Permian), southwestern New Mexico: Journal of Sedimentary Petrology, v. 50, p. 635-647.
Mack, G. H., Giles, K. A. and Durr, C. W., 2013, Sequence stratigraphy of the lower-middle Hueco transition interval (Lower Permian, Wolfcampian), Robledo Mountains, New Mexico: New Mexico Geology, v. 35, p. 27-37.
Mack, G. H., Tabor, N. J. and Zollinger, H. J., 2010, Paleosols and sequence stratigraphy of the Lower Permian Abo Member, south-central New Mexico, USA. Sedimentology, v. 2010, p. 1-18.
Masse, P. and Vachard, D., 1996, A crustacean coprolite, *Palaxius salataensis*, in the Upper Carboniferous of the southern Urals: Neues Jahrbuch für Geologie und Paläontologie Monatshefte, v. 8, p. 490-494.
Melnyk, D. H. and Maddocks, R. F., 1988, Ostracode biostratigraphy of the Permo-Carboniferous of central and north-central Texas, part II: Ostracode zonation: Micropaleontology, v. 34, p. 21-40.
Minter, N. J. and Braddy, S. J., 2009, Ichnology of an Early Permian intertidal flat: The Robledo Mountains Formation of southern New Mexico, USA: Special Papers in Palaeontology, vol. 82, p. 1-107.
Muir-Wood, H. M. and Cooper, G. A., 1960, Morphology, classification and life habits of the Productoidea (Brachiopoda): Geological Society of America, Memoir 81, 447 p.
Pray, L. C., 1961, Geology of the Sacramento Mountains escarpment, Otero County, New Mexico: New Mexico Bureau of Mines and Mineral Resources, Bulletin 35, 144 p.
Richardson, G. B., 1904, Report of a reconnaissance in Trans-Pecos Texas north of the Texas and Pacific Railway: Univeristy of Texas, Mineral Survey, Bulletin 9, 119 p.
Ross, C. A. and Ross, J. P., 2012, Sequence evolution and sequence extinction: Fusulinid biostratigraphy and species-level recognition of depositional sequences, Lower Permian, Glass Mountains, West Texas, U. S. A.: SEPM Special Publication 75, p. 317-359.
Sanders, D. and Krainer, K., 2005, Taphonomy of Early Permian benthic assemblages (Carnic Alps, Austria): Carbonate dissolution versus biogenic carbonate precipitation: Facies, v. 51, p. 522-540.
Schult, M.F., 1995a, Comparisons between the Las Cruces ichnofauna and other Permian ichnofaunas, including inferred trackmakers: New Mexico Museum of Natural History and Science, Bulletin 6, p. 127-133.
Schult, M.F., 1995b, Vertebrate trackways from the Robledo Mountains Member of the Hueco Formation, south-central New Mexico: New Mexico Museum of Natural History and Science, Bulletin 6, p. 115-126.
Seager, W.R., Kottlowski, F.E. and Hawley, J.W., 2008, Geologic map of the Robledo Mountains and vicinity, Doña Ana County, New Mexico: New Mexico Bureau of Geology and Mineral Resources, Open-file Report 509, scale 1:24,000.
Seager, W.R., Hawley, J.W., Kottlowski, F.E. and Kelly, S.A., 1987, Geology of east half of Las Cruces and northeast El Paso 1° by 2° sheets: New Mexico Bureau of Mines and Mineral Resources, Geologic Map 57.
Senowbari-Daryan, B., Weidlich, O. and Flügel, E., 1992, Erster Nachweis von «Favreinen» (Crustaceen-Koprolithen) aus dem Perm: Oberperm, Oman-Berge: Paläontologische Zeitschrift, v. 66, p. 187-196.
Simpson, R. D., 1976, Systematic paleontology and paleoenvironmental analysis of the upper Hueco Formation, Robledo and Doña Ana Mountains, Doña Ana County, New Mexico [M. S. thesis]: El Paso, University of Texas, 253 p.
Simpson, R. D., 1984, Permian Brachiopoda from far west Texas and southwestern New Mexico [Ph.D. dissertation]: El Paso, University of Texas, 401 p.
Spielmann, J. A., Lucas, S. G. and Krainer, K., 2005, Early Permian (Wolfcampian) marine invertebrate assemblage from the Hueco Group, Shalem Colony Formation, Doña Ana Mountains, New Mexico: New Mexico Museum of Natural History and Science, Bulletin 31, p. 170-173.
Stevens, C. H., 1966, Paleoecological implications of Early Permian fossil communities in eastern Nevada and western Utah: Geological Society of America Bulletin, v. 77, p. 1121-1130.
Thompson, M. L, 1942, Pennsylvanian System in New Mexico: New Mexico School of Mines, Bulletin 17, 90 p.
Thompson, M. L., 1954, American Wolfcampian fusulinids: University of Kansas, Paleontological Contributions, Protozoa, Article 5, 226 pp.
Tidwell, W.D., and Munzing, G.E., 1995, Gymnospermous woods from the Lower Permian Hueco Formation of south-central New Mexico: New Mexico Museum of Natural History and Science, Bulletin 6, p. 91–100.
Vachard, D. and Krainer, K., 2001a, Smaller foraminifers of the late Carboniferous Auernig Group, Carnic Alps (Austria/Italy): Rivista Italiana de Paleontologia e Stratigrafia, v. 107, p. 147-168.
Vachard, D. and Krainer, K., 2001b, Smaller foraminifers, characteristic algae and pseudo-algae of the latest Carboniferous/Early Permian Rattendorf Group, Carnic Alps (Austria/ Italy): Rivista Italiana de Paleontologia e Stratigrafia, v. 107, p. 169-195.
Vachard, D., Krainer, K. and Lucas, S., 2015, Kungurian (late Early Permian) algae, microproblematica, and smaller foraminifers from the Yeso Group and San Andres Formation (New Mexico; USA): Palaeontologia Electronica (in press).
Voigt, S., Lucas, S. G. and Krainer, K., 2013, Coastal-plain origin of trace-fossil bearing red beds in the Early Permian of southern New Mexico, U. S. A.: Palaeogeography, Palaeoclimatology, Palaeoecology, v. 369, p. 323-334.
Wahlman, G.P. and King, W.E., 2002, Latest Pennsylvanian and earliest Permian fusulinid biostratigraphy, Robledo Mountains and adjacent ranges, south-central New Mexico: New Mexico Bureau of Geology and Mineral Resources, Circular 208, p. 1-26.
Wardlaw, B. R., 2005, Age assignment of the Pennsylvanian-Early Permian succession of north central Texas: Permophiles, no. 46, p. 21-22.
Wilde, G. L., 1990, Practical fusulinid zonation: The species concept; with Permian basin emphasis: West Texas Geological Society Bulletin, v. 29, no. 7, p. 5-34.

Wilde, G. L., 2002, The Newwellian Substage: Rejection of the Bursumian Stage: Permophiles, no. 41, p. 53-62.
Wilde, G. L., 2006, Pennsylvanian-Permian fusulinaceans of the Big Hatchet Mountains, New Mexico: New Mexico Museum of Natural History and Science, Bulletin 38, 331 p.
Williams, T. E., 1963, Fusulinidae of the Hueco Group (Lower Permian), Hueco Mountains, Texas: Peabody Museum of Natural History, Yale University, Bulletin 18, 122 p.
Wilson, J. L., 1975, Carbonate facies in geologic history: Springer Verlag, Berlin-Heidelberg, 471 p.

TABLE 1. Location of measured stratigraphic sections of Hueco Group strata in and around the Prehistoric Trackways National Monument (Fig. 4). GPS coordinates are UTMs in NAD 83 datum.

number	name	base	top	Section, township, range
1.	Flood	322929, 3583032	322943, 3582834	NE ¼ NW ¼ sec. 30, T22S, R1E
2.	Orin	320928, 3584632	320963, 3584305	NW ¼ NW ¼ sec. 24, T22S, R1W
3.	Type Apache Dam	323328, 3582331	323288, 3582304	NE ¼ SW ¼ sec. 30, T22S, R1E
4.	Community Pit	323562, 3583577	323546, 3583337	SW ¼ SW ¼ sec. 20, T22S, R1W
5.	Scorpion Hill B	320556, 3584732	320416, 3584604	NE ¼ NE ¼ sec. 23, T22S, R1W
6.	Monument North	321209, 3585490	320779, 3585521	NW ¼ SW ¼ sec. 13, T22S, R1W
7.	North Apache Canyon	319476, 3583824	319416, 3583776	NW ¼ SW ¼ sec. 23, T22S, R1W
8.	Mack 4	320364, 3583801	320325, 3583660	SW ¼ SE ¼ sec. 23, T22S, R1W
9.	Scorpion Hill A	320583, 3584981	320556, 3584732	NE ¼ NE ¼ sec. 23, T22S, R1W
10.	Upper Apache Canyon	319886, 3583242	319958, 3583229	SE ¼ SW ¼ sec. 23, T22S, R1W
11.	Middle Apache Canyon	320464, 3583389	320457, 3583364	SE ¼ SE ¼ sec. 23, T22S, R1W
12.	Lower Apache Canyon	320925, 3582590	320914, 3582545	SE ¼ NE ¼ sec. 26, T22S, R1W
13.	Apache Dam	322359, 3580791	322515, 3580805	NE ¼ SE ¼ sec. 36, T22S, R1W
14.	Flood A	322806, 3582960		same as section 1
15.	Flood B	322815, 3582955		same as section 1
16.	Flood C	322838, 3582669		same as section 1
17.	Flood D	322846, 3582972		same as section 1
18.	Flood E	322935, 3583013		same as section 1
19.	Flood F	322944, 3583036		same as section 1
20.	Apache Canyon sabkha	320710, 3582669	320310, 3582680	SE ¼ NE ¼ sec. 26, T22S, R1W
21.	Flood G	322886, 3583003		same as section 1
22.	Branson Canyon	323294, 3582546	323084, 3582750	SE ¼ NW ¼ sec. 30, T22S, R1W
23.	Excavation	323300, 3583815	323252, 3583822	same as section 4
24.	Upper Branson Canyon	321693, 3583060	361640, 3582998	SE ¼ SW ¼ sec. 24, T22S, R1W
25.	Dead Man’s Curve	321927, 3583814	321619, 3583417	NW ¼ SE ¼ sec. 24, T22S, R1W
26.	Indian Springs Canyon	317299, 3587751	318591, 3586829	S ½ NE ¼ sec. 9, S ½ NW ¼ sec. 10 and NW ¼ SE ¼ sec. 10, T22S, R1W
27.	Robledo Mountain	See Krainer et al. (this volume)		NE ¼ SW ¼ sec. 35, T22S, R1W



Lucas, S. G. and DiMichele, W. A., eds., 2015, Carboniferous-Permian Transition in the Robledo Mountains, Southern New Mexico. New Mexico Museum of Natural History and Science Bulletin 65.

GEOLOGY OF PREHISTORIC TRACKWAYS NATIONAL MONUMENT, DOÑA ANA COUNTY, NEW MEXICO

SPENCER G. LUCAS[1], KARL KRAINER[2], W. JOHN NELSON[3] AND SCOTT ELRICK[3]

[1]New Mexico Museum of Natural History, 1801 Mountain Road NW, Albuquerque, NM 87104;
[2]Institute of Geology, Innsbruck University, Innrain 52, Innsbruck, A-6020 Austria;
[3]Illinois State Geological Survey, 615 East Peabody Drive, Champaign, IL 61820

Abstract—The Prehistoric Trackways National Monument (PTNM) is approximately 2137 hectares (5280 acres) of land in the Robledo Mountains of Doña Ana County, southern New Mexico, protected primarily because of its world-class Early Permian trace-fossil assemblages. Most of the bedrock exposed in the PTNM can be assigned to the Lower Permian Hueco Group comprising four formations: Shalem Colony (oldest), Community Pit, Robledo Mountains and Apache Dam (youngest). Hueco Group strata are mostly limestone and mudstone of shallow marine origin, but the Robledo Mountains Formation also includes red-bed siliciclastic coastal plain deposits that yield the trace fossil assemblages that justified creation of the PTNM. Rocks of Cenozoic age crop out much less extensively in the PTNM than the Hueco Group strata, and they are either Eocene fluvial, playa and volcaniclastic deposits of the Laramide orogeny (Love Ranch and Palm Park formations) or Miocene to Pliocene alluvial sediments (Rincon Valley and Camp Rice formations) or igneous rocks (Bell Top Formation, Robledo rhyolite, basalt) associated with late Cenozoic development of the Rio Grande rift. Quaternary rocks are mostly superficial alluvial and terrace deposits. The Rio Grande rifting event, which commenced in the Miocene, determined the current geological structure of the Robledo Mountains and the PTNM. The geological history of the PTNM can thus be divided into two principal phases—Early Permian shoreline and shallow marine environments of the Hueco seaway and late Cenozoic continental rifting and basin-margin sedimentation. The more than 250 million years that divide these two phases left little geological evidence in the PTNM.

INTRODUCTION

The Prehistoric Trackways National Monument (PTNM) is approximately 2137 hectares (5280 acres) of land administered by the U. S. Bureau of Land Management in the Robledo Mountains of Doña Ana County, southern New Mexico (Fig. 1). In 2008, the U. S. Congress created the national monument, primarily because of the world-class Early Permian trace-fossil assemblages preserved in the southern Robledo Mountains (Lucas et al., 2011 and references cited therein).

These trace fossils come from Lower Permian strata of the Hueco Group. The rugged and barren topography of the PTNM is primarily developed in these strata, which are uplifted and faulted along the western edge of the Rio Grande rift, a late Cenozoic structural feature. Thus, two geological events—Early Permian deposition of the Hueco Group and late Cenozoic extensional tectonism—determined most of the geology of the PTNM, which we describe here.

ROBLEDO MOUNTAINS: OVERVIEW

The Robledo Mountains are an isolated fault block mountain range just northwest of Las Cruces in southern New Mexico (Fig. 1). Triangular in map view, the range trends north and is about 15 km long, widening from an apex on the north to about 8 km wide at the southern end. The highest point is Robledo Mountain at 1795 m elevation, compared with 1205 m along the Rio Grande skirting the eastern side of the range. Picacho Mountain (elevation 1511 m) is a landmark at the southern end of the range.

Paleozoic strata are the primary bedrock exposed by the Robledo Mountains (Figs. 1-2). Older Paleozoic strata, rocks of Ordovician-Mississippian age, are only exposed at the northern end of the range and have an aggregate thickness of ~ 330 m (Fig. 2). Pennsylvanian strata (Horquilla Formation) are also exposed at the northern end of the range, and along part of its western side, and are as much as 300 m thick (see Krainer et al., this volume). Overlying Permian strata of the Hueco Group are as much as 565 m thick and crop out across most of the central and southern parts of the Robledo Mountains (see Lucas et al., this volume). Cenozoic rocks, of both igneous and sedimentary origin, are found throughout the range, but are a minor part of the bedrock except near the southern terminus of the Robledo Mountains (Seager et al., 2008).

Structurally and physiographically, the Robledos reside within the Rio Grande rift of the Basin and Range Province, which has been the scene of ongoing crustal extension since Miocene time. As a result, this area exhibits typical basin-and-range topography. Fault-bounded mountain ranges mostly trend north and are separated by broad valleys filled with sediments thousands of meters thick. Rifting has been accompanied by widespread volcanism, creating a variety of lava flows, cinder and composite cones, maars, and other volcanic features. To the east of the Robledo Mountains, the Rio Grande and its tributaries incise the Mesilla basin of the Rio Grande rift. To the west, an essentially uneroded late Cenozoic basin is the Corralitos graben. The Robledos thus can be seen as a horst block between these two basins.

The Robledo Mountains are situated in the northern Chihuahuan Desert, where scrub vegetation such as creosote bush, yuccas, and various cacti prevails. Sparse junipers grow at high elevation and in sheltered canyons. Average daily high temperatures range from 14°C in January to 35°C in July; lows are -2°C to 19°C, respectively. Average annual rainfall is 167.5 mm, most of which falls between July and October in the form of brief and often violent thunderstorms (www.worldclimate.com). The Rio Grande is the only perennial stream near the range.

PTNM: STRATIGRAPHY, SEDIMENTOLOGY AND PALEONTOLOGY

Most of the bedrock exposed in the PTNM can be assigned to the Lower Permian Hueco Group of Early Permian age, ~ 280 Ma (Figs. 3-4). Indeed, the Permian rocks of the Robledo Mountains have been assigned to the Hueco Limestone or Formation for many years (e. g., Thompson, 1942, 1954; Kottlowski, 1960, 1963; Jordan, 1971, 1975). Until recently, geologists divided the Hueco informally into lower, middle, Abo tongue, and upper members. Lucas et al. (1998) elevated the Hueco strata in the Robledo Mountains to a group comprising four formations: Shalem Colony (oldest), Community Pit, Robledo Mountains and Apache Dam (also see Lucas et al., this volume). Most of the boundaries of the named formations correspond to those of the informal members.

Hueco Group

Shalem Colony Formation (Psc)

The oldest unit of the Hueco Group, the Shalem Colony Formation is about 130-160 m thick, but only the upper 40-45 m are exposed in the PTNM (Fig. 5). The type section, north of the PTNM in section 12, T22S, R1W, is 106 m thick, with the base covered (Lucas et al., 1998). In the PTNM, the Shalem Colony Formation is composed of relatively thick beds or intervals of limestone intercalated with mostly covered slopes that represent either shale or nodular limestone.

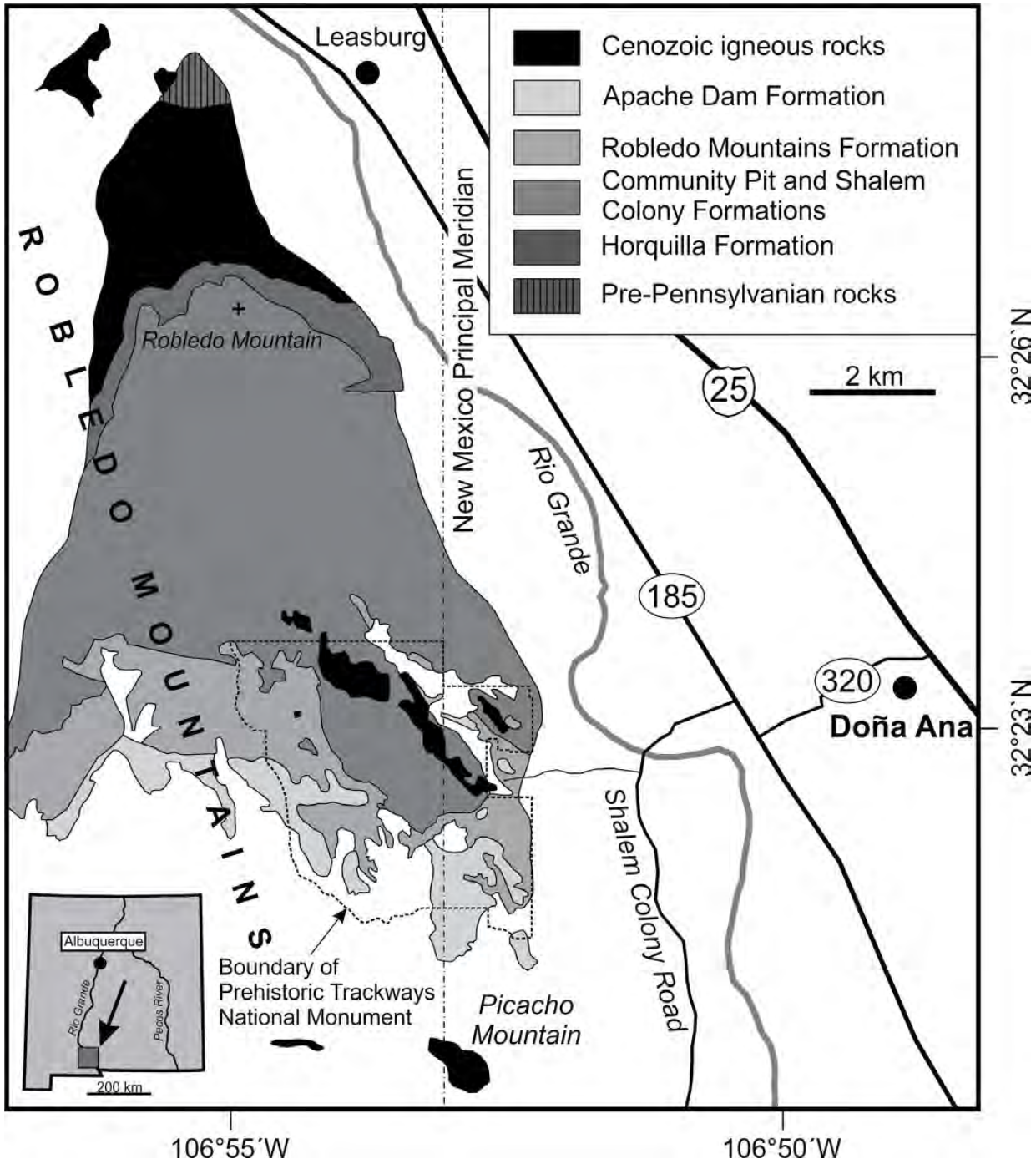


FIGURE 1. Simplified geological map of the Robledo Mountains showing location of the Prehistoric Trackways National Monument (PTNM).

A characteristic section of the upper part of the Shalem Colony Formation is exposed near the northern edge of the PTNM, where the upper 44 m of this formation are exposed (Fig. 5). The section is composed of thin- to medium-bedded limestone, wavy bedded, rare nodular limestone intervals 0.1-6.2 m thick, and covered intervals 0.2-2.9 m thick. Typical limestone microfacies are wackestone, packstone and grainstone (Fig. 6A-F). Calcareous algae are present in limestone near the top and near the base of the exposed section. Fusulinids of Early Permian (middle Wolfcampian-Nealian) age are present in two limestone beds in the lower part (Fig. 5, units 1 and 7). Chert is rare in the limestone facies. A carbonate conglomerate bed is present at the top of the section. Colors are mostly shades of gray, but some beds weather pale red to orange. Shale and siltstone, which are poorly exposed, are mostly grayish orange and laminated.

The Shalem Colony Formation crops out extensively southward from Robledo Mountain along both flanks of the range. Within the PTNM, the main belt of outcrops begins just west of the Community Pit and extends to the northwest (Fig. 3), but these rocks are thoroughly intruded by Tertiary rhyolite sills. More Shalem Colony outcrops occur at the northeastern corner of the Monument (see Lucas et al. this volume).

Community Pit Formation (Pcp)

This formation takes its name from a flagstone quarry just south of the type section, which is along the large canyon that passes through the center of section 18, T22S, R1E (Fig. 3). Outcrops are plentiful in this area, and also in a belt extending southeastward through sections 14, 24, and 25 of T22S, R1W. The formation is 90-180 m thick (Fig. 7). The Community Pit Formation is mostly a slope-forming interval of shale beds intercalated with relatively thin intervals of limestone, many of which are lime mudstones and dolomitic lime mudstones. The formation has a characteristic brownish gray to grayish orange color

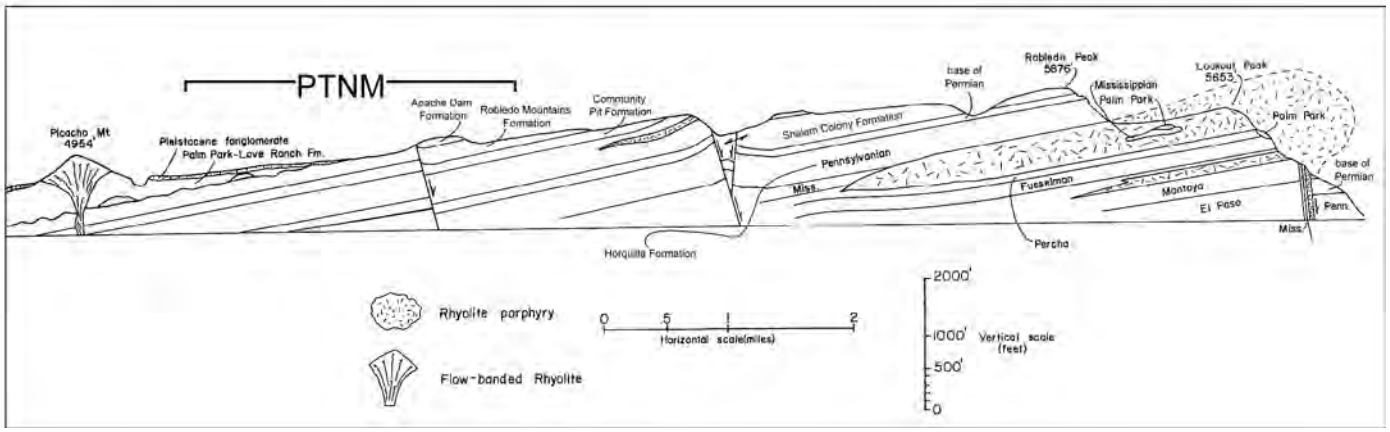


FIGURE 2. Diagrammatic cross section through the Robledo Mountains (modified from Hawley et al., 1975). The Prehistoric Trackways National Monument (PTNM) is located in the southern portion of the diagram as indicated.

and forms thick slopes between the cliff- and ledge-forming outcrops of the Shalem Colony and Robledo Mountains formations. Typically, its base is a shale slope above the stratigraphically highest, relatively thick (3-5 m) limestone interval of the Shalem Colony Formation (Fig. 5). The top of the Community Pit Formation is mapped at the base of the lowest red mudstone, siltstone, or sandstone assigned to the overlying Robledo Mountains Formation (Fig. 7).

In the PTNM (Fig. 7), the Community Pit Formation consists of bedded limestone intervals and thicker limestone beds alternating with shale intervals and covered intervals. Bedded limestone intervals are 0.2 to 5.9 m thick. Limestone is dominantly thin bedded (5-30 cm), although, rarely, thicker-bedded and massive limestone beds up to 1.2 m thick also occur. Limestone is dominantly gray to dark gray lime mudstone, and subordinate grainy limestone (wackestone to packstone). Microfacies include wackestone, packstone, grainstone and spiculite (Figs. 6G-H, 8A-B). Bedded cherty limestone intervals are rare. In the lower part of the section, two sandy carbonate conglomerate beds are intercalated. Shale intervals occur in the lower part of the section and are up to 2.2 m thick; covered intervals (most are probably shale) are up to 5.8 m thick. Fossils observed on outcrop are brachiopods, gastropods, calcareous algae, rare bryozoans, and plant fossils, mostly conifer cones and fossil wood (Falcon-Lang et al., 2014; DiMichele et al., this volume; Falcon-Lang et al., this volume).

Silicified wood occurs in two stratigraphic intervals of the Community Pit Formation (Figs. 7, 9; Falcon-Lang et al., 2014). At one locality, several logs that average about 15 cm in diameter lie flat to bedding in microgranular, dolomitic limestone. These logs are replaced by crystalline calcite, obliterating original grain. Foliage of a voltzian conifer and the callipterid *Lodevia oxydata*, unidentified stems, and bivalves occur in the same stratum (DiMichele et al., this volume). At a different site, Tidwell and Munzing (1995) reported fossil wood flat to bedding in gray, calcareous shale. They identified a gingkophyte, the coniferophyte *Dadoxylon*, and another conifer similar to *Walchia*. However, Falcon-Lang et al. (2014) reinterpreted all of these specimens as likely *Macdonalodendron*, a walchian conifer wood type. Fossil wood in the Community Pit Formation is interpreted as driftwood that floated a short distance from shore, became waterlogged, and buried in sediment. The likely setting was near the mouths of shallow bays or estuaries along the shores of which trees grew.

Microfossils (especially fusulinids) of the Community Pit Formation indicate it is mostly of Sakmarian (late Wolfcampian) age (see Lucas et al., this volume).

Robledo Mountains Formation (Prm)

The Robledo Mountains Formation is composed of approximately two-thirds drab-colored marine limestone and shale interbedded with one-third red terrestrial mudstone, siltstone and sandstone. The type section is on a steep, north-facing hillside about 1 km south of the Community Pit, mostly in the N½ NW¼ SE¼ of sec. 30, T22S, R1E (Lucas et al., 1995, 1998). At this site the formation measures 125 m thick; Seager et al. (2008) reported an average thickness of 120 m.

A complete section of the Robledo Mountains Formation in Branson Canyon is characteristic of its outcrops in the PTNM (Figs. 10-11). Most prominent are beds of siltstone to fine-grained sandstone, which are calcareous, partly micaceous, and commonly display horizontal lamination and ripple lamination. A few thin sandstone beds (0.1 m) appear massive. Rarely, mudcracks are present on the bedding surface. In one bed, bi-directional current ripples occur. Other sedimentary structures rarely observed are low-angle crossbedding and soft sediment deformation. This lithofacies is commonly red, and individual siltstone-sandstone beds are commonly 0.1-0.5 m thick. Alternating with the siltstone-sandstone beds are thinly laminated siltstone to mudstone, a few cm up to 1.6 m thick (mostly 0.1-0.5 m), the colors of which are greenish gray (in the lowermost 5 m) and red. Siltstone-sandstone and intercalated mudstone are common in the lowermost 5 m of the section, between 11 and 32 m, and in the uppermost part (80-90 m). Between 32 and 80 m, siltstone to fine-grained sandstone is very rare (one interval, 0.7 m thick).

Limestone in the lower part of the section (5-11 m) is limestone beds and bedded limestone units 0.2-1 m thick. Most beds are composed of lime mudstone; some beds are arenitic limestone containing crinoidal debris. A few lime mudstone beds contain calcite nodules (replaced gypsum) or are bioturbated. A few beds also contain myalinid bivalves on top. Characteristic microfacies include wackestone, grainstone and floatstone (Fig. 8C-E).

Limestone beds alternate with greenish and gray shale, which is partly laminated. Shale intervals are 0.1-0.7 m thick. Between 11 and 32 m, limestone is rare and occurs as thin limestone beds (0.2-0.3 m) that alternate with thin mudstone beds (0.1-0.3 m). Muddy and sandy limestone beds also are present. Between 32 and 80 m the section is mainly composed of limestone and covered intervals. Limestone crops out as thin limestone beds and bedded limestone units up to 1.8 m thick. Bedding is mostly even, although wavy bedding is observed rarely. Bed thickness is 0.1-0.3 m. Between 32 and 43 m many limestone beds are dolomitic, and some limestone beds contain crinoidal debris. Wavy bedded limestone (units 132, 136) contains abundant echinoid spines up to 5 cm long. Gastropods are present in limestone units 124 and 130. Limestone units 138 and 140 contain crinoidal debris, brachiopods and bryozoans. Algae are present in unit 142.

Limestone units are separated by covered intervals up to 5.2 m thick. Covered interval 131 is underlain by nodular limestone and shale containing brachiopods. Interval 137 is a mostly shaly slope containing abundant brachiopods, bryozoans, bivalves and rare ammonoids. This interval produced most of the extensive invertebrate fossil assemblage described by Kues (1995), who listed more than 70 fossil taxa, including those named above together with sponges, corals, crinoids, echinoids, nautiloids, scaphopods, ostracods, trilobites, conodonts, and shark remains.

The siliciclastic red beds yield trace fossils and fossil plants (mostly walchian conifers; see DiMichele et al., this volume), mud cracks, and raindrop impressions. Measured sections (Lucas et al. 1995, this volume; Mack, 2007) show much lateral variability. Nearly all of the tetrapod trackways, however, occur at a common level in the mid-lower part of the formation, overlying a "highly distinctive limestone bed" (Lucas et al. 1995). Nearly 50 known localities span an area of about 20 km^2 (8 square miles). The deposit is remarkable not only for the abundance and diversity of vertebrate traces, but for the co-occurrence of invertebrate traces (insect, spider, scorpion, eurypterid)

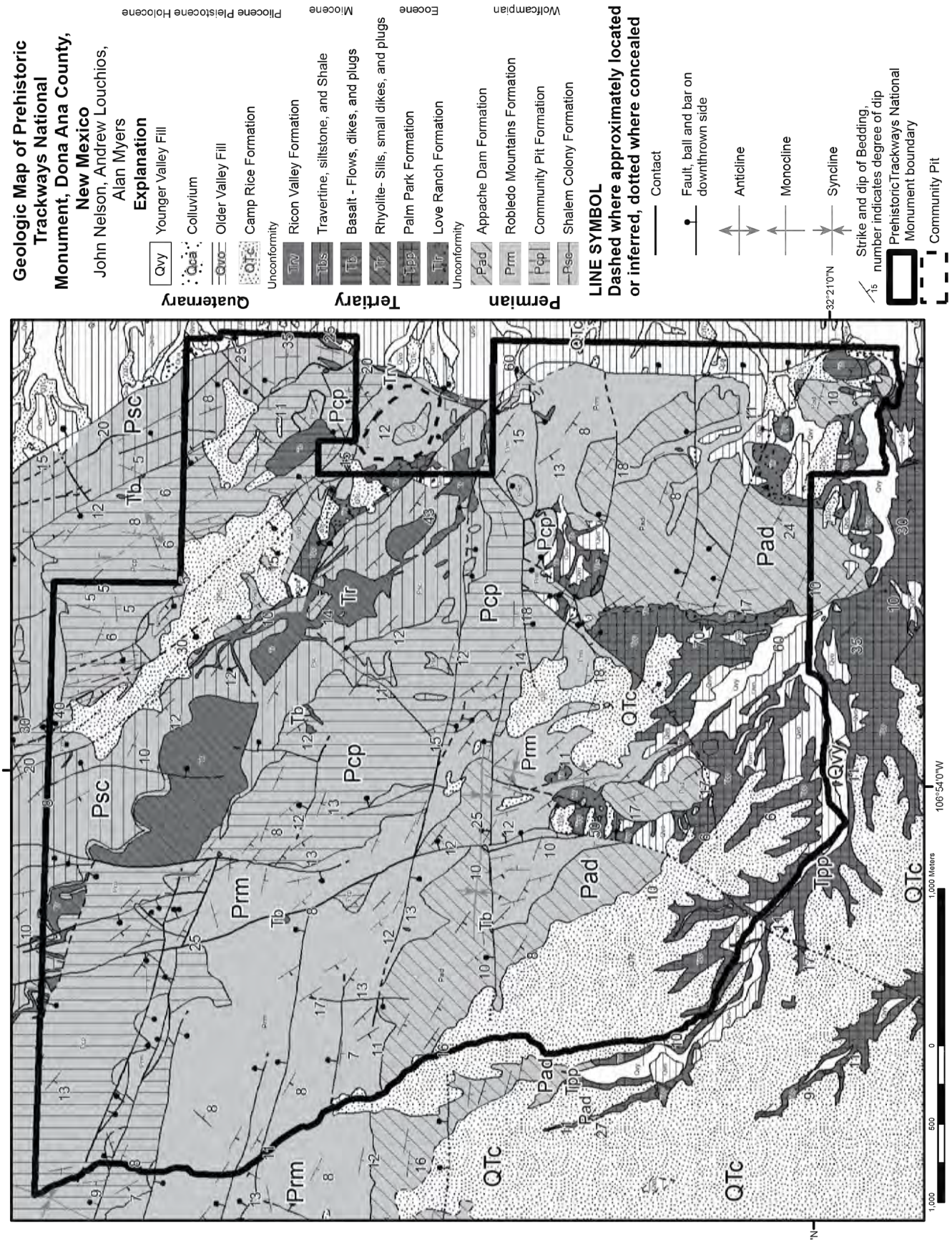


FIGURE 3. Geological map of the Prehistoric Trackways National Monument (based, in part, on Seager et al., 2008).

age		formation	maximum thickness	principal lithologies
PLIOCENE/ QUATERNARY		younger valley fill	21 m	gravel, sand, silt
		older valley fill	40 m	
MIOCENE	Santa Fe Group	Camp Rice Formation	90 m	conglomerate
		Rincon Valley Formation	199 m	conglomeratic sandstone, sandstone, mudstone
		travertine, siltstone, shale	9 m	travertine, siltstone, shale
		basalt		basalt
EOCENE		Robledo rhyolite	50 m	rhyolite
		Bell Top Formation		flow-banded rhyolite
		Palm Park Formation	380+ m	volcaniclastic rocks (upper part) and red siltstone and gypsum (lower part)
		Love Ranch Formation	60 m	mudstone, siltstone, sandstone, boulder conglomerate
PERMIAN	Hueco Group	Apache Dam Formation	107+ m	algal limestone and shale
		Robledo Mountains Formation	125 m	grainy limestone, shale and red-bed siliciclastics (sandstone, siltstone, mudstone)
		Community Pit Formation	177 m	shale, muddy limestone, dolomitic limestone
		Shalem Colony Formation	156 m	thick-bedded, coarse-grained limestone (wackestone, grainstone, etc.)

FIGURE 4. Summary of stratigraphic and volcanic rock units exposed in the Prehistoric Trackways National Monument.

and for accurate dating based on intercalated marine strata (Lucas and Heckert, 1995; Lucas et al., 1995, 2011 and references cited therein; Minter and Braddy, 2009).

Most workers had long interpreted the red beds of the Robledo Mountains Formation in the PTNM as tidal flat deposits (e. g., Jordan, 1975; LeMone et al., 1975; Mack and James, 1986; Lucas et al., 1995). However, Voigt et al. (2013) recently argued that these sediments formed on a coastal floodplain during alternating wet and dry conditions. They based this on detailed sedimentological and ichnological analysis that indicates that most of the trace fossils found in the Robledo Mountains Formation red beds were preserved on mud-draped surfaces within distal crevasse-splay siltstone to fine-grained sandstone. Interbedded mudstone with well-preserved macrofloral remains and a lungfish estivation burrow represent overbank fines. Both environmental subzones were at least loosely covered with low-growing plants and experienced common periods of subaerial exposure. None of the physical and biological structures recorded in their study indicate tidal influence, but instead they support the reconstruction of a freshwater ecosystem dominated by arthropods and tetrapods. Given their proximity to carbonates of unambiguous subtidal origin, Voigt et al. (2013) concluded that the trace-fossil-bearing red beds of the Robledo Mountains Formation formed in distal parts of an extensive coastal floodplain during alternating wet and dry conditions. None of the red beds records evidence of marine or tidal influence; instead they support the interpretation of a fluvially-controlled freshwater ecosystem with sparse plant cover and predominantly arthropod and tetrapod inhabitants.

Both contacts of the Robledo Mountains Formation are conformable, and are mapped at the highest and lowest occurrences of red siliciclastic rocks. Based particularly on its microfossils, the age of the Robledo Mountains Formation is Artinskian, so it is Leonardian on the North American provincial timescale (see Lucas et al., this volume).

Apache Dam Formation (Pad)

The youngest Paleozoic unit in the Robledo Mountains, the Apache Dam Formation, crops out extensively in the southern part of the Monument (Fig. 3). The type section is adjacent to that of the Robledo Mountains Formation, at the top of a steep, north-facing slope in the NE¼ SW¼ of sec. 30, T22S, R1E. The formation measured 61.7 m thick at this site (Lucas et al. 1998), but elsewhere in the area the Apache Dam Formation attains a thickness of 122 m, with the top eroded.

The Apache Dam Formation (Figs. 12-13) is composed of limestone intervals alternating with covered (shale) intervals. The following limestone lithotypes are present: (1) wavy-bedded limestone, thin to medium bedded (5-40 cm); (2) nodular to wavy bedded limestone; (3) even-bedded limestone, medium bedded; (4) thin-bedded limestone with thin shale intercalations (rare); (5) indistinctly bedded to massive limestone, up to 2 m thick; (6) thicker limestone beds containing crinoidal debris (up to 0.7 m thick); and (7) crossbedded arenitic limestone (very rare). Limestone units are up to 5.6 m thick, and covered intervals up to 4 m. In some of the limestone units, chert occurs as chert nodules, and rarely as thin chert bands. The most common microfacies types are bioclastic wackestone to packstone and algal wackestone to floatstone (Figs. 8F-H, 13). Packstone to rudstone is rare. All microfacies contain a diverse fossil assemblage. Gastropods, brachiopods, echinoids, corals, and phylloid algae are the most common elements. The Apache Dam is overlain with major unconformity by various Tertiary and Quaternary units.

Tertiary System

Rocks of Tertiary age crop out much less extensively in the PTNM than the Hueco Group strata (Fig. 3). These rocks are also much less studied locally than are the Permian strata.

Love Ranch Formation (Tlr)

The Love Ranch Formation consists of red to grayish-red mudstone, siltstone, sandstone, and conglomerate that has clasts of Permian limestone and siltstone up to boulder size. Because the Love Ranch pre-dates volcanic activity in the Las Cruces area, it is a sedimentary unit that generally lacks volcanic rock fragments. Outcrops occur in several areas, including the north side of Apache Canyon near its mouth and ravines and hillsides immediately west of the Community Pit (Fig. 3).

In southern New Mexico, the Love Ranch Formation is more than 600 m thick and crops out primarily in the San Andres and Caballo Mountains of Doña Ana and Sierra Counties. It represents syntectonic deposition during the Laramide orogeny in a basin (Love Ranch basin) north of a Laramide uplift (Rio Grande uplift) that has been inferred to have extended from about the southern tip of the Black Range to the Organ Mountains (Seager and Mack, 1986, 2003, fig. 53). The Love Ranch is a fluvial unit, filling south-trending paleovalleys as deep as 60 m (Seager and Mack, 1986; Krainer and Lucas, 2012). It can be assigned an Eocene age because of its stratigraphic relationship to the overlying upper Eocene Palm Park Formation, with which it interfingers, and because it contains clasts of what appear to be Eocene siliceous volcanic rocks. Evidence of an older age has been suggested from correlation to similar rocks outside of the Love Ranch basin, but we are skeptical of this correlation.

Palm Park Formation (Tpp)

This formation crops out extensively in the southern part of the PTNM along Apache Canyon, and also farther south around the slopes of Picacho Mountain (Fig. 3). Seager et al. (2008) divided the Palm Park into two facies, which are combined here (Figs. 3-4). The lower facies consists of interbedded red siltstone and gypsum up to about 80 m thick. Overlying these alluvial plain and playa sediments are volcaniclastic strata more than 300 m thick. These include gray, green, purple and maroon tuffaceous mudstone, siltstone, sandstone, and conglomerate with clasts up to boulder size, together with lahar (mud-flow) breccias.

The Palm Park is a primarily volcaniclastic deposit that records widespread andesitic volcanic activity along the apron of the mid-Cenozoic Mogollon-Datil volcanic field (e.g., Smith et al., 1985). In the Caballo Mountains of Sierra County, an early Chadronian age of about 36-37 Ma is indicated by the fossil mammals from the upper part of the Palm Park Formation (Lucas and Williamson, 1993; Lucas and Spielmann, 2012). Older K/Ar ages of 42, 43 and 51 Ma have

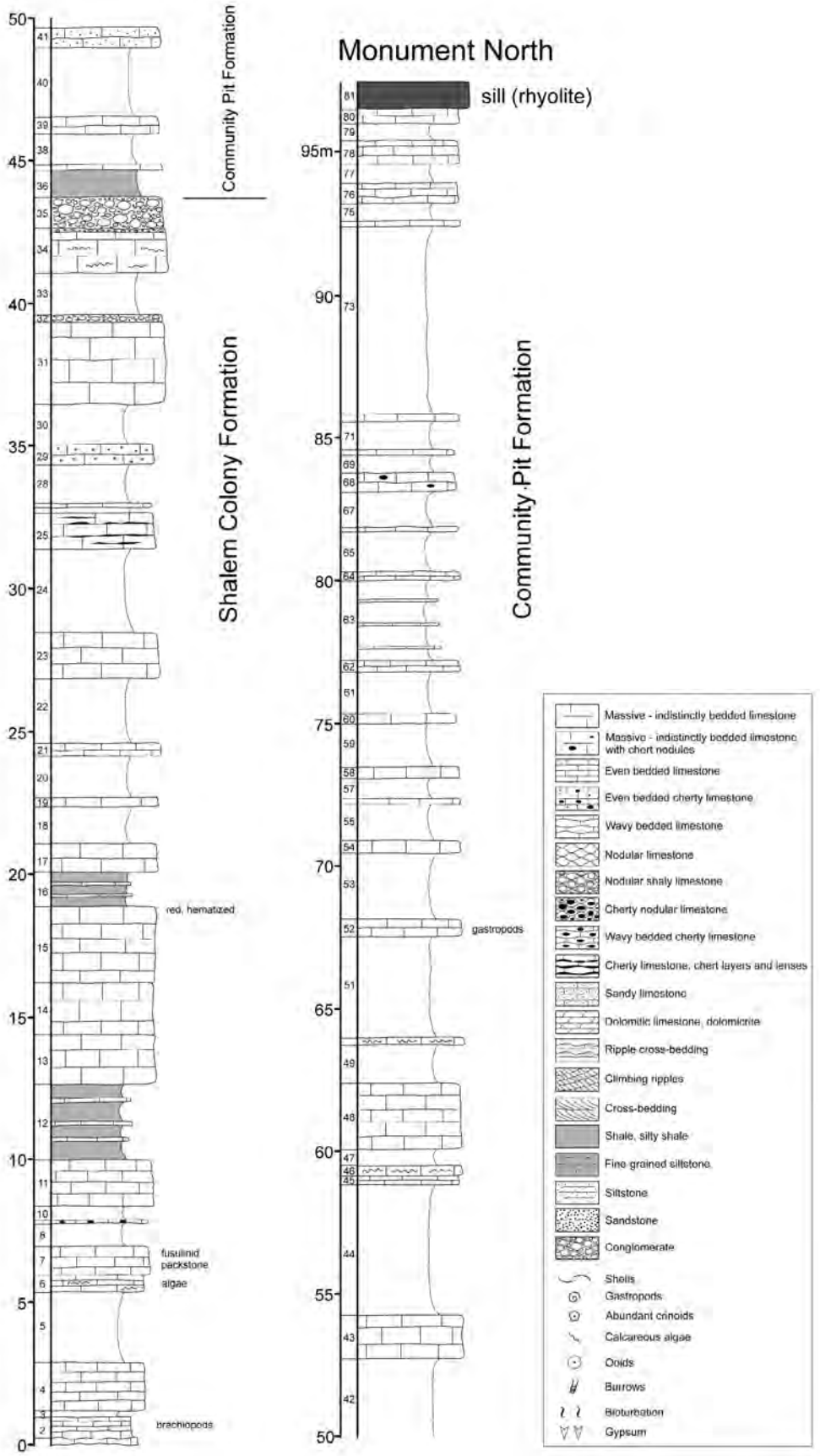


FIGURE 5. Measured stratigraphic section of the upper part of the Shalem Colony and lower part of the Community Pit formations in the Prehistoric Trackways National Monument. Section is located in the NW ¼ SW ¼ sec. 13, T22S, R1W. Numbers on left side of column are distance in meters above base of section.

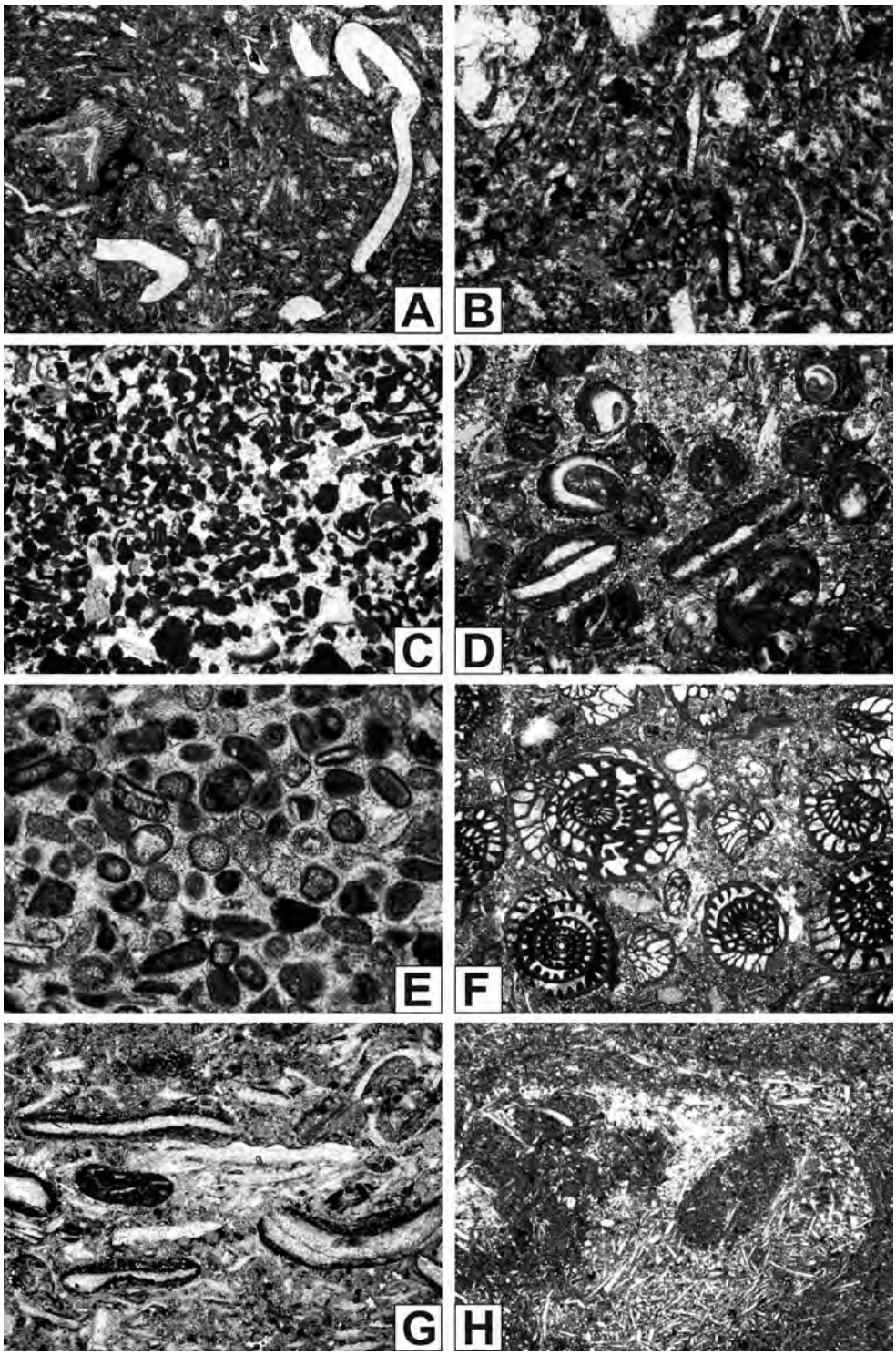


FIGURE 6. Thin section photographs of common microfacies types of the Shalem Colony (A-F) and Community Pit formations (G-H), Prehistoric Trackways National Monument. All photographs under plane light. **Shalem Colony Formation A,** Bioclastic wackestone containing a moderately diverse fossil assemblage (mainly foraminifers, ostracods, trilobite fragments and recrystallized skeletons) and many peloids. Indian Springs Canyon, unit 9, width of photograph is 6.3 mm. **B,** Bioclastic wackestone to packstone containing a moderately diverse fossil assemblage (mainly foraminifers, ostracods, bivalves) and many peloids. Indian Springs Canyon, unit 17, width of photograph is 3.2 mm. **C,** Grainstone containing abundant tubular foraminifers, peloids and micritic intraclasts and a few other fossil fragments. Indian Springs Canyon, unit 80, width of photograph is 6.3 mm. **D,** Oncoidal wackestone. Oncoids (mostly 1–2 mm) are encrusted by *Girvanella* and tubular foraminifers. Locally peloids and peloidal micrite are present. Indian Springs Canyon, unit 87, width of photograph is 6.3 mm. **E,** Oolitic grainstone containing abundant ooids (0.2 – 0.5 mm). Many ooids are micritized or recrystallized. Subordinate are micritic intraclasts and recrystallized fossil fragments. Indian Springs Canyon, unit 127, width of photograph is 1.2 mm. **F,** Fusulinid wackestone containing partly abraded and fragmented tests of fusulinids and subordinately other fossil fragments. Monument North, unit 1, width of photograph is 6.3 mm. **Community Pit Formation G,** Floatstone-rudstone composed of a diverse fossil assemblage with fragments up to several mm across. Many fragments display micritic envelopes or are encrusted by cyanobacteria to form oncoids. Monument North, unit 52, width of photograph is 6.3 mm. **H,** Spiculite containing abundant small monaxone and rare triaxone sponge spicules in micritic matrix. Monument North, unit 76, width of photograph is 3.2 mm.

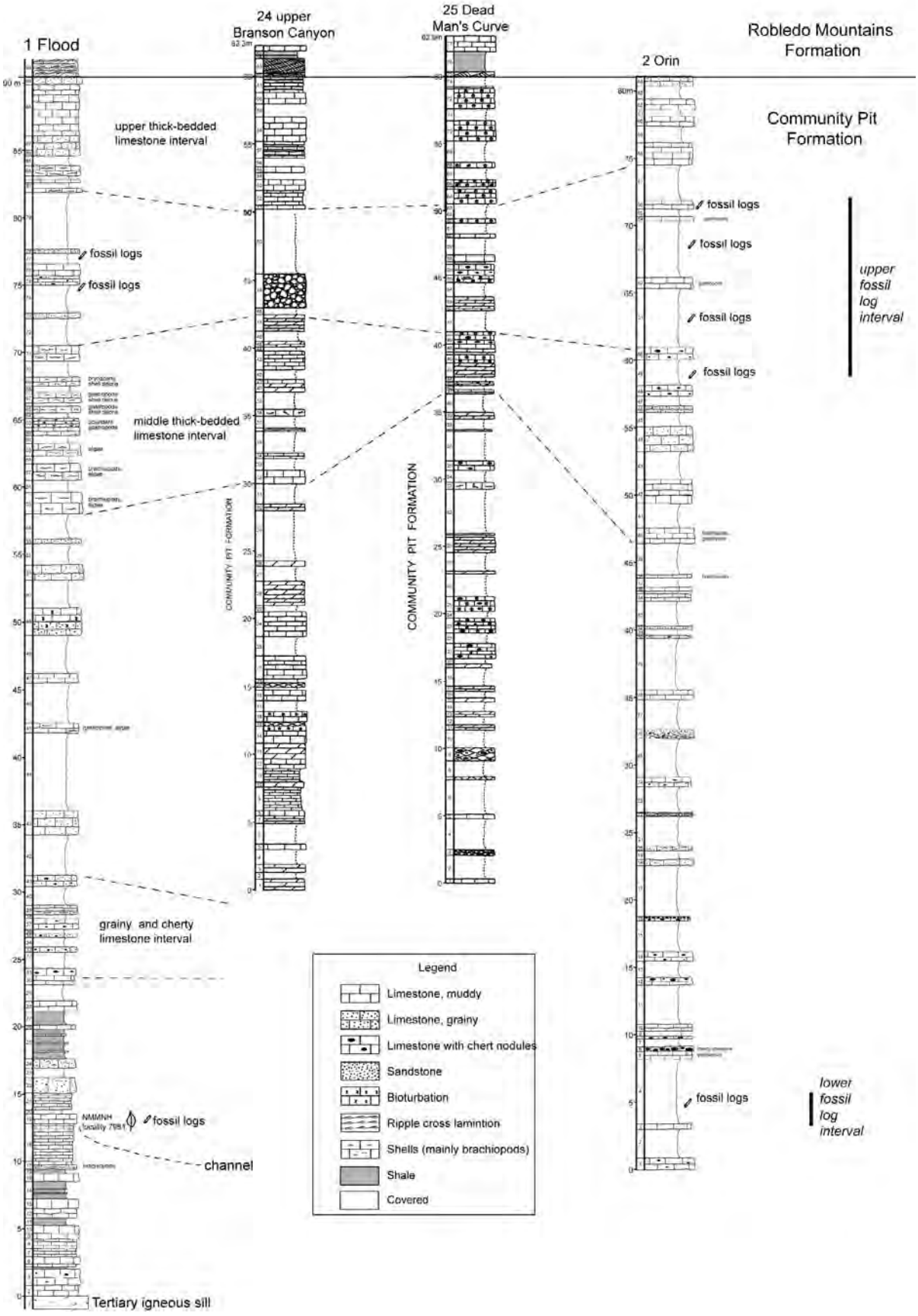


FIGURE 7. Correlated measured sections of most of the Community Pit Formation in the Prehistoric Trackways National Monument. Sections were measured in NW ¼ NW ¼ sec. 30 (Flood), SE ¼ SW ¼ sec. 24 (upper Branson Canyon), NW ¼ SE ¼ sec. 24 (Dead Man's Curve) and NW ¼ NW ¼ sec. 24 (Orin), T22S, R1W.

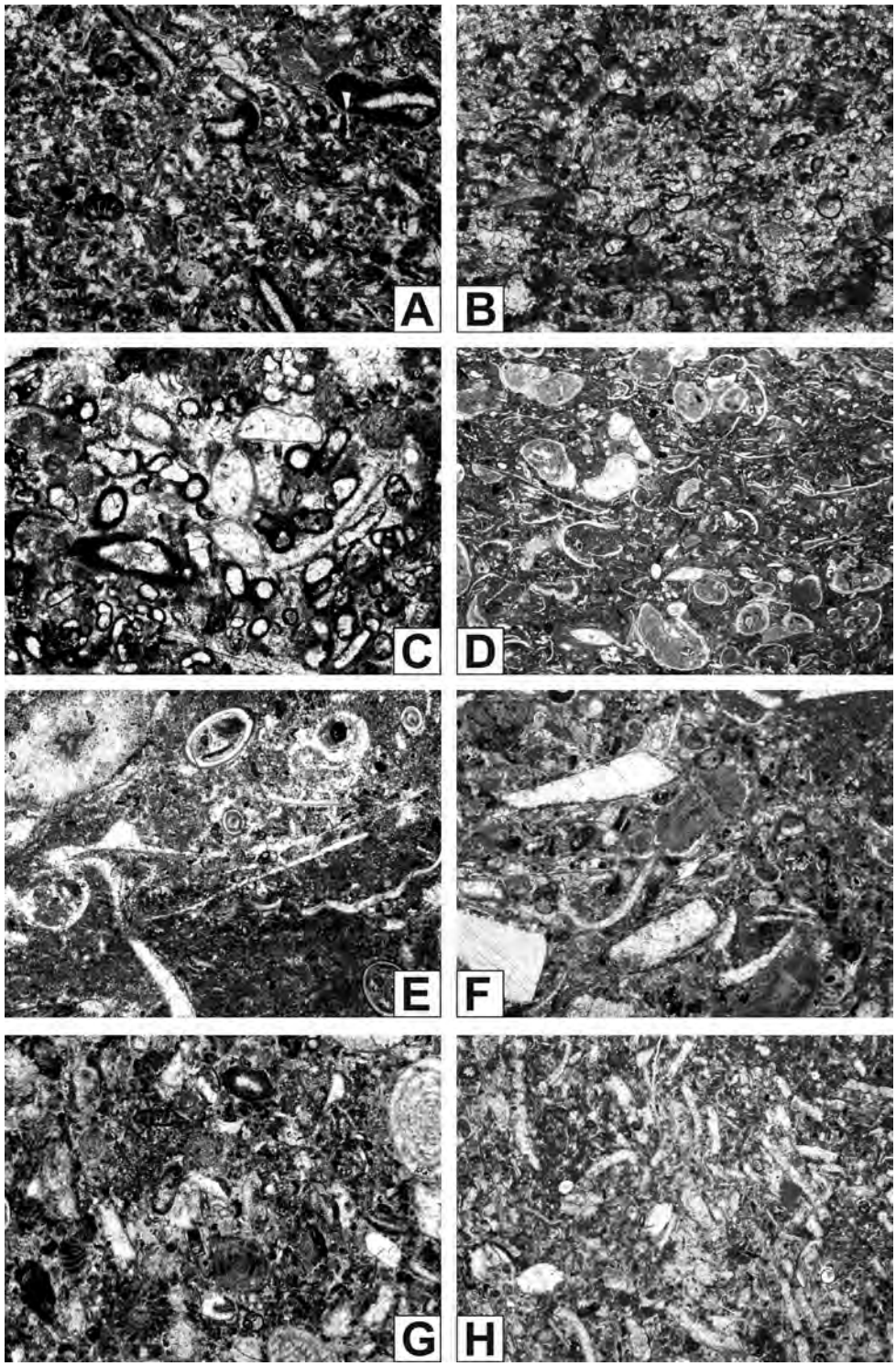


FIGURE 8. Thin section photographs of common microfacies types of the Community Pit Formation (A-B), Robledo Mountains Formation (C-E) and Apache Dam Formation (F-H), Robledo Mountains. All photographs under plane light. **Community Pit Formation A,** Grainstone to packstone composed of peloids, intraclasts, and diverse bioclasts, some encrusted by cyanobacteria and tubular foraminifers. Indian Springs Canyon, unit 133, width of photograph is 6.3 mm. **B,** Foraminiferal wackestone to packstone composed of abundant tubular foraminifers, many ostracods and few other fossil fragments. Indian Springs Canyon, unit 199, width of photograph is 3.2 mm. **Robledo Mountains Formation C,** Foraminiferal wackestone to grainstone, composed of abundant tubular foraminifers, subordinate ostracods and rare fossils of other types. Locally micrite is present. Branson Canyon, BRC 2, width of photograph is 3.2 mm. **D,** Ostracodal wackestone containing abundant ostracods, subordinate tubular foraminifers and *Spirorbis*. Branson Canyon, BRC 4, width of photograph is 6.3 mm. **E,** Wackestone to floatstone containing a few larger and many small bioclasts of a diverse fossil assemblage. Branson Canyon, BRC 10, width of photograph is 6.3 mm. **Apache Dam Formation F,** Bioclastic wackestone containing a moderately diverse fossil assemblage, including echinoderms, phylloid algae and foraminifers. Branson Canyon, BRC 13, width of photograph is 6.3 mm. **G,** Bioclastic wackestone to floatstone containing some larger and many small fossil fragments (echinoderms, phylloid algae, bivalves, brachiopods, foraminifers, bryozoans). A few of these are encrusted by cyanobacteria. Branson Canyon, BRC 16, width of photograph is 6.3 mm. **H,** Algal wackestone containing abundant recrystallized dasycladacean algae (*Epimastopora*), foraminifers and a few other fossils. Type Apache Dam, unit 21, width of photograph is 6.3 mm.



FIGURE 9. Photograph of a fossil log in the Community Pit Formation in the Prehistoric Trackways National Monument (courtesy of Jerry MacDonald).

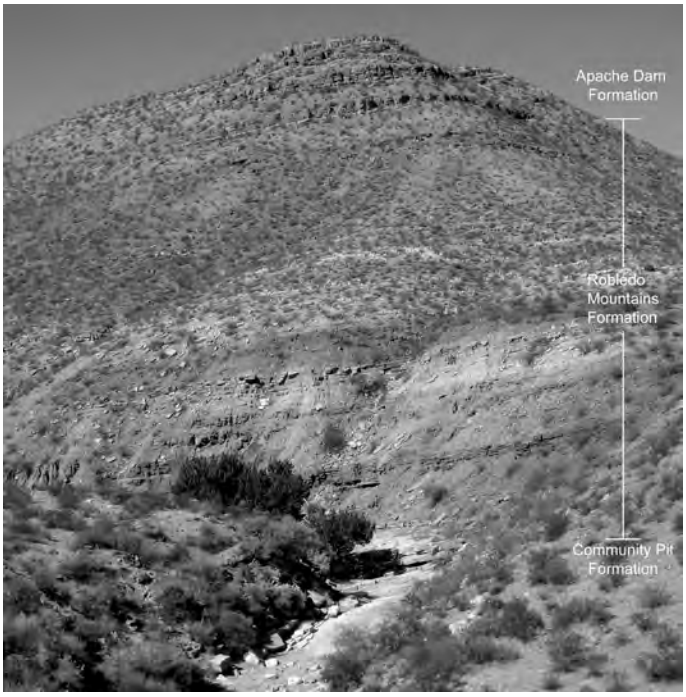


FIGURE 10. Photograph of the complete section of the Robledo Mountains Formation exposed in Branson Canyon (compare to Figure 11).

been reported from the Palm Park Formation (Seager et al., 1975, table 1), but these appear to be too old, though the oldest age of the Palm Park Formation is not certain. However, it is likely to be no older than the lithologically very similar Rubio Peak Formation in the Black Range, which is in the same stratigraphic interval as the Palm Park Formation. The Rubio Peak Formation has been radioisotopically dated at no older than ~38 Ma (Chapin et al., 2004) and has yielded early Chadronian fossil mammals and a fossil of the Duchesnean brontothere *Duchesneodus* (Morgan and Lucas, 2012). Therefore, we conclude that the Palm Park Formation is of middle-late Eocene age (late Duchesnean-early Chadronian), ~38-36 Ma, based on radioisotopic ages and mammalian biochronology.

Bell Top Formation (Tbt)

Picacho Mountain is a plug of flow-banded rhyolite assigned to the Bell Top Formation. The rock mostly lacks phenocrysts, but some outcrops show crystals of sanidine, oligoclase, and biotite. Intrusions commonly have glassy margins. The oldest published radioisotopic age of tuffs in the Bell Top Formation, which overlies the Palm Park Formation, is ~35.8 Ma, which is late Eocene (Chapin et al., 2004).

Robledo rhyolite (Tr)

The rock informally named Robledo rhyolite forms conspicuous sills and small dikes and plugs in the Robledo Mountains (Seager et al., 2008). The Lookout Peak sill at the northern end of the range is roughly 300 m thick, separating Silurian and older rocks below from Pennsylvanian above (Fig. 2). Devonian and Mississippian rocks were largely consumed by the intrusion. Another series of sills extends southeastward from the northwestern corner of the PTNM (Fig. 3). Largely injected into the Shalem Colony and lower Community Pit formations, these sills rapidly pinch and swell, reaching at least 50 m thick in the NW¼ of sec. 25, T22S, R1W. Small sills intrude the Robledo Mountains Formation in the NE¼ of sec. 30, T22S, R1E.

As Seager et al. (2008) report, the Robledo rhyolite is largely pink, tan, and cream-colored and massive to slightly porphyritic, with phenocrysts of orthoclase, biotite, and quartz. Flow banding is not developed. Kottlowski et al. (1969) reported an age of 35 Ma (latest Eocene), based on a single whole-rock K/Ar analysis.

Basalt (Tb)

Small to moderate-sized intrusions and flows of Tertiary basalt are found within the Monument and elsewhere in the Robledo Mountains. One of the largest of such bodies, a flow that displays columnar jointing, is just north of the Community Pit in the SW¼ NE¼ of sec. 19, T22S, R1E (Fig. 14). A steep conical hill near Apache Canyon in the NE¼ NW¼ of sec. 36, T22S, R1W represents a basalt (?) 100+ m across. A northeast-trending dike is well exposed along Apache Canyon in the NE ¼ of sec. 26, T22S, R1W; two more intrusions crop out along the ravine just north of the center of sec. 24 in the same township.

Seager et al. (2008) called the rock olivine mellilite. The basalt north of the Community Pit yielded a whole-rock K/Ar age of 7.1 Ma (late Miocene). This igneous activity reflects a phase of rift development during which most of the basins and ranges in southern New Mexico assumed their present forms (Seager et al., 1984).

Travertine, siltstone, and shale (Tbs)

Seager et al. (2008) mapped a small area of "travertine mounds and calcareous, laminated, buff-colored siltstone/shale, which unconformably overlies an eroded plug of basalt," southwest of the Community Pit in the west-central part of sec. 30, T22S, R1E. Reported thickness is about 9 m. The authors did not discuss the origin of the deposit, although travertine implies the former presence of hot springs. G. Mack (personal commun., 2011) suggests that these are lacustrine deposits. These relatively unconsolidated rocks overlie an eroded basalt plug and may be substantially younger than the Rincon Valley Formation, so their placement in the stratigraphic column here (Fig. 4) is tentative, after Seager et al. (2008).

Our study of these rocks on outcrop and in thin section (Fig. 15) supports the interpretation of a lacustrine origin. These beds are thinly bedded, intercalated siltstone and sandstone. The siltstone is indistinctly laminated and composed of fine-grained matrix in which abundant small feldspar and rare quartz grains occur. The diameter of the feldspar and quartz grains is mostly 0.01-0.02 mm, rarely up to 0.05 mm. This siltstone may be a volcanic ash layer (it contains a large amount of volcanic material). The sandstone is mixed siliciclastic-carbonate in composition and poorly sorted. Abundant carbonate grains and fresh plagioclase grains, rare quartz grains and many volcanic rock fragments, including volcanic chert grains, are embedded in fine-grained carbonate matrix. Rarely, reworked siltstone fragments are present. The plagioclase grains display twins and are angular. Plagioclase and quartz grains are of volcanic origin.

One sample is composed of laminated carbonate siltstone with a few small feldspar grains embedded; siltstone composed of carbonate matrix in which abundant fresh plagioclase grains and some volcanic chert grains, rare quartz grains and muscovite are embedded; and sandstone containing abundant recrystallized carbonate grains, many angular fresh plagioclase grains and some quartz grains, and a few volcanic rock fragments (including volcanic chert). All samples contain volcanic material (mainly fresh plagioclase grains, also volcanic rock fragments, volcanic chert, quartz) in varying amounts; fine-grained layers may be volcanic ash layers.

Rincon Valley Formation (Trv)

Seager et al. (2008) mapped small areas of this unit along the

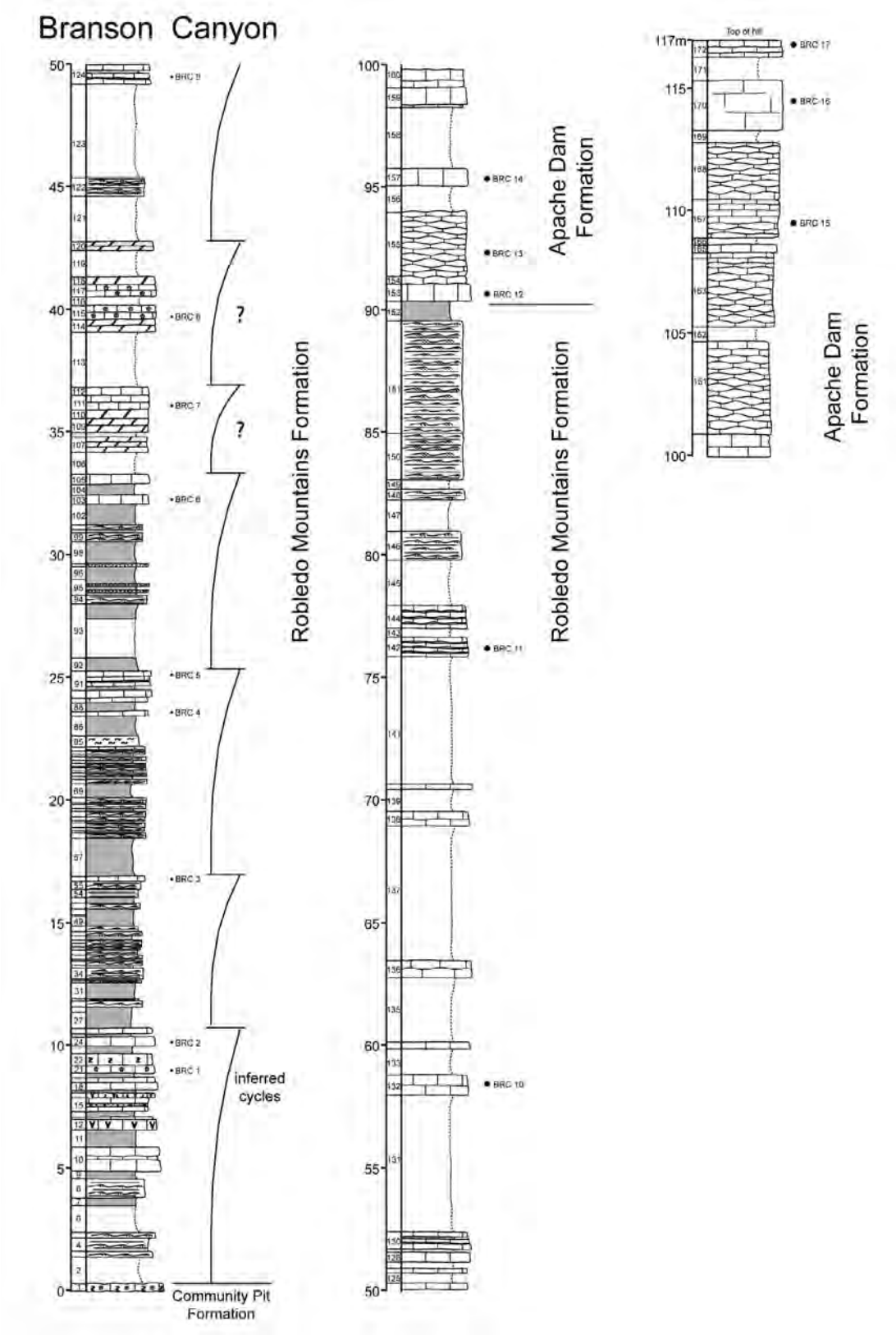


FIGURE 11. Measured section of the Robledo Mountains Formation exposed in Branson Canyon (compare to Figure 10). Numbers on left side of columns indicate distance in meters above base. Section measured in SE ¼ NW ¼ sec. 30, T22S, R1W. For lithologic legend see Figure 5.



FIGURE 12. Photograph of representative outcrop of the Apache Dam Formation in the PTNM (SE ¼ SW ¼ sec. 23, T22S, R1W). Inset shows characteristic algal limestone (algal plates about 5 cm long)

northeast-trending fault just east of the Community Pit (Fig. 3). They described the Rincon Valley Formation as "fanglomerate (tan) with interbedded conglomeratic sandstone, sandstone, and mudstone, all derived primarily from the underlying Bell Top and Palm Park volcanic and intrusive rocks." The Rincon Valley Formation represents "early rift" alluvial fan deposits. Locally, it is generally rotated by block faulting, with dips as much as 40 degrees and is as much as 198.2 m thick. A few fossil mammals, K-Ar dates and regional correlations indicate it is late Miocene to early Pliocene in age, between about 4 and 9 Ma (Seager et al., 1984; Morgan et al., 1998).

Tertiary and Quaternary Systems

Camp Rice Formation (QTc)

The Camp Rice Formation comprises varied middle Pliocene to early Pleistocene sediments of the ancestral Rio Grande and piedmont alluvial fans that drained into the river system. Most of the Camp Rice Formation represents fluvial channels and alluvial fans, but floodplain and eolian deposits also are present.

These deposits surround the Robledo Mountains and locally overlie pediment surfaces within the mountains (Fig. 3). Thickness ranges to more than 90 m on outcrop and may exceed 200 m in the subsurface. Locally, around the PTNM, the Camp Rice Formation is largely gravel, with clasts ranging up to boulder size cemented by pedogenic carbonate (caliche). Sand, silt, and loamy deposits, also cemented by caliche, are subordinate. Fossil mammals are fairly common in the basinal facies to the south and southeast, dating the deposits as Plio-Pleistocene (e. g., Morgan and Lucas, 2003).

Quaternary System

Older Valley Fill (Qvo)

Seager et al. (2008) mapped several kinds of older (Pleistocene) valley fill sediments, which have been combined into a single unit (Qvo) on our map. Within the PTNM, these deposits are largely "older valley-border alluvium" along the dissected, sloping surface (alluvial apron) that separates the Robledo Mountains from the modern Rio Grande floodplain. Valley-border deposits mantle the Camp Rice Formation and are inset into younger alluvium along the edge of the floodplain (Fig. 3). These deposits are as thick as 40 m and extend to an elevation of as much as 76 m above the river. The diverse sediments consist of crudely stratified gravel, sand, silt and loam. Some of the older surfaces contain layers of pedogenic carbonate (caliche).

Younger Valley Fill (Qvy)

Holocene alluvium of the Rio Grande and its tributaries is mapped as younger valley fill (map symbol Qvy: Fig. 3). Seager et al. (2008) separately mapped "valley-floor fluvial facies" along the Rio Grande and "valley-border alluvium" of tributary arroyos, terraces, and fans. Along the Rio Grande, river channel and floodplain sediments are at least 21 m thick and range in composition from gravel to fine sand, silt and clay. The valley bottom, which varies from a little over 1 km to more than 4 km wide, is irrigated and intensively farmed. Valley-border deposits occupy sloping aprons that border both sides of the valley bottom, together with the sediments of minor intermittent streams that flow out of the mountains. These deposits range from coarse gravel and rock debris to sand and loam. The areas covered by younger valley fill support limited grazing and non-agricultural uses.

PTNM: STRUCTURAL GEOLOGY

During the Phanerozoic, southern New Mexico experienced three major episodes of tectonic deformation. These are: (1) the Ancestral Rocky Mountains (ARM) orogeny, which took place during Pennsylvanian and Early Permian time; (2) the Laramide orogeny, which formed the Rocky Mountains between Late Cretaceous and middle Eocene time; and (3) the Rio Grande rifting event, which commenced in the Miocene (or late Oligocene) and is still in progress today. Among these, only the last has had any significant effect on the current geological structure of the Robledo Mountains and the PTNM.

Ancestral Rocky Mountains (ARM) Orogeny

The unification of Pangea, more specifically the collision of Gondwana with Laurussia, is generally agreed on as the cause of the ARM orogeny (e.g., Kluth and Coney, 1981; Dickinson and Lawton, 2003). This caused the creation of a series of north- to west-trending elongate basins and basement-cored uplifts, the "ancestral Rockies," across a broad part of the southern and western United States. The structural style of the uplift bounding faults of the ARM has proven difficult to decipher, either because the faults are buried or (more often) they have been reactivated by later deformation(s). Therefore, the synorogenic sediments – primarily of Middle Pennsylvanian to Early Permian age in New Mexico – are key to interpreting ARM history.

In the PTNM, a feature that may be related to a late phase of the ARM deformation crops out along the eastern side of Apache Canyon near the center of the W½ of sec. 25, T22S, R1W (Fig. 16). Limestone in the Robledo Mountains Formation exhibits a small, west-facing monocline, with bedding nearly vertical near the upper hinge. Above the limestone, beds of red siltstone are tilted 30° to the west, beveled to a flat surface, and overlain by horizontal siltstone like that below. Younger limestone layers pass above these structures without changing dip.

Lucas et al. (1995, fig. 5F) illustrated this outcrop and suggested the steeply dipping strata are delta foresets overlain by nearly horizontal sheetflood deposits. However, given the fold in limestones beneath the steeply dipping red beds, we prefer a syndepositional tectonic explanation that identifies this as an angular unconformity that resulted from Early Permian tilting and subsequent truncation of the steeply dipping strata.

Laramide Orogeny

The Laramide orogeny of the Late Cretaceous-Eocene culminated in crustal shortening and thickening that during the Mesozoic had characterized the western convergent margin of North America. Although models are not fully agreed upon, the result in New Mexico and adjacent Rocky Mountain states was a complex amagmatic deformation that resulted in basement-cored uplifts surrounded by basins in which fluvial and lacustrine clastic sediments accumulated (Cather, 2004).

In the PTNM, in what has been termed the Love Ranch basin, Eocene? red beds of the Love Ranch Formation accumulated adjacent to the Laramide Rio Grande uplift (Seager and Mack, 1986, 2003). Thrust faults of likely Laramide origin are present in the Doña Ana Mountains, 5 to 10 km northeast of the PTNM.

Basin and Range

The extensional orogeny (taphrogeny) that produced the western American Basin and Range reflects major crustal thinning and extension locally seen on the western margin of the Mesilla basin of the Rio Grande rift, which borders the eastern PTNM. This began at about the beginning of the Miocene (~25 Ma) and continues at present. Thus, crustal extension created an array of faults, the great majority of which trend more or less north-south locally. The two largest faults, simply named East and West Robledo faults, outline the south-tilted crustal block that comprises the Robledo Mountains. These faults join at the north end of the range and diverge southward, continuing beyond the southern end of the mountains beneath valley-fill sediments. The West Robledo fault is not exposed, but its presence is evident from the steep, linear western escarpment of the range. In contrast, the East Robledo fault may be inspected in many places where canyons and arroyos cut across its trace. Most easily accessible is a deep arroyo

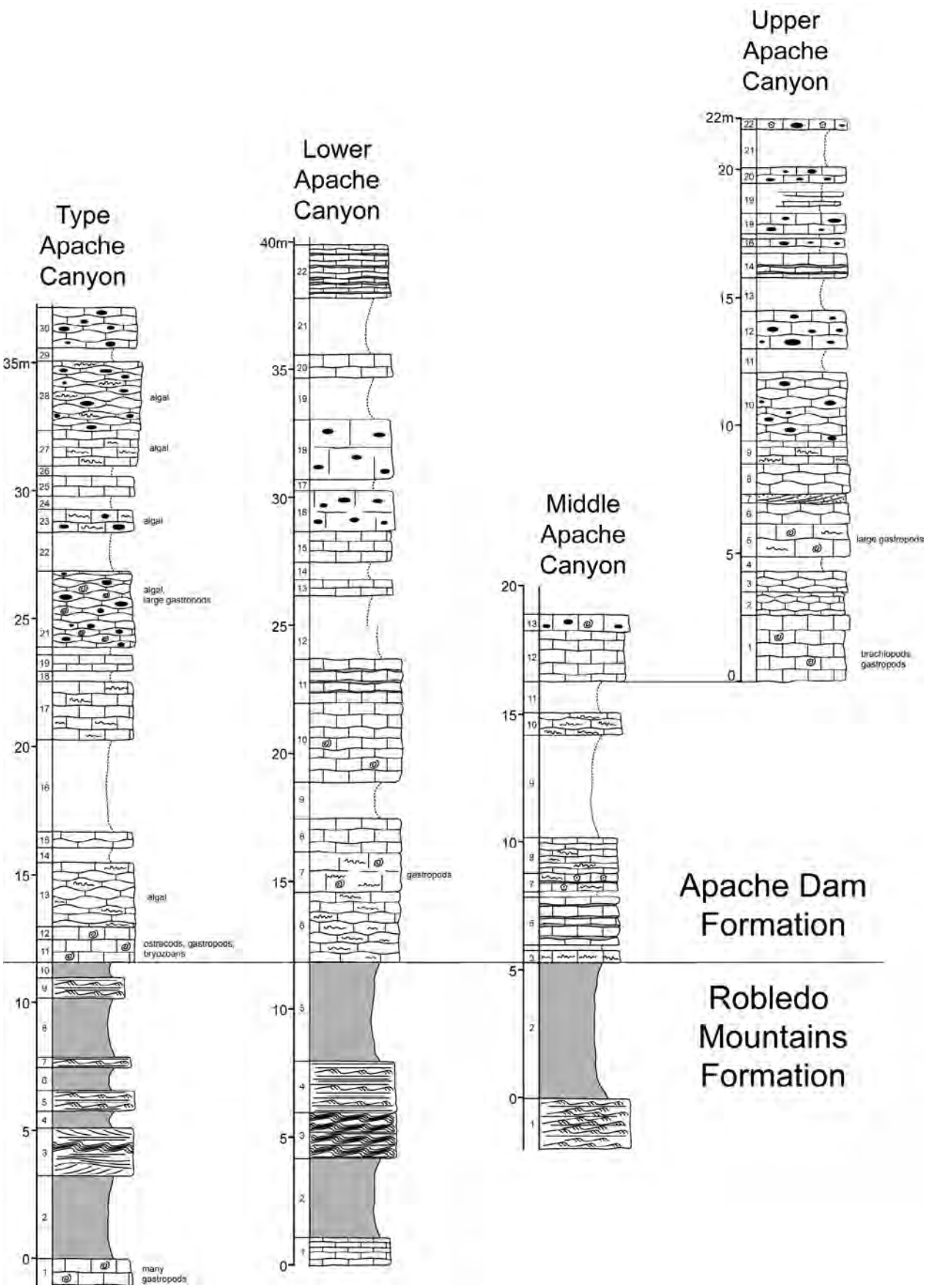


FIGURE 13. Measured stratigraphic sections of the Apache Dam Formation in the PTNM. See Figure 5 for lithologic legend. Sections were measured in the NE ¼ SW ¼ sec. 30 (type Apache Canyon), SE ¼ NE ¼ sec. 26 (Lower Apache Canyon), SE ¼ SE ¼ sec. 23 (Middle Apache Canyon) and SE ¼ SW ¼ sec. 23 (Upper Apache Canyon), T22S, R1W.



FIGURE 14. Photograph of Miocene basalt flow that displays columnar jointing, just north of the Community Pit in the SW¼ NE¼ of sec. 19, T22S, R1E.

along the access road at the southern edge of Community Pit. At this spot, Permian sedimentary rocks and Eocene rhyolite dip steeply, and are faulted into direct contact with Quaternary alluvium. As Seager et al. (2008) mapped, all of the Cenozoic units are offset along the East Robledo fault, and this faulting likely took place most recently during the late Pleistocene. Although not seismically active at present, this fault obviously has potential for further movement.

Other faults in the Robledo Mountains largely strike parallel with the two boundary faults (Fig. 3). Most have displacements measured in meters to tens of meters; a few exceed 100 m. The greatest offsets within the PTNM are along a graben that extends north-northwest from the Community Pit. A thick deposit of Camp Rice Formation fills this graben, which apparently formed a linear valley during Pliocene to early Pleistocene time. At the southern end of the Robledos, only a few faults visibly offset the Camp Rice and younger formations; but mapped absence of faults is largely a function of poor exposure. A number of faults that strike slightly north of west crosscut the more prevalent north-trending ones. All of the faults described above are of the high-angle normal variety.

GEOLOGICAL HISTORY OF THE PTNM

We can divide the geological history of the PTNM into two principal phases—Early Permian and late Cenozoic. The more than 250 million years that divide these two phases left little geological evidence in the PTNM—just some minor sedimentary deposits and structures of early/middle Cenozoic age.

Early Permian

During the Early Permian, the location of the present PTNM was equatorial near the western edge of the Pangean supercontinent. The shallow marine Hueco seaway covered parts of southern New Mexico and West Texas. The oldest strata exposed in the PTNM (Shalem Colony and Community Pit formations) record a time when the entire PTNM was below sea level, covered by shallow marine waters (Fig. 17). However, land was not far away, as indicated by the fossil logs found in shallow marine strata of the Community Pit Formation in and around the PTNM (Falcon-Lang et al., 2014).

Gypsum and shallow limestone microfacies indicate that the Hueco seaway at the location of the PTNM was shallow and poorly circulated under a hot and dry climate. Many limestones are dolomitic, and others have bioclastic debris, primarily from ostracods, crinoids, brachiopods and bryozoans. The most normal marine fossil assemblage comes from shale and nodular limestone beds of the Robledo Mountains Formation. These assemblages are brachiopod dominated (Fig. 17).

Deposition of the Robledo Mountains Formation marks the interval of Early Permian time when terrestrial environments first appeared at the location of the PTNM. Red-bed sandstones and mudrock of the Robledo Mountains Formation represent deposition on the arid coastal plain near the shoreline of the Hueco seaway (Fig. 17). The intercalation of nonmarine red beds and marine limestone/shale of the Robledo Mountains Formation records that shoreline moving back and forth across the area of the PTNM.

The only record of animal life on that coastal plan is in the form of ichnofossils. Plants are a low diversity assemblage dominated by walchian conifers (DiMichele et al., this volume). Indeed, such a low diversity, drought-resistant paleoflora characterizes the Abo depositional system across much of New Mexico (DiMichele et al., 2007, 2013; Lucas et al., 2012, 2013).

The invertebrate trace fossils are dominated by arthropod trackways (*Dendroidichnites, Diplichnites, Diplopodichnus, Kouphichnium, Lithographus, Octopodichnus, Palmichnium* and *Stiaria*), arthropod resting traces (*Lockeia, Rotterodichium, Selenichnites, Tonganoxichnus*), arthropod jumping traces (some *Tonganoxichnus*) and arthropod grazing traces (*Stiallia, Striatichnium*). Invertebrate feeding traces (*Treptichnus*), grazing tracers (*Cochlichnus*), graphoglyptids and helical-shaped burrows (*Augerinoichnus*) are less common. Vertebrate footprints are mostly of small temnospondyls (*Batrachichnus*), araeoscelids (*Dromopus*) and pelycosaurs (*Dimetropus*). Tracks of larger amphibians (*Limnopus*) and of primitive amniotes (*Hyloidichnus, Varanopus, Robledopus*) are much less common, and swim tracks (*Lunichnium, Characichnos*) are present. Fish swimming traces (*Undichna*) are also present. The trace fossil assemblage is largely of predators. Exceptions are invertebrate traces made by detritivores such as myriapods, rare diadectomorph tracks and some (or all?) of the larger pelycosaur tracks, which may have been made by edaphosaurs. The Robledo Mountains Formation trace fossil assemblages well represent the *Scoyenia* ichnoguild of the *Scoyenia* ichnofacies (Minter and Braddy, 2009).

Permian-Cenozoic—a 250 Million Year Hiatus

From Permian to late Cenozoic time (between about 280 and 30 million years), much happened to the area of the PTNM but left little geological record there. Most significant was the Late Cretaceous-Eocene Laramide orogeny and subsequent mid-Cenozoic caldera collapse volcanism. Some geological structures and red-bed conglomerates of the Eocene Love Ranch Formation represent the effects of the Laramide orogeny. The volcaniclastic rocks of the Palm Park Formation record the early phase of the mid-Cenozoic volcanism. They represent part of the Mogollon-Datil volcanic field, which covered much of southwestern New Mexico from middle Eocene through early Miocene time.

Late Cenozoic

The current landscape of the PTNM formed during the late Cenozoic along the edge of the Rio Grande rift, which extends from central Colorado to Mexico along the drainage of the Rio Grande. In the rift, vast thicknesses (locally thousands of meters) of alluvial, fluvial and lacustrine siliciclastic sediments accumulated throughout much of the late Cenozoic. Extensive volcanic fields of late Cenozoic age also are present in New Mexico, in and around the rift, and are well represented by the younger igneous rocks in and around the PTNM (Figs. 3-4).

Regional crustal extension began in central New Mexico during the Oligocene and forced the Colorado Plateau of the Four Corners region away from the craton, so that it began to move westward and southward. A high-standing welt that had been created by the Laramide orogeny then began to collapse, so that by the beginning of the Miocene the Laramide topography had been structurally inverted, and the lows began to accumulate fluvial and eolian sediments (Pazzaglia et al., 1999; Mack, 2004). The rift basins thus formed along a north-south trend that extended from Colorado to Mexico, including the Mesilla basin, which borders the Robledo Mountains on the east. The rift basins began as relatively broad, shallow closed basins, but as extension continued they deepened and became (simply speaking) a series of narrow, asymmetric grabens. Locally, the flanks of the rift basins were elevated and bowed outward, probably as a result of isostatic uplift along major extensional faults (May et al., 1994; Roy et al., 1999). Structurally, complex accomodation zones also border parts of the rift basins.

The sedimentary fill of the rift is broadly referred to as the Santa Fe Group, including the Rincon Valley and Camp Rice formations of the PTNM (Lucas and Ingersoll, 1981; Mack, 2004). In general, the rift basins have a temporally tripartite Santa Fe Group stratigraphy that well reflects the tectonic evolution of the rift system:

1. Early basin fills are eolian, alluvial fan and basin-floor playa deposits of late Oligocene? through middle Miocene age. These diverse

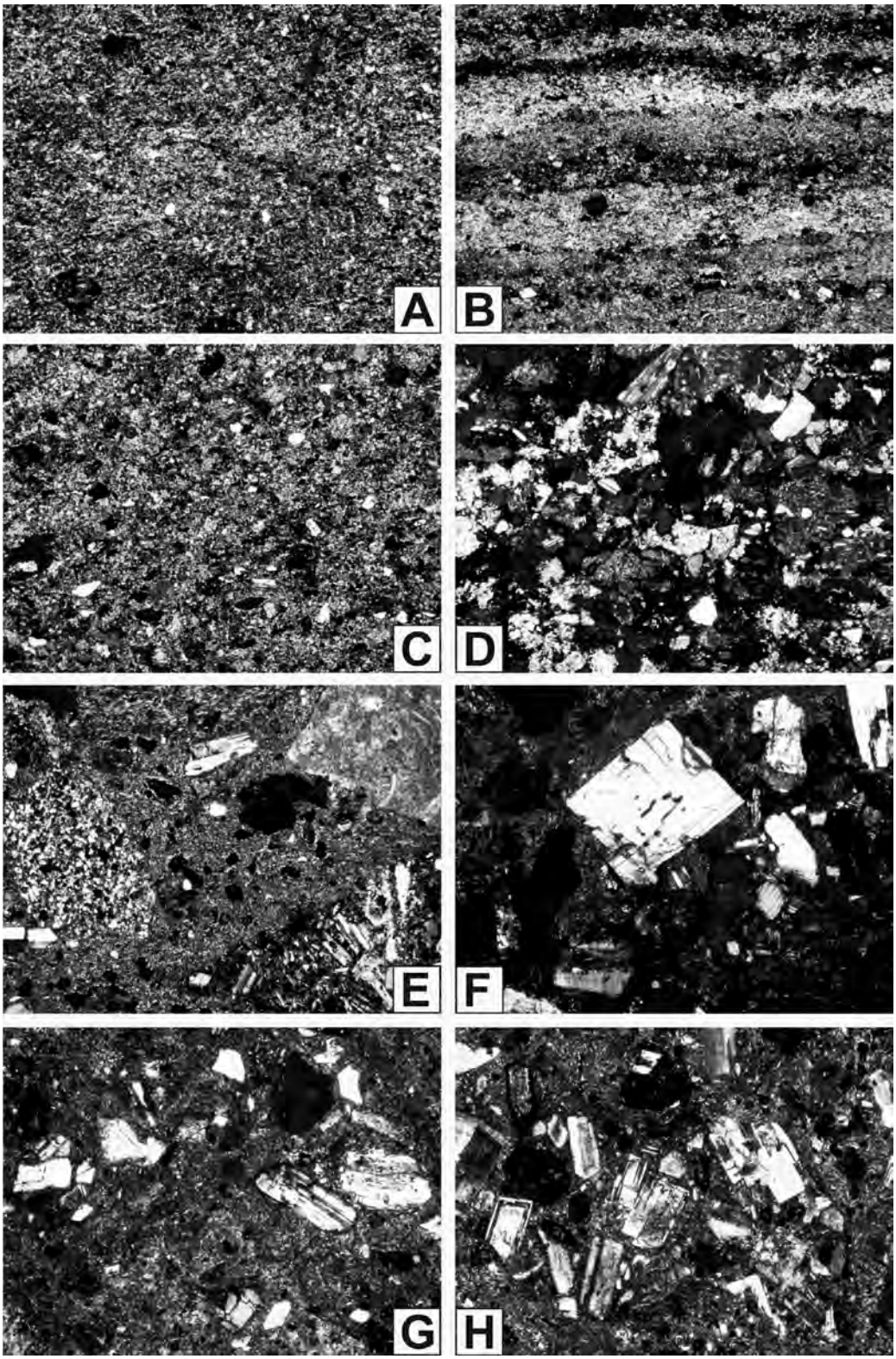


FIGURE 15. Thin section photographs of lacustrine sediments, Robledo Mountains (all under polarized light). Strata are part of the unit Seager et al. (2008) mapped as "Travertine, siltstone, and shale (Tbs)." **A,** Siltstone containing small angular feldspar grains (width of photograph is 1.2 mm). **B,** Laminated carbonate mudstone containing silt-sized angular feldspar grains (width of photograph is 3.2 mm). **C,** Fine-grained, mixed siliciclastic-carbonate sandstone composed of carbonate grains and abundant angular fresh feldspar grains embedded in carbonate matrix (width of photograph is 3.2 mm). **D,** Sandstone containing carbonate grains, abundant plagioclase grains and subordinate volcanic rock fragments and chert grains (width of photograph is 3.2 mm). **E,** Pebbly sandstone containing carbonate clasts (upper right), volcanic rock fragments (lower right) and a reworked siltstone fragment (left) embedded in silty to sandy matrix (width of photograph is 3.2 mm). **F,** Sandstone containing abundant volcanic material (mainly fresh plagioclase grains, subordinate volcanic rock fragments and chert grains, rare quartz grains; width of photograph is 3.2 mm). **G-H,** Sandstone containing abundant grains of volcanic origin (many fresh plagioclase grains, volcanic rock fragments with abundant plagioclase, and volcanic chert grains) and carbonate grains embedded in carbonate matrix (width of photograph is 3.2 mm).

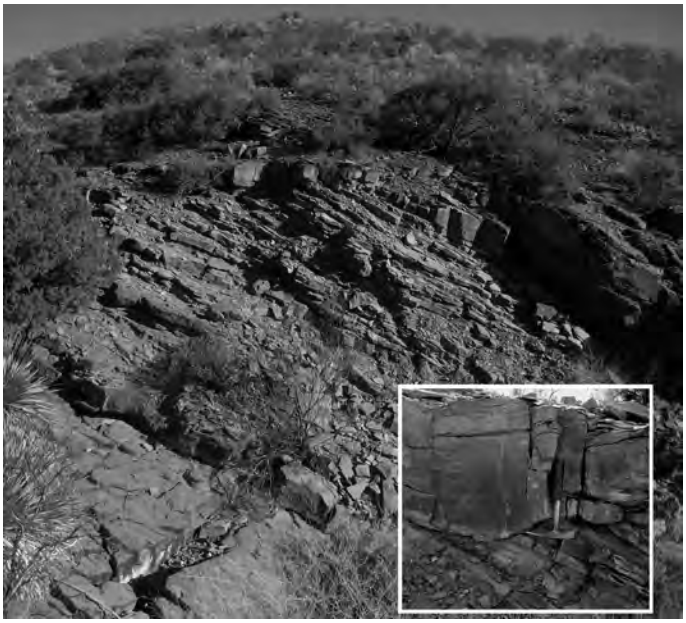


FIGURE 16. Photograph showing angular unconformity within red beds of the Robledo Mountains Formation along Apache Canyon (UTM zone 13, 321196E, 3582410N, NAD 83). View is looking south. Inset shows detail at contact of steeply dipping siltstone beds truncated by overlying horizontal siltstone beds of Robledo Mountains Formation.

deposits were laid down in the early broad and shallow extensional basins prior to graben formation, and are not exposed/preserved in the area of the PTNM.

2. Thick fluvial and lacustrine deposits of late Miocene-Pliocene age accumulated in the rapidly deepening graben system. In the PTNM, the Rincon Valley Formation represents this interval.

3. A through-flowing Rio Grande began to integrate drainage in all the rift basins during the Pliocene, so that basin stratigraphy changes to that of axial river and tributary deposits that are laterally intertongued with piedmont deposits shed from the basin margins. In the Robledo Mountains, the Camp Rice Formation well represents this interval.

Pleistocene ("Quaternary") rocks cover more than 25% of New Mexico and are a diverse array of continental sediments and lavas. Most of these rocks formed as the continuation of the Miocene-Pliocene depositional and volcanic processes associated with the Rio Grande rift. A striking characteristic of New Mexico's Pleistocene record is its erosive landscape. This is particularly evident in the Rio Grande valley adjacent to the PTNM, where the Miocene-Pliocene acccumulation of vast thicknesses of sediments has been followed by extensive fluvial incision that largely reflect changes in hydrology and sediment yield controlled by Pleistocene climate fluctuations and integration of the upper and lower Rio Grande so that the entire river system reached the Gulf of Mexico, in other words a drop in base level (e. g., Hawley, 1978; Pazzaglia et al.,1999; Pazzaglia and Hawley, 2004).

ACKNOWLEDGMENTS

The U. S. Bureau of Land Management provided generous financial and logistical support of our research in the PTNM. Among the many BLM staff who helped us, we are particularly grateful to McKinney Briske, Phil Gensler and Pat Hester. Collaboration and assistance in the field by various colleagues is also gratefully acknowledged, especially Dan Chaney, Bill DiMichele, Larry Rinehart, Justin Spielmann and Sebastian Voigt. Jerry MacDonald showed us fossil localities and otherwise assisted us in diverse ways. Bruce Allen and Bill DiMichele provided helpful reviews of the manuscript.

REFERENCES

Cather, S. M., 2004, Laramide orogeny in central and northern New Mexico and southern Colorado; *in* Mack, G. H. and Giles, K. A., eds., The geology of New Mexico: A geologic history: New Mexico Geological Society, Special Publication 11, p. 203-248.

Chapin, C.E., McIntosh, W.C. and Chamberlin, R.M., 2004, The late Eocene-Oligocene peak of Cenozoic volcanism in southwestern New Mexico; *in* Mack, G. and Giles, K., eds., The geology of New Mexico: A geologic history: New Mexico Geological Society, Special Publication, p. 271-293.

Dickinson, W. R. and Lawton, T. F., 2003, Sequential intercontinental suturing as the ultimate control for Pennsylvanian ancestral Rocky Mountain deformation: Geology, v. 31, p. 609-612.

DiMichele, W.A., Chaney, D.S., Lucas, S.G., Kerp, H. and Voigt, S., 2013, Flora of the Lower Permian Abo Formation red beds, western equatorial Pangea, New Mexico: New Mexico Museum of Natural History and Science, Bulletin 59, p.265-288.

DiMichele, W.A., Chaney, D.S., Nelson, W.J., Lucas, S.G., Looy, C.V., Quick, K. and Jun, W., 2007, A low diversity, seasonal tropical landscape dominated by conifers and peltasperms: Early Permian Abo Formation, New Mexico: Review of Palaeobotany and Palynology 145, p. 249-273.

Falcon-Lang, H.J., Kurzawe, F., and Lucas, S.G., 2014, Coniferopsid tree-trunks preserved in sabkha facies in the Permian (Sakmarian) Community Pit Formation in south-central New Mexico, U.S.A.: Systematics and Palaeoecology: Review of Palaeobotany and Palynology, v. 200, p. 138–160.

Hawley, J. W., ed., 1978, Guidebook to the Rio Grande rift in New Mexico and Colorado: New Mexico Bureau of Mines and Mineral Resources, Circular 163, 241 p.

Hawley, J. W., Seager, W. R. and Clemons, R. E., 1975, Third day road log from Las Cruces to North Mesilla Valley, Cedar Hills, San Diego Mountain, and Rincon area: New Mexico Geological Society, Guidebook 26, p. 35-53

Jordan, C. F., 1971, Lower Permian stratigraphy of southern New Mexico and West Texas [Ph.D. dissertation]: Houston, Rice University, 140 p.

Jordan, C. F., 1975, Lower Permian (Wolfcampian) sedimentation in the Orogrande basin, New Mexico: New Mexico Geological Society, Guidebook p. 109-117.

Kluth, C. F. and Coney, P. J., 1981, Plate tectonics of the ancestral Rocky Mountains: Geology, v. 9, p. 10-15.

Kottlowski, F. E., 1960, Reconnaissance geologic map of Las Cruces thirty-minute quadrangle: New Mexico Bureau of Mines and Mineral Resources, Geologic Map 14.

Kottlowski, F., 1963, Paleozoic and Mesozoic strata of southwestern and south-central New Mexico: State Bureau of Mines and Mineral Resources, New Mexico Institute of Mining & Technology, Bulletin 79, 100 p.

Kottlowski, F.E., Weber, R.H., and Willard, M.E., 1969, Tertiary intrusive-volcanic mineralization episodes in the New Mexico region: Geological Society of America, Abstracts with Programs, Annual Meeting, v. 1, part 7, p. 278-280.

Krainer, K. and Lucas, S.G., 2012, Alluvial fan sedimentation of the Eocene Love Ranch Formation, southern Caballo Mountains, Sierra County, New Mexico: New Mexico Geological Society, Guidebook 63, p. 45-46.

Kues, B.S., 1995, Marine fauna of the Early Permian (Wolfcampian) Robledo Mountains Member, Hueco Formation, southern Robledo Mountains, New Mexico: New Mexico Museum of Natural History and Science, Bulletin 6, p. 63-90.

LeMone, D.V., Simpson, R.D. and Klement, K.W., 1975, Wolfcampian upper Hueco Formation of the Robledo Mountains, Doña Ana County, New Mexico: New Mexico Geological Society, Guidebook 26, p. 119-121.

Lucas, S.G. and Heckert, A.B., eds., 1995, Early Permian footprints and facies: New Mexico Museum of Natural History and Science, Bulletin 6, 301 pp.

Lucas, S. G. and Ingersoll, R. M., 1981, Cenozoic continental deposits of New Mexico: An overview: Geological Society of America Bulletin, v. 92, p. 917-932.

Lucas, S. G. and Spielmann, J. A., 2012, Late Eocene (Chadronian) fossil mammals from the Palm Park Formation, Caballo Mountains, Sierra county, New Mexico: New Mexico Geological Society, Guidebook 63, p. 519-524.

Lucas, S. G. and Williamson, T. E., 1993, Eocene vertebrates and late Laramide stratigraphy of New Mexico: New Mexico Museum of Natural History and Science, Bulletin 2, p. 145-158.

Lucas, S.G., Anderson, O.J., Heckert, A.B. and Hunt, A.P., 1995, Geology of Early Permian tracksites, Robledo Mountains, south-central New Mexico: New Mexico Museum of Natural History and Science, Bulletin 6, p. 13-32.

Lucas, S. G., Heckert, A. B., Estep, J. W. and Cook, C. W., 1998, Stratigraphy of the Lower Permian Hueco Group in the Robledo Mountains, Doña Ana County, New Mexico: New Mexico Museum of Natural History and Science, Bulletin 12, p. 43-54.

Lucas, S. G., Voigt, S., Lerner, A. J., MacDonald, J. P., Spielmann, J. A. and Celeskey, M. D., 2011, The Prehistoric Trackways National Monument, Permian of southern New Mexico, U. S. A.: Ichnology Newsletter, no. 28, p. 10-14.

Lucas, S. G., Krainer, K., Chaney, D. S., DiMichele, W. A., Berman, Voigt, S., Berman, D. S, Henrici, A. C., 2012, The Lower Permian Abo Formation



FIGURE 17. Reconstructions of Hueco seafloor in Prehistoric Trackways National Monument (above) and Hueco shoreline/coastal plain (below) in Prehistoric Trackways National Monument (artwork by Mary Sundstrom).

in the Fra Cristobal and Caballo mountains, Sierra County, New Mexico: New Mexico Geological Society, Guidebook 63, p. 345-376.

Lucas, S. G., Krainer, K., Chaney, D. S., DiMichele, W. A., Voigt, S., Berman, D. S and Henrici, A. C., 2013, The Lower Permian Abo Formation in central New Mexico: New Mexico Museum of Natural History and Science, Bulletin 59, p. 161-179.

Mack, G. H., 2004, Middle and late Cenozoic crustal extension, sedimentation, and volcanism in the southern Rio Grande rift, Basin and Range, and southern transition zone of southwestern New Mexico; *in* Mack, G. H. and Giles, K. A., eds., The geology of New Mexico: a geologic history: New Mexico Geological Society, Special Publication 11, p. 389-406.

Mack, G. H., 2007, Sequence stratigraphy of the Lower Permian Abo member in the Robledo and Doña Ana Mountains near Las Cruces, New Mexico: New Mexico Geology, v. 29, p. 3-12.

Mack, G. H. and James, W. C., 1986, Cyclic sedimentation in the mixed siliclastic-carbonate Abo-Hueco transitional zone (Lower Permian), southwestern New Mexico: Journal of Sedimentary Petrology, v. 50, p. 635-647.

May, S. J., Kelley, S. A. and Russell, L. R., 1994, Footwall unloading and rift shoulder uplifts in the Albuquerque basin: Their relation to syn-rift fanglomerates and apatite fission-track ages: Geological Society of America, Special Paper 291, p. 125-134.

Minter, N.J. and Braddy, S.J., 2009, Ichnology of an Early Permian intertidal flat: The Robledo Mountains Formation of southern New Mexico, USA:

The Palaeontological Association, Special Papers in Palaeontology 82, p. 1-107.

Morgan, G. S. and Lucas, S. G., 2003, Mammalian biochronology of Blancan and Irvingtonian (Pliocene and early Pleistocene) faunas from New Mexico: Bulletin of the American Museum of Natural History, v. 278, p. 269-320.

Morgan, G. S. and Lucas, S. G., 2012, Cenozoic vertebrates from Sierra County, southwestern New Mexico: New Mexico Geological Society, Guidebook 63, p. 525-540.

Morgan, G. S., Lucas, S. G. and Estep, J. W., 1998, Pliocene (Blancan) vertebrate fossils from the Camp Rice Formation near Tonuco Mountain, Doña Ana County, southern New Mexico: New Mexico Geological Society, Guidebook 49, p. 237-249.

Pazzaglia, F. J. and Hawley, J. W., 2004, Neogene (rift flank) and Quaternary geology and geomorphology; *in* Mack, G. H. and Giles, K. A., eds., The geology of New Mexico: A geologic history: New Mexico Geological Society, Special Publication 11, p. 407-437.

Pazzaglia, F. J., Woodward, L. A., Lucas, S. G., Anderson, O. J., Wegmann, K. W. and Estep, J. W., 1999, Phanerozoic geologic evolution of the Albuquerque area: New Mexico Geological Society, Guidebook 50, p. 97-114.

Roy, M., Karlstrom, K., Kelley, S., Pazzaglia, F. and Cather, S., 1999, Topographic setting of the Rio Grande rift, New Mexico: Assessing the role of flexural "rift-flank uplift" in the Sandia Mountains: New Mexico Geological Society, Guidebook 50, p. 167-174.

Seager, W. R., and Mack, G. H., 1986, Laramide paleotectonics of southern New Mexico: American Association of Petroleum Geologists, Memoir 41, p. 669-685.

Seager, W. R. and Mack, G. H., 2003, Geology of the Caballo Mountains, New Mexico: New Mexico Bureau of Geology and Mineral Resources, Memoir 49, 136 p.

Seager, W.R., Clemons, R.E. and Hawley, J.W., 1975, Geology of Sierra Alta Quadrangle, Doña Ana County, New Mexico: New Mexico Bureau of Mines and Mineral Resources, Bulletin 102, 56 p.

Seager, W.R., Kottlowski, F.E., and Hawley, J.W., 2008, Geologic map of the Robledo Mountains and vicinity, Doña Ana County, New Mexico: New Mexico Bureau of Geology and Mineral Resources, Open File Report 509, 3 sheets, scale 1:24,000.

Seager, W.R., Shafiqullah, M., Hawley, J.W., and Marvin, R.F., 1984, New K/Ar dates from basalts and the evolution of the southern Rio Grande rift: Geological Society of America Bulletin, v. 95, p. 87-99.

Smith, L. N., Lucas, S. G. and Elston, W. E., 1985, Paleogene stratigraphy, sedimentation and volcanism of New Mexico; *in* Flores, R. M. and Kaplan, S. S., eds., Cenozoic paleogeography of west-central United States: Denver, RMS-SEPM, p. 293-315.

Thompson, M. L., 1942, Pennsylvanian System in New Mexico: New Mexico Bureau of Mines and Mineral Resources, Bulletin 17, 92 p.

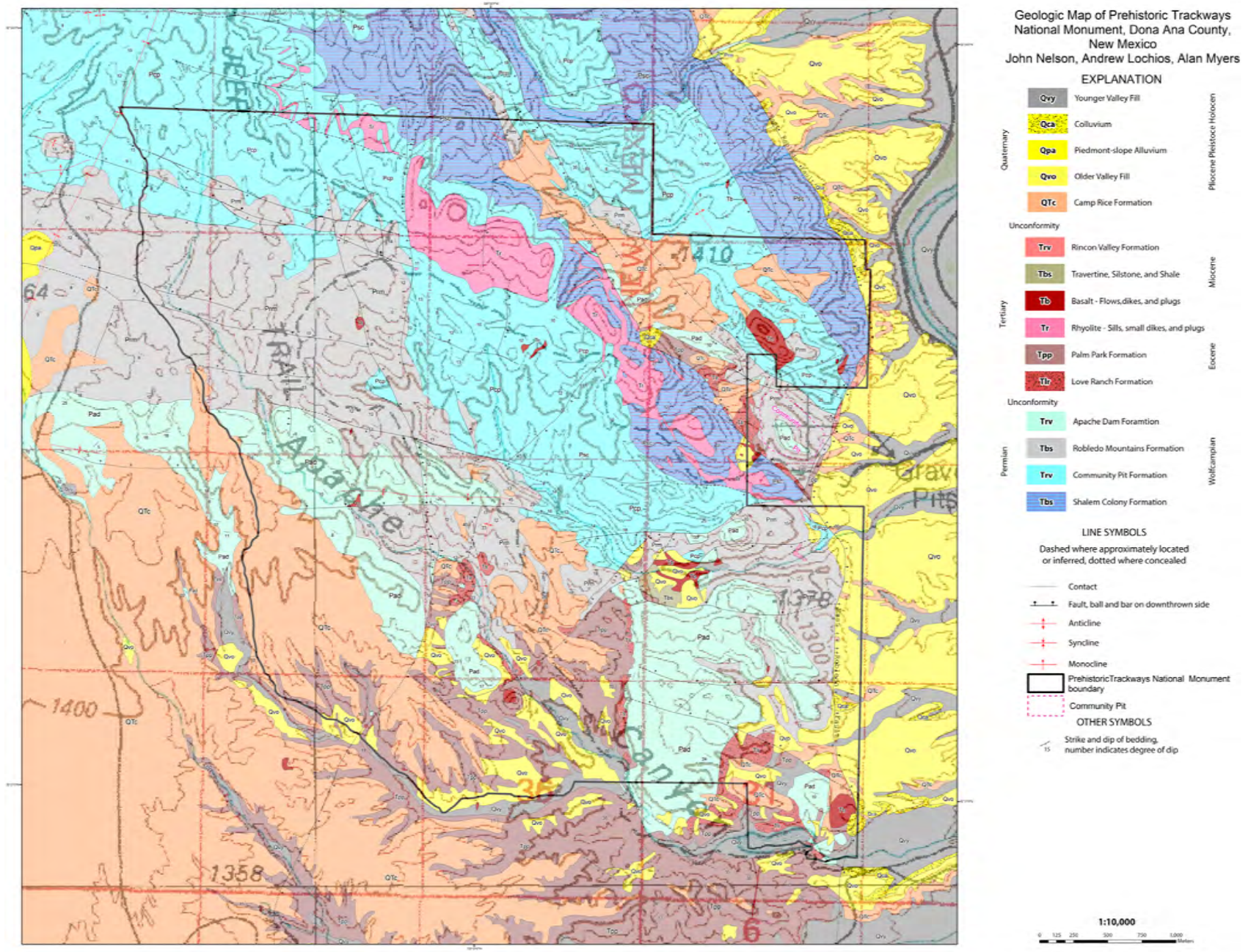
Thompson, M. L., 1954, American Wolfcampian fusulinids: University of Kansas, Paleontological Contributions, Protozoa, Article 5, 226 p.

Tidwell, W.D. and Munzing, G.E., 1995, Gymnopsermous woods from the Lower Permian Hueco Formation of south-central New Mexico: New Mexico Museum of Natural History and Science, Bulletin 6, p. 91-100.

Voigt, S., Lucas, S. G. and Krainer, K., 2013, Coastal-plain origin of trace-fossil bearing red beds in the Early Permian of southern New Mexico, U. S. A.: Palaeogeography, Palaeoclimatology, Palaeoecology, v. 369, p. 323-334.



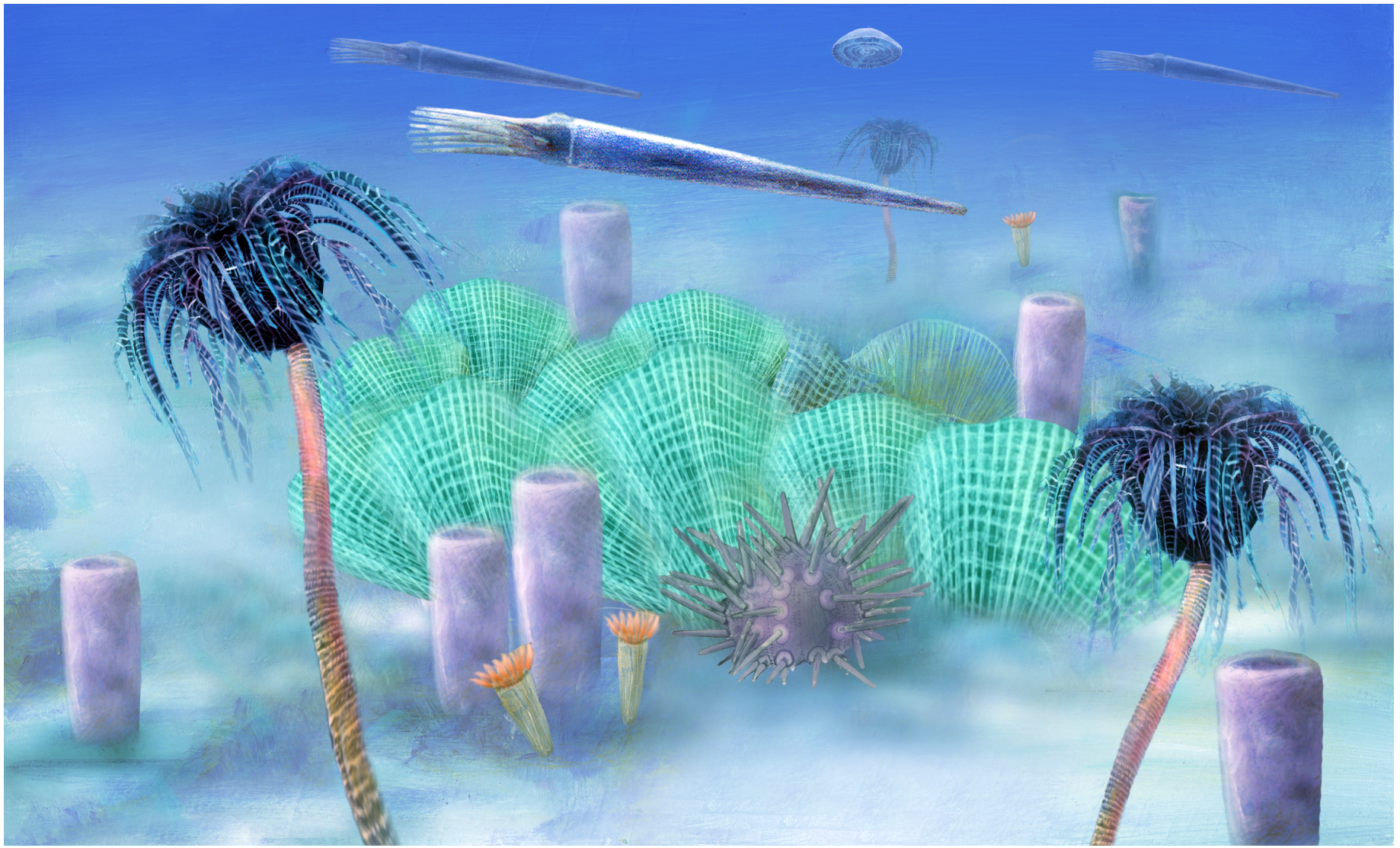
Outcrop of the trace-fossil-bearing Robledo Mountains Formation in “Branson Canyon” (SE ¼ NW ¼ sec. 30, T22S, R1W) in the Prehistoric Trackways National Monument. In the foreground, the yellow limestone beds in the canyon floor are the uppermost strata of the Community Pit Formation. The hill is capped with thick, gray limestone beds of the lower part of the Apache Dam Formation. Intervening strata are a complete, approximately 90-m-thick section of the Robledo Mountains Formation consisting of red-bed siltstones, sandstones and mudstones interbedded with gray/yellow shale and limestone.



Geologic map of the Prehistoric Trackways National Monument; this is a color version of the map in the article by Lucas, Krainer, Nelson and Elrick, this volume.



Bird’s-eye view of the Early Permian Hueco seacoast in the area of the Prehistoric Trackways National Monument, looking south. Montage by Mary Parrish using photographs by Candy Feller.



Nautiloids swim above a bryozoan and crinoid meadow on a Hueco seafloor in the area of the Prehistoric Trackways National Monument. Artwork by Mary Parrish.



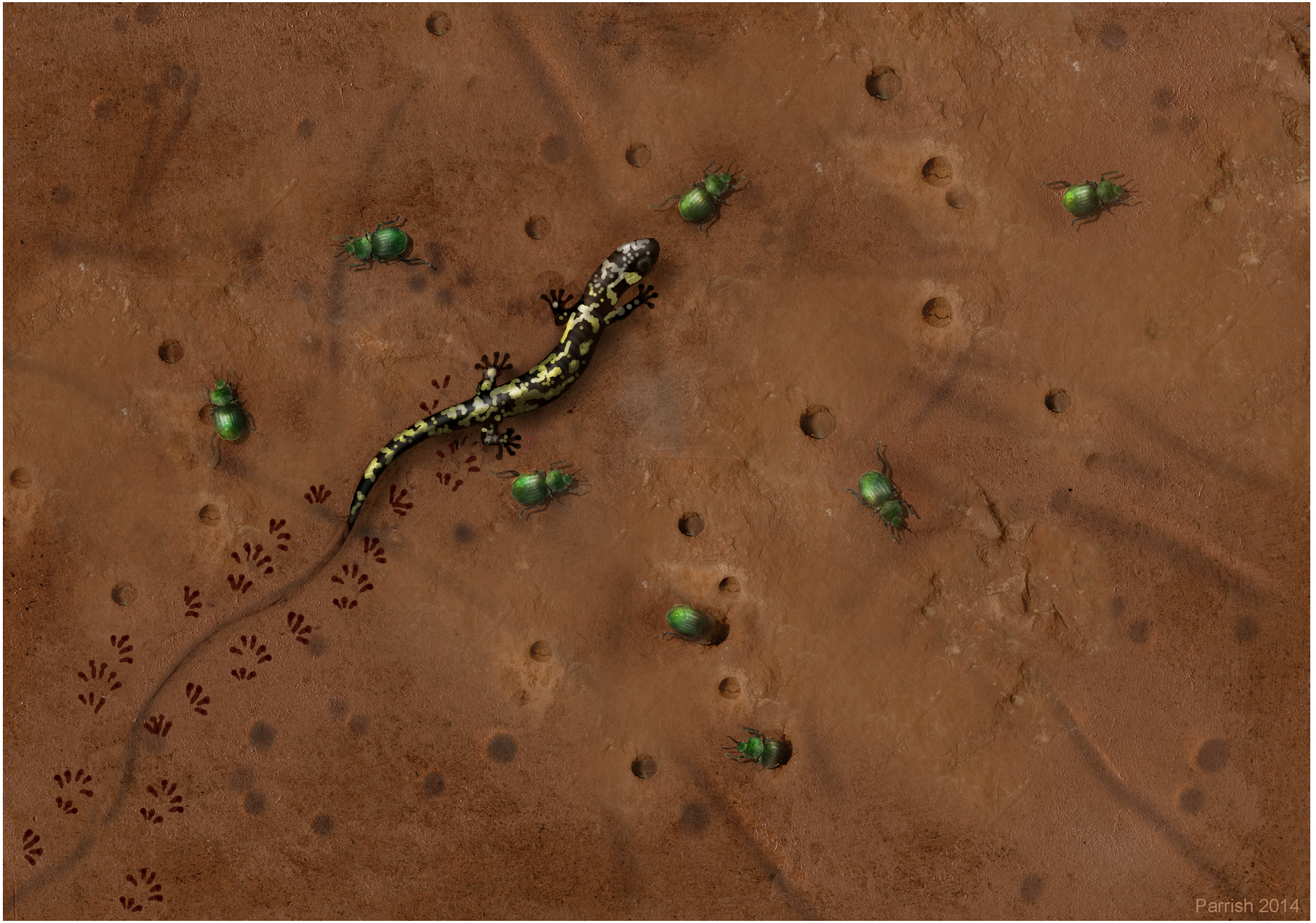
A shark swims among conifer logs and foliage that have been washed from land to the shallow, tropical Hueco seafloor in the area of the Flood locality of the Prehistoric Trackways National Monument. Artwork by Mary Parrish.



Dimetrodon, a large predatory pelycosaur, prowls a tidal flat along the Hueco seacoast, in the area of the Prehistoric Trackways National Monument. Artwork by Mary Parrish.



In the forest near the Hueco seacoast in the area of the Prehistoric Trackways National Monument, a large amphibian (*Eryops*) flushes smaller amphibians (*Diplocaulus*) out of the underbrush. Artwork by Mary Parrish.



A salamander-like temnospondyl amphibian chases a beetle on a sand flat near the Hueco seacoast in the area of the Prehistoric Trackways National Monument. Artwork by Mary Parrish.

Lucas, S. G. and DiMichele, W. A., eds., 2015, Carboniferous-Permian Transition in the Robledo Mountains, Southern New Mexico. New Mexico Museum of Natural History and Science Bulletin 65.

WALCHIAN CHARCOALIFIED WOOD FROM THE EARLY PERMIAN COMMUNITY PIT FORMATION IN PREHISTORIC TRACKWAYS NATIONAL MONUMENT, NEW MEXICO, U.S.A., AND ITS PALAEOECOLOGICAL IMPLICATIONS

HOWARD J. FALCON-LANG[1], FRANCINE KURZAWE[1] AND SPENCER G. LUCAS[2]

[1] Department of Earth Sciences, Royal Holloway, Egham, Surrey TW20 0EX, UK;
[2] New Mexico Museum of Natural History and Science, 1801 Mountain Rd. NW, Albuquerque, NM 87104, USA

Abstract—We describe the anatomy of large chunks of charcoalified wood, attributed to walchian conifers, found in the Lower Permian deposits of Prehistoric Trackways National Monument (PTNM), Robledo Mountains, New Mexico, U.S.A. The fossils are associated with a limestone conglomerate in the base of a fluvio-estuarine channel ~ 140 m wide and 5–6 m deep, incised into a shallow marine carbonate platform succession. When viewed with a Scanning Electron Microscope, charcoalified wood shows dominantly uniseriate, contiguous tracheid pits, cupressoid cross-field pits that are solitary or, if paired, show an opposite arrangement, and short uniseriate rays, 1–18 cells high. These anatomical characters match closely the wood of *Macdonaldodendron*, recently described from other sites in PTNM, which is demonstrably a walchian conifer based on aspects of its pith with sclerotic nests, endarch cauline bundles, triangular leaves, and whorled branch pattern. Therefore – while accepting that precise identification of isolated pieces of wood is fraught with difficulties – the overwhelming likelihood is that the new charcoalified material is, similarly, walchian. Its occurrence within an incised fluvio-estuarine channel suggests that fire-prone walchian trees grew at a time when sea-level was temporarily lowered and the shoreline of the Hueco Seaway had regressed southward, perhaps during glacial maximum. Paleosol data indicate that this coastline was subject to strongly seasonal rainfall; however, a remarkable feature of the charcoalified woods is that they completely lack growth rings. These facts can be reconciled if the walchian conifers were somehow buffered against seasonal drought, and the most likely explanatory hypothesis, consistent with taphonomic considerations, is that they were growing along wet riparian corridors, where elevated water tables provided a reliable year-round water supply. High fuel loads might be expected to have accumulated in these "wet spots" on an otherwise dry landscape, which would have been vulnerable to conflagration in the event of extreme droughts; this fire dynamic may explain the predominant preservation of fossil wood as charcoal.

INTRODUCTION

Compared to our knowledge of Pennsylvanian vegetation (DiMichele and Phillips, 1994; DiMichele and Falcon-Lang, 2011), the composition and ecology of Early Permian plant communities are less well understood (DiMichele et al., 2001a, 2010). In this paper, we focus our attention on Early Permian seasonal tropical plant communities that are preserved in the southwestern U.S.A. (especially New Mexico and Texas), on what was then the western coast of Euramerica (DiMichele et al., 2001a, b, 2007; Falcon-Lang et al., 2011a), which was subject to a seasonally dry tropical climate or, perhaps even, a semi-arid climate based on paleosol studies (Tabor and Montañez, 2004; Tabor, 2007; Tabor et al., 2008, 2013; Mack et al., 2013). Over the past two decades, many new fossil plant localities have been discovered in this area, revealing the existence of a low-diversity vegetation that was dominated, in local patches, by either walchian conifers, peltasperms (callipterids, comioids, supaioids), gigantopterids, tree ferns, or a combination of taxa (DiMichele et al., 2000, 2001a, 2004a,b, 2005a,b,c, 2006, 2008, 2013; DiMichele and Chaney, 2005; Chaney and DiMichele, 2007; Mamay et al., 2009; Chaney et al., 2009, 2012; Lucas et al., 2012; Voigt et al., 2013). These heterogeneous communities formed the vegetation of well-drained alluvial plains (e.g., DiMichele et al., 2007), or, locally, grew within coastal zones (e.g., DiMichele et al., 2000, 2001b). While such plant assemblages undoubtedly reflect taphonomic bias towards wetter sites where the growth and the preservation of plants were optimized (Gastaldo and Demko, 2010), they permit general insight into the vegetation structure of the region, provided facies context is critically analyzed (Falcon-Lang et al., 2009, 2011b). To further improve knowledge of the vegetation ecology of western tropical Euramerica, here we describe a new plant assemblage, comprising charcoalified wood, preserved in a particularly unusual facies context, within the Lower Permian strata of south-central New Mexico, U.S.A.

GEOLOGICAL CONTEXT

The fossil plant assemblages reported here occur in Lower Permian strata of Prehistoric Trackways National Monument (PTNM), Robledo Mountains, near Las Cruces, New Mexico (Fig. 1). The



FIGURE 1. County map of New Mexico highlighting the location of Prehistoric Trackways National Monument in Doña Ana County (gray), where the fossils were obtained (index map: location of New Mexico in the U.S.A.).

geological context is the same incised channel ~ 140 m wide and 5-6 m deep, described in detail in another paper in this volume, and found at NMMNHS locality 7981 (DiMichele et al., this volume). Consequently, we only briefly recap the main aspects of the geological context of this fossil site here.

The channel occurs in the middle part of the Community Pit Formation (Hueco Group), and bracketing fusulinid assemblages suggest an Early Permian (Sakmarian) age (Voigt et al., 2013; Falcon-Lang et al., 2014; Lucas et al., this volume). The channel is incised into a succession of shallow marine limestones, and the channel-fill contains three units. The lowermost unit comprises pebble-to-cobble limestone conglomerate with a matrix of medium- to coarse-grained carbonate and siliciclastic sandstone. The middle unit comprises carbonate mudstone showing undulatory or wavy lamination and scattered pterinopectinoids and linguloids, among other brackish fauna. The uppermost unit comprises an unfossiliferous dolomite, locally showing prominent calcite-filled vugs and nodular gypsum.

The plant assemblage that forms the focus of this paper consists of large (20-50 mm) chunks of charcoalified wood, with rounded corners, within the basal conglomerate. This conglomerate includes subangular pebbles and cobbles of marine limestone that were clearly indurated at the time of denudation and transport. Consequently, we interpret this feature as a fluvial channel incised during a lowering of sea-level and subsequent sub-aerial exposure of the marine shelf, rather than representing a submarine channel. Middle and upper units are interpreted as representing the subsequent flooding of the channel to form a coastal estuary, which later gradually silted up. The charcoalified fossil wood in the lowermost part of the channel-fill accumulated at, or shortly after, sea-level lowstand. If sea-level drawdown was caused by glacioeustasy, then the plant assemblage probably represents a record of vegetation that was growing around glacial maximum. A glacioeustatic origin for the channel is plausible because this part of the Early Permian (middle Asselian-early Artinskian) comprised the last major episode in the Late Paleozoic Ice Age (Fielding et al., 2008; Montañez and Poulsen, 2013).

CHARCOALIFIED WALCHIAN CONIFER WOOD

Material and Methods

Four charcoal specimens (20-50 mm) accessioned in the collections of the New Mexico Museum of Natural History and Science (NMMNH P-68181-P-68184) were studied. All four specimens comprise pycnoxylic wood, and mostly show a somewhat wedge-shaped cross-section. In preparation for observation and imaging, specimens were treated with 10% HCl (1 day) and 35% HF (7 days) to remove carbonate and siliciclastic material, respectively, fixed to aluminum stubs using Electrodag 550 (a nickel acrylic colloid), and coated in 150 Å of gold palladium using an ISI Sputter coater. Material was then observed at 15 kv with a Hitachi S-3500N Scanning Electron Microscope, with each specimen being imaged on transverse, radial, longitudinal, and tangential longitudinal surfaces (TS, RLS, and TLS, respectively). Several wood anatomical characters (i.e., number of rows of pits per tracheid, the number of pits per cross-field, ray height in number of cells, and radial/tangential tracheid diameter) were quantified based on a population of 25 measurements (cf. Falcon-Lang and Cantrill, 2000).

Description of Wood Anatomy

Viewed on RLS, tracheids show uniseriate, or more rarely biseriate, alternate bordered pitting (means of 1.1 to 1.3 rows of pits per tracheid; Fig. 2.1-2.3). Bordered pits are circular, ~ 6-9 µm in diameter, show circular apertures (~ 3-4 µm in diameter), and have a contiguous arrangement. Cross-field pits are cupressoid and 5-7 µm in diameter, with dominantly 1, or rarely 2-4 pits per field (means of 1.1 to 1.7 pits per cross-field), arranged side-by-side where multiple pits are present (Fig. 2.4). Viewed on TLS, rays are almost exclusively uniseriate (a few rays have short biseriate portions) and 1-18 cells high (means of 2.2 to 4.1 cells high; although these data are likely an underestimate due to poor preservation of taller rays; Fig. 2.7). Rays are commonly preserved in a tangentially expanded (ruptured) state (Fig. 2.6). Viewed on TS, tracheids are 18-25 µm in radial diameter, 16-24 µm in tangential diameter, and the middle lamella of adjacent tracheids is always homogenized (Fig. 2.4). In TS, tracheids show a distinctly rounded outline, and locally show spiral thickening. Growth rings are absent over observed radii of > 4 mm (Fig. 2.5).

Comparison with *Macdonaldodendron*

The charcoalified wood anatomy conforms to the Type II Paleozoic wood of Doubinger and Marguerier (1975), which is generally regarded as coniferous rather than cordaitalean. The charcoalified material is particularly closely similar, if not identical, to the wood of *Macdonaldodendron* described from the upper part of the Community Pit Formation (Falcon-Lang et al., 2014). This genus is interpreted as a walchian conifer based on aspects of its large pith with prominent sclerotic nests (Fig. 3.1), endarch cauline bundles (Fig. 3.2), triangular leaves (Fig. 3.3) and whorled branches (Fig. 3.4; Falcon-Lang et al., 2014). The close match between the charcoalified wood anatomy reported here and that of *Macdonaldodendron* includes dominantly uniseriate, contiguous tracheid pits (Fig. 3.5), cuppressoid cross-field pits that are mostly solitary, or if paired, show an opposite arrangement (Fig. 3.6), short uniseriate rays (Fig. 3.7) and a general absence of growth rings (Fig. 3.8). The charcoal is also similar to other Permian woods of suspected (Reymanowna, 1962; Tidwell and Munzing, 1995) or confirmed (Lemoigne and Tyroff, 1967) walchian affinity.

The wedge-shaped cross-sectional morphology of most of the charcoal fragments indicates that they derived from small-diameter axes rather than from trunk wood. Distinguishing between juvenile upright leader-axes and lateral branch axes is challenging and based on the recognition of reaction (compression) wood that develops when secondary xylem forms perpendicular to gravity (Chapman, 1994). A key feature of reaction (compression) wood is tracheids that have a distinctly rounded cross-section and spiral thickening; as such, the material discussed here is most likely to be branch wood.

Preservation as Charcoal

The observation of homogenized cell wall lamellae (Fig. 2.4) is the key feature that confirms that this material is fossil charcoal (fusain), the product of wildfire (Jones and Chaloner, 1991). Also consistent with a charcoalified preservational state is that the material shows reduced anatomical dimensions (e.g., tracheid diameter) when compared to most other permineralized walchian fossil wood specimens (Tidwell and Munzing, 1995) because wood undergoes significant contraction during the charring process (McGinnes et al., 1971). For example, in *Macdonaldodendron* tracheids are typically 43-47 µm in radial diameter, whereas in the charcoalified material, they are only 18-25 µm in diameter (Fig. 2.5). However, these reduced diameters could also reflect ontogeny because juvenile wood, as inferred for the charcoalified material, typically comprises tracheids of relatively small diameter.

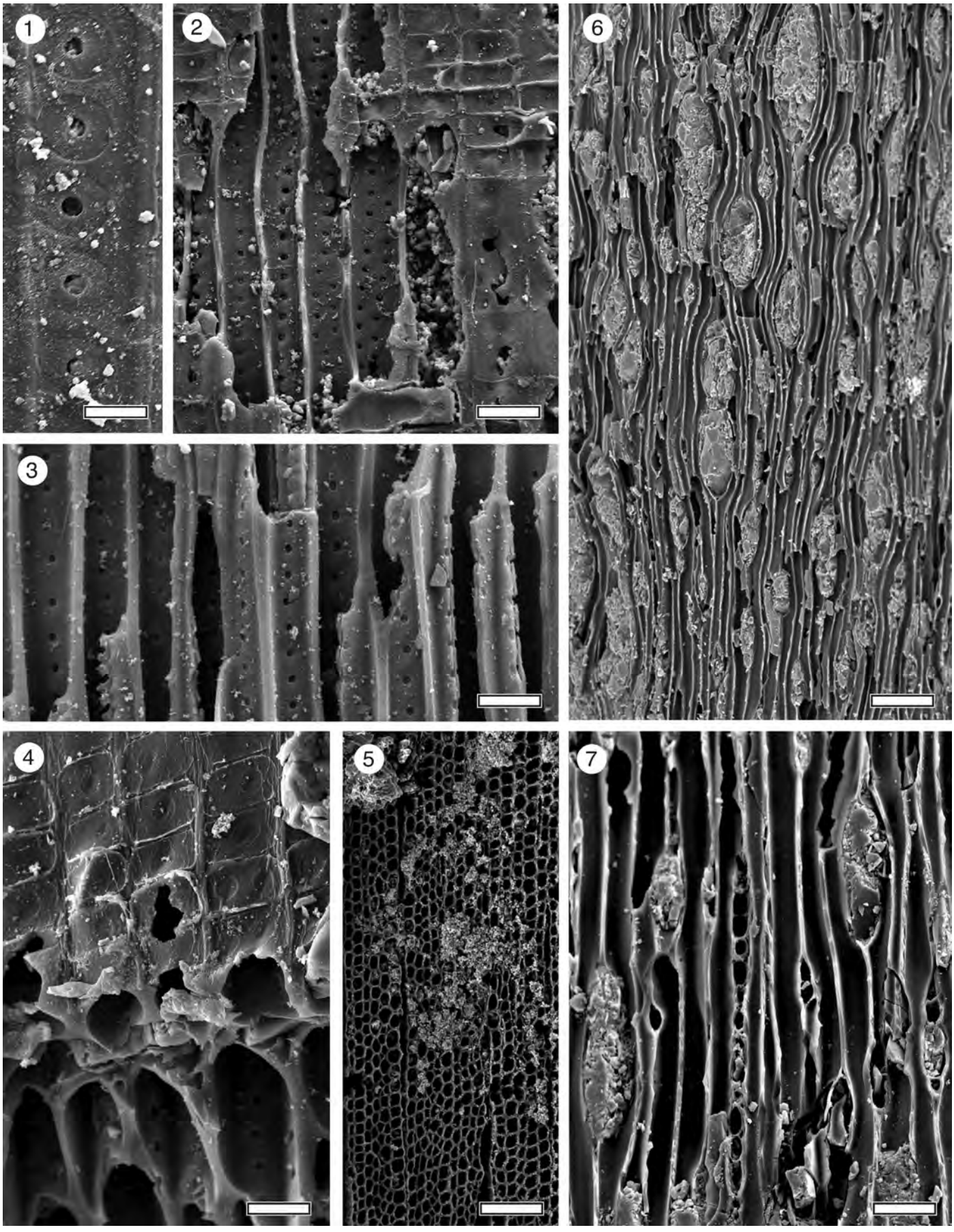
WALCHIAN PALEOECOLOGY

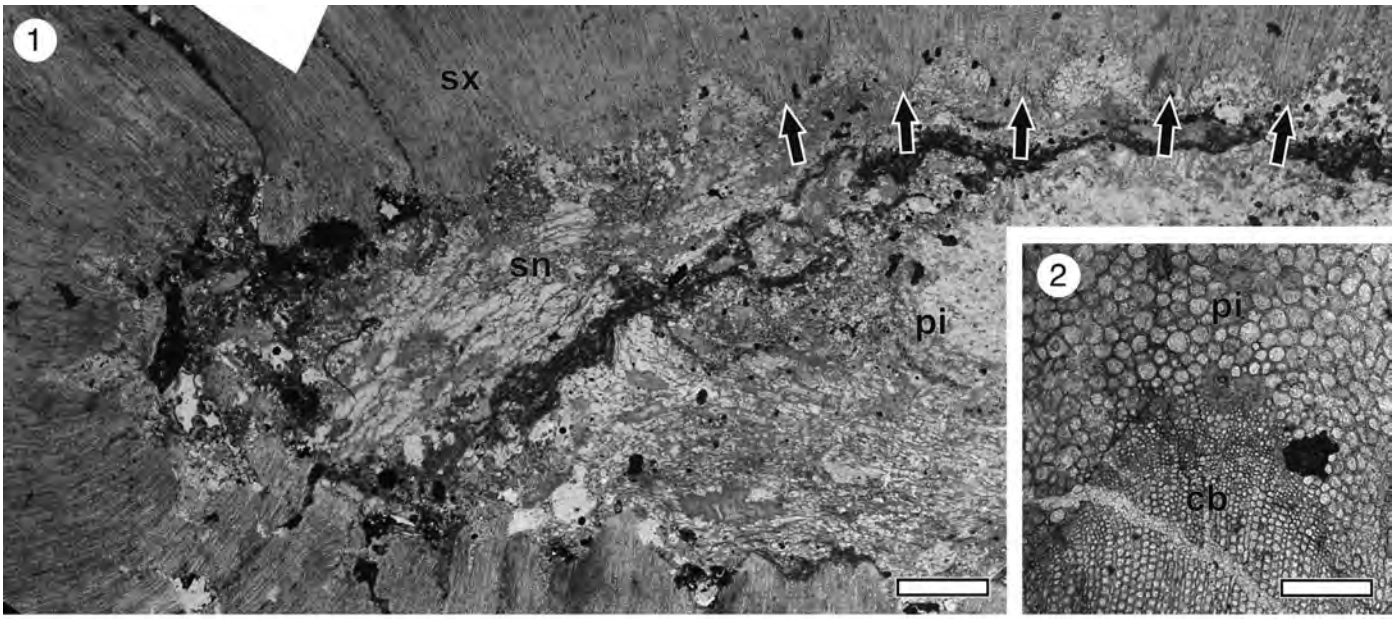
What does this charcoalified assemblage tell us about the Permian paleoecology of the seasonally dry regions of western tropical Euramerica, and about walchian communities in particular? In this discussion, we make the assumption that the walchian charcoal fragments are identical to the more complete tree-trunk specimens described as *Macdonaldendron* that dominate at other sites and stratigraphic intervals in the Community Pit Formation. This assumption is very likely, but obviously cannot be proven. Trunks referred to *Macdonaldendron* attain a diameter of 0.28 m or, possibly, up to 0.91 m, and these walchian conifers were relatively large, long-lived, evergreen trees with a monopodial trunk (Falcon-Lang et al., 2014).

Inferred Riparian Habitat

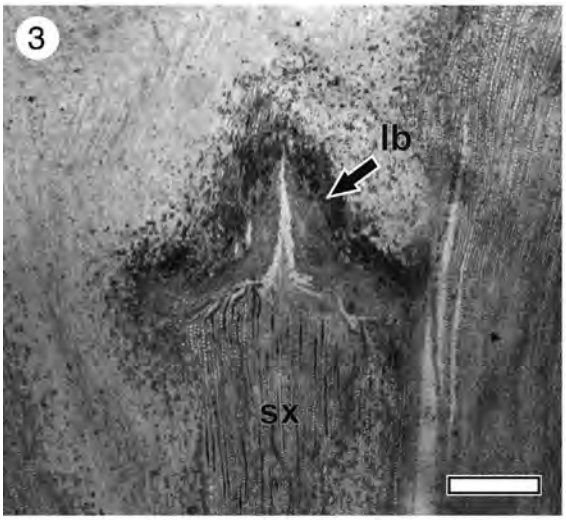
The facies context of the walchian charcoal indicates that plant remains were transported from their original site of growth and deposited downstream within a fluvio-estuarine channel. However, assessing the degree of transport, and constraining the original site of growth is not straightforward. Charcoal can be repeatedly reworked in fluvial channels for thousands of years, and transported hundreds of kilometers, prior to final burial (Blong and Gillespie, 1978). However, such highly allochthonous remains are typically small (sub millimeter-

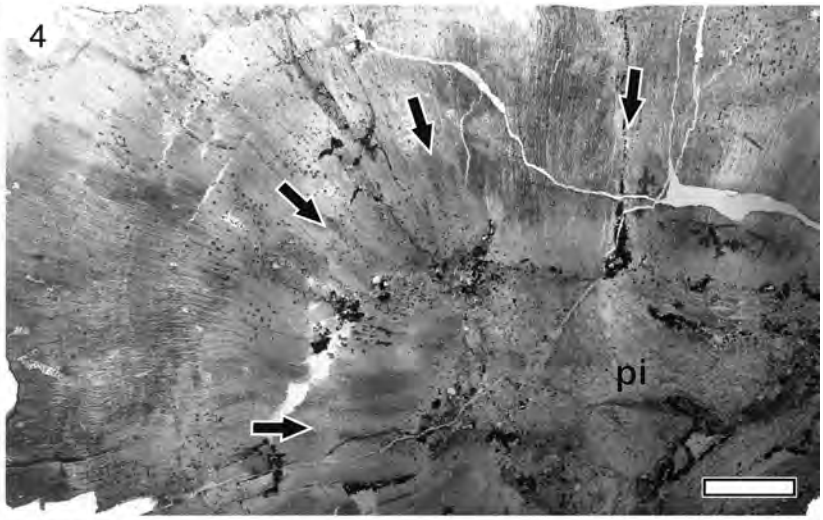
FIGURE 2 (facing page). Charcoalified walchian conifer wood from the Community Pit Formation, viewed with a Scanning Electron Microscope, all NMMNH P-68181; **2.1**, Uniseriate bordered tracheid pits, scale: 20 µm; **2.2**, Rare occurrence of 1–2-seriate bordered tracheid pits, scale: 30 µm; **2.3**, Uniseriate bordered tracheid pits, scale: 25 µm; **2.4**, Cupressoid cross-field pits, 1 – 2, opposite, scale: 15 µm; **2.5**, Growth rings absent, scale: 150 µm; **2.6**, exploded rays, scale: 150 µm, specimen; **2.7**, uniseriate rays up to 18 cells high, scale: 75 µm.

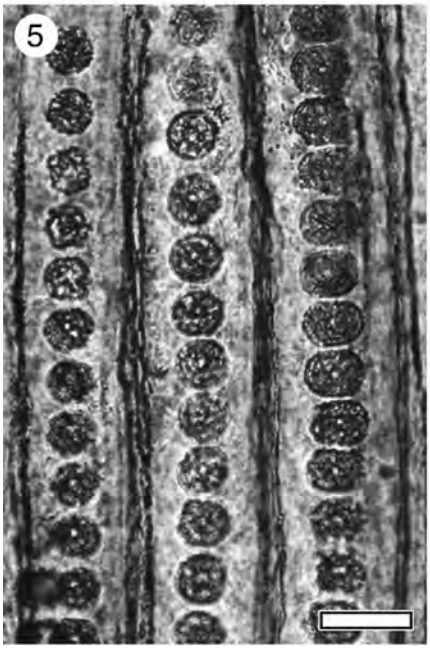

1
2
3
4
5
6
7

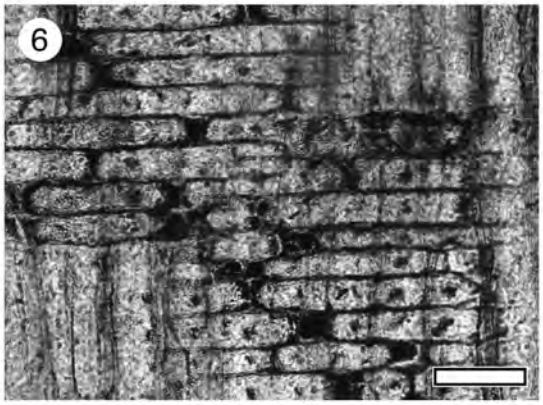

1
sx
sn
pi

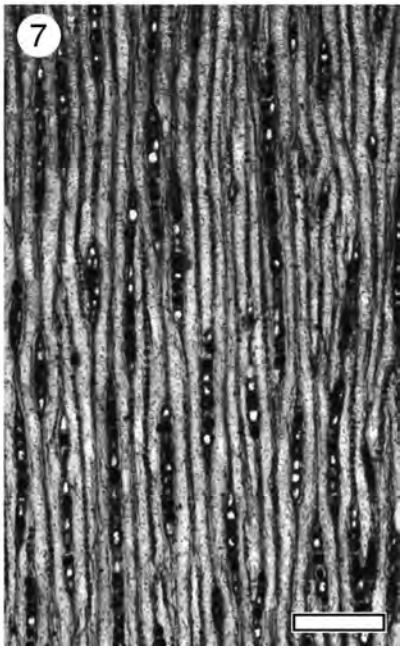
2
pi
cb

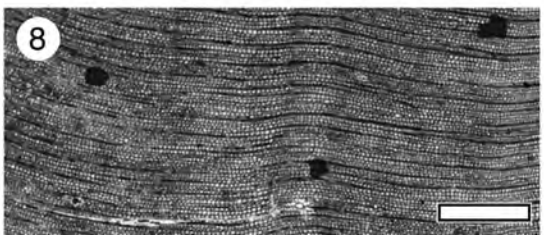

3
lb
sx


4
pi


5


6


7


8

size) because charcoalified wood has a strong fabric and easily splinters during bedload transport (Nichols et al., 2000). In contrast, the exceptionally large chunks of charcoal (20-50 mm diameter) reported here, with rounded corners, indicate saltative bedload transport (Gee et al., 2005) of limited distance.

Furthermore, plant taphocoenoses in fluvio-estuarine channels are generally of riparian origin, with trees stripped from the channel levees upstream (Scheihing and Pferfferkorn, 1984), and we note that walchian megafloral remains most commonly occur in Early Permian fluvial facies in the southwestern U.S.A. (DiMichele et al., 2007). Synthesizing these taphonomic data, the likelihood is that the charcoalified wood assemblage originated from riparian vegetation developed on coastal plains, just a few kilometers to the north of the study site, in a region bordering the Hueco seaway. It is far less likely that the material was transported long-distance from environments outside this regional context.

Inferred Edaphic Conditions

The climate of the coastal plains that bordered the Hueco Seaway is believed to have exhibited a strong rainfall seasonality, and at times, may have been semi-arid, based on regional studies of paleosols (Mack, 2003; Tabor, 2007; Tabor et al., 2008). However, as noted above, short radii of wood (20-50 mm) in multiple specimens of walchian charcoal do not show growth rings; we note either a similar lack of growth rings, or the presence of irregular growth interruptions only, in specimens of even larger radii (c. 100 mm) preserved in *Macdonalodendron* silicified tree-trunks higher in the succession (Falcon-Lang et al., 2014). This observation is unexpected because under seasonal tropical climates today, conifers almost always produce growth rings (Falcon-Lang, 2003), although such rings may not be strictly annual in distribution but reflect the vagaries of drought occurrence (Rozendaal and Zuidema, 2011).

This unusual growth phenomenon observed in the walchian conifers is probably not an indication that primitive conifers of this age were "incapable" of making growth rings (as has been argued by Brison et al., 2001) because other conifer taxa in the same assemblage show marked growth rings (Falcon-Lang et al., 2014). Furthermore, although some extant evergreen conifers with high leaf retention times (i.e., having a similar phenology to that envisaged for *Macdonalodendron*) are known to produce relatively subdued rings under seasonal climates (Falcon-Lang, 2000), the lack of growth rings observed in this study is still remarkable when compared to growth patterns in extant araucarians in the seasonal tropics (e.g., Ash, 1983).

Therefore, excluding these intrinsic influences, the absence of growth rings probably suggests that walchian trees were growing in an area where they were somehow buffered against the prevailing seasonally dry climate. Today we see such climate buffering in two settings: (1) in coastal settings prone to fog, where trees harvest moisture from the atmosphere; and (2) in riparian zones, where trees obtain moisture from the locally elevated water table. Both these settings can provide a year-round source of water even during times of drought, and trees in such areas may not produce rings (Jacoby, 1989; Cherubini et al., 1993; Gibling et al., 1998). Given the taphonomic inferences cited above, we favor the latter riparian hypothesis.

Fossil trees that occur in geological contexts suggestive of seasonal aridity, but lacking growth rings, have been reported with surprising frequency in the fossil record (Ash and Creber, 1992; Falcon-Lang, 2003; Parrish and Falcon-Lang, 2007), and they are mostly associated with fluvial deposits (Demko et al., 1998; Falcon-Lang et al., 2011b). This frequency probably reflects a taphonomic bias towards wetland settings, with the preservation potential of genuinely water-stressed vegetation, which may have colonized dry interfluve areas, being low (Gastaldo and Demko, 2010). Therefore, walchian charcoal material described here probably also represents a record of Early Permian vegetation biased towards the plants growing on the wettest spots of the landscape.

FIGURE 3 (facing page). *Macdonaldodendron* from the Community Pit Formation (after Falcon-Lang et al., 2014); **3.1**, Cross-section of axis showing sclerotic nests (sn) in the pith (pi) and secondary xylem (sx) cylinder; arrows show spacing of cauline bundles, NMMNH 539411a, TS, scale: 1 mm; **3.2**, Close-up of an endarch cauline bundle (cb) and parenchyma cells in pith (pi), NMMNH 539420, TS, scale: 300 µm; **3.3,** Close-up showing triangular leaf base (lb) embedded in the secondary xylem (sx), close to the pith edge (pi), NMMNH 539416, TS, scale: 750 µm; **3.4,** General cross-section of axis showing pith (pi) and whorl of departing branchlet traces (arrows mark the point at which traces leave the plane of section), NMMNH 539411b, TS, scale: 4 mm; **3.5**, Circular to slightly flattened tracheid pits, NMMNH 539411a, RLS, scale: 30 µm; **3.6**, Mainly solitary cupressoid cross-field pits, NMMNH 539411a, RLS, scale: 50 µm; **3.7**, Uniseriate rays with short biseriate portions, filled with resin, NMMNH 539411a, TLS, scale: 150 µm; **3.8**, Absence of clearly developed growth rings, NMMNH 539411a, TS, scale: 1 mm.

Inferred Fire Ecology

Despite this apparent access to a reliable year-round water supply, the dominant preservation of walchians as charcoal indicates that wildfires were an important ecosystem process (Jones and Chaloner, 1991). Although somewhat counter-intuitive, riparian vegetation is particularly prone to wildfire because the local availability of water allows the buildup of rather more substantial accumulations of fuel than would normally occur on a seasonally dry landscape (Pettit and Naiman, 2007). Such accumulations then become vulnerable to conflagration when sustained drought strikes. Of course, during the Early Permian, elevated levels of atmospheric oxygen may have accentuated the frequency and intensity of wildfires as well (Glasspool and Scott, 2010).

Walchians were, probably, one of the most fire-prone trees of the Late Paleozoic tropics because the leaves, twigs and wood of such conifers dominate charcoal assemblages of this age at many sites (Lyons and Darrah, 1989; Cunningham et al., 1993; Calder et al., 1999; Scott et al., 2010; Falcon-Lang et al., 2014). Kerp et al. (1990) suggested that some walchian conifers may have aperiodically abscised their ultimate branchlets, and Looy (2013) further hypothesized that abscission of entire lower branch systems may have acted as a fire-adaption, by creating a fuel-gap between the litter layer and canopy biomass. This kind of "self-pruning" in seen in extant *Araucaria araucana* and is probably similarly a fire adaptation (Falaschi et al., 2011).

However, the charcoalified wood fragments reported here likely originated from small diameter branches, and two pieces of information suggest that fires involved living canopy biomass rather than litter deadwood. Both the absence of "checking" structures (Jones, 1993), and the presence of large, radially oriented ruptures along rays in tangential section formed by expulsion of steam from moisture-rich parenchyma (Scott et al., 2010) indicate green sapwood was burned. These observations indicate that either this particular species of walchian conifer did not employ a fire-gap strategy or that existence of a fire-gap was not always sufficient to protect the canopy from conflagration.

ACKNOWLEDGMENTS

We thank the staff of the Bureau of Land Management (BLM Las Cruces District Office and Patricia Hester, BLM Regional Paleontologist) for permitting access to Prehistoric Trackways National Monument, and for generous financial support of this project. HFL gratefully acknowledges a NERC Advanced Fellowship (NE/F014120/2) held at Royal Holloway, University of London. FK gratefully acknowledges a Conselho Nacional de Desenvolvimento Científico e Tecnológico (CNPq, Brazil) Postdoctoral Fellowship (202078/2011-6). Jerry MacDonald originally discovered the locality described here. We also acknowledge helpful reviews by John Nelson and an anonymous reviewer.

REFERENCES

Ash, J., 1983, Growth rings in *Agathis robusta* and *Araucaria cunninghami* from tropical Australia: Australian Journal of Botany, v. 31, p. 269–275.

Ash, S.R., and Creber, G.T., 1992, Palaeoclimatic interpretation of the wood structures of the trees in the Chinle Formation (Upper Triassic), Petrified Forest National Park, Arizona, USA.: Palaeogeography, Palaeoclimatology, Palaeoecology, v. 96, p. 299–317.

Blong, R.J., and Gillespie, R., 1978, Fluvial transported charcoal gives erroneous ^{14}C ages for recent deposits: Nature, v. 271, p. 739–741.

Brison, A.L., Philippe, M., and Thevenard, F., 2001, Are Mesozoic wood growth rings climate-induced?: Paleobiology, v. 27, p. 531–538.

Chaney, S., and DiMichele, W.A., 2007, Paleobotany of the classic redbeds (Clear Fork Group - Early Permian) of north central Texas: Proceedings of the XVth International Congress on Carboniferous and Permian Stratigraphy, v. 1, p. 357–366.

Chaney, D.S., Mamay, S.H., DiMichele, W.A., and Kerp, H., 2009, *Auritifolia* gen. nov., probable seed plant foliage with comioid affinities from the Early Permian of Texas, U.S.A.: International Journal of Plant Sciences, v. 170, p. 247–266.

Chaney, D.S., DiMichele, W.A., Lucas, S.G., Voigt, S., and Looy, C.V., 2012, Floras from the Prehistoric Trackways National Monument, Pennsylvanian-Permian boundary, southern New Mexico: Geological Society of America, Abstracts with Programs, v. 44, p. 90.

Cherubini, P., Gartner, B.L., Tognetti, R., Braker, O.U., Schoch, W., Innes, J.L., 2003, Identification, measurement and interpretation of tree-rings in woody species from Mediterranean climates: Biological Reviews, v. 78, p. 119–148.

Demko, T.M., Dubiel, R.F., and Parrish, J.T., 1998, Plant taphonomy in incised valleys: Implications for interpreting paleoclimate from fossil plants: Geology, v. 26, p. 1119–1122.

DiMichele, W.A., and Chaney, D.S., 2005, Pennsylvanian-Permian fossil floras from the Cutler Group, Cañon del Cobre and Arroyo del Agua areas, in northern New Mexico: New Mexico Museum of Natural History and Science, Bulletin 31, p. 27–33.

DiMichele, W.A., and Falcon-Lang, H.J., 2011, Fossil forests in growth position (T^0 assemblages): Origin, taphonomic biases and palaeoecological significance: Journal of the Geological Society, v. 168, p. 585–605.

DiMichele, W.A., and Phillips, T.L., 1994, Paleobotanical and paleoecological constraints on models of peat formation in the Late Carboniferous of Euramerica: Palaeogeography, Palaeoclimatology, Palaeoecology, v. 106, p. 39–90.

DiMichele, W.A., Cecil, C.B., Montañez, I.P., and Falcon-Lang, H.J., 2010, Cyclic changes in Pennsylvanian paleoclimate and effects on floristic dynamics in tropical Pangaea: International Journal of Coal Geology, v. 83, p. 329–344.

DiMichele, W.A., Chaney, D.S., Dixon, W.H., Nelson, W.J., and Hook, R.W., 2000, An Early Permian coastal flora from the Central Basin Platform of Gaines County, West Texas: Palaios, v. 15, p. 524–534.

DiMichele, W.A., Chaney, D.S., Falcon-Lang, H.J., Kerp, H., Looy, C., Lucas, S.G., Krainer, K., Voigt, V., this volume, A compositionally unique voltzian-callipterid flora from a carbonate-filled channel, Lower Permian, Robledo Mountains, New Mexico, and its broader significance: New Mexico Museum of Natural History and Science Bulletin, this volume.

DiMichele, W.A., Chaney, D.S., Nelson, W.J., Lucas, S.G., Looy, C.V., Quick, K., and Jun, W., 2007, A low diversity, seasonal tropical landscape dominated by conifers and peltasperms: Early Permian Abo Formation, New Mexico: Review of Palaeobotany and Palynology, v. 145, p. 249–273.

DiMichele, W.A., Chaney, D. S., Lucas, S. G., Kerp, H., and Voigt, S., 2013, Flora of the Lower Permian Abo Formation redbeds, western equatorial Pangea, New Mexico: New Mexico Museum of Natural History and Science, Bulletin 59, p. 265–288.

DiMichele, W.A., Hook, R.W., Nelson, W.J., and Chaney, D.S., 2004a, An unusual Middle Permian flora from the Blaine Formation (Pease River Group: Leonardian–Guadalupian Series) of King County, West Texas: Journal of Paleontology, v. 78, p. 765–782.

DiMichele, W.A., Kerp, H., and Chaney, D.S., 2004b, Tropical floras of the Late Pennsylvanian-Early Permian transition: Carrizo Arroyo in context: New Mexico Museum of Natural History and Science, Bulletin 25, p. 105–110.

DiMichele, W.A., Kerp, H., Krings, M., and Chaney, D.S., 2005c, The Permian peltasperm radiation: Evidence from the southwestern United States: New Mexico Museum of Natural History and Science, Bulletin 30, p. 67–79.

DiMichele, W.A., Kerp, H., Tabor, N.J., and Looy, C.V., 2008. The so-called "Paleophytic-Mesophytic" transition in equatorial Pangea – Multiple biomes and vegetational tracking of climate change through geological time: Palaeoecology, Palaeclimatology, Palaeogeography, v. 268, p. 152–163.

DiMichele, W.A., Mamay, S.H., Chaney, D.S., Hook, R.W., and Nelson, W.J., 2001b, An Early Permian flora with Late Permian and Mesozoic affinities from north-central Texas: Journal of Paleontology, v. 75, p. 449–460.

DiMichele, W.A., Pfefferkorn, H.W., and Gastaldo, R.A., 2001a, Response of Late Carboniferous and Early Permian plant communities to climate change: Annual Review of Earth and Planetary Sciences, v. 29, p. 461–487.

DiMichele, W.A., Tabor, N.J., and Chaney, D.S., 2005a, Outcrop-scale environmental heterogeneity and vegetational complexity in the Permo-Carboniferous Markley Formation of north-central Texas: New Mexico Museum of Natural History and Science, Bulletin 30, p. 60–66.

DiMichele, W.A., Van Konijnenburg-Van Cittert, H.A., Looy, C.V., and Chaney, D.S., 2005b, *Equisetites* from the Early Permian of north-central Texas: New Mexico Museum of Natural History and Science, Bulletin 30, p. 56–59.

DiMichele, W.A., Tabor, N.J., Chaney, D.S., and Nelson, W.J., 2006, From wetlands to wet spots: Environmental tracking and the fate of Carboniferous elements in Early Permian tropical floras: Geological Society of America, Special Paper 399, p. 223–248.

Doubinger, J., and Marguerier, J., 1975. Paléoxylogie: étude anatomique comparée de *Scleromedulloxylon aveyronense* n. gen. et sp., du Permien de St. Affrique (Aveyron, France): Considérations taxinomiques et stratigraphiques: Geobios, v. 8, p. 25–59.

Falaschi, P., Grosfield, J., Zamuner, A.B., Foix, N., Rivera, S.M., 2011, Growth architecture and silhouette of Jurassic conifers from La Matilde Formation, Patagonia, Argentina: Palaeogeography, Palaeoclimatology, Palaeoecology, v. 302, p. 122–141.

Falcon-Lang, H.J., 2000, The relationship between leaf longevity and growth ring markedness in modern conifer woods and its implications for palaeoclimatic studies: Palaeogeography, Palaeoclimatology, Palaeoecology, v. 160, p. 317–328.

Falcon-Lang, H.J., 2003, Growth interruptions in conifer woods from the Upper Cretaceous (Late Campanian) Two Medicine Formation, Montana, U.S.A.: implications for paleoclimate and dinosaur ecology: Palaeogeography, Palaeoclimatology, Palaeoecology, v. 199, p. 299–314.

Falcon-Lang, H.J., and Cantrill, D.J., 2000, Cretaceous (Late Albian) Coniferales of Alexander Island, Antarctica. Part 1: Wood taxonomy, a quantitative approach: Review of Palaeobotany and Palynology, v. 111, p. 1–17.

Falcon-Lang, H.J., Nelson, W.J., Elrick, S., Looy, C.V., Ames, P.R., and DiMichele, W.A., 2009, Incised channel fills containing conifers indicate that seasonally dry vegetation dominated Pennsylvanian tropical lowlands: Geology, v. 37, p. 923–926.

Falcon-Lang, H.J., Jud, N.A., Nelson, W.J., DiMichele, W.A., Chaney, D.S., and Lucas, S.G., 2011a, Pennsylvanian coniferopsid forests in sabkha facies reveal the nature of seasonal tropical biome: Geology, v. 39, p. 371–374.

Falcon-Lang, H.J., Pendleton, J.L., and Wellman, C.H., 2011b. Dryland plant communities in the Pennsylvanian (mid- to late Bolsovian) Winterbourne Formation of Bristol, southern Britain: Further evidence for taphonomic megabias: Review of Palaeobotany and Palynology, v. 166, p. 268–285.

Falcon-Lang, H.J., Kurzawe, F., and Lucas, S.G., 2014, Coniferopsid tree-trunks preserved in sabkha facies in the Permian (Sakmarian) Community Pit Formation in south-central New Mexico, U.S.A.: Systematics and palaeoecology: Review of Palaeobotany and Palynology, v. 200, p. 138–160.

Fielding, C.R., Frank T.D., and Isbell, J.L., 2008, The Late Paleozoic Ice Age – A review of current understanding and synthesis of global climate patterns: Geological Society of America, Special Publication 441, p. 343–354.

Gastaldo, R.A., and Demko, T.M., 2010, Long-term hydrology controls the plant fossil record; in Allison, P.A., and Bottjer, D.J, eds., Taphonomy: Processes and bias through time. Topics in Geobiology, v. 32, p. 249–286.

Gee, C.T., 2005, The genesis of mass carpological deposits (bedload carpodeposits) in the Tertiary of the Lower Rhine Basin, Germany: Palaios, v. 20, p. 464–479.

Gibling, M.R., Nanson, G.C., and Maroulis, J.C., 1998, Anastomosing river sedimentation in the Channel Country of central Australia: Sedimentology, v. 45, p. 595–619.

Glasspool, I.J., and Scott, A.C., 2010, Phanerozoic concentrations of atmospheric oxygen reconstructed from sedimentary charcoal: Nature Geoscience, *v.* 3, p. 627–630.

Jacoby, G.C., 1989, Overview of tree-ring analysis in tropical regions: International Association of Wood Anatomists Bulletin, v.10, p. 99–108.

Jones, T.P., 1993, New morphological and chemical evidence for a wildfire origin for fusain from comparisons with modern charcoal: Special Papers in Palaeontology, v. 49, p. 113–123.

Jones, T.P., and Chaloner, W.G., 1991, Fossil charcoal, its recognition and palaeoatmospheric significance: Palaeogeography, Palaeoclimatology, Palaeoecology, v. 97, p. 39–50.

Kerp, J.H.F., Poort, R.J., Swinkels, H.A.J.M., and Verwer, R., 1990, Aspects of Permian palaeobotany and palynology. IX. Conifer-dominated Rotliegend floras from the Saar-Nahe Basin (?Late Carboniferous-Early Permian; SW-Germany) with special reference to the reproductive biology of early conifers: Review of Palaeobotany and Palynology, v. 62, p. 205–248.

Lemoigne, Y., and Tyroff, H., 1967, Caractères anatomiques d'un fragment de bois appartenant à l'espèce *Walchia piniformis*: Comptes Rendus hebdomadaires des séances de l'Académie de Sciences, Paris, v. 265, p. 595–597.

Looy, C.V., 2013, Natural history of a plant trait: Branch system abscission in Paleozoic conifers and its environmental, autecological and ecosystem implications in a fire-prone world: Paleobiology, v. 39, p. 235–252.

Lucas, S.G., Harris, S.K., Spielmann, J.A., Berman, D.S., Henrici, A.C., Krainer, K., Rinehart, L.F., Dimichele, W.A., Chaney, D.S., and Kerp, J.H.F., 2012, Lithostratigraphy, paleontology, biostratigraphy, and age of the upper Paleozoic Abo Formation near Jemez Springs, northern New Mexico, U.S.A.: Annals of Carnegie Museum, v. 80, p. 323–350.

Mack, G.H., 2003, Lower Permian terrestrial paleoclimatic indicators in New Mexico and their comparison to paleoclimate models: New Mexico Geological Society, Guidebook 54, p. 231–240.

Mack, G.H., Giles, K.A., and Durr, C.W., 2013, Sequence stratigraphy of the lower-middle Hueco transition interval (lower Permian, Wolfcampian), Robledo Mountains, New Mexico: New Mexico Geology, v. 35, p. 27–37

Mamay, S.H., Chaney, D.S., and DiMichele, W.A., 2009, *Comia*, a seed plant possibly of peltaspermous affinity: A brief review of the genus and description of two new species from the Early Permian (Artinskian) of Texas, *C. greggii* sp. nov. and *C. craddockii* sp. nov.: International Journal of Plant Sciences, v. 170, p. 267–282.

McGinnes, E.A., Jr., Kandeel, S.A., and Szopa, P.S., 1971, Some structural changes observed in the transformation of wood into charcoal: Wood and Fiber, v. 3, p. 77–83.

Montañez, I. P., and Poulsen, C. J., 2013, The Late Paleozoic Ice Age: An evolving paradigm: Annual Review of Earth and Planetary Sciences, v. 41, p. 629–656.

Nichols, G.J., Cripps, J.A., Collinson, M.E., and Scott, A.C., 2000, Experiments in waterlogging and sedimentology of charcoal: Results and implications: Palaeogeography, Palaeoclimatolology, Palaeoecology, v. 164, p. 43–56

Parrish, J.T., and Falcon-Lang, H.J., 2007, Coniferous trees associated with interdune deposits in the Jurassic Navajo Sandstone Formation, Utah, U.S.A.: Palaeontology, v. 50, p. 829–843.

Pettit, N.E., and Naiman, R.J., 2007, Fire in the riparian zone: Characteristics and ecological consequences: Ecosystems, v. 10, p. 673-687.

Reymanowna, M., 1962, On *Dadoxylon schrollianum* with pith and other Dadoxyla from the Upper Carboniferous in South Poland: Acta Palaeobotanica, v. 3, p. 3–20.

Rozendaal, D.M., and Zuidema, P.A., 2011, Dendroecology in the tropics: A review: Trees, v. 25, p. 3–16.

Scheihing, M.H., and Pfefferkorn, H.W., 1984, The taphonomy of land plants in the Orinoco Delta: A model for the incorporation of plant parts in clastic sediments of Late Carboniferous age of Euramerica: Review of Palaeobotany and Palynology, v. 41, p. 205–240.

Scott, A.C., Kenig, F., Plotnick, R.E., Glasspool, I.J., Chaloner, W.G., and Eble, C.F., 2010, Evidence of multiple late Bashkirian to early Moscovian (Pennsylvanian) fire events preserved in contemporaneous cave fills: Palaeogeography, Palaeoclimatology, Palaeoecology, v. 91, p. 72–84.

Tabor, N.J., 2007, Permo–Pennsylvanian palaeotemperatures from Fe-Oxide and phyllsilicate $d^{18}O$ values: Earth and Planetary Science Letters, v. 253, p. 159–171.

Tabor, N.J., and Montañez, I.P., 2004, Morphology and distribution of fossil soils in the Permo-Pennsylvanian Wichia and Bowie Groups, north-central Texas, USA: Implications for western equatorial Pangean palaeoclimate during icehouse-greenhouse transition: Sedimentology, v. 51, p. 851–884.

Tabor, N.J., Montañez, I.P., Scotese, C.R., Poulsen, C.J., and Mack, G.H., 2008, Paleosol archives of environmental and climatic history in paleotropical western Pangea during the latest Pennsylvanian through Early Permian: Geological Society of America, Special Paper 441, p. 291–303.

Tabor, N.J., DiMichele, W.A., Montañez, I.P, and Chaney, D.S., 2013, Late Paleozoic continental warming of a cold tropical basin and floristic change in western Pangea: International Journal of Coal Geology, v. 119, p. 177-186.

Tidwell, W.D., and Munzing, G.E., 1995, Gymnospermous woods from the Lower Permian Hueco Formation of south-central New Mexico: New Mexico Museum of Natural History and Science, Bulletin 6, p. 91–100.

Voigt, S., Lucas, S.G., and Krainer, K., 2013, Coastal-plain origin of trace-fossil bearing red beds in the Early Permian of southern New Mexico, U.S.A.: Palaeogeography, Palaeoclimatology, Palaeoecology, v. 369, p. 323–334.



Lucas, S. G. and DiMichele, W. A., eds., 2015, Carboniferous-Permian Transition in the Robledo Mountains, Southern New Mexico. New Mexico Museum of Natural History and Science Bulletin 65.

A COMPOSITIONALLY UNIQUE VOLTZIAN CONIFER-CALLIPTERID FLORA FROM A CARBONATE-FILLED CHANNEL, LOWER PERMIAN, ROBLEDO MOUNTAINS, NEW MEXICO, AND ITS BROADER SIGNIFICANCE

WILLIAM A. DIMICHELE[1], DAN S. CHANEY[1], HOWARD FALCON-LANG[2], HANS KERP[3], CINDY V. LOOY[4], SPENCER G. LUCAS[5], KARL KRAINER[6] AND SEBASTIAN VOIGT[7]

[1] Department of Paleobiology, NMNH Smithsonian Institution, Washington, DC 20560, USA;[2] Department of Earth Sciences, Royal Holloway, Egham, Surrey TW20 0EX, UK;[3] Forschungsstelle für Paläobotanik, Westfälische Wilhelms-Universität Münster, Heisenbergstraße 2, 48149 Münster, Germany;[4] Department of Integrative Biology and Museum of Paleontology, University of California, 3060 Valley Life Sciences Building #3140, Berkeley, California 94720, USA;
[5] New Mexico Museum of Natural History and Science, 1801 Mountain Rd. NW, Albuquerque, NM 87104, USA;
[6]Institute of Geology and Paleontology, University of Innsbruck, Innsbruck A-6020 Austria; [7] Urweltmuseum GEOSKOP, Burg Lichtenberg (Pfalz), Burgstraße 19, D-66871 Thallichtenberg, Germany

Abstract—Among the Early Permian deposits in Prehistoric Trackways National Monument, Robledo Mountains, is a limestone-filled paleochannel in the Community Pit Formation, discovered by Jerry MacDonald. The paleochannel, which is ~ 140 m wide and 5-6 m maximum depth, contains a complex fill sequence, indicating a seasonally dry climate, and two distinct fossil plant assemblages. The base of the channel is a limestone conglomerate that contains permineralized logs and charcoal attributable to indeterminate walchian conifers. The middle channel fill consists of multiple lenses of lime mudstone with a sparse brackish-to-marine water invertebrate fauna and a macroflora consisting largely of an undescribed voltzian conifer and the callipterid *Lodevia oxydata*; the deposit also contains in situ fossil roots, indicating at least sporadic plant colonization of the micritic muds. The upper portion of the channel fill is a micritic, gypsiferous lime mudstone that lacks macrofossils.

The significance of this deposit, despite its low diversity, lies in the great caution it presents regarding interpretations of evolutionary patterns based on direct reading of the terrestrial fossil record. This is indicated by the spatio-temporal occurrences of the two rare elements that make up the mid-channel flora. The voltzian conifer is the earliest member of this evolutionary lineage yet described, extending the known range by approximately 25 million years from the previously known occurrence, which itself extended the range approximately 10 million years. Similarly, the geographic range of *Lodevia oxydata* at the Late Pennsylvanian-Early Permian transition, is extended nearly 2500 km, from its previously most westerly known occurrence in West Virginia, USA. Together with the only other report from the Rotliegendes of Poland, it gives this species a total known range, based on these three widely separated and localized occurrences, of approximately 9000 km on today's earth. Clearly, prior to the latest Permian, when such conifers were abundant, the voltzians were significant tropical landscape elements somewhere, but have been incorporated into the fossil record rarely and thus their early history remains largely unknown. For the callipterid, temporal continuity throughout its known range cannot be established, so it cannot be determined if the plant occupied the full range at any given time, or only portions thereof. Nonetheless, the geographic sparseness of its appearances, in light of the high density of plant remains from the sites where it does occur, indicate that its fossil record also is highly incomplete. Such patterns of occurrence, if used in conjunction with indicators of climate and environment, serve to support inferences about where and under what conditions these plants lived and the kinds of taphonomic factors that influenced their preservation.

INTRODUCTION

There are instances, in the course of geological fieldwork, when the hand of fortune reveals the unanticipated and, often, the unimagined. Such discoveries may have significance that goes far beyond their seemingly miniscule spatio-temporal scope. They can open the way to consider possibilities not previously envisioned, and change understandings of pattern and process in significant ways.

In recent years, discoveries in the plant fossil record of what might be termed "outliers," either biogeographically or stratigraphically, have increased awareness that much more of evolutionary interest was happening outside the preservational window of the fossil record than anticipated. Major lineages have been shown to have evolved earlier and appeared in geographic locations quite distinct from what their zeniths in the fossil record might indicate. As a few examples, consider the discovery of the typically Late Triassic, high southern latitude genus *Dicroidium* in Late Permian, equatorial latitudes (Kerp et al., 2006; Abu Hamad et al., 2008); the appearance of *Dioonitocarpidium*, another Late Triassic and Early Jurassic taxon, in the Early Permian equatorial realm (DiMichele et al., 2001); or the occurrence of a voltzialean conifer in the latest Early Permian (Looy, 2007), a lineage previously known, and abundantly so, no earlier than the Late Permian. Other examples of either early or unexpectedly late occurrences can be extended to the Peltaspermales, both of the group as a whole (Kerp, 1988) and of the more derived, typically Mesozoic forms with radially symmetrical reproductive morphologies (Kerp et al., 2001), or even to the wholesale survival of a Middle Pennsylvanian-type Euramerican wetland flora into the Early Permian of the Cathaysian realm of western Pangea (Hilton and Cleal, 2007; Wang et al., 2012). All of these occurrences, and many others, suggest that great caution is necessary when using the fossil record of terrestrial organisms as a direct chronicle of first and last occurrences or as a template for a direct reading of the course of evolutionary history.

Here we report a small limestone-filled, channel-form deposit of Early Permian age from Prehistoric Trackways National Monument, in the Robledo Mountains of southern New Mexico. This channel is filled with carbonate sediments preserving plant fossils that greatly extend the stratigraphic and geographic ranges, respectively, of two taxa: the so-called "voltzian" voltzialean conifers and the callipterid *Lodevia oxydata*. These discoveries are important not only for understanding the evolutionary histories and biogeographies of these particular taxa. They serve as indications of just how great are the gaps in our understanding of ancient landscape dynamics and how we must be prepared to work among data sets and models as we develop mechanistic explanations of pattern.

GENERAL GEOLOGICAL CONTEXT

The fossil deposit under consideration was discovered by Mr. Jerry MacDonald, who first noted fossil wood (MacDonald, 1994). Later, one of the authors (SGL) found plant macrofossils in association with the wood while preparing a detailed measured section through this stratigraphic interval (Lucas et al., 1998a, b).

The channel is located in the Robledo Mountains in Doña Ana County, south-central New Mexico (Fig. 1). This exposure is within the Prehistoric Trackways National Monument, managed by the US Bureau of Land Management. Stratigraphically, it is within the Community Pit Formation of the Hueco Group (Fig. 1), which can be age-constrained, based on a variety of paleontological lines of evidence, particularly fusulinids, conodonts and ammonoids, to between the late Asselian and early Artinskian, Early Permian (Falcon-Lang et al., submitted).

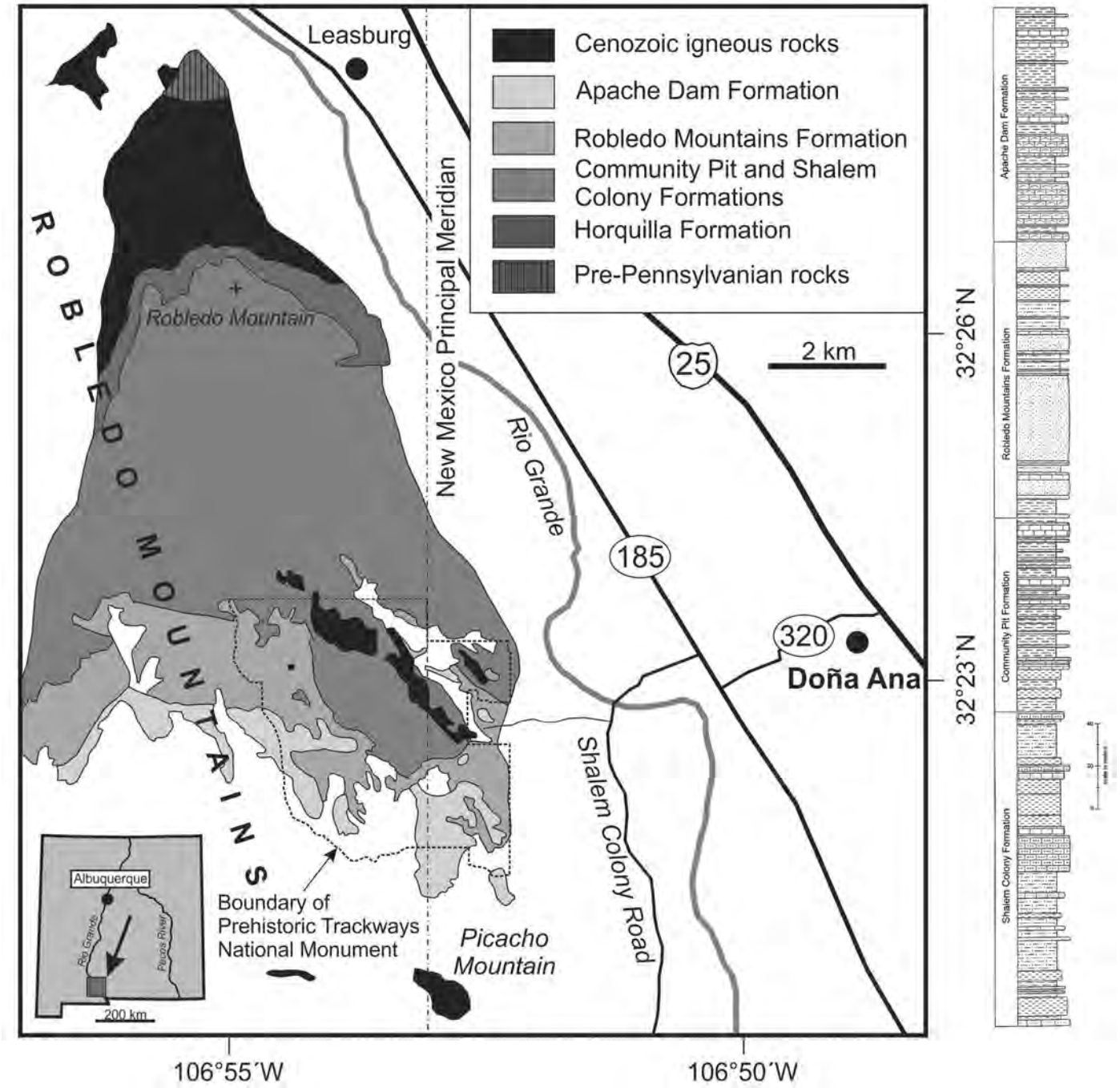


FIGURE 1. Location of the Prehistoric Trackways National Monument in southern New Mexico, within the Robledo Mountains. The fossiliferous channel deposit is within the lower part of the Community Pit Formation.

The Community Pit Formation is correlative with the lower part of the Abo Formation, which crops out prominently throughout central New Mexico (Lucas et al., 2011, 2013).

Throughout most of its outcrop area, the Abo Formation consists entirely of terrestrial red beds – mostly channelized siltstones and sandstones within and between pedogenically overprinted siltstones and, in some cases, claystones (volumetrically, most of the Abo Formation is mudrock). Rare carbonates represent either thin non-marine limestones or calcareous pedogenic horizons. Paleosols indicate a seasonal climate, likely dry subhumid to semiarid (Mack et al., 2010; Tabor et al., 2008). In south-central New Mexico, Early Permian terrestrial red beds interfinger with marine rocks of the Hueco seaway (Mack and James, 1986). These rocks comprise the mixed terrestrial-marine, siliciclastic-carbonate Hueco Group, consisting of (in ascending order) the Shalem Colony, Community Pit, Robledo Mountains and Apache Dam formations (Lucas et al., 1998b, 2002). Paleosols and depositional environments suggest a climatic background that was semi-arid on average (Mack et al., 2003, 2013). At the time of deposition, the area of Hueco Group deposition was peri-equatorial, perhaps 2° North (Tabor et al., 2008).

The Abo Formation flora (Hunt, 1983; DiMichele et al., 2001, 2012, 2013a) is composed nearly entirely of walchian conifers and the probable peltasperm, *Supaia* (White, 1929; Wang, 1997), with rare occurrences of the callipterids *Autunia conferta* and *Rhachiphyllum schenkii*, sphenophylls, pecopterid ferns, the pteridosperm *Neuropteris*, and the possible cycadophyte *Taeniopteris*. This flora is entirely different from that of the carbonate-filled channel in the Robledo Mountains, with which it is broadly contemporaneous.

PALEOCHANNEL-FILL GEOLOGICAL SETTING

The study site consists of a small paleochannel filled principally with carbonates. Paleozoic plant fossils are known and reported from

both marine and non-marine carbonates (e.g., DiMichele et al., 2013b), but such an environmental setting is not one from which such fossils are generally expected or sought. Micritic carbonates are primarily biogenic precipitates forming under climatic conditions chemically conducive to such activity – primarily strongly seasonally dry settings with high evapotranspiration, but with regular influxes of carbonate-rich waters. Such precipitates "set up," that is they harden rapidly following exposure to air or to flushing by fresh water (e.g., Larrahondo et al., 2011), subsequent to which the incorporation of plant debris would be excluded. Thus, plant remains found as fossils in such carbonate muds had to be incorporated into the substrate while it was still under aqueous cover. Under such conditions, the growth environment of the parent plants was most likely one from which fossilized organic remains are rarely found.

The top of the paleochannel lies approximately 15.5 m above the local base of the Community Pit Formation. It is approximately 140 m wide and 5-6 m deep. The width is an approximation because of possible obliquity in the angle across which the paleochannel face is exposed by erosion. The paleochannel is somewhat asymmetrical in shape, with the eastern edge being steeper and more deeply incised than the western margin.

The paleochannel fill consists of three distinct facies. (1) In a restricted area in the center, and deepest portion of the channel, the 0.05-1.1 m thick fill is composed of an intraformational conglomerate composed mainly of marine limestone clasts most likely derived from the channel walls and local drainage basin. This unit also contains the remains of fossilized logs of walchian conifers, partially to completely preserved as charcoal (Fig. 2.1). (2) The middle unit is up to 4 m thick and consists of micritic limestone beds containing a sparse macrofauna of linguloids and pectinids, a microfauna of ostracodes, foraminiferans and possibly sponge spicules, and a macroflora dominated by voltzian conifers and the callipterid *Lodevia oxydata* (Fig. 2.2), and including unidentifiable tree trunks. This interval also contains scattered occurrences of fossilized fibrous root masses, which appear to have been preserved in situ, indicating rooting into the carbonate muds during the time of active accretion. (3) The uppermost 1.2 m of the channel is filled with a dolomite containing gypsum nodules that lacks fossils.

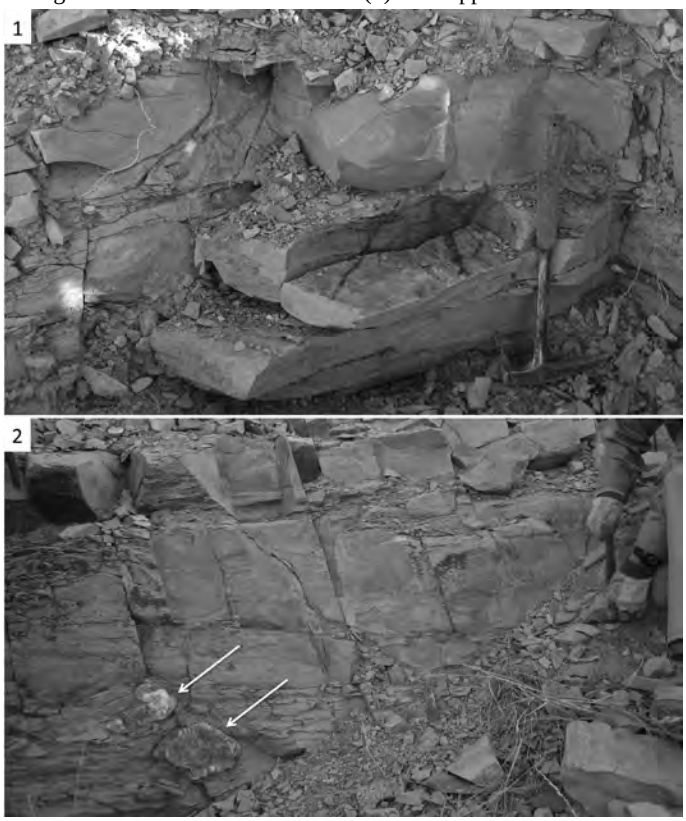


FIGURE 2. Geology of channel-fill deposit. **2.1**, Micritic carbonates from mid-channel with plant fossils, visible on bedding surface. Hammer is 40 cm in length. **2.2**, Lower portion of channel fill with silicified coniferophyte stems (white arrows) and micritic carbonates of middle channel fill above.

FOSSIL FLORA

There are two distinct floras in the strata that compose the paleochannel. These floras are preserved in different facies, are compositionally distinct and preserved differently. They appear to be derived from spatio-temporally distinct kinds of vegetation and to reflect growth of the plants under different kinds of environmental conditions.

The older flora consists entirely of logs and wood fragments, some preserved as charcoal, and located exclusively in the basal-most conglomeratic unit. The anatomical characteristics of those specimens that could be studied, which are preserved mainly as charcoalified wood, indicate a walchian conifer affinity. In the absence of pith and detailed vascular features, a more confident assignment cannot be made. These specimens are described in detail in Falcon-Lang et al. (this volume). Walchian conifers are common and widespread in Early Permian deposits throughout western equatorial Pangea. The walchian conifer stem *Macdonaldodendron* Falcon-Lang, Kurzawe & Lucas (Falcon-Lang et al., 2014), has been described from allochthonous specimens preserved in offshore carbonate facies of the Community Pit Formation, but 50 or more meters above the carbonate channel-fill horizon.

The second flora is preserved in the middle unit of the paleochannel fill, in a micritic lime mudstone. Specimens are sparse and variably disposed within the micrites, and include foliage, branch fragments with attached foliage, carbonate permineralized trunks, and in situ fossil fibrous roots. The majority of the specimens are attributable to an undescribed form of voltzian voltzialean conifer (Fig. 3.1). These specimens consist of several vegetative morphotypes, some of which are probably assignable to the same species, and rare specimens of reproductive structures. Less abundant, but nonetheless common, is foliage of the callipterid plant *Lodevia oxydata* (Göppert) Haubold & Kerp (Fig. 3.2). Also notable in this assemblage are masses of taxonomically unattributable fibrous roots that must have penetrated the carbonate muds while they were still soft – and hence, almost certainly, water covered (Fig. 3.3). Rare elements of the flora include a few specimens of sphenopterid fern foliage, some fragmentary remains possibly assignable to *Walchia* sp., and a single specimen attributable to the sphenopsid *Annularia spicata* (Gutbier) Schimper. This flora is described in greater detail in Falcon-Lang et al. (submitted).

DISCUSSION

The fossil floras discussed herein are of importance for several reasons: depositional environment, inferred environmental circumstances, and floristic composition. All descends from the first – the peculiar depositional context of the fossils. The presence of fossil plants in micritic carbonate deposits may not be as unusual as it first appears; however, this is not a search image that most field-oriented researchers have in mind, and, consequently, may be frequently overlooked. An equally unusual example of a fossil deposit is one from the Middle Permian of North Texas, described in the literature as South Ash Pasture (DiMichele et al., 2004), which is preserved in a small, siltstone-filled channel that is incised into thick, primary gypsum beds and is overlain by oolitic limestone. Basically, the South Ash Pasture deposit would have been overlooked or bypassed for detailed examination but for the fortuitous find of fossil wood by a property owner. There is no simple "cure" for this problem, other than the prescription of "more field work."

The fossil deposit in the Robledos is preserved in a small, incised paleochannel, cut through marine carbonate and siliciclastic strata (Fig. 4). The channel is, as far as we can determine, an isolated feature and thus unlikely to have resulted from channel switching. It may signal a drop in base level as an initiator of incision. Whether the change in base level was due to a eustatic sea-level drop or local to regional tectonism cannot be determined satisfactorily from the evidence at hand. Eustasy, in particular, should have had a widespread effect. Mapping throughout the Prehistoric Trackways National Monument has not revealed any additional features of this nature in the same stratigraphic interval. The Asselian-Sakmarian time period, however, was within the Early Permian glacial interval (Montañez et al., 2007; Fielding et al., 2008), so a eustatic cause must remain a possibility. Tectonism is a significant unknown in this instance. The Robledo Mountains area was in the then tectonically active Orogrande Basin, though a more broadly visible physical fingerprint might be expected were local tectonism the cause

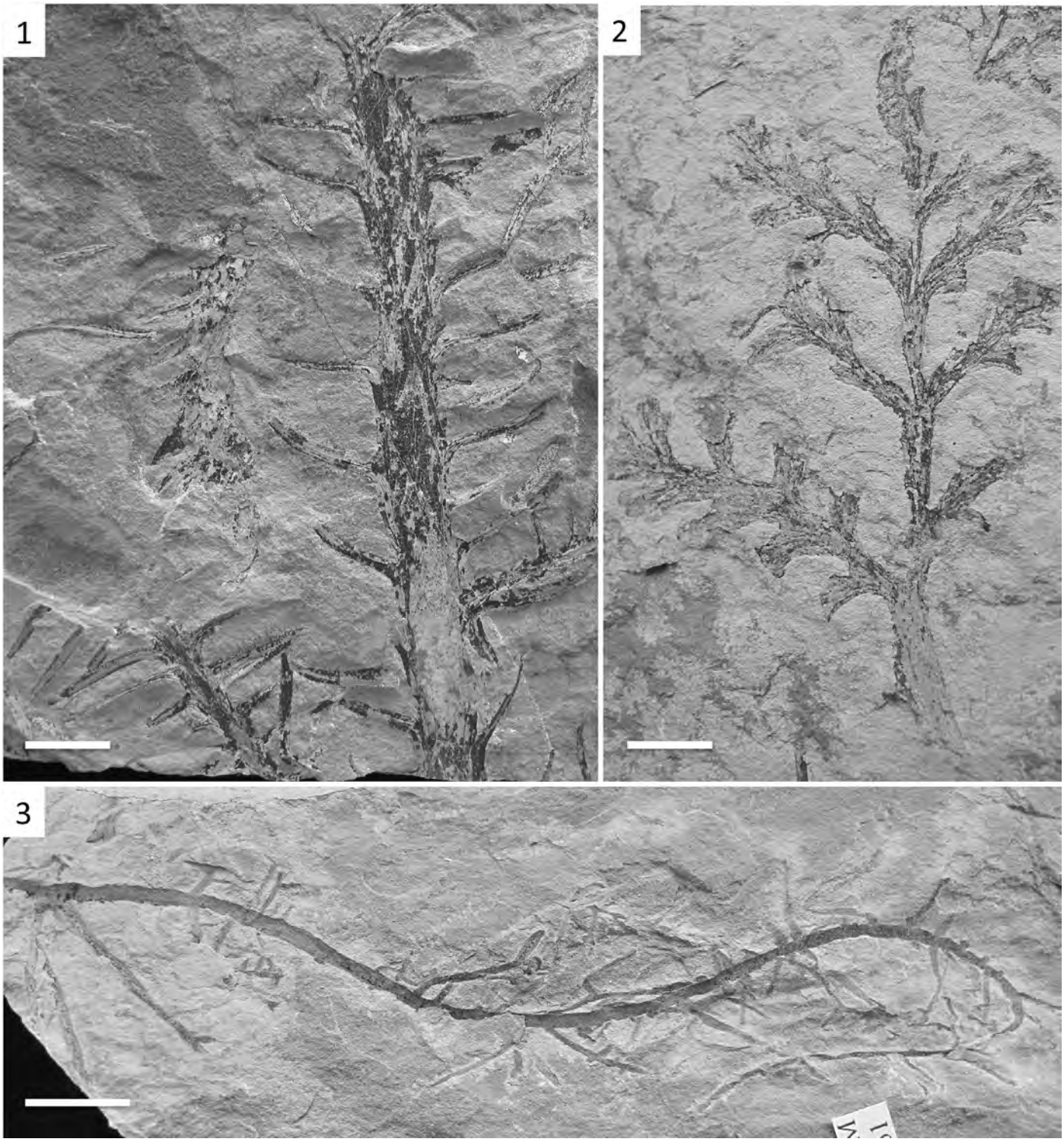


FIGURE 3. Channel-fill plants. **3.1**, Voltzialean conifer branch with attached foliage. NMMNH Specimen P-68872, NMMNH locality 3016 (USNM locality 43550). **3.2**, *Lodevia oxydata*, callipterid foliage. NMMNH Specimen P-68873, NMMNH locality 9123 (USNM locality 43554). **3.3**, Roots of indeterminate affinity. NMMNH Specimen P-68874, NMMNH locality 9124 (USNM locality 43551). All scale bars = 1 cm.

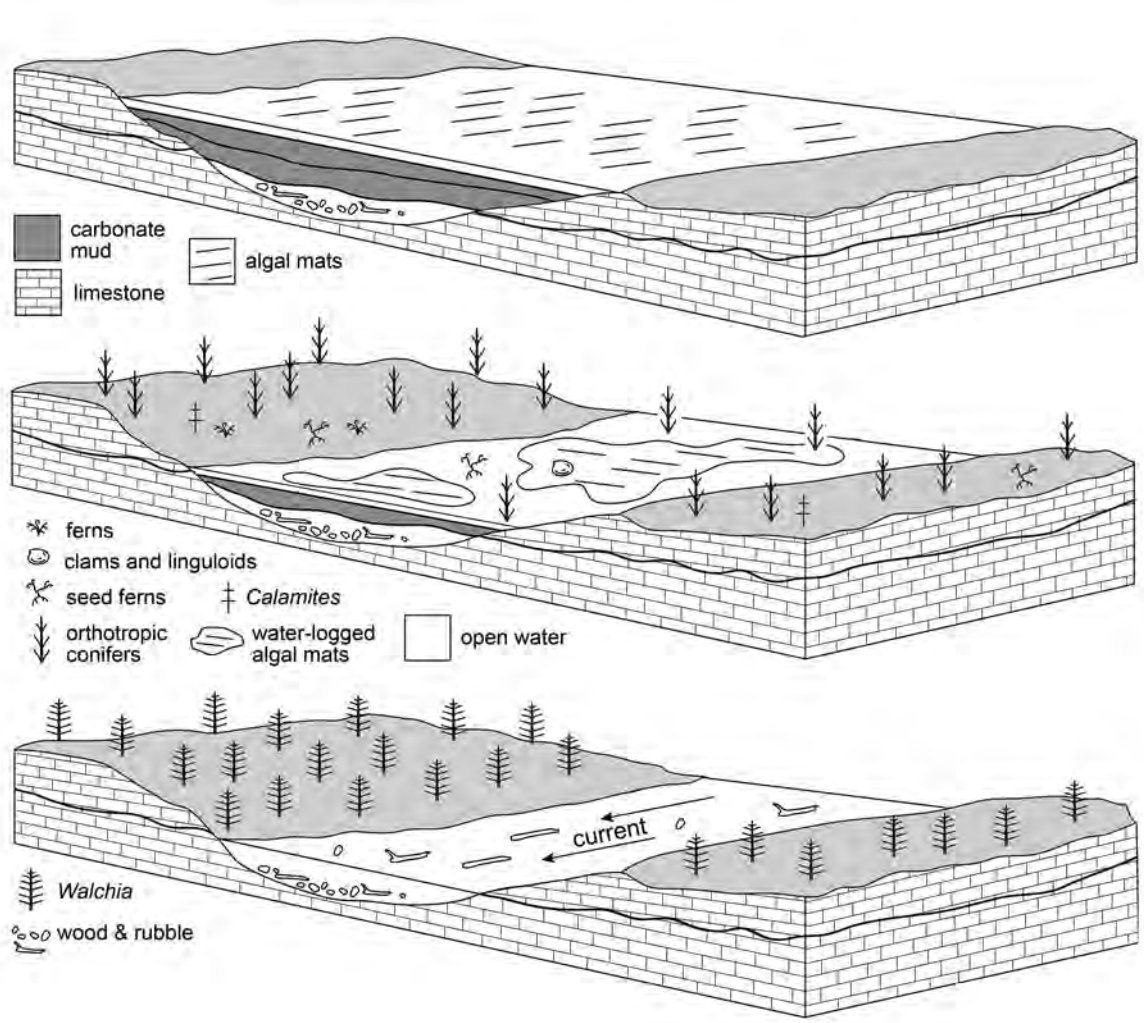


FIGURE 4. Channel-fill progression model. **Bottom**. Active flow during incision phase and early back filling. **Middle**. As the channel fills flow volume decreases and carbonate precipitation ensues; surrounding flora changes and plants are incorporated into the micritic muds. **Top**. Evaporitic conditions intensify in final channel fill phases and gypsum is deposited in association with micritic muds.

of subsidence-initiated channel incision.

In terms of glacial-interglacial cycles, there are reasonable expectations that lowstand coastal deposits are among the most likely to be preserved on intermediate-term time scales because they can be buried by marine incursions, isolating organic material from degradation for tens of thousands of years. Such intermediate-term burial gives regional tectonism time to create long-term accommodation space, if the area is within a basinal setting (Gastaldo and Demko, 2011). It might be hypothesized, therefore, that a eustatic rise in sea level following incision would most likely result in preservation of a fossil flora composed of the most commonly encountered taxa found in the area surrounding the deposit. Alternatively, if the cause of channel incision were tectonic, it presents the possibility that accommodation space was created at a portion of the glacial-interglacial cycle not usually conducive to intermediate and long-term preservation of organic debris, such as during high-stand or falling stages of sea level. Under such circumstances, the possibility arises of capturing a terrestrial flora not normally preserved in the fossil record.

Another peculiar aspect of the depositional conditions of the paleochannel fill is the preservation of the mid-channel flora within brackish-to-marine micritic carbonates. The presence of sparse linguloid and pectinid invertebrates, and the composition of the microfauna within the micrites suggests such salinities. This flora is composed of two very unusual taxa, a voltzian voltzialean conifer and *Lodevia oxydata*. In order for these fossils to be incorporated into a micritic mud, the substrate would need to have been soft and actively accumulating. This would require water cover, given that such muds almost certainly reflect the activities of carbonate-generating organisms and that such micrites would have solidified to a concrete-like texture within a very short time (days to weeks) once exposed to the air or flushed with fresh water. Thus, the plants were either growing on the margins of the paleochannel or, given the presence of fibrous roots in the micritic carbonates, perhaps even in the paleochannel itself, which may have been mostly sediment filled and under shallow water cover during the middle and later phases of backfilling.

The environmental conditions recorded by the paleochannel deposit suggest climatic aridity, during base-level rise and channel filling (Fig. 4). The oldest deposits in the channel are composed of an intraformational, marine-carbonate conglomerate, composed of clasts similar compositionally to the channel walls. This kind of deposit indicates enough moisture on the landscape, at least periodically, to contribute to streams that could locally transport clasts of large size. In addition, the deposit contains some walchian-like coniferophyte logs, which are most likely to have grown under seasonally dry, subhumid to, perhaps, semi-arid climate (Bashforth et al., 2014). This basal-most deposit most likely formed as a lag in the channel bottom during incision or as back-filling was initiated.

The middle part of the paleochannel is composed of micritic carbonates, which appear to be an in situ accumulation of lime muds most likely precipitated by biogenic activity. An environment suitable for such carbonate precipitation would have to have been able to support a community of bacteria and algae capable of creating such sediment, thus wet enough to maintain at least some surface water cover in the paleochannel, but with limited flow volumes compared to the earlier formed deposit. Local soil moisture also had to be sufficient enough to support trees, or at least shrubs, and some groundcover plants, either on the paleochannel margins or in shallow water portions of the channel, or both. The final phase of paleochannel filling (Fig. 4, top

panel) does not contain fossil flora, and the micritic carbonate matrix includes concentrations of gypsum, suggesting that this final phase may have become semi-arid to arid, though the gypsum is not primary and thus may not be a direct reflection of climate at the time of limestone formation. Nonetheless, the paleochannel provides an unusual look at changing environmental circumstances and the vegetational changes that accompanied this.

From the biological viewpoint, the flora from the middle unit of the paleochannel is exceptional. The conifer occurrence extends the range of this evolutionary lineage to an earlier time by approximately 25 million years, the previously earliest occurrence being at the Early-Middle Permian boundary (Looy, 2007). The *Lodevia oxydata* fossils extend the geographic range of that taxon by approximately 2500 km, from an occurrence in the Appalachian Basin (DiMichele et al., 2013b), to a total range, based on only three occurrences (the eastern most from Poland), of over 9000 km (this would, of course, be a still substantial ~ 6000 km in the Early Permian world). These extensions, not the first of their kind, are both remarkable and serve as a warning. Previously reported outlying, early appearances of such plants as *Peltaspermum* (Kerp et al., 2001), *Dioonitocarpidium* (DiMichele et al., 2001), *Dicroidium* (Kerp et al., 2006), or voltzian voltzialean conifers (Looy, 2007) have changed both our understanding of the temporal and biogeographic distributions of these plants. Such patterns of fossil distribution in time and space indicate a great deal of undetected biological dynamics that must be inferred from isolated, often unique occurrences. As such, they serve as points of interaction with models of evolution and its relation to space and time more than they serve as parts of a well represented, direct record of the evolutionary process.

ACKNOWLEDGMENTS

This research was supported by a grant from the Bureau of Land Management, which is gratefully acknowledged. Additional support comes from the National Museum of Natural History Small Grants Program. We thank Jerry MacDonald, Las Cruces, NM, for his generous advice and assistance with this research. We gratefully acknowledge the field assistance of Scott Elrick, Vincent “Skip” Lyles, John Nelson, Larry Rinehart and Justin Spielmann. Mary Parrish, NMNH, prepared the artwork. We thank Blaine Cecil and Peter Holterhoff for their reviews of an earlier draft of this paper.

REFERENCES

Abu Hamad, A., Kerp, J.H.F., Vörding, B. and Bandel, K., 2008 A Late Permian flora with *Dicroidium* from the Dead Sea region, Jordan: Review of Palaeobotany and Palynology, v. 149, p. 85-130.

Bashforth, A.R., Cleal, C.J., Gibling, M.R., Falcon-Lang, H.J. and Miller, R.F., 2014. Paleoecology of Early Pennsylvanian vegetation on a seasonally dry tropical landscape (Tynemouth Creek Formation, New Brunswick, Canada): Review of Palaeobotany and Palynology, v. 200, p. 229-263.

DiMichele, W.A., Mamay, S.H., Chaney, D.S., Hook, R.W. and Nelson, W.J., 2001. An Early Permian flora with Late Permian and Mesozoic affinities from north-central Texas: Journal of Paleontology, v. 75, p. 449–460.

DiMichele, W.A., Chaney, D.S., Nelson, W.J., Lucas, S.G., Looy, C.V., Quick, K. and Jun, W., 2007. A low diversity, seasonal tropical landscape dominated by conifers and peltasperms: Early Permian Abo Formation, New Mexico: Review of Palaeobotany and Palynology, v. 145, p. 249–273.

DiMichele, W. A., Lucas, S. G. and Krainer, K., 2012. Vertebrate trackways among a stand of *Supaia* White plants on an Early Permian floodplain, New Mexico: Journal of Paleontology, v. 86, p. 584-594.

DiMichele, W.A., Chaney, D. S., Lucas, S. G., Kerp, H. and Voigt, S., 2013a. Flora of the Lower Permian Abo Formation redbeds, western equatorial Pangea, New Mexico: New Mexico Museum of Natural History and Science Bulletin, v. 59, p. 265–288.

DiMichele, W.A., Kerp, H., Sirmons, R., Fedorko, N., Skema, V., Blake, B.M. and Jr., Cecil, C.B., 2013b. Callipterid peltasperms of the Dunkard Group, Central Appalachian Basin: International Journal of Coal Geology, v. 119, p. 56–78.

Falcon-Lang, H.J., Kurzawe, F. and Lucas, S.G., 2014. Coniferopsid tree trunks preserved in sabkha facies in the Permian (Sakmarian) Community Pit Formation in south-central New Mexico, U.S.A.: Systematics and palaeoecology: Review of Palaeobotany and Palynology, v. 200, p. 138-160.

Falcon-Lang, H.J., DiMichele, W.A., Kurzawe, F., Looy C.V., Lucas, S.G., Chaney D.S., Contreras, D.L., Elrick, S.D., Kerp, H., Krainer, K., Nelson, W.J. and Vachard, D., submitted. Vegetation of an Early Permian (Asselian) seasonally dry coast in western equatorial Pangaea: palaeoecology and evolutionary significance. Palaeogeography, Palaeoclimatology, Palaeoecology.

Fielding, C.R., Frank T.D. and Isbell, J.L., 2008. The Late Paleozoic ice age – a review of current understanding and synthesis of global climate patterns: Geological Society of America Special Publication, v. 441, p. 343–354.

Gastaldo, R.A. and Demko, T.M., 2011. Long term hydrology controls the plant fossil record; in Allison, P.A. and Bottjer, D.J., eds., Taphonomy: Processes and bias through time: Topics in Geobiology, v. 32, p. 249–286.

Hilton, J. and Cleal, C.J., 2007. The relationship between Euramerican and Cathaysian tropical floras in the Late Palaeozoic: Palaeobiogeographical and palaeogeographical implications: Earth Science Reviews, v. 85, p. 85–116.

Hunt, A., 1983. Plant fossils and lithostratigraphy of the Abo Formation (Lower Permian) in the Socorro area and plant biostratigraphy of Abo red beds in New Mexico: New Mexico Geological Society, Guidebook 34, p. 157-163.

Kerp, H., Broutin, J., Lausberg, S., Aassoumi, H. 2001. Discovery of latest Carboniferous-Early Permian radially symmetrical peltaspermaceous megasporophylls from Europe and North Africa: Comptes Rendus de l’Académie des Sciences de Paris. Série IIa, v. 322, p: 513-519.

Kerp, H., Abu Hamad, A., Vörding, B. and Bandel, K., 2006. Typical Triassic Gondwanan floral elements in the Upper Permian of the paleotropics: Geology, v. 34, p. 265–268.

Kerp, J.H.F., 1988. Aspects of Permian palaeobotany and palynology. X. The West- and Central European species of the genus *Autunia* Krasser emend. Kerp (Peltaspermaceae) and the form-genus *Rhachiphyllum* Kerp (callipterid foliage): Review of Palaeobotany and Palynology, v. 54, p. 249-360.

Larrahondo, J.M., Burns, S.E. and Gutierrez, B., 2011, Early marine diagenesis in Calcium Carbonate rich sediments: A review of implications for geotechnical systems; in Han, J. and Alazamora, D.J., eds., Geo-Frontiers 2011, Advances in geotechnical engineering: American Society of Civil Engineers, Reston, Virginia, p. 3956-3965.

Looy, C.V., 2007, Extending the range of derived Late Paleozoic conifers: *Lebowskia* gen. nov. (Majonicaceae): International Journal of Plant Sciences, v. 168, p. 957–972.

Lucas, S.G., Heckert, A.B., Estep, J.W., Hunt, A.P. and Anderson, O.J., 1998a, Stratigraphy, paleontology and depositional environments of the Lower Permian Robledo Mountains Formation of the Hueco Group, Robledo Mountains, New Mexico: New Mexico Museum of Natural History and Science, Bulletin 12, p. 29–41.

Lucas, S.G., Heckert, A.B., Estep, J.W., Hunt, A.P. and Anderson, O.J., 1998b, Stratigraphy, of the Lower Permian Hueco Group in the Robledo Mountains, Doña Ana County, New Mexico: New Mexico Museum of Natural History and Science, Bulletin12, p. 43–54.

Lucas, S.J., Krainer, K. and Kues, B.S., 2002. Stratigraphy and correlation of the Lower Permian Hueco Group in the southern San Andres Mountains, Doña Ana County, New Mexico: New Mexico Geological Society, Guidebook 53, p. 223–240.

Lucas, S.G., Voigt, S., Lerner, A.J., MacDonald, J.P. Spielmann, J.A. and Celeskey, M.D., 2011, The Prehistoric Trackways National Monument, Permian of southern New Mexico, U.S.A: Ichnology Newsletter, v. 28, p. 10–14.

Lucas, S.G., Krainer, K., Chaney, D.S., DiMichele, W.A., Voigt, S., Berman, D.S. and Henrici, A.C., 2013, The Lower Permian Abo Formation in central New Mexico: New Mexico Museum of Natural History and Science, Bulletin 59, p. 161-179.

MacDonald, J.P., 1994. Late Paleozoic (Early Permian) petrified wood from the Robledo Mountains of New Mexico, U.S.A.: A summary of findings: Unpublished Report, U. S. Bureau of Land Management, Las Cruces, New Mexico, 79 p.

Mack, G.H. and James, W.C., 1986. Cyclic sedimentation in the mixed siliciclastic-carbonate Abo–Hueco transitional zone (Lower Permian), southwestern New Mexico: Journal of Sedimentary Petrology, v. 56, p. 635–647.

Mack, G.H., Leeder, M., Perez-Arlucea, M. and Baily, B.D.J., 2003. Sedimentology, paleontology, and sequence stratigraphy of Early Permian estuarine deposits, south-central New Mexico, USA: Palaios, v. 18, p. 403–420.

Mack, G.H., Tabor, N.J. and Zollinger, H.J., 2010, Palaeosols and sequence stratigraphy of the Lower Permian Abo Member, south-central New Mexico, USA: Sedimentology 57, p. 1566-1583.

Mack, G.H., Giles, K.A. and Durr, C.W., 2013, Sequence stratigraphy of the lower-middle Hueco transition interval (Lower Permian, Wolfcampian), Robledo Mountains, New Mexico: New Mexico Geology, v. 35, p. 27-37.

Montañez, I.P., Tabor, N.J, Niemeier, D., DiMichele, W.A., Frank, T.D., Fielding, C.R., Isbell, J.L., Birgenheier, L.P. and Rygel, M.C., 2007, CO_2-forced climate and vegetation instability during Late Paleozoic deglaciation: Science, v. 315, p. 87-91.

Tabor, N.J., Montañez, I.P., Scotese, C.R., Poulsen, C.J. and Mack, G.H., 2008, Paleosol archives of environmental and climatic history in paleotropical western Pangea during the latest Pennsylvanian through Early Permian: Geological Society of America Special Paper, v. 441, p. 291–303.

Wang, J., Pfefferkorn, H.W., Zhang, Y. and Feng, Z., 2012. Permian vegetational Pompeii from Inner Mongolia and its implications for landscape paleoecology and paleobiography of Cathaysia: Proceedings of the National Academy of Sciences of the USA, v. 109, p. 4927–4932.

Wang Z.-Q., 1997. Permian *Supaia* fronds and an associated *Autunia* fructification from Shanxi, China: Palaeontology, v. 40, p. 245–277.

White, D., 1929. Flora of the Hermit Shale, Grand Canyon, Arizona: Bulletin of the Carnegie Institution of Washington, 221 p.

Lucas, S. G. and DiMichele, W. A., eds., 2015, Carboniferous-Permian Transition in the Robledo Mountains, Southern New Mexico. New Mexico Museum of Natural History and Science Bulletin 65.

EARLY PERMIAN FOSSIL FLORAS FROM THE RED BEDS OF PREHISTORIC TRACKWAYS NATIONAL MONUMENT, SOUTHERN NEW MEXICO

WILLIAM A. DIMICHELE[1], SPENCER G. LUCAS[2], CINDY V. LOOY[3], DAN S. CHANEY[1] AND SEBASTIAN VOIGT[4]

[1] Department of Paleobiology, NMNH Smithsonian Institution, Washington, DC 20560 USA; [2] New Mexico Museum of Natural History and Science, 1801 Mountain Rd. NW, Albuquerque, NM 87104, USA; [3]Department of Integrative Biology and Museum of Paleontology, University of California, 3060 Valley Life Sciences Building #3140, Berkeley, California 94720, USA; [4]Urweltmuseum GEOSKOP, Burg Lichtenberg (Pfalz), Burgstraße 19, D-66871 Thallichtenberg, Germany

Abstract—Early Permian (Wolfcampian), fossiliferous terrestrial red beds of the Abo Formation crop out in a north-to-south band through central New Mexico. Abo strata were deposited in entirely terrestrial settings and only in southern portions of the state do they intertongue with marine rocks of the Hueco Group. Here we focus on fossil floras from one of the areas where this close spatio-temporal intercalation of marine rocks and terrestrial red beds has been recognized, the Prehistoric Trackways National Monument located in the Robledo Mountains in Doña Ana County, south-central New Mexico. These strata are assigned to the Robledo Mountains Formation and are part of the upper Hueco Group. They are laterally equivalent to the upper part of the Abo Formation identified elsewhere in the state.

The floras of the Robledo Mountains Formation red beds are compositionally similar to those found in the Abo Formation. They are dominated by walchian conifers most similar to *Walchia piniformis*, a form taxon that may represent a number of distinct biological species. Isolated occurrences of other taxa include the peltasperm *Supaia thinnfeldioides*, the possible peltasperm *Gigantopteridium* sp., the cycadophyte *Taeniopteris* and callipterid peltasperms. The monotony of these Early Permian red-bed floras over a very large area is noteworthy and perplexing. Other facies from strata within this same time interval, elsewhere in the region, preserve either strikingly different floras or floras of considerably higher diversity. The red-bed floras do not appear to reflect a persistent preservational bias, but suggest that large areas were covered by low diversity forests of conifers. The proximity of the red-bed facies to marine conditions bordering the Hueco seaway does not seem to have had any discernible effect on their composition.

INTRODUCTION

The Early Permian was marked by a series of glaciations separated by periods of global warmth (e.g., Montañez et al., 2007; Fielding et al., 2008). In addition, the geological record indicates episodically increasing seasonality and climatic dryness around the equatorial regions of central and western Pangea (Kerp, 1996; Tabor and Poulsen, 2008; Tabor et al., 2013; Opluštil et al., 2013), a trend that began in the late Middle Pennsylvanian (Cecil et al., 1985). During this period of warming, terrestrial floras became increasingly heterogeneous spatially, which might be argued is an expectation in a world where generally increasing aridity magnifies habitat variability at all scales from the local landscape to broad regions.

One of the most westerly known Early Permian equatorial Pangean floras is found in the red beds of central New Mexico. These strata are terrestrial in origin and where there is no intercalation with marine strata are assigned to the Abo Formation (Lucas et al., 2005, 2013). In the southern parts of their outcrop area, however, along the Hueco seaway, Early Permian terrestrial red beds occur between beds of marine carbonate, recording oscillating cycles of climate and sea level (Mack et al., 2010). In this area, strata equivalent to the Abo Formation are classified as the Hueco Group. Of several Hueco Group formations, red beds and their associated plant and animal fossil assemblages are known only from the Robledo Mountains Formation, equivalent to the upper Abo and of Artinskian age.

In this paper we examine the flora of the Robledo Mountains Formation as preserved in the Prehistoric Trackways National Monument of southern New Mexico. These floras are of interest because they occur in terrestrial red beds preserved between marine strata. Evidence from trace fossils suggests that these red beds were deposited in relatively close proximity to marine environments (Voigt et al., 2013). They reemphasize the observation that the Abo Formation red beds, and their correlatives, contain a low diversity flora that is characteristic of this region, overwhelmingly dominated by walchian conifers.

LOCATION

The exposures examined in this study are located in the Prehistoric Trackways National Monument (PTNM). The PTNM is located within the Robledo Mountains, a small mountainous area to the northwest of Las Cruces, New Mexico, in Doña Ana County (Fig. 1). The PTNM is approximately 2140 hectares (approximately 8.25 square miles) in which principally Early Permian strata are exposed. It is administered by the US Bureau of Land Management.

GEOLOGICAL BACKGROUND

Lower Permian exposures in the Prehistoric Trackways National Monument are classified as the Hueco Group, a mixed marine carbonate – terrestrial siliciclastic unit. The Hueco Group is subdivided into four formations (Fig. 1) that are, from the base, the Shalem Colony, Community Pit, Robledo Mountains and Apache Dam (Lucas et al., 2005). The Shalem Colony, Community Pit and Apache Dam formations are composed predominantly of marine rocks; the Robledo Mountains Formation is mixed marine and terrestrial.

The Hueco Group is the lateral equivalent of the Abo and Yeso formations to the north (Lucas et al., 2013). The Abo Formation is divided into two members (Lucas et al., 2005), the lower Scholle Member and the upper Cañon de Espinoso Member. Both members are composed entirely of terrestrial lithofacies, primarily siliciclastics; carbonates in these rocks are pedogenic in origin. Within the Hueco Group, the Shalem Colony Formation is approximately correlative with the Scholle Member. The Community Pit, Robledo Mountains and lower quarter of the Apache Dam formations are the approximate correlatives of the Cañon de Espinoso Member. The upper portion of the Apache Dam Formation is laterally equivalent to the Yeso Group to the north. The Abo correlatives are considered to be of Wolfcampian age, and the Yeso equivalents of Leonardian age. Conodonts from the lower part of the Robledo Mountains Formation indicate an early Artinskian age for that formation (Lucas et al., 1998). This places the red beds and their floras in a time period variously classified as the end of Permian Glaciation II (Montañez et al., 2007), which is known by its proximate record primarily in western Australia (Fielding et al., 2008).

Fossiliferous red beds occur in one formation of the Hueco Group, the Robledo Mountains. At present, there are no known red-bed floras from the Shalem Colony, Community Pit or Apache Dam formations; floras from a brackish-water carbonate facies in the Community Pit Formation include allochthonous assemblages of walchian coniferophyte logs (Falcon-Lang et al., this volume) and a parautochthonous foliar macroflora (Falcon-Lang et al., submitted; DiMichele et al., this volume) of unique composition and depositional character. Floras are known from the red-bed facies through the entire

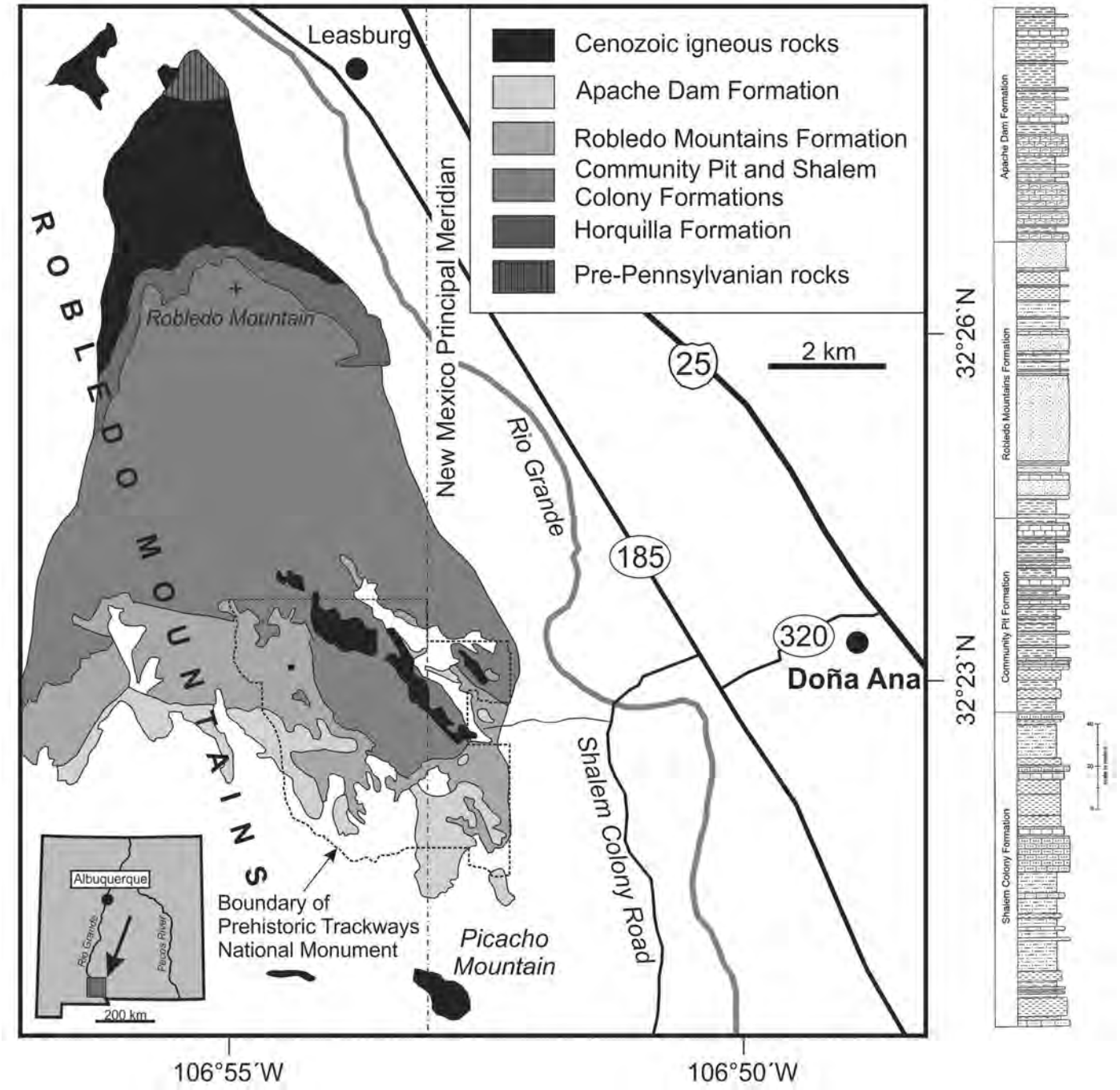


FIGURE 1. Location of the Prehistoric Trackways National Monument in southern New Mexico, within the Robledo Mountains. The fossiliferous red-bed deposits are within the Robledo Mountains Formation.

125 m thickness of the Robledo Mountains Formation.

Where it is best exposed, Robledo Mountains Formation characteristics suggest a strong background of external allogenic controls on large-scale patterns of sedimentation and sea level (Mack and James, 1986). At the highest level there is an alternation of marine and terrestrial facies; distinct red-bed successions, each 5 or more meters in thickness, alternate with marine carbonate beds. The red beds account for about one-third of the entire thickness of the formation and occur in approximately 5-7 discrete intervals (Voigt et al., 2013). Within the red-bed units (Figs. 2.1, 2.2), fluvial sandstone, siltstone and claystone (Mack, 2007) alternate with pedogenic horizons. Sandstone bodies indicate a predominance of sheet flow, with generally southerly flow directions (Voigt et al., 2013). Pedogenic horizons are variously developed, but comprise largely calcic Vertisols of polygenetic character indicative of long periods of surface exposure (Mack et al., 2010). The sandstone-siltstone-claystone layers, particularly where plant macrofossils and ichnofossil assemblages are most common, consist of alternating beds of siltstone to fine sandstone of tabular shape, generally flat bottomed, and thin clay layers, often little more than a few mm in thickness but in places up to several cm (Figs. 2.3, 2.4). The fossils are concentrated in the claystone layers (Fig. 3), but occur in the sandstones and siltstones at some places. The claystone beds show evidence of exposure in the form of mudcracks (Fig. 4), raindrop imprints, and rill marks; trackways of both invertebrates and vertebrates also are common and likely formed on wet exposed surfaces or in shallow water (Braddy, 1998; Lucas and Hunt, 2006; Minter and Braddy, 2009; Voigt et al., 2013). Plant fossils were found in three of the red bed intervals. These intervals account for a total thickness of approximately 25 m. Contacts between the red bed siliciclastics and limestones are abrupt. The carbonates appear to have formed in settings with poor circulation and or high salinity (Voigt et al., 2013). Overall, the features of both the siliciclasitics and carbonates are in conformance

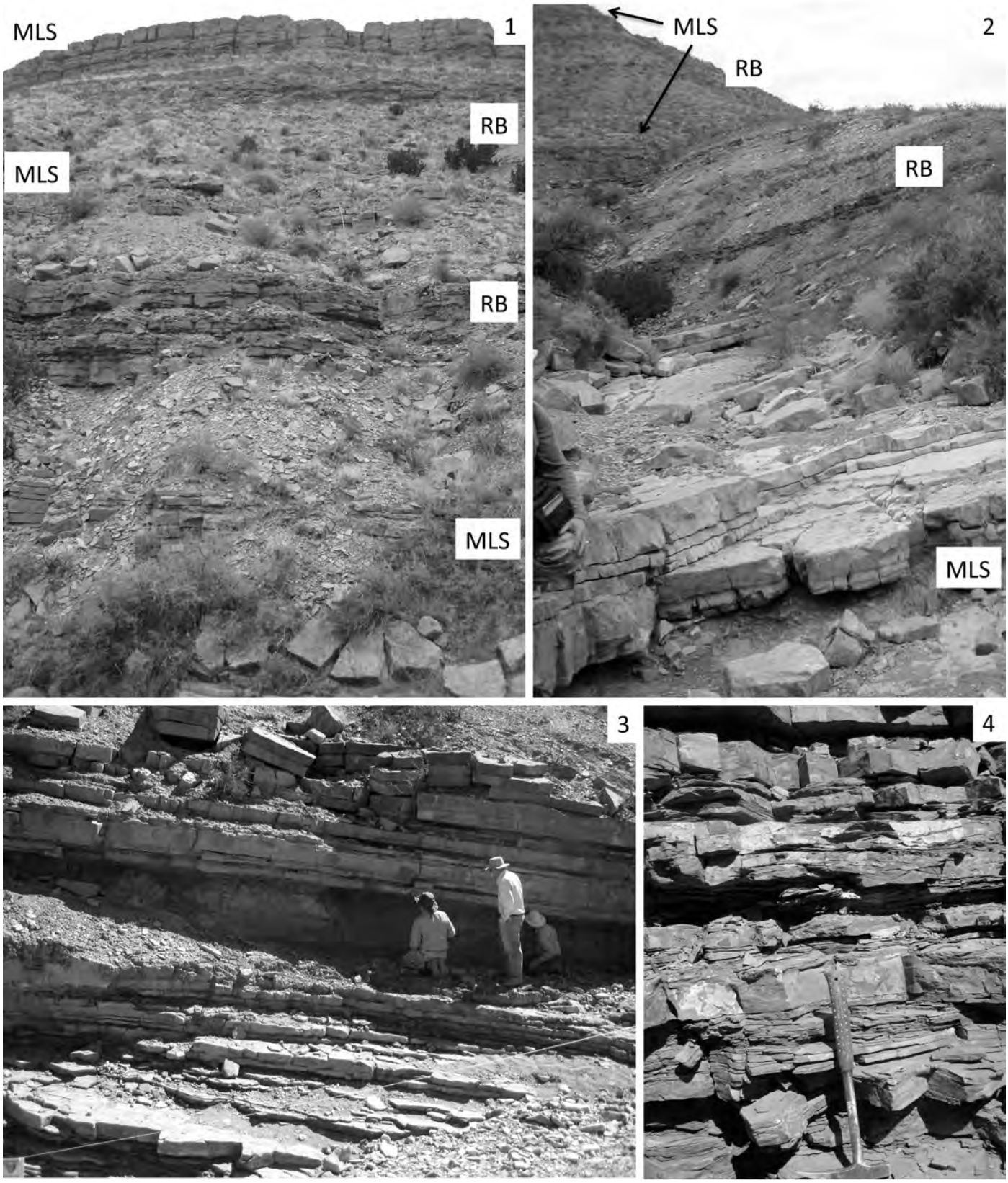


FIGURE 2. Robledo Mountains Formation geology. **2.1,** Branson Canyon, Robledo Mountains Formation, alternating marine carbonates (MLS) and siliciclastic red beds (RB). **2.2,** Branson Canyon, Robledo Mountains Formation, alternating marine carbonates (MLS) and red beds (RB). **2.3,** Branson Canyon, Robledo Mountains Formation, alternating siltstone and claystone beds. **2.4,** Branson Canyon, Robledo Mountains Formation, alternating siltstone and claystone beds; hammer is 40 cm in length.



FIGURE 3. Mat of *Walchia* branches encased in a claystone drape. Branches and branch debris lack preferential orientation and comprise multiple layers. Field photograph. Padded portion of hammer handle is 19 cm in length.

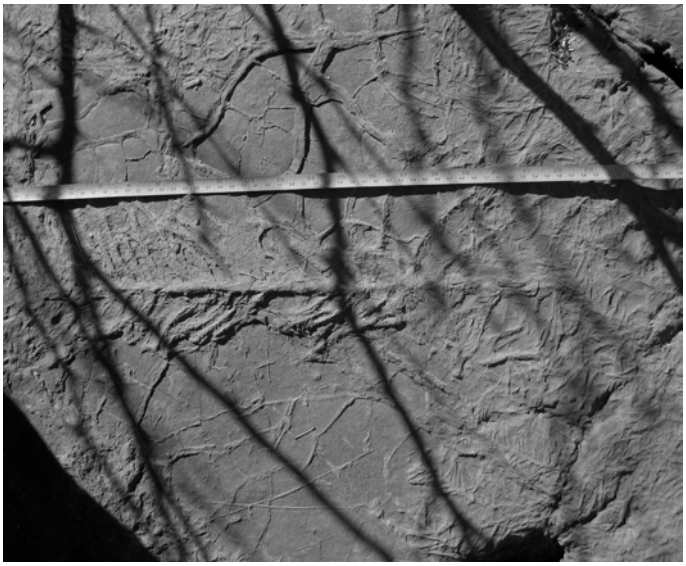


FIGURE 4. *Walchia piniformis* branch and fragmentary remains embedded in a thin claystone layer with mudcracks. Looking up from the bottom. Field photograph. Scale in centimeter and inches.

with a generally hot and dry background climate.

Paleogeographically, the PTNM lies at the southern edge of the Robledo shelf (Fig. 1), between the deeper Orogrande Basin and the Abo coastal plain (Mack et al., 1995; Lucas et al., 2012). In the Robledo Mountains, Hueco Group strata are somewhat transitional between the terrestrial Abo-Yeso strata to the north and the more marine Hueco strata of the Hueco seaway in southern and southeastern New Mexico (Krainer and Lucas, 1995). The alternation of terrestrial red beds and marine carbonates in the Robledo Mountains Formation does not mean, however, that the red bed floras grew in settings fringing the coastline. Physical proximity within a stratigraphic section is not necessarily indicative of physical proximity in space. In fact, the maturity and thickness of many of the paleosols (Mack et al, 2010) suggests long periods of development in a fluvial, floodplain setting, distant from the coastline. Plus, flatness of the landscape could permit significant variations in the marine coverage of the area with relatively minor changes in sea level. The absence or minor representation of fluvial channels in the red bed succession, combined with sheet flood deposits, may reflect the development of distal fan deposits, from which unchannelized or weakly channelized flow proceeded to the coastal regions during wetter periods. Fan deposits correlative with the Robledo Mountains Formation have been documented to the east of the PTNM in the Sacramento Mountains (Lucas et al., 2014). These thin rapidly toward the Hueco seaway, where they are correlative with mudstones and finer sandstones that interfinger with marine rocks. These deposits lend some credence to the possibility of sheet flood sources in nearby tectonically active areas. Such a scenario could account for Abo/Robledo Mountain sheet flood deposits more parsimoniously than crevasse splays from unidentified fluvial channels on the coastal plain (Mack et al., 2010; Voigt et al. 2013).

FOSSIL-PLANT COLLECTIONS

Fossil plants from the Robledo Mountains Formation were collected in eight geographically distinct sites in the PTNM. At a number of these sites, the exposures were areally widespread enough that several sub-collections were made. The informal names applied to these sites, and the collection numbers are listed below (NMMNH-New Mexico Museum of Natural History, USNM-National Museum of Natural History). Exact sites of these areas are on file at the respective museums.

(1) Community Pit: NMMNH 8220, USNM43564
(2) Apache Canyon: USNM43557, USNM43558, USNM43559, USNM43560, USNM43561
(3) Mouth of Apache Canyon: USNM43556
(4) Tributary of Apache Canyon: USNM43555
(5) Discovery Site: USNM43565
(6) Branson Canyon: USNM43575, USNM43576, USNM43577
(7) Apache Dam: USNM43553
(8) Triangle Intersection: USNM43562

The collections, in all cases other than that described by Voigt et al. (2013), are what may be described as "surface collections" – obtained largely from outcrop but with little or no excavation. Even though the plant remains are concentrated in finer grained layers of the siltstone-claystone facies, the rocks are highly indurated and not conducive to excavation with hand tools. Plants are located by surface prospecting to find bedding-plane exposures of sufficient extent that fossiliferous content is revealed. Minor working with hand tools was necessary to extract particular specimens. In many instances, however, plant remains could not be removed from the outcrop surfaces and only photographic documentation was possible (e.g., Fig. 5). Only in exceptional instances, where no fossils in place could be found, were collections made from loose pieces, so-called "float," that could not be connected directly with any particular in situ bed.

RED-BEDS FOSSIL FLORA, PTNM

The fossil flora from the red beds in the PTNM is of low diversity and generally the same from one collecting site to another, with exceptions. In addition, it is closely similar to that found in the Abo Formation in the central and northern parts of New Mexico, wherein there is no proximity to marine conditions (Hunt, 1983; DiMichele et al., 2007, 2013a). The flora is overwhelmingly dominated by the walchian conifer *Walchia piniformis* Sternberg, with some specimens possibly of *Otovicia* (*Walchia*) *hypnoides* (Brongniart) Kerp et al. and a variety of unattributable morphologies. There are minor occurrences of other plants including *Supaia* cf. *thinnfeldioides* White, *Taeniopteris* Brongniart, callipterids, perhaps attributable to *Rhachiphyllum schenckii* Kerp, and an undescribed gigantopterid with venation intermediate between *Gigantopteridium* Koidzumi and *Cathaysiopteris* Koidzumi. There also are rare fragments of fern-like foliage, roots, seeds and polliniferous organs.

Description of a flora from the PTNM is presented in Voigt et al. (2013), from the Community Pit site. Plant fossils, principally conifers, are mentioned in Lucas et al. (1995), Braddy (1998) and DiMichele et al. (2013a), among others. Below we briefly describe the main floral elements of that assemblage specific to the Robledo Mountains red-bed facies, interlayered siltstone-claystone.



FIGURE 5. *Walchia piniformis* branches in a claystone layer above a thicker layer of siltstone. Branches show no preferential orientation. Field photograph. Hammer is 28 cm in length.

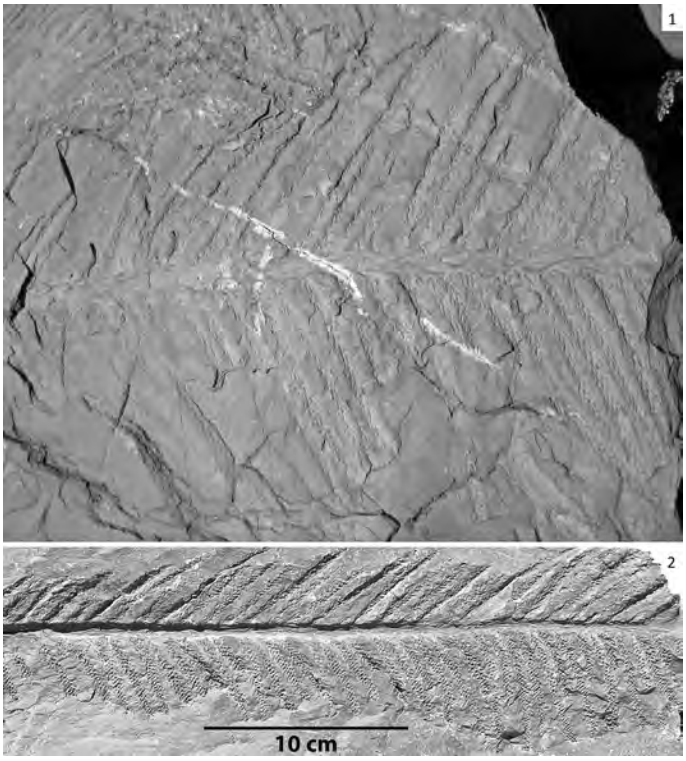


FIGURE 6. *Walchia piniformis*. **6.1**, Large branch showing planate form, typical needle-like, spreading leaves. Discovery Site. Field photograph. USNM locality 43565. **6.2**, Large branch mold, showing planate form and arrangement of foliage. This specimen was found oriented at right angles to bedding in a siltstone, indicating rapid burial and considerable stiffness (possibly due to drying) of the specimen at the time of burial. Insect Hill subsite, Apache Canyon, USNM Specimen 558251, USNM locality 43557. Scale bar = 10 cm.

Walchian Conifers

Walchian conifers are the most abundant plants in the PTNM red-bed floras. It could be stated confidently that they are the overwhelmingly dominant elements of these floras. We assign the most commonly encountered morphotype to *Walchia piniformis*, though the fit with that species is not exact. This form also bears similarity to Morphotype IVA of Looy and Duijnstee (2013), from younger Permian strata in the north-central Texas redbeds. The Robledo Mountains Formation form is characterized by plagotropic branches (Figs. 3-6) of lengths approaching 50 cm. The bases of some branches are consistent with a deciduous-branch habit of the parental tree (Fig. 4) (Looy, 2013). The branches bear elongate, narrow, upturned, acuminate, scoop-like leaves that are not closely adpressed to the parent axis (Fig. 6.2, see also Voigt et al., 2013, their figure 8H). There are less common specimens with small, triangular, adpressed leaves, borne on plagiotropic branches. Such specimens are usually preserved as three-dimensional casts or molds (Figs. 7.2-7.4), which can make their leaves appear to be more adpressed than is, in fact, the case. And some specimens appear to have intermediate morphologies (see Fig. 7.1 – some leaves appear adpressed and others are free and ascendant – at white arrows). These small-leaved forms may be compared with *Otovicia hypnoides* (Kerp et al., 1990), but likely are distinct from that species (Fig. 7). They also bear some similarity to Morphotype II of Looy and Duijnstee (2013). Other kinds of conifer remains are encountered rarely and are likely morphological variants of these two more commonly encountered forms.

Supaia thinnfeldioides

Specimens assignable to *Supaia thinnfeldioides* were found at several sites, but always as isolated, poorly preserved elements (Fig. 8.1). *S. thinnfeldioides* occurs at many other locations in the Abo Formation red beds, often in great abundance (e.g., DiMichele et al., 2007). In the Abo Formation walchian conifers and *Supaia* do not occur together in equal proportions. Generally they are found in completely distinct populations or co-occur as minor elements of the biomass in assemblages dominated by the other form.. It is probable that *Supaia* is a peltasperm (Wang, 1997, 2005). An occurrence elsewhere in the Abo Formation of upright stems in association with *Supaia* foliage suggests a small tree or shrub stature and opportunistic life history, colonizing disturbed sites and living in areas subject to disturbance (DiMichele et al., 2012).

Callipterids

There is only a single specimen reported from the PTNM red beds attributable to the callipterids, a group of peltaspermous seed plants (Kerp, 1988). This specimen, described and illustrated by Voigt et al. (2013, their figure 8I) as callipterid foliage of uncertain affinity is reillustrated here as Figure 8.2. We have found no additional specimens during our collecting and prospecting in the PTNM red beds.

The callipterid identification of Voigt et al. (2013) is consistent with the presence of rachial pinnules and the high-angle venation of the laminate segments. The specimen most closely resembles the genus *Rhachiphyllum* Kerp. This genus is typified by pinnules/laminate portions of the frond that are of flat aspect, have steeply ascending lateral veins, and relatively weakly developed midribs that are superficial on the lamina. In these features, it contrasts sharply with the somewhat similar form *Autunia* Krasser emend Kerp, which also has steeply ascending lateral venation, but in which the pinnule lamina is vaulted, resulting in a sunken, well delimited midvein in the pinnules (Kerp , 1988). *Rhachiphyllum* has not been found in connection or in a statistically demonstrable association with callipterid reproductive organs so, at this time, its peltaspermacean affinity is conjectural, but seems highly likely.

Callipterids are significant components of Early Permian floras throughout Europe (Kerp and Fichter, 1985; Opluštil, 2013) and in the Texas and Oklahoma portions of the southwestern United States (Chaney and DiMichele, 2007; DiMichele et al., 2013b; Tabor et al., 2013). They are not, however, a significant component of Early Permian red-bed floras of the Abo Formation and its correlatives in New Mexico (DiMichele et al., 2013a). Callipterids, particularly *Autunia conferta* (Sternberg) Kerp, are present in these floras, but are rare and have not been found to be abundant at any particular site where they are known to occur. Elsewhere in the PTNM, in the stratigraphically lower Community Pit Formation of the Hueco Group, a flora containing the callipterid *Lodevia oxydata* (Goeppert) Kerp has been found in a channel filled with brackish-water limestone, possibly formed during a period of strongly seasonally dry to xeric conditions (Falcon-Lang et al., this volume; DiMichele et al., this volume). These occurrences, the rarity of callipterids in the red beds, and the extremely unusual occurrence of *Lodevia oxydata* in abundance but in a rarely

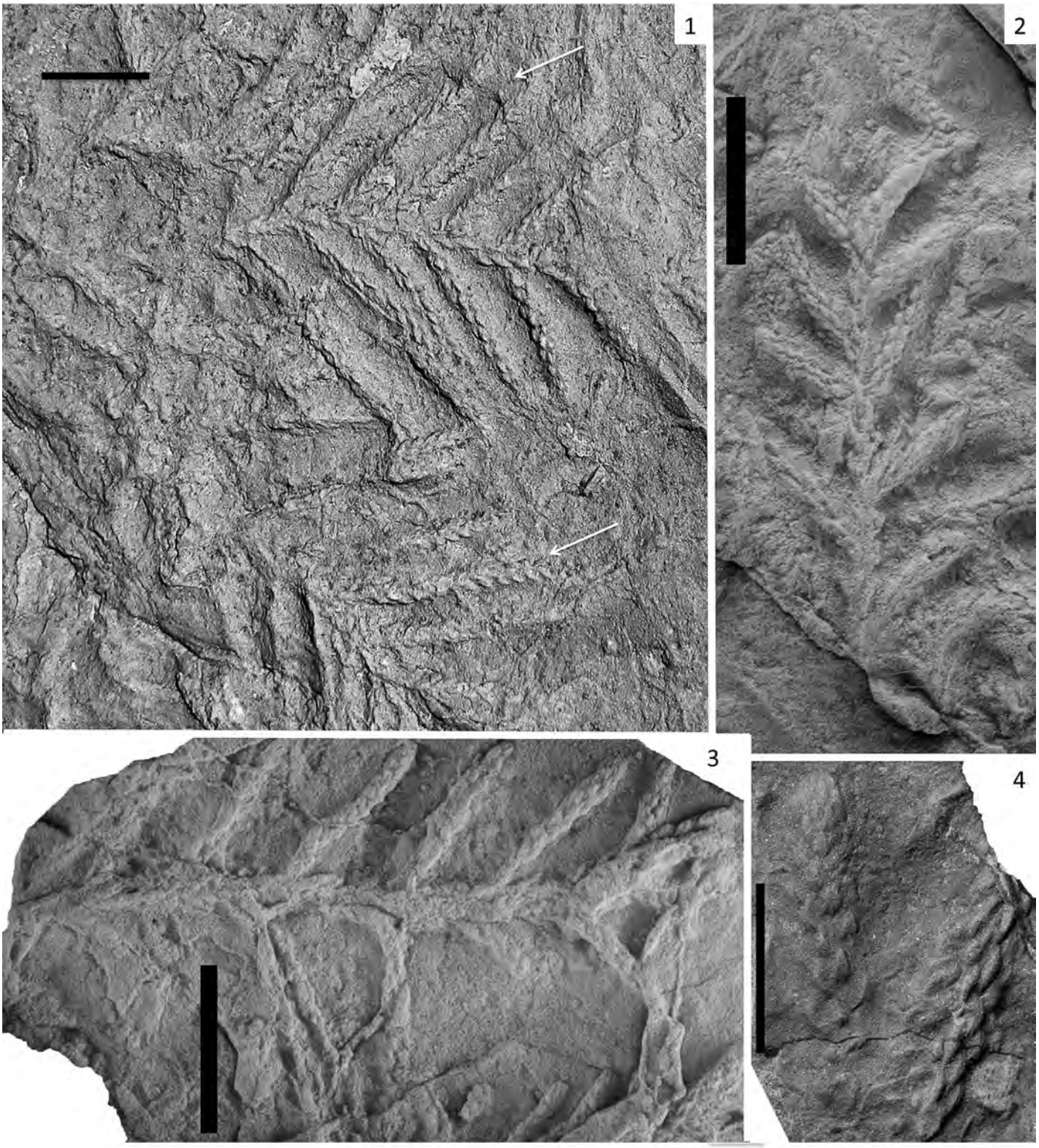


FIGURE 7. cf. *Otovicia hypnoides*. All of these specimens may, in fact, be morphological variants of *Walchia piniformis*. All are characterized my small, triangular, seemingly adpressed leaves (but note specimen illustrated in image 7.1). **7.1**, Branches with variation in foliage morphology ranging between that typical of *W. piniformis* (white arrows) and *O. hypnoides*. Apache Canyon, Field photograph, USNM locality 43559. **7.2**, Very small branch. Apache Canyon, USNM Specimen 596867, USNM locality 43560. **7.3**, Very small branch. Mouth of Apache Canyon, USNM specimen 596872, USNM locality 43556. **7.4**, Branch tip casts. Apache Canyon, USNM Specimen 596869, USNM locality 43560. All scale bars = 1 cm.

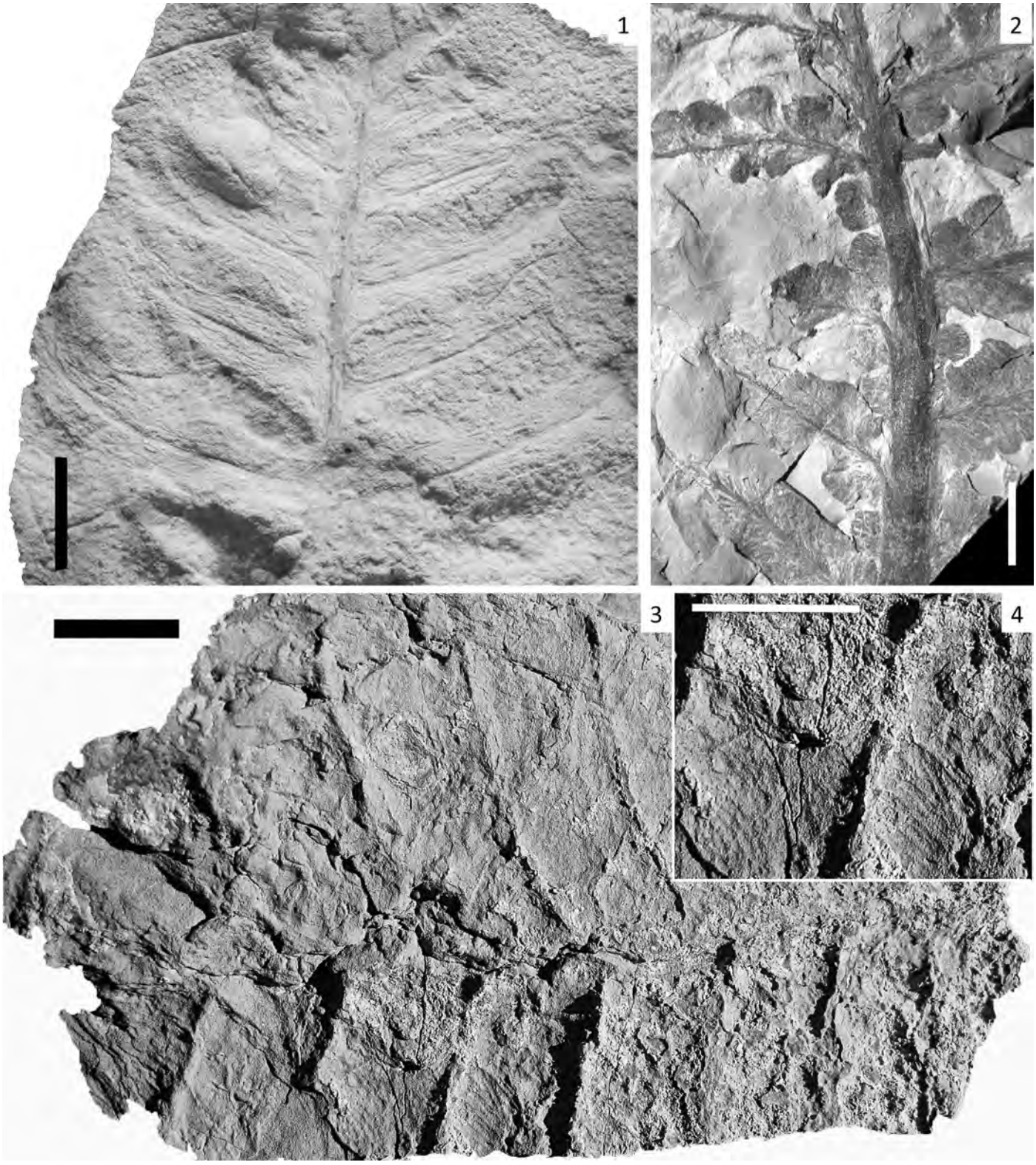


FIGURE 8. Peltasperms. **9.1**, *Supaia thinnfeldioides* with thick lamina obscuring secondary veins. Apache Dam, USNM Specimen 596870, USNM locality 43553. **9.2**, Callipterid, cf. *Rhachiphyllum*. Voigt et al. (2013) Figure 8I. Community Pit, NMMNHS Specimen number NMMNH P-62610. NMMNH locality 8220. **9.3**, *Gigantopteridium*, form with venation intermediate between *Gigantopteridium* and *Cathaysiopteris*. Triangle Intersection, USNM Specimen 558281, USNM locality 43562. **9.4**, Detail of venation in specimen illustrated in 9.3. All scale bars = 1 cm.

encountered depositional setting, indicate that callipterids were part of the Early Permian landscape in western Pangea, but were, for various taphonomic reasons, typically not preserved in the fossil record.

Gigantopterids

Several gigantopterid specimens were found at the Triangle Intersection locality. This is the only occurrence of gigantopterids that we have encountered in any Abo Formation or equivalent red-bed deposits in the course of fieldwork. Similarly, we have not identified gigantopterids in either the NMNH or NMMNH collections from any Abo Formation or equivalent strata. Read and Mamay (1964) report an occurrence of a single fragmentary specimen of "*Gigantopteris*", presumably *Gigantopteridium*, from the Abo Formation near Orogrande, NM, which is in the environs of Alamogordo, and thus, like the PTNM occurrence, in the southern part of the state and Abo outcrop belt. We could not locate any evidence of the specimen in the USNM collections from this site.

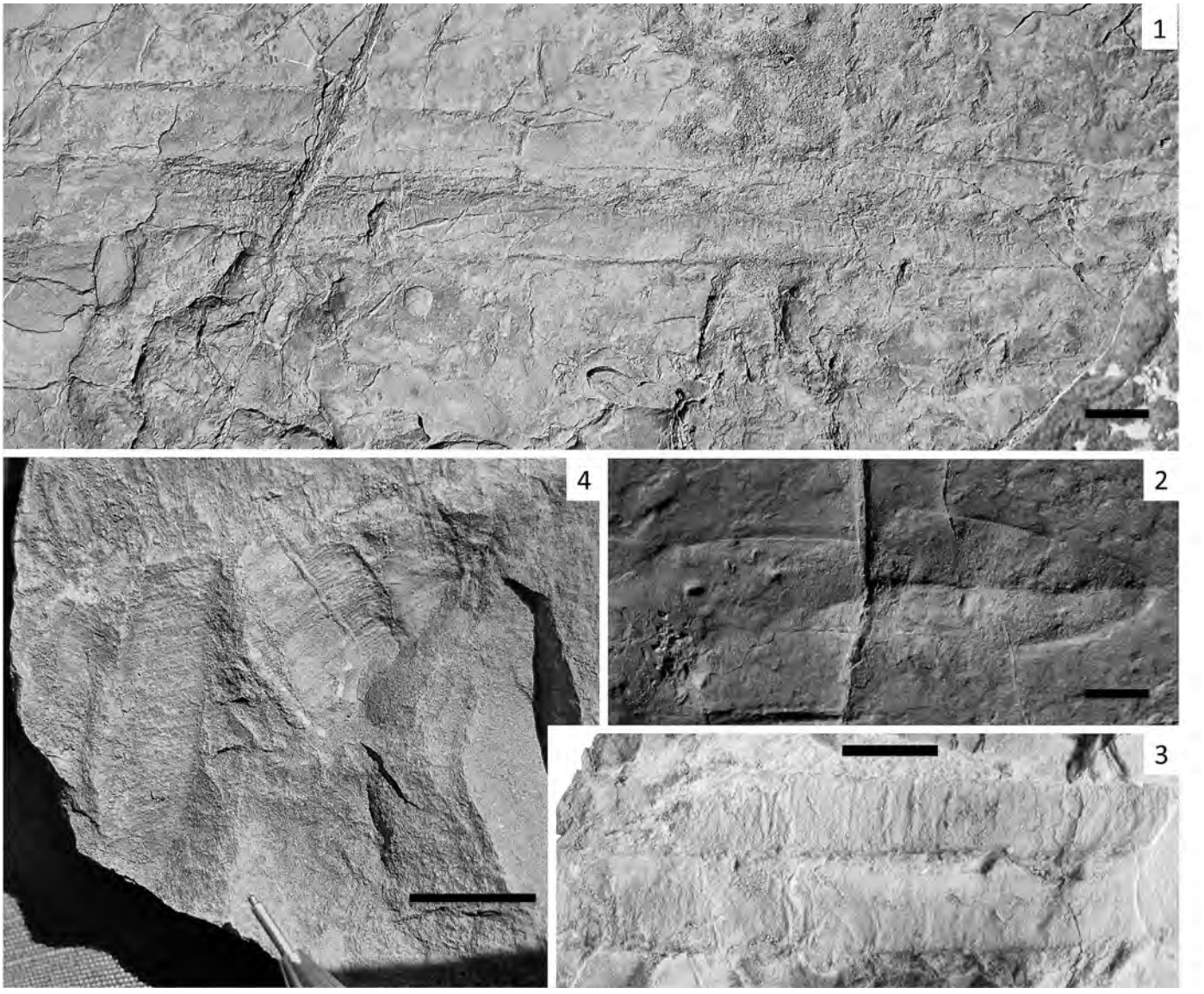
The gigantopterid specimens from the PTNM are poorly preserved in sandstone (Figure 8.3), a lithology in which gigantopterids are commonly preserved, particularly the earliest occurring North American genera *Gigantopteridium* and *Cathaysiopteris*. The PTNM specimens most closely resemble *Gigantopteridium*, but particularly an undescribed form that is somewhat intermediate in its morphology between *Gigantopteridium* and *Cathaysiopteris*. In this form, the tertiary venation is not as well organized into fascicles as in *Gigantopteridium*, but is somewhat more seriate, and suture veins are more prominent than in *Gigantopteridium*, as in *Cathaysiopteris* (Fig. 8.4).

Stratigraphically, in north-central Texas, the first gigantopterids, of the *Gigantopteridium* form, appear around the horizon of the Elm Creek Limestone (Read and Mamay, 1964; Hentz, 1987). The Elm Creek traditionally marks the base of the Leonardian in the north-Texas section (using fususlinids: Myers, 1968), which, based on conodonts, is of early Artinskian age (e.g. Wardlaw, 2005). This is congruent with the age determined for the Robledo Mountains Formation based on conodonts and other marine invertebrates.

Taeniopteris

Taeniopteris is a rare element in the PTNM red-bed floras, as it is in the Abo Formation throughout New Mexico. *Taeniopteris* is not a "natural" genus and includes both ferns and what are suspected to be seed plants (Remy and Remy, 1975). Some of the larger, more robust forms have been suggested to be ancestors of cycads, or of broadly cycadophytic affinity (Mamay, 1976; Gillespie and Pfefferkorn, 1986), though more recent research has brought that interpretation into question (Axsmith et al., 2003). There are many described species of *Taeniopteris*, and the genus was widespread in the equatorial tropics during the Permian, but appears to be significantly less common in the European portions of Euramerica than in the more westerly regions (e.g., Voigt and Röβler, 2004).

The PTNM *Taeniopteris*, to the extent that can be determined from the few preserved fragments, is predominantly of one kind, a narrow, elongate form with long, tapering terminal portions (Fig. 9.1), bluntly rounded apices (Fig. 9.2), leathery texture (Fig. 9.3) and secondary venation that is seriate and makes a right angle with the midvein or may be slightly inclined toward the apex of the leaf (acroscopically) (Fig. 9.4). At one site, Mouth of Apache Canyon, high in the Robledo



Mountains Formation, *Taeniopteris* is the dominant element. Voigt et al. (2013) illustrated a fragmentary specimen with similar morphology from stratigraphically low in the formation (re-illustrated here as Fig. 9.2).

Miscellaneous Plant Remains

There are several occurrences of unattributable reproductive organs or vegetative remains in the PTNM red-bed collections. These include clusters of what appear to be sporangia of a type not found at other localities throughout the Abo Formation (Fig. 10.1). These organs were found at the Mouth of Apache Canyon locality, solely in association with *Taeniopteris* of a narrow form. Seeds are extremely rare in Abo Formation floras and this is equally true in the Robledo Mountains Formation. Voigt et al. (2013, their figure 8F) reported small, winged seeds of a walchian-conifer-type, reillustrated here as Figure 10.2. These are very similar to seeds associated with conifer cones from some Early Permian localities in north-central Texas (Chaney, personal observation) and similar seeds have been described for other walchians by Rothwell et al. (2005).

The presence of upright stems, buried in flood sediments, has rarely been reported in Abo strata and their equivalents. Voigt et al. (2013, their figure 5C) illustrate a longitudinal section through a stem of approximately 1 cm diameter from the lower Robledo Mountains Formation, reillustrated here as Figure 10.3. Mack et al. (2010) also mention, but do not illustrate, small, upright stems in association with buried paleosol surfaces, also in what can be inferred to be the Robledo Mountains Formation (they use different stratigraphic terminology). These reported stems are congruent in size and depositional setting with stems reported in association with *Supaia* foliage and tetrapod trackways from the Abo Formation in the vicinity of the Mud Springs Mountains, near Truth or Consequences, NM (DiMichele et al., 2012).

Fossil roots of fibrous character occur throughout the Robledo Mountains Formation at various locations in red-bed siltstones.

DISCUSSION

The flora of the Lower Permian red beds in PTNM is compositionally closely similar to that of the corrrelative Abo Formation found throughout the central portion of New Mexico (DiMichele et al., 2013a). The dominant elements of the flora are walchian conifers, of a form similar to *Walchia piniformis*, found most often in low diversity assemblages lacking other kinds of plants. Although present in the PTNM, the probable peltasperm *Supaia* is quite rare; elsewhere, in the Abo Formation, *Supaia* is locally abundant and dominates low diversity fossil assemblages that commonly lack conifers (e.g., DiMichele et al., 2007). The patterns of distribution and relatively rare co-occurrence of these plants suggest spatial separation of their populations on the original landscape. Other rare elements in the Robledo Mountains Formation flora, such as *Taeniopteris*, callipterids, and gigantopterids, are equally rare throughout the Abo Formation.

The PTNM red-bed floras of the Robledo Mountains Formation are of significance because they occur within a mixed marine-terrestrial stratigraphic sequence. The close proximity of marine strata has led to interpretations of the Hueco terrestrial red beds as tidal flats (e.g., Mack and James, 1986; Lucas et al., 1995; Minter et al., 2006; Minter and Braddy, 2009). This has been reassessed recently based on studies of paleosols (Mack et al., 2010) and on detailed sedimentological analysis of the terrestrial siliciclastics in combination with analysis of ichofossil assemblages, neither of which are of peritidal character (Voigt et al., 2013). These more recent studies suggest that the terrestrial red beds represent distal, coastal floodplain settings characterized by sheet-flood crevasse splays and mud-dominated overbank deposits that formed under a seasonally dry climatic regime (Mack et al., 2010). The larger scale alternation of terrestrial and marine rocks is suggestive of allogenic drivers (Mack, 2007;Mack et al., 2010), possibly Southern Hemisphere ice-volume fluctuations during the waning of Permian Glacial II in the late Artinskian (Montañez et al., 2007).

From a paleobotanical viewpoint, the Robledo Mountains Formation simply exacerbates the enigma of the low-diversity and monotonous composition of the flora of the Early Permian siliciclastic red beds. Here, in an interval characterized by interbedded marine and terrestrial strata, there are no detectable differences in the floristic composition from coeval strata to the north that experienced no detectable marine influence. The red-bed facies extends from northern New Mexico, in the Zuni Mountains, to the southern portions of the state, bordering the Hueco seaway, where interbedded red beds and carbonate rocks have been designated the Hueco Group and encompass the Robledo Mountains Formation. Throughout this vast area, the composition of the flora of the Abo Formation and equivalent strata is the closely similar (Hunt, 1983; DiMichele et al., 2007, 2013a). The dominant plants at most sites are walchian conifers, generally attributable to *Walchia piniformis*, but also to other taxa, and locally deposits may be found that are dominated by *Supaia thinnfeldioides*.

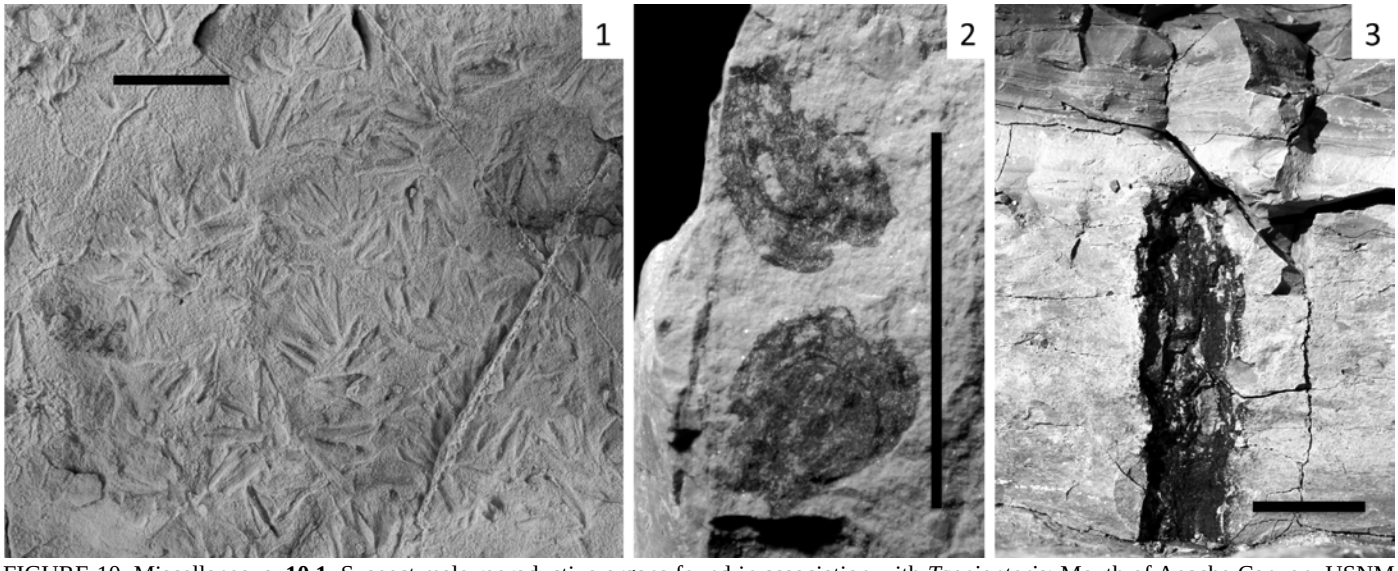


FIGURE 10. Miscellaneous. **10.1**, Suspect male reproductive organs found in association with *Taeniopteris*; Mouth of Apache Canyon, USNM Specimen 596873, USNM locality 43556. **10.2**, Winged, playspermic seeds of a form commonly found in association with conifer remains, Voigt et al. (2013) Figure 8F. Community Pit, NMMNHS Specimen number NMMNH P-62502. NMMNH locality 8220. **10.3**, Small upright stem similar to stems attributed to *Supaia* by DiMichele et al. (2012), Voigt et al. (2013, figure 5C). Community Pit. Field photograph, NMMNH locality 8220. All scale bars = 1 cm.

FIGURE 9 (facing page). *Taeniopteris*. **8.1**, General shape, elongate, gradually tapering toward the apex. Mouth of Apache Canyon, USNM Specimen 596871, USNM locality 43556. **8.2**, Blunt tip. Voigt et al. (2013) Figure 8C. Community Pit, NMMNHS Specimen number NMMNH P-62607. NMMNH locality 8220. **8.3**, Thick, probably xeromorphic lamina. Mouth of Apache Canyon, USNM Specimen 596874, USNM locality 43556. **8.4**, Secondary venation at nearly right angles to the midvein. Mouth of Apache Canyon, USNM Specimen 558417, USNM locality 43556. All scale bars = 1 cm.

Other plants clearly were part of this assemblage, indicated by scattered, rare occurrences of various taxa, nearly all seed plants of xeromorphic morphology. Yet there are other facies within the Abo Formation and correlatives. These include those composed of gray shales and sandstones (e.g., Lucas 2012a, b) that contain quite different, more diverse floras that include a significant component of lower vascular plants and medullosan seed ferns, or a unique flora preserved in limestones composed of voltzian coniferophytes and callipterids (DiMichele et al., this volume). Equivalent age floras from farther to the east, along the paleoequator, also are significantly more diverse and less dominated by conifers than the Abo red-bed floras (e.g., Chaney and DiMichele, 2007; Tabor et al., 2013). Thus, the Abo red beds stand out regionally as encompassing a peculiar plant assemblage, both in terms of diversity and composition.

There are no clearly identifiable taphonomic filters that might have created a so-called megabias (Behrensmeyer et al., 2000) in the formation of these fossil assemblages. It appears that the environments represented by the Abo red beds were indeed populated by vast forests of conifers, as suggested by the fossil assemblages. Locally, particularly in areas of disturbance, stands of small *Supaia* plants were abundant. Within this landscape there also were populations of a few other kinds of plants, particularly callipterids and taeniopterids, though nowhere have these plants been found in abundance. To date, gigantopterids have only been found in areas bordering the Hueco seaway, but the number of occurrences is so small that this cannot be taken as statistically meaningful. Ground cover plants have rarely been identified and are confined to small ferns and sphenophylls, which may suggest selective preservation of arborescent taxa. Thus, the Robledo Mountains Formation floras from the PTNM strengthen the interpretation that floras from the Early Permian New Mexico red beds are unique among known Early Permian assemblages from the Pangean equatorial regions.

ACKNOWLEDGMENTS

We thank Jerry MacDonald of Las Cruces, New Mexico for his kind guidance and assistance with many aspects of this project. The fieldwork on which this study is based was supported by a grant from the US Bureau of Land Management, and they are gratefully acknowledged. We thank Scott Elrick, Howard Falcon-Lang, Karl Krainer, Vincent “Skip” Lyles, John Nelson, Mary Parrish, Larry Rinehart and Justin Speilmann for their assistance in the field. B. Mitchell Blake, Jr. and Martin Gibling are thanked for their helpful comments on an earlier version of this manuscript.

REFERENCES

Axsmith, B. J., Serbet, R., Krings, M., Taylor, T. N., Taylor, E. L. and Mamay, S. H., 2003, The enigmatic Paleozoic plants *Spermopteris* and *Phasmatocycas* reconsidered: American Journal of Botany, v. 90, p. 1585-1595.

Behrensmeyer, A.K., Kidwell, S.M. and Gastaldo, R.A., 2000, Taphonomy and paleobiology: Paleobiology, p. 103-147.

Braddy, S. J., 1998, An overview of the invertebrate ichnotaxa from the Robledo Mountains ichnofauna (Lower Permian), southern New Mexico: New Mexico Museum of Natural History and Science, Bulletin 12, p. 93-98.

Cecil, C. B., 1990, Paleoclimate controls on stratigraphic repetition of chemical and siliciclastic rocks: Geology, v. 18, p. 533-536.

Cecil, C.B., Stanton, R.W., Neuzil, S.G., Dulong, F.T., Ruppert, L.F. and Pierce, B.S., 1985, Paleoclimate controls on late Paleozoic sedimentation and peat formation in the central Appalachian Basin (USA): International Journal of Coal Geology, v. 5, p. 195-230.

Chaney, D.S. and DiMichele, W.A., 2007, Paleobotany of the classic redbeds (Clear Fork Group – Early Permian) of north central Texas: Proceedings of the XVth International Congress on Carboniferous and Permian Stratigraphy, p. 357-366.

DiMichele, W.A., Kerp, H., Krings, M. and Chaney, D.S., 2005, The Permian peltasperm radiation: Evidence from the southwestern United States: New Mexico Museum of Natural History and Science, Bulletin 30, p. 67-79.

DiMichele, W.A., Chaney, D.S., Nelson, W.J., Lucas, S.G., Looy, C.V., Quick, K. and Jun, W., 2007, A low diversity, seasonal tropical landscape dominated by conifers and peltasperms: Early Permian Abo Formation, New Mexico: Review of Palaeobotany and Palynology, v. 145, p. 249-273.

DiMichele, W.A., Lucas, S.G. and Krainer, K., 2012, Vertebrate trackways among a stand of *Supaia* White plants on an Early Permian floodplain, New Mexico: Journal of Paleontology, v. 86, p. 584-594.

DiMichele, W.A., Chaney, D.S., Lucas, S.G., Kerp, H. and Voigt, S., 2013a, Flora of the Lower Permian Abo Formation redbeds, western equatorial Pangea: New Mexico: New Mexico Museum of Natural History and Science, Bulletin 59, p. 265-287.

DiMichele, W.A., Kerp, H., Sirmons, R., Fedorko, N., Skema, V., Blake Jr, B.M. and Cecil, C.B., 2013b, Callipterid peltasperms of the Dunkard Group, Central Appalachian Basin: International Journal of Coal Geology, v. 119, p. 56-78.

DiMichele, W.A., Chaney, D.S., Falcon-Lang, H.W., Kerp, H., Looy, C.V., Lucas, S.G., Krainer, K. and Voigt, S., 2014, A compositionally unique voltzian conifer-callipterid flora from a carbonate-filled channel, Lower Permian, Robledo Mountains, New Mexico, and its broader significance: New Mexico Museum of Natural History and Science Bulletin, this volume.

Falcon-Lang, H. J., Kurzawe, F. and Lucas, S. G., 2014, Coniferopsid tree trunks preserved in sabkha facies in the Permian (Sakmarian) Community Pit Formation in south-central New Mexico, USA: Systematics and palaeoecology: Review of Palaeobotany and Palynology, v. 200, p. 138-160.

Falcon-Lang, H.J., DiMichele, W.A., Kurzawe, F., Looy C.V., Lucas, S.G., Chaney D.S., Contreras, D.L., Elrick, S.D., Kerp, H., Krainer, K., Nelson, W.J. and Vachard, D., submitted, Vegetation of an early Permian (Asselian) seasonally dry coast in western equatorial Pangaea: palaeoecology and evolutionary significance: Palaeogeography, Palaeoclimatology, Palaeoecology.

Fielding, C.R., Frank, T.D. and Isbell, J.L., 2008, The late Paleozoic ice age—A review of current understanding and synthesis of global climate patterns: Geological Society of America, Special Paper 441, p. 343-354.

Gillespie, W.H. and Pfefferkorn, H.W., 1986, Taeniopterid lamina on *Phasmatocycas* megasporophylls (Cycadales) from the Lower Permian of Kansas, U.S.A.: Review of Palaeobotany and Palynology, v. 49, p. 99-116.

Hentz, T.F., 1988, Lithostratigraphy and paleoenvironments of upper Paleozoic continental red beds, north-central Texas: Bowie (new) and Wichita (revised) Groups: Texas Bureau of Economic Geology, Report of Investigations 170, p. 1-49.

Hunt, A., 1983, Plant fossils and lithostratigraphy of the Abo Formation (Lower Permian) in the Socorro area and plant biostratigraphy of Abo red beds in New Mexico: New Mexico Geological Society, Guidebook 34, p. 157-163.

Kerp, H., 1996, Post-Variscan late Palaeozoic Northern Hemisphere gymnosperms: The onset to the Mesozoic: Review of Palaeobotany and Palynology, v. 90, p. 263-285.

Kerp, H. and Fichter, J., 1985, Die Makrofloren des saarpfälzischen Rotliegenden (? Ober-Karbon-Unter-Perm; SW-Deutschland): Mainzer Geowissenschaftliche Mitteilungen, v. 14, p. 159-286.

Kerp, J.H.F., 1988, Aspects of Permian palaeobotany and palynology. X. The West- and Central European species of the genus *Autunia* Krasser emend. Kerp (Peltaspermaceae) and the form-genus *Rhachiphyllum* Kerp (callipterid foliage): Review of Palaeobotany and Palynology, v. 54, p. 249-360.

Kerp, J.H.F. and Haubold, H., 1988, Aspects of Permian palaeobotany and palynology. VIII. On the reclassification of the West-and central European species of the form-genus *Callipteris* Brongniart 1849: Review of Palaeobotany and Palynology, v. 54, p. 135-150.

Kerp, J.H.F., Poort, R.J., Swinkels, H.A.J.M. and Verwer, R., 1990, Aspects of Permian palaeobotany and palynology. IX. Conifer-dominated Rotliegend floras from the Saar-Nahe Basin (? Late Carboniferous-Early Permian; SW-Germany) with special reference to the reproductive biology of early conifers: Review of Palaeobotany and Palynology, v. 62, p. 205-248.

Krainer, K. and Lucas, S.G., 1995, The limestone facies of the Abo–Hueco transitional zone in the Robledo Mountains, southern New Mexico: New Mexico Museum of Natural History and Science, Bulletin 6, p. 33-38.

Looy, C. V., 2013, Natural history of a plant trait: Branch-system abscission in Paleozoic conifers and its environmental, autecological, and ecosystem implications in a fire-prone world: Paleobiology, v. 39, p. 235-252.

Looy, C.V. and Duijnstee, I.A., 2013, Characterizing morphologic variability in foliated Paleozoic conifer branches – A first step in testing its potential as proxy for taxonomic position: New Mexico Museum of Natural History and Science, Bulletin 60, p. 215-223.

Lucas, S.G. and Hunt, A.P., 2006, Permian tetrapod footprints: biostratigraphy and biochronology; *in* Lucas, S. G., Cassinis, G. and Schneider, J. W., eds., Non-Marine Permian biostratigraphy and biochronology: Geological Society, London, Special Publications 265**,** p. 179–200.

Lucas, S.G., Heckert, A.B., Estep, J.W., Hunt, A.P. and Anderson, O.J., 1998, Stratigraphy, paleontology and depositional environments of the Lower Permian Robledo Mountains Formation of the Hueco Group, Robledo Mountains, New Mexico: New Mexico Museum of Natural History and Science, Bulletin 12, p. 29–41.

Lucas, S.G., Krainer, K. and Colpitts, R.M., Jr., 2005, Abo-Yeso (Lower Permian) stratigraphy in central New Mexico: New Mexico Museum of Natural History and Science, Bulletin 31, p. 101-117.

Lucas, S.G., Krainer, K., Chaney, D.S., DiMichele, W.A., Voigt, S., Berman, D.S and Henrici, A.C., 2012a, The Lower Pemian Abo Formation in the Fra Cristobal and Caballo Mountains, Sierra County, New Mexico: New Mexico Geological Society, Guidebook 63, p. 345-376.

Lucas, S.G., Harris, S.K., Spielmann, J.A., Berman, D.S, Henrici, A.C., Krainer, K., Rinhart, L.F., DiMichele, W.A., Chaney, D.S. and Kerp, H., 2012b, Lithostratigraphy, paleontology, biostratigraphy and age of the upper Paleozoic Abo Formation near Jemez Springs, northern New Mexico, USA: Annals of the Carnegie Museum, v. 80, p. 323-350.

Lucas, S.G., Krainer, K., Chaney, D.S., DiMichele, W.A., Voigt, S., Berman, D.S and Henrici, A.C., 2013, The Lower Permian Abo Formation in central New Mexico: New Mexico Museum of Natural History and Science, Bulletin 59, p. 161-180.

Lucas, S.G., Krainer, K., Voigt, S., Berman, D.S and Henrici, A., 2014, The Lower Permian Abo Formation in the northern Sacramento Mountains, southern New Mexico. New Mexico Geological Society, Guidebook 65, p. 287-302.

Mack, G. H., 2007, Sequence stratigraphy of the Lower Permian Abo Member in the Robledo and Doña Ana Mountains near Las Cruces, New Mexico: New Mexico Geology, v. 29, p. 3-12.

Mack, G.H. and James, W.C., 1986, Cyclic sedimentation in the mixed siliciclastic-carbonate Abo–Hueco transitional zone (Lower Permian), southwestern New Mexico: Journal of Sedimentary Petrology, v. 56, p. 635–647.

Mack, G. H., Lawton, T. F. and Sherry, C. R., 1995, Fluvial and estuarine depositional environments of the Abo Formation (Early Permian), Caballo Mountains, south-central New Mexico: New Mexico Museum of Natural History and Science, Bulletin 6, p. 181-187.

Mack, G.H., Tabor, N.J. and Zollinger, H.J., 2010, Palaeosols and sequence stratigraphy of the Lower Permian Abo Member, south-central New Mexico, USA: Sedimentology, v. 57, p. 1566-1583.

Mamay, S.H., 1976, Paleozoic origin of the cycads: U.S. Geological Survey, Professional Paper 934, p. 1-48.

Minter, N. and Braddy, S., 2009, Ichnology of an Early Permian intertidal flat: The Robledo Mountains Formation of southern New Mexico, USA: Palaeontological Association Special Papers in Palaeontology, v. 82, p 1-107.

Minter, N., Buatois, L., Lucas, S., Braddy, S. and Smith, J., 2006, Spiral-shaped graphoglyptids from an Early Permian intertidal flat: Geology, v. 34, p. 1057-1060.

Montañez, I. P., Tabor, N. J., Niemeier, D., DiMichele, W. A., Frank, T. D., Fielding, C. R., Isbell, J.L., Birgenheier, L.P. and Rygel, M. C., 2007, CO_2-forced climate and vegetation instability during Late Paleozoic deglaciation: Science 315, p. 87-91.

Myers, D. A., 1968, *Schwagerina crassitectoria* Dunbar and Skinner, 1937, a fusulinid from the upper part of the Wichita Group, Lower Permian, Coleman County, Texas: U.S. Geological Survey, Professional Paper 600-B, p. 133-139.

Opluštil, S., Šimůnek, Z., Zajíc, J. and Mencl, V., 2013, Climatic and biotic changes around the Carboniferous/Permian boundary recorded in the continental basins of the Czech Republic: International Journal of Coal Geology, v. 119, p. 114-151.

Read, C.B. and Mamay, S.H., 1964, Upper Paleozoic floral zones andfloral provinces of the United States: U.S. Geological Survey, Professional Paper 454K, p. 1-35.

Remy, W. and Remy, R., 1975, Beitrage zur Kenntnis des Morpho-Genus *Taeniopteris* Brongniart: Argumenta Palaeobotanica, v. 4, p. 31-37.

Rothwell, G.W., Mapes, G. and Hernandez-Castillo, G.R., 2005, *Hanskerpia* gen. nov. and phylogenetic relationships among the most ancient conifers (Voltziales): Taxon, v. 54, p. 733-750.

Tabor, N.J. and Poulsen, C.J., 2008, Palaeoclimate across the Late Pennsylvanian–Early Permian tropical palaeolatitudes: a review of climate indicators, their distribution, and relation to palaeophysiographic climate factors: Palaeogeography, Palaeoclimatology, Palaeoecology, v. 268, p. 293-310.

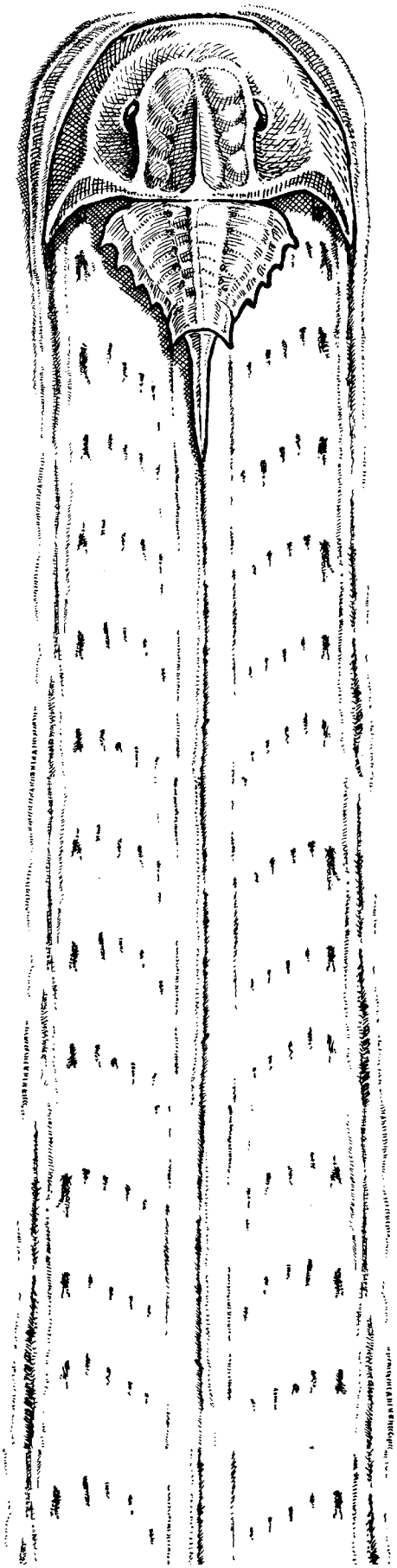
Tabor, N. J., DiMichele, W. A., Montañez, I. P. and Chaney, D. S., 2013, Late Paleozoic continental warming of a cold tropical basin and floristic change in western Pangea: International Journal of Coal Geology, v. 119, p. 177-186.

Voigt, S. and Röβler, R., 2004, Taeniopterid-type leaf fragments – the first record of macrophytic remains from the Eisenach Formation (Rotliegend, Permian, Thuringian Forest): Hallesches Jahrbuch für Geowissenschaften, v. 18B, p. 27-37.

Voigt, S., Lucas, S. G. and Krainer, K., 2013, Coastal-plain origin of trace-fossil bearing red beds in the Early Permian of Southern New Mexico, USA: Palaeogeography, Palaeoclimatology, Palaeoecology, v. 369, p. 323-334.

Wang, Z.Q., 1997, Permian *Supaia* frond and an associated *Autunia* fructification from Shanxi, China: Palaeontology, v. 40, p. 24–277.

Wardlaw. B.R., 2005, Age assignment of the Pennsylvanian-Permian succession of north central Texas: Permophiles, no. 46, p. 21-22.



Lucas, S. G. and DiMichele, W. A., eds., 2015, Carboniferous-Permian Transition in the Robledo Mountains, Southern New Mexico. New Mexico Museum of Natural History and Science Bulletin 65.

A *SELENICHNITES* ICHNOASSOCIATION FROM EARLY PERMIAN TIDAL FLATS OF THE PREHISTORIC TRACKWAYS NATIONAL MONUMENT OF SOUTH-CENTRAL NEW MEXICO

ALLAN J LERNER AND SPENCER G. LUCAS

New Mexico Museum of Natural History and Science, 1801 Mountain Road N.W., Albuquerque, New Mexico 87104 USA

Abstract—A newly recognized local ichnoassociation containing vertebrate and invertebrate ichnotaxa from near the eastern border of the Prehistoric Trackways National Monument in south-central New Mexico, USA, is stratigraphically high in the Lower Permian Robledo Mountains Formation in a siliclastic facies that was deposited paralic to the Hueco seaway. Specimens were collected both in situ and as float blocks from a sandstone bed exposed in the adjacent flagstone quarry known as the Community Pit. The vertebrate ichnotaxa of this ichnoassociation include *Characichnos* isp. and *Undichna unisulca*. The invertebrate ichnotaxa are *Cochlichnus anguineus*, *Helminthopsis hieroglyphica*, *Kouphichnium* isp. and *Selenichnites rossendalensis*. This is the first record of *S. rossendalensis* from New Mexico. This ichnoassociation formed subaqueously in two differing nearshore settings: (1) a lower energy setting that contains relatively abundant *Selenichnites* and (2) a higher energy setting, in which *Selenichnites* is scarce but pot casts are common. The low energy setting seen at the in situ locality may have served as a nursery area for paleolimulids (*Paleolimulus*). The higher energy setting is preserved on float blocks collected from the Community Pit. These blocks contain allochthonous bivalves and possible storm indicators (pot casts), which are not found at the in situ locality. The ichnogeneric composition and depositional settings of this local *Selenichnites* ichnoassociation distinguish it from those well-known nonmarine Robledo Mountain Formation red bed ichnoassemblages that formed on the distal parts of an extensive coastal plain.

INTRODUCTION

The Prehistoric Trackways National Monument (PTNM) near Las Cruces, in Doña Ana County, south-central New Mexico (Fig. 1), encompasses scientifically important sedimentary deposits containing Early Permian vertebrate and invertebrate trace fossils (Lucas and Heckert, 1995; Lucas et al., 1995, 1998; Minter and Braddy, 2009). These ichnoassemblages were formed on a vast coastal plain along part of the Pangean near-equatorial and tropical shoreline during the early Leonardian (see Lucas et al., this volume). We add to this record by describing and discussing a newly recognized local *Selenichnites* ichnoassociation. The ichnogeneric composition and nearshore depositional setting of this ichnoassociation distinguish it from the well-known nonmarine Robledo Mountains Formation red-bed ichnoassemblages that are now considered to have formed on the distal parts of an extensive coastal floodplain (Voigt et al., 2013).

The referred specimens in this paper are in the collection of the New Mexico Museum of Natural History and Science (NMMNH) in Albuquerque, New Mexico. The ichnofossils described here were collected in place at NMMNH locality 8641 and as float blocks from a lithofacies exposed by rock quarrying in the nearby Community Pit (NMMNH localities 7966, 7967, 7968, 7982), a now abandoned flagstone quarry adjacent to the PTNM.

STRATIGRAPHIC CONTEXT

The ichnofossils discussed in this paper occur approximately in the middle of an 11.3-m-thick succession of red beds intercalated in bedded limestone in the upper part of the Robledo Mountains Formation (Fig. 2) in the Robledo Mountains. The ichnofossils from locality 8641, which produced the majority of the referred specimens, are preserved on reddish brown mud-draped sandstone slabs as positive hyporelief impressions.

The strata immediately below the productive level are brownish and red micaceous, ripple-laminated sandstone (Fig. 2, unit 69). Overlying strata are red, coarse-grained siltstone to fine-grained sandstone and red micaceous shale (units 70-71). The main sedimentary structure of one of the uppermost fine-grained sandstone horizons (unit 69) is ripple-drift cross lamination. The referred ichnofossils are found at the base a sandstone that is thinly laminated.

Siliciclastic red beds in the Robledo Mountains Formation have generally been interpreted as tidal flat deposits (e.g., Mack and James, 1986; Lucas et al., 1995). In this interpretation, the mudstones and ripple-laminated sandstones in our measured section represent the "ripple laminated sandstone facies" and "mixed sandstone-shale facies" of Mack and James (1986). According to Mack and James (1986) the ripple-laminated sandstones were deposited on intertidal sand flats near mean low tide.

However, according to Voigt et al. (2013), trace-fossil bearing red beds of the Robledo Mountains Formation were deposited in the distal parts of an extensive coastal flood plain during alternating dry and wet climatic conditions, with little to no marine influence. Flaser- to wavy-bedded siltstone and fine-grained sandstone were interpreted to represent distal crevasse splay deposits. Most of the trace fossils in the Robledo Mountains Formation occur on mud-draped bedding planes of this lithofacies. The red-bed intervals generally do not show any evidence of marine or tidal influence, but the ichnoassemblage documented here (Figs. 3-7) is an exception.

SYSTEMATIC INVERTEBRATE ICHNOLOGY

Ichnogenus *Cochlichnus* Hitchcock, 1858
Cochlichnus anguineus Hitchcock, 1858
Fig. 6A

Referred specimens: P-68502, P-68503, P-68476, P-64533, P-64535, P-70232.

Description: The referred specimens are preserved as horizontal, smooth, non-branching, regularly sinusoidal burrows. The diameters of these specimens vary from 0.5 to 1.0 mm, and show sine curves with a wavelength of 2 mm and an amplitude of 1 mm. Specimen lengths extend upward to 26 mm. The burrow courses are generally straight, with occasional crosscutting between specimens. The burrow fill is the same as the bedding sediment. No annulations or ornamentation are seen.

Remarks: These referred specimens are assigned to *Cochlichnus anguineus* based on their characteristic sinusoidal form and smooth surfaces. *Cochlichnus* is a long ranging ichnogenus (Cambrian to Holocene) that appears in widely varied facies (Minter and Braddy, 2009). *Cochlichnus anguineus* has previously been reported from two localities in Robledo Mountains Formation red beds (Braddy, 1998; Minter and Braddy, 2009), but it is relatively uncommon overall in that ichnofacies. In contrast, slabs from the local *Selenichnites* ichnoassociation are often profusely covered by tiny *Cochlichnus* trails.

Modern producers of sinusoidal trails resembling *Cochlichnus* include nematodes (Sandstedt et al., 1961; Moussa, 1970; Chamberlain, 1975), insect larvae (Metz, 1987) and a polychaete (Behrends and Michaelis, 1977; Buatois and Mángano, 2011). The referred *Cochlichnus* specimens may perhaps have been produced by nemertines, nematodes and annelids. Body fossils of these invertebrates, although rare, are known from nearshore deposits of the Mississippian Bear Gulch fauna of Montana and the Middle Pennsylvanian Mazon Creek Essex fauna of Illinois (Schram, 1979).

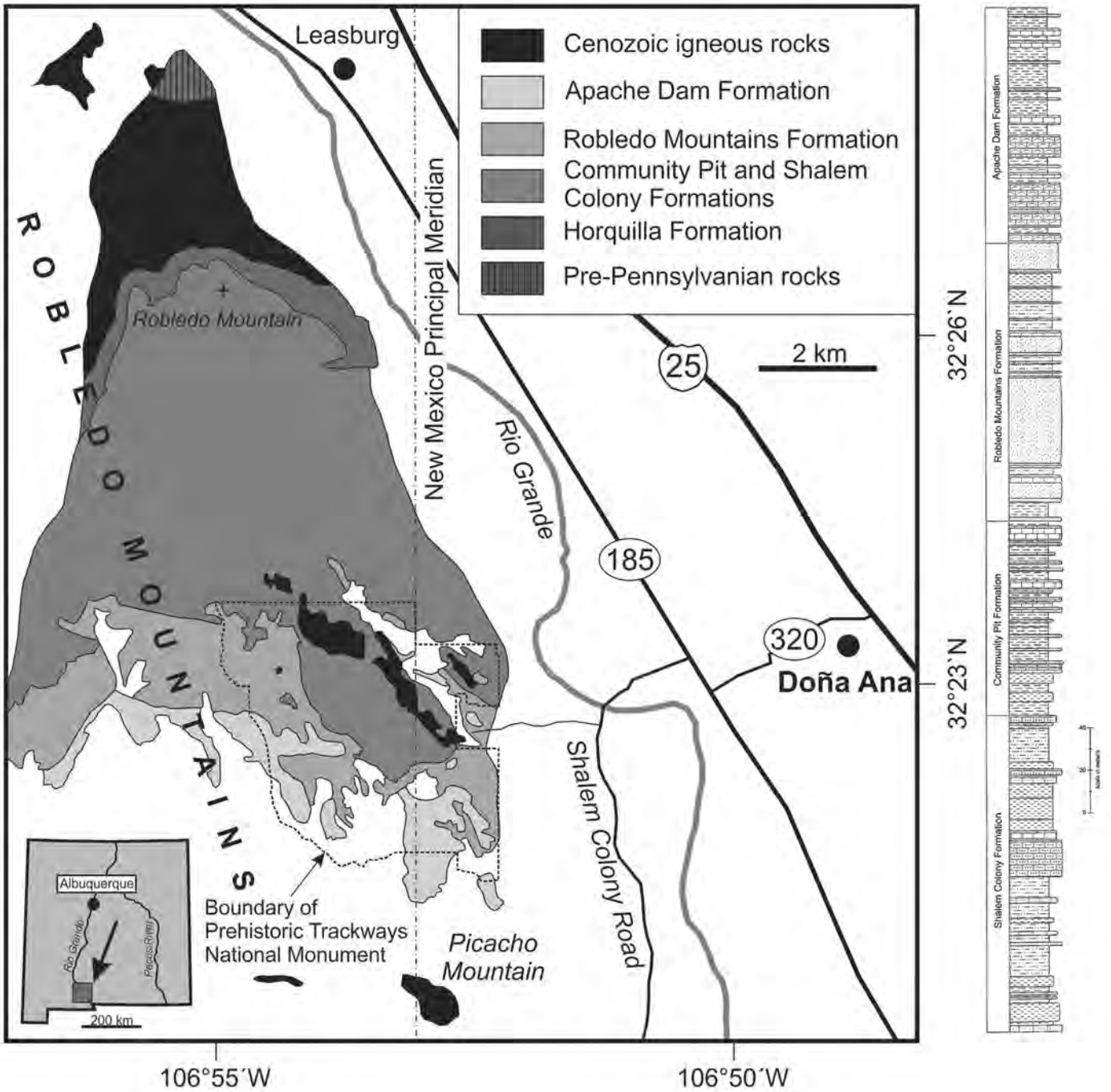


FIGURE 1. Location of the Prehistoric Trackways National Monument in the southern Robledo Mountains, south-central New Mexico, and generalized Hueco Group stratigraphic column. Stratigraphic column in Figure 2 is at boundary of Robledo Mountains and Apache Dam formations.

Ichnogenus *Helminthopsis* Heer, 1877
***Helminthopsis hieroglyphica* Wetzel and Bromley, 1966**
Fig. 7E

Referred specimens: P-64533, P-64534, P-64535, P-64536, P-64537, P-64539 (Fig. 7E), P-64543, P-64545, P-64547, P-70230, P-70231.

Description: The referred specimens are preserved as horizontal, rounded to flattened, non-branching, simple burrows. The burrow fill is the same as the bedding sediment. The specimens are generally ~1 mm wide, although smaller examples also occur. The specimens have courses that alternate between straight and winding segments, and some have portions with sharp angles. Occasional crosscutting of adjacent specimens occurs, but none self-overcross. Specimen lengths extend to as much as 36 mm.

Remarks: We assign the referred specimens to *Helminthopsis hieroglyphica*, a grazing trail characterized by alternating winding and straight segments, crosscutting, and sharp angles (Buatois and Mángano, 1993). The absence of self-overcrossing excludes placement within *Gordia indianaensis* (Buatois et al., 1998), which they otherwise closely resemble. *Helminthopsis* is a facies-crossing ichnotaxon that ranges from Precambrian to Holocene (Buatois et al., 1998). There has been an increase of *Helminthopsis hieroglyphica* reports since the 1990's, primarily from nonmarine facies (Lerner et al., 2007). The probable producers of *H. hieroglyphica* in nonmarine settings include insect larvae and nematomorphs (Buatois et al., 1997), although sphaeriid bivalves have also been reported as having produced *Helminthopsis*-like traces in contemporary fluvial settings (Lawfield and Pickerill, 2006). We conjecture that the referred specimens, which are from intertidal sandflat settings, may have been produced by

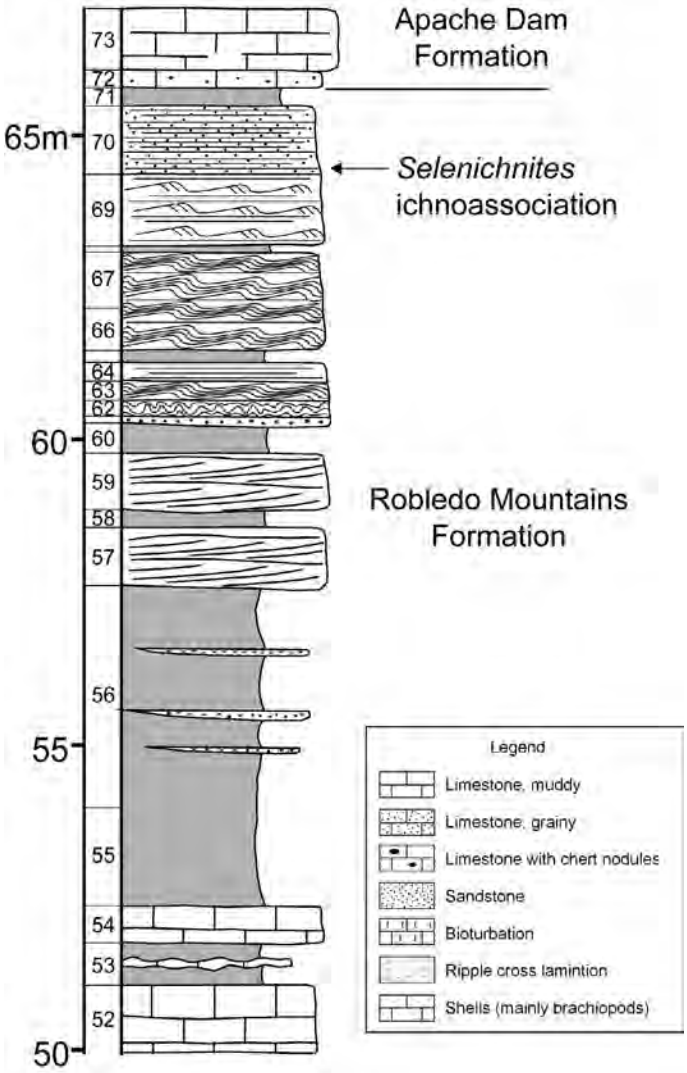


FIGURE 2. Measured stratigraphic section in the upper part of the Community Pit of the Prehistoric Trackways National Monument. The *Selenichnites* ichnoassociation fossils described here come from the lower part of unit 70.

nemertines, nematodes or annelids. Abundant *Helminthopsis*, as well as the previously mentioned *Cochlichnus*, serve as a useful overall marker for the local *Selenichnites* ichnoassociation beds.

Ichnogenus *Kouphichnium* Nopsca, 1923
***Kouphichnium* isp.**
Figs. 7B, D

Referred specimens: P-64541, P-64550, P-64551 (Fig. 7B), P-64552 (Fig. 7D), P-68473, P-68476, P-68477, P-68492, P-68493, P-68494, P-68495, P-68496, P-68500, P-68506.

Description: Specimens are highly variable in morphology and range from trackway preservation to isolated imprints. Preserved trackways have external widths that range from 18 to 28 mm, although an unusually small uncatalogued trackway on *Selenichnites* slab P-64554 has an external width of about 10 mm. Referred trackways show two track rows containing variably overstepped imprint series. These may sometimes be arranged *en echelon* with up to five imprints in each series. The imprints are mostly punctate to comma shaped, but with the outermost imprints in a series often being larger and more irregular than the others. There are isolated bifid or trifid "pusher" imprints on some specimen slabs, but these are rare overall. A medial linear feature is present within some trackway specimens. Trackway courses are generally straight to gently curved and may reach up to 200 mm in length.

Remarks: We assign the referred specimens to *Kouphichnium* based on their characteristic morphology. However, we leave the ichnospecific assignment of these specimens in open nomenclature. The current ichnotaxonomic status of *Kouphichnium* is confused and in need of revision. *Kouphichnium* is a relatively abundant ichnofaunal element within the local *Selenichnites* ichnoassociation but it often consists of incomplete groups of undertrack fallout (*sensu* Goldring and Seilacher, 1971). The referred trackways collected in situ from locality 8641 are relatively better preserved than those from the Community Pit, which are generally weathered.

A few *Kouphichnium* specimens have previously been reported from the Robledo Mountains Formation, but assignment was questionable as most specimens are poorly preserved (Minter and Braddy, 2009). *Kouphichnium* occurs in various settings including deltaic, estuarine, tidal flats, floodplains, and lacustrine margins (Minter and Braddy, 2009). Numerous authors have attributed *Kouphichnium* to xiphosurid producers (e.g., Caster, 1938, 1944; King 1965, Hardy, 1970; Gaillard, 2009). *Mesolimulus* has famously been documented at the end of some *Kouphichnium* trackways from the Upper Jurassic Solnhofen limestones of Germany (Seilacher, 2007; Buatois and Mángano, 2011; Lomax and Racay, 2012), which provides evidence for this attribution.

Ichnogenus *Selenichnites* Romano and Whyte, 1990
***Selenichnites rossendalensis* Hardy, 1970**
Figs. 3-5, 7A

Referred specimens: P-63475 (Fig. 4D), P-64510 (Fig. 3A), P-64538, P-64540 (Fig. 4B), P-64542, P-64544, P-64545, P-64546, P-64548 (Fig. 4A), P-64549, P-64554 (Fig. 4C), P-66373, P-66532 (Fig. 7A), P-68478, P-68488, P-68489 (Fig. 4E), P-68490 (Fig. 3B, 3C), P-68491.

Description: All specimens demonstrate a lunate (horseshoe) morphology consisting of a rounded anterior margin and occasionally separate lateral lobes (*sensu* Romano and Whyte, 1987). The specimens appear as single casts (P-64538, P-64544, P-64545, P-64546, P-68478) or as casts arranged into series (P-64510, P-64540, P-64548, P-64549, P-64554, P-66373, P-68488, P-68490, P-68491). There are as few as two casts within a series (P-64554) and as many as about 20 (P-68491). Most casts in series (P-64540, P-68488, P-68490, P-68491, P-64510) have irregular meanders along their courses. The repeat distance between casts in series is varied, with some barely separated (P-64540) and others separated by up to 45 mm (P-68490). Most casts are between 15 to 18 mm wide, although P-64548 and P-68478 are 26 mm wide. The narrowest cast (P-64544) is 13 mm wide, and the widest casts (P-64542, P-66532) are 55 to 60 mm wide. The horseshoe casts are generally deepest at the anterior. The lateral lobes are generally parallel to the midline or turned slightly outward (P-64554). Single lunate impressions vary in overall length from 13 mm (P-64510) to 18 mm (P-68490). Some horseshoe casts show a varied range of medial impressions between the lateral lobes. P-64548 has a raised medial structure with a relatively wide base that posteriorly narrows into a spatulate form. P-64546 shows at its posterior a thin, 12 mm long, medially offset, telson impression. P-63475 is proportionately xiphosurid-like in outline and includes a telson impression. Most of the specimens are associated with appendage imprints of varied morphology at their posterior (P-64510, P-64546, P-64548, P-68488, P-68490) or in near proximity on the slab surfaces (P-64540, P-64554, P-68478, P-68491).

Remarks: The referred specimens, which display a high degree of morphological variability, are assigned to *Selenichnites*. This ichnogenus is composed of suboval traces with a rounded anterior margin, strongly convex lunate or paired crescent lobes, with or without scratch marks or a posterior ridge, which may occur either as isolated traces or within a series (Romano and Whyte, 1987). Of the numerous (9) ichnospecies (Hardy, 1970; Fischer, 1978; Chisholm, 1985; Romano and Whyte, 1987; Trewin and McNamara, 1995; Poiré and Del Valle, 1996; Weber and Braddy, 2004; Minter and Braddy, 2009; Gibb et al., 2011) available within *Selenichnites*, the referred specimens most resemble *S. rossendalensis* (=*Kouphichnium rossendalensis* Hardy, 1970). We thus assign the specimens to *S. rossendalensis*, recognizing that although the referred specimens differ in some regard from the holotype material they are still within the preservational variation limits of the ichnospecies (*sensu* Bengtson, 1988).

The ichnospecific diagnosis for *Selenichnites rossendalensis* given by Hardy (1970, p. 189) simply stated that it consists of trails composed of lunate casts corresponding in outline to the shape of the xiphosuran prosoma, that it is often in series, and is associated with appendage and telson marks. Although not included in the ichnospecific diagnosis, Hardy (1970) added in his text that *S. rossendalensis* was preserved as an irregularly meandering series of lunate casts. Several of the

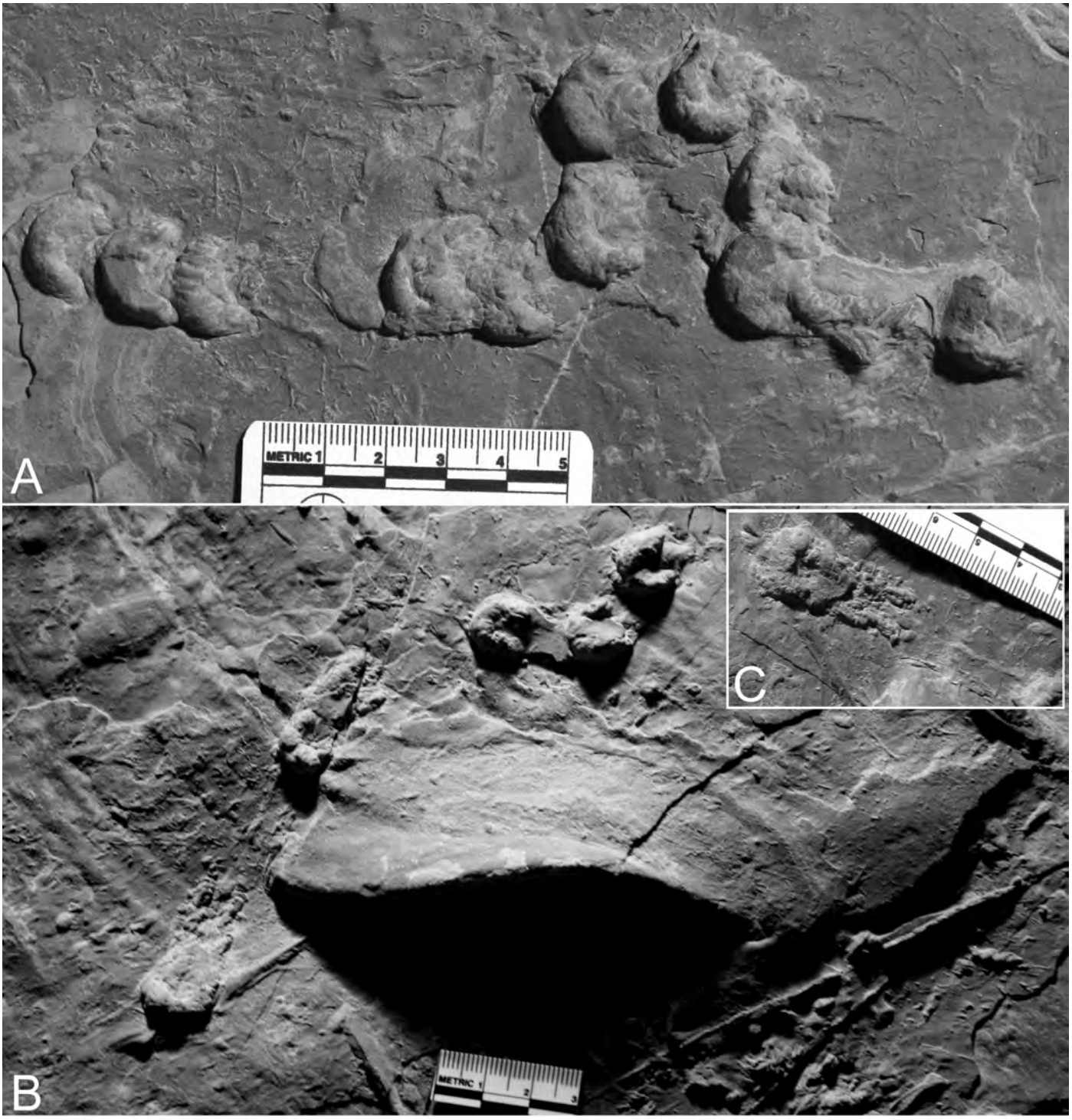


FIGURE 3. *Selenichnites rossendalensis*. **A**, P-64510, a series of casts that have a meandering course. **B**, P-68490, a series of casts that meanders around a large, convex tetrapod swimming track. **C**, P-68490 (inset), detail of anteriormost cast.

referred specimens (P-64540, P-68488, P-68490, P-68491, P-64510) have meanders that much resemble those seen on the *S. rossendalensis* holotype slab (Hardy, 1970, pl. 40; Eagar et al., 1985, pl. 11). The *S. rossendalensis* type locality material is preserved in convex hyporelief on sandstone blocks from the Namurian (Upper Mississippian) Upper Haslingden Flags of northern England (Hardy, 1970). Hardy attributed these traces to a xiphosurid (*Bellinurus*) and considered them to have been produced in a nonmarine, sandbank depositional setting.

Hardy (1970) assigned the material to *Kouphichnium* based on an inferred xiphosurid trace producer, and erected a new ichnospecies, *K. rossendalensis.* This ichnospecies was later reassigned by Miller (1982) to a new ichnogenus *Limulicubichnus*, which she had established for limulid resting traces. *L. rossendalensis* was reassigned by Romano and Whyte (1987) to another new ichnogenus, *Selenichnus*, which they had erected based on the morphology of the trace fossils rather than the inferred producers. The ichnogeneric name *Selenichnus* was preoccupied, and Romano and Whyte (1990) subsequently proposed the replacement name *Selenichnites*.

Eagar et al. (1995) later reassessed the Upper Haslingden Flags ichnofauna. These authors concluded that *Selenichnites rossendalensis* is a nonmarine shoreline indicator and speculated that the burrowing behavior seen in *S. rossendalensis* resulted from xiphosurids having become stranded on mudflats due to periodic fluctuations of water level. In their interpretation, *S. rossendalensis* was produced subaerially by

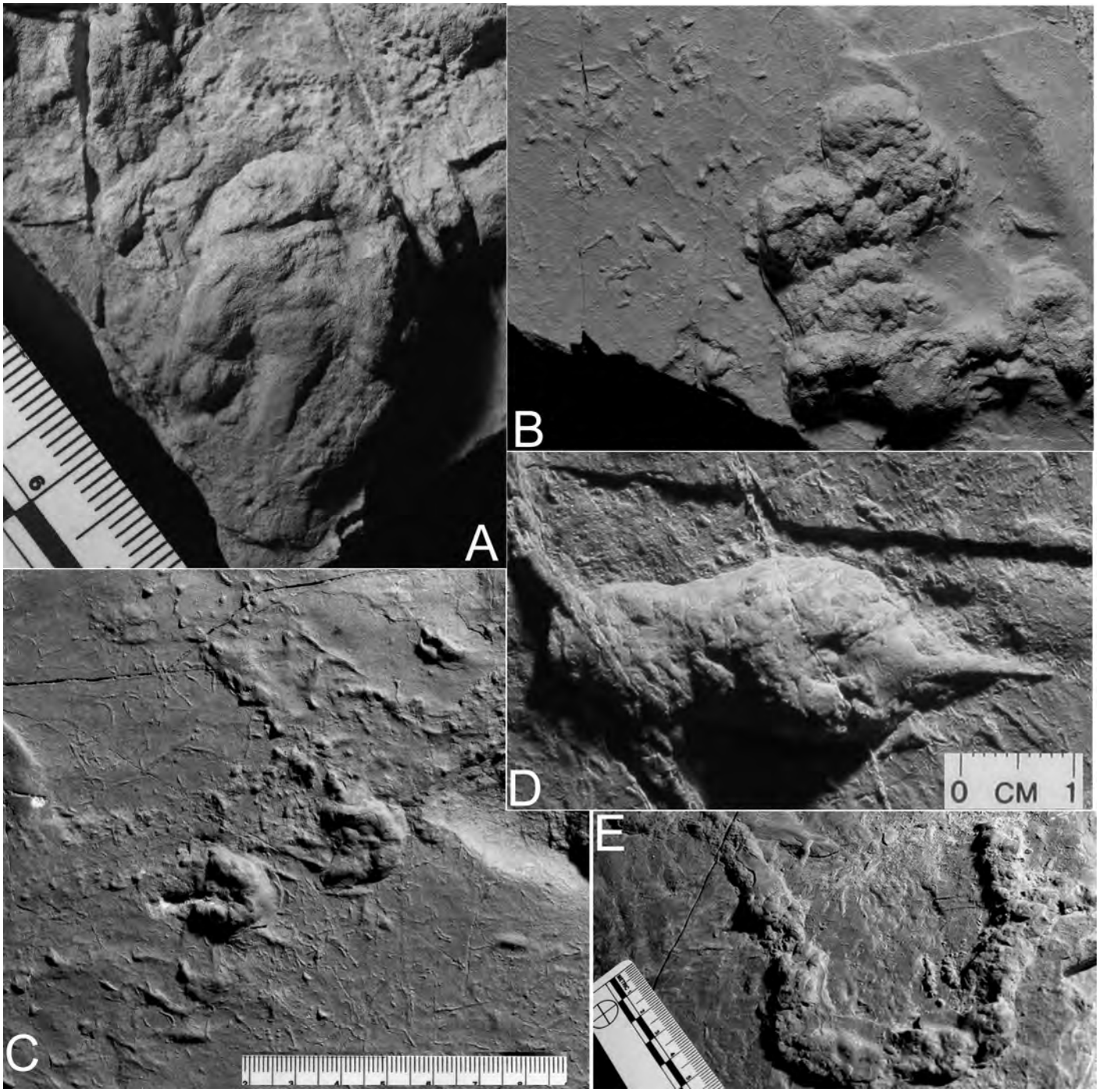


FIGURE 4. *Selenichnites rossendalensis.* **A**, P-64548, a cast with a medial feature that posteriorly narrows into a spatulate form. **B**, P-64540, deeply impressed casts with *Kouphichnium*. **C**, P-64554, casts with invertebrate trails and *Kouphichnium*. **D**, P-63475, cast with telson impression. **E**, P-68489 resembles *Selenichnites bradfordensis* but lacks oblique penetration structures. Note the meandering course.

stranded xiphosurids that burrowed into the sediment in order to avoid dehydration while waiting until the water level rose again.

This is the first record of *Selenichnites rossendalensis* from New Mexico. Another *Selenichnites* ichnospecies, *S. belosis*, is endemically known from limited material that was collected from nonmarine redbeds of the Robledo Mountains Formation (Minter and Braddy, 2009). *Selenichnites* ranges from Cambrian to Jurassic. It is generally regarded as having been produced by xiphosurans (Draganits et al., 2001). Other producers such as crustaceans, eurypterids, anomalocarids, trilobites, and euthycarcinoids (Fischer, 1978; Trewin and McNamara, 1995; Poiré and Del Valle, 1996; Weber and Braddy, 2004; Gibb et al, 2011) have also been proposed, particularly for the Cambrian through Silurian occurrences. *Selenichnites* is usually considered to be a resting trace (cubichnia), an ethological category that can incorporate behaviors such as temporarily digging, seeking protection from predators or simply a cessation of usual activities (Buatois and Mángano, 2011). Trewin and McNamara (1995) considered the repeated digging seen in *Selenichnites* to represent feeding behaviors akin to those seen in modern *Limulus*.

SYSTEMATIC VERTEBRATE ICHNOLOGY

Ichnogenus *Characichnos* Whyte and Romano, 2001
Characichnos isp.
Fig. 7C

Referred specimens: P-68505, P-68509, P-68499 (Fig. 7C), P-70233, P-70234, P-70235, P-70236.

Description: The referred traces are relatively large and composed of two or three parallel imprints of long, thin, slightly arcuate scratch

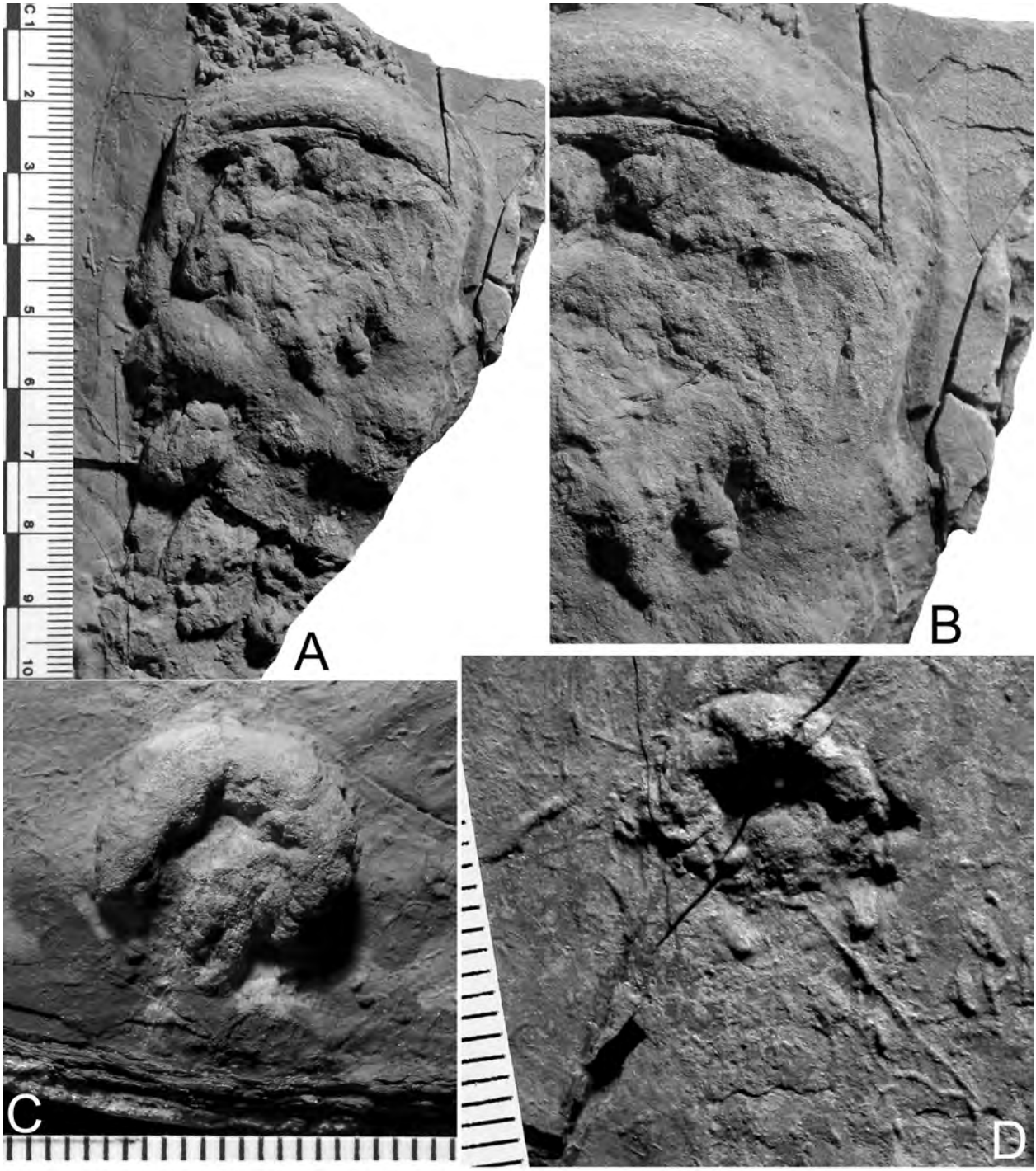


FIGURE 5. *Selenichnites rossendalensis*. **A**, P-64542 is the largest specimen collected from locality 8641 and preserves unusual features. **B,** P-64542, detail showing a genal spine impression and a bifid limb impression (arrows). **C**, P-64544, is the narrowest collected specimen. **D**, P-64546, a cast with telson impression.

marks. The scratch marks are up to 120 mm long and up to 12 mm wide. A maximum of four sets of imprints have been identified in series. A few specimens show a rounded "heel" imprint.

Remarks: We regard the current ichnotaxonomic status of tetrapod "swim traces" or "swim tracks" as highly problematic. Indeed, referring to such traces as swim tracks is somewhat questionable, as a swimming tetrapod generally would leave no traces. The term swim trace/track thus is based on the perception that these are digit scratch marks left by a partially buoyant tetrapod, much as *Undichna* is perceived to be the scratch marks left by the fin(s) of a fish swimming just above (but also touching) the sediment-water interface. The "swim tracks" described here nicely correspond to Whyte and Romano's (2001, p. 232) definition of *Characichnos* as "two to four elongate, parallel hypichnial ridges (or epichnial grooves) which may be straight, gently curved or slightly sinuous. The termination of the ridges (or grooves) may be straight or slightly flexed."

Ichnogenus *Undichna* Anderson, 1976
***Undichna unisulca* Gibert et al., 1999**
Fig. 6E

Referred specimen: P- 64553 (Fig. 6E).

Description: The specimen consists of a single, sinusoidal trail preserved in convex hyporelief along the bedding surface. The wavelength of the component sinusoidal forms is about 44 mm, and the amplitude ranges from 8 to 13 mm. The length of the sinusoidal trail is 160 mm, and its width varies from 1 to 2 mm. The course of the trail

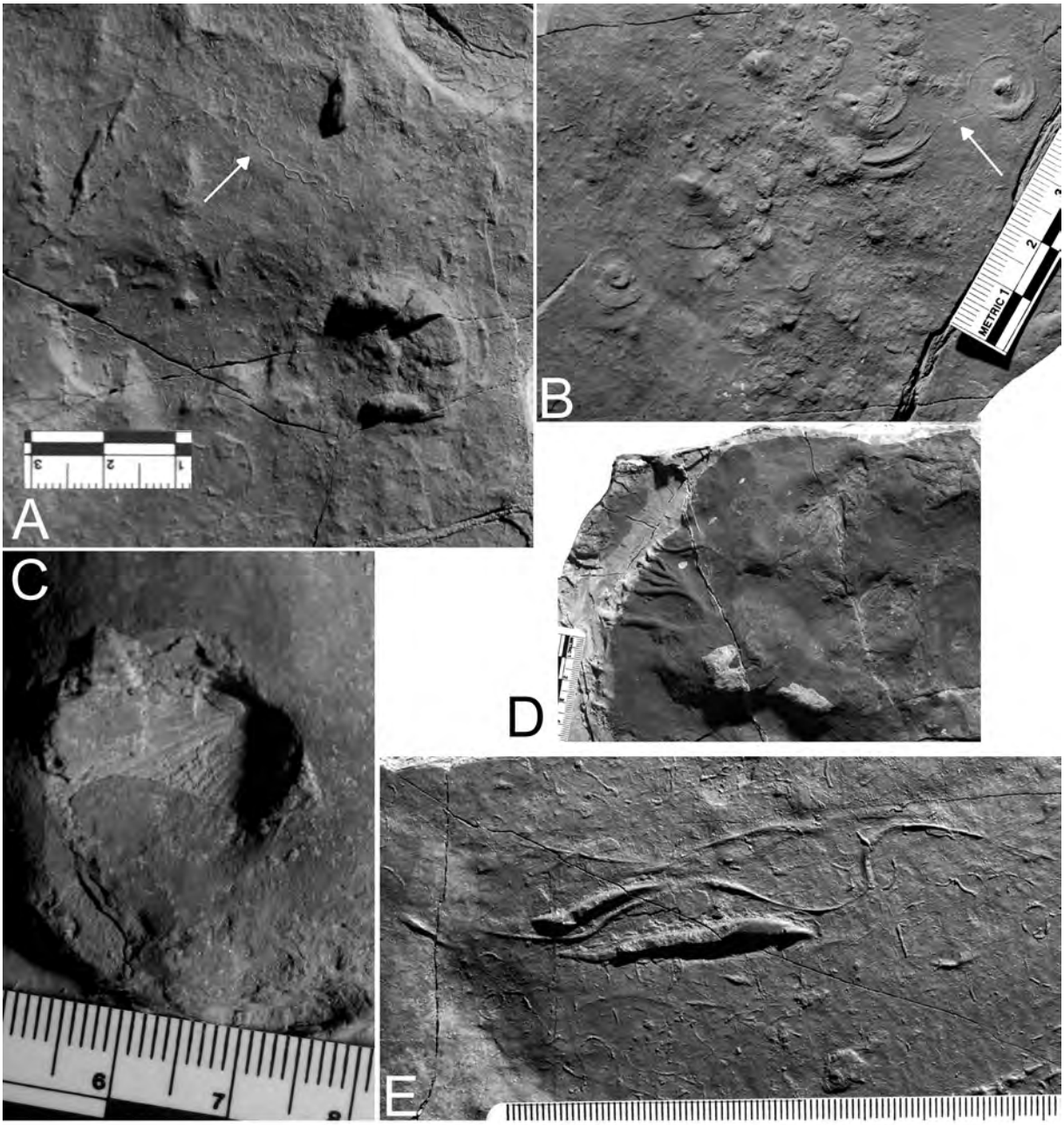


FIGURE 6. Selected fossils and sedimentary structures from the *Selenichnites* ichnoassociation. **A**, Small *Cochlichnus anguineus* (arrow) with *Selenichnites* (P-64549) and *Kouphichnium*. **B**, P-60676, scratch circles? Note the linear form with a rounded terminus (arrow), which strongly resembles a hydrozoan capitate tentacle. **C**, P-64502, *Aviculopecten* valve from the Community Pit. **D,** P-64498, *Bergaueria*-like structure (pot cast) with branched rill marks resembling tentacles. **E**, P-64553, *Undichna unisulca.*

is generally straight. There is a single pair of relatively large scratch marks on either side of a single sinusoidal form along the trail course. One of these scratch marks is about 4 mm wide with tapered ends, and its position and length coincides almost exactly with that of the adjacent sinusoidal form. The opposite scratch is also about 4 mm wide with tapered ends. It closely follows from a short distance the contour of the adjacent sinusoidal form and intergrades with the sinusoidal form at its peak amplitude. There is another faintly impressed sinusoidal trail seen in proximity on the bedding surface, but a close association with the referred specimen is not certain.

Remarks: We assign this trace to *Undichna unisulca* due to it consisting of a single sinusoidal wave, but recognize that it shows some additional complexity. The scratch marks seen on either side of the trail were probably made by pelvic or anal fins of the producer having momentarily contacted the substrate, but we consider these to have little ichnotaxonomic significance to the overall assignment. The referred *Undichna* specimen is much larger than other sinusoidal trails (*Cochlichnus*) commonly seen within the local *Selenichnites* ichnoassociation.

With regard to the fish that produced the referred specimen, there has only been a single vertebrate body fossil recovered from the Robledo Mountains Formation. This is a small chondrichthyan tooth assigned to the marine edestid shark *Agassizodus* (Kues, 1995). There is, however, a diverse ichthyofauna known from the Upper Carboniferous to Lower Permian Abo and Cutler formations of New Mexico, which contain xenacanths, acanthodians, lungfish and rhipidistians (Berman, 1993; Minter and Braddy, 2006). *Undichna* has previously been reported from the Robledo Mountains Formation as *U. bina*, *U. britannica* and *U. unisulca* (Minter and Braddy, 2006, 2009).

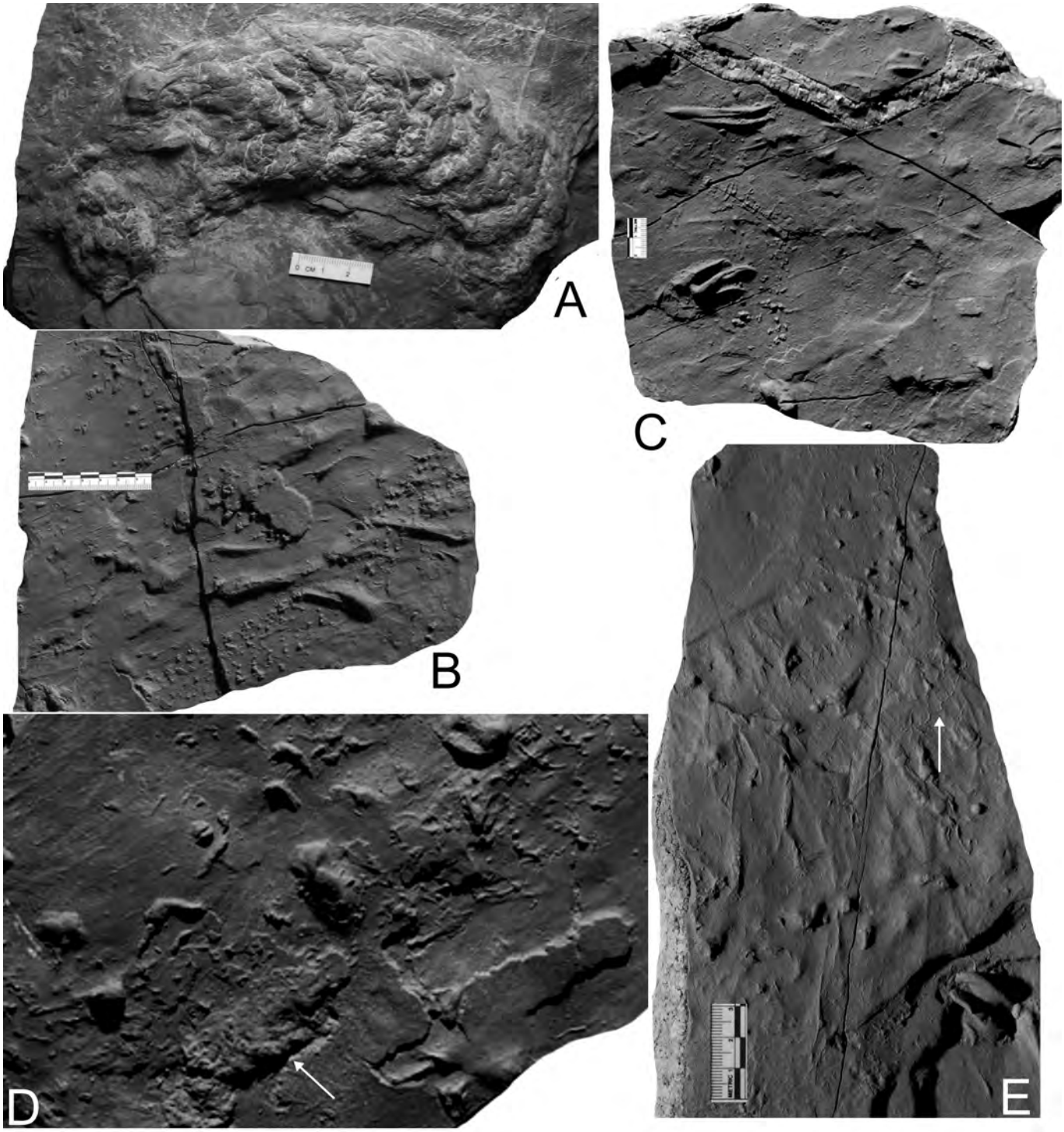


FIGURE 7. Selected trace fossils from the *Selenichnites* ichnoassociation. **A,** P-66532, a large *S. rossendalensis* specimen collected from the Community Pit. **B,** P-64551, *Kouphichnium* with vertebrate swim traces (*Characichnos*). **C**, P-68499, *Characichnos* with *Kouphichnium*. **D**, P-64552, *Kouphichnium* with poorly preserved *S. rossendalensis*. **E**, P-64539, *Helminthopsis hieroglyphica* (arrow).

SEDIMENTARY STRUCTURES

Scratch circles? (Problematic impressions) Fig. 6B

Referred specimens: P-60676 (Fig. 6B), P-60677, P-61279, P-61280.

Description: The referred specimens are circular in form and have diameters that range from 3 to 60 mm. Specimens may have a raised central boss that is surrounded at variable intervals by raised concentric rings. Some of these rings show small, outwardly radiating striae. P-60676 contains several circular impressions that display unusual morphology including a structure that resembles a hydrozoan capitate tentacle (Fig. 6B, arrow).

Remarks: These circular specimens are particularly abundant on float blocks from the Community Pit. Indeed, they serve as another bed marker for the local *Selenichnites* ichnoassociation. When first reported these circular impressions were all thought to be porpitid (chondrophorine) pneumatophores (Lerner and Lucas, 2010; Lerner et al., 2010). P-60676 (Fig. 6B), which was uniquely collected as float from below locality 8641, may indeed be representative of these soft-bodied animals. Circular impressions on this slab contain structures

that show resemblance to hydrozoan anatomy (velum, ring canals and manubrium) and should receive further study.

However, we now consider a porpitid affinity for most of these circular forms to be unlikely. A more parsimonious explanation is that at least some of these interesting structures are scratch circles. We will present a more comprehensive treatment of these enigmatic structures in a later publication.

Bergaueria-like mounds and related structures
Fig. 6D

Referred specimens: P-64490, P-64491, P-64490, P-64492, P-64493, P-64494, P-64495, P-64496, P-64497, P-64498 (Fig. 6D), P-64499, P-64500, P-64501, P-64502.

Description: We have divided the referred specimens into three informally termed categories; *Bergaueria*-like mounds, cupcake-mounds, and tentacle-like structures. The *Bergaueria*-like mounds are simple to complex structures that are generally rounded to elliptical in outline. Specimens may have thin constrictions or sloped expansions at the bedding plane. Mound diameters range from 39 to 250 mm and height from the bedding plane ranges from 9 to 55 mm. Surface textures are rough and some show small bulges. Ornamentation or linings are not seen. Distal terminations lack a central depression. Pectinacean valves (*Aviculopecten*) sometimes occur as inclusions in *Bergaueria*-like mounds.

Cupcake-type mounds are less abundant than *Bergaueria*-like mounds and generally smaller. They also differ by having rounded outlines, inwardly tapered sides, and flattened tops. Cupcake-type mounds are generally perpendicular to the bedding plane in orientation. Rarely, specimens may show dense, small invertebrate trails on their surfaces.

Tentacle-like structures appear as raised ridges in association with a *Bergaueria*-like mound or separately on shallow ripple slopes. These structures have rounded tops and are 1 mm wide or less. Both branched and unbranched forms occur. Tentacle-like structures are generally straight along their length, but may also curve or follow vertical contours on the slab surface. Some of the tentacle-like structures are covered by small invertebrate grazing trails at their base.

Remarks: It is difficult at times to determine whether certain forms represent biogenic ichnofossils or are sedimentary pseudofossils. When discovered, these *Bergaueria*-like mounds were thought to represent bergauerian anemone burrows (Lerner and Lucas 2010; Lerner et al., 2010). A biogenic origin for these mounds was furthered by the tentacle-like structures that emanated from some specimens (Fig. 6D). Tentacle impressions are rare in the fossil record, although Neoproterozoic forms such as *Eoporpita medusa* and *Hiemalora stellaris* are known (Lipps and Valentine, 2004). The co-occurrence of the referred specimens with undoubted biogenically produced trace fossils such as *Selenichnites* and *Kouphichnium* added to the consideration that these were bergauerian anemone burrows.

Of the various revised bergauerian ichnotaxa recognized by Pemberton et al. (1988), the referred material outwardly resembles *Bergaueria hemispherica.* This ichnospecies was described from the Cambrian of Spain as essentially a hemispherical trace lacking a central depression (Crimes et al., 1977), and the referred material generally matches this description. The preservation of the referred *Bergaueria*-like mounds as hyporelief structures on the soles of sandstone beds overlying mudstones is similar to the preservational mode of the *B. hemispherica* holotype material (Crimes et al., 1977). Some of the referred specimens additionally show a narrow constriction at the bedding surface. This feature likewise appears on the *B. hemispherica* holotype (Pemberton et al., 1988, fig. 8). Pemberton et al. (1988) further noted that small shells fill some *Bergaueria* burrows. Bivalve (*Aviculopecten*) inclusions similarly occur within some of the referred specimens.

However, a criterion for the recognition of *Bergaueria hemispherica* is that the specimen has a distinctive thin lining (Pemberton et al., 1988), and this feature is not present on the referred material. *B. hemispherica* is, moreover, a simple form, and the referred specimens show a range of morphological complexity. *B. hemispherica* is considered a relatively large bergauerian measuring 43-60 mm wide (Mángano et al., 2005). Only the smallest of the referred specimens having a 45 mm diameter fits within this range. Most of the other *Bergaueria*-like mounds would be considered gigantic, showing diameters that range from 88 mm to 250 mm.

We now consider the referred material, which occurs exclusively on float blocks from the Community Pit and not from locality 8641, to be inorganically produced sedimentary structures (pseudofossils). The *Bergaueria*-like mounds are now reinterpreted as pot casts. The tentacle-like structures are likely rills or dewatering structures that were formed by fluidization within the sediment or by run off (W. Hagadorn, pers. comm.). A similarity between dewatering or degassing structures and some conical structures thought to have been produced by anemones was noted by Buck and Goldring (2003), and consequently Gingras et al. (2008) advised that caution be used when interpreting potential anemone trace fossils.

DISCUSSION

Selenichnites

Judging from Hardy's (1970) figures of a holotype slab containing multiple casts, and a single paratype, there appears to be a high degree of morphological variation within this little studied ichnospecies. This high degree of morphological variation is also well demonstrated within the relatively large sample of newly collected material from New Mexico. We briefly note that we attribute the referred *Selenichnites rossendalensis* specimens to a paleolimulid producer whose identity will be discussed in a following section (Xiphosurid Trace Fossil Producer).

P-64542 (Fig. 5A) is the single largest specimen from locality 8641, and it displays unusual features. The anterior of the trace contains a horseshoe cast that is about 55 mm wide. Based on its large size, this trace specimen is interpreted as representing a fully adult producer. The right lateral lobe of the cast has at its posterior a well preserved impression of a paleolimulid genal spine (Fig. 5B, arrow). In near proximity, but closer to the midline, is a walking limb impression with a bifid pincer (Fig. 5B, arrow). Using Van der Hammen's (1986) terminology this xiphosuran leg impression likely records an apotele, tibiotarsus and patella. Compared to the walking legs of *Limulus polyphemus*, the subequal size of the bifid impression most resembles the pincers on walking legs 2-5, rather than those on the distinctive "pusher" leg 6, which contains the flabellum. The posterior region of this variant specimen is complex, but composed of forms that were likely produced by contact of the paleolimulid's ventral abdomen with the underlying sediment. There is a heavily bioturbated area at the anterior margin of the horseshoe form that is composed of numerous irregular imprints. This disturbed area likely represents the producer's continuation of forward movement through the sediment after having rested, or is possibly feeding activity.

P-66532 is the single largest *Selenichnites* specimen collected from the Community Pit (Fig. 7A). It may have been produced by an adult paleolimulid foraging along the water/sediment interface. *Limulus* individuals use their prosoma in bulldozer fashion to plow through the sediment and grasp prey with their pincers (Barthel, 1974; Walls et al., 2002). The repetitive crescentic ridges seen in the referred specimen are interpreted as prosomal prod marks. The churned areas within the structure may have resulted from the paleolimulid producer having used its cephalothoracic appendages as it burrowed through the sediment in search of prey.

P-63475 is preserved as a full-bodied resting impression that is recognizably xiphosurid-like in outline, although there is an extended anterior portion (Fig 4D). Eldredge (1970) provided a detailed description of the burrowing behavior of *Limulus polyphemus* under laboratory conditions. He noted that this predominantly nocturnal species is dormant and concealed by a thin layer of substrate during daylight hours. P-63475 likely records analogous behavior of a Permian paleolimulid. The extended anterior portion of the referred specimen appears to have resulted from the animal having repositioned itself.

P-68489 (Fig. 4E) shows some resemblance to *Selenichnites bradfordensis* Chisholm, 1985, which is of controversial validity (Romano and Whyte, 1987; Gibb et al., 2011). *Selenichnites bradfordensis* is considered to represent the bedding plane expression of burrows that are oriented oblique to the bedding in the vertical plane (Chisholm, 1985; Minter and Braddy, 2009). There is no indication that the referred specimen is linked to oblique penetration structures, so we consider this specimen to be a poorly preserved *S. rossendalensis*.

P-64548 shows at its posterior region a narrowing spatulate form (Fig. 4A). We do not interpret this as a telson imprint, but rather as a ventral opisthosomal impression. This impression closely corresponds to the shape of the abdominal branchial appendage region on *Limulus polyphemus* (see Suzuki et al., 2008, fig. 1), a modern horseshoe crab. Indeed, some of the triangular medial to posterior markings on other referred *S. rossendalensis* specimens likely

resulted from the paleolimulid producer's opisthosoma contacting the underlying sediment. Nevertheless, we choose not to erect yet another *Selenichnites* ichnospecies based on these variations. We consider this specimen, and other variants within the referred material, to be within a preservational continuum, pending the outcome of a study of *Selenichnites rossendalensis* reportedly being undertaken by others (M. Romano, pers. comm.).

Xiphosurid Trace Fossil Producer

Synziphosurines are not considered as producers of the referred trace fossils (*Selenichnites* and *Kouphichnium*), as the youngest member of this group is from the Late Mississippian (Moore et al., 2007). Xiphosurids (Order Xiphosurida), the true horseshoe crabs, have a fossil record that ranges from the present to the Late Ordovician (Rudkin and Young, 2009), and we consider these to have been the most likely producers. Xiphosurids have an overall poor body fossil record, which is due in part to their having a sclerotized but non-biomineralized exoskeleton (Fernández and Pazos, 2013; Rudkin and Young, 2009). There is also a poor representation in the fossil record of depositional environments in which most fossil xiphosurids occur (Babcock et al., 2000).

Recently, a combined field party from the United States National Museum and the New Mexico Museum of Natural History discovered two partial *Euproops* specimens from a coastal lake setting within the Missourian interval of the Beeman Formation of southeastern New Mexico (Lucas et al., 2014). Although there are a few North American records of *Euproops* from Virgilian Stage strata, it does not range into the Permian (Babcock and Merriam, 2000). We therefore do not consider euproopids as having produced the referred material.

The Permian xiphosurid record consists of a single bellinurine and two limuline genera (Rudkin and Young, 2009). The Permian bellinurine record is restricted to Europe, but some of the limuline records are geographically close to New Mexico. Limulacean paleolimulids are therefore considered to have been the likeliest producer of the referred material. The limuline Paleolimulidae ranged from Desmoinesian through Leonardian, and paleolimulid specimens are known from Illinois, Kansas and Texas (Babcock and Merriam, 2000; Allen and Feldmann, 2005). Paleolimulidae contains two genera; *Panduralimulus* and *Paleolimulus*. *Panduralimulus* contains a single species, *P. babcocki* (Allen and Feldmann, 2005). There is disagreement as to whether *Paleolimulus* contains one or two species. Babcock and Merriam (2000) consider *Paleolimulus avitus* to be a junior synonym of *Paleolimulus signatus*, whereas Allen and Feldmann (2005) retained *P. avitus* as a distinct species. *Paleolimulus* is best known from exceptionally preserved specimens found within several late Virgilian to early Leonardian Lagerstätten of eastern Kansas (Babcock et al., 2000). The depositional environments reported by Babcock et al. (2000) for the Kansas localities yielding multiple *Paleolimulus* specimens are lacustrine (Wellington Formation insect beds), and an estuarine/tidal flat setting (Pony Creek Shale). *Paleolimulus* has also been reported from the nearshore marine Essex fauna of Mazon Creek, Illinois (Mikulic, 1997), but this record is not well studied. *Panduralimulus babcocki* is known from a single locality in the Early Permian (Leonardian) of Baylor County, Texas, in deposits that were thought to represent a mixed, marginal marine-deltaic setting (Allen and Feldmann, 2005).

The generic diagnosis of *Panduralimulus babcocki* states that these are very small forms, with prosomal widths that range from 4.5 to 13.4 mm (Allen and Feldman, 2005). The widest *Panduralimulus babcocki* specimen (13.4 mm) is comparatively equal to the narrowest of the referred *Selenichnites* specimens (13 mm). This relational size difference strongly suggests that *P. babcocki* was not the producer of the referred material. *Paleolimulus*, in contrast, is a larger form that could well accommodate the widest of the referred *Selenichnites* specimens (60 mm). Indeed, a plastoholotype restoration of *Paleolimulus signatus* by Babcock et al. (2000) indicates a prosomal width of 75 mm. The genal spine impression (Fig. 5B, arrow) seen on P-64542 compares well to genal spines of *Paleolimulus* (e.g., Dunbar, 1923, fig. 2), but this in itself is inconclusive because there was a range of genal spine variation within *Paleolimulus* (Allen and Feldman, 2005). Of the two genera considered, we conclude that the referred *Selenichnites* and *Kouphichnium* traces were most likely produced by *Paleolimulus.*

Depositional Settings and Paleoecology

We consider the Robledo Mountains Formation *Selenichnites* ichnoassociation to have been formed subaqueously. One indicator of this is *Undichna*, which is a well-recognized trace fossil produced by fishes. The minimum water depth at deposition could have been as low as just several centimeters based on the relatively small *Undichna* from locality 8641. The *Characichnos* specimens in this ichnoassociation, particularly from the Community Pit, indicate that there was sufficient water depth at deposition to have provided buoyancy for relatively large animals to have produced "swimming" marks on the bottom sediment. There is an absence of subaerial indicators such as mud cracks or rain impressions on any of the specimen slabs from either locality 8641 or the Community Pit. This absence of subaerial indicators shows that locality 8641, presumably more landward than were the Community Pit localities, was not at the uppermost limits of a tidal sandflat setting at deposition.

There is an entire absence of fossil plant material, or its impressions, within the local *Selenichnites* ichnoassociation. This is another tidal flat indicator, as tidal flats are non-vegetated. This stands in contrast to the important plant record from red bed ichnoassociations within the Robledo Mountains Formation.

It's probable that locality 8641 served as a nearshore paleolimulid nursery area. Hardy (1970) gave the widths of the *Selenichnites rossendalensis* type material as generally being between 16-17 mm. This is similar to the majority of the referred *S. rossendalensis*, although two specimens are much wider, being in the 55-60 mm range. There are a total of 18 *Selenichnites* specimens in the New Mexico sample (those in series are counted only once). These have widths that cluster into distinctive population groups; 14 specimens are 13-18 mm wide, two specimens are 25-26 mm wide, and two specimens are 55-60 mm wide. This suggests that different age groups are represented in the New Mexico sample. Assuming that all of the *Selenichnites* specimens were produced by a single paleolimulid species (*Paleolimulus*), we infer that specimens 13-18 mm wide were produced by juveniles, specimens 25-26 mm wide were produced by sub-adults, and specimens 55-60 mm wide were produced by adults. Strikingly, the most populous group within the total sample therefore consists of probable juvenile paleolimulids (14 out of 18 specimens).

The high number of specimens considered to have been produced by juvenile paleolimulids supports interpretation of locality 8641 as having been a protected nursery. *Limulus polyphemus* adults migrate from offshore depths to the intertidal zone, where the females dig excavations and deposit eggs on estuarine beaches (Walls et al., 2002; Botton et al., 2010). *L. polyphemus* juveniles, once hatched, move progressively farther from shore along tidal flats as they mature, and those in the lowest intertidal zones are close in prosomal width to sexually mature adults (Rudloe, 1981). The single largest specimen (55 mm) collected from locality 8641 may have been produced by an adult that had migrated nearshore to spawn (Fig. 5A).

There is a sparse invertebrate fossil fauna that occurs exclusively with referred trace fossils from the Community Pit. This faunal record consists entirely of pectinacean bivalves (P-70237, P-70238, P-68508, P-68510, P-70239), which we identify as *Aviculopecten* (Fig. 6C). *Aviculopecten* is a typical taxon in shallow marine facies of the Robledo Mountains Formation (Kues, 1995). We thus consider it to have been an allochthonous element that was transported into the Community Pit tidal flat depositional setting. We consider the referred *Aviculopecten* to be an indicator that there was a relatively higher energy regime in place at deposition than there was at locality 8641, where bivalves are absent.

If the circular impressions commonly found on Community Pit float blocks are eventually determined to be scratch circles, then these too are an indicator of a relatively high energy hydrologic regime having been in place at deposition. Currents could have been a prime factor that created rotating tools of some sort that led to the formation of scratch circles on the sediment surface. If the circular impressions are eventually determined to be trace fossil-like molds of echinoid interambulacral plates, then it's possible that these shallow marine faunal elements were transported by relatively high energy currents into the Community Pit tidal flat depositional setting. Further study is planned of these interesting structures.

Sedimentary pot casts, which we consider to be another higher energy indicator, also occur exclusively from the Community Pit depositional setting. Myrow (1992) described a diverse suite of erosional structures from a shallow subtidal zone in the Late Precambrian-Early Cambrian of Newfoundland. He considered the pot casts found within these deposits to have been storm-generated features. A large Early Permian coastal storm could conceivably have created sufficient current scour to have caused the pot casts and ripple structures seen on Community Pit slabs. The pot cast cavities may have acted as traps as indicated by *Aviculopecten* inclusions. These bivalve inclusions

may also have acted as rotating tools that contributed to the pot cast formation. Interestingly, P-64490 from the Community Pit shows a *Kouphichnium* trackway with an otherwise straight course that deviates and closely follows the curved and sloped periphery of a pot cast. This indicates that the pot cast was temporally emplaced prior to the formation of the trackway. The *Kouphichnium* trackway may represent a return to more normal tidal conditions after a storm event had passed.

The trophic relationships among the vertebrate and invertebrate producers of the diverse ichnogenera contained within the discussed ichnoassociation can likely be inferred with some degree of confidence. Hence, we interpret the ichnoassociation as constituting an ichnoguild. The apex predators within this ichnoguild were terrestrial tetrapods, as represented by *Characichnos*. The large and small tetrapods that produced these "swim" traces apparently hunted in shallow nearshore waters and probably fed on fishes and paleolimulids. The fishes within this ichnoguild, represented by *Undichna*, likely fed on paleolimulid juveniles and vermiform invertebrates (nemertines, nematodes and annelids). Although modern limulids feed on worms and bivalve mollusks (Walls et al., 2002), the earliest limulid likely to have been durophagous is from the Triassic (Signor and Brett, 1984). The paleolimulids within this ichnoguild, as represented by *Selenichnites* and *Kouphichnium*, thus likely fed on the vermiform invertebrates that produced the highly abundant invertebrate trails (*Helminthopsis* and *Cochlichnus*).

CONCLUSIONS

As demonstrated by their relatively abundant trace fossils (*Selenichnite*s and *Kouphichnium*), paleolimulid horseshoe crabs were active on the Early Permian equatorial coast of New Mexico. As can be seen from the newly described and important New Mexico *Selenichnites rossendalensis* sample, we concur with Eagar et al. (1995) that *S. rossendalensis* is a xiphosurid-produced nonmarine shoreline indicator, at least during the Late Carboniferous–Early Permian. The tidal flat depositional settings and ichnogeneric composition of the local *Selenichnites* ichnoassociation distinguishes it from those better known nonmarine Robledo Mountain Formation red bed ichnoassemblages that formed on the distal parts of an extended coastal floodplain. Abundant *Cochlichnus anguineus* and *Helminthopsis hieroglyphica* serve as a useful overall marker for the local *Selenichnites* ichnoassociation beds. These invertebrate trails are largely absent from Robledo Mountains Formation red beds. Abundant circular impressions (scratch circles?) commonly found on Community Pit float blocks also serve as a useful overall marker for this ichnoassociation and are likewise absent from Robledo Mountains Formation red beds.

ACKNOWLEDGMENTS

Mike Romano and Matt Stimson generously provided reviews that substantially improved this paper. Thank you. We also wish to thank Whitey Hagadorn and Soren Jensen for helpful discussion concerning sedimentary structures and pseudofossils. Lauren Babcock and Sebastian Voigt are also acknowledged for discussion, encouragement, and diverse assistance. Larry Rinehart provided invaluable field contributions that significantly added to the scope of this paper. Amanda Cantrell provided assistance as NMMNH Collections Manager. Jerry P. MacDonald is acknowledged for having collected many of the referred specimens and for his long dedication to the successful establishment of the Prehistoric Trackways National Monument.

REFERENCES

Allen, J. G., and Feldmann, R. M., 2005, *Panduralimulus babcocki* n. gen. and sp., a new limulacean horseshoe crab from the Permian of Texas: Journal of Paleontology, v. 79, p. 594-600.

Anderson, A., 1976, Fish trails from the Early Permian of South Africa: Palaeontology, v. 19, p. 397-409.

Babcock, L. E. and Merriam, D. E., 2000, Horseshoe crabs (Arthropoda: Xiphosurida) from the Pennsylvanian of Kansas and elsewhere: Transactions of the Kansas Academy of Science, v. 103, p. 76-94.

Babcock, L. E., Merriam, D. F. and West, R., 2000, *Paleolimulus*, an early limuline (Xiphosurida), from Pennsylvanian-Permian Lagerstätten of Kansas, and taphonomic comparison with modern *Limulus*: Lethaia, v. 33, p. 129-141.

Barthel, K. W., 1974, *Limulus*: a living fossil: Naturawissenschaften, v. 61, p. 428-433.

Bengtson, P., 1988, Open nomenclature: Palaeontology, v. 31, p. 223-227.

Behrends, G., and Michaelis, H, 1977, Zur Deutung der Lebensspuren des Polychaeten *Scolelepis squamata*: Senckenbergiana Maritima, v. 9, p. 47-57.

Berman, D. S., 1993, Lower Permian vertebrate localities of New Mexico and their assemblages: New Mexico Museum of Natural History and Science, Bulletin, 2, p. 11-21.

Botton, M. L., Tankersley, R. A., and Loveland, R. E., 2010, Developmental ecology of the American horseshoe crab: Current Zoology, v. 56, p. 550-562.

Braddy, S. J., 1998, An overview of the invertebrate ichnotaxa from the Robledo Mountains ichnofauna (Lower Permian), southern New Mexico: New Mexico Museum of Natural History and Science, Bulletin 12, p. 93-98.

Buatois, L. A., Jalfin, G. and Aceñolaza, F. G., 1997, Permian nonmarine invertebrate trace fossils from southern Patagonia, Argentina; ichnologic signatures of substrate consolidation and colonization sequences: Journal of Paleontology, v. 71, p. 324-336.

Buatois, L. A., and Mángano, 1993, Trace fossils from a Carboniferous turbiditic lake: Implications for the recognition of additional nonmarine ichnofacies: Ichnos, v. 2, p. 237-258.

Buatois, L. A., and Mángano, M. G., 2011, Ichnology: organism-substrate interactions in space and time. Cambridge University Press, 358 p.

Buatois, L. A., Mángano, M. G., Maples, C. G. and Lanier, W. P., 1998, Ichnology of an Upper Carboniferous fluvio-estuarine paleovalley: The Tonganoxie Sandstone, Buildex Quarry, eastern Kansas, USA: Journal of Paleontology, v. 72, p. 152-180.

Buck, S. G., and Goldring, R., 2003, Conical sedimentary structures. Trace fossils or not? Observations, experiments, and review: Journal of Sedimentary Research, v. 73, p. 338-353.

Caster, K. E., 1938, A restudy of the tracks of *Paramphibius*: Journal of Paleontology, v. 12, p. 3-60.

Caster, K. E., 1944, Limuloid trails from the Upper Triassic (Chinle) of the Petrified Forest National Monument, Arizona: American Journal of Science, v. 242, p. 74-84.

Chamberlain, C. K., 1975, Recent Lebensspurren in nonmarine aquatic environments; *in* Frey, R. W., ed., The study of trace fossils. New York, Springer-Verlag, p. 431-458.

Chisholm, J. I., 1985, Xiphosurid burrows from the Lower Coal Measures (Westphalian A) of West Yorkshire: Palaeontology, v. 28, p. 619-662.

Crimes, T. P., Legg, I., Marcos, and Arboleya, M., 1977, ?Late Precambrian-low Lower Cambrian trace fossils from Spain; *in* Crimes, T. P. and Harper, J. C., eds.,Trace fossils 2: Geological Journal, Special Issue 9, p. 91-138.

Dunbar, C. O., 1923, Kansas Permian insects. Part 2. *Paleolimulus*, a new genus of Paleozoic Xiphosura, with notes on other genera: American Journal of Science, 5th Series, v. 5, p. 443-454.

Draganits, E., Braddy, S. J. and Briggs, D. E. G., 2001, A Gondwanan coastal arthropod ichnofauna from the Muth Formation (Lower Devonian, Northern India): Paleoenvironment and trace maker behavior: Palaios, v. 16, p. 126-147.

Eagar, R. M. C., Baines, J. G., Collinson, J. D., Hardy, P. G., Okolo, S. A. and Pollard, J. E., 1985, Trace fossil assemblages and their occurrence in Silesian (mid-Carboniferous) deltaic sediments of the Central Pennine Basin, England; *in* Curran, H. A., ed., Biogenic structures: Their use in interpreting depositional environments: Society of Economic Paleontologists and Mineralogists, Special Publication 35, p. 99-149.

Eldredge, N., 1970, Observations on burrowing behavior in *Limulus polyphemus* (Chelicerata, Merostomata), with implications for the functional anatomy of trilobites: American Museum Novitates, no. 2436, p. 1-17.

Fernández, D. E. and Pazos, P. J., Xiphosurid trackways in a Lower Cretaceous tidal flat in Patagonia: Palaeoecological implications and the involvement of microbial mats in trace-fossil preservation: Palaeogeography, Palaeoclimatology, Palaeoecology, v. 375, p. 16-29.

Fischer, W. A., 1978, The habitat of the early vertebrates: Trace and body fossil evidence from the Harding Formation (Middle Ordovician), Colorado: The Mountain Geologist, v. 15, p. 1-26.

Gaillard, C., 2009, A giant limulid trackway (*Kouphichnium lithographicum*) from the lithographic limestones of Cerin (Late Kimmeridgian, France): Ethological and environmental implications: Swiss Journal of Geosciences, v. 104, p. 57-72.

Gibb, S., Chatterton, B. D. E., and Pemberton, S. G., 2011, Prod traces (*Selenichnites*) from the Middle Cambrian of Morocco, with hypotheses on the ethology of the tracemaker(s): Ichnos, v. 18, p. 156-165.

Gibert, J. M. De, Buatois, L. A., Fregenal-Martínez, M. A., Mangano, M. G., Ortega, F., Poyato-Ariza, F. J. and Wenz, S., 1999, The fish trace fossil *Undichna* from the Cretaceous of Spain: Palaeontology, v. 42, p. 409-427.

Gingras, M. K., Dashtgard, S. E., MacEachern, J. A. and Pemberton, S. G., 2008, Biology of shallow marine ichnology: A modern perspective: Aquatic Biology, v. 2, p. 255-268.

Goldring, R. and Seilacher, A., 1971, Limulid undertracks and their sedimentological implication: Neues Jarhbuch für Geologie und Paläontologie Abhandlungen, v. 137, p. 422-442.
Goldring, R., Pollard, J. E. and Radley, J. D., 2005, Trace fossils and pseudofossils from the Wealden strata (non-marine Lower Cretaceous) of southern England: Cretaceous Research, v. 26, p. 665-685.
Hardy, P. G., 1970, New xiphosurid trails from the Upper Carboniferous of northern England: Palaeontology, v. 13, p. 188-190.
Heer, O., 1877, Florafossils Helvetias: Die vorweltliche Flora der Schweiz. Zurich, J. Wurster and Co., 182 p.
Hitchcock, E., 1858, Ichnology of New England: Report on the sandstone of the Connecticut Valley, especially its fossil foot marks: Boston, W. White, 220 p.
Hou, X.-G., Stanley, G. D., Jr, Zhao, J. and Ma, X.-Y., 2005, Cambrian anemones with preserved soft tissue from the Chengjiang biota, China: Lethaia, v. 38, p. 193-203.
King, A. F., 1965, Demonstration: Xiphosurid trails from the Upper Carboniferous of Bude, north Cornwall: Proceedings of the Geological Society of London, v. 1626, p. 162-165.
Kues, B. S., 1995, Marine fauna of the Early Permian (Wolfcampian) Robledo Mountains Member, Hueco Formation, southern Robledo Mountains, New Mexico: New Mexico Museum of Natural History and Science, Bulletin 6, p. 63-90.
Lawfield, A. M. W., and Pickerill, R. K., 2006, A novel contemporary fluvial ichnocoenose: Unionid bivalves and the *Scoyenia-Mermia* ichnofacies transition: Palaios, v. 21, p. 391-396.
Lerner, A. J. and Lucas, S. G., 2010, An unusual cnidarian-dominated trace and body fossil assemblage from the Lower Permian Robledo Mountains Formation, south-central New Mexico, USA: Abstracts Volume, 18th International Sedimentological Congress, Mendoza, Argentina, p. 538.
Lerner, A. J., Lucas, S. G., MacDonald, J. P. and Spielmann, J. A., 2010, A new association of Early Permian invertebrate trace and body fossils from the Prehistoric Trackway National Monument of south-central New Mexico: Abstracts Volume, A Decade of Discovery; National Landscape Conservation System, Bureau of Land Management Science Symposium, p. 22-23.
Lerner, A. J, Lucas, S. G. and Spielmann, J. A., 2007, Invertebrate ichnoassemblage from the Triassic Moenkopi Group in north-central Utah: New Mexico Museum of Natural History and Science, Bulletin 40, p. 203-207.
Lipps, J. H. and Valentine, J. W., 2004, Late Neoproterozoic Metazoa: Weird, wonderful, and ghostly: The Paleontology Society Papers, v. 10, p. 51-66.
Lomax, D. R. and Racay, C. A., 2012, A long mortichnial trackway of *Mesolimulus walchi* from the Upper Jurassic Solnhofen lithographic limestone near Wintershof, Germany: Ichnos, v. 19, p. 175-183.
Lucas, S. G., Estep, J. W. and Hoffer, J. M., eds., 1998, Permian stratigraphy and paleontology of the Robledo Mountains, New Mexico: New Mexico Museum of Natural History and Science, Bulletin 12, 98 p.
Lucas, S. G., Anderson, O. J., Heckert, A. B. and Hunt, A. P., 1995, Geology of Early Permian tracksites, Robledo Mountains, south-central New Mexico: New Mexico Museum of Natural History and Science, Bulletin 6, p. 13-32.
Lucas, S.G. and Heckert, A.B., eds. 1995, Early Permian footprints and facies: New Mexico Museum of Natural History and Science, Bulletin 6, 301 p.
Lucas, S. G., Lerner, A. J, DiMichele, W. A., Cantrell, A. K., Suazo, T. L. and Chaney, D. S., 2014, Xiphosaurid fossils from the Pennsylvanian Beeman Formation, Otero County, New Mexico: New Mexico Geological Society, Guidebook 65, p. 311-314.
Mack, G.H. and James, W.C., 1986, Cyclic sedimentation in the mixed siliciclastic-carbonate Abo-Hueco transitional zone (Lower Permian), southwestern New Mexico: Journal of Sedimentary Petrology, v. 56, p. 635-647.
Mángano, M. G., Buatois, L. A. and Guinea, F. M., 2005, Ichnology of the Alfarcito Member (Santa Rosita Formation) of northwestern Argentina; animal-substrate interactions in a lower Paleozoic wave-dominated shallow sea: Ameghiniana, v. 42, p. 641-668.
Meglitsch, P. A. and Schram, F. R., 1991, Invertebrate Zoology, 3rd ed., Oxford University Press, 409 p.
Metz, R. 1987, Insect traces from nonmarine ephemeral puddles: Boreas, v. 16, p. 330-348.
Mikulic, D. G., 1995, Xiphosura; *in* Shabica, C. W. and Hay, A. A., eds., Richardson's guide to the fossil fauna of Mazon Creek: Northeastern Illinois University Press, p. 134-139.
Miller, M. F., 1982, *Limulicubichnus*: A new ichnogenus of limulid resting traces: Journal of Paleontology, v. 56, p. 429-433.
Minter, N. J. and Braddy, S. J., 2006, The fish and amphibian swimming traces *Undichna* and *Lunichnium*, with examples from the Lower Permian of New Mexico, USA: Palaeontology, v. 49, p. 1123-1142.
Minter, N. J. and Braddy, S. J., 2009, Ichnology of an Early Permian intertidal flat: The Robledo Mountains Formation of southern New Mexico, USA: Special Papers in Palaeontology, v. 82, 107 p.
Moore, R. A., McKenzie, S. C. and Lieberman, B. S., 2007, A Carboniferous synziphosurine (Xiphosura) from the Bear Gulch Limestone, Montana, USA: Palaeontology, v. 50, p. 1013-1019.
Moussa, M. T., 1970, Nematode trails of the Green River Formation (Eocene) in the Uinta Basin, Utah: Journal of Paleontology, v. 44, p. 304-307.
Myrow, P. M., 1992, Pot gutter casts from the Chapel Island Formation, southeast Newfoundland: Journal of Sedimentary Petrology, v. 62, p. 992-10007.
Nopsca, F. B., 1923, Die Familien der Reptilien: Forschritte de Geologie und Paläontologie, v. 2, p. 1-210.
Pemberton, S. G., Frey, R. W. and Bromley, R. G., 1988, The ichnotaxonomy of *Conostichus* and other plug-shaped ichnofossils: Canadian Journal of Earth Sciences, v. 25, p. 866-892.
Poiré, D. G. and Del Valle, A., 1996, Trazas fosiles en barras submareales de la Formacion Balcarce (Cambrico/Ordovicico), Cabo Corrientes, Mar del Plata, Argentina: Asociación Paleontológica Argentina, Publicación Especial 4, p. 89-102.
Romano, M. and Whyte, M. A., 1987, A limulid trace fossil from the Scarborough Formation (Jurassic) of Yorkshire; its occurrence, taxonomy and interpretation: Proceedings of the Yorkshire Geological Society. v. 46, p. 85-95.
Romano, M. and Whyte, M. A., 1990, *Selenichnites*, a new name for the ichnogenus *Selenichnus* Romano and Whyte, 1987: Proceedings of the Yorkshire Geological Society, v. 48, p. 221.
Rudkin, D. M. and Young, G. A., 2009, Horseshoe crabs. An ancient ancestry revealed; *in* Tanacredi, J., Botton, M. L. and Smith, D. R., eds., Biology and conservation of horseshoe crabs: Berlin, Springer, p. 25-44.
Rudloe, A., 1981, Aspects of the biology of juvenile horseshoe crabs, *Limulus polyphemus*: Bulletin of Marine Science, v. 31, p. 125-133.
Sandstedt, R., Sullivan, T. and Schuster, M., 1961, Nematode tracks in the study of movement of *Meloidogyne incognita incognita*: Nematologica, v. 6, p. 261-265.
Schram, F. R., 1979, Worms of the Mississippian Bear Gulch Limestone of central Montana, USA: Transactions of the San Diego Society of Natural History, v. 19, p. 107-120.
Seilacher, A., 2007, Trace fossil analysis. Heidelberg; Springer-Verlag, 358 p.
Signor, P. W. III and Brett, C. E., 1984, The mid-Paleozoic precursor to the Mesozoic marine revolution: Paleobiology, v. 10, p. 229-245.
Suzuki, Y., Kondo, A. and Bergström, 2008, Morphological requirements in limulid and decapod gills: A case study in deducing the function of lamellipedian exopod lamellae: Acta Palaeontologica Polonica, v. 53, p. 275-283.
Trewin, N. H. and McNamara, K. J., 1995, Arthropods invade the land: Trace fossils and palaeoenvironments of the Tumblagooda Sandstone (?Late Silurian) of Kalbarri, Western Australia: Transactions of the Royal Society of Edinburgh: Earth Sciences, v. 85, p. 177-210.
Van der Hammen, L., 1986, Comparative studies in Chelicerata IV. Apatellata, Arachnida, Scorpionida, Xiphosura: Zoologische Verhandenlingen, v. 226, p. 1-52.
Voigt, S., Lucas, S. G. and Krainer, K., 2013, Coastal-plain origin of trace-fossil bearing red beds in the Early Permian of southern New Mexico: Palaeogeography, Palaeoclimatology, Palaeoecology, v. 369, p. 323-334.
Walls, E. A., Berkson, J., and Smith, S. A., 2002, The horseshoe crab, *Limulus polyphemus*: 200 million years of existence, 100 years of study: Reviews in Fisheries Science, v. 101, p. 39-73.
Weber, B., and Braddy, S. J., 2004, A marginal marine ichnofauna from the Blaiklock Glacier Group (?Lower Ordovician) of the Shackleton Range, Antarctica: Transactions of the Royal Society of Edinburgh: Earth Sciences, v. 94, p. 1-20.
Wetzel, A., and Bromley, R. G., 1996, Re-evaluation of the ichnogenus *Helminthopsis*- a new look at the type material: Palaeontology, v. 39, p. 1-19.
Whyte, M. A., and Romano, M., 2001, A dinosaur ichnocoenosis from the Middle Jurassic of Yorkshire, UK: Ichnos, v. 8, p. 223-234.

Lucas, S. G. and DiMichele, W. A., eds., 2015, Carboniferous-Permian Transition in the Robledo Mountains, Southern New Mexico. New Mexico Museum of Natural History and Science Bulletin 65.

PERMIAN TETRAPOD ICHNODIVERSITY OF THE PREHISTORIC TRACKWAYS NATIONAL MONUMENT (SOUTH-CENTRAL NEW MEXICO, U.S.A.)

SEBASTIAN VOIGT[1] AND SPENCER G. LUCAS[2]

[1]Urweltmuseum GEOSKOP / Burg Lichtenberg (Pfalz), Burgstr. 19, 66871 Thallichtenberg, Germany, s.voigt@pfalzmuseum.bv-pfalz.de;
[2]New Mexico Museum of Natural History and Science, 1801 Mountain Road N.W., Albuquerque, New Mexico 87104, U.S.A., spencer.lucas@state.nm.us

Abstract—The Early Permian (early Leonardian) Robledo Mountains Formation of the Prehistoric Trackways National Monument (PTNM) near Las Cruces, south-central New Mexico, contains one of the most abundant and most extensively discussed assemblages of Paleozoic tetrapod footprints in the world. More than 700 specimens with tetrapod footprints from this place, housed at the New Mexico Museum of Natural History and Science, Albuquerque, have recently been subjected to an anatomical-feature-based ichnotaxonomic analysis. Based on the results of this study, the tracks belong to eight tetrapod ichnotaxa *Matthewichnus caudifer* Kohl and Bryant, 1994, *Batrachichnus salamandroides* (Geinitz, 1861), *Amphisauropus kablikae* (Geinitz and Deichmüller, 1882), *Dimetropus leisnerianus* (Geinitz, 1863), *Notalacerta missouriensis* Butts, 1891, *Robledopus macdonaldi* Voigt, Lucas, Buchwitz and Celeskey, 2013, *Hyloidichnus bifurcatus* Gilmore, 1927, and *Dromopus lacertoides* Marsh, 1894, which can be referred to lepospondyl, temnospondyl, seymouriamorph, pelycosaurian-grade synapsid, protorothyridid, captorhinid, and araeoscelid trackmakers. About 90% of the material comprises tracks of *Batrachichnus*, *Dimetropus*, and *Dromopus*, suggesting that temnospondyl amphibians, pelycosaurs, and early diapsids represented the most common individuals of the ancient terrestrial tetrapod fauna of the study area. The ichnoassemblage is of typical Early Permian aspect and, in view of the low number and diversity of advanced captorhinomorph footprints (*Hyloidichnus*), supports assignment to the Artinskian stage. Notable features are the rare occurrence of two more typically Pennsylvanian ichnotaxa (*Matthewichnus*, *Notalacerta*) as well as the only occurrence of the proposed basal non-diapsid eureptilian track *Robledopus*. The exceptional status of the PTNM track assemblages is paleoecologically based, rather than reflecting a biostratigraphic acme, as the Robledo Mountains Formation in the Robledo Mountains yields the best studied marginal marine vertebrate footprint assemblage of Early Permian age.

INTRODUCTION

The Early Permian (early Leonardian) Robledo Mountains Formation in south-central New Mexico contains one of the most abundant and diverse assemblages of nonmarine Paleozoic trace fossils in the world (MacDonald, 1992, 1994; Hunt et al., 1993; Lucas and Heckert, 1995; Lucas et al., 1998a; Minter and Braddy, 2009). As a first-class ichnofossil Lagerstätte, the stratum typicum area was protected by law as the Prehistoric Trackways National Monument (PTNM) in March 2009, and this stimulated an intensification of research activities in this area (e. g., Lucas et al., 2010, 2013a; Voigt et al., 2013a, b; Falcon-Lang et al., 2014).

A recently finished conservative revision of invertebrate trace fossil collections from the PTNM shows 22 assigned taxa, while treating nine other forms in open nomenclature (Minter and Braddy, 2009). Invertebrate traces from the PTNM are mostly arthropod walking and shallow feeding traces. Though much more work has always been dedicated to the vertebrate tracks of the study area, their taxonomy is still obscure, given that 34 different binominal names are available in the literature for tetrapod footprints from the Robledo Mountains (Schult, 1994, 1995; Haubold et al., 1995; Hunt et al., 1995; Lucas et al., 1998a; Braddy et al., 2003; Minter and Braddy, 2006, 2009; Voigt et al., 2013a, b). Results of an anatomical-feature-based ichnotaxonomic revision performed in 2010 to 2012 and presented here for the first time point to a moderately diverse ichnofauna. The faunistic interpretation of this extensive footprint record gives new perspective to our understanding of the evolution and ecology of early tetrapods.

LOCALITY AND GEOLOGICAL CONTEXT

The Robledo Mountains are a wedge-shaped, southward-dipping horst of Paleozoic and Cenozoic rocks on the western margin of the Rio Grande rift near Las Cruces, New Mexico (Fig. 1; LeMone et al., 1975; Lucas et al., 1995, 1998a). The majority of strata exposed in the PTNM are early Leonardian (Early Permian, Artinskian) sedimentary rocks that occupy a geographic position between the marine carbonates and shales of the Hueco Group to the south and the nonmarine siliciclastics of the Abo Formation to the north (Lucas et al., 1998a-c, 2011, 2012, 2013b). An approximately 125-m-thick section of interbedded shallow marine carbonates, tidal flat sandstones, and coastal plain mudstones has been assigned to the Robledo Mountains Formation (Lucas et al., 1998b; Voigt et al., 2013a). These marginal marine deposits are extraordinarily rich in fossil tracks and traces. Plant impressions, petrified wood, and abundant root traces point to a heterogeneous, vegetated tropical coastline with a variety of microhabitats and specialized biota.

MATERIAL AND METHODS

This study is based on a revision of about 1000 catalogued specimens with tetrapod footprints from the PTNM housed in the New Mexico Museum of Natural History and Science (NMMNH) in Albuquerque, New Mexico. The material comes from marginal marine and continental strata of 48 different localities in the Robledo Mountains Formation and was mainly collected by Jerry P. MacDonald, Las Cruces, New Mexico, between 1987 and 2010 (MacDonald, 1994, 1995). Each specimen of PTNM tetrapod footprints at the NMMNH was described in detail and photographed for the purpose of this work. Outline drawings were made of true trackways in order to quantify parameters of the imprint morphology and trackway pattern according to standard procedures in vertebrate ichnology (Haubold, 1971; Leonardi et al., 1987; Voigt and Haubold, 2000). The ichnotaxonomy applied here is strongly based on anatomically-controlled features of the imprint morphology and trackway pattern (Haubold, 1996). This study benefits from a comparative analysis carried out between 2010 and 2012 of all Paleozoic tetrapod footprints from New Mexico housed in the New Mexico Museum of Natural History. All specimens discussed here are housed at NMMNH where the map coordinates of fossil localities are on file.

ICHNOTAXONOMY

The NMMNH collection includes about 775 specimens with tetrapod footprints from 48 fossil localities of the Robledo Mountains Formation at PTNM (Table 1). Almost 60% of these specimens (443 by number) only preserve tracks that cannot be identified. The remaining 332 specimens of the PTNM tetrapod footprint collection at

NMMNH can be assigned to eight ichnotaxa: *Matthewichnus caudifer*, *Batrachichnus salamandroides*, *Amphisauropus kablikae*, *Dimetropus leisnerianus*, *Notalacerta missouriensis*, *Robledopus macdonaldi*, *Hyloidichnus bifurcatus*, and *Dromopus lacertoides*. About 300 specimens (90%) of all specimens with assignable tracks belong to only three ichnotaxa *Batrachichnus salamandroides*, *Dimetropus leisnerianus*, and *Dromopus lacertoides*. In this section we briefly describe each of the eight PTNM tetrapod ichnotaxa based on the best preserved material at NMMNH. An overview of the subjective ichnotaxonomic synonymy of previously studied specimens of the same collection is given in Table 2.

Matthewichnus caudifer Kohl and Bryant, 1994 (Figs. 2, 10A)

Material: NMMNH P-23046, incomplete step cycle, convex hyporelief, NMMNH locality 846; NMMNH P-23312, trackway with continuous tail trace, convex hyporelief, NMMNH locality 2817; NMMNH P-23377, incomplete trackway, convex hyporelief, NMMNH locality 846; NMMNH P-23511, trackway with continuous tail trace, concave epirelief, NMMNH locality 846; NMMNH P-24342, short trackway, concave epirelief, NMMNH locality 846; NMMNH P-62087, long trackway, concave epirelief, NMMNH locality 7934.

Description: Trackways of quadrupedal tetrapods with tetradactyl manus and pentadactyl pes imprints up to 2 cm long. Manus imprints about one third shorter than pes imprints, with long digits II and III and short digits I and IV. Digit length of the pes imprint increases from I to IV, with digit V about as long as II. Digit impressions are usually straight or slightly curved inward and distally rounded. Trackways sometimes with distinct and continuous tail or body trace. Manus and pes imprints seem to be randomly positioned along trackways except: (1) manus imprints are often inwardly rotated, pes imprints either forward or outwardly rotated; (2) left and right manus imprints are narrower than the related pes imprints; and (3) pes imprints are in front of closely associated or partially overstepped manus imprints.

Discussion: This kind of track is most similar to *Matthewichnus caudifer* Kohl and Bryant, 1994. The most striking feature of the tracks is the highly irregular trackway pattern pointing to trackmakers with long glenoacetabular distances and low pace angulation of 90° or less (Kohl and Bryant, 1994; Haubold et al., 2005). Solely based on characters of the imprint morphology, *M. caudifer* is indistinguishable from *Batrachichnus salamandroides*. Separation of the two ichnotaxa is only tenable as long as there is no specimen recording the transition from the highly irregular trackway pattern of *M. caudifer* to the regular trackway pattern of alternately arranged manus-pes couples that are usually preserved in *B. salamandroides*. Considering the small size of the imprints and the inferred high coupling value, microsaurs are among the most likely trackmakers of *M. caudifer* from the Robledo Mountains Formation at PTNM.

Batrachichnus salamandroides (Geinitz, 1861) (Figs. 3, 10B)

Material: NMMNH P-23060, two manus-pes couples of two trackways, concave epirelief, from NMMNH locality 2821; NMMNH P-23065, shallow undertracks of a single trackway, convexe hyporelief, from NMMNH locality 2852; NMMNH P-23174, longer trackway segment with distinct undertracks, part and counterpart, from NMMNH locality 2821; NMMNH P-23315, numerous surface to near-surface tracks of at least three different trackways, part and counterpart, from NMMNH locality 2818; NMMNH P-23400, trackway with tail/body trace, part and counterpart, from NMMNH locality 846; NMMNH P-23593, surface to near-surface tracks of a single trackway with discontinuous tail/body trace, part and counterpart, from NMMNH locality 2851; NMMNH P-47800, trackway of well-preserved tracks with continuous tail/body trace, convex hyporelief, from NMMNH locality 846; NMMNH P-62184, longer trackway of shallow near-surface tracks with faint tail/body trace, concave epirelief, from NMMNH locality 2821; NMMNH P-62199, random association of several larger tracks, concave epirelief, from NMMNH locality 7934; NMMNH P-62212, single trackway with continuous tail/body trace, from NMMNH locality 7924.

Description: Tracks of quadrupedal tetrapods with tetradactyl, plantigrade manus imprints up to 25 mm long. Manus imprints are slightly wider than long and exhibit a serial increase in digit length from I to III. Digit IV is about as long as II, and the longest digit is about half the length of the manus imprint. Pes imprints pentadactyl and semiplantigrade, usually as long as wide, with digit proportions I<II~V<III<IV. Trackway pattern with regularly arranged manus and pes tracks, mostly with alternating coupled manus-pes sets. The pes imprint is positioned posteriorly to the manus imprint or proximally overstepping it. Manus imprint pointed inward, pes mainly pointed outward. Continuous to discontinuous tail drag mark common.

Discussion: The described footprints are characterized by the tetradactyl manus imprint, small track size and an often very regular trackway pattern matching all characteristics of *Batrachichnus*

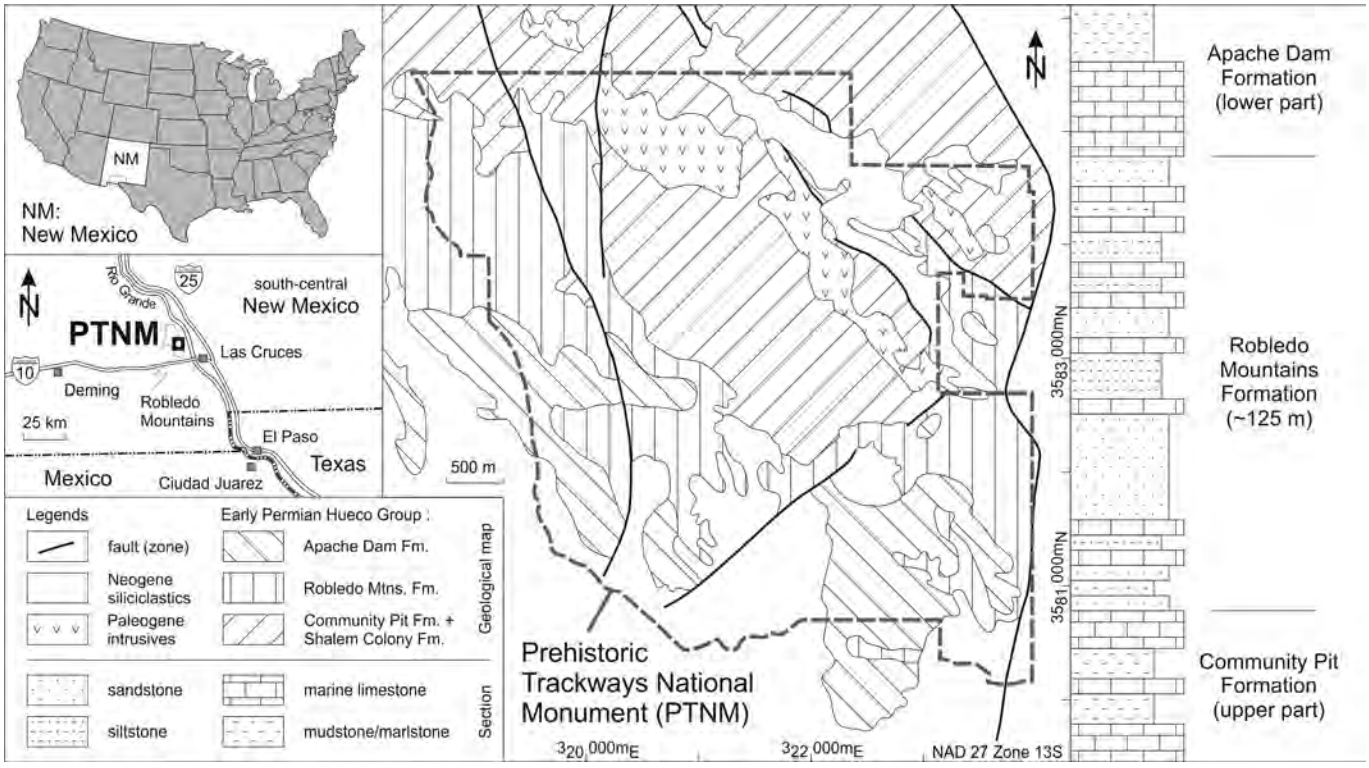


FIGURE 1. Simplified geological framework of the Prehistoric Trackways National Monument, Robledo Mountains, south-central New Mexico (after Lucas et al., 1995, 1998b; Voigt et al., 2013a).

TABLE 1. NMMNH tetrapod footprint localities and tetrapod ichnodiversity of the Robledo Mountains Formation at PTNM.

NMMNH Locality	*Matthew-ichnus*	*Batrach-ichnus*	*Amphi-sauropus*	*Dime-tropus*	*Nota-lacerta*	*Robledo-pus*	*Hyloid-ichnus*	*Dromo-pus*	Specimens indet.	Total specimens
L-846	+	+	+	+	-	-	-	+	139	320
L-2811	-	-	-	+	-	-	-	+	5	10
L-2812	-	-	-	+	-	-	-	+	3	6
L-2813	-	+	-	+	-	-	-	+	7	14
L-2814	-	+	-	+	-	-	-	+	8	11
L-2815	-	+	-	-	-	-	-	+	1	3
L-2816	-	+	-	+	-	-	-	-	4	5
L-2817	+	+	-	+	-	-	-	+	48	52
L-2818	-	+	-	+	-	-	-	+	18	31
L-2819	-	+	-	+	-	-	-	-	5	7
L-2820	-	-	-	-	-	-	-	-	3	3
L-2821	-	+	-	+	-	+	+	+	29	51
L-2823	-	+	-	+	-	-	-	-	8	12
L-2824	-	-	-	-	-	+	-	+	5	7
L-2825	-	-	-	-	-	-	-	-	2	2
L-2828	-	+	-	+	-	-	-	+	21	31
L-2829	-	-	-	-	-	-	-	+	2	3
L-2830	-	+	-	-	-	-	-	-	0	1
L-2835	-	+	-	-	-	-	-	-	12	16
L-2851	-	+	-	-	-	-	-	+	23	37
L-2852	-	+	-	+	-	-	-	+	53	63
L-7903	-	-	-	-	-	-	-	-	2	2
L-7920	-	+	-	-	-	-	-	-	0	1
L-7922	-	-	-	-	-	-	-	+	0	1
L-7923	-	+	-	-	-	-	-	-	0	1
L-7924	-	-	-	-	-	-	-	+	0	2
L-7925	-	-	-	-	-	-	-	+	0	1
L-7926	-	-	-	-	-	-	-	+	0	1
L-7927	-	+	-	-	-	-	-	-	0	1
L-7928	-	+	-	-	-	-	-	+	0	2
L-7929	-	+	-	+	-	-	-	-	1	4
L-7930	-	+	-	-	-	-	-	-	0	1
L-7931	-	+	-	-	-	-	-	-	0	1
L-7934	+	+	-	-	-	-	-	+	2	10
L-7959	-	+	-	+	-	-	-	+	1	5
L-7966	-	-	-	-	-	-	-	-	9	9
L-7967	-	-	-	-	-	-	-	-	2	2
L-7969	-	-	-	+	-	-	-	+	3	5
L-7970	-	-	-	-	-	-	-	-	1	1
L-8020	-	-	-	-	-	-	-	-	1	1
L-8211	-	-	-	-	-	-	-	-	18	18
L-8212	-	+	-	+	-	-	-	-	0	3
L-8220	-	+	-	-	+	-	-	+	2	7
L-8257	-	-	-	-	-	-	-	-	1	1
L-8259	-	-	-	+	-	-	-	-	0	1
L-8261	-	-	-	-	-	-	-	-	1	1
L-8542	-	+	-	-	-	-	-	+	1	6
L-8641	-	-	-	-	-	-	-	-	2	2
48 localities	+	+	+	+	+	+	+	+	443	775

TABLE 2. Subjective ichnotaxonomic synonymy of important PTNM tetrapod footprint specimens at NMMNH, including inorganic markings that have been interpreted to be tetrapod footprints by previous workers. *Serpentichnus* is rejected as a trace fossil based on recent PTNM facies analyses (Voigt et al., 2013a).

NMMNH specimen	Assignation by reference	Reference	this paper
P-4000	*Lunichnium rotterodium*	Minter and Braddy (2006: fig. 5A)	indet.
P-4000	*Lunichnium rotterodium*	Minter and Braddy (2009: fig. 44B)	indet.
P-23001	*Batrachichnus delicatulus*	Haubold et al. (1995: fig. 2B)	*Batrachichnus salamandroides*
P-23060	*Limnopus* sp.	Haubold et al. (1995: fig. 7C)	*Batrachichnus salamandroides*
P-23066	cf. *Gilmoreichnus hermitanus*	Haubold et al. (1995: fig. 21B)	*Dimetropus leisnerianus*
P-23072	*Gilmoreichnus* sp.	Haubold et al. (1995: fig. 22A)	*Robledopus macdonaldi*
P-23072	*Erpetopus*, cf. *E. willistoni*	Hunt et al. (1995: fig. 3A)	*Robledopus macdonaldi*
P-23088	*Hyloidichnus bifurcatus*	Haubold et al. (1995: fig. 9A)	*Hyloidichnus bifurcatus*
P-23138	*Batrachichnus delicatulus*	Haubold et al. (1995: fig. 5B)	*Batrachichnus salamandroides*
P-23169	*Serpentichnus*? *robledoensis*	Minter and Braddy (2009: fig. 46G)	tool marks
P-23171	*Dromopus agilis*	Haubold et al. (1995: fig. 14C)	*Dromopus lacertoides*
P-23174	*Batrachichnus delicatulus*	Haubold et al. (1995: fig. 2C)	*Batrachichnus salamandroides*
P-23269	*tracks of large amphibian*	Hunt et al. (1995: fig. 3B)	*Amphisauropus kablikae*
P-23277	*Batrachichnus delicatulus*	Haubold et al. (1995: fig. 2A)	*Batrachichnus salamandroides*
P-23305	*Dimetropus leisnerianus*	Hunt et al. (1995: fig. 7B)	*Dimetropus leisnerianus*
P-23315	*Batrachichnus delicatulus*	Haubold et al. (1995: fig. 4A)	*Batrachichnus salamandroides*
P-23317	*Serpentichnus*? *robledoensis*	Minter and Braddy (2009: fig. 46E)	tool marks
P-23320	*Gilmoreichnus hermitanus*	Hunt et al. (1995: fig. 5E, F)	indet. (probably captorhinomorph manual undertracks)
P-23322	*Gilmoreichnus* sp.	Haubold et al. (1995: fig. 22B)	*Robledopus macdonaldi*
P-23329	*Dromopus lacertoides*	Minter and Braddy (2009: fig. 43D)	*Dromopus lacertoides*
P-23424	cf. *Gilmoreichnus hermitanus*	Haubold et al. (1995: fig. 21A)	*Robledopus macdonaldi*
P-23443	*Serpentichnus* cf. *robledoensis*	Minter and Braddy (2009: fig. 45C)	tool marks
P-23487	*Serpentichnus*? *robledoensis*	Minter and Braddy (2009: fig. 46D)	tool marks
P-23489	*Serpentichnus*? *robledoensis*	Minter and Braddy (2009: fig. 46F)	tool marks
P-23490	*Serpentichnus*? *robledoensis*	Minter and Braddy (2009: fig. 46H)	tool marks
P-23493	*Serpentichnus*? *robledoensis*	Minter and Braddy (2009: fig. 46A)	tool marks
P-23510	*Batrachichnus delicatulus*	Haubold et al. (1995: fig. 5A)	*Matthewichnus caudifer*
P-23548	*Serpentichnus*? *robledoensis*	Minter and Braddy (2009: fig. 46C)	tool marks
P-23667	*Batrachichnus delicatulus*	Braddy et al. (2003: fig. 2A)	indet.
P-23667	*Batrachichnus salamandroides*	Minter and Braddy (2009: fig. 41C)	indet.
P-23716	*Dimetropus nicolasi*	Minter and Braddy (2009: fig. 43B)	*Dimetropus leisnerianus*
P-23719	*Dimetropus* sp., cf. *D. nicolasi*	Haubold et al. (1995: fig. 23B)	*Dimetropus leisnerianus*
P-23719	*Dimetropus nicolasi*	Minter and Braddy (2009: fig. 43A)	*Dimetropus leisnerianus*
P-23723	*Dimetropus* sp., cf. *D. nicolasi*	Haubold et al. (1995: fig. 24C)	*Dimetropus leisnerianus*
P-23941	*Gilmoreichnus hermitanus*	Hunt et al. (1995: fig. 5C, D)	*Dimetropus leisnerianus*
P-23979	*Dromopus lacertoides*	Minter and Braddy (2009: fig. 43C)	*Dromopus lacertoides*
P-24144/24148	*Serpentichnus robledoensis*	Braddy et al. (2003: fig. 4)	tool marks
P-24144/24148	*Serpentichnus robledoensis*	Minter and Braddy (2009: fig. 45A)	tool marks
P-24149	*Serpentichnus sigmoidalis*	Minter and Braddy (2009: fig. 48B)	tool marks
P-24153	*Serpentichnus sigmoidalis*	Minter and Braddy (2009: fig. 48C)	tool marks
P-24172	*Serpentichnus sigmoidalis*	Minter and Braddy (2009: fig. 48A)	tool marks
P-24195	*Serpentichnus robledoensis*	Minter and Braddy (2009: fig. 45B)	tool marks
P-24360	*Serpentichnus* cf. *robledoensis*	Minter and Braddy (2009: fig. 45D)	tool marks
P-29186	*Serpentichnus*? *robledoensis*	Minter and Braddy (2009: fig. 46B)	tool marks
P-45658	*Limnopus vagus*	Minter and Braddy (2009: fig. 44A)	*Batrachichnus salamandroides*
P-47798	*Serpentichnus* cf. *robledoensis*	Minter and Braddy (2009: fig. 45E)	tool marks
P-47800	*Batrachichnus salamandroides*	Minter and Braddy (2009: fig. 41C)	*Batrachichnus salamandroides*
P-62216	*Notalacerta missouriensis*	Voigt et al. (2013a: fig. 9E)	*Notalacerta missouriensis*

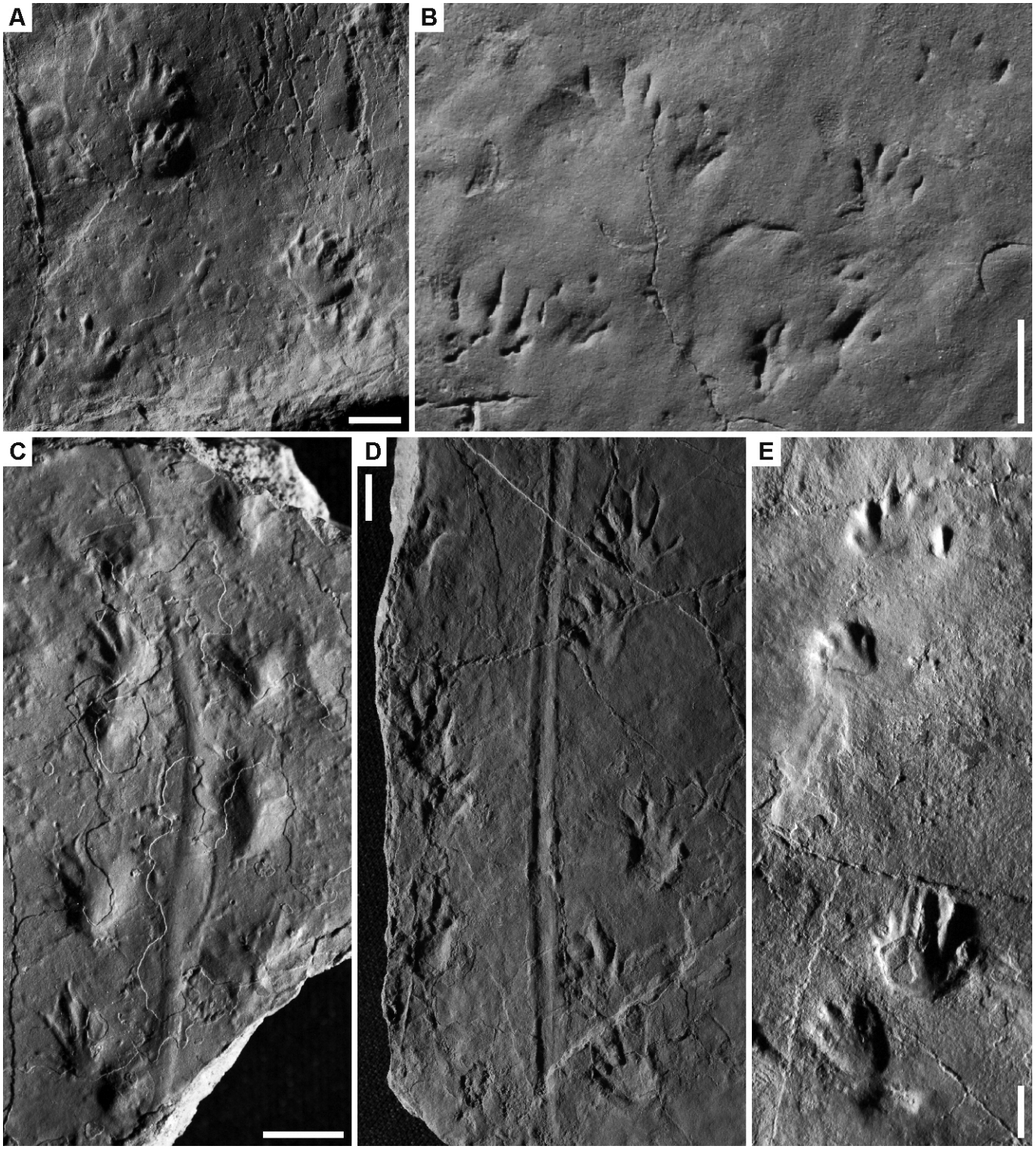


FIGURE 2. *Matthewichnus caudifer* Kohl and Bryant, 1994: (A) NMMNH P-23046; (B) NMMNH P-24342; (C) NMMNH P-23312; (D) NMMNH P-23511; (E) NMMNH P-23377. Scale bars equal 1cm.

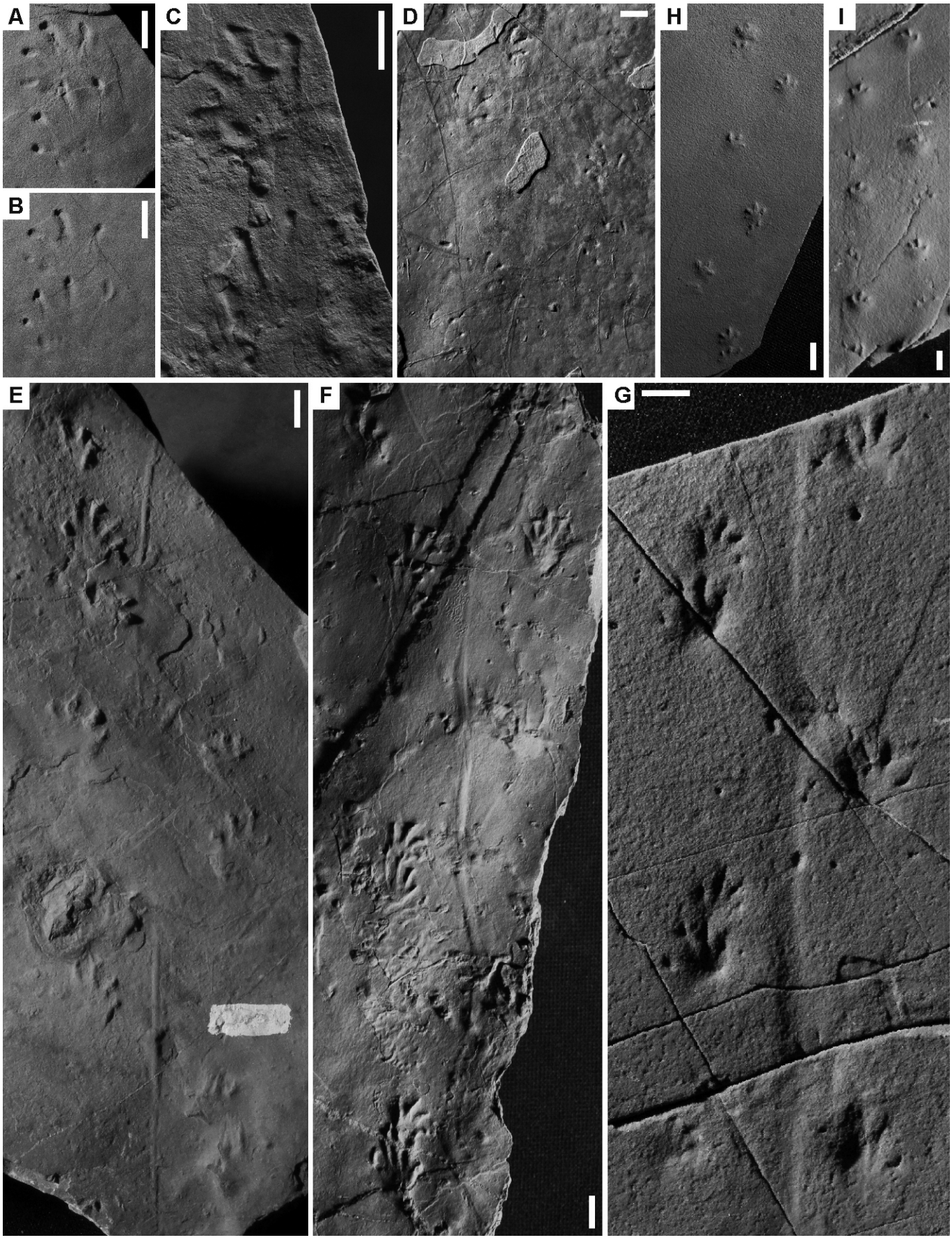


FIGURE 3. *Batrachichnus salamandroides* (Geinitz, 1861): (A-B) NMMNH P-23060; (C) NMMNH P-62199; (D) NMMNH P-62184; (E) NMMNH P-23400; (F) NMMNH P-47800; (G) NMMNH P-62212; (H) NMMNH P-23174; (I) NMMNH P-23065. Scale bars equal 1cm.

Woodworth, 1900. *Limnopus* Marsh, 1894 is very similar except for track size and relatively shorter manual digits, a feature that, however, becomes more significant only in larger tracks (Haubold, 1996; Voigt, 2005). The most important difference from specimens of *Matthewichnus caudifer* is the more regular trackway pattern of *Batrachichnus*, suggesting that the latter tracks have been made by animals with a short coupling value (= ratio of trunk and limb length). *Batrachichnus* is considered to be a monospecific ichnogenus because anatomically controlled differences in the digit proportions and trackway parameters have not been established. The first named ichnospecies of the ichnogenus is *B. salamandroides* (Geinitz, 1861) from the Early Permian of the Czech Republic. Tracks of *Batrachichnus* are usually referred to temnospondyls (Haubold, 1970, 1971, 1996, 2000; Gand, 1988; Gand and Durand, 2006; Voigt, 2005, 2007, 2012).

Among the PTNM track material at NMMNH is an uncounted number of specimens with undertracks that might belong to *Batrachichnus* based on the small size of the tracks and the relatively regular trackway pattern, but usually the tetradactyl manus imprint cannot be confirmed due to the indistinct preservation of the imprints (cf. Haubold et al., 1995: fig. 3, 4B, C). Independent of this questionable material, *Batrachichnus* seems to be the most common tetrapod track of the Robledo Mountains Formation at PTNM. Tracks of the ichnotaxon are known from 27 of 48 NMMNH PTNM tetrapod footprint localities (Table 1).

Amphisauropus kablikae (Geinitz and Deichmüller, 1882) (Fig. 4, 10C)

Material: NMMNH P-23269, isolated manus-pes couple; NMMNH P-62576, seven indistinct tracks of the same trackway; NMMNH P-62577, three manus-pes couples of a single trackway. All tracks are preserved in concave epirelief and come from NMMNH locality 846.

Description: Tracks of quadrupedal tetrapods with pentadactyl, plantigrade imprints up to 70 mm in length. Pes imprint about as long as wide with straight, distally rounded digits of the following proportions: I<V≤II<III<IV. Sole imprint indistinct due to a significant decrease in relief proximo-laterally. Manus imprint similar in width to the pes, but about one fifth shorter than the pes imprint; digit lengths increase from I to III, IV equals III, V is a little bit shorter than II. Trackways (NMMNH P-62576, -62577) show alternating arrangements of coupled manus-pes sets with a strongly inwardly rotated manus and outwardly pointing pes imprints; the manus imprint may be partially overstepped proximally by the pes. No evidence of tail or body traces.

Discussion: *Amphisauropus* is an extremely rare tetrapod ichnotaxon of the Robledo Mountains Formation at PTNM. The only known material is poorly preserved, but there is no doubt of the assignment based on the number, shape and proportions of digits and the divergent orientation of manus and pes imprints within coupled tracks. All of the discussed tracks are relatively large, at the upper size limit of *Amphisauropus* according to the abundant material of the Early Permian of central Germany (Voigt, 2005). Considering the low number of exclusively large tracks from a single locality, *Amphisauropus* likely represents an atypical element of the PTNM tetrapod ichnofauna. *Amphisauropus* is usually referred to seymouriamorph trackmakers (Haubold, 2000; Lucas et al., 2001; Voigt, 2005, 2012; Voigt et al., 2011; Marchetti et al., 2014).

Dimetropus leisnerianus (Geinitz, 1863) (Fig. 5, 10D)

Material: NMMNH P-14653, 21 pieces with undertracks of a single long trackway, concave epirelief, from NMMNH locality 846; NMMNH P-23066, six manus-pes couples with small tracks of a single trackway, convex hyporelief, from NMMNH locality 2852; NMMNH P-23133, two isolated tracks, concave epirelief and convex hyporelief in one slab indentifying the hyporelief to be a deep undertrack, from NMMNH locality 846; NMMNH P-23145, isolated, shallow near-surface track, concave epirelief, from NMMNH locality 846; NMMNH P-23119/23395, isolated undertrack, part and counterpart, from NMMNH locality 846; NMMNH P-23536, isolated manus-pes couple in deep undertrack preservation, concave epirelief, from NMMNH locality 2819; NMMNH P-23622, incomplete left manus-pes couple, concave epirelief, from NMMNH locality 2828; NMMNH P-23719, part of a longer trackway, concave epirelief, from NMMNH locality 846.

Description: Tracks of quadrupedal tetrapods with pentadactyl, plantigrade to semiplantigrade footprints up to about 150 mm long. Manus and pes imprints are similar in shape but different in size. Imprints are always longer than wide, with distally pointed slender digits and proximally elongated heel. Digits I to IV of both manus and pes imprint exhibit a moderate serial increase in length; digit V is about as long as II or III, shorter in the manus and longer in the pes imprint. Manus imprint positioned anteriorly to the pes imprint, about one third

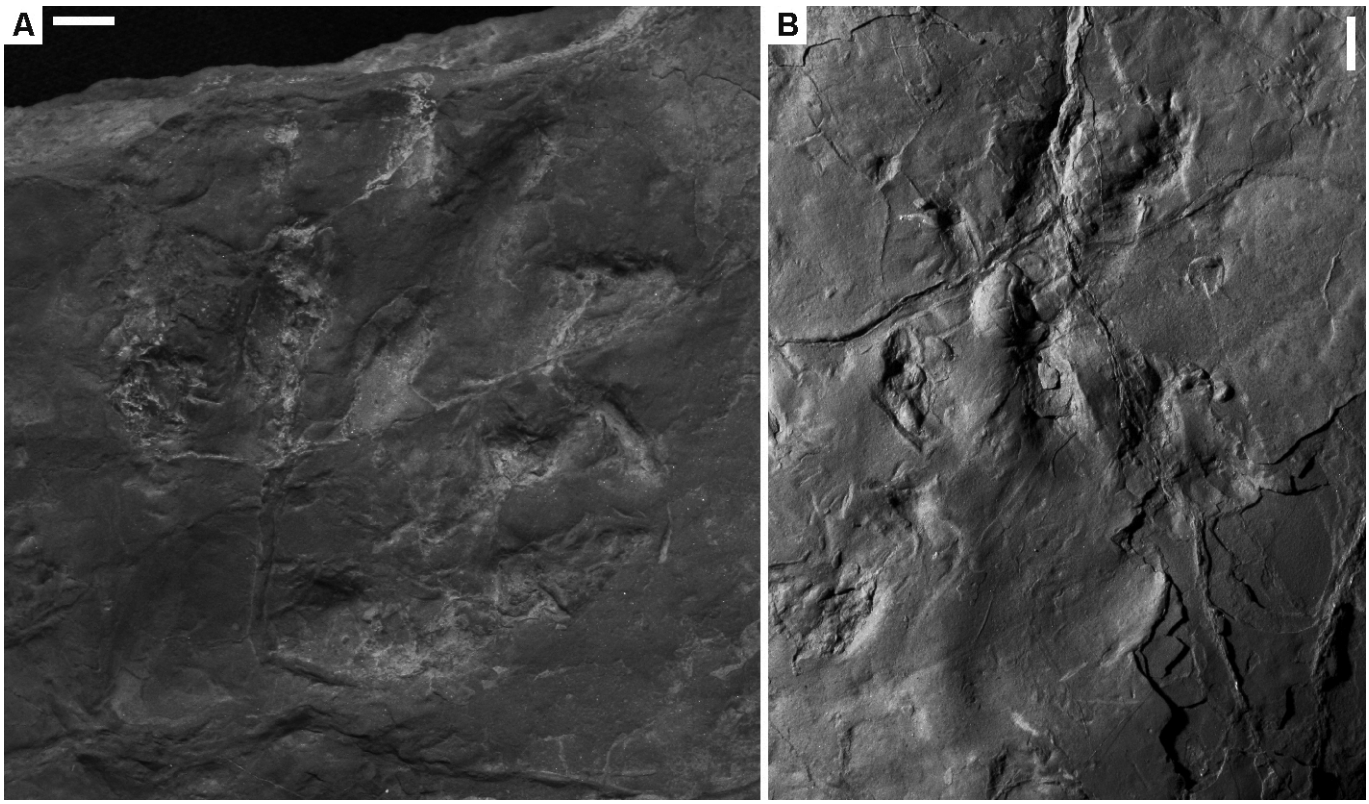


FIGURE 4. *Amphisauropus kablikae* (Geinitz and Deichmüller, 1882): (A) NMMNH P-23269; (B) NMMNH P-62577. Scale bars equal 1cm.

shorter than the pes imprint. The trackway pattern most commonly shows a clearly alternating arrangement of coupled manus-pes tracks, with the manus imprints being pointed more inwardly than the latter. No tail trace or other track accessories such as skin impressions have been observed.

Discussion: The elongated heel as well as the shape, orientation, and proportion of the digits strongly support assignment of the discussed tracks to *Dimetropus* Romer and Price, 1940. This is confirmed by two specimens (NMMNH P-23145, -23622; Figs. 5A−B), which show typical characteristics of shallow near-surface tracks of the ichnotaxon, particularly the hemispherical imprints of the metatarsal-/metacarpal-phalangeal pads and isolated claw marks.

Globally, *Dimetropus* is almost exclusively known from undertracks. Without well-preserved material, a separation of different ichnospecies is not reasonable (Voigt, 2005). Therefore we refer the studied material to *D. leisnerianus* (Geinitz, 1863) as the first available ichnospecies. *Dimetropus* is considered to be the track morphotype of many Late Carboniferous and Early Permian non-therapsid synapsids such as caseids, edaphosaurids, ophiacodontids, and sphenacodonts (Haubold, 2000; Voigt, 2005; Voigt and Ganzelewski, 2010).

The PTNM competes with the Bromacker locality of central Germany for the most important site regarding the abundance of Pennsylvanian-Permian pelycosaurian tracks and trackways. However, 99% of *Dimetropus* from the PTNM lack details of the imprint morphology (digit proportions, heel shape, skin impression etc.) due to preservation as undertracks. To date, there is not a single complete near-surface manus imprint of the ichnotaxon known from the study area. The scientific importance of the material is more or less restricted to the pure number of tracks, the total length of trackways and certain information gained from the trackway pattern (Hunt et al., 1993; Hunt and Lucas, 1998).

Notalacerta missouriensis Butts, 1891 (Figs. 6, 10E)

Material: NMMNH P-62216, 10 or more tracks of a single trackway with discontinues tail trace, preserved by part and counterpart, NMMNH locality 8220 (Voigt et al., 2013a).

Description: Trackway of quadrupedal tetrapod with pentadactyl, semiplantigrade to digitigrade tracks up to 2.7 cm in length. Tracks about as long as wide, with long and slender, distally pointed digits. Manus imprint two-thirds to three-fourths of the length of the pes imprint; manual digit proportions: I<V<II<III<IV, pedal digit proportions: I<II~V<III<IV. Trackway with alternating arrangement of manus-pes couples with relatively short stride and low pace angulation. Both manus and pes imprints are forwardly directed or slightly inwardly rotated with respect to the trackway midline. Very faint, discontinuous, partially bent tail trace.

Discussion: The imprint and digit proportions of the discussed tracks correspond to captorhinomorph footprints such as *Notalacerta* Butts, 1891, *Varanopus* Moodie, 1929, *Hyloidichnus* Gilmore, 1927 and *Erpetopus* Moodie, 1929. A more detailed analysis of the ichnotaxonomic relationships and distinction of these tracks was published recently (Voigt et al., 2013b). NMMNH P-62216 is most similar to tracks of *Notalacerta missouriensis* Butts, 1891 based on the relative length of the fifth digit of the pes imprint, the presence of a tail trace, and the orientation of the tracks to the trackway midline. A notable feature of the discussed specimen is the narrowly spaced digits III and IV of the manus imprint, which is in accordance with tracks of *N. missouriensis* from the Middle Pennsylvanian McAlester Formation of Oklahoma (Fig. 6). This feature has not yet been observed in any other captorhinomorph footprint.

Notalacerta is well known from Pennsylvanian strata of Missouri (Butts, 1891), Kansas (Chesnut et al., 1994), Alabama (Haubold et al., 2005), and Oklahoma (Lucas et al., 2004). A possible Early Permian record of this ichnotaxon was described from redbeds of Prince Edward Island, Canada (Calder et al., 2004). *Notalacerta* is supposed to be the tracks of early non-diapsid eureptiles, e.g., Protorothyrididae (Chesnut et al., 1994; Calder et al., 2004; Haubold et al., 2005).

Robledopus macdonaldi Voigt, Lucas, Buchwitz and Celeskey, 2013 (Figs. 7, 10F)

Material: NMMNH P-23120 (including specimens formerly numbered NMMNH P-23424, -23425, and -23679), holotype, two trackways with 38 tracks in total, preserved as part and partial counterpart from NMMNH locality 2824; NMMNH P-23072, 32 imprints of five mainly faint trackways, concave epirelief, from NMMNH locality 2821; NMMNH P–23322, a single trackway consisting of 15 distinct imprints and two sets of faint manus and pes impressions of another trackway, both preserved as part and counterpart, from NMMNH locality 2821.

Description: Trackway of a small quadrupedal tetrapod with pentadactyl manus and pes imprints that range from 9 to 25 mm in length; manus and pes as long as wide or slightly wider than long; pes about one fourth longer than the manus; digit impressions straight, slightly tapering distally to terminate in hook-like claw imprints. Manus imprints: Digits increase in length from I to III, IV about as long as III, and V as long as II; without heel impression, proximal margin of sole indistinctly concave; sole approximately one third of imprint's total length. Pes imprints: Mediolaterally decrease in relief, digits IV and V missing or as tip marks only; digits increase in length from I to IV, V about as long as III; all tips except V commonly with drag marks; no heel impression, proximal margin of sole indistinctly concave or straight, sole less than one third as long as the entire imprint. Trackways exhibit alternating sets of manus and pes imprints; pes outwardly rotated (β = 18–53°); manus inwardly or forward-directed (β = -25.7°). Width of pedal pace slightly exceeds that of the manus. Continuous, straight to slightly sinuous tail/body traces are common; some trackways exhibit double-lined (body and tail) traces either well separated from each other or superimposed.

Discussion: *Robledopus* is a unique type of Paleozoic tetrapod footprint with captorhinomorph affinities (Voigt et al., 2013b). It is only known from the Robledo Mountains Formation of the PTNM. Tracks of *Robledopus* were previously assigned to *Gilmoreichnus* (Haubold et al., 1995), *Erpetopus* (Hunt et al., 1995), and *Gilmoreichnus* or *Hyloidichnus* (Minter and Braddy, 2009). *Gilmoreichnus* Haubold, 1971 is a junior subjective synonym of *Varanopus* and, later, was often attributed to poorly preserved tracks of *Amphisauropus* as well (Voigt, 2005). The former assignments of *Robledopus* tracks are not surprising, as the ichnotaxon is most similar to *Notalacerta*, *Varanopus*, *Hyloidichnus*, *Erpetopus* and *Amphisauropus*. However, it differs from *Notalacerta* in the outward-directed pes imprint with a relatively short digit IV (non-lacertoid track); from *Varanopus* by the relatively longer manual digit impression III, the outward-directed pes imprint and the presence of a body/tail trace; from *Hyloidichnus* by the relatively much longer pedal digit impression V, significantly diverging pes and manus imprints and the presence of a body/tail trace; from *Erpetopus* in the relatively short manus and pes digit impression IV, the relatively long pedal digit impression V, the lack of partial overstepping of the manus imprint by the pes and presence of a body/tail trace; and from *Amphisauropus* by having relatively longer and thinner digit imprints with claw marks at the tips. Tracks of *Robledopus* show a predominance of features that characterize footprints of Pennsylvanian non-diapsid eureptiles, supporting interpretation of *Robledopus* as the track of "protorothyridids" (Voigt et al., 2013b).

Hyloidichnus bifurcatus Gilmore, 1927 (Figs. 8, 10G)

Material: NMMNH P-23088 and NMMNH P-23233, each specimen with an isolated manus-pes couple preserved in concave epirelief, from NMMNH locality 2821. NMMNH P-23668 from NMMNH locality 2821, showing 10 undertracks of a single trackway preserved in convex hyporelief, is compared to the ichnotaxon.

Description: Tracks of quadrupedal tetrapods with pentadactyl, semiplantigrade to digitigrade imprints up to 40 mm in length. Manus and pes imprints are more or less similar in size and digit proportions. Both imprints are about as long as wide and show relatively long, straight and slender digits that increase in size from I to IV. Digit V is about as long as digit I in the manus and the pes imprint. Digits have claw-mark-like tapering tips, which are often curved inward in the first four digits, but rotated outward in digit V. Bifurcated digit tips (I–IV) may be common. Sole or palm impressions are very short or not preserved (undertracks). Trackway pattern, as far as can be assessed on the basis of the limited material, without specific features: more or less regular arrangement of manus and pes imprints, similar trackway width of manus and pes, slightly to strongly alternating arrangement of manus-pes couples, including marginal (primarily) overstepping of the manus imprint by the pes, and no evidence of a tail or body trace.

Discussion: Based on the shape and proportions of the digits, the described tracks correspond well with *Hyloidichnus* Gilmore, 1927. *Hyloidichnus* is similar to *Varanopus* Moodie, 1929. Both ichnotaxa, however, are clearly distinguished by the relative length of the fifth digit of the pes imprint (Voigt et al., 2009, 2010, 2013; Hminna et al., 2012; Marchetti et al., 2013). Pedal digit V equals the length of digit I in *Hyloidichnus*, whereas it is at least as long as digit II in *Varanopus*. The assignment of the described tracks to *Hyloidichnus* is supported

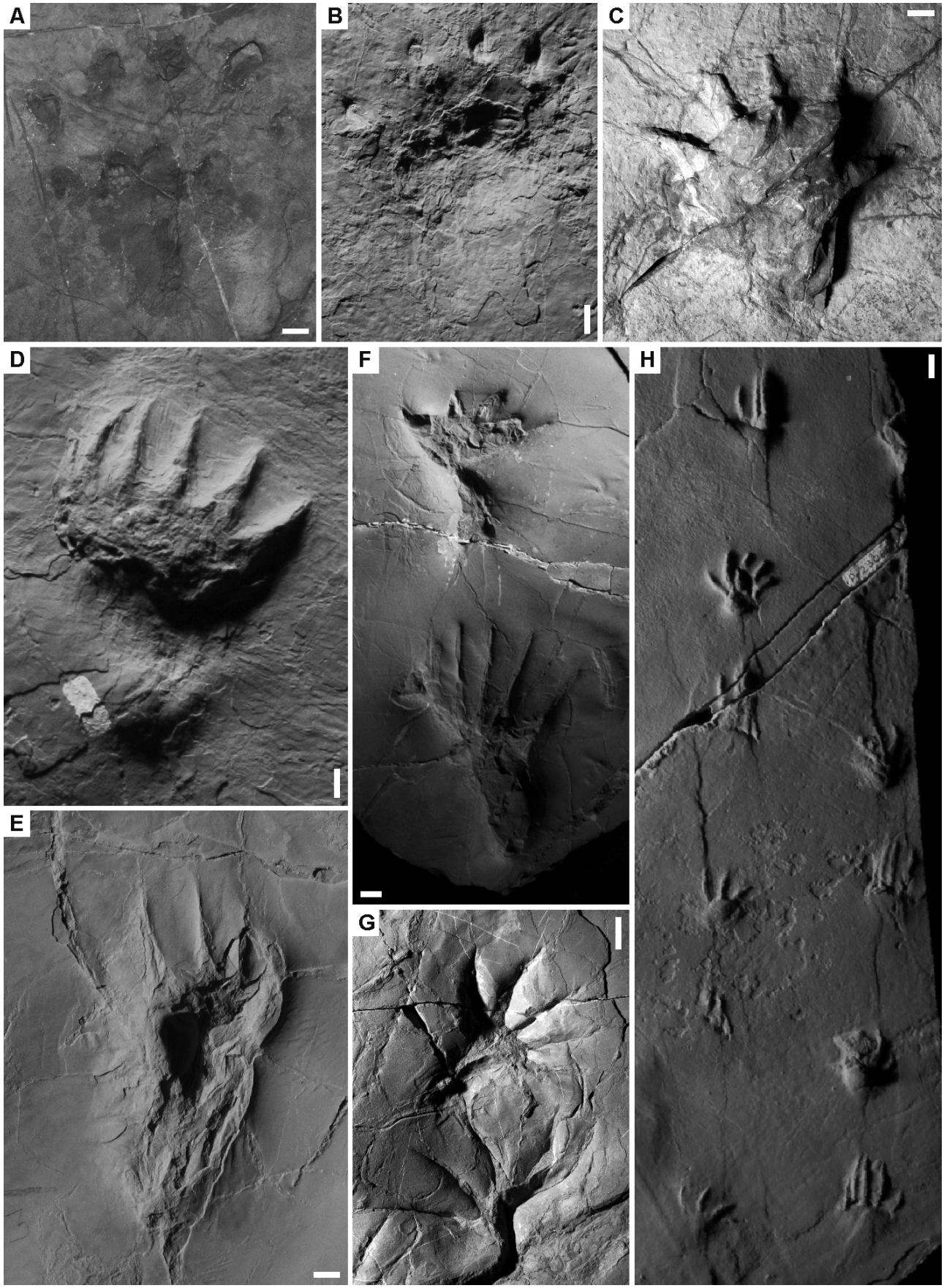


FIGURE 5. *Dimetropus leisnerianus* (Geinitz, 1863): (A) NMMNH P-23145; (B) NMMNH P-23622; (C) NMMNH P-23133; (D) NMMNH P-23119/23395; (E) NMMNH P-14653; (F) NMMNH P-23719; (G) NMMNH P-23536; (H) NMMNH P-23066. Scale bars equal 1cm.

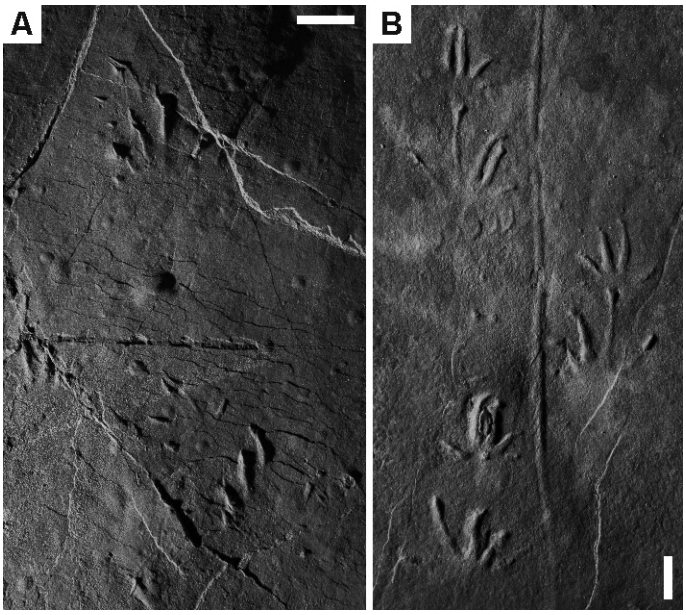


FIGURE 6. *Notalacerta missouriensis* Butts, 1891: (A) NMMNH P-62216, Robledo Mountains Formation, Early Permian, New Mexico; (B) NMMNH P-31746, Middle Pennsylvanian, Oklahoma. Scale bars equal 1cm.

by the extramorphologically bifurcated digit tips that can be seen in some of the specimens (e.g., NMMNH P-23088). Though this feature is principally known from almost all Paleozoic tetrapod ichnotaxa, it is most common in *Hyloidichnus*, including the holotype of *H. bifurcatus* (Gilmore, 1927; Haubold et al., 1995). NMMNH P-23668 is only compared to *H. bifurcatus* because its undertracks do not unequivocally indicate the digit proportions. Tracks of *Hyloidichnus* and *Varanopus* are usually referred to captorhinids (Haubold, 1971; Gand, 1988; Haubold and Lucas, 2001, 2003; Voigt, 2005; Gand and Durand, 2006). More specifically, Voigt et al. (2009, 2010) argued for a track-trackmaker relationship of *Hyloidichnus* and moradisaurine captorhinids.

Dromopus lacertoides (Geinitz, 1861) (Figs. 9, 10H)

Material: There are almost 120 specimens showing undertracks of the ichnotaxon. Specimens with this kind of preservation have been described and figured extensively by previous workers (MacDonald, 1992, 1994, 1995; Hunt et al., 1993, 1995; Schult, 1994, 1995; Haubold et al., 1995; Lucas et al., 1998a, b, 2010; Minter and Braddy, 2009; Voigt et al., 2013a). In contrast, there is a very low number of surface to near-surface tracks of the ichnotaxon, including the following specimens (Fig. 9): NMMNH P-23754, three tracks of the same trackway, convex hyporelief, NMMNH locality 846; NMMNH P-62093, -62094, -62095, three manus-pes couples probably of the same trackmaker, tracks partially with skin impressions (all specimens come from NMMNH locality 7934 and are preserved in convex hyporelief); NMMNH P-62215, manus-pes couple, concave epirelief, from NMMNH locality 7934.

Description: Trackways of quadrupedal tetrapods with pentadactyl, plantigrade to digitigrade tracks that are up to 70 mm long and one fourth longer than wide. Manus and pes imprints of similar shape, but different in size, with the manus measuring about three-fourths of the length of the pes. Digit impressions are long, slender, and distally curved, with distinct claw marks at their tips; digit impressions increase in length from I to IV, V is about as long as II. Trackways usually show distinctly alternating arrangements of manus-pes sets; manus imprints often partially overstepped by the pes proximo-laterally. No evidence of tail or body traces.

Discussion: Overall shape and imprint proportions of these tracks are in accordance with *Dromopus* Marsh, 1894. *Dromopus* is among the most common and most easily recognizable tetrapod tracks of the study area. This is in accordance with the majority of Late Pennsylvanian to Early Permian tetrapod footprint sites of North America and Europe (Haubold, 1971, 1996, 2000; Gand, 1988; Voigt, 2005, 2012; Lucas, 2007). A differentiation of *Dromopus* tracks based on anatomically-controlled features has not yet been demonstrated (Voigt, 2005). Therefore, we assign the PTNM material to *D. lacertoides* (Geinitz, 1861) as the first available, valid ichnospecies of *Dromopus*. *Dromopus* is generally referred to small- and medium-sized sauropsids with

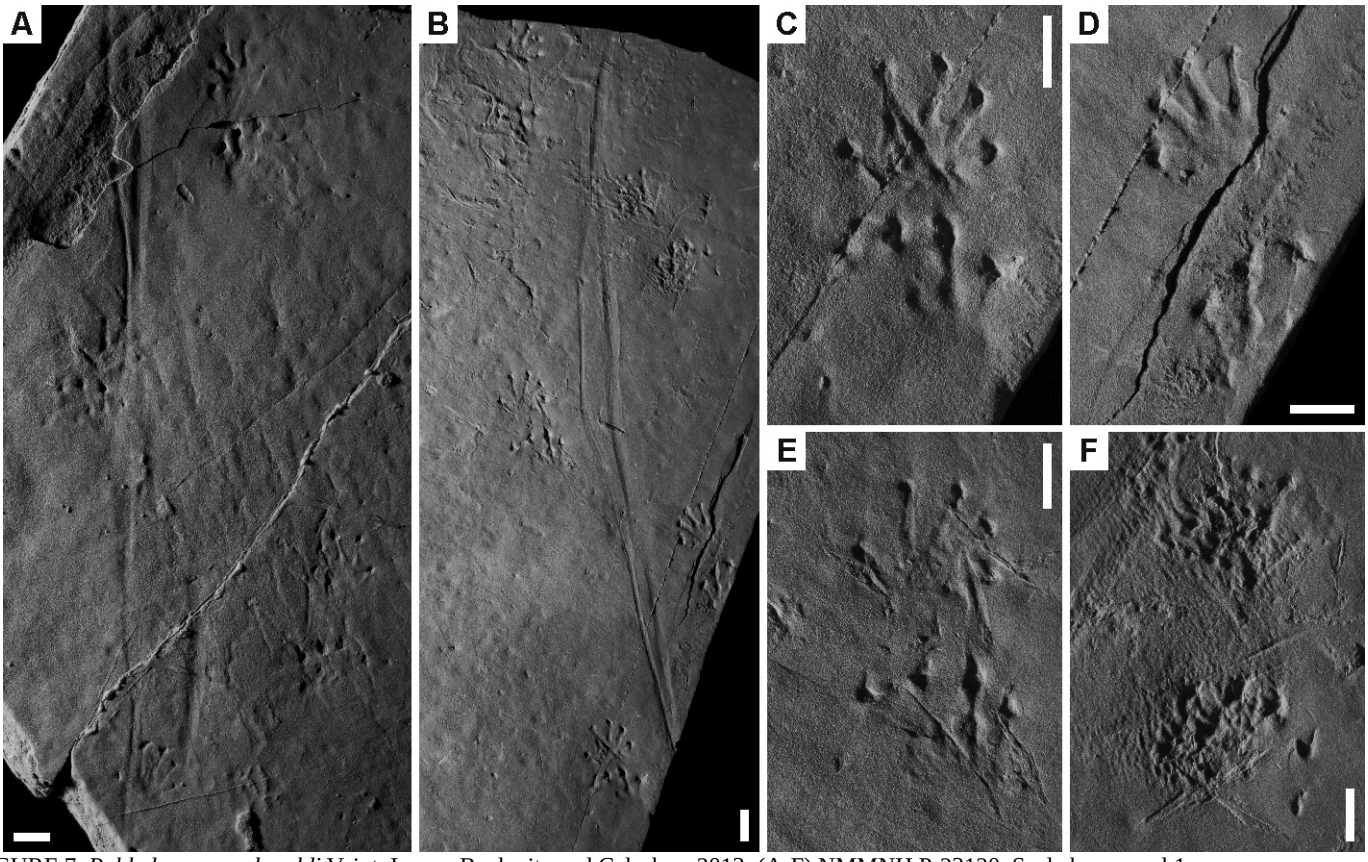


FIGURE 7. *Robledopus macdonaldi* Voigt, Lucas, Buchwitz and Celeskey, 2013: (A-F) NMMNH P-23120. Scale bars equal 1cm.

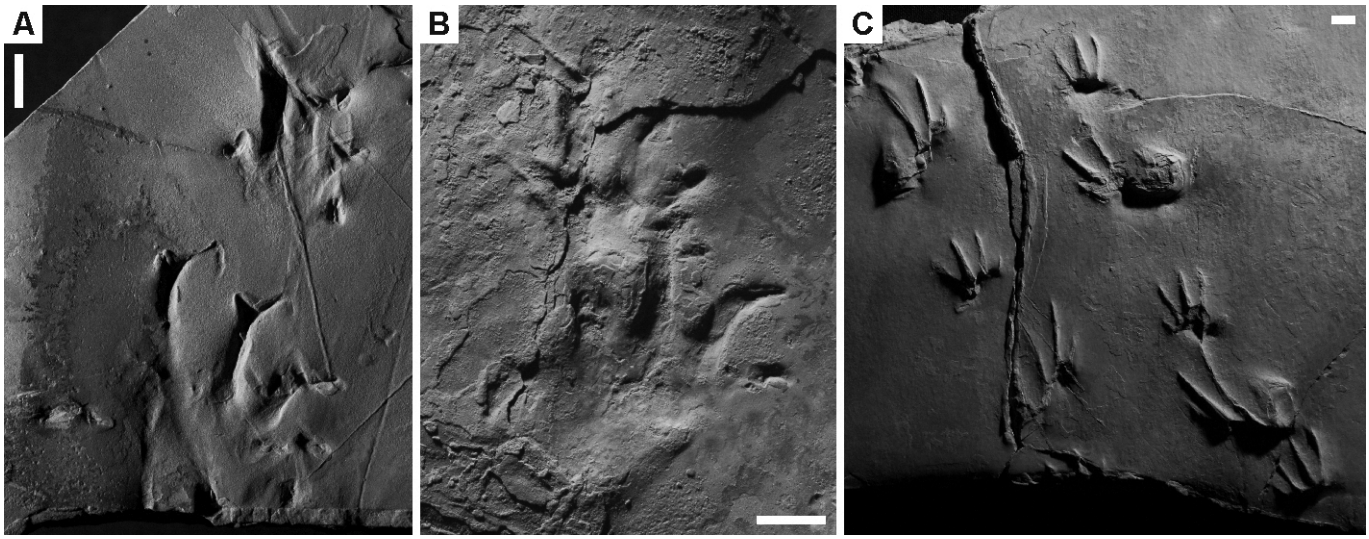


FIGURE 8. *Hyloidichnus bifurcatus* Gilmore, 1927: (A) NMMNH P-23088; (B) NMMNH P-23233; (C) NMMNH P-23668. Scale bars equal 1cm.

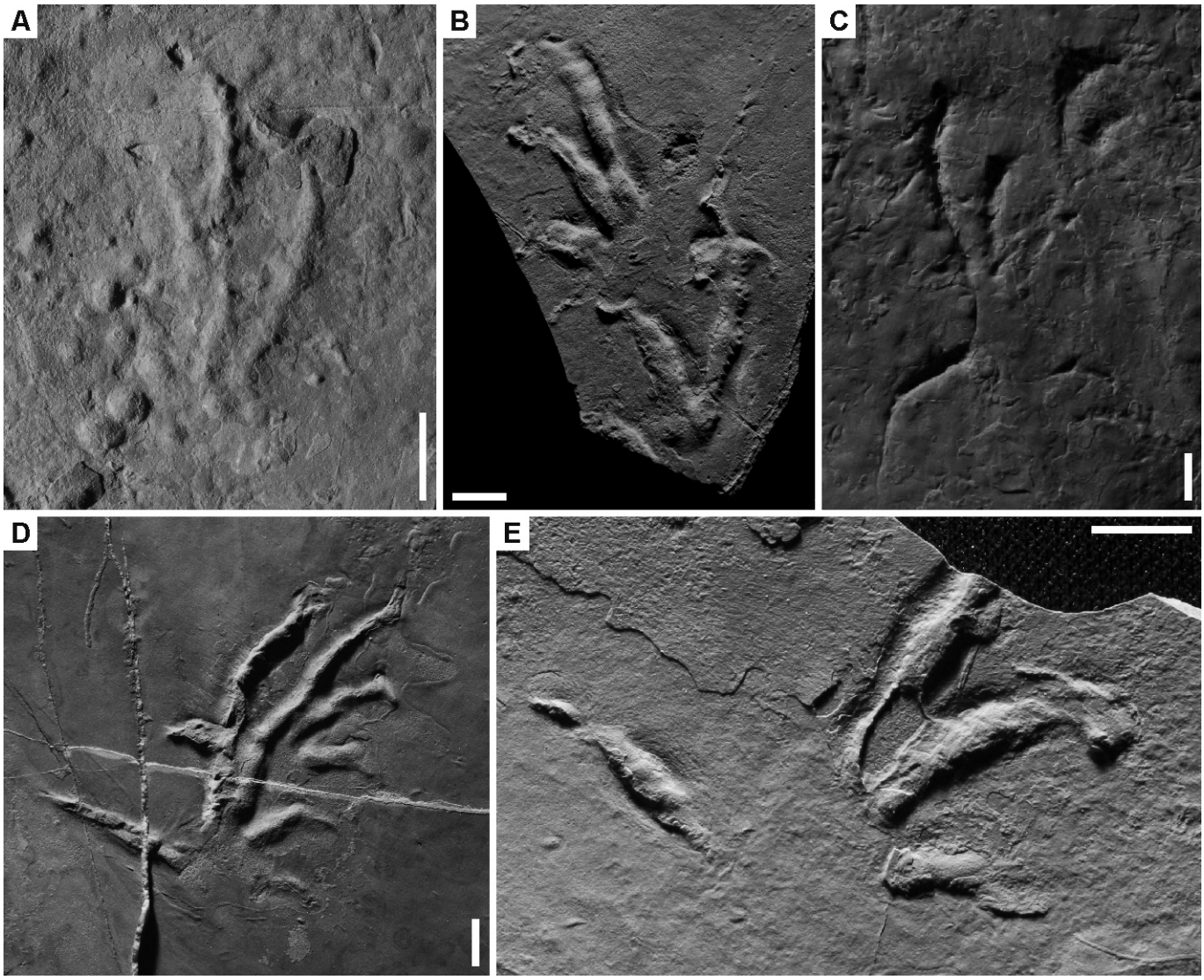


FIGURE 9. *Dromopus lacertoides* Marsh, 1894: (A) NMMNH P-23754; (B) NMMNH P-62093; (C) NMMNH P-62215; (D) NMMNH P-62095; (E) NMMNH P-62094. Scale bars equal 1cm.

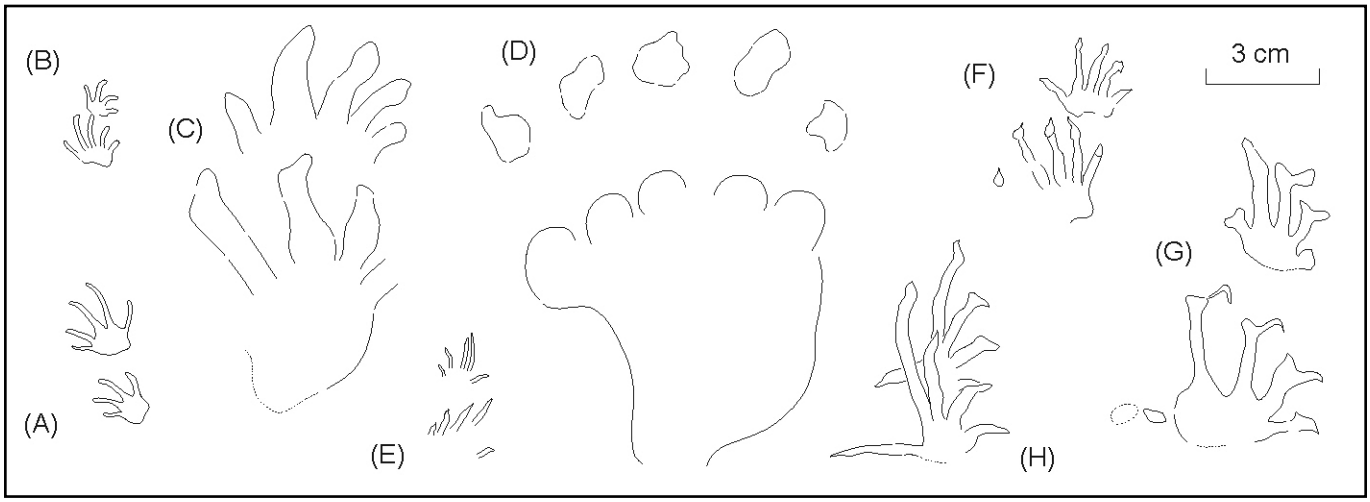


FIGURE 10. Outline drawings of manus-pes couples of characteristic PTNM tetrapod footprints: (A) *Matthewichnus caudifer*, (B) *Batrachichnus salamandroides*, (C) *Amphisauropus kablikae*, (D) *Dimetropus leisnerianus*, (E) *Notalacerta missouriensis*, (F) *Robledopus macdonaldi*, (G) *Hyloidichnus bifurcatus*, (H) *Dromopus lacertoides*.

autopods of lacertoid type, i.e., araeoscelids, in particular (Haubold, 1971, 1996, 2000; Gand, 1988; Haubold and Lucas, 2003; Voigt, 2005; Gand and Durand, 2006).

STRATIGRAPHIC, FAUNISTIC AND PALEOECOLOGICAL IMPLICATIONS

The PTNM tetrapod ichnofaunal assemblage provides evidence for the presence of lepospondyls, temnospondyls, seymouriamorphs, pelycosaurian-grade synapsids, captorhinomorphs and early diapsids along the northern coast of an extensive epicontinental seaway that existed during Pennsylvanian-Permian time in what is part of the United States today (Blakey, 2005). Regarding the ichnotaxonomic composition, the studied assemblage is exceptional in the co-occurrence of more typical Pennsylvanian (*Matthewichnus*, *Notalacerta*) and more typical or even exclusively Permian tetrapod ichnotaxa (*Batrachichnus*, *Amphisauropus*, *Dimetropus*, *Hyloidichnus*, *Dromopus*). In addition, *Robledopus* is only known from the Robledo Mountains Formation of the PTNM. As 90% of all PTNM tetrapod footprints at NMMNH belong to *Batrachichnus*, *Dimetropus*, and *Dromopus* we assume that the terrestrial tetrapod fauna of the Robledo Mountains Formation at PTNM was numerically dominated by temnospondyl amphibians, "pelycosaurs" and early diapsids. The track assemblage is broadly coeval with part of the nonmarine Abo Formation in central and north-central New Mexico, which yields bone assemblages dominated by fossils of lepospondyls, temnospondyls, diadectomorphs and primitive amniotes (e.g., Berman et al., 2014). Thus, there is general overlap between trackmakers of the PTNM ichnoassemblage and the Abo bone assemblages, though relative abundances of various taxa are very different, for example the abundance of early diapsids indicated by the track record and their relative rarity in the bone assemblage.

Only three specimens with tracks of *Amphisauropus* have been found at PTNM and because all of them are large tracks of adult individuals it is most likely that seymouriamorphs just occasionally or even accidently roamed the distal coastal plain to shoreline environments. Tracks of supposed lepospondyls (*Matthewichnus*) and especially captorhinomorphs (*Notalacerta*, *Robledopus*, *Hyloidichnus*) are much more common than tracks of seymouriamorphs, considering that the NMMNH collection includes several tracks (e.g., NMMNH P-23242, -23292, -23320, -23457, -62183) that show captorhinomorph affinities but are not sufficiently preserved in order to allow ichnogeneric assignation. According to the tracks, the captorhinomorphs were represented by the basal Protorothyrididae (*Notalacerta*, *Robledopus*) as well as advanced Captorhinidae (*Hyloidichnus*).

As well as aiding in faunal analysis, tetrapod footprints can be a useful biostratigraphic tool in Carboniferous-Permian continental deposits (e.g.; Haubold, 1996, 2000; Haubold and Lucas, 2003; Voigt, 2005, 2012; Lucas, 2007; Voigt et al., 2011; Marchetti et al., 2014). *Amphisauropus* tracks first occur in the global tetrapod footprint record with the onset of the Permian (Haubold, 2000; van Allen et al., 2005; Voigt, 2005; Lucas, 2007). Footprints of advanced captorhinomorphs such as *Hyloidichnus* Gilmore, 1927 and *Erpetopus* Moodie, 1929 first occur in late Early Permian strata (Haubold, 2000; Haubold and Lucas, 2001, 2003; Gand and Durand, 2006; Voigt et al., 2011; Marchetti et al., 2014). The presence and partial abundance of *Batrachichnus*, *Amphisauropus*, *Dimetropus*, *Hyloidichnus*, and *Dromopus* tracks within the tetrapod ichnofauna of the Robledo Mountains Formation at PTNM suggests an Early Permian age for those beds. As there is no evidence of *Erpetopus* tracks, which seem to be indicative of Kungurian and younger Permian strata (Gand and Durand, 2006; Hminna et al., 2012; Marchetti et al., 2014) an Artinskian age is most likely for the Robledo Mountains Formation at PTNM based on tetrapod footprints (Fig. 11). This is consistent with other age data for Hueco Group strata in the Robledo Mountains (see Lucas et al., this volume).

The relatively unusual composition of the PTNM tetrapod ichnoassemblage with its mixture of Pennsylvanian and Early Permian ichnotaxa, the presence of two different kinds of supposed protorothyridid tracks, and the presence of an apparently endemic ichnotaxon (*Robledopus*), may be explained by the fact that there are no reliable data on contemporaneous Early Permian vertebrate track faunas from marginal marine settings.

Voigt et al. (2013a) argued that most of the PTNM tetrapod footprints preserved in true red-beds have been made by animals walking on extensive coastal floodplains. This includes the most prolific PTNM track site, NMMNH locality 846. Notably, this is the only site with tracks of *Amphisauropus*, suggesting it is the most terrestrially influenced one. On the other hand, the Robledo Mountains Formation clearly includes intertidal and even subtidal deposits that preserve, among various kinds of aquatic invertebrate traces, swimming and scratch marks of tetrapods (e.g., NMMNH P-64497, -66530, from NMMNH locality 7966; NMMNH P-64491, from NMMNH locality 7967; NMMNH P-64512, -64517, -64524 to -64527, -64530, from NMMNH locality 8211; NMMNH P-64545 from NMMNH locality 8641). These tetrapod swimming and scratch marks are much larger than of the most common PTNM amphibian tracks *Matthewichnus* and *Batrachichnus*, and because there are no associations with any tetrapod walking track it is possible that these scratch and swimming tracks (many of which may be assignable to the tetrapod "swim track" form ichnogenus *Characichnos* Whyte and Romano, 2001) come from marine tetrapods similar to Early Permian mesosaurs (Modesto, 2010). This possibility gives a new perception of this outstanding tetrapod ichnofossil assemblage and indicates that there is still more work to do in analysis of the ichnofaunas of the PTNM.

CONCLUSIONS

1. The PTNM is one of the most extensively collected areas with Paleozoic tetrapod footprints in the world. At least 775 specimens with tetrapod footprints from the study area are housed at the NMMNH, which houses the most important reference collection of vertebrate tracks from the PTNM.

2. About 40% of the NMMNH PTNM tetrapod footprint collection includes tracks that can be assigned to an ichnospecies with certainty. These tracks can be referred to eight ichnotaxa, i.e. *Matthewichnus caudifer*, *Batrachichnus salamandroides*, *Amphisauropus kablikae*, *Dimetropus leisnerianus*, *Notalacerta missouriensis*, *Robledopus*

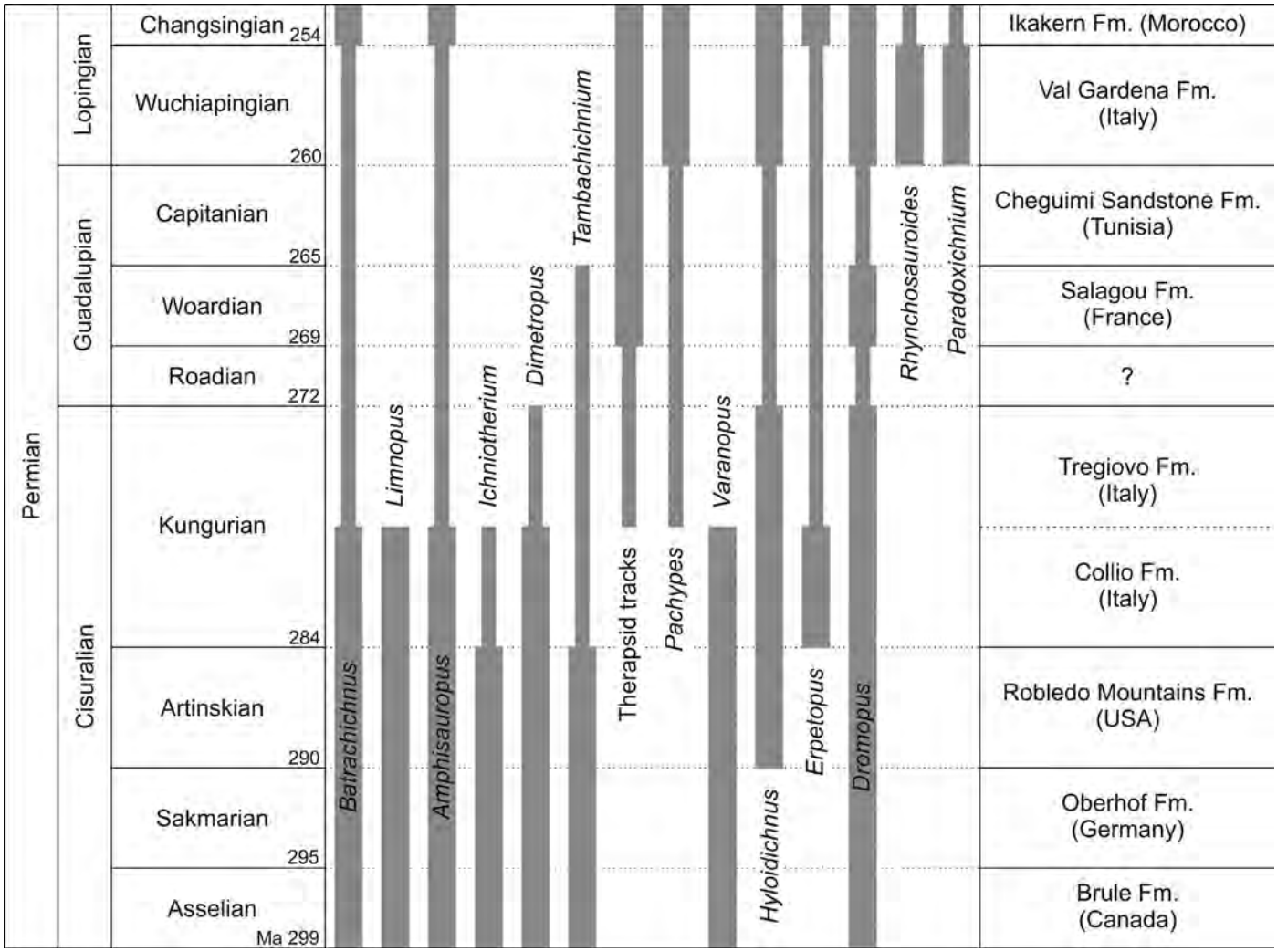


FIGURE 11. Stratigraphic range of common and well-known Permian tetrapod ichnotaxa (thick bar = fossil evidence; thin bar = distribution supposed). Formation names exemplify footprint-bearing deposits of the respective time interval. Data are compiled from Haubold (2000), Van Allen et al. (2005), Voigt (2005), Gand and Durand (2006), Lucas (2007), Voigt et al. (2010, 2013b), Hminna et al. (2012), and Marchetti (2014).

macdonaldi, *Hyloidichnus bifurcatus*, and *Dromopus lacertoides*.

3. The PTNM vertebrate ichnofauna is numerically dominated by tracks of *Batrachichnus salamandroides*, *Dimetropus leisnerianus*, and *Dromopus lacertoides*. Tracks of these ichnotaxa make up 90% of all specimens with identifiable footprints.

4. Based on the tetrapod ichnofauna, the Permian tropical seacoast represented by the Robledo Mountains Formation at PTNM was populated (ordered by decreasing number of tracks) by temnospondyl amphibians, araeoscelids, pelycosaurian-grade synapsids, captorhinomorphs, and lepospondyls. Seymouriamorph tracks are extremely rare and only known by large imprints of adult individuals suggesting that marginal marine environments did not belong to the natural habitat of these animals.

5. The PTNM tetrapod ichnofauna supports an Early Permian (most likely Artinskian) age for the Robledo Mountains Formation of the study area.

6. The PTNM represents the best studied tetrapod ichnofauna of an Early Permian seacoast and thus is an important baseline for the distribution and taxonomic composition of early terrestrial tetrapod communities in this kind of depositional environment.

ACKNOWLEDGMENTS

This contribution is in honor of Jerry P. MacDonald, who collected most of the footprints from the Robledo Mountains at PTNM and donated them to the NMMNH as part of the Jerry MacDonald Paleozoic Trackway Collection. The U.S. Bureau of Land Management granted access to the footprint localities in the Prehistoric Trackways National Monument during field work in 2009 to 2012. Financial support from the BLM also made this research possible. We acknowledge diverse help from Lori Allen, McKinney Briske, Amanda Cantrell, Phil Gensler, Patricia Hester, Larry Rinehart and Justin Spielmann. We appreciate helpful reviews by Adrian Hunt and Hendrik Klein.

REFERENCES

Berman, D. S, Henrici, A. C. and Lucas, S. G., 2014, Pennsylvanian-Permian red bed vertebrate localities of New Mexico and their assemblages: New Mexico Museum of Natural History and Science, Bulletin 64, p. 65-76.

Blakey, R., 2005, Paleogeography and geologic evolution of ancestral rocky mountains —Early Permian (285 Ma): online http://www2.nau.edu/rcb7/garmgeolhist.html.

Braddy, S. J., Morrissey, L. B., and Yates, A. M., 2003, Amphibian swimming traces from the Lower Permian of southern New Mexico: Palaeontology, v. 46, p. 671–683.

Butts, E., 1891, Recently discovered footprints of the amphibian age in the Upper Coal Measure Group of Kansas City, Missouri: Kansas City Scientist, v. 5, p. 17–19.

Calder, J.H., Baird, D., and Urdang, E.B., 2004, On the discovery of tetrapod trackways from Permo-Carboniferous redbeds of Prince Edward Island and their biostratigraphic significance: Atlantic Geology, v. 40, p. 217–226.

Chesnut, D.R., Baird, D., Smith, J.H. and Lewis, R.Q., 1994, Reptile trackway from the Lee Formation (Lower Pennsylvanian) of south-central Kentucky: Journal of Paleontology, v. 68, p. 154–158.

Falcon-Lang, H.J., Kurzawe, F., and Lucas, S.G., 2014, Coniferopsid tree-trunks preserved in sabkha facies in the Permian (Sakmarian) Community Pit Formation in south-central New Mexico, U.S.A. — systematics and palaeoecology: Review of Palaeobotany and Palynology, v. 200, p. 138–160.

Gand, G., 1988, Les traces de vertébrés tétrapodes du Permien français: [Ph.D. Thesis]: Université de Bourgogne Edition Centre des Sciences de la Terre, Dijon. 341 pp.

Gand, G., and Durand, M., 2006, Tetrapod footprint ichno-associations from French Permian basins. Comparisons with other Euramerican ichnofaunas: Geological Society London, Special Publications, v. 265, p. 157–177.

Geinitz, H.B., 1861, Dyas oder die Zechsteinformation und das Rothliegende (Permische Formation zum Theil): W. Engelmann, Leipzig. 130 pp.

Geinitz, H.B., 1863, Beiträge zur Kenntnis der organischen Überreste in der Dyas (oder permischen Formation zum Theil) und über den Namen Dyas: Neues Jahrbuch für Mineralogie, Geologie und Paläontologie, v. 1863, p. 385–398.

Geinitz, H.B., and Deichmüller, J.V., 1882, Die Saurier der unteren Dyas von Sachsen: Palaeontographica, v. 29, p. 1–46.

Gilmore, G.W., 1927, Fossil footprints from the Grand Canyon II: Smithsonian Miscellaneous Collections, v. 80, p. 1–78.

Haubold, H., 1970, Versuch der Revision der Amphibien-Fährten des Karbon und Perm: Freiberger Forschungshefte C, v. 260, p. 83–117.

Haubold, H., 1971, Ichnia Amphibiorum et Reptiliorum fossilium: Encyclopedia of Palaeoherpetology, v. 18, p. 1–124.

Haubold, H., 1996, Ichnotaxonomie und Klassifikation von Tetrapodenfährten aus dem Perm: Hallesches Jahrbuch für Geowissenschaften B, v. 18, p. 23–88.

Haubold, H., 2000, Tetrapodenfährten aus dem Perm - Kenntnisstand und Progress 2000: Hallesches Jahrbuch für Geowissenschaften B, v. 22, p. 1–16.

Haubold, H. and Lucas, S.G., 2001, Die Tetrapodenfährten der Choza Formation (Texas) und das Artinsk-Alter der Redbed-Ichnofaunen des Unteren Perm: Hallesches Jahrbuch für Geowissenschaften B, v. 23, p. 79–108.

Haubold, H. and Lucas, S.G., 2003, Tetrapod footprints of the Lower Permian Choza Formation: Paläontologische Zeitschrift, v. 77, p. 247–261.

Haubold, H., Hunt, A.P., Lucas, S.G. and Lockley, M.G., 1995, Wolfcampian (Early Permian) vertebrate tracks from Arizona and New Mexico: New Mexico Museum of Natural History and Science, Bulletin 6, p. 135–165.

Haubold, H., Allen, A., Atkinson, T.P., Buta, R.J., Lacefield, J.A., Minkin, S.C. and Relihan, B.A., 2005, Interpretation of the tetrapod footprints from the Early Pennsylvanian of Alabama; in Buta, R.J., Rindsberg, A.K. and Kopaska-Merkel, D.C. eds., Pennsylvanian footprints in the Black Warrior Basin of Alabama, Alabama Paleontological Society, Birmingham. p. 75–111.

Hminna, A., Voigt, S., Saber, H., Schneider, J.W. and Hmich, D., 2012, On a moderately diverse continental ichnofauna from the Permian Ikakern Formation (Argana Basin, Western High Atlas, Morocco): Journal of African Earth Sciences, v. 68, p. 15–32.

Hunt, A.P. and Lucas, S.G., 1998, Vertebrate tracks and the myth of the belly-dragging, tail-dragging tetrapods of the Late Paleozoic**:** New Mexico Museum of Natural History and Science, Bulletin 12, p. 67–69.

Hunt, A.P., Lucas, S.G., Haubold, H. and Lockley, M.G., 1995, Early Permian (Late Wolfcampian) tetrapod tracks from the Robledo Mountains, south-central New Mexico: New Mexico Museum of Natural History and Science, Bulletin 6, p. 167–180.

Hunt, A.P., Lockley, M.G., Lucas, S.G., MacDonald, J.P., Hotton, N. and Kramer, J., 1993, Early Permian tracksites in the Robledo Mountains, south-central New Mexico: New Mexico Museum of Natural History and Science, Bulletin 2, p. 23–31.

Kohl, M.S. and Bryan, J.R., 1994, A new Middle Pennsylvanian (Westphalian) amphibian trackway from the Cross Mountain Formation, east Tennessee Cumberlands: Journal of Paleontology, v. 68, p. 655–663.

LeMone, D.V., Simpson, R.D. and Klement, K.W., 1975, Wolfcampian upper Hueco Formation of the Robledo Mountains, Doña Ana County, New Mexico: New Mexico Geological Society Guidebook, 26, p. 119–121.

Leonardi, G., 1987, Glossary and Manual of Tetrapod Footprint Palaeoichnology: Ministerio Minas Energie, Departemento Nacional da Produçao Mineral, Brasilia, 117 p.

Lucas, S.G., 2007, Tetrapod footprint biostratigraphy and biochronology: Ichnos, v. 14, p. 5–38.

Lucas, S.G. and Heckert, A.B., eds., 1995, Early Permian footprints and facies: New Mexico Museum of Natural History and Science, Bulletin 6, 301 p.

Lucas, S.G., Estep, J.W. and Hoffer, J.M., eds., 1998a, Permian stratigraphy and paleontology of the Robledo Mountains, New Mexico: New Mexico Museum of Natural History and Science Bulletin, v. 12, 98 p.

Lucas, S. G., Lerner, A. J and Voigt, S., 2013a, Scorpionid resting trace from the Lower Permian of southern New Mexico, USA: Ichnos, v. 20, p. 195-201.

Lucas, S.G., Lerner, A.J., Bruner, M. and Shipman, P., 2004, Middle Pennsylvanian ichnofauna from eastern Oklahoma, USA: Ichnos, v. 11, p. 45–55.

Lucas, S.G., Anderson, O.J., Heckert, A.B. and Hunt, A.P., 1995, Geology of Early Permian tracksites, Robledo Mountains, south-central New Mexico: New Mexico Museum of Natural History and Science, Bulletin 6, p. 13–32.

Lucas, S.G., Heckert, A.B., Estep, J.W., Hunt, A.P. and Anderson, O.J., 1998b, Stratigraphy, paleontology and depositional environments of the Lower Permian Robledo Mountains Formation of the Hueco Group, Robledo Mountains, New Mexico: New Mexico Museum of Natural History and Science, Bulletin 12, p. 29–41.

Lucas, S.G., Heckert, A.B., Estep, J.W., Hunt, A.P. and Anderson, O.J., 1998c, Stratigraphy, of the Lower Permian Hueco Group in the Robledo Mountains, Doña Ana County, New Mexico: New Mexico Museum of Natural History and Science, Bulletin 12, p. 43–54.

Lucas, S.G., Krainer, K., Corbitt, L., DiBenedetto and J., Vachard, D., 2011, The Trans Mountain Road Member, a new stratigraphic unit of the Lower Permian Hueco Group, northern Franklin Mountains, Texas: New Mexico Museum of Natural History and Science, Bulletin 53, p. 93–109.

Lucas, S.G., Voigt, S., Lerner, A.J., MacDonald, J.P., Spielmann, J.A. and Celeskey, M.D., 2010, The Prehistoric Trackways National Monument, Permian of southern New Mexico, USA: Ichnology Newsletter, v. 28, p. 10–14.

Lucas, S. G., Krainer, K., Chaney, D. S., DiMichele, W. A., Voigt, S., Berman, D. S, and Henrici, A. C., 2012, The Lower Permian Abo Formation in the Fra Cristobal and Caballo mountains, Sierra County, New Mexico: New Mexico Geological Society, Guidebook 63, p. 345-376.

Lucas, S.G., Krainer, K., Chaney, D., DiMichele, W.A., Voigt, S., Berman, D.S, and Henrici, A.C., 2013b, The Lower Permian Abo Formation in central New Mexico: New Mexico Museum of Natural History and Science, Bulletin 59, p. 161-179.

MacDonald, J.P., 1992, Footprints from the dawn of time: Science Probe, v. 2, p. 32–47.

MacDonald, J.P., 1994, Earth's first steps: Tracking life before the dinosaurs: Johnson Printing, Boulder, 290 p.

MacDonald, J.P., 1995, History of the discovery of fossil footprints in southern New Mexico, USA: New Mexico Museum of Natural History and Science, Bulletin 6, p. 1–12.

Marchetti, L., 2014, Early Permian vertebrate ichnofauna from South Alpine Region (Northern Italy): Ichnosystematics, paleoecology and stratigraphic meaning: [Ph.D. Thesis], Università degli Studi di Padova Dipartimento di Geoscienze, Padova, 128 p.

Marchetti, L., Avanzini, M. and Conti, M.A., 2013, *Hyloidichnus bifurcatus* Gilmore, 1927 and *Limnopus heterodactylus* (King, 1845) from the Early Permian of the Southern Alps (N Italy): A new equilibrium in the ichnofauna: Ichnos, v. 20, p. 202–217.

Marsh, O.C., 1894, Footprints of vertebrates in the Coal Measures of Kansas: American Journal of Science, v. 48, p. 81–84.

Minter, N.J. and Braddy, S.J., 2006, The fish and amphibian swimming traces *Undichna* and *Lunichnium*, with examples from the Lower Permian of New Mexico, USA: Palaeontology, v. 49, p. 1123–1142.

Minter, N.J. and Braddy, S.J., 2009, Ichnology of an Early Permian intertidal flat: The Robledo Mountains Formation of southern New Mexico, USA: Special Papers in Palaeontology, v. 82, p. 1–107.

Modesto, S.P., 2010, The postcranial skeleton of the aquatic parareptile *Mesosaurus tenuidens* from the Gondwanan Permian: Journal of Vertebrate Paleontology, v. 30, p. 1378–1395.

Moodie, R.L., 1929, Vertebrate footprints from the red beds of Texas: American Journal of Science, v. 97, p. 352–368.

Romer, A.S. and Price, L.I., 1940, Review of the Pelycosauria: Geological Society of America Special Papers, v. 28, p. 1–538.

Schult, M.F., 1994, Paleoecology and paleoenvironment of an Early Permian vertebrate trace fossil fauna, Las Cruces, New Mexico: [Ph.D. Thesis]: Bloomington, Indiana University, 192 p.

Schult, M.F., 1995, Vertebrate trackways from the Robledo Mountains Member of the Hueco Formation, south-central New Mexico: New Mexico Museum of Natural History and Science, Bulletin, 6, p. 115–126.

Van Allen, H.E.K., Calder, J.H. and Hunt, A.P., 2005, The trackway record of a tetrapod community in a walchian conifer forest from the Permo-Carboniferous of Nova Scotia: New Mexico Museum of Natural History and Science, Bulletin 30, p. 322–332.

Voigt, S., 2005, Die Tetrapodenichnofauna des kontinentalen Oberkarbon und Perm im Thüringer Wald - Ichnotaxonomie, Paläoökologie und Biostratigraphie: Cuvillier Verlag, Göttingen. 305 p.

Voigt, S., 2007, Auf den Spuren der Saurier: Die Tetrapodenfährten aus dem Oberkarbon und Unterperm des Saar-Nahe-Beckens; *in*, Schindler, T. and Heidtke, U. H. C., 2007, ed., Kohlesümpfe, Seen und Halbwüsten - Dokumente einer rund 300 Millionen Jahre alten Lebewelt zwischen Saarbrücken und Mainz: POLLICHIA Sonderveröffentlichung, v. 10, p. 288–303.

Voigt, S., 2012, Tetrapodenfährten: Schriftenreihe der Deutschen Gesellschaft für Geowissenschaften, v. 61, p. 92−106.

Voigt, S. and Ganzelewski, M., 2010, Toward the origin of amniotes: Diadectomorph and synapsid footprints from the early Late Carboniferous of Germany: Acta Palaeontologica Polonica, v. 55, p. 57–72.

Voigt, S. and Haubold, H., 2000, Analyse zur Variabilität der Tetrapodenfährte *Ichniotherium cottae* aus dem Tambacher Sandstein (Rotliegend, Unterperm, Thüringen): Hallesches Jahrbuch für Geowissenschaften B, v. 22, p. 17–58.

Voigt, S., Lucas, S.G. and Krainer, K., 2013a, Coastal-plain origin of trace-fossil bearing red beds in the Early Permian of southern New Mexico, U.S.A.: Palaeogeography, Palaeoclimatology, Palaeoecology, v. 369, p. 323–334.

Voigt, S., Lucas, S.G., Buchwitz, M. and Celeskey, M., 2013b, *Robledopus macdonaldi*, a new kind of basal eureptile footprint from the Early Permian of New Mexico: New Mexico Museum of Natural History and Science, Bulletin 60, p. 445–459.

Voigt, S., Hminna, A., Saber, H., Schneider, J.W. and Klein, H., 2010, Tetrapod footprints from the uppermost level of the Permian Ikakern Formation (Argana Basin, Western High Atlas, Morocco): Journal of African Earth Sciences, v. 57, p. 470–478.

Voigt, S., Lagnaoui, A., Hminna, A., Saber, H. and Schneider, J.W., 2011, Revisional notes on the Permian tetrapod ichnofauna from the Tiddas Basin, central Morocco: Palaeogeography, Palaeoclimatology, Palaeoecology, v. 302, p. 474–483.

Voigt, S., Saber, H., Schneider, J., Hminna, A., Hmich, D. and Klein, H., 2009, Large imprints of *Hyloidichnus* Gilmore, 1927 from the Permian of Morocco in the light of captorhinid phylogeny and biogeography: Abstract Volume, First International Congress on North African Vertebrate Palaeontology, Marrakech, May 25–27, 2009, p. 22.

Whyte, M.A. and Romano, M., 2001, A dinosaur ichnocoenosis from the Middle Jurassic of Yorkshire, UK: Ichnos, v. 8, p. 233–234.

Woodworth, J.B., 1900, Vertebrate footprints on Carboniferous shales of Plainville, Massachusetts: Bulletin of the Geological Society of America, v. 11, p. 449–454.

